World Journal of Gastroenterology®

Volume 12 Number 14
April 14, 2006

Supported by NSFC
2005-2006

National Journal Award
2005

The WJG Press

The WJG Press, Apartment 1066 Yishou Garden, 58 North Langxinzhuang Road, PO Box 2345, Beijing 100023, China
Telephone: +86-10-85381901
Fax: +86-10-85381893
E-mail: wjg@wjgnet.com
http: //www.wjgnet.com

ISSN 1007-9327 CN 14-1219/R Local Post Offices Code No. 82-261

World Journal of Gastroenterology www.wjgnet.com Volume 12 Number 14 Apr 14 2006

ISSN 1007-9327
CN 14-1219/R

WJG

World Journal of Gastroenterology®

Indexed and Abstracted in:
Index Medicus, MEDLINE, PubMed, Chemical Abstracts, EMBASE/Excerpta Medica, Abstracts Journals, Nature Clinical Practice Gastroenterology and Hepatology, CAB Abstracts and Global Health.

Volume 12 Number 14
April 14, 2006

World J Gastroenterol
2006 April 14; 12(14): 2149-2312
Online Submissions
www.wjgnet.com/wjg/index.jsp
www.wjgnet.com
Printed on Acid-free Paper

A Weekly Journal of Gastroenterology and Hepatology

World Journal of Gastroenterology®

Editorial Board

2004-2006

Published by The WJG Press, PO Box 2345, Beijing 100023, China
Fax: +86-10-85381893 E-mail: wjg@wjgnet.com http://www.wjgnet.com

Canada

Matthew Bjerknes, *Toronto*
Michael F Byrne, *Vancouver*
Wang-Xue Chen, *Ottawa*
Hugh J Freeman, *Vancouver*
Chantal Guillemette , *Québec*
Samuel S Lee, *Calgary*
Gerald Y Minuk, *Manitoba*
Morris Sherman, *Toronto*
Alan BR Thomson, *Edmonton*
Eric M Yoshida, *Vancouver*

China

Henry LY Chan, *Hongkong*
Xiao-Ping Chen, *Wuhan*
Jun Cheng, *Beijing*
Chi-Hin Cho, *Hong Kong*
Zong-Jie Cui, *Beijing*
Da-Jun Deng, *Beijing*
Er-Dan Dong, *Beijng*
Sheung-Tat Fan, *Hong Kong*
Xue-Gong Fan, *Changsha*
Jin Gu, *Beijing*
De-Wu Han, *Taiyuan*
Ming-Liang He, *Hong Kong*
Fu-Lian Hu, *Beijing*
Wayne HC Hu, *Hong Kong*
Guang-Cun Huang, *Shanghai*
Xiao-Long Ji, *Beijing*
Ching Lung Lai, *Hong Kong*
Kam Chuen Lai, *Hong Kong*
Yuk Tong Lee, *Hong Kong*
Suet Yi Leung, *Hong Kong*
Wai-Keung Leung, *Hong Kong*
Zhi-Hua Liu, *Beijing*
Ai-Ping Lu, *Beijing*
Jing-Yun Ma, *Beijing*
Lun-Xiu Qin, *Shanghai*
Yu-Gang Song, *Guangzhou*
Qin Su, *Beijing*
Yuan Wang, *Shanghai*
Benjamin Chun-Yu Wong, *Hong Kong*
Wai-Man Wong, *Hong Kong*
Hong Xiao, *Shanghai*
Dong-Liang Yang, *Wuhan*
Yuan Yuan, *Shenyang*
Man-Fung Yuen, *Hong Kong*
Jian-Zhong Zhang, *Beijing*
Xin-Xin Zhang, *Shanghai*
Zhi-Rong Zhang, *Chengdu*
Shu Zheng, *Hangzhou*

Croatia

Tamara Cacev, *Zagreb*
Marko Duvnjak, *Zagreb*

Czech

Milan Jirsa, *Praha*

Denmark

Peter Bytzer, *Copenhagen*
Hans Gregersen, *Aalborg*
Jens H Henriksen, *Hvidovre*
Fin Stolze Larsen, *Copenhagen*
SØren MØller, *Hvidovre*

Egypt

Abdel-Rahman El-Zayadi, *Giza*
Sanaa Moharram Kamal, *Cairo*
Ayman Yosry, *Cairo*

Finland

Pentti Sipponen, *Espoo*

France

Corlu Anne, *Rennes*
Denis Ardid, *Clermont-Ferrand*
Charles Paul Balabaud, *Bordeaux*
Jacques Belghiti, *Clichy*
Pierre Brissot, *Rennes*
Patrice Philippe Cacoub, *Paris*
Franck Carbonnel, *Besancon*
Laurent Castera, *Pessac*
Bruno Clément, *Rennes*
Jacques Cosnes, *Paris*
Thomas Decaens, *Cedex*
Francoise Lunel Fabiani, *Angers*
Gérard Feldmann, *Paris*
Jean Fioramonti, *Toulouse*
Chantal Housset, *Paris*
Juan Lucio Iovanna, *Marseille*
Rene Lambert, *Lyon*
Francis Mégraud, *Bordeaux*
Richard Moreau, *Clichy*
Thierry Piche, *Nice*
Jean Rosenbaum, *Bordeaux*
Jose Sahel, *Marseille*
Jean-Yves Scoazec, *Lyon*
Khalid Ahnini Tazi, *Clichy*
MC Vozenin-brotons, *Villejuif*
Jean-Pierre Henri Zarski, *Grenoble*
Jessica Zucman-Rossi, *Paris*

Germany

HD Allescher, *Garmisch-Partenkirchen*
Martin Anlauf, *Kiel*
Rudolf Arnold, *Marburg*
Max G Bachem, *Ulm*
Thomas F Baumert ,*Freiburg*
Daniel C Baumgart, *Berlin*
Hubert Blum, *Freiburg*
Katja Breitkopf, *Mannheim*
Markus W Büchler, *Heidelberg*
Reinhard Buettner, *Bonn*
Elke Cario, *Essen*
Uta Dahmen, *Essen*
CF Dietrich, *Bad Mergentheim*
Paul Enck, *Tuebingen*
Fred Fändrich, *Kiel*
Ulrich Robert Fölsch, *Kiel*
Peter R Galle, *Mainz*
Andreas Geier, *Aache*
Dieter Glebe, *Giessen*
Burkhard Göke, *Munich*
Florian Graeple, *Tuebingen*
Axel M Gressner, *Aachen*
Veit Gülberg, *Munich*
Rainer Haas, *Munich*
Eckhart Georg Hahn, *Erlangen*
Stephan Hellmig, *Kiel*
ohannes Herkel, *Hamburg*
Eberhard Hildt, *Berlin*
Joerg C Hoffmann, *Berlin*
Werner Hohenberger, *Erlangen*
RG Jakobs, *Ludwigshafen*
Jutta Keller, *Hamburg*
Stefan Kubicka, *Hannover*
Joachim Labenz, *Siegen*
Michael Peter Manns, *Hannover*
Stephan Miehlke, *Dresden*
Sabine Mihm, *Göttingen*
Silvio Nadalin, *Essen*
Markus F Neurath, *Mainz*
Johann Ockenga, *Berlin*
Gustav Paumgartner, *Munich*
Ulrich Ks Peitz, *Magdeburg*
Steffen Rickes, *Magdeburg*
Gerhard Rogler, *Regensburg*
Tilman Sauerbruch, *Bonn*
Andreas Schäffler, *Regensburg*
Hans Scherubl, *Berlin*
Roland M Schmid, *München*
AG Schreyer, *Regensburg*
Tobias Schroeder, *Essen*
Hans Seifert, *Oldenburg*
J Ruediger Siewert, *Munich*
Manfred V Singer, *Mannheim*
Gisela Sparmann, *Rostock*
Jurgen M Stein, *Frankfurt*
Manfred Stolte, *Bayreuth*
Rainer Straub, *Regensburg*
WR Stremmel, *Heidelberg*
Harald F Teutsch, *Ulm*
HL Tillmann, *Leipzig*
Tung-Yu Tsui, *Regensburg*
Axel Ulsenheimer, *Munich*
Patrick Veit, *Essen*
Siegfried Wagner, *Deggendorf*
Henning Walczak, *Heidelberg*
Fritz von Weizsacker, *Berlin*
Jens Werner, *Heidelberg*
Bertram Wiedenmann, *Berlin*
Reiner Wiest, *Regensburg*
Stefan JP Zeuzem, *Homburg*

Greece

Elias A Kouroumalis, *Heraklion*

Hungary

Peter Laszlo Lakatos, *Budapest*

Iceland

H Gudjonsson, *Reykjavik*

India

Sujit K Bhattacharya, *Kolkata*
Yogesh K Chawla, *Chandigarh*
Radha K Dhiman, *Chandigarh*
Sri Prakash Misra, *Allahabad*
ND Reddy, *Hyderabad*

Iran

Reza Malekzadeh, *Tehran*
Seyed Alireza Taghavi, *Shiraz*

Ireland

Anthony P Moran, *Galway*

Israel

Simon Bar-Meir, *Hashomer*
Abraham Rami Eliakim, *Haifa*
Yaron Ilan , *Jerusalem*
Yaron Niv, *Pardesia*
Ran Oren, *Tel Aviv*

Italy

Giovanni Addolorato, *Roma*
Domenico Alvaro, *Rome*
Annese V, *San Giovanni Rotond*
Adolfo Francesco Attili, *Roma*
Giovanni Barbara, *Bologna*
Gabrio Bassotti, *Perugia*
Franco Bazzoli, *Bologna*
Stefano Bellentani, *Carpi*
Antomio Benedetti, *Ancona*
Mauro Bernardi, *Bologna*
Luigi Bonavina, *Milano*
Giovanni Cammarota, *Roma*
Antonino Cavallari, *Bologna*
Giuseppe Chiarioni, *Valeggio*
Massimo Conio, *Sanremo*
Dario Conte, *Milano*
Gino Roberto Corazza, *Pavia*
Francesco Costa, *Pisa*
Antonio Craxi, *Palermo*
Roberto De Giorgio, *Bologna*

Giovanni D De Palma, *Naples*
Fabio Farinati, *Padua*
Andrea Galli, *Firenze*
Valeria Ghisett , *Turin*
Edoardo G Giannini, *Genoa*
Paolo Gionchetti, *Bologna*
Mario Guslandi, *Milano*
Giacomo Laffi, *Firenze*
Giovanni Maconi, *Milan*
ED Mangoni, *Napoli*
Giulio Marchesini, *Bologna*
Giuseppe Montalto, *Palermo*
Giovanni Monteleone, *Rome*
Gerardo Nardone, *Napoli*
Luisi Pagliaro, *Palermo*
Fabrizio R Parente, *Milan*
F Perri, *San Giovanni Rotondo*
Raffaele Pezzilli, *Bologna*
A Pilotto, *San Giovanni Rotondo*
Paolo Del Poggio, *Treviglio*
Gabriele Bianchi Porro, *Milano*
Piero Portincasa, *Bari*
Bernardino Rampone, *Siena*
Claudio Romano, *Messina*
Mario Del Tacca, *Pisa*
Pier Alberto Testoni, *Milan*
Enrico Roda, *Bologna*
Vincenzo Savarino, *Genova*
Roberto Testa, *Genoa*
Dino Vaira, *Bologna*

Japan

Kyoichi Adachi, *Izumo*
Yasushi Adachi, *Sapporo*
Taiji Akamatsu, *Matsumoto*
Sk Md Fazle Akbar, *Ehime*
Takafumi Ando, *Nagoya*
Akira Andoh, *Otsu*
Taku Aoki, *Tokyo*
Masahiro Arai, *Tokyo*
Tetsuo Arakawa, *Osaka*
Yasuji Arase, *Tokyo*
Masahiro Asaka, *Sapporo*
Hitoshi Asakura, *Tokyo*
Takeshi Azuma, *Fukui*
Yoichi Chida, *Fukuoka*
Takahiro Fujimori, *Tochigi*
Jiro Fujimoto, *Hyogo*
Kazuma Fujimoto, *Saga*
Mitsuhiro Fujishiro, *Tokyo*
Yoshihide Fujiyama, *Otsu*
Hiroyuki Hanai, *Hamamatsu*
Kazuhiro Hanazaki, *Nagano*
Naohiko Harada, *Fukuoka*
Makoto Hashizume, *Fukuoka*
Tetsuo Hayakawa, *Nagoya*
Kazuhide Higuchi, *Osaka*
Keiji Hirata, *Kitakyushu*
Yuji Iimuro, *Nishinomiya*
Kenji Ikeda, *Tokyo*
Fumio Imazeki, *Chiba*
Yasuhiro Inokuchi, *Yokohama*
Haruhiro Inoue, *Yokohama*
Masayasu Inoue, *Osaka*
Hiromi Ishibashi, *Nagasaki*
Shunji Ishihara, *Izumo*
Toru Ishikawa, *Niigata*
Kei Ito, *Sendai*
Masayoshi Ito, *Tokyo*
Hiroaki Itoh, *Akita*
Ryuichi Iwakiri, *Saga*
Hiroshi Kaneko, *Aichi-Gun*
Takashi Kanematsu, *Nagasaki*
Junji Kato, *Sapporo*
Mototsugu Kato, *Sapporo*
Shinzo Kato, *Tokyo*
Sunao Kawano, *Osaka*
Mitsuhiro Kida, *Kanagawa*
Yoshikazu Kinoshita, *Izumo*
Tsuneo Kitamura, *Chiba*
Seigo Kitano, *Oita*
Kazuhiko Koike, *Tokyo*
Norihiro Kokudo, *Tokyo*
Satoshi Kondo, *Sapporo*
Shoji Kubo, *Osaka*
Shigeki Kuriyama, *Kagawa*
Masato Kusunoki, *Tsu Mie*
Katsunori Iijima, *Sendai*
Shin Maeda, *Tokyo*
Masatoshi Makuuchi, *Tokyo*
Osamu Matsui, *Kanazawa*
Yasushi Matsuzaki, *Tsukuba*
Kiyoshi Migita ,*Omura*
Tetsuya Mine, *Kanagawa*
Hiroto Miwa, *Hyogo*
Masashi Mizokami, *Nagoya*
Motowo Mizuno, *Hiroshima*
Morito Monden, *Suita*
Hisataka S Moriwaki, *Gifu*
Yoshiharu Motoo, *Kanazawa*
Akihiro Munakata, *Hirosaki*
Kazunari Murakami, *Oita*
Kunihiko Murase, *Tusima*
Yujl Naito, *Kyoto*
Hisato Nakajima, *Tokyo*
Hiroki Nakamura, *Yamaguchi*
Shotaro Nakamura, *Fukuoka*
Mikio Nishioka, *Niihama*
Susumu Ohmada, *Maebashi*
Masayuki Ohta, *Oita*
Tetsuo Ohta, *Kanazawa*
Kazuichi Okazaki, *Osaka*
Katsuhisa Omagari, *Nagasaki*
Saburo Onishi, *Nankoku*
Morikazu Onji, *Ehime*
Satoshi Osawa, *Hamamatsu*
Yutaka Inagaki , *Kanagawa*
Hiromitsu Saisho, *Chiba*
Isao Sakaida, *Yamaguchi*
Michiie Sakamoto, *Tokyo*
Yasushi Sano, *Chiba*
Iwao Sasaki, *Sendai*
Motoko Sasaki, *Kanazawa*
Chifumi Sato, *Tokyo*
Shuichi Seki, *Osaka*
Hiroshi Shimada, *Yokohama*
Mitsuo Shimada, *Tokushima*
Tomohiko Shimatan, *Hiroshima*
Hiroaki Shimizu, *Chiba*
Ichiro Shimizu, *Tokushima*
Tooru Shimosegawa, *Sendai*
Tadashi Shimoyama, *Hirosaki*
Ken Shirabe, *Iizuka City*
Yoshio Shirai, *Niigata*
Katsuya Shiraki, *Mie*
Yasushi Shiratori, *Okayama*
Yasuhiko Sugawara, *Tokyo*
Hidekazu Suzuki, *Tokyo*
Tadatoshi Takayama, *Tokyo*
Tadashi Takeda, *Osaka*
Kiichi Tamada, *Tochigi*
Akira Tanaka, *Kyoto*
Eiji Tanaka, *Matsumoto*
Noriaki Tanaka, *Okayama*
Shinji Tanaka, *Hiroshima*
Wei Tang, *Tokyo*
Kyuichi Tanikawa, *Kurume*
Akira Terano, *Shimotsugagun*
Hitoshi Togash, *Yamagata*
Kazunari Tominaga, *Osaka*
Minoru Toyota, *Sapporo*
Akihito Tsubota, *Chiba*
Shingo Tsuji, *Osaka*
Takato Ueno, *Kurume*
Shinichi Wada, *Tochigi*
Hiroyuki Watanabe, *Kanazawa*
Toshio Watanabe, *Osaka*
Yuji Watanabe, *Ehime*
Chun-Yang Wen, *Nagasaki*
Koji Yamaguchi, *Fukuoka*
Takayuki Yamamoto, *Yokkaichi*
Takashi Yao, *Fukuoka*
Masashi Yoneda, *Tochigi*
Hiroshi Yoshida, *Tokyo*
Masashi Yoshida, *Tokyo*
Norimasa Yoshida, *Kyoto*
Kentaro Yoshika, *Toyoake*
Masahide Yoshikawa, *Kashihara*

Lebanon

Ala I Sharara, *Beirut*
Joseph Daoud Boujaoude, *Beirut*

Lithuania

Sasa Markovic, *Japljeva*

Macedonia

Vladimir Cirko Serafimoski, *Skopje*

Malaysia

Andrew Seng Boon Chua, *Ipoh*
Khean-Lee Goh, *Kuala Lumpur*
Jayaram Menon, *Sabah*

Mexico

Saúl Villa-Trevio, *México*
JKY Furusho, *Mexico*

Monaco

Patrick Rampal, *Monaco*

Netherlands

Lee Bouwman, *Leiden*
Rick Greupink, *Groningen*
Janine K Kruit, *Groningen*
Ernst Johan Kuipers, *Rotterdam*
Yi Liu, *Amsterdam*
Chris JJ Mulder, *Amsterdam*
Michael Müller, *Wageningen*
Amado Salvador Peña, *Amsterdam*
Robert J Porte, *Groningen*
Andreas Smout, *Utrecht*
RW Stockbrugger, *Maastricht*
Renate G Van der Molen, *Rotterdam*
Karel van Erpecum, *Utrecht*
GV Henegouwen, *Utrecht*

New Zealand

Ian David Wallace, *Auckland*

Nigeria

Samuel Babafemi Olaleye, *Ibadan*

Norway

Trond Berg, *Oslo*
Helge Lyder Waldum, *Trondheim*

Pakistan

Muhammad S Khokhar, *Lahore*

Poland

Tomasz Brzozowski, *Cracow*
Robert Flisiak, *Bialystok*
Hanna Gregorek, *Warsaw*
Hanna Gregorek, *Warsaw*
DM Lebensztejn, *Bialystok*
Wojciech G Polak ,*Wroclaw*

Portugal

Miguel Carneiro De Moura, *Lisbon*

Russia

Vladimir T Ivashkin, *Moscow*
Leonid Lazebnik, *Moscow*
Vasiliy I Reshetnyak, *Moscow*

Singapore

Bow Ho, *Kent Ridge*
Khek-Yu Ho, *Singapor*
Francis Seow-Choen, *Singapore*

Slovakia

Anton Vavrecka, *Bratislava*

South Africa

Michael C Kew, *Parktown*

South Korea

Byung Ihn Choi, *Seoul*
Ho Soon Choi, *Seoul*
Jae J Kim, *Seoul*
Jin-Hong Kim, *Suwon*
Myung-Hwan Kim, *Seoul*
Jong Kyun Lee, *Seoul*
Eun-Yi Moon, *Taejeon City*
Jae-Gahb Park, *Seoul*
Dong Wan Seo, *Seoul*

Spain

Juan G Abraldes, *Barcelona*
Agustin Albillos, *Madrid*
Raul J Andrade, *Málaga*
Luis Aparisi, *Valencia*
Fernando Azpiroz, *Barcelona*
Ramon Bataller, *Barcelona*
Josep M Bordas, *Barcelona*
Xavier Calvet, *Sabadell*
Vicente Carreño, *Madrid*
Antoni Castells, *Barcelona*
Vicente Felipo, *Valencia*
Juan C Garcia-Pagán, *Barcelona*
Jaime Bosch Genover, *Barcelona*
Jaime Guardia, *Barcelona*
Angel Lanas, *Zaragoza*
María Isabel Torres López, *Jaén*
José M Mato, *Derio*
MAM Navas, *Pamplona*
Julian Panes, *Barcelona*
Miguel Minguez Perez, *Valencia*
Miguel Perez-Mateo, *Alicante*
Josep M Pique, *Barcelona*
Jesus M Prieto, *Pamplona*
Sabino Riestra, *Pola De Siero*
Luis Rodrigo, *Oviedo*
Manuel Romero-Gómez, *Sevilla*

Sweden

Curt Einarsson, *Huddinge*
Xupeng Ge, *Stockholm*
Hanns-Ulrich Marschall, *Stockholm*
Lars Christer Olbe, *Molndal*
Xiao-Feng Sun, *Linkoping*
Ervin Tóth, *Malmö*

Switzerland

Chrish Beglinger, *Basel*
Pierre A Clavien, Zurich
Jean-Francois Dufour, *Bern*
Franco Fortunato, *Zürich*
Jean Louis Frossard, *Geneva*
Gerd A Kullak-Ublick, *Zurich*
Bruno Stieger, *Zurich*
Arthur Zimmermann, *Berne*

Turkey

Yusuf Bayraktar, *Ankara*
Figen Gurakan, *Ankara*
Aydin Karabacakoglu, *Konya*
Serdar Karakose, *Konya*
Hizir Kurtel, *Istanbu*
Osman Cavit Ozdogan, *Istanbul*
Cihan Yurdaydin, *Ankara*

United Arab Emirates

Sherif M Karam, *Al-Ain*

United Kingdom

Anthony TR Axon, *Leeds*
Mairi Brittan, *London*
Andrew Kenneth Burroughs, *London*
Paul Jonathan Ciclitira, *London*
Amar Paul Dhillon, *London*
Elizabeth Furrie, *Dundee*
Daniel Richard Gaya, Edinburgh
Subrata Ghosh, *London*
William Greenhalf, *Liverpool*
Peter Clive Hayes, Edinburgh
Gwo-Tzer Ho, *Edinburgh*
Anthony R Hobson, *Salford*
David Paul Hurlstone, *Sheffield*
Brian T Johnston, *Belfast*
David EJ Jones, *Newcastle*
Michael A Kamm, *Harrow*
Patricia F Lalor, *Birmingham*
Hong-Xiang Liu, *Cambridge*
Dermot Patrick Mcgovern, *Oxford*
Giorgina Mieli-Vergani, *London*
Nikolai V Naoumov, *London*
John P Neoptolemos, *Liverpool*
James Neuberger, *Birmingham*
Mark S Pearce, *Newcastle Upon Tyne*
Marco Senzolo, *Padova*
Robert Sutton, *Liverpool*
Simon D Taylor-Robinson, *London*
Ulrich Thalheimer, *London*
Nick Paul Thompson, *Newcastle*
David Tosh, *Bath*
Frank Ivor Tovey, *Basingstoke*
Diego Vergani, *London*
Peter James Whorwell, *Manchester*
Karen Leslie Wright, *Bath*
Min Zhao, *Foresterhill*

United States

Christian Cormac Abnet, *Maryland*
Gary A Abrams, *Birmingham*
Golo Ahlenstiel, *Bethesda*
Gavin Edward Arteel, *Louisville*
Jasmohan Singh Bajaj, *Milwaukee*
Jamie S Barkin, *Miami Beach*
Kim Elaine Barrett, *San Diego*
Jennifer D Black, *Buffalo*
Alan Cahill, *Philadelphia*
David L Carr-Locke, *Boston*
Ravi S Chari, *Nashville*
Jiande Chen, *Galveston*
Xian-Ming Chen, *Rochester*
Parimal Chowdhury, *Arkansas*
Raymond T Chung,Boston
James M Church, *Cleveland*
Vincent Coghlan, *Beaverton*
John Cuppoletti, *Cincinnati*
Peter V Danenberg, *Los Angeles*
Kiron Moy Das, *New Brunswick*
Vincent Paul Doria-Rose, *Seattle*
Bijan Eghtesad, *Cleveland*
Hala El-Zimaity, *Houston*
Michelle Embree-Ku, *Providence*
Ronnie Fass, *Tucson*
Chris E Forsmark, *Gainesville*
Scott L Friedman, *New York*
John Geibel, *New Haven*
Ignacio Gil-Bazo, *New York*
David Y Graham, *Houston*
Anna S Gukovskaya, *Los Angeles*
Stephen B Hanauer, *Chicago*
Gavin Harewood, *Rochester*
Alan W Hemming, *Gainesville*
Jamal A Ibdah, *Columbia*
Atif Iqbal, *Omaha*
Hajime Isomoto, *Rochester*
Hartmut Jaeschke, *Tucson*
Dennis M Jensen, *Los Angeles*
Leonard R Johnson, *Memphis*
Peter James Kahrilas, *Chicago*
AN Kalloo, *Baltimore*
Neil Kaplowitz, Los Angeles
Ali Keshavarzian, *Chicago*
Joseph B Kirsner, *Chicago*
Burton I Korelitz, *New York*
Robert J Korst, *New York*
Richard A Kozarek, *Seattle*
Shiu-Ming Kuo, *Buffalo*
Daryl Tan Yeung Lau, *Galvesto*
Glen A Lehman, *Indianapolis*
Frederick H Leibach, *Augusta*
Alex B Lentsch, *Cincinnati*
Andreas Leodolter, *La Jolla*
Gene LeSage, *Houston*
Ming Li, *New Orleans*
LM Lichtenberger, *Houston*
GR Lichtenstein, *Philadelphia*
Martin Lipkin, *New York*
Josep M Llovet, *New York*
Edward V Loftus, *Rocheste*
Robin G Lorenz, *Birmingham*
JD Luketich, *Pittsburgh*
Henry Thomson Lynch, *Omaha*
John Frank Di Mari, *Texas*
John M Mariadason, *Bronx*
WM Mars, *Pittsburgh*
George W Meyer, *Sacramento*
G Michalopoulos, *Pittsburgh*
S Pal Singh S Monga, *Pittsburgh*
Timothy H Moran, *Baltmore*
Hiroshi Nakagawa, *Philadelphia*
Douglas B Neison, *Minneaplis*
Curtis T Okamoto, *Los Angeles*
Stephen J Pandol, *Los Angeles*
Pankaj Jay Pasricha, *Gaveston*
Zhiheng Pei, *New York*
Michael A Pezzone, *Pittsburgh*
CS Pitchumoni, *New Brunswiuc*
Jay Pravda, *Gainesville*
M Raimondo, *Jacksonville*
Adrian Reuben, *Charleston*
Victor E Reyes, *Galveston*
Richard Rippe, *Chapel Hill*
Marcos Rojkind, *Washington*
Hemant Kumar Roy, *Evanston*
Shawn David Safford, *Norfolk*
NJ Shaheen, *Chapel Hill*
Stuart Sherman, *Indianapolis*
Shivendra Shukla, *Columbia*
Alphonse E Sirica, *Virginia*
Michael Steer, *Boston*
Gary D Stoner, *Columbus*
Yvette Tache, *Los Angeles*
Jayant Talwalkar, *Rochester*
K-M Tchou-Wong, *New York*
PJ Thuluvath, *Baltimore*
Swan Nio Thung, *New York*
RA Travagli, *Baton Rouge*
G Triadafilopoulos, *Stanford*
Chung-Jyi Tsai, *Lexington*
Hugo E Vargas, *Scottsdale*
Jian-Ying Wang, *Baltimore*
Steven David Wexner, *Weston*
Keith Tucker Wilson, *Baltimore*
Jackie Wood, *Ohio*
George Y Wu, *Farmington*
Jian Wu, *Sacramento*

Samuel Wyllie, Houston
Wen Xie, *Pittsburgh*
Yoshio Yamaoka, *Texas*
Liqing Yu, *Winston-Salem*
David Yule, *Rochester*
Ruben Zamora, *Pittsburgh*
Michael Zenilman, *Brooklyn*
Zhi Zhong, *Chapel Hill*

Yugoslavia
DM Jovanovic, *Sremska Kamenica*

National Journal Award
2005

World Journal of Gastroenterology®

Volume 12 Number 14
April 14, 2006

Supported by NSFC
2005-2006

Contents

World Journal of Gastroenterology
Volume 12 **Number** 14 **April** 14, 2006

Contents

World Journal of Gastroenterology (*World J Gastroenterol* , *WJG*), a leading international journal in gastroenterology and hepatology, has an established reputation for publishing first class research on esophageal cancer, gastric cancer, liver cancer, viral hepatitis, colorectal cancer, and *Helicobacter pylori* infection, providing a forum for both clinicians and scientists, and has been indexed and abstracted in *Index Medicus*, MEDLINE, PubMed, Chemical Abstracts, EMBASE, Abstracts Journals, Nature Clinical Practice Gastroenterology and Hepatology, CAB Abstracts and Global Health. *WJG* is a weekly journal published by The *WJG* Press. The publication date is on 7th, 14th, 21st, and 28th every month. The *WJG* is supported by The National Natural Science Foundation of China, No. 30224801 and No.30424812, which was founded with a name of *China National Journal of New Gastroenterology* on October 1,1995, and renamed as *WJG* on January 25, 1998.

PRINTED BY
Printed in Beijing on acid-free paper by Beijing Kexin Printing House

Print ISSN 1007-9327 CN 14-1219/R.

EDITORIAL OFFICE
World Journal of Gastroenterology,
The WJG Press, Apartment 1066 Yishou Garden, 58 North Langxinzhuang Road, PO Box 2345, Beijing 100023, China
Telephone: +86-10-85381901
Fax: +86-10-85381893
E-mail: wjg@wjgnet.com
http://www.wjgnet.com

SUBSCRIPTION AND AUTHOR REPRINTS

Jing Wang
The WJG Press, Apartment 1066 Yishou Garden, 58 North Langxinzhuang Road, PO Box 2345, Beijing 100023, China
Telephone: +86-10-85381901
Fax: +86-10-85381893
E-mail: j.wang@wjgnet.com
http://www.wjgnet.com

Institutional Rates
2006 rates: USD 1500.00

Personal Rates
2006 rates: USD 700.00

INSTRUCTIONS TO AUTHORS
Full instructions are available online at http://www.wjgnet.com/wjg/help/instructions.jsp. If you do not have web access please contact the editorial office.

PO Box 2345, Beijing 100023, China
www.wjgnet.com
wjg@wjgnet.com

World J Gastroenterol 2006 April 14; 12(14): 2149-2160
World Journal of Gastroenterology ISSN 1007-9327

EDITORIAL

Role of Toll-like receptors in health and diseases of gastrointestinal tract

Greg Harris, Rhonda KuoLee, Wangxue Chen

Greg Harris, Rhonda KuoLee, Wangxue Chen, Institute for Biological Sciences, National Research Council Canada, 100 Sussex Drive, Ottawa, ON, K1A 0R6, Canada
Supported by the National Research Council Canada and the National Institutes of Health, United States
Correspondence to: Dr. Wangxue Chen, National Research Council Canada, Institute for Biological Sciences, 100 Sussex Drive, Room 3100, Ottawa, ON K1A 0R6, Canada. wangxue.chen@nrc.gc.ca
Telephone: +1-613- 9910924 Fax: +1-613-9529092
Received: 2005-10-03 Accepted: 2005-12-22

Abstract

The human gastrointestinal (GI) tract is colonized by non-pathogenic commensal microflora and frequently exposed to many pathogenic organisms. For the maintenance of GI homeostasis, the host must discriminate between pathogenic and non-pathogenic organisms and initiate effective and appropriate immune and inflammatory responses. Mammalian toll-like receptors (TLRs) are members of the pattern-recognition receptor (PRR) family that plays a central role in the initiation of innate cellular immune responses and the subsequent adaptive immune responses to microbial pathogens. Recent studies have shown that gastrointestinal epithelial cells express almost all TLR subtypes characterized to date and that the expression and activation of TLRs in the GI tract are tightly and coordinately regulated. This review summarizes the current understanding of the crucial dual roles of TLRs in the development of host innate and adaptive immune responses to GI infections and the maintenance of the immune tolerance to commensal bacteria through down-regulation of surface expression of TLRs in intestinal epithelial cells.

Key words: Toll-like receptor; Gastrointestinal tract; Intestinal disease

Harris G, KuoLee R, Chen W. Role of Toll-like receptors in health and diseases of gastrointestinal tract. *World J Gastroenterol* 2006; 12(14): 2149-2160

http://www.wjgnet.com/1007-9327/12/2149.asp

INTRODUCTION

Innate immunity is considered to be important for the elimination of invading microbes from the gastrointestinal tract and for the control of their systemic dissemination. Mammalian toll-like receptors (TLRs) are members of the pattern-recognition receptor (PRR) family and play a central role in the initiation of innate cellular immune responses and the subsequent adaptive immune responses to microbial pathogens[1,2]. The capacity to recognize diverse pathogen-associated molecular patterns (PAMPs) that are unique to microorganisms and therefore absent from host cells makes TLRs well-suited to act as an early warning system against invading pathogens. Activation of the TLR signal transduction pathway leads to the induction of numerous genes that function in host defense, including those for inflammatory cytokines, chemokines, antigen-presenting molecules, and costimulatory molecules[1,2]. Recognition of PAMPs by TLRs differs from the recognition of microorganism-specific antigens by the adaptive immune system, in that PAMPs are typically highly conserved across several species of microorganisms, such as surface lipoproteins common to several bacterial species, or genetic material from an entire family of viruses. The ability of TLRs to recognize a broad spectrum of microbial molecules enables the host to detect the presence of pathogens rapidly, before a more widespread infection occurs.

In this review, we have briefly summarized the recent progress in the understanding of the role of TLRs in the host defense against gastrointestinal pathogens and in the maintenance of immune tolerance to commensal microflora. For more general information on the biological functions of TLRs and the TLR signaling pathway, the readers are referred to a number of excellent review articles in this field[3-7].

TLRs, TLR LIGANDS AND TLR SIGNALING PATHWAYS

To date, 11 related TLR genes have been identified and characterized (*tlr1* to *tlr11*) (Table 1)[3,4,7-9]. Some TLRs, such as TLR3, TLR5 and TLR9, only recognize one type of PAMP, while others, such as TLR2, appear to recognize several different microbial molecules. Among these, TLR4 is the signal-transducing element of the

Table 1 Toll-like receptors and known microbial ligands[4,7,18]

TLR family	Microbial ligands
Lipid ligands	
TLR1	Tri-acyl lipopeptides (bacteria, mycobacteria)
TLR2	Lipoprotein/lipopeptides (a variety of pathogens)
	Peptidoglycan (Gram-positive bacteria)
	Lipoteichoic acid (Gram-positive bacteria)
	Lipoarabinomannan (mycobacteria)
	A phenol-soluble modulin (*Staphylococcus epidermidis*)
	Glycoinositolphospholipids (*Trypanosoma Cruzi*)
	Glycolipids (*Treponema maltophilum*)
	Porins (*Neisseria*)
	Zymosan (fungi)
	Atypical LPS (*Leptospira interrogans* and *Porphyromonas gingivalis*)
	Hemagglutinin (measles)
TLR4	LPS (Gram-negative bacteria)
	Fusion protein (respiratory syncytial virus)
	Envelope proteins (mouse mammary tumor virus)
	HSP60 (*Chlamydia pneumoniae*)
TLR6	Di-acyl lipopeptides (mycoplasma)
Nucleic acid ligand	
TLR3	Double-stranded RNA (virus)
TLR7 or 8	U-rich ssRNA
TLR9	CpG DNA (bacteria)
Protein ligand	
TLR5	Flagellin (bacteria)
Uropathogenic bacteria	
TLR11	Uropathogenic bacteria
Ligand unknown	
TLR10	?

lipopolysaccharide (LPS) receptor complex, and is also involved in the signaling response to other exogenous stimuli [*e.g.*, bacterial HSP60 and fimbriae, *Streptococcus pneumoniae* pneumolysin, lipoteichoic acid (LTA) from gram-positive bacteria, and respiratory syncytial virus coat protein][10,11]. TLR2 binds to bacterial lipoproteins, LTA and peptidoglycan[11-13], although some recent studies have argued that peptidoglycan recognition does not occur through TLR2[14], or that TLR2 alone is not sufficient to detect peptidoglycan[15]. Flagellin, a bacterial protein involved in motility, binds TLR5[16]. CpG, a repetitive sequence of unmethylated nucleic acids found in high quantities in bacterial DNA, is recognized by TLR9[17]. Also, although the specific ligand is not yet known, murine TLR11 is involved in protection from uropathogenic bacterial infection in mice[18]. Certain bacterial virulence factors, such as fimbriae or enterotoxins, have been shown to activate TLR2 and/or TLR4[19-23]. Some viruses are also recognized by TLRs. Double-stranded RNA (dsRNA), which is found in many types of virus, elicits immune responses through TLR3[24] and probably another PRR[25, 26]. Human TLR7 and/or TLR8 are known to bind single-stranded RNA (ssRNA) from viruses, such as human immunodeficiency virus (HIV)-1, influenza and human parechovirus-1[27-29]. TLR specificity is not limited to bacterial or viral PAMPs. TLR2 and/or TLR4 have been implicated in the detection of *Candida albicans* and *Entamoeba histolytica*[30-34]. In addition, some TLRs also bind endogenous molecules, such as HSP60, fibronectin, surfactant protein A, and β-defensin-2[4, 9].

TLRs vary from one another by their ligand specificity, determined by the extracellular portion of the receptor. The cytoplasmic tails of TLRs appear to be associated with the tails of other TLRs in a process known as TLR cooperation[35]. This can occur between receptors of similar or different specificity. For example, TLR2 requires association with TLR6 in order to propagate the correct intracellular signal after binding peptidoglycan or zymosan (a yeast cell-wall particle)[35]. In the cytoplasmic domain of TLRs, the element common to all TLRs is the Toll-interleukin-1-related (TIR) domain. After homo- or heterodimerization of TLRs, the intracellular TIR domains self-associate, and bind TIR domains of intracellular adaptor molecules. All TLRs except TLR3 associate with the TIR-containing myeloid differentiation factor (MyD) 88[36], which upon activation mediates a signaling cascade leading to activation of the NF-κB transcription factor[6]. The end result of TLR signaling is an upregulation of pro-inflammatory cytokines and chemokines, such as TNF-α and IL-8, and the induction of a localized immune response.

TLR4 was the first PRR to be properly identified as having a specific ligand[10], and the mechanism of TLR/LPS interaction is thus the best studied. LPS is transferred to cell-surface CD14 by LPS-binding protein (LBP)[37,38]. CD14 does not signal LPS presence directly to the cell because it lacks a cytoplasmic domain. Instead, the proximity of CD14 to TLR4 allows CD14 to "present" LPS to TLR4[10,39,40], which itself is bound to MD-2 on the cell surface. A physical association on the cell surface between MD-2 and TLR4 is essential for TLR4 function[41], and MD-2 is in fact essential for TLR4 to be trafficked to the cell surface in the first place[42].

TLR ACTIVITY IN THE GASTROINTESTINAL (GI) TRACT

Emerging evidence has shown that TLR expression and activation is specially regulated in the GI tract. This is probably due to the continuous presence of physiological microflora in the gut. It is essential that TLRs do not react to PAMPs expressed by commensal microflora, yet retain the ability to detect and mount effective immune responses against invading pathogens. This is mainly accomplished by the down-regulation of surface expression of TLRs, such as TLR2, TLR4 and MD-2, in the gut epithelium[5,43-47]. Although intestinal epithelial cells (IEC) can and sometimes do express TLR2 and/or TLR4[46,48-50], these TLRs usually relocate to either intracellular compartments such as the Golgi apparatus, or to the basolateral membrane of the cell as a result of the continuous stimulation by varying components of the commensal bacteria[50-53]. Indeed, *in vitro* studies of an IEC line have shown that LPS or peptidoglycan stimulation relocates the constitutive surface expression

of TLR2 and TLR4 into intracellular compartments near the basolateral membrane[51]. Others have shown that both primary and immortalized IEC responded to TLR ligand stimulation, and that prolonged exposure to these ligands reduced surface expression of TLRs without reducing mRNA levels[49]. It is important to note that intracellular TLR4 retains its full signaling capability, and detects both internalized LPS and intracellular bacteria[52,53]. This mechanism allows the host to detect the pathogenic organisms that have penetrated the intestinal epithelium without overreaction to commensal bacteria on the surface of intestinal epithelium.

There have been some debates over the precise cellular localization of TLR5, the receptor for flagellin, in IEC[54-57]. One group has shown that TLR5 was only expressed on the basolateral membrane[55], whereas another group using a different cell line showed both basolateral and apical TLR5 expression following the stimulation with *Escherichia coli* flagellin[54]. Apical TLR5 expression has also been demonstrated *ex vivo* in the murine ileum[54]. In addition, *Salmonella typhimurium* flagellin can translocate across epithelial cells to the basolateral membrane, a process that is essential for *S. typhimurium* flagellin to induce inflammatory responses[55,58,59]. These data strongly suggest the possibility that under normal circumstances TLR5 is only expressed at the basolateral membrane in IEC. The basolateral expression of TLR5 may be important for the maintenance of GI homeostasis since flagellin from commensal bacteria generally does not translocate to the basolateral membrane and thereby does not induce an inflammatory response[58].

The intestinal epithelium also uses specific tissue distribution and compartmentalization of TLR-expressing cells to avoid unnecessary TLR activation and at the same time allow the development of rapid and efficient host defense against invasion by pathogenic organisms. In this regard, intestinal myofibroblasts are capable of upregulating TLR2, TLR3, TLR4, TLR6 and TLR7 expression after LPS or LTA stimulation, thereby allowing a functional TLR response to invasive pathogens in the subepithelial compartment[60]. It has also been shown that crypt epithelial cells express TLR2 and TLR4, whereas mature IEC express TLR3 only[44]. Since crypt epithelial cells do not come into direct contact with commensal bacteria, their expression of TLR2 and TLR4 should not be detrimental to the host. TLR3 expression in the intestinal lumen is also non-detrimental because the TLR3 ligand, viral dsRNA, is not a natural presence in the gut microflora.

Another strategy in the regulation of TLR activities in the GI mucosa is through high expression of TLR-antagonists to suppress the activation of these TLRs still present at the cell surface. For example, TLR9 is constitutively expressed in IEC, but remains completely unresponsive to CpG[61]. In this regard, various proteins, termed TLR-attenuating factors, are known to attenuate TLR signaling, and this was extensively reviewed by Liew *et al*[6]. Some of these TLR-attenuating factors have been shown to be highly expressed in TLR-hyporesponsive IEC, or to be lacking in cases of intestinal inflammation. Toll-interacting protein (TOLLIP) inhibits TLR signaling by interfering with IL-1 receptor-associated kinase (IRAK), an important component of the TLR signaling cascade[62]. TOLLIP was found to be upregulated in TLR-hyporesponsive primary and immortalized IEC after prolonged exposure to TLR ligands[45,49], and TOLLIP mRNA was highly expressed in healthy colonic mucosa[49]. Peroxisome proliferator-activated receptor γ (PPARγ) limits TLR activity by inhibiting NF-κB activation[63,64]. PPARγ was more highly expressed in the colon compared to the small intestine[65], and has been shown to have a crucial role in the induction of tolerance to commensal bacteria[66]. Stimulation of IEC by TLR ligands or by intestinal microflora extracts increased PPARγ expression[67]. Thus, TOLLIP and PPARγ appear to down-regulate TLR activity in direct response to the continual exposure of IEC to commensal bacteria.

It has recently been identified that TIR8/single Ig IL-1-related receptor (SIGIRR) can negatively regulate TLR activity, possibly by interfering with TLR4 and IRAK signaling[68,69]. Studies in TIR8$^{-/-}$ mice showed that these mice developed more severe intestinal inflammation than wild-type control mice after LPS treatment[70], implicating the role of TIR8 in the suppression of the intestinal inflammatory response. In addition, it has been shown in a mouse model of colitis that vasoactive intestinal peptide (VIP) treatment can restore the overexpressed TLR2 and TLR4 to baseline levels[71]. The mechanism of action was unknown, but might involve either VIP-mediated suppression of NF-κB activation (leading to a cessation of further TLR expression) or suppression of cytokines known to contribute to TLR upregulation in IEC[71]. This appears to be a novel mechanism by which a natural intestinal peptide suppresses TLR activity. Finally, macrophages isolated from the intestinal lamina propria of IL-10$^{-/-}$ mice, which develop inflammatory bowel disease (IBD)-like colitis, were shown to express reduced levels of IκBNS, an inhibitor of NFκB activation[72]. IκBNS is responsible for suppression of LPS-induced cytokine production by lamina propria macrophages[72]. The lamina propria macrophages are normally hyporesponsive to TLR stimulation except in cases of intestinal inflammation[73], but these from IL-10$^{-/-}$ mice were responsive.

There are some known cases where commensal bacteria actually enhance anti-inflammatory activity in the intestinal epithelium. One example is the aforementioned upregulation of TOLLIP and PPARγ by commensal bacteria[45,49,66]. Others have shown that non-pathogenic *S pullorum* could block the activation of NF-κB by *S typhimurium*[74]. Furthermore, Backhed *et al*[75] showed that hypo-acylated LPS was less stimulatory towards TLR4 compared to normally acylated LPS, and that it actually inhibited the pro-inflammatory effects of wild-type LPS. Several species of commensal bacteria produce hypo-acylated LPS, which may contribute to the down-regulation of TLR4 activities[75].

TLRs AND INFLAMMATORY BOWEL DISEASE

IBD, comprising Crohn's disease (CD) and ulcerative colitis (UC), is a chronic, relapsing GI disorder of

unknown etiology. The development of IBD is hypothesized to be the result of dysregulated immune responses to one or more intestinal luminal antigens (loss of tolerance) in genetically predisposed individuals. While the pathophysiological features of IBD are uncontrolled, excessive inflammation in the GI mucosa and the upregulation of a host of pro-inflammatory and T cell cytokines[76,77], the root of the problem may lie in the defective immune tolerance to commensal bacteria and other intestinal luminal antigens. Experimental and clinical studies suggest that the over-expression of certain TLRs and down-regulation of TLR antagonists in IEC can be one of the underlying mechanisms leading to an improper reaction to commensal bacteria by the host. In this regard, TLR4 expression was reported to be elevated in colonic tissue of UC and CD patients[47], and TLR4 polymorphisms at Asp299Gly and Thr399Ile have been linked to the development of both CD and UC[78,79]. It was also shown that TLR2 activity was increased in a mouse model of colitis[80]. The presence of high titers of flagellin-specific antibodies in the serum of CD patients raises the possibility that flagellin from commensal bacteria might trigger an improper immune response in the GI mucosa through TLR5[81,82] and that TLR5 may also play an important role in the pathogenesis of IBD. In addition, as discussed above, intestinal myofibroblasts express TLR2 and TLR4 and respond to LPS and LTA stimulation, and have been implicated in the development of CD-associated fibrosis[60]. Moreover, PPARγ was found to be decreased in intestinal epithelial tissue of UC patients[67]. Thus, TLR mutations and dysregulation are likely major contributing factors in the predisposition and perpetuation of IBD.

More recently, it has been shown that TLRs may contribute to the pathogenesis of IBD in conjunction with another family of PRRs termed nucleotide-binding oligomerization domain proteins (Nod). Specific genetic variations in Nod2 have been strongly linked to the development of CD[83,84] and to excessive NF-κB activity[85]. Interestingly, the Nod2 variations may also have a direct effect on TLR-mediated control of intestinal inflammation. In IEC from Nod2-variant patients, TLR2 stimulation led to excessive production of both pro-inflammatory and Th1 cytokines[15,86,87]. These cytokines are heavily involved in the pathogenesis of IBD[77]. It appears that the association between Nod2 and TLRs seen in normal intestinal tissue[88] is important for intestinal homeostasis. Alteration of this association by genetic variation in Nod2 leads to the development of chronic intestinal inflammation. Further exploration into how Nod2 mutations affect TLR function will undoubtedly shed light on novel interactions between Nod1/2 and TLRs in the GI mucosa.

TLRs AND *HELICOBACTER PYLORI* INFECTION

Helicobacter pylori (*H pylori*) is a Gram-negative bacterium that colonizes the gastric mucosa and causes chronic gastritis and gastric ulcers. The bacterium adheres strongly to the surface of gastric epithelial cells (GEC) without actually invading them[89,90]. As is the case with IBD, the host inflammatory response to *H pylori* infection directly contributes to disease pathogenesis[91]. Although the host mounts a strong specific immune response to the pathogen, this response is for the most part ineffective[92]. *H pylori* infection is relatively common worldwide, yet less than one quarter of infected individuals progress to disease[93]. Whether or not an individual proceeds to a disease state might be influenced by any combination of host, bacterial and environmental factors.

Because of the clinical significance of *H pylori* infection, the interaction between TLR and *H pylori* is probably the most extensively studied. Since the first step in *H pylori* infection is the adherence to GEC by the bacterium, it is logical to postulate that TLRs would play a role in *H pylori* detection, as well as the subsequent mounting of the deleterious cellular and inflammatory immune response. Despite extensive studies on this subject, as yet there is no clear consensus as to which TLR(s) is involved in the detection of *H pylori* by GEC. Several groups have shown the apical and basolateral expression of TLR4 in *H pylori*-infected GEC[94,95]. TLR5 and TLR9 were also expressed both apically and basolaterally in the GEC of healthy individuals, but the apical expression of these TLRs was lost in *H pylori*-induced gastritis[95]. GEC expression of TLR2, another important receptor for bacterial PAMPs, has yet to be fully characterized.

Several studies have suggested that TLR4 may play an important role in the recognition of *H pylori* infection by gastric mucosa[94,96] as TLR4 and MD-2 expression, as well as responsiveness to *H pylori* LPS stimulation, in gastric biopsy samples of patients with *H pylori* infection were up-regulated[94]. However, others have reported that the detection of *H pylori* by primary GEC is TLR4-independent[97]. Interestingly, Smith *et al*[98] found that the gastric epithelium recognizes *H pylori* LPS through TLR2 rather than TLR4, suggesting the possible disassociation between the up-regulation of TLR4 and the pro-inflammatory potential of *H pylori* LPS. Similarly, Mandell *et al*[99] showed that whole *H pylori* elicited an immune response through TLR2, not TLR4, in mice. These findings are not entirely surprising since it has been long recognized that *H pylori* LPS does not share all the characteristics of other Gram-negative GI bacteria.

Although *H pylori* flagellin was initially shown to be able to interact with TLR5[100], more recent studies have found that TLR5 was unresponsive to *H pylori* flagellin, suggesting the low immunogenicity of this molecule[101-103]. Anderson-Nissen *et al*[101] have recently mapped low TLR5 responsiveness to a specific area of the amino acid sequence in the *H pylori* flagellin. Introduction of this sequence into *Salmonella* flagellin renders the new construct devoid of all TLR5-activating activity[101]. Thus, it is possible that *H pylori* uses TLR5 evasion to avoid immune detection. The ability of *H pylori* to induce chronic and persistent gastric inflammation suggests that PAMP(s) other than flagellin may be involved in the pathogenesis of the infection. Indeed, Takenaka *et al*[104] have shown that *H pylori* heat shock protein (HSP) 60 is able to activate TLR2 and TLR4 and increase NF-κB activity and IL-8 production in GEC.

Evidently, there is still much to be discovered regarding the interactions of *H pylori* with TLRs in the gastric epithelium. While it is likely that host factors in the

immune response might play a role in disease pathogenesis, there does not appear to be any evidence in the literature demonstrating an association between genetic variation in TLRs and *H pylori* disease progression, as is the case in IBD.

TLRs AND INFECTIONS WITH INTESTINAL BACTERIA

Despite a relatively large amount of information available concerning the roles of TLRs in the GI tract, there is surprisingly little data showing the actual *in vivo* role for TLRs in combating enteric pathogens. The obvious assumption is that invasive pathogens expressing known bioactive PAMPs will trigger a TLR-mediated immune response upon invasion of the IEC barrier. However, *in vivo* models of this scenario are scarce. Of the most common enteric pathogens, the interplay between TLRs and *S typhimurium* has been most extensively studied.

Invasion of IEC by *S typhimurium* leads to bacterial replication in intracellular vacuoles, localized inflammation, and lysis of infected cells. Several TLRs (TLR2, TLR4 and TLR5) appear to play a crucial role in the host defense against *S typhimurium* infection. Allelic variation in chicken TLR4 has been linked to the susceptibility to *S typhimurium*[105]. Studies of systemic *S typhimurium* infection in TLR4-deficient mice have also shown an important role for TLR4 in controlling the infection, TNF-α and chemokine production, and cellular immune responses[106-108]. Moreover, results from several recent studies have implicated TLR4 in the immediate detection of *S typhimurium* and early macrophage responses, and TLR2 as a key player in late responses after cellular invasion and intracellular replication have occurred[109,110].

S typhimurium flagellin induces a strong, TLR5-mediated inflammatory response in IEC[55,59]. Interestingly, this phenomenon does not require cellular invasion; adherence to IEC is sufficient[55,58,111]. The fact that IECs do not express TLR5 on the apical membrane[55,58] implies that *S typhimurium* actually has to translocate flagellin molecules through IEC to the basolateral membrane where TLR5 is expressed[55,58,59]. This process is dependent on the presence of *S typhimurium* pathogenicity island 2 (SPI2)[59,112], and probably also *S typhimurium* guanine nucleotide exchange factor, SopE2[113]. Therefore, it appears that the interplay between TLR5 and *S typhimurium* flagellin is a major determinant in the host response to IEC infection and the clinical outcome of the infection. Indeed, Sebastiani *et al*[114] linked the murine TLR5 gene to an *S typhimurium* susceptibility locus, and showed that susceptible mice expressed decreased levels of TLR5. Also, Zeng *et al*[115] found that *S typhimurium* strains lacking flagellin expression induced minimal inflammatory responses, suggesting that flagellin is the primary cause of inflammation in enteric *S typhimurium* infection.

The important role of TLRs in the immunopathogenesis of *Salmonella* infection is further verified in infection with *S typhi*, the etiological agent of typhoid fever. Unlike *S typhimurium*, *S typhi* infection fails to induce IL-8 production or neutrophil recruitment to the intestinal epithelium that is characteristic of *S typhimurium* infection, thereby allowing the systematical dissemination of the infection. It has been suggested that the ability of the *S typhi* capsular antigen (Vi, a virulence factor not expressed in *S typhimurium*) to inhibit the TLR4 and TLR5 response to the infection may partially contribute to its pathogenesis[116].

The role of TLRs in the pathogenesis of and immunity to other enteric bacterial infections remains largely unexplored. Recognition of LPS by TLR4 is unlikely to be a major contributing factor in diarrheagenic *E coli* infection because lipid A, the structure within LPS which activates TLR4, is highly conserved, and is therefore common to both pathogenic strains and non-pathogenic commensal strains of *E coli*. Although the O antigen of *E coli* LPS is more variant between strains, this antigen does not activate TLR4[75]. In addition, commensal bacteria-derived LPS is known to induce the intracellular relocalization of TLR4 in IEC[51]. It is, therefore, reasonable to assume that IECs do not react to LPS from *E coli* adhered to the outer apical membrane of the cell. However, other *E coli* PAMPs may play a role in the up-regulation of TLR activities in IEC. In this regard, it has been shown that flagellin from several strains of pathogenic *E coli* can induce NF-κB activation and IL-8 production through TLR5[117-119]. In addition, it has recently been shown that aggregative adherence fimbriae (AAF), an EAEC virulence factor, is involved in cell adhesion and contribute to inflammation and IL-8 production in IEC[120], although it is unclear whether this effect is TLR-mediated. Since both *Porphymonas gingivalis* fimbriae and *E coli* P fimbriae, a virulence factor in uropathogenic *E coli*, can activate TLR2 and/or TLR4[20,22,121,122], it is possible that the inflammatory response induced by EAEC AAF is mediated through TLR recognition as well. Furthermore, it has been shown that the *E coli* type II heat-labile (LT-II) enterotoxin, expressed by ETEC, activates TLR2 *via* its B subunit[21].

Campylobacter jejuni infection is one of the most common causes of food-born gastroenteritis. *C jejuni* infection leads to adhesion to IEC, followed by cellular damage due to invasion, toxins and excessive inflammation[123,124]. Infection of IEC by *C jejuni* leads to an enhanced IL-8 production, which is dependent on bacterial adhesion to IEC[125]. However, it is not known whether this inflammatory response is TLR-mediated and, if so, which TLR(s) and ligand(s) are involved. Studies of TLR4 and CD14 polymorphisms commonly associated with susceptibility to other infections showed no link to *C jejuni* infection or disease progression, suggesting that TLR4 does not play a role in the immune response to this pathogen. Moreover, *C jejuni* flagellin failed to stimulate TLR5[101,125], as it possesses the same site-specific mutations as *H pylori* that allow it to avoid TLR5 recognition[101]. One possible candidate for the induction of the inflammatory responses seen in the above study could be *C jejuni* fimbriae, as is the case with the fimbriae of other bacterial species[20,22,121,122]. However, it remains controversial whether *C jejuni* expresses any sort of fimbriae[126,127].

Shigella flexneri , the causative agent of dysentery, is able to survive in a highly acidic environment such as the stomach. As a result, a relatively low dose of *S flexneri* can initiate an intestinal infection[128]. *S flexneri* lipoproteins

can activate TLR2 in non-intestinal epithelial cell lines[129], but TLR2 reactivity to *S flexneri* lipoproteins in IEC remains to be demonstrated. The ability of *S flexneri* to invade IEC plays an important role in the induction of inflammation[130]. Cellular invasion by *S flexneri* induces NF-κB activation and IL-8 production in both IEC and non-intestinal epithelial cells[130-133]. However, this response appears to be independent of TLR and MyD88, and is mediated by Nod1[132]. Some clinical isolates of *S flexneri* have been shown to express a type I fimbriae[134], which could potentially be detected by TLRs similar to fimbriae of other enteric bacteria[20,22,121,122].

TLRs AND INTESTINAL VIRAL INFECTIONS

Viral infection in the GI tract can lead to invasion and destruction of IEC and gastrointestinal inflammation. In most cases, an individual becomes immune to reinfection, suggesting that an effective adaptive immune response occurs in viral gastroenteritis[135]. Although it has been proposed that TLR3, TLR7 and TLR8 are likely to play a major role in sensing the viral infection in the GI tract and initiating an effective mucosal immune response, there is little published evidence to support this notion. The four most common viruses associated with viral gastroenteritis are rotavirus, calicivirus, astrovirus and adenovirus (serotype 40, 41). Of these, only rotavirus infection of IEC has been examined for TLR involvement. It appears that extracellular TLR3 was not involved in the response to rotavirus dsRNA since dendritic cells pretreated with TLR3-blocking antibodies, thereby blocking the surface TLR3, remained responsive to rotavirus dsRNA[136]. Because viruses are intracellular pathogens, the viral genetic material is more likely to be exposed after invasion of the cell. Indeed, intracellular expression of TLR3 has been demonstrated in several cell types[136-138]. However, studies on TLR3-deficient mice showed that responses to infection by reovirus, a dsRNA virus which is known to infect the gastrointestinal epithelium, were TLR3-independent[26]. Therefore, it seems that despite its constitutive expression in IEC[44], TLR3 may not play an important role in the host defense against GI infection by dsRNA viruses.

The role of TLR7 and TLR8 in the GI infection with ssRNA viruses, such as calicivirus, has not been directly investigated, despite the importance of these TLRs in the recognition of ssRNA viruses. It is worth noting that of the four major types of viral gastroenteritis, calicivirus infection tends to occur equally in adults and children, whereas infections with rotavirus, astrovirus and adenovirus are mostly seen in children. Glass *et al*[135] suggested that this could be caused by short-lived immunity to calicivirus or because of antigenic variation, rendering the adaptive immune response less effective in the face of future infection. If the former is the case, it would be interesting to know if the short-lived immune response could be attributed to a unique property of TLR7 and/or TLR8-mediated detection of calicivirus in IEC, compared to detection of the other three dsRNA viruses.

TLRs IN PARASITIC GASTROINTESTINAL INFECTION

Despite the high incidence and economic significance of parasitic GI infections, particularly in the developing countries, there is very limited information in literature on the role of TLRs in the parasitic GI infection, with the exception of *E histolytica* infection. *E histolytica* can be ingested with contaminated food or water, and colonize the colon. The infection can sometimes remain asymptomatic, but can also cause diarrhea, vomiting and ulcers. Studies performed prior to the discovery of TLRs showed that *E histolytica* infection induced neutrophil influx into the site of infection[139,140] in mice and IL-8 production in IEC lines as well as in human IEC xenografted into immunodeficient mice[141,142]. In the IEC cell line, the IL-8 response was contact-independent, and presumably mediated by *E histolytica* soluble factors[142]. It has recently been shown that *E histolytica* lipopeptidophosphoglycan (LPPG) induces TLR2- and TLR4-dependent IL-8 production in human kidney cell lines and monocytes[33,34]. These studies also suggest that LPPG might be a novel PAMP, and the factor responsible for induction of IL-8 and the neutrophil response seen in previous studies of *E histolytica* infection.

CONCLUSION AND PROSPECTIVE

Emerging experimental and clinical evidence have shown that TLR expression and activation are specially regulated in the GI tract, probably due to its unique environment (the presence of commensal microflora and the exposure to invading pathogens). This is mainly accomplished by: (1) the down-regulation of surface expression of TLRs by the gut epithelium; (2) the specific tissue distribution and compartmentalization of TLR-expressing cells in the gut; and (3) the high expression of TLR-antagonists/attenuating factors that suppress the activation of these TLRs still present at the cell surface. These mechanisms render the GI mucosa able to avoid unnecessary TLR activation to commensal microflora yet retain the ability to detect and mount rapid and efficient immunity against the invasion of pathogens.

TLRs are expressed by both epithelial and non-epithelial cells throughout the entire GI tract. The unique patterns of cellular localization and tissue distribution of TLRs in GI tract allow the host to differentiate between commensal non-pathogenic and pathogenic microbes. Recent studies strongly suggest that dysfunction or dysregulation of TLR expression and activation in IEC is one of the underlying mechanisms leading to the development of IBD. Although there is little doubt now that TLRs play important roles in both the predisposition and perturbation of IBD, caution must be exercised in the interpretation of the clinical and experimental data on TLR studies because it remains to be determined whether the TLR dysregulation seen in patients with IBD is the pathological consequence or the underlying cause of the chronic inflammation. In addition, conflicting results have been reported in regard to the TLR4 activity[80], and the

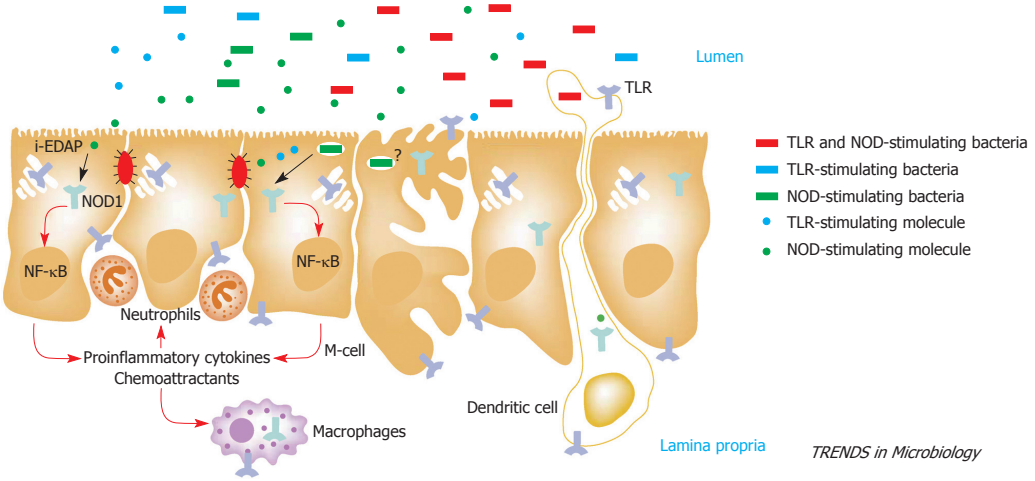

Figure 1 Host sensing of enteropathogenic bacteria. Enteroinvasive bacteria are sensed by specific cells (intestinal epithelial cells, M cells, macrophages and dendritic cells) located in the intestinal mucosa. Resident and invasive bacteria and their molecules released into the intestinal lumen could be recognized by host cells. Sensing of bacteria and their products are mediated by surface Toll-like receptors (TLRs) and cytosolic Nod1 receptors. Intestinal epithelial cells lack functional TLR2 and TLR4 but they might express TLR5 at the basolateral surface. Thus, some entero-invasive flagellate bacteria might stimulate epithelial cells through both TLR5 and Nod1 (depicted in red), whereas other invasive bacteria might activate Nod1 but not TLRs (depicted in green). Flagellate Gram-positive bacteria lacking Nod1-stimulating molecules are expected to trigger TLRs but not Nod1 signaling (depicted in blue). Soluble TLR- and Nod1-stimulating products are found in the intestinal contents but their role in host defense is unknown. Certain TLRs might be also localized to intracellular compartments (e.g., Golgi apparatus for TLR4), but the relevance of intracellular TLR signaling in the intestinal mucosa remains elusive. Reprinted from Chamaillard *et al*. Battling enteroinvasive bacteria: Nod1 comes to the rescue.*Trends Microbiol* 12:529-532[154]. Copyright (2004), with permission from Elsevier.

expression of some TLRs by IEC was found unchanged (TLR9) in patients with IBD[47,61]. This is hardly surprising and probably reflects the complexity of the nature of the disease, the diversified patient populations, and the different research approaches employed.

Despite the demonstrated roles of TLRs in host defense against many microbial infections, there is surprisingly little data on the actual *in vivo* role for TLRs in combating GI pathogens, particularly in viral and parasitic infections. For bacterial pathogens, although the interaction between *H pylori* and GEC has been extensively studied, there is no clear consensus as to which TLR(s) is involved in the recognition of *H pylori* by the host, or the role of TLRs in the pathogenesis of *H pylori*-induced gastritis and gastric ulcer. *S typhimurium* is another well-studied GI pathogen although many studies regarding the interaction between TLR and this pathogen were conducted in animal models where the infection was initiated by systemic injection rather than the natural GI route. In this regard, studies on systemic and respiratory infections have shown that the requirement of different subtypes of TLRs in host defense against microbes appears to be dependent on the type of pathogen, the route of infection, and the initial dose of infection[143-145].

Many virulent strains of pathogens have evolved multiple mechanisms to evade recognition by TLRs. In this regard, a new family of PRRs, the NACHT-LRRs (NLRs), which include both nucleotide-binding oligomerization domains (NODs) and NALPs [NACHT-, LRR- and pyrin domain (PYD)-containing proteins], has been recently identified and implicated in the recognition of bacterial components in the cytosol[146]. It has been suggested that the Nod family of proteins is a major contributor to innate immunity in IEC when TLR activity is attenuated[147-149]. The intracellular location of NODs allows the detection of invasive pathogens in a similar fashion to intracellular or basolateral TLR expression (Figure 1). In addition, Nod1/2 can activate NF-κB through a different signaling pathway from TLRs[150-152], thus rendering them functional even in the presence of TLR-attenuating factors such as TOLLIP and TIR8/SIGGIR that are highly expressed in IEC. Furthermore, Nod1/2 can positively influence TLR activity[15,88,153], and may contribute to the pathogenesis of IBD in conjunction with TLRs. The discovery of the NLR family definitely adds further complexities to the host immune regulation but is also likely to shed new insights into the pathogenesis of GI disorders and provide additional opportunities for the development of novel immunotherapeutic strategies.

TLRs were discovered relatively recently, and their involvement in health and diseases of the GI tract remains a new and exciting field of study. Future work in this field will lead to a better understanding of the unique mechanisms involved in the fine balance between tolerance and immune response. An array of new treatment options for IBD, *H pylori* infection, and other GI disorders could involve tissue-specific suppression of TLR signaling pathways by either chemical means, introduction of natural TLR suppressors and antagonists such as PPARγ, or use of gene therapy to correct TLR gene defects. In this regard, further exploration of the recently characterized negative regulatory mechanisms, that have evolved to attenuate TLR signaling by the host, may be fruitful for the development of new generation of more effective immunotherapeutic agents for the treatment of GI disorders.

ACKNOWLEDGMENTS

We apologise to all authors whose contributions could not be cited here because of space limitations.

REFERENCES

1 **Chaudhary PM,** Ferguson C, Nguyen V, Nguyen O, Massa

HF, Eby M, Jasmin A, Trask BJ, Hood L, Nelson PS. Cloning and characterization of two Toll/Interleukin-1 receptor-like genes TIL3 and TIL4: evidence for a multi-gene receptor family in humans. *Blood* 1998; **91**: 4020-4027
2 **Rock FL**, Hardiman G, Timans JC, Kastelein RA, Bazan JF. A family of human receptors structurally related to Drosophila Toll. *Proc Natl Acad Sci USA* 1998; **95**: 588-593
3 **Kopp E**, Medzhitov R. Recognition of microbial infection by Toll-like receptors. *Curr Opin Immunol* 2003; **15**: 396-401
4 **Takeda K**, Kaisho T, Akira S. Toll-like receptors. *Annu Rev Immunol* 2003; **21**: 335-376
5 **Abreu MT**, Thomas LS, Arnold ET, Lukasek K, Michelsen KS, Arditi M. TLR signaling at the intestinal epithelial interface. *J Endotoxin Res* 2003; **9**: 322-330
6 **Liew FY**, Xu D, Brint EK, O'Neill LA. Negative regulation of toll-like receptor-mediated immune responses. *Nat Rev Immunol* 2005; **5**: 446-458
7 **Kaisho T**, Akira S. Pleiotropic function of Toll-like receptors. *Microbes Infect* 2004; **6**: 1388-1394
8 **Vasselon T**, Detmers PA. Toll receptors: a central element in innate immune responses. *Infect Immun* 2002; **70**: 1033-1041
9 **Sabroe I,** Read RC, Whyte MK, Dockrell DH, Vogel SN, Dower SK. Toll-like receptors in health and disease: complex questions remain. *J Immunol* 2003; **171**: 1630-1635
10 **Hoshino K**, Takeuchi O, Kawai T, Sanjo H, Ogawa T, Takeda Y, Takeda K, Akira S. Cutting edge: Toll-like receptor 4 (TLR4)-deficient mice are hyporesponsive to lipopolysaccharide: evidence for TLR4 as the Lps gene product. *J Immunol* 1999; **162**: 3749-3752
11 **Takeuchi O**, Hoshino K, Kawai T, Sanjo H, Takada H, Ogawa T, Takeda K, Akira S. Differential roles of TLR2 and TLR4 in recognition of gram-negative and gram-positive bacterial cell wall components. *Immunity* 1999; **11**: 443-451
12 **Aliprantis AO**, Yang RB, Mark MR, Suggett S, Devaux B, Radolf JD, Klimpel GR, Godowski P, Zychlinsky A. Cell activation and apoptosis by bacterial lipoproteins through toll-like receptor-2. *Science* 1999; **285**: 736-739
13 **Underhill DM**, Ozinsky A, Smith KD, Aderem A. Toll-like receptor-2 mediates mycobacteria-induced proinflammatory signaling in macrophages. *Proc Natl Acad Sci USA* 1999; **96**: 14459-14463
14 **Travassos LH**, Girardin SE, Philpott DJ, Blanot D, Nahori MA, Werts C, Boneca IG. Toll-like receptor 2-dependent bacterial sensing does not occur via peptidoglycan recognition. *EMBO Rep* 2004; **5**: 1000-1006
15 **Netea MG**, Ferwerda G, de Jong DJ, Jansen T, Jacobs L, Kramer M, Naber TH, Drenth JP, Girardin SE, Kullberg BJ, Adema GJ, Van der Meer JW. Nucleotide-binding oligomerization domain-2 modulates specific TLR pathways for the induction of cytokine release. *J Immunol* 2005; **174**: 6518-6523
16 **Hayashi F**, Smith KD, Ozinsky A, Hawn TR, Yi EC, Goodlett DR, Eng JK, Akira S, Underhill DM, Aderem A. The innate immune response to bacterial flagellin is mediated by Toll-like receptor 5. *Nature* 2001; **410**: 1099-1103
17 **Hemmi H**, Takeuchi O, Kawai T, Kaisho T, Sato S, Sanjo H, Matsumoto M, Hoshino K, Wagner H, Takeda K, Akira S. A Toll-like receptor recognizes bacterial DNA. *Nature* 2000; **408**: 740-745
18 **Zhang D**, Zhang G, Hayden MS, Greenblatt MB, Bussey C, Flavell RA, Ghosh S. A toll-like receptor that prevents infection by uropathogenic bacteria. *Science* 2004; **303**: 1522-1526
19 **Calkins CM**, Barsness K, Bensard DD, Vasquez-Torres A, Raeburn CD, Meng X, McIntyre RC Jr. Toll-like receptor-4 signaling mediates pulmonary neutrophil sequestration in response to gram-positive bacterial enterotoxin. *J Surg Res* 2002; **104**: 124-130
20 **Frendeus B**, Wachtler C, Hedlund M, Fischer H, Samuelsson P, Svensson M, Svanborg C. Escherichia coli P fimbriae utilize the Toll-like receptor 4 pathway for cell activation. *Mol Microbiol* 2001; **40**: 37-51
21 **Hajishengallis G**, Tapping RI, Martin MH, Nawar H, Lyle EA, Russell MW, Connell TD. Toll-like receptor 2 mediates cellular activation by the B subunits of type II heat-labile enterotoxins. *Infect Immun* 2005; **73**: 1343-1349
22 **Ogawa T**, Asai Y, Hashimoto M, Uchida H. Bacterial fimbriae activate human peripheral blood monocytes utilizing TLR2, CD14 and CD11a/CD18 as cellular receptors. *Eur J Immunol* 2002; **32**: 2543-2550
23 **Park JM**, Ng VH, Maeda S, Rest RF, Karin M. Anthrolysin O and other gram-positive cytolysins are toll-like receptor 4 agonists. *J Exp Med* 2004; **200**: 1647-1655
24 **Alexopoulou** L, Holt AC, Medzhitov R, Flavell RA. Recognition of double-stranded RNA and activation of NF-kappaB by Toll-like receptor 3. *Nature* 2001; **413**: 732-738
25 **Hoebe K**, Janssen EM, Kim SO, Alexopoulou L, Flavell RA, Han J, Beutler B. Upregulation of costimulatory molecules induced by lipopolysaccharide and double-stranded RNA occurs by Trif-dependent and Trif-independent pathways. *Nat Immunol* 2003; **4**: 1223-1229
26 **Edelmann KH**, Richardson-Burns S, Alexopoulou L, Tyler KL, Flavell RA, Oldstone MB. Does Toll-like receptor 3 play a biological role in virus infections? *Virology* 2004; **322**: 231-238
27 **Diebold SS**, Kaisho T, Hemmi H, Akira S, Reis e Sousa C. Innate antiviral responses by means of TLR7-mediated recognition of single-stranded RNA. *Science* 2004; **303**: 1529-1531
28 **Heil F**, Hemmi H, Hochrein H, Ampenberger F, Kirschning C, Akira S, Lipford G, Wagner H, Bauer S. Species-specific recognition of single-stranded RNA via toll-like receptor 7 and 8. *Science* 2004; **303**: 1526-1529
29 **Triantafilou K,** Vakakis E, Orthopoulos G, Ahmed MA, Schumann C, Lepper PM, Triantafilou M. TLR8 and TLR7 are involved in the host's immune response to human parechovirus 1. *Eur J Immunol* 2005; **35**: 2416-2423
30 **Blasi E,** Mucci A, Neglia R, Pezzini F, Colombari B, Radzioch D, Cossarizza A, Lugli E, Volpini G, Del Giudice G, Peppoloni S. Biological importance of the two Toll-like receptors, TLR2 and TLR4, in macrophage response to infection with Candida albicans. *FEMS Immunol Med Microbiol* 2005; **44**: 69-79
31 **Netea MG**, Van Der Graaf CA, Vonk AG, Verschueren I, Van Der Meer JW, Kullberg BJ. The role of toll-like receptor (TLR) 2 and TLR4 in the host defense against disseminated candidiasis. *J Infect Dis* 2002; **185**: 1483-1489
32 **Villamon E**, Gozalbo D, Roig P, O'Connor JE, Fradelizi D, Gil ML. Toll-like receptor-2 is essential in murine defenses against Candida albicans infections. *Microbes Infect* 2004; **6**: 1-7
33 **Maldonado C**, Trejo W, Ramirez A, Carrera M, Sanchez J, Lopez-Macias C, Isibasi A. Lipophosphopeptidoglycan of Entamoeba histolytica induces an antiinflammatory innate immune response and downregulation of toll-like receptor 2 (TLR-2) gene expression in human monocytes. *Arch Med Res* 2000; **31**: S71-S73
34 **Maldonado-Bernal C**, Kirschning CJ, Rosenstein Y, Rocha LM, Rios-Sarabia N, Espinosa-Cantellano M, Becker I, Estrada I, Salazar-Gonzalez RM, Lopez-Macias C, Wagner H, Sanchez J, Isibasi A. The innate immune response to Entamoeba histolytica lipopeptidophosphoglycan is mediated by toll-like receptors 2 and 4. *Parasite Immunol* 2005; **27**: 127-137
35 **Ozinsky A**, Underhill DM, Fontenot JD, Hajjar AM, Smith KD, Wilson CB, Schroeder L, Aderem A. The repertoire for pattern recognition of pathogens by the innate immune system is defined by cooperation between toll-like receptors. *Proc Natl Acad Sci USA* 2000; **97**: 13766-13771
36 **Fitzgerald KA**, Rowe DC, Golenbock DT. Endotoxin recognition and signal transduction by the TLR4/MD2-complex. *Microbes Infect* 2004; **6**: 1361-1367
37 **Schumann RR,** Leong SR, Flaggs GW, Gray PW, Wright SD, Mathison JC, Tobias PS, Ulevitch RJ. Structure and function of lipopolysaccharide binding protein. *Science* 1990; **249**: 1429-1431
38 **Yu B,** Wright SD. Catalytic properties of lipopolysaccharide (LPS) binding protein. Transfer of LPS to soluble CD14. *J Biol Chem* 1996; **271**: 4100-4105
39 **Poltorak A**, He X, Smirnova I, Liu MY, Van Huffel C, Du X, Birdwell D, Alejos E, Silva M, Galanos C, Freudenberg M, Ricciardi-Castagnoli P, Layton B, Beutler B. Defective LPS

signaling in C3H/HeJ and C57BL/10ScCr mice: mutations in Tlr4 gene. *Science* 1998; **282**: 2085-2088
40 **Qureshi ST**, Lariviere L, Leveque G, Clermont S, Moore KJ, Gros P, Malo D. Endotoxin-tolerant mice have mutations in Toll-like receptor 4 (Tlr4) *J Exp Med* 1999; **189**: 615-625
41 **Shimazu R,** Akashi S, Ogata H, Nagai Y, Fukudome K, Miyake K, Kimoto M. MD-2, a molecule that confers lipopolysaccharide responsiveness on Toll-like receptor 4. *J Exp Med* 1999; **189**: 1777-1782
42 **Nagai Y**, Akashi S, Nagafuku M, Ogata M, Iwakura Y, Akira S, Kitamura T, Kosugi A, Kimoto M, Miyake K. Essential role of MD-2 in LPS responsiveness and TLR4 distribution. *Nat Immunol* 2002; **3**: 667-672
43 **Abreu MT**, Vora P, Faure E, Thomas LS, Arnold ET, Arditi M. Decreased expression of Toll-like receptor-4 and MD-2 correlates with intestinal epithelial cell protection against dysregulated proinflammatory gene expression in response to bacterial lipopolysaccharide. *J Immunol* 2001; **167**: 1609-1616
44 **Furrie E**, Macfarlane S, Thomson G, Macfarlane GT. Toll-like receptors-2, -3 and -4 expression patterns on human colon and their regulation by mucosal-associated bacteria. *Immunology* 2005; **115**: 565-574
45 **Melmed G**, Thomas LS, Lee N, Tesfay SY, Lukasek K, Michelsen KS, Zhou Y, Hu B, Arditi M, Abreu MT. Human intestinal epithelial cells are broadly unresponsive to Toll-like receptor 2-dependent bacterial ligands: implications for host-microbial interactions in the gut. *J Immunol* 2003; **170**: 1406-1415
46 **Naik S**, Kelly EJ, Meijer L, Pettersson S, Sanderson IR. Absence of Toll-like receptor 4 explains endotoxin hyporesponsiveness in human intestinal epithelium. *J Pediatr Gastroenterol Nutr* 2001; **32**: 449-453
47 **Cario E**, Podolsky DK. Differential alteration in intestinal epithelial cell expression of toll-like receptor 3 (TLR3) and TLR4 in inflammatory bowel disease. *Infect Immun* 2000; **68**: 7010-7017
48 **Ortega-Cava CF**, Ishihara S, Rumi MA, Kawashima K, Ishimura N, Kazumori H, Udagawa J, Kadowaki Y, Kinoshita Y. Strategic compartmentalization of Toll-like receptor 4 in the mouse gut. *J Immunol* 2003; **170**: 3977-3985
49 **Otte JM**, Cario E, Podolsky DK. Mechanisms of cross hyporesponsiveness to Toll-like receptor bacterial ligands in intestinal epithelial cells. *Gastroenterology* 2004; **126**: 1054-1070
50 **Tohno M**, Shimosato T, Kitazawa H, Katoh S, Iliev ID, Kimura T, Kawai Y, Watanabe K, Aso H, Yamaguchi T, Saito T. Toll-like receptor 2 is expressed on the intestinal M cells in swine. *Biochem Biophys Res Commun* 2005; **330**: 547-554
51 **Cario E**, Brown D, McKee M, Lynch-Devaney K, Gerken G, Podolsky DK. Commensal-associated molecular patterns induce selective toll-like receptor-trafficking from apical membrane to cytoplasmic compartments in polarized intestinal epithelium. *Am J Pathol* 2002; **160**: 165-173
52 **Hornef MW**, Frisan T, Vandewalle A, Normark S, Richter-Dahlfors A. Toll-like receptor 4 resides in the Golgi apparatus and colocalizes with internalized lipopolysaccharide in intestinal epithelial cells. *J Exp Med* 2002; **195**: 559-570
53 **Hornef MW**, Normark BH, Vandewalle A, Normark S. Intracellular recognition of lipopolysaccharide by toll-like receptor 4 in intestinal epithelial cells. *J Exp Med* 2003; **198**: 1225-1235
54 **Bambou JC**, Giraud A, Menard S, Begue B, Rakotobe S, Heyman M, Taddei F, Cerf-Bensussan N, Gaboriau-Routhiau V. *In vitro* and *ex vivo* activation of the TLR5 signaling pathway in intestinal epithelial cells by a commensal Escherichia coli strain. *J Biol Chem* 2004; **279**: 42984-42992
55 **Gewirtz AT**, Navas TA, Lyons S, Godowski PJ, Madara JL. Cutting edge: bacterial flagellin activates basolaterally expressed TLR5 to induce epithelial proinflammatory gene expression. *J Immunol* 2001; **167**: 1882-1885
56 **Kim JG**, Lee SJ, Kagnoff MF. Nod1 is an essential signal transducer in intestinal epithelial cells infected with bacteria that avoid recognition by toll-like receptors. *Infect Immun* 2004; **72**: 1487-1495
57 **Tallant T**, Deb A, Kar N, Lupica J, de Veer MJ, DiDonato JA. Flagellin acting via TLR5 is the major activator of key signaling pathways leading to NF-kappa B and proinflammatory gene program activation in intestinal epithelial cells. *BMC Microbiol* 2004; **4**: 33
58 **Gewirtz AT**, Simon PO Jr, Schmitt CK, Taylor LJ, Hagedorn CH, O'Brien AD, Neish AS, Madara JL. Salmonella typhimurium translocates flagellin across intestinal epithelia, inducing a proinflammatory response. *J Clin Invest* 2001; **107**: 99-109
59 **Lyons S**, Wang L, Casanova JE, Sitaraman SV, Merlin D, Gewirtz AT. Salmonella typhimurium transcytoses flagellin via an SPI2-mediated vesicular transport pathway. *J Cell Sci* 2004; **117**: 5771-5780
60 **Otte JM**, Rosenberg IM, Podolsky DK. Intestinal myofibroblasts in innate immune responses of the intestine. *Gastroenterology* 2003; **124**: 1866-1878
61 **Pedersen G**, Andresen L, Matthiessen MW, Rask-Madsen J, Brynskov J. Expression of Toll-like receptor 9 and response to bacterial CpG oligodeoxynucleotides in human intestinal epithelium. *Clin Exp Immunol* 2005; **141**: 298-306
62 **Zhang G**, Ghosh S. Negative regulation of toll-like receptor-mediated signaling by Tollip. *J Biol Chem* 2002; **277**: 7059-7065
63 **Desreumaux P**, Dubuquoy L, Nutten S, Peuchmaur M, Englaro W, Schoonjans K, Derijard B, Desvergne B, Wahli W, Chambon P, Leibowitz MD, Colombel JF, Auwerx J. Attenuation of colon inflammation through activators of the retinoid X receptor (RXR)/peroxisome proliferator-activated receptor gamma (PPARgamma) heterodimer. A basis for new therapeutic strategies. *J Exp Med* 2001; **193**: 827-838
64 **Gupta RA**, Polk DB, Krishna U, Israel DA, Yan F, DuBois RN, Peek RM Jr. Activation of peroxisome proliferator-activated receptor gamma suppresses nuclear factor kappa B-mediated apoptosis induced by *Helicobacter pylori* in gastric epithelial cells. *J Biol Chem* 2001; **276**: 31059-31066
65 **Lefebvre M**, Paulweber B, Fajas L, Woods J, McCrary C, Colombel JF, Najib J, Fruchart JC, Datz C, Vidal H, Desreumaux P, Auwerx J. Peroxisome proliferator-activated receptor gamma is induced during differentiation of colon epithelium cells. *J Endocrinol* 1999; **162**: 331-340
66 **Kelly D**, Campbell JI, King TP, Grant G, Jansson EA, Coutts AG, Pettersson S, Conway S. Commensal anaerobic gut bacteria attenuate inflammation by regulating nuclear-cytoplasmic shuttling of PPAR-gamma and RelA. *Nat Immunol* 2004; **5**: 104-112
67 **Dubuquoy L**, Jansson EA, Deeb S, Rakotobe S, Karoui M, Colombel JF, Auwerx J, Pettersson S, Desreumaux P. Impaired expression of peroxisome proliferator-activated receptor gamma in ulcerative colitis. *Gastroenterology* 2003; **124**: 1265-1276
68 **Polentarutti N**, Rol GP, Muzio M, Bosisio D, Camnasio M, Riva F, Zoja C, Benigni A, Tomasoni S, Vecchi A, Garlanda C, Mantovani A. Unique pattern of expression and inhibition of IL-1 signaling by the IL-1 receptor family member TIR8/SIGIRR. *Eur Cytokine Netw* 2003; **14**: 211-218
69 **Wald D**, Qin J, Zhao Z, Qian Y, Naramura M, Tian L, Towne J, Sims JE, Stark GR, Li X. SIGIRR, a negative regulator of Toll-like receptor-interleukin 1 receptor signaling. *Nat Immunol* 2003; **4**: 920-927
70 **Garlanda C**, Riva F, Polentarutti N, Buracchi C, Sironi M, De Bortoli M, Muzio M, Bergottini R, Scanziani E, Vecchi A, Hirsch E, Mantovani A. Intestinal inflammation in mice deficient in Tir8, an inhibitory member of the IL-1 receptor family. *Proc Natl Acad Sci USA* 2004; **101**: 3522-3526
71 **Gomariz RP**, Arranz A, Abad C, Torroba M, Martinez C, Rosignoli F, Garcia-Gomez M, Leceta J, Juarranz Y. Time-course expression of Toll-like receptors 2 and 4 in inflammatory bowel disease and homeostatic effect of VIP. *J Leukoc Biol* 2005; **78**: 491-502
72 **Hirotani T,** Lee PY, Kuwata H, Yamamoto M, Matsumoto M, Kawase I, Akira S, Takeda K. The nuclear IkappaB protein IkappaBNS selectively inhibits lipopolysaccharide-induced IL-6 production in macrophages of the colonic lamina propria. *J Immunol* 2005; **174**: 3650-3657
73 **Hausmann M**, Kiessling S, Mestermann S, Webb G, Spottl T, Andus T, Scholmerich J, Herfarth H, Ray K, Falk W, Rogler G.

Toll-like receptors 2 and 4 are up-regulated during intestinal inflammation. *Gastroenterology* 2002; **122**: 1987-2000
74 **Neish AS,** Gewirtz AT, Zeng H, Young AN, Hobert ME, Karmali V, Rao AS, Madara JL. Prokaryotic regulation of epithelial responses by inhibition of IkappaB-alpha ubiquitination. *Science* 2000; **289**: 1560-1563
75 **Backhed F**, Normark S, Schweda EK, Oscarson S, Richter-Dahlfors A. Structural requirements for TLR4-mediated LPS signalling: a biological role for LPS modifications. *Microbes Infect* 2003; **5**: 1057-1063
76 **Reaves TA**, Chin AC, Parkos CA. Neutrophil transepithelial migration: role of toll-like receptors in mucosal inflammation. *Mem Inst Oswaldo Cruz* 2005; **100 Suppl 1**: 191-198
77 **Reuter BK**, Pizarro TT. Commentary: the role of the IL-18 system and other members of the IL-1R/TLR superfamily in innate mucosal immunity and the pathogenesis of inflammatory bowel disease: friend or foe? *Eur J Immunol* 2004; **34**: 2347-2355
78 **Franchimont D**, Vermeire S, El Housni H, Pierik M, Van Steen K, Gustot T, Quertinmont E, Abramowicz M, Van Gossum A, Deviere J, Rutgeerts P. Deficient host-bacteria interactions in inflammatory bowel disease? The toll-like receptor (TLR)-4 Asp299gly polymorphism is associated with Crohn's disease and ulcerative colitis. *Gut* 2004; **53**: 987-992
79 **Torok HP**, Glas J, Tonenchi L, Mussack T, Folwaczny C. Polymorphisms of the lipopolysaccharide-signaling complex in inflammatory bowel disease: association of a mutation in the Toll-like receptor 4 gene with ulcerative colitis. *Clin Immunol* 2004; **112**: 85-91
80 **Singh JC**, Cruickshank SM, Newton DJ, Wakenshaw L, Graham A, Lan J, Lodge JP, Felsburg PJ, Carding SR. Toll-like receptor-mediated responses of primary intestinal epithelial cells during the development of colitis. *Am J Physiol Gastrointest Liver Physiol* 2005; **288**: G514-G524
81 **Sitaraman SV**, Klapproth JM, Moore DA 3rd, Landers C, Targan S, Williams IR, Gewirtz AT. Elevated flagellin-specific immunoglobulins in Crohn's disease. *Am J Physiol Gastrointest Liver Physiol* 2005; **288**: G403-G406
82 **Lodes MJ**, Cong Y, Elson CO, Mohamath R, Landers CJ, Targan SR, Fort M, Hershberg RM. Bacterial flagellin is a dominant antigen in Crohn disease. *J Clin Invest* 2004; **113**: 1296-1306
83 **Hugot JP**, Chamaillard M, Zouali H, Lesage S, Cezard JP, Belaiche J, Almer S, Tysk C, O'Morain CA, Gassull M, Binder V, Finkel Y, Cortot A, Modigliani R, Laurent-Puig P, Gower-Rousseau C, Macry J, Colombel JF, Sahbatou M, Thomas G. Association of NOD2 leucine-rich repeat variants with susceptibility to Crohn's disease. *Nature* 2001; **411**: 599-603
84 **Ogura Y**, Bonen DK, Inohara N, Nicolae DL, Chen FF, Ramos R, Britton H, Moran T, Karaliuskas R, Duerr RH, Achkar JP, Brant SR, Bayless TM, Kirschner BS, Hanauer SB, Nunez G, Cho JH. A frameshift mutation in NOD2 associated with susceptibility to Crohn's disease. *Nature* 2001; **411**: 603-606
85 **Maeda S**, Hsu LC, Liu H, Bankston LA, Iimura M, Kagnoff MF, Eckmann L, Karin M. Nod2 mutation in Crohn's disease potentiates NF-kappaB activity and IL-1beta processing. *Science* 2005; **307**: 734-738
86 **Netea MG**, Kullberg BJ, de Jong DJ, Franke B, Sprong T, Naber TH, Drenth JP, Van der Meer JW. NOD2 mediates anti-inflammatory signals induced by TLR2 ligands: implications for Crohn's disease. *Eur J Immunol* 2004; **34**: 2052-2059
87 **Watanabe T**, Kitani A, Murray PJ, Strober W. NOD2 is a negative regulator of Toll-like receptor 2-mediated T helper type 1 responses. *Nat Immunol* 2004; **5**: 800-808
88 **van Heel DA**, Ghosh S, Hunt KA, Mathew CG, Forbes A, Jewell DP, Playford RJ. Synergy between TLR9 and NOD2 innate immune responses is lost in genetic Crohn's disease. *Gut* 2005; **54**: 1553-1557
89 **Clyne M**, Drumm B. Adherence of *Helicobacter pylori* to primary human gastrointestinal cells. *Infect Immun* 1993; **61**: 4051-4057
90 **el-Shoura SM**. *Helicobacter pylori*: I. Ultrastructural sequences of adherence, attachment, and penetration into the gastric mucosa. *Ultrastruct Pathol* 1995; **19**: 323-333
91 **Dixon MF**. Histological responses to *Helicobacter pylori* infection: gastritis, atrophy and preneoplasia. *Baillieres Clin Gastroenterol* 1995; **9**: 467-486
92 **Ferrero RL**. Innate immune recognition of the extracellular mucosal pathogen, *Helicobacter pylori*. *Mol Immunol* 2005; **42**: 879-885
93 **Nguyen TN**, Barkun AN, Fallone CA. Host determinants of *Helicobacter pylori* infection and its clinical outcome. *Helicobacter* 1999; **4**: 185-197
94 **Ishihara S**, Rumi MA, Kadowaki Y, Ortega-Cava CF, Yuki T, Yoshino N, Miyaoka Y, Kazumori H, Ishimura N, Amano Y, Kinoshita Y. Essential role of MD-2 in TLR4-dependent signaling during *Helicobacter pylori*-associated gastritis. *J Immunol* 2004; **173**: 1406-1416
95 **Schmausser B**, Andrulis M, Endrich S, Lee SK, Josenhans C, Muller-Hermelink HK, Eck M. Expression and subcellular distribution of toll-like receptors TLR4, TLR5 and TLR9 on the gastric epithelium in *Helicobacter pylori* infection. *Clin Exp Immunol* 2004; **136**: 521-526
96 **Kawahara T**, Kuwano Y, Teshima-Kondo S, Kawai T, Nikawa T, Kishi K, Rokutan K. Toll-like receptor 4 regulates gastric pit cell responses to *Helicobacter pylori* infection. *J Med Invest* 2001; **48**: 190-197
97 **Backhed F**, Rokbi B, Torstensson E, Zhao Y, Nilsson C, Seguin D, Normark S, Buchan AM, Richter-Dahlfors A. Gastric mucosal recognition of *Helicobacter pylori* is independent of Toll-like receptor 4. *J Infect Dis* 2003; **187**: 829-836
98 **Smith MF Jr**, Mitchell A, Li G, Ding S, Fitzmaurice AM, Ryan K, Crowe S, Goldberg JB. Toll-like receptor (TLR) 2 and TLR5, but not TLR4, are required for *Helicobacter pylori*-induced NF-kappa B activation and chemokine expression by epithelial cells. *J Biol Chem* 2003; **278**: 32552-32560
99 **Mandell L**, Moran AP, Cocchiarella A, Houghton J, Taylor N, Fox JG, Wang TC, Kurt-Jones EA. Intact gram-negative *Helicobacter pylori*, Helicobacter felis, and Helicobacter hepaticus bacteria activate innate immunity via toll-like receptor 2 but not toll-like receptor 4. *Infect Immun* 2004; **72**: 6446-6454
100 **Torok AM**, Bouton AH, Goldberg JB. *Helicobacter pylori* induces interleukin-8 secretion by Toll-like receptor 2- and Toll-like receptor 5-dependent and -independent pathways. *Infect Immun* 2005; **73**: 1523-1531
101 **Andersen-Nissen E,** Smith KD, Strobe KL, Barrett SL, Cookson BT, Logan SM, Aderem A. Evasion of Toll-like receptor 5 by flagellated bacteria. *Proc Natl Acad Sci U S A* 2005; **102**: 9247-9252
102 **Lee SK**, Stack A, Katzowitsch E, Aizawa SI, Suerbaum S, Josenhans C. *Helicobacter pylori* flagellins have very low intrinsic activity to stimulate human gastric epithelial cells via TLR5. *Microbes Infect* 2003; **5**: 1345-1356
103 **Gewirtz AT**, Yu Y, Krishna US, Israel DA, Lyons SL, Peek RM Jr. *Helicobacter pylori* flagellin evades toll-like receptor 5-mediated innate immunity. *J Infect Dis* 2004; **189**: 1914-1920
104 **Takenaka R,** Yokota K, Ayada K, Mizuno M, Zhao Y, Fujinami Y, Lin SN, Toyokawa T, Okada H, Shiratori Y, Oguma K. *Helicobacter pylori* heat-shock protein 60 induces inflammatory responses through the Toll-like receptor-triggered pathway in cultured human gastric epithelial cells. *Microbiology* 2004; **150**: 3913-3922
105 **Leveque G**, Forgetta V, Morroll S, Smith AL, Bumstead N, Barrow P, Loredo-Osti JC, Morgan K, Malo D. Allelic variation in TLR4 is linked to susceptibility to Salmonella enterica serovar Typhimurium infection in chickens. *Infect Immun* 2003; **71**: 1116-1124
106 **O'Brien GC**, Wang JH, Redmond HP. Bacterial lipoprotein induces resistance to Gram-negative sepsis in TLR4-deficient mice via enhanced bacterial clearance. *J Immunol* 2005; **174**: 1020-1026
107 **Vazquez-Torres A**, Vallance BA, Bergman MA, Finlay BB, Cookson BT, Jones-Carson J, Fang FC. Toll-like receptor 4 dependence of innate and adaptive immunity to Salmonella: importance of the Kupffer cell network. *J Immunol* 2004; **172**: 6202-6208
108 **Li Q**, Cherayil BJ. Role of Toll-like receptor 4 in macrophage

activation and tolerance during Salmonella enterica serovar Typhimurium infection. *Infect Immun* 2003; **71**: 4873-4882
109 **Weiss DS**, Raupach B, Takeda K, Akira S, Zychlinsky A. Toll-like receptors are temporally involved in host defense. *J Immunol* 2004; **172**: 4463-4469
110 **Lembo A,** Kalis C, Kirschning CJ, Mitolo V, Jirillo E, Wagner H, Galanos C, Freudenberg MA. Differential contribution of Toll-like receptors 4 and 2 to the cytokine response to Salmonella enterica serovar Typhimurium and Staphylococcus aureus in mice. *Infect Immun* 2003; **71**: 6058-6062
111 **Eaves-Pyles T**, Szabo C, Salzman AL. Bacterial invasion is not required for activation of NF-kappaB in enterocytes. *Infect Immun* 1999; **67**: 800-804
112 **Hapfelmeier S**, Stecher B, Barthel M, Kremer M, Muller AJ, Heikenwalder M, Stallmach T, Hensel M, Pfeffer K, Akira S, Hardt WD. The Salmonella pathogenicity island (SPI)-2 and SPI-1 type III secretion systems allow Salmonella serovar typhimurium to trigger colitis via MyD88-dependent and MyD88-independent mechanisms. *J Immunol* 2005; **174**: 1675-1685
113 **Huang FC**, Werne A, Li Q, Galyov EE, Walker WA, Cherayil BJ. Cooperative interactions between flagellin and SopE2 in the epithelial interleukin-8 response to Salmonella enterica serovar typhimurium infection. *Infect Immun* 2004; **72**: 5052-5062
114 **Sebastiani G**, Leveque G, Lariviere L, Laroche L, Skamene E, Gros P, Malo D. Cloning and characterization of the murine toll-like receptor 5 (Tlr5) gene: sequence and mRNA expression studies in Salmonella-susceptible MOLF/Ei mice. *Genomics* 2000; **64**: 230-240
115 **Zeng H**, Carlson AQ, Guo Y, Yu Y, Collier-Hyams LS, Madara JL, Gewirtz AT, Neish AS. Flagellin is the major proinflammatory determinant of enteropathogenic Salmonella. *J Immunol* 2003; **171**: 3668-3674
116 **Raffatellu M**, Chessa D, Wilson RP, Dusold R, Rubino S, Baumler AJ. The Vi capsular antigen of Salmonella enterica serotype Typhi reduces Toll-like receptor-dependent interleukin-8 expression in the intestinal mucosa. *Infect Immun* 2005; **73**: 3367-3374
117 **Berin MC**, Darfeuille-Michaud A, Egan LJ, Miyamoto Y, Kagnoff MF. Role of EHEC O157:H7 virulence factors in the activation of intestinal epithelial cell NF-kappaB and MAP kinase pathways and the upregulated expression of interleukin 8. *Cell Microbiol* 2002; **4**: 635-648
118 **Khan MA**, Kang J, Steiner TS. Enteroaggregative Escherichia coli flagellin-induced interleukin-8 secretion requires Toll-like receptor 5-dependent p38 MAP kinase activation. *Immunology* 2004; **112**: 651-660
119 **Steiner TS,** Nataro JP, Poteet-Smith CE, Smith JA, Guerrant RL. Enteroaggregative Escherichia coli expresses a novel flagellin that causes IL-8 release from intestinal epithelial cells. *J Clin Invest* 2000; **105**: 1769-1777
120 **Harrington SM**, Strauman MC, Abe CM, Nataro JP. Aggregative adherence fimbriae contribute to the inflammatory response of epithelial cells infected with enteroaggregative *Escherichia coli*. *Cell Microbiol* 2005; **7**: 1565-1578
121 **Asai Y**, Ohyama Y, Gen K, Ogawa T. Bacterial fimbriae and their peptides activate human gingival epithelial cells through Toll-like receptor 2. *Infect Immun* 2001; **69**: 7387-7395
122 **Hajishengallis G**, Sojar H, Genco RJ, DeNardin E. Intracellular signaling and cytokine induction upon interactions of Porphyromonas gingivalis fimbriae with pattern-recognition receptors. *Immunol Invest* 2004; **33**: 157-172
123 **Butzler JP**. Campylobacter, from obscurity to celebrity. *Clin Microbiol Infect* 2004; **10**: 868-876
124 **Ketley JM.** Pathogenesis of enteric infection by Campylobacter. *Microbiology* 1997; **143 (Pt 1)**: 5-21
125 **Watson RO**, Galan JE. Signal transduction in Campylobacter jejuni-induced cytokine production. *Cell Microbiol* 2005; **7**: 655-665
126 **Dolg P**, Yao R, Burr DH, Guerry P, Trust TJ. An environmentally regulated pilus-like appendage involved in Campylobacter pathogenesis. *Mol Microbiol* 1996; **20**: 885-894
127 **Gaynor EC**, Ghori N, Falkow S. Bile-induced 'pili' in Campylobacter jejuni are bacteria-independent artifacts of the culture medium. *Mol Microbiol* 2001; **39**: 1546-1549
128 **Gorden J**, Small PL. Acid resistance in enteric bacteria. *Infect Immun* 1993; **61**: 364-367
129 **Aliprantis AO**, Weiss DS, Radolf JD, Zychlinsky A. Release of Toll-like receptor-2-activating bacterial lipoproteins in Shigella flexneri culture supernatants. *Infect Immun* 2001; **69**: 6248-6255
130 **Sansonetti PJ**, Arondel J, Huerre M, Harada A, Matsushima K. Interleukin-8 controls bacterial transepithelial translocation at the cost of epithelial destruction in experimental shigellosis. *Infect Immun* 1999; **67**: 1471-1480
131 **Dyer RB**, Collaco CR, Niesel DW, Herzog NK. Shigella flexneri invasion of HeLa cells induces NF-kappa B DNA-binding activity. *Infect Immun* 1993; **61**: 4427-4433
132 **Girardin SE**, Tournebize R, Mavris M, Page AL, Li X, Stark GR, Bertin J, DiStefano PS, Yaniv M, Sansonetti PJ, Philpott DJ. CARD4/Nod1 mediates NF-kappaB and JNK activation by invasive Shigella flexneri. *EMBO Rep* 2001; **2**: 736-742
133 **Philpott DJ**, Yamaoka S, Israel A, Sansonetti PJ. Invasive Shigella flexneri activates NF-kappa B through a lipopolysaccharide-dependent innate intracellular response and leads to IL-8 expression in epithelial cells. *J Immunol* 2000; **165**: 903-914
134 **Snellings NJ**, Tall BD, Venkatesan MM. Characterization of Shigella type 1 fimbriae: expression, FimA sequence, and phase variation. *Infect Immun* 1997; **65**: 2462-2467
135 **Glass RI**, Noel J, Ando T, Fankhauser R, Belliot G, Mounts A, Parashar UD, Bresee JS, Monroe SS. The epidemiology of enteric caliciviruses from humans: a reassessment using new diagnostics. *J Infect Dis* 2000; **181 Suppl 2**: S254-S261
136 **Matsumoto** M, Funami K, Tanabe M, Oshiumi H, Shingai M, Seto Y, Yamamoto A, Seya T. Subcellular localization of Toll-like receptor 3 in human dendritic cells. *J Immunol* 2003; **171**: 3154-3162
137 **Funami K**, Matsumoto M, Oshiumi H, Akazawa T, Yamamoto A, Seya T. The cytoplasmic 'linker region' in Toll-like receptor 3 controls receptor localization and signaling. *Int Immunol* 2004; **16**: 1143-1154
138 **Guillot L**, Le Goffic R, Bloch S, Escriou N, Akira S, Chignard M, Si-Tahar M. Involvement of toll-like receptor 3 in the immune response of lung epithelial cells to double-stranded RNA and influenza A virus. *J Biol Chem* 2005; **280**: 5571-5580
139 **Martinez-Palomo A**, Tsutsumi V, Anaya-Velazquez F, Gonzalez-Robles A. Ultrastructure of experimental intestinal invasive amebiasis. *Am J Trop Med Hyg* 1989; **41**: 273-279
140 **Shibayama M**, Navarro-Garcia F, Lopez-Revilla R, Martinez-Palomo A, Tsutsumi V. *In vivo* and *in vitro* experimental intestinal amebiasis in Mongolian gerbils (Meriones unguiculatus). *Parasitol Res* 1997; **83**: 170-176
141 **Seydel KB**, Li E, Swanson PE, Stanley SL Jr. Human intestinal epithelial cells produce proinflammatory cytokines in response to infection in a SCID mouse-human intestinal xenograft model of amebiasis. *Infect Immun* 1997; **65**: 1631-1639
142 **Yu Y**, Chadee K. Entamoeba histolytica stimulates interleukin 8 from human colonic epithelial cells without parasite-enterocyte contact. *Gastroenterology* 1997; **112**: 1536-1547
143 **Chen W**, Kuolee R, Shen H, Busa M, Conlan JW. Toll-like receptor 4 (TLR4) plays a relatively minor role in murine defense against primary intradermal infection with Francisella tularensis LVS. *Immunol Lett* 2005; **97**: 151-154
144 **Reiling N**, Holscher C, Fehrenbach A, Kroger S, Kirschning CJ, Goyert S, Ehlers S. Cutting edge: Toll-like receptor (TLR)2- and TLR4-mediated pathogen recognition in resistance to airborne infection with Mycobacterium tuberculosis. *J Immunol* 2002; **169**: 3480-3484
145 **Takeuchi O**, Hoshino K, Akira S. Cutting edge: TLR2-deficient and MyD88-deficient mice are highly susceptible to Staphylococcus aureus infection. *J Immunol* 2000; **165**: 5392-5396
146 **Martinon F**, Tschopp J. NLRs join TLRs as innate sensors of pathogens. *Trends Immunol* 2005; **26**: 447-454
147 **Girardin SE**, Boneca IG, Carneiro LA, Antignac A, Jehanno M, Viala J, Tedin K, Taha MK, Labigne A, Zahringer U, Coyle AJ, DiStefano PS, Bertin J, Sansonetti PJ, Philpott DJ. Nod1 detects a unique muropeptide from gram-negative bacterial peptido-

glycan. *Science* 2003; **300**: 1584-1587
148 **Girardin SE**, Boneca IG, Viala J, Chamaillard M, Labigne A, Thomas G, Philpott DJ, Sansonetti PJ. Nod2 is a general sensor of peptidoglycan through muramyl dipeptide (MDP) detection. *J Biol Chem* 2003; **278**: 8869-8872
149 **Viala J**, Chaput C, Boneca IG, Cardona A, Girardin SE, Moran AP, Athman R, Memet S, Huerre MR, Coyle AJ, DiStefano PS, Sansonetti PJ, Labigne A, Bertin J, Philpott DJ, Ferrero RL. Nod1 responds to peptidoglycan delivered by the *Helicobacter pylori* cag pathogenicity island. *Nat Immunol* 2004; **5**: 1166-1174
150 **Inohara N**, Koseki T, del Peso L, Hu Y, Yee C, Chen S, Carrio R, Merino J, Liu D, Ni J, Nunez G. Nod1, an Apaf-1-like activator of caspase-9 and nuclear factor-kappaB. *J Biol Chem* 1999; **274**: 14560-14567
151 **Kobayashi K**, Inohara N, Hernandez LD, Galan JE, Nunez G, Janeway CA, Medzhitov R, Flavell RA. RICK/Rip2/CARDIAK mediates signalling for receptors of the innate and adaptive immune systems. *Nature* 2002; **416**: 194-199
152 **Ogura Y**, Inohara N, Benito A, Chen FF, Yamaoka S, Nunez G. Nod2, a Nod1/Apaf-1 family member that is restricted to monocytes and activates NF-kappaB. *J Biol Chem* 2001; **276**: 4812-4818
153 **van Heel DA**, Ghosh S, Butler M, Hunt K, Foxwell BM, Mengin-Lecreulx D, Playford RJ. Synergistic enhancement of Toll-like receptor responses by NOD1 activation. *Eur J Immunol* 2005; **35**: 2471-2476
154 **Chamaillard M**, Inohara N, Nunez G. Battling enteroinvasive bacteria: Nod1 comes to the rescue. *Trends Microbiol* 2004; **12**: 529-532

S- Editor Wang J **L- Editor** Kumar M **E- Editor** Liu WF

PO Box 2345, Beijing 100023, China
www.wjgnet.com
wjg@wjgnet.com

World J Gastroenterol 2006 April 14; 12(14): 2161-2167
World Journal of Gastroenterology ISSN 1007-9327

REVIEW

Treatment of nonalcoholic fatty liver disease

Juergen Siebler, Peter R Galle

Juergen Siebler, Peter R Galle, Department of Internal Medicine, University Hospital of Mainz, Langenbeckstr.1, 55131 Mainz, Germany
Correspondence to: Juergen Siebler, MD, Department of Internal Medicine, University Hospital of Mainz, Langenbeckstr. 1, 55131 Mainz, Germany. siebler@uni-mainz.de
Telephone: +49-6131-175740 Fax: +49-6131-175583
Received: 2005-11-10 Accepted: 2005-12-07

Abstract

Nonalcoholic fatty liver disease (NAFLD) is the most common cause for elevated liver enzymes in the developed nations. Beyond prevention programs which are of particular interest because of the increasing number of overweight children, treatment should be focussed on the most important risk factors, obesity and insulin resistance. As a consequence of elucidating the pathomechanisms of NAFLD, the number of potential therapeutic options increased. However, many studies investigating the therapeutic effect show shortcomings in at least one of the following points: lack of a serial liver biopsy, short term of treatment and limited number of included patients. The second generation insulin sensitizer pioglitazone and rosiglitazone show the most promising improvements in NAFLD, but weight gain and potential hepatotoxicity calls for attention. In conclusion, a general recommendation for the application of specific drugs cannot be given. Besides controlled clinical trials, weight reduction and physical activity to improve insulin sensitivity in obese patients should be the priority objective.

Key words: Nonalcoholic fatty liver disease; Treatment

Siebler J, Galle PR. Treatment of nonalcoholic fatty liver disease. *World J Gastroenterol* 2006; 12(14): 2161-2167

http://www.wjgnet.com/1007-9327/12/2161.asp

INTRODUCTION

Insulin resistance and obesity represent the most important risk factors for development of NAFLD[1]. Fatty liver has a benign prognosis, whereas up to 20% of patients with NASH develop cirrhosis[2, 3]. Risk factors for development of fibrosis are age, BMI>30, glutamic-oxaloacetic transaminase (AST)/glutamic-pyruvic transaminase (ALT)>1, and diabetes[4]. In addition, the risk for development of hepatocellular carcinoma (HCC) is comparable to that of patients with hepatitis C infection[5]. The pathophysiology of NAFLD is described as a "two hit model". The first hit is supposed to be the increase of free fatty acids in hepatocytes which results in a decrease of β-oxidation. Downregulation of β-oxidation further aggravates accumulation of fatty acids. The second step includes all mechanisms contributing to the development of inflammation and fibrosis[6]. In detail, increase of fatty acids enhances the expression of cytochrome peroxidase 2E1 (CYP2E1). CYP2E1 stimulates generation of oxidative species and thereby enhances lipid peroxidation of the hepatocyte membrane[7, 8]. Endotoxin and TNF-α have been demonstrated to play a harmful role in development of alcoholic steatohepatitis[9]. Injection of lipopolysaccharide (LPS) in leptin-deficient, obese ob/ob mice resulted in a significantly more severe liver injury probably caused by TNF-α compared to lean control animals[10]. Administration of anti-TNF-α-antibody ameliorated liver damage in this model of NAFLD[11]. Both endotoxin and oxidative stress upregulate expression of CD95 ligand and contribute to apoptotic cell death[12]. In fact, increased hepatocyte apoptosis correlating with disease severity was described in patients with NASH[13].

Here we discuss the role of a drug-free management in improvement of insulin resistance and NASH and give a critical summary of recent data on medical treatment. The potential concepts of treatment are summarized in Figure 1.

REDUCTION OF BODY WEIGHT

Although insulin resistance occurs in patients with normal BMI and anthropometric measurements, the majority of these patients are adipose with increased visceral fat. So, in overweight or obese patients, weight loss is usually recommended as the first line management[14]. The American Gastroenterological Association recommends a target of 10% of baseline weight as an initial goal of weight loss if BMI exceeds 25 kg/m^2. Weight loss should proceed at a rate of 1-2 lb/wk. Rapid weight loss due to a very low energy diet (<500 kcal daily) or jejunoileal bypass has been associated with exacerbation of steatohepatitis in obese patients[15-17]. Weight loss should be achieved by restricting calorie intake and physical exercise. Both have been shown to improve insulin resistance[18]. Physical exercise is proven to be beneficial for coronary heart disease and peripheral vascular disease. Rollins demonstrated that moderate to high-intensity exercise (30 min 3-5 times/wk) reduces the

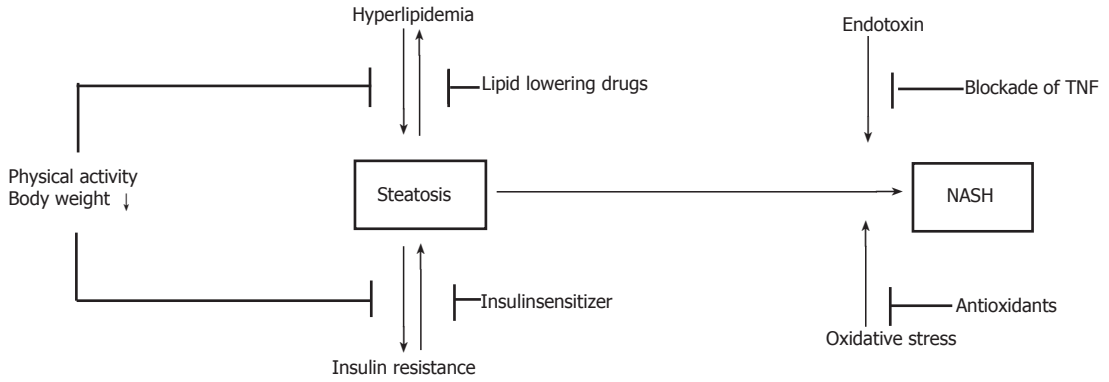

Figure 1 Potential treatment options of NAFLD

risk of complications associated with obesity[19]. However, it is not clear whether patients with NAFLD would benefit from merely increasing physical activity. The goal of weight management is to induce a negative calorie balance. A calorie deficit of 500-1 000 calories/d for those who are overweight or obese appears to be rational, although there are no specific studies on this subject. Dietary recommendation should include reduction of dietary carbohydrates, because lipid profile of overweight patients improves[20, 21]. However, weight loss is rarely achieved or maintained over a long period. Most studies to date have been short term with a small number of patients included. Children with NASH may benefit from weight loss, because serum liver enzymes normalized and sonographic abnormalities disappeared[22]. Another study investigated 48 patients with elevated liver enzymes and clinical, histological, and sonographic characteristics of fatty liver disease[23]. Eighty-one percent of these patients were obese, 73% were glucose-intolerant or diabetic, and 85% had dyslipidemia. Dietary intervention as well as lipid-lowering medication and oral antidiabetics as needed were included into the treatment protocol. These dietary interventions resulted not only in a moderate weight loss, but also in a reduction of serum liver enzymes in 96% of patients. However, it remains unclear, if improved liver enzymes were accompanied by an improvement of liver histology, because serial liver biopsies were not performed. In another study, 15 obese patients followed a restricted diet (25 calories per kilogram ideal body weight) and exercise regimen over a 3 mo period[24]. Liver enzymes decreased in all patients and steatosis determined by biopsy was reduced compared with patients from control group.

A recently published study analyzed the effect of short term weight loss on liver histology[25]. Twenty-three obese patients (BMI>25kg/m^2) with biopsy-proven NASH received standardized nutritional counseling to reduce insulin resistance and body weight. Each subject received individualized nutrition counseling in order to achieve dietary goals. The dietary adjustments included increased intake of fiber and a decreased intake of calories. The daily calory intake consists of 40%-45% carbohydrates with an emphasis on complex carbohydrates with fiber, 35%-40% fat with emphasis on mono- and polyunsaturated fats, and 15%-20% protein. In addition, all participants were encouraged to increase their physical activity to achieve a heart rate of 70% of the calculated target heart rate. Food frequency questionnaires were performed to assess dietary intake and the Paffenberger Activity Questionnaire was used to evaluate the level of physical activity. Sixteen patients successfully completed 12 mo of intense dietary intervention. Mean weight decreased from 98.3 kg to 95.4 kg. There was also a reduction of mean waist circumference, visceral fat, fasting glucose, insulin resistance, triglycerides, serum levels of liver enzymes and histological score, but the differences were not statistically significant. Fifteen patients underwent repeat liver biopsy. Nine of these 15 patients had a histological response, 6 patients had a stable score and none had worsened.

Pharmacological treatment of obesity may be applied to patients with a BMI>27 kg/m^2 and obesitiy-associated comorbidities. Sibutramine is a serotonin reuptake antagonist which should not be used in patients with coronary heart disease and moderate or severe hypertension[26]. The intake of orlistat results in fat malabsorption. Sabuncu and coworkers analyzed the effects of orlistat and sibutramine in obese patients with clinically presumed NASH. Both orlistat and sibutramine improved liver enzymes and decreased the sonographic hallmarks of fatty liver. However, liver biopsies were not performed and the level of alkaline phosphatase increased[27].

Those patients with a BMI>35 kg/m^2 and obesity-associated comorbidities may be considered for more aggressive weight management, including bariatric surgery. Because liver failure occurs after jejuno-ileal bypass, the later has been replaced by the proximal gastric bypass operation. Two studies demonstrated improvement of liver histology after weight reduction and stabilization of weight for long term[28, 29]. However, occasional cases of worsening liver function can also occur during period of rapid weight loss following this procedure. The results of studies investigating the safety of such surgery in patients with severe NASH have to be awaited. Patients considered for this procedure should be monitored carefully and the pros and cons should be discussed with the patient in detail.

ANTIOXIDANTS

Oxidative stress is proposed to act as the "second hit" in

the pathogenesis from steatosis to NASH and fibrosis. Therefore, using antioxidant substances seems to be rational in the treatment of steatohepatitis. Several *in vitro* and animal *in vivo* studies revealed that application of vitamin E decreased levels of profibrogenic TGF beta, improved liver histology and inhibited hepatic stellate cell activation[30-32]. Two open-label pilot trials examined the effect of vitamin E in patients with NAFLD[33, 34]. Eleven pediatric patients with presumed NASH were prescribed 400-1 200 IU of oral vitamin E. Diagnosis was based on the presence of chronically elevated levels of AST and ALT, and fatty liver on ultrasound. Other causes for hepatitis were excluded. Two patients had biopsy-proven NASH. Treatment resulted in normalization of liver function test. However, serial biopsies were not performed, liver remained increased echogenic during treatment and improvement of enzymatic values was not sustained after discontinuation of vitamin E[33]. In another study[34], 10 patients with the clinical diagnosis of NAFLD and 12 patients with biopsy proven NASH were treated with vitamine E (300 mg/d) for 1 year. Treatment resulted in a significant improvement of liver enzymes. In the nine patients with steatohepatitis who had a posttreatment liver biopsy, the degree of steatosis, inflammation, or fibrosis also improved or remained unchanged. The plasma levels of TGF-β decreased significantly with vitamin E. However, these promising results were not confirmed in a subsequent randomized, double-blind, placebo-controlled trial[35]. In this study, vitamin E (1 000 IU/d) in combination with vitamin C (1 000 mg/d) to potentially enhance the regeneration of oxidized vitamin E was given to 23 patients with NASH, while 22 patients were randomized to placebo. The duration of treatment was 6 mo. In addition, a low fat, low calorie diet in combination with increased physical activity was recommended. The degree of adherence to these recommendations remained unclear. The results showed a significant improvement of ALT levels in the placebo group but not in the treatment group. The fibrosis stage of 11 (48%) patients of the vitamin group and 9 (41%) of the placebo group improved by at least one stage. The authors concluded from this within group comparison that vitamin C and vitamin E are effective in improving liver fibrosis, although only two more patients in the vitamin group showed a regression of fibrosis. Adams and Angulo[36] criticized that the effect of placebo treatment was ignored, because no comparison between groups was performed. A between group analysis revealed that 6 mo of therapy with the combination of vitamin E and C is not better than placebo for patients with NASH.

URSODEOXYCHOLIC ACID

This hydrophilic bile acid is approved for the treatment of primary biliary cirrhosis. Ursodeoxycholic acid (UDCA) has been shown to reduce the portion of hydrophobic bile acids which contribute to oxidative stress. This is of particular importance, because fatty hepatocytes reveal an increased sensitivity to hydrophobic bile acids[37]. A pilot study published in 1996 analyzing the effect of UDCA on serum liver enzymes and histology in patients with NAFLD showed promising results[38]. The hepatic steatosis decreased on repeat liver biopsy in 12 of 19 patients and there was also a statistically significant improvement in liver enzymes, but there were no changes in the histological grade of inflammation or fibrosis. In a subsequent controlled trial 166 patients were randomized with liver-biopsy proven NASH to receive 13 and 15 mg/kg of UDCA daily[39]. One hundred and twenty-six patients completed 2 years of therapy and serial liver biopsies were available in 107 patients. Analysis of serum liver chemistry, changes in the degree of steatosis, necro-inflammation or fibrosis revealed no significant difference between the verum and placebo-treated groups. However, the results from this study showed a high rate of spontaneous improvement in hepatic steatosis in the placebo arm probably explaining in part why the data were negative. In addition, the dose of 13 and 15mg/kg pre day was possibly insufficient to improve NAFLD, so effect of higher doses needs to be evaluated in further studies.

INSULINSENSITIZER

The association of insulin resistance and hyperinsulinemia with NAFLD suggests a possibility of therapeutical intervention. The first evidence came from leptin-deficient, obese ob/ob mice. Metformin, a biguanide that reduces hyperinsulinemia and improves hepatic insulin resistance, reduced hepatomegaly and hepatic steatosis in ob/ob mice, whereas caloric restriction did not result in a substantial improvement[40]. The authors postulated that metformin improve hepatic insulin resistance by decreasing hepatic expression of TNF-α, a cytokine that promotes insulin resistance. A pilot study evaluated the effect of metformin in 20 patients with histological proven NASH[41]. When compared with the six patients not complying with treatment, intake of metformin for 4 mo significantly reduced levels of transaminases. They normalized in 50% of treated individuals. Also, insulin sensitivity improved significantly and liver volume decreased by 20%. Metformin was well tolerated and there was no case of lactic acidosis. However, the authors did not provide a serial liver biopsy to evaluate the effect of metformin on liver histology. These promising results were only in part supported by another open label trial [42]. Fifteen patients with biopsy proven NAFLD completed 12 mo of treatment with metformin (20 mg/kg). During the initial 3 mo, liver enzymes improved significantly. There was also an improvement in insulin sensitivity detectable. However, after 3 mo, insulin sensitivity did not further improve and levels of AST and ALT gradually increased back to pretreatment levels. Among the 10 patients with posttreatment biopsy, three showed improvement in steatosis, two showed improvement in inflammation score and one in fibrosis.

Another trial evaluating the effect of metformin was performed by a Turkish group from Ankara[43]. Uygun and coworkers randomized 36 patients with NASH into two groups. The first group was given lipid and calorie-restricted diet alone, while the second group was treated with metformin in addition to the diet for a period of 6 mo. The comparison between both groups showed no

significant differences in inflammatory activity or fibrosis, although more patients in the treatment group showed an improved liver histology. The improvements of liver enzymes, insulin, insulin resistance index and c-peptide levels in the metformin group were significantly greater than those detected in the group with dietary treatment alone. The most recently published controlled trial by Bugianesi and colleagues demonstrated a better effect of metformin on improvement of liver enzymes compared to a prescriptive diet or the administration of vitamin E[44]. Unfortunately, the histological data were limited to support an association between improvement of liver chemistry and histological findings.

Another class of agents presumably improving insulin sensitivity is the thiazolinediones. These compounds are ligands for the peroxisome proliferator-activated receptor gamma (PPAR gamma), which is expressed at high levels in adipocytes. Troglitazone, a first generation thioglitazone, and metformin were shown to inhibit the expression of sterol regulatory element binding protein-1 (SREBP-1), a key regulator of lipogenic enzymes[40, 45]. Troglitazone was investigated in a pilot study including 6 patients with biopsy-proven NASH[46]. Patients received 200 mg of troglitazone twice daily, which was well tolerated. Levels of ALT normalized in 4 of 6 patients on therapy and they persisted in normal range 3 mo after discontinuation of troglitazone. However, the Food and Drug Administration removed troglitazone from the market in March 2000 because of serious hepatotoxicity[47, 48]. The second-generation thioglitazones rosiglitazone and pioglitazone appear to be safer, although their use is currently contraindicated in the presence of active liver disease or of ALT more than 2.5 times normal. An open label trial including 26 biopsy-proven NASH patients analyzed the effect of rosiglitazone, 4 mg twice daily for 48 wk[49]. All patients were overweight, and 23% had a BMI>35 kg/m^2. Twenty-six patients had posttreatment biopsy. The mean necro-inflammatory score significantly improved with treatment and biopsies of 10 patients did not fulfill published criteria for NASH anymore after treatment . Twenty-five patients completed 48 wk of treatment and showed a significant improvement in liver enzymes and insulin resistance. However, 3 patients had to be withdrawn because of adverse events. One of these individuals discontinued because of increased ALT levels. In addition, weight gain occurred in more than two-thirds of participants and liver enzyme levels increased to near pretreatment level 6 mo after discontinuation of study medication. Another pilot study demonstrated similar results in 18 patients with biopsy proven NASH, who were treated with pioglitazone[50]. By 48 wk, levels of ALT normalized in 72% of patients. Hepatic fat content and size decreased which was determined by magnetic resonance imaging. There was also a significant improvement in liver histology regarding features of steatosis, inflammation and fibrosis. Histological improvement occurred in two-thirds of patients. The main side effect in this study was also weight gain and increase in total body adiposity.

In a recently published pilot study by Sanyal and coworkers 20 nondiabetic patients with biopsy-confirmed NASH were randomized to take the combination of pioglitazone (30 mg daily) and vitamin E or vitamin E (400 IU daily) alone for a period of 6 mo[51]. ALT levels normalized in all patients within 6 mo. Compared to baseline, treatment with vitamin E alone resulted in a significant decrease in steatosis, whereas the combination therapy produced a significant improvement in steatosis, cytologic ballooning, Mallory´s hyaline and pericellular fibrosis. Although vitamin E did not have any significant effects on metabolic endpoints, combination therapy improved insulin sensitivity, lowered fasting free fatty acid (FFA) levels and decreased metabolites of FFA oxidation. However, like in the previous trial by Neuschwander-Tetri and coworkers[49] , one of 10 patients receiving pioglitazone plus vitamin E had a significant increase in ALT level and was withdrawn from the study.

LIPID LOWERING DRUGS

Because NAFLD frequently occurs with a disordered lipid homeostasis, lipid-lowering drugs are considered as possible treatment for NAFLD. Hypertriglyceridemia and reduced HDL-cholesterol level are typical dyslipidemias associated with NAFLD. Gemfibrozil reduces very low-density lipoprotein triglyceride production. In a small controlled study of 46 patients with NASH, levels of AST were significantly decreased in 74% of the gemfibrozil group compared with 30% in the control group after 4 wk of treatment[52]. There was no correlation with pretreatment serum triglyceride levels. Posttreatment liver biopsies were not performed and the duration of biochemical response was not evaluated.

In NASH patients with hyperlipidemia statins are another potential treatment option. However, existing data are predominantly uncontrolled with a small number of patients. One study analyzed 28 hyperlipidemic patients with biopsy-proven NASH. Patients were given atorvastatin 20 mg daily for 24 wk. Both significant reduction of LDL-cholesterol and liver enzymes were detectable after treatment[53]. Statin-induced hepatoxicity did not occur and the risk seems to be not increased in patients with presumed NAFLD[54]. However, controlled trials with a bigger number of patients are required to demonstrate the benefit and elucidate potential risks of administrating statins.

BLOCKADE OF TNF-α

Adipose tissue produces several cytokines and biologically active proteins, denoted as adipokines, regulating hepatic and peripheral glucose and lipid metabolism. These adipokines include leptin, resistin, adiponectin and TNF-α. Expression of resistin is not increased in patients with insulin resistance, although resistin inhibits insulin action in animal models[55]. NASH patients show increased serum leptin levels, suggesting the attempt to overcome hepatic leptin resistance to stimulate hepatic lipid turnover[56]. In several studies investigating the pathomechanisms of fatty liver disease increased TNF-α levels have also been demonstrated[57, 58]. TNF-α contributes to insulin resistance and thereby increases hepatic steatosis and plays a

potentially proinflammatory role[59]. This was supported by studies in leptin deficient ob/ob mice. Treatment of anti-TNF-α antibody improved liver histology, reduced hepatic total fatty acid content, and decreased ALT levels[11]. However, studies of ob/ob mice lacking type I and II TNF receptors have suggested that TNF-α is not involved in the liver disease[60]. Further evidence of the involvement of TNF-α came from studies of pentoxifylline which acts as an inhibitor of TNF-α[61, 62]. In these two studies 20 patients and 18 patients, respectively, with biopsy confirmed NASH were enrolled. Pentoxifylline was given for 6 or 12 mo. Both studies demonstrated a significant improvement of AST and ALT levels after application of pentoxifylline in patients with NASH, although histological evidence of its benefit remains unknown.

Adiponectin is exclusively secreted from adipose tissue in inverse proportion to BMI[63, 64]. Although the three dimensional structure of adiponectin closely resembles that of TNF-α[65], these two proteins have completely opposite effects. Adiponectin and TNF-α suppress each other´s production and antagonize their biological effects[66]. Adiponectin acts to reduce body fat[67], improve hepatic and peripheral insulin sensitivity[68] and decrease fatty acid levels[69]. Adiponectin has also antiinflammatory effects which could prevent liver disease. Xu and coworkers replenished recombinant adiponectin in mice fed with a high fat ethanol containing diet and in obese ob/ob mice with NASH. In both mice, administration of adiponectin ameliorated hepatomegaly, steatosis, and elevated ALT levels[70]. Both hepatic TNF-α expression and serum levels of TNF-α significantly decreased, which is further evidence for a harmful role of TNF-α.

This concept was further supported by a study of over 100 patients with NAFLD[71]. Multivariate analysis revealed that decreased serum adiponectin levels and increased TNF-α and soluble TNFR2 levels correlated with the presence of NASH independent of the presence of insulin resistance. NASH patients showed lower adiponectin levels than patients with simple steatosis. Levels of adiponectin correlated with the degree of hepatic necroinflammation. These data provide evidence for the involvement of TNF-α and adiponectin in human NAFLD. Therefore, studies evaluating the effect of adiponectin in treatment of NASH are required.

LIVER TRANSPLANTATION

NASH is considered the most common cause of cryptogenic cirrhosis[72]. Patients with pure steatosis have a benign prognosis, whereas the risk for developing cirrhosis and hepatocellular carcinoma in NASH patients is increased[73, 74]. Complications of cirrhosis or hepatocellular carcinoma may require liver transplantation. In one study by Laurin and colleagues six of eight patients who underwent transplantation for NASH developed recurrent NASH. In three of these six patients, perivenular fibrosis recurred[75]. The patients with recurrences revealed post-transplant hyperlipidemia and increases in body weight. In two subsequent studies the recurrence rate of steatosis was between 60 to 100% of transplant recipients[76, 77]. In one third of these patients progression to steatohepatitis occurred.

CONCLUSIONS

Because of increasing incidence of obesity and insulin resistance NAFLD has become increasingly the focus of basic and clinical research. Whereas fatty liver shows a benign prognosis, patients with NASH should be treated. Progress in understanding the pathomechanisms which contribute to aggravation of fatty liver pathology offers potential treatment options. However, a standard therapy has not been established. The most promising results came from trials with second generation insulin sensitizer in obese patients with insulin resistance. Blockade of TNF-α by adiponectin showed impressive improvement of NASH in an animal model. Clinical trials investigating therapeutic effect of inhibiting TNF-α in NAFLD have to be awaited. So, beyond clinical studies, the first step in treatment should be improvement of insulin sensitivity by weight loss and physical activity.

REFERENCES

1 **Chitturi S**, Abeygunasekera S, Farrell GC, Holmes-Walker J, Hui JM, Fung C, Karim R, Lin R, Samarasinghe D, Liddle C, Weltman M, George J. NASH and insulin resistance: Insulin hypersecretion and specific association with the insulin resistance syndrome. *Hepatology* 2002; **35**: 373-379

2 **Lee RG**. Nonalcoholic steatohepatitis: a study of 49 patients. *Hum Pathol* 1989; **20**: 594-598

3 **Powell EE**, Cooksley WG, Hanson R, Searle J, Halliday JW, Powell LW. The natural history of nonalcoholic steatohepatitis: a follow-up study of forty-two patients for up to 21 years. *Hepatology* 1990; **11**: 74-80

4 **Angulo P**, Keach JC, Batts KP, Lindor KD. Independent predictors of liver fibrosis in patients with nonalcoholic steatohepatitis. *Hepatology* 1999; **30:** 1356-1362

5 **Ratziu V**, Bonyhay L, Di Martino V, Charlotte F, Cavallaro L, Sayegh-Tainturier MH, Giral P, Grimaldi A, Opolon P, Poynard T. Survival, liver failure, and hepatocellular carcinoma in obesity-related cryptogenic cirrhosis. *Hepatology* 2002; **35**: 1485-1493

6 **Day CP**, James OF. Steatohepatitis: a tale of two "hits"? Gastroenterology 1998; **114:** 842-845

7 **Esterbauer H**, Schaur RJ, Zollner H. Chemistry and biochemistry of 4-hydroxynonenal, malonaldehyde and related aldehydes. *Free Radic Biol Med* 1991; **11**: 81-128

8 **Osmundsen H**, Bremer J, Pedersen JI. Metabolic aspects of peroxisomal beta-oxidation. *Biochim Biophys Acta* 1991; **1085**: 141-158

9 **Uesugi T**, Froh M, Arteel GE, Bradford BU, Wheeler MD, Gabele E, Isayama F, Thurman RG. Role of lipopolysaccharide-binding protein in early alcohol-induced liver injury in mice. *J Immunol* 2002; **168**: 2963-2969

10 **Faggioni R**, Fantuzzi G, Gabay C, Moser A, Dinarello CA, Feingold KR, Grunfeld C. Leptin deficiency enhances sensitivity to endotoxin-induced lethality. *Am J Physiol* 1999; **276:** R136-R142

11 **Li Z**, Yang S, Lin H, Huang J, Watkins PA, Moser AB, Desimone C, Song XY, Diehl AM. Probiotics and antibodies to TNF inhibit inflammatory activity and improve nonalcoholic fatty liver disease. *Hepatology* 2003; **37**: 343-350

12 **Hug H**, Strand S, Grambihler A, Galle J, Hack V, Stremmel W, Krammer PH, Galle PR. Reactive oxygen intermediates are involved in the induction of CD95 ligand mRNA expression by cytostatic drugs in hepatoma cells. *J Biol Chem* 1997; **272**: 28191-28193

13 **Feldstein AE**, Canbay A, Angulo P, Taniai M, Burgart LJ, Lindor KD, Gores GJ. Hepatocyte apoptosis and fas expression are prominent features of human nonalcoholic steatohepatitis. *Gastroenterology* 2003; **125**: 437-443

14 American Gastroenterological Association medical position statement: nonalcoholic fatty liver disease. *Gastroenterology* 2002; **123**: 1702-1704

15 **Andersen T**, Gluud C, Franzmann MB, Christoffersen P. Hepatic effects of dietary weight loss in morbidly obese subjects. *J Hepatol* 1991; **12**: 224-229

16 **Luyckx FH**, Scheen AJ, Desaive C, Dewe W, Gielen JE, Lefebvre PJ. Effects of gastroplasty on body weight and related biological abnormalities in morbid obesity. *Diabetes Metab* 1998; **24**: 355-361

17 **Drenick EJ**, Simmons F, Murphy JF. Effect on hepatic morphology of treatment of obesity by fasting, reducing diets and small-bowel bypass. *N Engl J Med* 1970; **282**: 829-834

18 **Cox KL**, Burke V, Morton AR, Beilin LJ, Puddey IB. Independent and additive effects of energy restriction and exercise on glucose and insulin concentrations in sedentary overweight men. *Am J Clin Nutr* 2004; **80**: 308-316

19 **Rollins G**. Moderate exercise reduces the risk of heart disease and death in men with type 2 diabetes. *Rep Med Guidel Outcomes Res* 2003; **14**: 10, 12

20 **Archer WR**, Lamarche B, Deriaz O, Landry N, Corneau L, Despres JP, Bergeron J, Couture P, Bergeron N. Variations in body composition and plasma lipids in response to a high-carbohydrate diet. *Obes Res* 2003; **11**: 978-986

21 **Sondike SB**, Copperman N, Jacobson MS. Effects of a low-carbohydrate diet on weight loss and cardiovascular risk factor in overweight adolescents. *J Pediatr* 2003; **142**: 253-258

22 **Vajro P**, Fontanella A, Perna C, Orso G, Tedesco M, De Vincenzo A. Persistent hyperaminotransferasemia resolving after weight reduction in obese children. *J Pediatr* 1994; **125**: 239-241

23 **Knobler H**, Schattner A, Zhornicki T, Malnick SD, Keter D, Sokolovskaya N, Lurie Y, Bass DD. Fatty liver--an additional and treatable feature of the insulin resistance syndrome. *QJM* 1999; **92**: 73-79

24 **Ueno T**, Sugawara H, Sujaku K, Hashimoto O, Tsuji R, Tamaki S, Torimura T, Inuzuka S, Sata M, Tanikawa K. Therapeutic effects of restricted diet and exercise in obese patients with fatty liver. *J Hepatol* 1997; **27**: 103-107

25 **Huang MA**, Greenson JK, Chao C, Anderson L, Peterman D, Jacobson J, Emick D, Lok AS, Conjeevaram HS. One-year intense nutritional counseling results in histological improvement in patients with non-alcoholic steatohepatitis: a pilot study. *Am J Gastroenterol* 2005; **100**: 1072-1081

26 **Ryan DH**. Use of sibutramine to treat obesity. *Prim Care* 2003; **30**: 405-426, viii

27 **Sabuncu T**, Nazligul Y, Karaoglanoglu M, Ucar E, Kilic FB. The effects of sibutramine and orlistat on the ultrasonographic findings, insulin resistance and liver enzyme levels in obese patients with non-alcoholic steatohepatitis. *Rom J Gastroenterol* 2003; **12**: 189-192

28 **Luyckx FH**, Scheen AJ, Desaive C, Thiry A, Lefebvre PJ. Parallel reversibility of biological markers of the metabolic syndrome and liver steatosis after gastroplasty-induced weight loss in severe obesity. *J Clin Endocrinol Metab* 1999; **84**: 4293

29 **Luyckx FH**, Desaive C, Thiry A, Dewe W, Scheen AJ, Gielen JE, Lefebvre PJ. Liver abnormalities in severely obese subjects: effect of drastic weight loss after gastroplasty. *Int J Obes Relat Metab Disord* 1998; **22**: 222-226

30 **Parola M**, Muraca R, Dianzani I, Barrera G, Leonarduzzi G, Bendinelli P, Piccoletti R, Poli G. Vitamin E dietary supplementation inhibits transforming growth factor beta 1 gene expression in the rat liver. *FEBS Lett* 1992; **308**: 267-270

31 **Parola M**, Leonarduzzi G, Biasi F, Albano E, Biocca ME, Poli G, Dianzani MU. Vitamin E dietary supplementation protects against carbon tetrachloride-induced chronic liver damage and cirrhosis. *Hepatology* 1992; **16**: 1014-1021

32 **Houglum K**, Venkataramani A, Lyche K, Chojkier M. A pilot study of the effects of d-alpha-tocopherol on hepatic stellate cell activation in chronic hepatitis C. *Gastroenterology* 1997; **113**: 1069-1073

33 **Lavine JE**. Vitamin E treatment of nonalcoholic steatohepatitis in children: a pilot study. *J Pediatr* 2000; **136**: 734-738

34 **Hasegawa T**, Yoneda M, Nakamura K, Makino I, Terano A. Plasma transforming growth factor-beta1 level and efficacy of alpha-tocopherol in patients with non-alcoholic steatohepatitis: a pilot study. *Aliment Pharmacol Ther* 2001; **15**: 1667-1672

35 **Harrison SA**, Torgerson S, Hayashi P, Ward J, Schenker S. Vitamin E and vitamin C treatment improves fibrosis in patients with nonalcoholic steatohepatitis. *Am J Gastroenterol* 2003; **98**: 2485-2490

36 **Adams LA**, Angulo P. Treatment of nonalcoholic steatohepatitis: antioxidants or insulin sensitizers? *Clin Gastroenterol Hepatol* 2004; **2**: 1059-1060

37 **Angulo P**. Use of ursodeoxycholic acid in patients with liver disease. *Curr Gastroenterol Rep* 2002; **4**: 37-44

38 **Laurin J**, Lindor KD, Crippin JS, Gossard A, Gores GJ, Ludwig J, Rakela J, McGill DB. Ursodeoxycholic acid or clofibrate in the treatment of non-alcohol-induced steatohepatitis: a pilot study. *Hepatology* 1996; **23**: 1464-1467

39 **Lindor KD**, Kowdley KV, Heathcote EJ, Harrison ME, Jorgensen R, Angulo P, Lymp JF, Burgart L, Colin P. Ursodeoxycholic acid for treatment of nonalcoholic steatohepatitis: results of a randomized trial. *Hepatology* 2004; **39**: 770-778

40 **Lin HZ**, Yang SQ, Chuckaree C, Kuhajda F, Ronnet G, Diehl AM. Metformin reverses fatty liver disease in obese, leptin-deficient mice. *Nat Med* 2000; **6**: 998-1003

41 **Marchesini G**, Brizi M, Bianchi G, Tomassetti S, Zoli M, Melchionda N. Metformin in non-alcoholic steatohepatitis. *Lancet* 2001; **358**: 893-894

42 **Nair S**, Diehl AM, Wiseman M, Farr GH Jr, Perrillo RP. Metformin in the treatment of non-alcoholic steatohepatitis: a pilot open label trial. *Aliment Pharmacol Ther* 2004; **20**: 23-28

43 **Uygun A**, Kadayifci A, Isik AT, Ozgurtas T, Deveci S, Tuzun A, Yesilova Z, Gulsen M, Dagalp K. Metformin in the treatment of patients with non-alcoholic steatohepatitis. *Aliment Pharmacol Ther* 2004; **19**: 537-544

44 **Bugianesi E**, Gentilcore E, Manini R, Natale S, Vanni E, Villanova N, David E, Rizzetto M, Marchesini G. A randomized controlled trial of metformin versus vitamin E or prescriptive diet in nonalcoholic fatty liver disease. *Am J Gastroenterol* 2005; **100:** 1082-1090

45 **Kakuma T**, Lee Y, Higa M, Wang Z, Pan W, Shimomura I, Unger RH. Leptin, troglitazone, and the expression of sterol regulatory element binding proteins in liver and pancreatic islets. *Proc Natl Acad Sci USA* 2000; **97**: 8536-8541

46 **Caldwell SH**, Hespenheide EE, Redick JA, Iezzoni JC, Battle EH, Sheppard BL. A pilot study of a thiazolidinedione, troglitazone, in nonalcoholic steatohepatitis. *Am J Gastroenterol* 2001; **96**: 519-525

47 **Kohlroser J**, Mathai J, Reichheld J, Banner BF, Bonkovsky HL. Hepatotoxicity due to troglitazone: report of two cases and review of adverse events reported to the United States Food and Drug Administration. *Am J Gastroenterol* 2000; **95**: 272-276

48 **Menon KVN**, Angulo P, Lindor KD. Severe cholestatic hepatitis from troglitazone in a patient with nonalcoholic steatohepatitis and diabetes mellitus. *Am J Gastroenterol* 2001; **96**: 1631-1634

49 **Neuschwander-Tetri BA**, Brunt EM, Wehmeier KR, Oliver D, Bacon BR. Improved nonalcoholic steatohepatitis after 48 weeks of treatment with the PPAR-gamma ligand rosiglitazone. *Hepatology* 2003; **38**: 1008-1017

50 **Promrat K**, Lutchman G, Uwaifo GI, Freedman RJ, Soza A, Heller T, Doo E, Ghany M, Premkumar A, Park Y, Liang TJ, Yanovski JA, Kleiner DE, Hoofnagle JH. A pilot study of pioglitazone treatment for nonalcoholic steatohepatitis. *Hepatology* 2004; **39**: 188-196

51 **Sanyal AJ**, Mofrad PS, Contos MJ, Sargeant C, Luketic VA, Sterling RK, Stravitz RT, Shiffman ML, Clore J, Mills AS. A pilot study of vitamin E versus vitamin E and pioglitazone for the treatment of nonalcoholic steatohepatitis. *Clin Gastroenterol Hepatol* 2004; **2**: 1107-1115

52 **Basaranoglu M**, Acbay O, Sonsuz A. A controlled trial of gem-

fibrozil in the treatment of patients with nonalcoholic steatohepatitis. *J Hepatol* 1999; **31**: 384
53 **Hatzitolios A**, Savopoulos C, Lazaraki G, Sidiropoulos I, Haritanti P, Lefkopoulos A, Karagiannopoulou G, Tzioufa V, Dimitrios K. Efficacy of omega-3 fatty acids, atorvastatin and orlistat in non-alcoholic fatty liver disease with dyslipidemia. *Indian J Gastroenterol* 2004; **23**: 131-134
54 **Chalasani N**, Aljadhey H, Kesterson J, Murray MD, Hall SD. Patients with elevated liver enzymes are not at higher risk for statin hepatotoxicity. *Gastroenterology* 2004; **126**: 1287-1292
55 **Nagaev I**, Smith U. Insulin resistance and type 2 diabetes are not related to resistin expression in human fat cells or skeletal muscle. *Biochem Biophys Res Commun* 2001; **285**: 561-564
56 **Chitturi S**, Farrell G, Frost L, Kriketos A, Lin R, Fung C, Liddle C, Samarasinghe D, George J. Serum leptin in NASH correlates with hepatic steatosis but not fibrosis: a manifestation of lipotoxicity? *Hepatology* 2002; **36**: 403-409
57 **Kugelmas M**, Hill DB, Vivian B, Marsano L, McClain CJ. Cytokines and NASH: a pilot study of the effects of lifestyle modification and vitamin E. *Hepatology* 2003; **38**: 413-419
58 **Wigg AJ**, Roberts-Thomson IC, Dymock RB, McCarthy PJ, Grose RH, Cummins AG. The role of small intestinal bacterial overgrowth, intestinal permeability, endotoxaemia, and tumour necrosis factor alpha in the pathogenesis of non-alcoholic steatohepatitis. *Gut* 2001; **48**: 206-211
59 **Crespo J**, Cayon A, Fernandez-Gil P, Hernandez-Guerra M, Mayorga M, Dominguez-Diez A, Fernandez-Escalante JC, Pons-Romero F. Gene expression of tumor necrosis factor alpha and TNF-receptors, p55 and p75, in nonalcoholic steatohepatitis patients. *Hepatology* 2001; **34**: 1158-1163
60 **Memon RA**, Grunfeld C, Feingold KR. TNF-alpha is not the cause of fatty liver disease in obese diabetic mice. *Nat Med* 2001; **7**: 2-3
61 **Satapathy SK**, Garg S, Chauhan R, Sakhuja P, Malhotra V, Sharma BC, Sarin SK. Beneficial effects of tumor necrosis factor-alpha inhibition by pentoxifylline on clinical, biochemical, and metabolic parameters of patients with nonalcoholic steatohepatitis. *Am J Gastroenterol* 2004; **99**: 1946-1952
62 **Adams LA**, Zein CO, Angulo P, Lindor KD. A pilot trial of pentoxifylline in nonalcoholic steatohepatitis. *Am J Gastroenterol* 2004; **99**: 2365-2368
63 **Berg AH**, Combs TP, Scherer PE. ACRP30/adiponectin: an adipokine regulating glucose and lipid metabolism. *Trends Endocrinol Metab* 2002; **13**: 84-89
64 **Arita Y**, Kihara S, Ouchi N, Takahashi M, Maeda K, Miyagawa J, Hotta K, Shimomura I, Nakamura T, Miyaoka K, Kuriyama H, Nishida M, Yamashita S, Okubo K, Matsubara K, Muraguchi M, Ohmoto Y, Funahashi T, Matsuzawa Y. Paradoxical decrease of an adipose-specific protein, adiponectin, in obesity. *Biochem Biophys Res Commun* 1999; **257**: 79-83
65 **Shapiro L**, Scherer PE. The crystal structure of a complement-1q family protein suggests an evolutionary link to tumor necrosis factor. *Curr Biol* 1998; **8**: 335-338
66 **Maeda N**, Shimomura I, Kishida K, Nishizawa H, Matsuda M, Nagaretani H, Furuyama N, Kondo H, Takahashi M, Arita Y, Komuro R, Ouchi N, Kihara S, Tochino Y, Okutomi K, Horie M, Takeda S, Aoyama T, Funahashi T, Matsuzawa Y. Diet-induced insulin resistance in mice lacking adiponectin/ACRP30. *Nat Med* 2002; **8**: 731-737
67 **Shklyaev S**, Aslanidi G, Tennant M, Prima V, Kohlbrenner E, Kroutov V, Campbell-Thompson M, Crawford J, Shek EW, Scarpace PJ, Zolotukhin S. Sustained peripheral expression of transgene adiponectin offsets the development of diet-induced obesity in rats. *Proc Natl Acad Sci USA* 2003; **100**: 14217-14222
68 **Berg AH**, Combs TP, Du X, Brownlee M, Scherer PE. The adipocyte-secreted protein Acrp30 enhances hepatic insulin action. *Nat Med* 2001; **7**: 947-953
69 **Fruebis J**, Tsao TS, Javorschi S, Ebbets-Reed D, Erickson MR, Yen FT, Bihain BE, Lodish HF. Proteolytic cleavage product of 30-kDa adipocyte complement-related protein increases fatty acid oxidation in muscle and causes weight loss in mice. *Proc Natl Acad Sci USA* 2001; **98**: 2005-2010
70 **Xu A**, Wang Y, Keshaw H, Xu LY, Lam KS, Cooper GJ. The fat-derived hormone adiponectin alleviates alcoholic and non-alcoholic fatty liver diseases in mice. *J Clin Invest* 2003; **112**: 91-100
71 **Hui JM**, Hodge A, Farrell GC, Kench JG, Kriketos A, George J. Beyond insulin resistance in NASH: TNF-alpha or adiponectin? *Hepatology* 2004; **40**: 46-54
72 **Caldwell SH**, Oelsner DH, Iezzoni JC, Hespenheide EE, Battle EH, Driscoll CJ. Cryptogenic cirrhosis: clinical characterization and risk factors for underlying disease. *Hepatology* 1999; **29**: 664-669
73 **Matteoni CA**, Younossi ZM, Gramlich T, Boparai N, Liu YC, McCullough AJ. Nonalcoholic fatty liver disease: a spectrum of clinical and pathological severity. *Gastroenterology* 1999; **116**: 1413-1419
74 **Marrero JA**, Fontana RJ, Su GL, Conjeevaram HS, Emick DM, Lok AS. NAFLD may be a common underlying liver disease in patients with hepatocellular carcinoma in the United States. *Hepatology* 2002; **36**: 1349-1354
75 **Kim WR**, Poterucha JJ, Porayko MK, Dickson ER, Steers JL, Wiesner RH. Recurrence of nonalcoholic steatohepatitis following liver transplantation. *Transplantation* 1996; **62**: 1802-1805
76 **Charlton M**, Kasparova P, Weston S, Lindor K, Maor-Kendler Y, Wiesner RH, Rosen CB, Batts KP. Frequency of nonalcoholic steatohepatitis as a cause of advanced liver disease. *Liver Transpl* 2001; **7**: 608-614
77 **Contos MJ**, Cales W, Sterling RK, Luketic VA, Shiffman ML, Mills AS, Fisher RA, Ham J, Sanyal AJ. Development of nonalcoholic fatty liver disease after orthotopic liver transplantation for cryptogenic cirrhosis. *Liver Transpl* 2001; **7**: 363-373

S- Editor Wang J **L- Editor** Zhu LH **E- Editor** Bai SH

PO Box 2345, Beijing 100023, China
www.wjgnet.com
wjg@wjgnet.com

World J Gastroenterol 2006 April 14; 12(14): 2168-2173
World Journal of Gastroenterology ISSN 1007-9327

GASTRIC CANCER

Mechanisms inactivating the gene for E-cadherin in sporadic gastric carcinomas

Yao-Chi Liu, Chen-Yang Shen, Hurng-Sheng Wu, Tsai-Yuan Hsieh, De-Chuan Chan, Cheng-Jueng Chen, Jyh-Cherng Yu, Cheng-Ping Yu, Horng-Jyh Harn, Peng-Jen Chen, Chung-Bao Hsieh, Teng-Wei Chen, Huan-Mieng Hsu

Yao-Chi Liu, De-Chuan Chan, Cheng-Jueng Chen, Jyh-Cherng Yu, Chung-Bao Hsieh, Teng-Wei Chen, Huan-Mieng Hsu, Division of General Surgery, Department of Surgery, Tri-Service General Hospital, National Defense Medical Center, Taipei, Taiwan, China
Tsai-Yuan Hsieh, Peng-Jen Chen, Division of Gastroenterology, Department of Internal Medicine, Tri-Service General Hospital, National Defense Medical Center, Taipei, Taiwan, China
Cheng-Ping Yu, Department of Pathology, Tri-Service General Hospital, National Defense Medical Center, Taipei, Taiwan, China
Horng-Jyh Harn, Department of Pathology, Buddhist Tzu-Chi General Hospital, Hualien, Taiwan, China
Hurng-Sheng Wu, Department of Surgery, Show Chwan Memorial Hospital, Changhua, Taiwan, China
Chen-Yang Shen, Institute of Biomedical Sciences, Academia Sinica, Taipei, Taiwan, China
Supported by Clinical Research Fund of the Tri-Service General Hospital and C.Y.Fundation for Advancement of Education, Science and Medicine, Taipei, Taiwan, China
Correspondence to: Dr. Yao-Chi Liu, Division of General Surgery, Tri-Service General Hospital. No. 325, Sec 2, Cheng-Kung Road, Neihu 114, Taipei, Taiwan, China. dlyaochi@yahoo.com.tw
Telephone: +886-2-87927191 Fax: +886-2-87927372
Received: 2005-03-29 Accepted: 2005-07-20

Abstract

AIM: To study the role of *CDH1/E-cadherin* (E-cad) gene alteration profiles including mutation, loss of heterozygosity (LOH), promoter polymorphism and hypermethylation in mechanisms of *CDH1* inactivation in gastric carcinoma (GC).

METHODS: Specimens were collected surgically from 70 patients with GC. Allelotyping PCR and detection of LOH, denaturing high pressure liquid chromatography and DNA sequencing, restriction fragment length polymorphism analysis, methylation specific PCR, and immunohistochemical staining were used.

RESULTS: Promoter polymorphism was not a major mechanism of E-cad inactivation. Only one truncating mutation was found in a diffuse type tumor (3%). Both LOH and promoter hypermethylation were major mechanisms of E-cad inactivation, but interestingly, there was a negative association between the fraction of allelic loss (LOH) in tumors and hypermethylation of *CDH1*. Therefore LOH and hypermethylation were two different tumorigenic pathways involved in GC.

CONCLUSION: Given the findings that somatic mutation was extremely low and the relationship between LOH and hypermethylation was inverse, any two combinations of these three factors cannot fulfill the classical two-hit hypothesis of *CDH1* inactivation. Thus, other mechanisms operating at the transcriptional level or at the post-translational level might be required to induce E-cadherin inactivation.

Key words: Gastric carcinoma; E-cadherin gene alteration profiles; Inactivation of E-cadherin

Liu YC, Shen CY, Wu HS, Hsieh TY, Chan DC, Chen CJ, Yu JC, Yu CP, Harn HJ, Chen PJ, Hsieh CB, Chen TW, Hsu HM. Mechanisms inactivating the gene for E-cadherin in sporadic gastric carcinomas. *World J Gastroenterol* 2006; 12(14): 2168-2173

http://www.wjgnet.com/1007-9327/12/2168.asp

INTRODUCTION

CDH1/E-cadherin (E-cad) is a member of the family of transmembrane glycoproteins expressed on epithelial cells and is responsible for calcium-dependent cell-to-cell adhesion[1]. E-cad forms complexes and connects actin filaments with α-, β-, and γ-catenins[2,3], which are essential to neoplastic transformation and metastasis[4, 5]. Loss of cell adhesion may contribute to loss of contact inhibition of growth, which is an early step in the neoplastic process. Furthermore, loss of cadherin activity may result in cancer cell detachment and metastasis[6, 7].

Gastric carcinogenesis is a multi-step process with morphological progression involving multiple genetic and epigenetic events. E-cad gene (*CDH1)* is an important putative tumor suppressor gene. In gastric carcinomas (GCs), the reduction in E-cad expression activation of *E-cad* gene varies from 17% to 92%, and is more frequent in diffuse type than in intestinal type tumors[8-13]. Germline mutation of the *CDH1* gene is found in all familial GCs[14, 15]. Somatic mutations of *CDH1* are found in more than

50% of diffuse type GCs but are not found in intestinal type GCs in Caucasians and Japanese populations[16-19]. The rate of loss of heterozygosity (LOH) ranges from 2.8% to 60% in diffuse and intestinal type tumors[16-20]. In addition to the well-known 'two-hit'inactivation mechanism proposed by Knudson (1971), *CDH1* can be silenced in GC by epigenetic promoter hypermethylation[17, 21]. Besides, Li *et al*[22] reported that the-60C/A polymorphism has a direct effect on the transcriptional regulation of *CDH1*. All above previous studies of the inactivation of this gene in patients with GC have been limited in their analyses. In this study, we investigated a range of alterations in *CDH1* expression profiles, including genetic mutations, LOH, promoter polymorphism, promoter hypermethylation, and immunohistochemical stain of E-cad protein together to determine possible genetic and epigenetic mechanisms of *CDH1* inactivation.

MATERIALS AND METHODS

Patients and samples

Specimens were collected surgically from 70 Taiwanese patients with GC between July 1999 and July 2002 at the Division of General Surgery, Department of Surgery, Tri-Service General Hospital, Taipei, Taiwan. None of the subjects received preoperative anticancer therapy. Clinical information was obtained from medical records. Samples were taken from representative cancerous lesions and the adjacent non-cancerous epithelial parts of the tissues were flash frozen in liquid nitrogen and stored at -80℃. All tumor DNA samples were obtained by micro-dissection from 5-μm thick hematoxylin and eosin stained and paraffin embedded tissue sections[23]. Non-cancerous DNA was extracted from tissues which were flash-frozen in liquid nitrogen and stored at -80℃. All 70 samples were classified according to the Lauren's criteria[23]: 27 were intestinal and 43 were diffuse types. The tumors were staged at the time of surgery using the standard criteria by TNM staging, with the unified international gastric cancer staging classification[24].

Allelotyping PCR and detection of allelic loss or loss of heterozygosity (LOH) of CDH1

DNA samples from tumor and normal mucosal specimens were used for allelotyping PCR with fluorescent primers (markers). Three micro-satellite markers (D16S3043, D16S3050, and D16S3021) at 16q22.1 were used to detect LOH at the CDH1 locus. PCR amplification was carried out as previously described[26]. PCR products were separated electrophoretically on an ABI PRISM 377 DNA sequencer, and fluorescent signals from the differently sized alleles were recorded and analyzed using Genotyper version 2.1 and GeneScan version 3.1 software packages. A given informative marker was considered to display LOH when a threefold or greater difference was seen in the relative allele intensities of the tumor and normal DNA samples.

Denaturing high pressure liquid chromatography (DHPLC) analysis and DNA sequencing for CDH1 mutation analysis

We used DHPLC and direct sequencing to determine inactivating mutations responsible for the loss of *CDH1* expression. The promoter region and 16 exons including the exon-intron boundaries were analyzed using the previously described protocol and primer pairs[26]. The optimal conditions for DHPLC analysis of each amplicon were available as requested. All variants detected by DHPLC were re-amplified and the site of variation was identified by direct DNA sequencing using an ABI PRISM 377 DNA sequencer.

Restriction-fragment length polymorphism (RFLP) analysis to identify nucleotide changes at –160 of the CDH1 promoter

The -160 polymorphic site contained either a C or A residue. The tumor type was determined by *Bst*EII digestion of the PCR products amplified using the primer set 5′-TGATCCCAGGTCTTAGTGAG-3′ (upstream) and 5′-AGTCTGAACTGACTT CCGCA-3′ (downstream). The 318-bp PCR product was cut into two fragments (208 and 110 bp) if it contained the A residue. To ensure that the observed polymorphism was specific and not an experimental artifact, the results were confirmed by direct DNA sequencing.

Methylation-specific PCR (MSP) and bisulfite-modified genomic sequencing to detect promoter hypermethylation of CDH1

Genomic DNA was modified by bisulfite treatment, converting unmethylated cytosines to uracils and leaving methylated cytosines unchanged. MSP was performed on the treated DNA to detect all three CpG islands in the *CDH1* promoter region as previously described[27]. Each unmethylated–methylated primer pair set was engineered to assess the methylation status of 4-6 CpGs with at least one CpG dinucleotide positioned at the 3′ end of each primer to discriminate between methylated and unmethylated alleles following bisulfite modification. Hs578t cells, which contain a heterogeneously methylated CpG island 1 and methylated CpG islands 2 and 3, served as the positive control, and MCF7 cells were used as the negative control.

Immunohistochemical staining and evaluation of E-cad expression

Sections (5 μm thick) were treated with monoclonal anti-E-cad antibody (Cappel, Aurora, OH, USA), then with secondary antibody. The signal was detected using a kit containing avidin–biotin complex and diaminobenzidine (DAB; Vector Laboratories, Burlingame, CA, USA). DAB produced a yellowish brown staining if the sample was positive. If more than 90% of the tumor cells exhibited intense membranous staining similar to that of normal cells, the result was considered positive (++). If the staining intensity was demonstrably reduced relative to that of normal cells and/or the staining pattern was heterogeneous (10%-90% positive), the result was deemed to be weakly positive (+). If IHC expression was completely lost or positive in less than 10% of cells, the result was defined as negative (–).

Statistical analysis

Analyses were performed using S-Plus® 2000 for

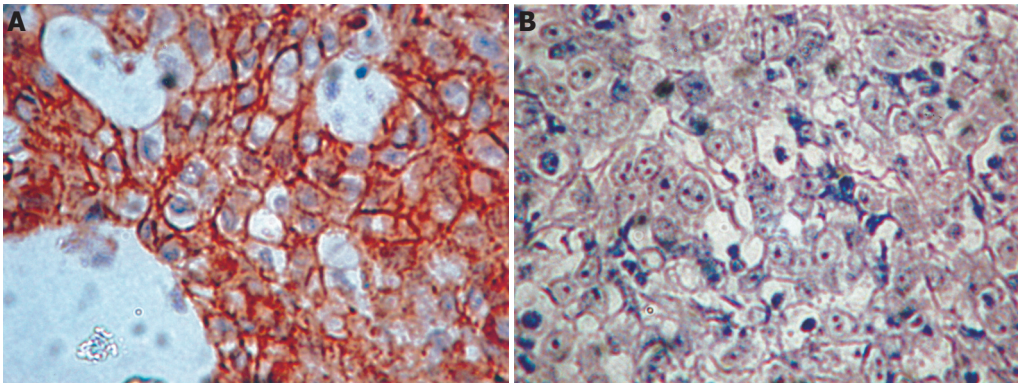

Figure 1 Immunohistochemical staining for positive (**A**) and negative (**B**) E-cad expression in diffuse type tumor.

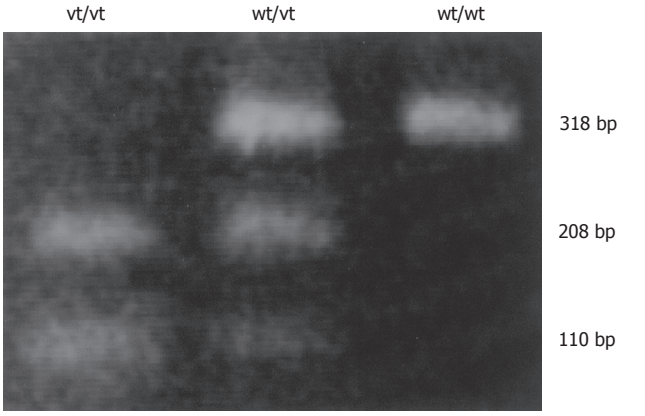

Figure 2 PCR-restriction fragment length polymorphism (RFLP) analysis of genetic polymorphism of the -160 site of the *E-cad* promoter. The C/A polymorphism was differentiated by *BstEII* digestion of PCR products homozygous for the wild-type (high-activity) allele (*wt/wt*, CC gentoype), heterozygous for the variant (low-activity) allele (*wt/vt*, CA genotype), and homozygous for the low-activity allele (*vt/vt*, AA genotype)

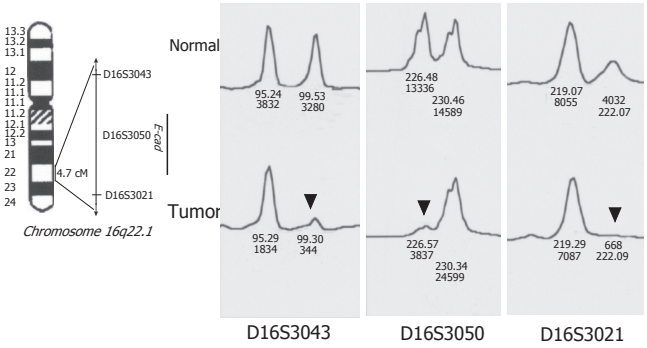

Figure 3 Allelic loss or loss of heterozygosity (LOH) of *CDH1*/*E-cad*. Left panel: *E-cad* detected by allelic loss or loss of heterozygosity (LOH) of the *E-cad* locus, reflected by three microsatellite markers (*D16S3043*, *D16SS3050* and *D16S3021*) at 16q22.1. *Right panel*: LOH in a representative GC. The locius of markers *D16S3043*, *D16S3050*, and *D16S3021* were considered to be informative when they were heterozygous in normal tissue (i.e. two alleles were seen), and showed LOH when a 3-fold or greater difference was seen in the relative allele intensity ratio between the tumor and normal DNA (arrow).

Windows statistical software (CANdiensten, Amsterdam, Netherlands). Significance was assumed at $P<0.05$ for all tests. Categorical variables were tested using Fisher's exact test.

RESULTS

Of the 70 patients, 52 were men and 18 were women. Their median age was 69.7 years (range 32-88 years). According to Lauren's classification, 27 and 43 tumors were intestinal and diffuse histotypes, respectively. Reduced gene expression was more frequent in diffuse type tumors (38/43, 88%) than in intestinal type tumors (13/27, 48%; $P=0.006$). Representative examples of immunohistochemical staining for E-cad expression in diffuse type tumors are shown in Figure 1.

Promoter polymorphism

Three of the 70 patients were omitted from our analysis of the -160C/A polymorphism due to insufficient samples. Among the other 67 patients, 29 were genotype C/C (43%), 24 were genotype A/C (36%) and 14 were genotype A/A (21%) (Figure 2). There was no significant difference in the frequency of the C/A + A/A genotypes between diffuse and intestinal type tumors (27/42, 64% *vs* 11/25, 44%). There was no significant difference in LOH between the C/C and C/A + A/A genotypes (10/25, 40% *vs* 13/33, 39%). There was also no significant difference in hypermethylation between C/C and C/A + A/A genotypes (20/29, 69% *vs* 24/37, 65%). There was no significant difference in the frequency of the C/A + A/A genotypes between tissues with reduced and normal E-cad expression (12/17, 71% *vs* 27/50, 54%).

Loss of heterozygosity

To detect allelic loss at *CDH1*, three micro-satellite markers (D16S3043, D16S3050, D16S3021) at 16q22.1 were used (Figure 3). The allelic status of this gene was reflected well by these three markers, because its locus was very close to the loci of these markers (LOD score > 4 estimated by linkage analysis). We considered the results for all three markers together and found heterozygosity in at least one. Of the 70 samples collected, 10 were omitted from the analysis or homozygous and could not be detected. A high frequency of allelic loss at *CDH1* was detected (23/60, 38%). The frequency of LOH at *CDH1* was similar between diffuse type tumors (15/38, 39%) and intestinal type tumors (8/22, 36%). Reduced E-cad expression was more frequent in LOH-positive tumors (21/23, 91%) than in LOH-negative tumors (24/37, 65%; $P=0.03$).

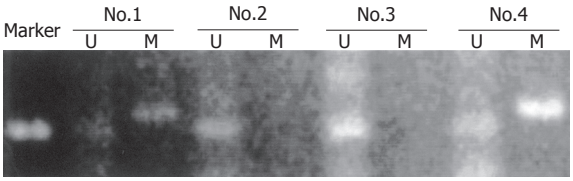

Figure 4 Promoter hypermethylation of the *CDH1/E-cad* detected by methylation-specific PCR (MSP). The presence of a visible PCR product in the lanes marked U indicates the presence of an unmethylated allele, while the presence of the product in the lanes marked M indicates the presence of a methylated allele. The intensity of each methylated band was further semi-quantitated, and as shown in the figure, cases 1 and 4 were defined as "hypermethylation"with "+"and "++", respectively, and cases 2 and 3 were defined as "unmethylation".

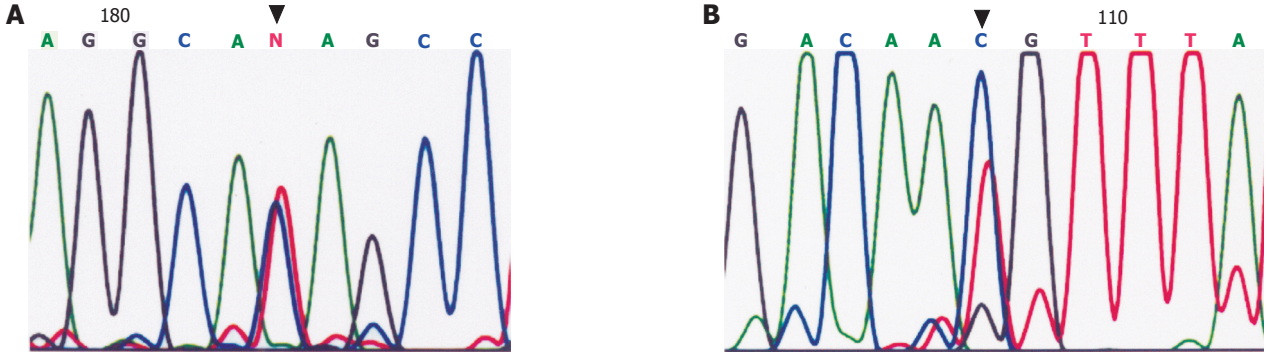

Figure 5 *CDH1*/E-cad mutation and polymorphism detected by direct DNA sequencing. Two tumors subjected to DNA sequencing were found to harbor C-to-T transversion in exon 13 (**A**), resulting in a truncated mutation (Gln to stop condon TAG) and C-to-T transversion in exon 14 (**B**), resulting in no amino acid change, which was considered to be polymorphism.

Promoter hypermethylation

The degree of hypermethylation estimated by MSP was defined as strongly detectable (+++, ++), detectable (+), or not detectable (–)(Figure 4). Three of the 70 samples were omitted from our analysis of hypermethylation due to insufficient samples. The *CDH1* promoter was hypermethylated in 45 of these 67 GCs (67%). Hypermethylation was more frequent in diffuse type tumors (31/41, 76%) than in intestinal type tumors (13/26, 50%; $P=0.03$ by Fisher's exact test). Furthermore, hypermethylation was more frequent in GCs with reduced E-cad expression than in those with normal levels (37/45, 82% *vs* 12/22, 55%; $P=0.02$). The fraction of allelic loss (FAL) of *CDH1*, calculated as the frequency of LOH at *CDH1* locus, was generally inverse to the degree of hypermethylation (Tables 1, 2).

Mutation

In these 70 patients, five diffuse type tumors (Case No. 15, 24, 29, 30, and 39) had a single-nucleotide polymorphism (SNP) at amino acid 692, and four diffuse type tumors (Case No. 35, 40, 59, and 63) had an SNP at position 755 . Case No.15 had a truncated mutation at position 699 (Figure 5). No *CDH1* mutation was found in intestinal type tumors.

DISCUSSION

In this study, 27 and 43 tumors were of the intestinal and diffuse histotypes, respectively. Inactivation of the *CDH1* gene and loss of normal E-cad expression were involved more frequently in diffuse type than in intestinal type tumors (88% *vs* 48%; $P=0.006$). However, the percentage of reduction in E-cad expression of GC varies from 17% to 92% in previous reports[8-13]

Promoter polymorphism

Li *et al*[22] reported that the A allele of the -160C/A promoter polymorphism alters transcriptional binding, resulting in a reduction in transcriptional efficiency of 68% relative to that of the C allele. In our study, there was no significant difference in the frequency of the C/A + A/A genotypes between diffuse and intestinal type tumors. There was no significant difference in LOH and hypermethylation between the C/C and C/A + A/A genotypes. There was also no significant difference in the frequency of the C/A + A/A genotypes between tumors with reduced and normal E-cad expression, suggesting that the A allele does not play a major role in the inactivation of *CDH1* and can not serve as the 'second hit'.

Mutations

Somatic mutations of *CDH1* are found in more than 50% of diffuse type GCs but not in intestinal type GCs in Caucasian and Japanese populations[16-19]. A review by Berx *et al*[28] noted that the predominant defects in diffuse type tumors are splice mutations causing skipping in exon 8 or 9, which account for in-frame deletions, whereas mis-sense and truncating mutations are less frequent in diffuse GCs. Moreover intragenic polymorphisms arise from changes in the third (wobble) position of the respective codons and are more frequent in codons 692 and 751. In the present study, five of the diffuse type tumors had a codon 692 polymorphism and four diffuse type tumors had a codon 755 polymorphism. Only one of 38 diffuse type tumors had a truncated codon 699 mutation. Because consistent findings have been obtained by repeated detection of the same specimens, we considered this finding to be valid. Therefore, this low rate of *CDH1* mutation in the Taiwanese GCs may suggest different tumorigenic mechanisms to inactivate this gene.

Table 1 Fraction of allelic loss (FAL) in tumors with different hypermethylation statuse

Promoter hypermethylation	FAL	
Yes (++,+++)	0.098	
Yes (+)	0.214	
No	0.377	$P=0.03$

FAL was estimated by allelic status at D16S3043, D16SS3050 and D16S3021. FAL (fraction of allelic loss) = number of loci showing LOH / number of informative loci in each tumor. The FALs of tumors with different hypermethylation status were calculated as the mean of FALs of individual tumors with the same hypermethylation status.

Table 2 Association between loss of heterozygosity and promoter hypermethylation of *CDH1*

	Loss of heterozygosity		
	Yes (%)	*n* (%)	Promoter
hypermethylation			
Yes (++,+++)	1 (9.1)	17 (34.7)	
Yes (+)	2 (18.2)	21 (42.9)	
No	8 (72.7)	11 (22.5)	$P=0.001$

LOH status is defined by D16S3043

Loss of heterozygosity

It was reported that the rate of LOH ranges from 2.8% to 60% in diffuse and intestinal type tumors [16-20]. A high frequency (38%) of allelic loss at *CDH1* was identified in our study. The frequency of LOH was similar between the diffuse and intestinal type tumors (39% *vs* 36%). Reduced E-cad expression demonstrated by immunohistochemical analysis was more frequent in LOH-positive tumors than in LOH-negative tumors (91% *vs* 65%; $P=0.03$), suggesting that LOH is a major mechanism for the inactivation of *CDH1*.

Promoter hypermethylation

Tamura *et al*[29] and Graziano *et al*[30] indicated that *CDH1* promoter methylation may play a major role together with mutations or deletions, in causing the inactivation of the *CDH1* gene in GCs, especially in diffuse type tumors. They also reported that *CDH1* promoter hypermethylation is associated with reduced E-cad expression detected immunohistochemically. In the present study, the *CDH1* promoter was hypermethylated in 67% of GCs. Hypermethylation was more frequent in diffuse type tumors than in intestinal type tumors ($P=0.03$). Furthermore, hypermethylation was more frequent in tumors with reduced E-cad expression than in normal E-cad expression (82% *vs* 55%; $P=0.02$), suggesting that *CDH1* promoter hypermethylation is a major mechanism for gene inactivation.

Methylation of the *CDH1* promoter has been documented as the 'second hit' responsible for the development of hereditary diffuse GCs[31] and sporadic diffuse GCs[17] among Caucasians. Because there was only one genetic mutation in diffuse type tumors and no mutation in intestinal type tumors in this series, we examined the hypermethylated status of tumors with or without LOH at the *CDH1* locus. We investigated the relationship between hypermethylation and FAL, which was estimated from the allelic status at D16S3043, D16S3050, and D16S3021. Hypermethylated tumors tended to have significantly lower FAL values (Table 1). This is contrary to the result predicted by the two-hit hypothesis. Further examination using individual markers to redefine the LOH status of tumors yielded similar results (Table 2). Therefore, cancers having lost one *CDH1* allele and those carrying hypermethylated *CDH1* alleles may be involved in two different tumorigenic pathways. Because the somatic mutation rate is extremely low, any two combination of these three factors cannot fulfill the classic 'two-hit' hypothesis. Other molecules involved in the E-cad-mediated cell-cell adhesion complex, such as the intracellular attachment proteins α, β, and γ-catenin, may be subjected to targeted inactivation[32-36]. Receptor tyrosine kinase (RTK), the main positive regulator of progression and tissue expansion, can repress E-cad function by transcriptional repression of *CDH1* via the transcription factor SNAI1[37,38], posttranscriptional repression via direct or indirect phosphorylation of adheren junction components such as β-catenin[39], or RTK-associated endocytosis and degradation of the E-cad protein[40]. This more flexible status achieved either by retaining an intact allele subsequent to LOH or by regulation via epigenetic mechanisms operating at the transcriptional or posttranslational levels, could provide an advantage in counteracting the changing microenvironment during tumor progression. Further investigation is needed at the transcriptional level and the post-translational level into E-cad inactivation of GC.

In conclusion, given the finding that somatic mutation was extremely low and the relationship between LOH and hypermethylation was inverse, any two combinations of these three factors can not fulfill the classical two-hit hypothesis of E-cadherin inactivation. Thus, other mechanisms operating at the transcriptional level or at the post-translational level, might be required to inactivate E-cadherin in GC.

ACKNOWLEDGMENTS

The authors are grateful to Miss Pei-Ei Wu and Miss Chien-Shi Wang for their technical assistance.

REFERENCES

1 **Takeichi M**. Cadherin cell adhesion receptors as a morphogenetic regulator. *Science* 1991; **251:** 1451-1455
2 **Takeichi M**. Cadherins: a molecular family important in selective cell-cell adhesion. *Annu Rev Biochem* 1990; **59:** 237-252
3 **Grunwald GB**. The structural and functional analysis of cadherin calcium-dependent cell adhesion molecules. *Curr Opin Cell Biol* 1993; **5**: 797-805
4 **Hirohashi S**. Inactivation of the E-cadherin-mediated cell adhesion system in human cancers. *Am J Pathol* 1998; **153:** 333-339
5 **Pignatelli M**, Vessey CJ. Adhesion molecules: novel molecular tools in tumor pathology. *Hum Pathol* 1994; **25:** 849-856
6 **Hashimoto M**, Niwa O, Nitta Y, Takeichi M, Yokoro K. Unstable expression of E-cadherin adhesion molecules in metastatic ovarian tumor cells. *Jpn Cancer Res* 1989; **80:** 459-463
7 **Bussemakers MJ**, van Moorselaar RJ, Giroldi LA, Ichikawa T, Isaacs JT, Takeichi M, Debruyne FM, Schalken JA. Decreased expression of E-cadherin in the progression of rat prostatic

cancer. *Cancer Res* 1992; **52:** 2916-2922
8 **Shimoyama Y**, Hirohashi S. Expression of E- and P-cadherin in gastric carcinomas. *Cancer Res* 1991; **51:** 2185-2192
9 **Oka H**, Shiozaki H, Kobayashi K, Tahara H, Tamura S, Miyata M, Doki Y, Iihara K, Matsuyoshi N, Hirano S. Immunohistochemical evaluation of E-cadherin adhesion molecule expression in human gastric cancer. *Virchows Arch A Pathol Anat Histopathol* 1992; **421:** 149-156
10 **Matsuura K**, Kawanishi J, Fujii S, Imamura M, Hirano S, Takeichi M, Niitsu Y. Altered expression of E-cadherin in gastric cancer tissues and carcinomatous fluid. *Br J Cancer* 1992; **66:** 1122-1130
11 **Mayer B**, Johnson JP, Leitl F, Jauch KW, Heiss MM, Schildberg FW, Birchmeier W, Funke I. E-cadherin expression in primary and metastatic gastric cancer: down-regulation correlates with cellular dedifferentiation and glandular disintegration. *Cancer Res* 1993; **53:** 1690-1695
12 **Gabbert H**. Mechanisms of tumor invasion: evidence from in vivo observations. *Cancer Metastasis Rev* 1985; **4:** 293-309
13 **Shun CT**, Wu MS, Lin JT, Wang HP, Houng RL, Lee WJ, Wang TH, Chuang SM. An immunohistochemical study of E-cadherin expression with correlations to clinicopathological features in gastric cancer. *Hepatogastroenterology* 1998; **45**: 944-949
14 **Guilford P**, Hopkins J, Harraway J, McLeod M, McLeod N, Harawira P, Taite H, Scoular R, Miller A, Reeve AE. E-cadherin germline mutations in familial gastric cancer. *Nature* 1998; **392:** 402-405
15 **Gayther SA,** Gorringe KL, Ramus SJ, Huntsman D, Roviello F, Grehan N, Machado JC, Pinto E, Seruca R, Halling K, MacLeod P, Powell SM, Jackson CE, Ponder BA, Caldas C. Identification of germ-line E-cadherin mutations in gastric cancer families of European origin. *Cancer Res* 1998; **58:** 4086-4089
16 **Becker KF**, Atkinson MJ, Reich U, Becker I, Nekarda H, Siewert JR, Hofler H. E-cadherin gene mutations provide clues to diffuse type gastric carcinomas. *Cancer Res* 1994; **54:** 3845-3852
17 **Machado JC**, Oliveira C, Carvalho R, Soares P, Berx G, Caldas C, Seruca R, Carneiro F, Sobrinho-Simoes M. E-cadherin gene (*CDH1*) promoter methylation as the second hit in sporadic diffuse gastric carcinoma. *Oncogene* 2001; **20:** 1525-1528
18 **Tamura G**, Sakata K, Nishizuka S, Maesawa C, Suzuki Y, Iwaya T, Terashima M, Saito K, Satodate R. Inactivation of the E-cadherin gene in primary gastric carcinomas and gastric carcinoma cell lines. *Jpn J Cancer Res* 1996; **87**: 1153-1159
19 **Ascano JJ**, Frierson H Jr, Moskaluk CA, Harper JC, Roviello F, Jackson CE, El-Rifai W, Vindigni C, Tosi P, Powell SM. Inactivation of the E-cadherin gene in sporadic diffuse-type gastric cancer. *Mod Pathol* 2001; **14**: 942-949
20 **Machado JC**, Soares P, Carneiro F, Rocha A, Beck S, Blin N, Berx G, Sobrinho-Simoes M. E-cadherin gene mutations provide a genetic basis for the phenotypic divergence of mixed gastric carcinomas. *Lab Invest* 1999; **79**: 459-465
21 **Chan AO**, Lam SK, Wong BC, Wong WM, Yuen MF, Yeung YH, Hui WM, Rashid A, Kwong YL. Promoter methylation of E-cadherin gene in gastric mucosa associated with Helicobacter pylori infection and in gastric cancer. *Gut* 2003; **52:** 502-506
22 **Li LC**, Chui RM, Sasaki M, Nakajima K, Perinchery G, Au HC, Nojima D, Carroll P, Dahiya R. A single nucleotide polymorphism in the E-cadherin gene promoter alters transcriptional activities. *Cancer Res* 2000; **60:** 873-876
23 **Moskaluk CA**, Kern SE. Microdissection and polymerase chain reaction amplification of genomic DNA from histological tissue sections. *Am J Pathol* 1997; **150**: 1547-1552
24 **Lauren P**. The two histological main types of gastric carcinoma: diffuse and so-called intestinal-type carcinoma. an attempt at a histo-clinical classification. *Acta Pathol Microbiol Scand* 1965; **64:** 31-49
25 **Sobin LH**, Wittekind CH (editors). International Union Against Cancers (UICC): TNM Classification of Malignant Tumors. 5th ed. *New York: John Wiley*, 1997
26 **Berx G**, Cleton-Jansen AM, Strumane K, de Leeuw WJ, Nollet F, van Roy F, Cornelisse C. E-cadherin is inactivated in a majority of invasive human lobular breast cancers by truncation mutations throughout its extracellular domain. *Oncogene* 1996; 13: 1919-1925
27 **Graff JR**, Herman JG, Myohanen S, Baylin SB, Vertino PM. Mapping patterns of CpG island methylation in normal and neoplastic cells implicates both upstream and downstream regions in de novo methylation. *J Biol Chem* 1997; **272**: 22322-22329
28 **Berx G**, Becker KF, Hofler H, van Roy F. Mutations of the human E-cadherin (CDH1) gene. *Hum Mutat* 1998; **12**: 226-237
29 **Tamura G**, Yin J, Wang S, Fleisher AS, Zou T, Abraham JM, Kong D, Smolinski KN, Wilson KT, James SP, Silverberg SG, Nishizuka S, Terashima M, Motoyama T, Meltzer SJ. E-Cadherin gene promoter hypermethylation in primary human gastric carcinomas. *J Natl Cancer Inst* 2000; **92**: 569-573
30 **Graziano F**, Arduini F, Ruzzo A, Mandolesi A, Bearzi I, Silva R, Muretto P, Testa E, Mari D, Magnani M, Scartozzi M, Cascinu S. Combined analysis of E-cadherin gene (CDH1) promoter hypermethylation and E-cadherin protein expression in patients with gastric cancer: implications for treatment with demethylating drugs. *Ann Oncol* 2004; **15:** 489-492
31 **Grady WM**, Willis J, Guilford PJ, Dunbier AK, Toro TT, Lynch H, Wiesner G, Ferguson K, Eng C, Park JG, Kim SJ, Markowitz S. Methylation of the CDH1 promoter as the second genetic hit in hereditary diffuse gastric cancer. *Nat Genet* 2000; **26**: 16-17
32 **Jawhari AU**, Noda M, Farthing MJ, Pignatelli M. Abnormal expression and function of the E-cadherin-catenin complex in gastric carcinoma cell lines. *Br J Cancer* 1999; **80**: 322-330
33 **Ohene-Abuakwa** Y, Noda M, Perenyi M, Kobayashi N, Kashima K, Hattori T, Pignatelli M. Expression of the E-cadherin/catenin (alpha-, beta-, and gamma-) complex correlates with the macroscopic appearance of early gastric cancer. *J Pathol* 2000; **192**: 433-439
34 **Yu J**, Ebert MP, Miehlke S, Rost H, Lendeckel U, Leodolter A, Stolte M, Bayerdorffer E, Malfertheiner P. alpha-catenin expression is decreased in human gastric cancers and in the gastric mucosa of first degree relatives. *Gut* 2000; **46**: 639-644
35 **Xiangming C**, Hokita S, Natsugoe S, Tanabe G, Baba M, Takao S, Kuroshima K, Aikou T. Cooccurrence of reduced expression of alpha-catenin and overexpression of p53 is a predictor of lymph node metastasis in early gastric cancer. *Oncology* 1999; **57**: 131-137
36 **Matsui S**, Shiozaki H, Inoue M, Tamura S, Doki Y, Kadowaki T, Iwazawa T, Shimaya K, Nagafuchi A, Tsukita S. Immunohistochemical evaluation of alpha-catenin expression in human gastric cancer. *Virchows Arch* 1994; **424**: 375-381
37 **Batlle E**, Sancho E, Franci C, Dominguez D, Monfar M, Baulida J, Garcia De, Herreros A. The transcription factor snail is a repressor of E-cadherin gene expression in epithelial tumour cells. *Nat Cell Biol* 2000; **2**: 84-89
38 **Cano A**, Perez-Moreno MA, Rodrigo I, Locascio A, Blanco MJ, del Barrio MG, Portillo F, Nieto MA. The transcription factor snail controls epithelial-mesenchymal transitions by repressing E-cadherin expression. *Nat Cell Biol* 2000; **2**: 76-83
39 **Potla L**, Boghaert ER, Armellino D, Frost P, Damle NK. Reduced expression of EphrinA1 (EFNA1) inhibits three-dimensional growth of HT29 colon carcinoma cells. *Cancer Lett* 2002; **175**: 187-195
40 **Kamei T**, Matozaki T, Sakisaka T, Kodama A, Yokoyama S, Peng YF, Nakano K, Takaishi K, Takai Y. Coendocytosis of cadherin and c-Met coupled to disruption of cell-cell adhesion in MDCK cells--regulation by Rho, Rac and Rab small G proteins. *Oncogene* 1999; **18**: 6776-6784

S- Editor Guo SY **L- Editor** Wang XL **E- Editor** Bai SH

PO Box 2345, Beijing 100023, China
www.wjgnet.com
wjg@wjgnet.com

World J Gastroenterol 2006 April 14; 12(14): 2174-2180
World Journal of Gastroenterology ISSN 1007-9327

Helicobacter pylori

Effect of NaCl and *Helicobacter pylori* vacuolating cytotoxin on cytokine expression and viability

Juan Sun, Kazuo Aoki, Jin-Xu Zheng, Bing-Zhong Su, Xiao-Hui Ouyang, Junichi Misumi

Juan Sun, Kazuo Aoki, Junichi Misumi, Department of Public Health and Hygiene(Ⅱ), Faculty of Medicine, Oita University Oita 879-5593, Japan
Jin-Xu Zheng, Department of Pulmonary Medicine, Affiliated Hospital, School of Medicine, Jiang Su University, Zhenjiang 212001,China
Bing-Zhong Su, Xiao-Hui Ouyang, First Affiliated Hospital of Inner Mongolia Medical College, Hohhot 010000, Inner Mongolia, China,
Co-correspondents: Juan Sun
Correspondence to: Junichi Misumi, Department of Public Health and Hygiene(Ⅱ), Faculty of Medicine, Oita University Oita 879-5593, Japan. misumijc@oita-med.ac.jp
Telephone: +81-97-5865742 Fax: +81-97- 5865749
Received: 2005-08-24 Accepted: 2005-11-18

Abstract

AIM: To determine whether *Helicobacter pylori* (*H pylori*) vacuolating cytotoxin (VacA) regulates release of pro-inflammatory cytokines (IL-1β, IL-8, TNF-α, and IL-6) or alters gastric epithelial cell viability and to determine whether NaCl affects these VacA-induced changes.

METHODS: Vacuolating activity was determined by measuring the uptake of neutral red into vacuoles of VacA-treated human gastric epithelial (AGS) cells. AGS cell viability was assessed by direct cell counting. Specific enzyme-linked immunosorbent assays (ELISA) and reverse transcriptase-polymerase chain reaction(RT-PCR) were performed to examine the effects of *H pylori* VacA and NaCl on cell pro-inflammatory cytokine production in AGS cells. Immunohistochemical staining of gastric tissue from Mongolian gerbils was used to confirm VacA-induced pro-inflammatory cytokine production and the effects of NaCl on this VacA-induced response.

RESULTS: Addition of VacA alone reduced AGS cell viability ($P < 0.05$), and this reduction was enhanced by high doses of NaCl ($P < 0.05$). VacA alone induced expression of TNF-α, IL-8 and IL-1β, while NaCl alone induced expression of TNF-α and IL-1β. Changes in mRNA levels in the presence of both VacA and NaCl were more complicated. For the case of TNF-α, expression was dose-dependent on NaCl. IL-6 mRNA was not detected. However, low levels of IL-6 were detected by ELISA. Positive immunohistochemical staining of IL-1, IL-6, and TNF-α was found in gastric tissue of *H pylori*-infected gerbils fed with either a normal diet or a high salt diet. However, the staining of these three cytokines was stronger in *H pylori*-infected animals fed with a 5g/kg NaCl diet.

CONCLUSION: VacA decreases the viability of AGS cells, and this effect can be enhanced by NaCl. NaCl also affects the production of pro-inflammatory cytokines induced by VacA, suggesting that NaCl plays an important role in *H pylori*-induced gastric epithelial cell cytotoxicity.

Key words: *Helicobacter pylori*; Vacuolating cytotoxin; Cytokine; Gerbil; AGS cell

Sun J, Aoki K, Zheng JX, Su BZ, Ouyang XH, Misumi J. Effect of NaCl and *Helicobacter pylori* vacuolating cytotoxin on cytokine expression and viability. *World J Gastroenterol* 2006; 12(14): 2174-2180

http://www.wjgnet.com/1007-9327/12/2174.asp

INTRODUCTION

Gastric cancer is one of the leading causes of cancer-related death[1, 2]. Epidemiological studies in humans and rodents have demonstrated that chronic gastritis caused by *Helicobacter pylori* (*H pylori*) is a strong risk factor for this malignancy[3]. Current models suggest that *H pylori* is not directly carcinogenic but rather acts indirectly on inducing cancer. For example, it may act through inflammatory mediators or by decreasing gastric acid secretion, thus favoring the formation of mutagenic adducts[4]. *H pylori* expresses several major proteins that are critical to the pathogenicity of the bacterium[5]. The vacuolating cytotoxin, VacA, is an *H pylori*-secreted virulence factor that induces the formation of large cytoplasmic vacuoles in epithelial cells, which precedes cultured cell death both *in vitro* and *in vivo*[6-9]. In the past decade, a considerable number of studies have contributed to our understanding of the mechanism of VacA-induced intracellular vacuolation[6].

Salt consumption is considered a risk factor for gastric cancer[10]. *H pylori*-associated mucosal atrophy is partially associated with a high salt diet[11]. Excessive NaCl intake enhances *H pylori* colonization in mice and humans, while chronic salt intake may exacerbate gastritis by increasing *H pylori* colonization[12]. Furthermore, salt intake may interfere with *H pylori* infection and modify the cancer risk[13]. The high prevalence of *H pylori* infection and high salt diets may significantly affect the rate of occurrence of gas-

tric carcinogenesis[14-17].

It has been reported that cytokines play an important role in gastric cancer. Proinflammatory cytokines such as interleukin-8 (IL-8) and tumor necrosis factor-α (TNF-α) may up regulate cyclooxygenase-2 (COX-2) during gastric carcinogenesis[18]. Genotypes of IL-1β (-511 T/T) and TNF-α (-308 A/A) are associated with the risk of non-cardia gastric cancer. The presence of TNF-α SNPs -308 and -1031 might favor *H pylori* infection and promote an inflammatory response in infected gastric mucosa[19]. IL-1β genotype has been found to increase the risk of distal gastric cancer[20]. IL-1β is one of the potent proinflammatory cytokines elicited by *H pylori* infection[21, 22]. In human gastric cancer cells, IL-1β induces vascular endothelial growth factor (VEGF), a dominant angiogenic factor in gastric cancer[23]. Moreover, levels of IL-1β and IL-8 have been found to be significantly higher in *H pylori*-positive gastric cancers compared with controls, and eradication of *H pylori* can significantly reduce the levels of these cytokines[24]. Genetic polymorphisms identified in *IL-6* can be attributed to ethnicity and appear to be independent of the clinical outcome of *H pylori* infections[25].

The present study was to examine the combined effects of VacA and NaCl on cell viability and pro-inflammatory cytokine expression both in AGS cells and in Mongolian gerbils.

MATERIALS AND METHODS

Preparation of VacA

The toxin-producing strain, *H pylori* ATCC49503, was used as the source of VacA. *H pylori* was grown under microaerophilic conditions on Columbia blood agar plates with vigorous shaking in a controlled microaerophilic atmosphere of 50 mL/L O_2 and 100 mL/L CO_2 at 37℃ for 3-4 d, harvested and re-suspended in brucella broth (Difco) supplemented with 100 mL/L fetal calf serum. *H pylori* cells were grown for 48 h at 37℃ in an Erlenmeyer flask with shaking at 60 r/min. Cells were then pelleted by centrifugation at 500 r/min for 20 min. The culture supernatants were collected and pooled. Solid ammonium sulfate was added to the pooled material at 4℃ to 50% saturation. The precipitate was collected by centrifugation at 12000 r/min for 20 min, dissolved in 60 mmol/L Tris-HCl (pH 7.7) containing 0.1 mol/L NaCl and subjected to liquid chromatography on a Superose 6 HR 10/30 column (1cm × 30 cm) equilibrated with 60 mmol/L Tris-HCl (pH 7.7) containing 0.1 mol/L NaCl. The material was eluted with the same buffer at a flow rate of 0.5 mL/min. The eluted protein was monitored by Western blotting using polyclonal anti-VacA (Santa Cruz Biotechnology, Inc., Santa Cruz, CA). The fractions containing VacA were collected, pooled, diluted with deionized water to the intended concentration and maintained at -20℃[26]. VacA concentration was determined by Micro-BCA assay (Bio-Rad, Hercules, CA).

Vacuolating activity assay

The human gastric epithelial cell line AGS (ATCC CRL 1739) was maintained in Ham's F-12 medium supplemented with 100 mL/L fetal calf serum and 50 mg/L penicillin-streptomycin (Life Technologies, Inc.) under 50mL/L CO_2 at 37℃. AGS cells were seeded in 96-well culture plates (5×10^3 cells/well in 90 μL) and cultured as monolayers for 20 h in a 50 mL/L CO_2 atmosphere at 37℃. Samples (10 μL) of VacA were added to achieve the indicated final concentrations and cells were incubated for an additional 2-8 h at 37℃[27]. Vacuolating activity was determined by measuring the uptake of neutral red into vacuoles in VacA-treated cells. Cells were incubated for 5 min at room temperature with 50 μL of freshly prepared 0.5 g/L neutral red in PBS containing 3 g/L BSA and washed three times with 0.1 mL of PBS containing 3 g/L BSA. After addition of 0.1 mL 700 mL/L ethanol in water containing 0.4 mL/L HCl, absorbance at 540 nm (A_{540}) was measured. Vacuolating activity was determined by subtracting the A_{540} of cells incubated without VacA from the A_{540} of VacA-treated cells. To evaluate the effect of NaCl on vacuolating activity, AGS cells were incubated with 40 mg/L VacA and 0-10 mmol/L NaCl for the indicated periods.

Assessment of AGS cell viability

AGS cells were seeded to a subconfluent density of 5×10^4 cells/well in 24-well plates and incubated at 37℃ overnight. The supernatant was discarded before co-incubation. AGS cells were grown with NaCl alone or in the presence of VacA and NaCl in F-12 medium supplemented with 100 mL/L FBS. Control cells were inoculated into F-12 and incubated for up to 72 h in triplicate. At the end of each time of incubation, cell viability was determined in a hemacytometer by trypan blue exclusion.

Cytokine and cytokine mRNA measurement

After AGS cells were incubated for 24 h. *H pylori* VacA (40 mg/L) and 10 mmol/L NaCl were added. The cells were incubated for an additional 4 h. The supernatants were then collected and stored at -20℃ until assay. The levels of IL-6, IL-8, IL-1β and TNF-α in the culture supernatants were determined by enzyme-linked immunosorbent assay (ELISA) using commercially available kits (Immunotech, France) according to the manufacturer's instructions. In these assays, the lower limits of detection were 3 ng/L for IL-6, 8 ng/L for IL-8, 1.5 ng/L for IL-1β and 5 ng/L for TNF-α.

Total RNA was extracted from AGS cells (incubated as indicated above, under cytokine measurement) using Isogen (Nippon Gene, Tokyo, Japan). Aliquots (2.5 μg) of total RNA were incubated at 70℃ for 5 min, chilled on ice and reverse transcribed in a final volume of 10 μL of a solution containing 200 MU/L Moloney murine leukemia virus reverse transcriptase (M-MLV RT) (Invitrogen Life Technologies), first-strand buffer (250 mmol/L Tris-HCl, pH 8.3 at room temperature, 375 mmol/L KCl, 15 mmol/L $MgCl_2$) containing 0.1 mol/L DTT and 2.5 mmol/L dNTPs plus random primer (6 mer) pd(N)6 (TaKaRa, Japan). Reactions were incubated at 22℃ for 10 min, at 37℃ for 60 min, heated to 80℃ for 5 min, and stored at -20℃ until use.

The resultant cDNA from above (1 μL) was added to a 29-μL reaction containing PCR reaction buffer, 1 μL of 4 nmol of each primer (IL-1 β, IL-6, IL-8, TNF-α),

Table 1 Viability of AGS cells grown in the presence of NaCl or VacA and NaCl (*P* value, *t*-test)

VacA (mg/L)	NaCl (mmol/L)	24 h	48 h	72 h
(-)				
	0	-	-	-
	2.5	0.12	0.07	0.22
	5	0.04	0.09	0.18
	10	0.06	0.11	0.15
50				
	0	0.03	0	0.01
	2.5	0.02	0	0.01
	5	0.01	0.02	0
	10	0	0	0
50				
	0	-	-	-
	2.5	0.45	0.36	0.13
	5	0.27	0.08	0.01
	10	0.12	0.01	0.04

0.1 μL of 5 MU/L of Taq DNA polymerase and water. Oligonucleotide primers were designed based on previous reports[28]. PCR was performed with an automatic thermal cycler using an initial denaturation step at 95 ℃ for 5 min followed by 36 cycles of denaturation at 94 ℃ for 1 min, annealing at 60 ℃ for 1 min, and an extension at 72 ℃ for 1 min. The final cycle included an extension for 7 min at 72 ℃ to ensure full extension of the products. Aliquots (5 μL) of each PCR product were analyzed by electrophoresis on 1.5 g/L agarose S gels (Wako Chemical Co., Ltd., Osaka, Japan) containing ethidium bromide, and the bands were examined under UV light to detect amplified DNAs.

Animal experiment

H pylori-infected and non-infected 7-wk-old male Mongolian gerbils (MGS/Sea; Seac Yoshitomi, Fukuoka, Japan) were housed in steel cages on hardwood chip bedding in an air-conditioned biohazard room with a 12 h light-12 h dark cycle. The animals were classified into four groups according to *H pylori* infection and NaCl diet ($n = 3$). *H pylori*-infected and non-infected gerbils were given autoclaved distilled water *ad libitum* and CE-2 irrigated with 50 g/kg NaCl (Kyudo Co. LTD, Japan) or CE-2 only (normal diet). After 4 mo, the gerbils were sacrificed and stomach tissue was obtained and frozen.

The frozen tissue blocks were sectioned (6 μm thick) as previously described[28] and the sections were fixed with 4 g/L paraformaldehyde and acetone for 10 min each. The sections were treated with 30 mL/L H_2O_2 (Wako, Japan) in methanol for 5 min followed by blocking with 10 ml/L normal rabbit serum (Vector Laboratories, Inc., Burlingame, CA) for 10 min. We used goat polyclonal antibodies as primary antibodies directed against the following mouse proteins: TNF-α, IL-1β, and IL-6 (R & D Systems, Inc.). Tissue sections were incubated for 60 min at room temperature in a moist chamber with the desired primary antibody diluted according to the manufacturer's instructions. Biotinylated rabbit anti-goat immunoglobulin G (Vector Laboratories) was then applied for 30 min at room temperature. After three times of 5-min rinse with PBS, the signals from the antibodies were amplified using an ABC kit (Vector Laboratories) for 30 min and visualized with DAB reagent (Vector Laboratories) for 5 min. The sections were counterstained with Mayer hematoxylin (Muto Pure Chemicals Co., Ltd., Tokyo, Japan), dehydrated and mounted using histological mounting medium (Fisher Scientific). Negative control reactions contained purified goat IgG (Vector Laboratories) instead of specific primary antibodies.

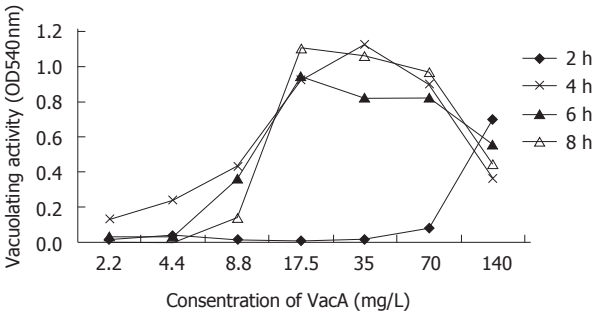

Figure 1 Activity of VacA-induced vacuolization.

Statistical analysis

All data in each experiment were expressed as the mean ± SE. The statistical significance of the response of cytokine production to VacA was evaluated using the Student's *t*-test. Differences between cytokine levels were considered significant at $P < 0.05$.

RESULTS

VacA visualization

VacA, partially-purified from a toxin-producing *H pylori* strain, was visualized on a Western blot with a VacA-specific antibody (Table 1). An antibody-reactive protein at 87 ku, the molecular weight expected for the mature toxin[26] was found.

VacA-induced vacuolation in AGS cells

AGS cells showed dose-dependent vacuolation induced by VacA (Figure 1). Different VacA concentrations were shown for the indicated incubation times. Vacuolization was quantified by measuring the uptake of neutral red into vacuoles. The experiments were carried out in triplicate. When VacA was incubated with AGS cells at 4, 6 and 8 h, its activity was stable in the range of 17-70 mg/L. Vacuolation was not seen in AGS cells in response to VacA after incubation for 2 h, except at the maximum concentration.

VacA-induced vacuolating activity was not influenced by NaCl

The time course for vacuolation within cultured cells in the presence of VacA and NaCl showed the effect of NaCl on the vacuolating activity (Figure 2). The vacuolating activity was shown as a function of incubation time at different NaCl concentrations. Cells were induced with 40 mg/L VacA. The experiments were carried out in triplicate.

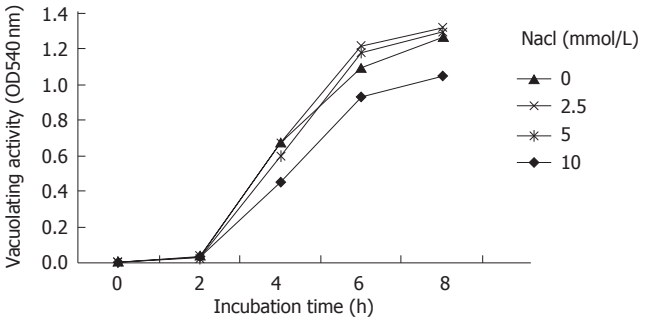

Figure 2 Time course of VacA-induced vacuolization of AGS cells at different NaCl concentrations.

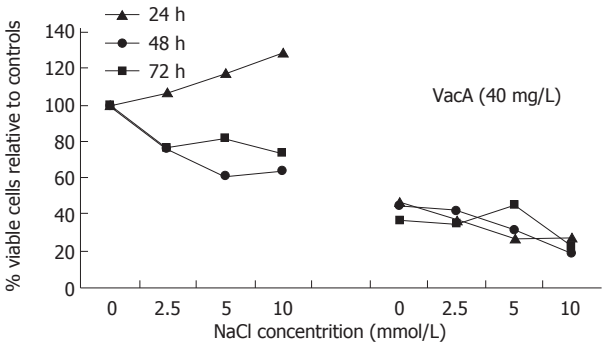

Figure 3 Viability of AGS cells grown in the presence of NaCl alone or VacA and NaCl.

At all NaCl concentrations, the vacuolating activity was minimal after incubation for 2 h. Time-dependent vacuolating activity increased linearly, doubling every two hours between 2 and 6 h of incubation. Because the curves at all NaCl concentrations were similar, NaCl did not appear to significantly affect VacA-induced vacuolation. As a control, the same concentrations of NaCl were added to AGS cells without VacA and no vacuolating activity was observed (data not shown).

Viability of AGS cells was decreased after coculture with VacA and NaCl

The effect of NaCl on AGS viability was assessed with and without VacA at the indicated incubation times. Cell viability was determined by trypan blue exclusion. The experiments were carried out in triplicate. Upon incubation with increasing levels of NaCl for 72 h, there was an apparent slight increase in the viability of AGS cells. However, culture for 24 or 48 h apparently decreased the viability of AGS cells (Figure 3). These results, however, were not statistically significant ($P > 0.05$) compared with control AGS cells at all incubation time (Table 1). Furthermore, the viability of AGS cells cultured with VacA and 10 mmol/L NaCl was significantly reduced ($P < 0.05$) compared with VacA alone after incubation for 48 and 72 h. Although the average viability values after incubation for 24 h were similar to those at 48 and 72 h, the viability at 10 mmol/L and 0 mmol/L NaCl was not significantly different ($P > 0.05$) because large variances were obtained for the 24-h samples. The reduced viability in the presence of VacA was similar at all three incubation times.

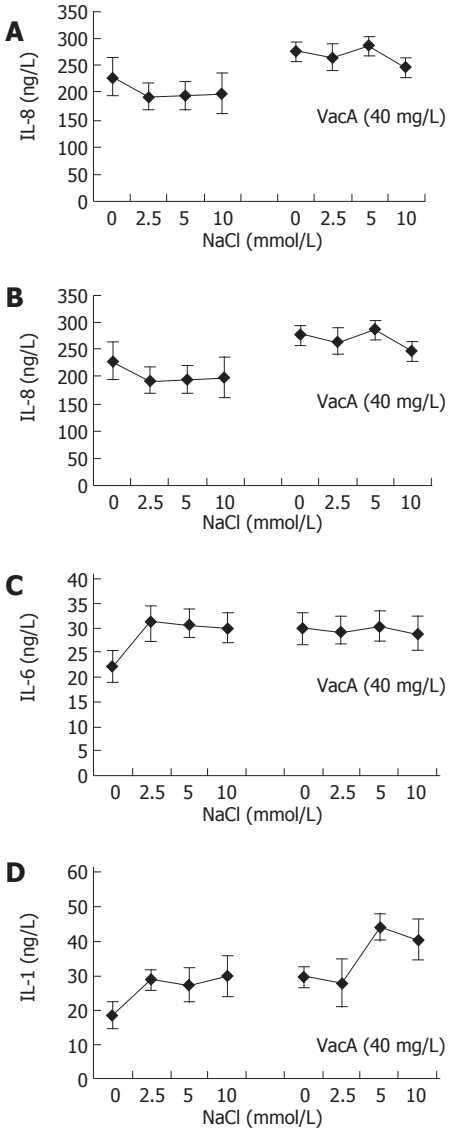

Figure 4 Production of cytokines induced by NaCl alone or VacA and NaCl.

VacA-induced cytokine production in AGS cells

To examine cytokine production after cell culture with VacA combined with NaCl, AGS cells were incubated with VacA or VacA and NaCl. The secretion of TNF-α, IL-8, IL-6 and IL-1β assessed by ELISA, is shown in Figure 4. The experiments were carried out in triplicate. In addition, we assessed the cytokine response of cultured human AGS cells to NaCl alone. The secretion of TNF-α increased in cells exposed to VacA, but this increase was inhibited in the presence of both VacA and NaCl. However, the secretion of TNF-α seemed to increase slightly in culture with NaCl alone ($P > 0.05$, Figure 4A). The secretion of IL-8 increased in cells exposed to VacA compared with cell-only control cultures or those exposed to NaCl alone. The secretion increased when VacA was combined with NaCl. However, NaCl did not appear to increase IL-8 secretion in the presence of VacA. NaCl did not induce IL-8 secretion from AGS cells at any concentration tested (Figure 4B). IL-6 secretion increased in cultures incubated with VacA or NaCl or both VacA and NaCl (Figure 4C). IL-1β secretion increased after culture with VacA or NaCl

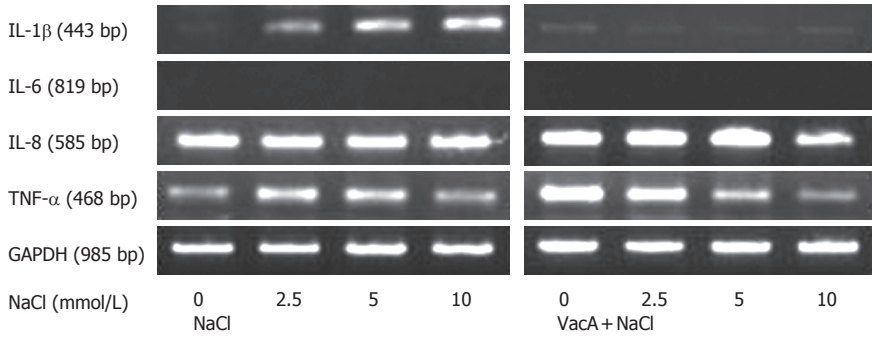

Figure 5 Expression of cytokines induced by NaCl or VacA with NaCl (RT-PCR) in gastric tissue of *H pylori*-infected gerbils (×200) fed with a normal diet (top) and a 50g/kg NaCl diet (bottom).

alone. The addition of 5 or 10 mmol/L NaCl enhanced VacA-induced IL-1β secretion, although it was not dose-dependent (Figure 4D).

Cytokine mRNA expression induced by VacA in AGS cells

To examine the ability of VacA combined with NaCl to induce the production of cytokines, cytokine-specific mRNA expression in AGS cells was analyzed by RT-PCR at 4 h post-induction. The expression of TNF-α, IL-8, IL-6 and IL-1β mRNAs is shown in Figure 5. TNF-α mRNA expression increased slightly after culture with NaCl, and there was a significant increase in TNF-α expression after culture with VacA. TNF-α mRNA expression decreased after culture with VacA combined with NaCl and displayed a significant NaCl dose-dependence. IL-8 mRNA expression was not stimulated by NaCl alone. However, the IL-8 mRNA PCR product increased after culture with VacA especially with VacA combined and NaCl, although a decrease was observed at the highest NaCl concentration. IL-6 mRNA was not detected in the control cells or upon exposure to any of the above conditions. IL-1β mRNA expression was induced in response to NaCl in a dose-dependent manner. Expression was also induced upon exposure to VacA, but this effect was not stimulated by NaCl.

Proinflammatory cytokine production in gastric tissue

Positive staining of IL-1β, IL-6, and TNF-α in gastric tissue was found in all but one of the *H pylori*-infected subjects ($n=6$) regardless of diet. However, we observed more staining of all three cytokines in *H pylori*-infected gerbils on a 50 g/kg NaCl diet than in infected gerbils on a normal diet, suggesting a potential role of NaCl in the up-regulation of VacA-induced pro-inflammatory cytokine production in gastric epithelium. IL-6 displayed less increase in staining than the other two cytokines, consistent with the *in vitro* ELISA results. There was no significant difference between the specific primary antibody staining and the IgG negative control staining in tissues from uninfected animals fed with 50 g/kg NaCl and positive staining was not observed in the untreated gerbils (data not shown).

DISCUSSION

The neutral red uptake assay is often used for quantitatively determining *H pylori* cytotoxicity *in vitro*[9]. Because the shortest time point at which vacuolation was induced in this study was 4 h, 4 h incubation was chosen for further experiments. The appropriate dose of VacA to induce vacuolation was determined to be 17.5 mg/L, and 40 mg/L VacA decreased AGS cell viability to 40% after 24 h. Therefore, 40 mg/L VacA was used in experiments to assess VacA-induced cytokine production.

Significant vacuolating activity is stimulated by acidic ($pH<5.5$) or alkaline ($pH>9.5$) conditions[27]. We evaluated the effect of high Na^+ and Cl^- concentrations on vacuolization induced by VacA. AGS cells exposed *in vitro* to VacA at various concentrations of NaCl had vacuolization rates similar to those exposed to VacA alone, suggesting that VacA may be activated by exposure to acidic or alkaline conditions but not under the osmotic conditions.

H pylori has been shown to either reduce or enhance gastric epithelial cell viability *in vitro*[29]. All strains of *H pylori* decrease cell viability of microvascular endothelial cells after 72 h[30]. Furthermore, co-culture of *H pylori* with AGS cells significantly decreases cell viability[29]. Consistent with these studies, our results demonstrated that VacA alone could reduce AGS cell viability ($P<0.05$), which was enhanced by high doses of NaCl ($P<0.05$).

Increased levels of proinflammatory cytokines induced by VacA in AGS cells and gerbils can be considered a cytotoxic effect. Consistent with our findings, others have noted that the damage caused by *H pylori* is partially attributed to the enhanced secretion of the proinflammatory cytokines IL-1β, IL-6, IL-8, and TNF-α, particularly in response to VacA-expressing *H pylori* strains[31,32]. It has been reported that gastric *H pylori* infections induce mucosal production of various cytokines, including IL-1β, IL-6, IL-8 and TNF-α[33]. Our study further confirmed the cytokine response to the combined effect of NaCl and VacA *in vitro* and *in vivo*. First, we examined the expression profile of proinflammatory cytokines in response to stimulation by NaCl alone. The addition of NaCl alone to AGS cells resulted in a dose-dependent increase in IL-1β mRNA level, whereas expression of the other three cytokine mRNAs did not change significantly both *in vitro* and *in vivo*. It has been reported that normal human dermal fibroblasts ele-vate IL-1β mRNA levels upon exposure to 0.5 mmoL/L NaCl and that normal human epidermal keratinocytes increase levels of IL-6 and IL-8 mRNA in response to NaCl[34]. These reported differences in IL-6 and IL-8 expression in response to NaCl exposure may be attributable to differences in cell types or the higher NaCl concentration used in the other studies, which was fivefold higher than that in our study. We found that NaCl could

not alter VacA-induced IL-8 expression. However, the induction of IL-8 by VacA alone is consistent with previous studies that *H pylori* infection increases mucosal production of IL-8 and interaction between viable *H pylori* and AGS cells increases levels of IL-8 mRNA expression and protein secretion[33, 35].

It has also been reported that polymorphisms within the IL-1β and TNF-α genes are associated with a risk for gastric carcinoma in individuals infected with *H pylori*[36]. Our study demonstrated that VacA-induced expression of IL-1β and TNF-α mRNAs could be up-regulated by NaCl in gerbils, whereas NaCl increased IL-1β expression and decreased VacA-induced TNF-α expression in AGS cells.

IL-6 is a multifunctional cytokine that plays a central role in host defense mechanisms[37-40]. IL-6 production upon *H pylori* infection could be induced in response to urease in human AGS cells[41]. IL-6 can also be induced by VacA in bone marrow-derived mast cells[42]. These findings are consistent with our ELISA results, but we were unable to detect IL-6 mRNA with RT-PCR under any of the conditions we tested.

VacA directly activates AGS cells to produce proinflammatory cytokines, which might be a host early innate immune response, suggesting that VacA plays a role in the pathogenesis of *H pylori*-infected gastritis although the cag pathogenicity island is closely related to induction of proinflammatory cytoikine[43]

High-salt diet (NaCl 75g/kg versus 2.5g/kg) intake enhances *H pylori* colonization in mice and humans, while chronic salt intake might exacerbate gastritis by increasing *H pylori* colonization[12]. Our study indicated that excessive dietary NaCl (50 g/kg) influenced cytokine production in the Mongolian gerbil model of *H pylori* infection. VacA may be regulated by NaCl to influence cytokine production through a variety of mechanisms. One mechanism might be through an effect on VacA channels, which are likely to be an important component in the mode of action of this toxin[36].

In conclusion, the virulent *H pylori* cytotoxin, VacA, decreases the viability of AGS cells, which can be enhanced by NaCl. NaCl also affects the production of proinflammatory cytokines induced by VacA. Our results suggest that NaCl plays an important role in *H pylori*-induced AGS cell cytotoxicity. However, the interactions between *H pylori*, NaCl and gastric cancer are complex, more studies are required to understand the mechanism by which NaCl affects the progression of *H pylori*-related gastric cancer.

ACKNOWLEDGMENTS

The authors thank Sakurai Mami for skillful technical assistance.

REFERENCES

1 **Sun J**, Misumi J, Shimaoka A, Aoki K, Esaki F. Stomach cancer-related mortality. *Eur J Cancer Prev* 2001; **10**: 61-67
2 **Sun J**, Misumi J, Shimaoka A, Aoki K, Kono A. Stomach cancer-related mortality rate is higher in young Japanese women than in men. *Public Health* 2002; **116**: 39-44
3 **Cover TL**, Krishna US, Israel DA, Peek RM Jr. Induction of gastric epithelial cell apoptosis by *Helicobacter pylori* vacuolating cytotoxin. *Cancer* Res 2003; **63**: 951-957
4 **Shirin H**, Sordillo EM, Oh SH, Yamamoto H, Delohery T, Weinstein IB, Moss SF. *Helicobacter pylori* inhibits the G1 to S transition in AGS gastric epithelial cells. *Cancer Res* 1999; **59**: 2277-2281
5 **Gobert AP**, Mersey BD, Cheng Y, Blumberg DR, Newton JC, Wilson KT. Cutting edge: urease release by *Helicobacter pylori* stimulates macrophage inducible nitric oxide synthase. *J Immunol* 2002; **168**: 6002-6006
6 **Patel HK**, Willhite DC, Patel RM, Ye D, Williams CL, Torres EM, Marty KB, MacDonald RA, Blanke SR. Plasma membrane cholesterol modulates cellular vacuolation induced by the *Helicobacter pylori* vacuolating cytotoxin. *Infect Immun* 2002; **70**: 4112-4123
7 **Vinion-Dubiel AD**, McClain MS, Cao P, Mernaugh RL, Cover TL. Antigenic diversity among *Helicobacter pylori* vacuolating toxins. *Infect Immun* 2001; **69**: 4329-4336
8 **Willhite DC**, Ye D, Blanke SR. Fluorescence resonance energy transfer microscopy of the *Helicobacter pylori* vacuolating cytotoxin within mammalian cells. *Infect Immun* 2002; **70**: 3824-3832
9 **Ricci V**, Galmiche A, Doye A, Necchi V, Solcia E, Boquet P High cell sensitivity to *Helicobacter pylori* VacA toxin depends on a GPI-anchored protein and is not blocked by inhibition of the clathrin-mediated pathway of endocytosis. Mol Biol Cell 2000; **11**: 3897-3909
10 **Ogimoto I**, Shibata A, Fukuda K. World Cancer Research Fund/American Institute of Cancer Research 1997 recommendations: applicability to digestive tract cancer in Japan. *Cancer Causes Control* 2000; **11**: 9-23
11 **Calam J**. *Helicobacter pylori* modulation of gastric acid. *Yale J Biol Med* 1999; **72**: 195-202
12 **Fox JG**, Dangler CA, Taylor NS, King A, Koh TJ, Wang TC. High-salt diet induces gastric epithelial hyperplasia and parietal cell loss, and enhances *Helicobacter pylori* colonization in C57BL/6 mice. *Cancer Res* 1999; **59**: 4823-4828
13 **Bretagne JF**. Could *Helicobacter pylori* treatment reduce stomach cancer risk? *Gastroenterol Clin Biol* 2003; **27**: 440-452
14 **Ngoan LT**, Yoshimura T. Work, salt intake and the development of stomach cancer. *Med Hypotheses* 2003; **60**: 552-556
15 **Nozaki K**, Tsukamoto T, Tatematsu M. Effect of high salt diet and *Helicobacter pylori* infection on gastric carcinogenesis. *Nippon Rinsho* 2003; **61**: 36-40
16 **Tsugane S**, Sasazuki S, Kobayashi M, Sasaki S. Salt and salted food intake and subsequent risk of gastric cancer among middle-aged Japanese men and women. *Br J Cancer* 2004; **90**: 128-134
17 **Xibin S**, Moller H, Evans HS, Dixing D, Wenjie D, Jianbang L. Residential Environment, Diet and Risk of Stomach Cancer: a Case-control Study in Linzhou, China. *Asian Pac J Cancer Prev* 2002; **3**: 167-172
18 **Konturek PC**, Konturek SJ, Bielanski W, Kania J, Zuchowicz M, Hartwich A, Rehfeld JF, Hahn EG. Influence of COX-2 inhibition by rofecoxib on serum and tumor progastrin and gastrin levels and expression of PPARgamma and apoptosis-related proteins in gastric cancer patients. *Dig Dis Sci* 2003; **48**: 2005-2017
19 **Zambon CF**, Basso D, Navaglia F, Falda A, Belluco C, Fogar P, Greco E, Gallo N, Farinati F, Cardin R, Rugge M, Di Mario F, Plebani M. Increased risk of noncardia gastric cancer associated with proinflammatory cytokine gene polymorphisms. *Gastroenterology* 2004; **126**: 382-384
20 **Garza-Gonzalez E,** Bosques-Padilla FJ, El-Omar E, Hold G, Tijerina-Menchaca R, Maldonado-Garza HJ, Perez-Perez GI. Role of the polymorphic IL-1B, IL-1RN and TNF-A genes in distal gastric cancer in Mexico. *Int J Cancer* 2005; **114**: 237-241
21 **Basak C, Pathak SK,** Bhattacharyya A, Mandal D, Pathak S, Kundu M. NF-kappaB- and C/EBPbeta-driven interleukin-1beta gene expression and PAK1-mediated caspase-1 activation play essential roles in interleukin-1beta release from *Helicobacter pylori* lipopolysaccharide-stimulated macrophages. *J Biol Chem* 2005; **280**: 4279-4288
22 **Nishi Y**, Isomoto H, Uotani S, Wen CY, Shikuwa S, Ohnita K, Mizuta Y, Kawaguchi A, Inoue K, Kohno S. Enhanced produc-

tion of leptin in gastric fundic mucosa with *Helicobacter pylori* infection. *World J Gastroenterol* 2005; **11**: 695-699

23 **Kawaguchi M**, Akagi M, Gray MJ, Liu W, Fan F, Ellis LM. Regulation of vascular endothelial growth factor expression in human gastric cancer cells by interleukin-1beta. *Surgery* 2004; **136**: 686-692

24 **Konturek PC,** Kania J, Kukharsky V, Raithel M, Ocker M, Rembiasz K, Hahn EG, Konturek SJ. Implication of peroxisome proliferator-activated receptor gamma and proinflammatory cytokines in gastric carcinogenesis: link to Helicobacter pylori-infection. *J Pharmacol Sci* 2004; **96**: 134-143

25 **Hwang IR**, Hsu PI, Peterson LE, Gutierrez O, Kim JG, Graham DY, Yamaoka Y. Interleukin-6 genetic polymorphisms are not related to *Helicobacter pylori*-associated gastroduodenal diseases. *Helicobacter* 2003; **8**: 142-148

26 **Yahiro K**, Niidome T, Hatakeyama T, Aoyagi H, Kurazono H, Padilla PI, Wada A, Hirayama T. *Helicobacter pylori* vacuolating cytotoxin binds to the 140-kDa protein in human gastric cancer cell lines, AZ-521 and AGS. *Biochem Biophys Res Commun* 1997; **238**: 629-632

27 **Yahiro K**, Niidome T, Kimura M, Hatakeyama T, Aoyagi H, Kurazono H, Imagawa K, Wada A, Moss J, Hirayama T. Activation of *Helicobacter pylori* VacA toxin by alkaline or acid conditions increases its binding to a 250-kDa receptor protein-tyrosine phosphatase beta. *J Biol Chem* 1999; **274**: 36693-36699

28 **Sun J**, Bi L, Chi Y, Aoki K, Misumi J. Effect of sodium acetate on cell proliferation and induction of proinflammatory cytokines: a preliminary evaluation. *Food Chem Toxicol* 2005; **43**: 1773-1778

29 **Peek RM Jr**, Blaser MJ, Mays DJ, Forsyth MH, Cover TL, Song SY, Krishna U, Pietenpol JA. *Helicobacter pylori* strain-specific genotypes and modulation of the gastric epithelial cell cycle. *Cancer Res* 1999; **59**: 6124-6131

30 **Kalia N**, Jones C, Bardhan DK, Reed MW, Atherton JC, Brown NJ. Effects of genotypically different strains of *Helicobacter pylori* on human microvascular endothelial cells in vitro. *Dig Dis Sci* 2001; **46**: 54-61

31 **Brzozowski T**, Konturek PC, Konturek SJ, Kwiecien S, Pajdo R, Karczewska E, Stachura J, Hahn EG. Water extracts of *Helicobacter pylori* delay healing of chronic gastric ulcers in rats: role of cytokines and gastrin-somatostatin link. *Digestion* 1999; **60**: 22-33

32 **Mitsuno Y**, Yoshida H, Maeda S, Ogura K, Hirata Y, Kawabe T, Shiratori Y, Omata M. *Helicobacter pylori* induced transactivation of SRE and AP-1 through the ERK signalling pathway in gastric cancer cells. *Gut* 2001; **49**: 18-22

33 **Sharma SA**, Tummuru MK, Miller GG, Blaser MJ. Interleukin-8 response of gastric epithelial cell lines to *Helicobacter pylori* stimulation in vitro. *Infect Immun* 1995; **63**: 1681-1687

34 **Terunuma A**, Aiba S, Tagami H. Cytokine mRNA profiles in cultured human skin component cells exposed to various chemicals: a simulation model of epicutaneous stimuli induced by skin barrier perturbation in comparison with that due to exposure to haptens or irritant. *J Dermatol Sci* 2001; **26**: 85-93

35 **Ohkusa T**, Okayasu I, Miwa H, Ohtaka K, Endo S, Sato N. *Helicobacter pylori* infection induces duodenitis and superficial duodenal ulcer in Mongolian gerbils. *Gut* 2003; **52**: 797-803

36 **Iwamoto H**, Czajkowsky DM, Cover TL, Szabo G, Shao Z. VacA from *Helicobacter pylori*: a hexameric chloride channel. *FEBS Lett* 1999; **450**: 101-104

37 **Sun J**, Tian Z, Zhang JH. Effect of recombinant Human Interleukin-6 on Mouse NK and CTL Cells in vitro and in vivo. *Zhongguo Zhongliu Shengwu Zhiliao* 1995; **2**: 188-190

38 **Sun J**, Tian Z, Zhang JH. Effect of recombinant Human Interleukin-6 on Mouse LAK Cells in vitro and in vivo. *Zhongguo Mianyixue Zazhi* 1996; **12**: 98-100

39 **Sun J**, Tian Z, Zhang JH. Effect of recombinant Human Interleukin-6 on Mouse blood system. *Zhongguo Shenghua Yaowu Zazhi* 1995; **16**: 154-156

40 **Sun J**, Tian Z, Zhang JH. Effect of recombinant Human Interleukin-6 on Mouse Microphage in vitro and in vivo. *Zhonghua Zhongliu Zazhi* 1995;**17**: 446-447

41 **Tanahashi T**, Kita M, Kodama T, Yamaoka Y, Sawai N, Ohno T, Mitsufuji S, Wei YP, Kashima K, Imanishi J. Cytokine expression and production by purified *Helicobacter pylori* urease in human gastric epithelial cells. *Infect Immun* 2000; **68**: 664-671

42 **Supajatura V,** Ushio H, Wada A, Yahiro K, Okumura K, Ogawa H, Hirayama T, Ra C. Cutting edge: VacA, a vacuolating cytotoxin of *Helicobacter pylori*, directly activates mast cells for migration and production of proinflammatory cytokines. J Immunol 2002; **168**: 2603-2607

43 **Censini S,** Lange C, Xiang Z, Crabtree JE, Ghiara P, Borodovsky M, Rappuoli R, Covacci A. cag, a pathogenicity island of *Helicobacter pylori*, encodes type I-specific and disease-associated virulence factors. Proc Natl Acad Sci USA 1996; **93**: 14648-14653

S- Editors Pan BR and Wang J **L- Editor** Wang XL **E- Editor** Liu WF

PO Box 2345, Beijing 100023, China
www.wjgnet.com
wjg@wjgnet.com

World J Gastroenterol 2006 April 14; 12(14): 2181-2186
World Journal of Gastroenterology ISSN 1007-9327

Helicobacter pylori and other *Helicobacter* species DNA in human bile samples from patients with various hepato-biliary diseases

Santosh K Tiwari, Aleem A Khan, Mohd Ibrahim, Mohd Aejaz Habeeb, C M Habibullah

Santosh K Tiwari, Aleem A Khan, Mohd. Ibrahim, Mohd Aejaz Habeeb, C M Habibullah, Center for Liver Research and Diagnostics, Deccan College of Medical Sciences, Kanchanbagh, Hyderabad 500 058, Andhra Pradesh, India
Mohd Aejaz Habeeb, C M Habibullah, Department of Gastroenterology, Deccan College of Medical Sciences Hyderabad 500 058, Andhra Pradesh, India
Supported by the Department of Biotechnology, Government of India
Co-correspondence: Aleem A Khan
Correspondence to: Professor C M Habibullah, Director, Centre for Liver Research and Diagnostics, Deccan College of Medical Sciences and Allied Hospitals Kanchanbagh, Hyderabad, Andhra Pradesh, 500 058, India. cmhabib@rediffmail.com.
Telephone: +91-40-24342954 Fax: +91-40-24342954
Received: 2005-09-29 Accepted: 2005-11-12

Abstract

AIM: To investigate the presence of *Helicobacter* species by nested PCR of 16S rRNA genes followed by the presence of *Helicobacter pylori* (*H pylori*) 16S rRNA, *ureA*, *cagA* genes in bile obtained at endoscopic retrograde cholangio-pancreatography (ERCP) from 60 Indian subjects.

METHODS: Sixty bile samples were obtained from patients diagnosed with various hepato-biliary diseases and control subjects at ERCP. PCR analysis was carried out using primers for *Helicobacter* genus 16S rRNA gene and *H pylori* (16S rRNA, *ureA* and *cagA*) genes. Gastric *H pylori* status was also assessed from biopsies obtained at endoscopy from patients with various hepato-biliary diseases and controls. The control group mainly consisted of subjects with gastric disorders. Sequencing analysis was performed to confirm that PCR products with 16S rRNA and *cagA* primers were derived from *H pylori*.

RESULTS No *Helicobacters* were grown in culture from the bile samples. *Helicobacter* DNA was detected in bile of 96.7% and 6.6% of groups I and II respectively. Ten from group I were positive for 16S rRNA and *ureA* and 9 were positive for *cagA* gene. In contrast of the 2 from the control, 1 amplified with 16S rRNA, *ureA* and *cagA* primers used. The sequences of the 16S rRNA genes and *cagA* were 99% similar to *Helicobacter pylori*.

CONCLUSION: *Helicobacters* are associated with the pathogenesis of various hepato-biliary disorders.

Key words: *Helicobacter pylori*; Bile; Hepato-biliary diseases; PCR, Sequence analysis

Tiwari SK, Khan AA, Ibrahim M, Habeeb MA, Habibullah CM. *Helicobacter pylori* and other *Helicobacter* species DNA in human bile samples from patients with various hepato-biliary diseases. *World J Gastroenterol* 2006; 12(14): 2181-2186

http://www.wjgnet.com/1007-9327/12/2181.asp

INTRODUCTION

The re-discovery of *Helicobacter pylori* (*H pylori*) as a curved bacterium in the stomach by histological examination of gastric biopsies[1, 2] and its subsequent first isolation by Warren & Marshall in 1983 have probably etched new avenues in the management of various gastro-duodenal disorders. Since its discovery, this microaerophilic Gram negative pathogen has been linked to various gastric pathologies including gastric carcinoma and mucosa associated lymphoid tissue (MALT) lymphoma[3, 4]. Numerous other *Helicobacter* species along with *Helicobacter pylori* have subsequently been isolated from sites other than the stomach, including oral cavity, liver and biliary tree of animals and humans[5-7]. Recent studies have implicated the association between *Helicobacter* infections with certain diseases of the liver of some animal species such as *H canis* in dogs[8] and *H hepaticus* & *H bilis* in mice[9-11].

In humans, other *Helicobacter* species including *H pylori* DNA has been detected in the liver of patients suffering from cholestatic diseases[12, 13]. In one study, a high frequency of *H pylori* and *H pullorum* sequences were detected by PCR, in the liver of patients with cirrhosis and superimposed hepatocellular carcinoma[14]. More recently, a study by Pellicano *et al* suggests that presence of *Helicobacter spp* in liver samples could possibly serve as a co-factor in the development of end-stage of liver disease in humans[15]. These concerns have spurred considerable interest in determining the mechanisms by which these extra cellular bacteria and the associated inflammatory response endorse hepatic and biliary disease.

Therefore, we investigated the presence of *Helicobacter*

Table 1 List of primers used for the study

Primer	Sequence (5′→3′)	Product size (bp)
Heli-nest S	5′ATTAGTGGCGCACGGGTGAGTAA 3′	1300
Heli-nest R	5′ TTTAGCATCCCGACTTAAGGC 3′	
Heli-S	5′ GAACCTTACCTAGGCTTGACATTG 3′	480
Heli-R	5′ GGTGAGTACAAGACCCGGGAA 3′	
16S-rRNA.F	5′ TAAGAGATCAGCCTATATGTCC 3′	534
16S-rRNA.R	5′ TCCCACGCTTTAAGCGCAAT 3′	
UreA-S	5′GCCAATGGTAAATTAGTT 3′	411
UreA-R	5′ CTCCTTAATTGTTTTTAC 3′	
CagA-S	5′ CCATGAATTTTTGATCCGTTCGG 3′	349
CagA-R	5′ GATAACAGGCAAGCTTTTGAGAGGGA 3′	

spp genomes in the bile specimens obtained from patients with different hepato-biliary diseases and among control group (without any hepatic and biliary disease but with different gastric disorders) at endoscopic retrograde cholangio-pancreatography (ERCP). We also evaluated the association between the presence of *Helicobacter* species with various hepato-biliary disorders.

MATERIALS AND METHODS

Subjects

The study population consisted of 60 subjects categorized into two groups (thirty in each) *viz*., Group I (those with hepato-biliary disorders) and Group II (those with no pathologically proven liver or biliary disease but with different gastric disorders, served as control). Patients of both sexes and age range: 23-68 years, average age: 48.1 years were included in the study. Subjects from either group underwent ERCP followed by upper gastrointestinal endoscopy at the Department of Gastroenterology, Deccan College of Medical Sciences, Hyderabad. The study protocol was approved by the Institutional Review Board (IRB) and Institutional Ethical Committee (IEC). Approval was obtained from IEC for the initiation of the study. Informed consent was obtained from all the patients before their enrolling in the study according to the Helsinki Declaration. None of the patients included for the study were on antibiotics prior to ERCP or endoscopy.

Patients' details and diagnoses were recorded and 5-10 mL bile samples were collected in glycerol by aspiration during the ERCP procedure and 3 gastric biopsies were collected during endoscopy from the same patient: one in urea solution for rapid urease test (RUT), one in brucella broth supplemented with fetal calf serum (FCS) for culture and 1 in phosphate buffered saline (PBS) for DNA isolation. Aspirated bile samples and the biopsy collected in PBS were stored at -80 °C until DNA was isolated.

Helicobacter culture

The gastric biopsy collected in supplemented brucella broth was immediately transported to the laboratory and streaked on the chocolate brucella agar supplemented with 70 mL/L sheep blood and 6 mg/L-vancomycin, 2 mg/L-amphoteracin-B and polymixin-B 2500/L (Sigma Chemicals, USA) and incubated at 37 °C in microaerobic conditions. A small aliquot (about 0.5 mL) of the collected bile sample was also instantaneously homogenized within half an hour of collection in 0.5 to 1 mL brucella broth (Becton and Dickinson, USA) containing 50 mL/L fetal calf serum (Gibco BRL, Germany) and streaked over the same medium for primary isolation of *H pylori* and incubated as described above. Approximately 50 μL of the sample was plated onto each plate and the remaining sample was used for DNA isolation.

DNA extraction

The genomic DNA from the gastric tissue, isolated culture and bile samples was isolated *as per* the standard protocol previously described[16]. In case of bile sample, briefly 450 μL of the sample was diluted with equal volume of PBS and centrifuged at 15000 g for 20 min. The supernatant was discarded and the pellet was again subsequently mixed with 250 μL of the PBS and DNA isolated by modified cetyl trimethyl ammonium bromide (CTAB) method. The DNA was extracted and preserved at -20°C until amplification was performed. Appropriate care was taken during extraction to remove the PCR inhibiting substances present in the bile[17]. Briefly as *Helicobacter* DNA was isolated from an unusual source, there is possibility of existence of specific inhibitors and competing substrates. For such situations, dilution of inhibited samples provides a rapid and straightforward way of permitting amplification. This dilution exploits the sensitivity of PCR by reducing the concentration of inhibitors relative to target DNA.

PCR amplification

Amplification was performed *as per* standard protocol described previously[13] with minor modifications. All primers were synthesized at Bioserve Biotechnologies Pvt Ltd, Hyderabad, India. Amplification was performed in a PTC 100 thermocycler (M J Research Inc. Water town, USA).

PCR amplification with Helicobacter genus-specific primers

Nested PCR was carried out using two oligonucleotide pairs previously reported by Pellicano *et al*[15] and designated as Heli in Table 1. The primers (Helinest-S & R, Heli-S & R) used in our study were reported to amplify 26 species of *Helicobacter* genus[15]. At each amplification, *H pylori* DNA was used as a positive control, while water instead of DNA served as a negative control.

First amplification

Amplification was carried out in a total volume of 20 μL containing 0.5 μL DNA, PCR buffer (1×), 200 μmol/L dNTPs, 1.5 mmol/L Mg^{2+}, 0.2 μmol/L primers (Heli-nest-S and Heli-nest-R), 1U Taq DNA polymerase (Invitrogen Life Technologies, Germany). Amplification conditions were optimized and are enlisted in Table 2. A sample was scored positive if an amplification product of 1300 bp could be resolved after electrophoresis on 15 g/L agarose gel.

Second amplification

One microliter of amplicon from the first amplification

Table 2 Conditions of polymerase chain reactions used in the study

Target gene	Initial denaturation step	Temperature o denaturation, annealing and	Cycle	Final extension step extension
Helicobacter Spp,16S rRNA	94 ℃ for 5 min	94℃ for 30 s 55℃ for 30 s	35	72℃ for 7 min 72℃ for 1.5 min
Second amplification step	94℃ for 5 min	94℃ for 30 s 60℃ for 30 s 72℃ for 30 s	35	72℃ for 7 min
Helicobacter pylori, 16S rRNA	95℃ f	94℃ for 30 s 56℃ for 30	40	72℃ for 5 min 2℃ for 1 min
ureA	95℃ for 5 min	94℃ for 30 s 52℃ for 30	35	72℃ for 6 min 72℃ for 1 min
cagA	95℃ for 5 min	94℃ for 1 min 52℃ for 1 min 72℃ for 2 min	35	72℃ for 10 min

step was used with primers Heli-S and Heli-R (Table 1) and amplification was repeated with minor alterations (Table 2). The expected product size of the amplicon was 480 bp.

Specificity test of genus specific primers

The specificity of genus specific primers *viz.,* Helinest-S, Helinest-R, Heli-S and Heli-R as well as primers specific to *H pylori* was assessed by using 6 bacterial strains. This included two different *Helicobacter pylori* strains along with 4 other enteric bacteria commonly residing the stomach.

H pylori specific 16S rRNA PCR

The samples positive with *Helicobacter* genus PCR were further analyzed for the presence of *H pylori* DNA in the culture, biopsy and bile samples by targeting the 16S rRNA gene using primers enlisted in Table 1. Amplification was carried out as per the mentioned protocol (Table 2). The amplification product size was 534 bp typical of *H pylori.*

Amplification of ureA gene

Samples positive for *H pylori* were subsequently analyzed with a different set of primers designated *ure*A, in Table 1. The sense and anti-sense primers of this gene were used for PCR as per the mentioned protocol in Table 2. The amplification product size was 411 bp typical of *H pylori.*

Amplification of cagA gene

Samples positive for *H pylori* were subsequently screened for the presence of *cag*A gene using specific primers (Table 1). Amplification was carried out as per the program given in Table 2 with minor alterations increasing the annealing time to 1 min and extension time to 2 min. The expected product size of the primers used was 349 bp.

Sequencing of the 16S rRNA products and cagA amplification product

The *H pylori* positive DNA fragments from the bile samples were sequenced. Comparison of DNA sequences of the genomic 16S rRNA amplicons and *cag*A amplicons with those of *H pylori* was performed using sequence alignment with the BLAST programme. The presence of *H pylori* sequence was thus confirmed in these bile samples.

Statistical analysis

Helicobacter genus positivity and negativity was compared using the Fisher's exact test. $P < 0.05$ was considered as significant.

RESULTS

Culture

Of the 60 gastric biopsies streaked, colonies could be isolated from 54(90%) subjects (26 from group I and 28 from group II). No *Helicobacter pylori* colonies could be grown of the 60 bile samples streaked, even after prolonged incubation for up to 2 wk under microaerophilic conditions.

Specificity test

Helicobacter genus specificity was tested using a panel of *H pylori* strains by PCR with specific primer sets used for this study. All the *H pylori* DNA gave a positive amplification with the expected product size. The non-*Helicobacter* species DNA extracts did not yield any result with the oligonucleotide primers used.

PCR amplification with Helicobacter genus-specific primers

Helicobacter DNA was detected by nested-PCR in 29(96.7%) of the 30 bile samples collected from group I patients and 2(6.6%) of the subjects from group II sub-group respectively. All the 29 samples from group I and 2 from group II amplified at both first and second amplification reactions. The amplification product sizes of both the PCR are shown in Figures 1A and 1B respectively. DNA isolated from 60 biopsy and 54 cultures, gave a positive amplification with the expected product size.

Screening for H pylori DNA in bile

Of the 29 *Helicobacter* genus positive samples from group I subjects, 10(33.3%) bile samples were amplified with the *H pylori* specific 16S rRNA primers, yielding a product size of 534 bp on electrophoresis (Figure 1C). While of the 2 *Helicobacter* genus positive from group II, only 1 was amplified with the *H pylori* 16S rRNA primers used (Table 3).

Confirmation of gastric H pylori colonization

Screening of the 60 biopsy DNA and 54 culture DNA from both the study groups gave positive amplification with the specified primers used, yielding a product size of 534 bp.

Analysis of ureA and cagA gene

Of the 29 subjects analyzed for the presence of *ure*A and *cag*A sequences from group I sub-group, we found that 10 (33.5%) were amplified with *ure*A gene while 9 (30%) amplified with the *cag*A primer. On the other hand, 1 sample which was amplified for *H pylori* 16S rRNA gene in group II, also gave positive amplification for *ure*A and *cag*A respectively (Table 3). The amplified products of these genes are represented in Figure 1D, E.

Table 3 Details of *Helicobacter* genus, *H pylori* 16S rRNA, ureA, cagA positivity in the study subjects

No	Category ($n=60$)	*Helicobacter* genus positivity *n* (%)	*H pylori* 16S rRNA positive *n* (%)	*ureA* positive *n* (%)	*CagA* positive *n* (%)
1	Group I	29(96.7)	10(33.3)	10(33.3)	09(30)
2	Group II	02(6.6)	01(3.3)	01(3.3)	01(3.3)

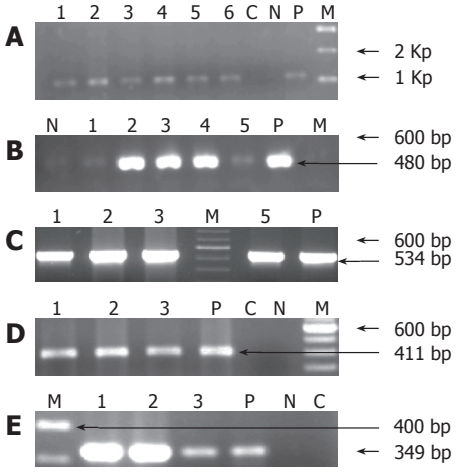

Figure 1 A schematic representation of the PCR products of the *Helicobacter spp* DNA. **A:** Gel image showing first amplification products of 16S rRNA PCR with *Helicobacter* genus specific primers at 1 300 bp. Lanes 1 to 6 represent *Helicobacter* DNA isolated from bile samples, 'P' represents positive control andLanes C, N and M represents negative control, reaction negative control and 1 Kb molecular weight marker. **B:** Second amplification products of 16S rRNA PCR with *Helicobacter* genus specific primers at 480 bp. Lanes 1 to 5 represent bile DNA, 'P' represents positive control. Lanes N and M represent reaction negative control and 100 bp molecular weight marker ladder respectively. **C:** Gel picture showing 16S rRNA amplification products specific to *H pylori* of bile samples at 534 bp. Lanes 1, 2, 3 and 5 represent bile DNA samples while Lanes M and P represent 100 bp ladder and positive control respectively. **D:** *ureA* amplification products at 411 bp. Lanes 1 to 3 represent bile DNA, Lane 'P' represents positive control and Lanes C, N and M represent negative control, reaction negative control and 100bp molecular weight ladder respectively. **E:** Gel picture illustrating the *cagA* amplification products at 349 bp. Lanes 1, 2 and 3 represent bile DNA while Lanes M, P, N and C represent 100bp molecular weight ladder, positive and reaction negative control, negative control respectively.

Sequence analysis of PCR product from bile DNA with 16S rRNA and cagA primers

To confirm that the PCR product obtained with the 16S rRNA and *cag*A primers belonged to *H pylori*, we examined the sequence of the PCR product in 4 bile samples (3 from Group I and 1 from Group II). The nucleotide sequence of the amplified products shared 99% identity with the 16S rRNA and *cag*A gene of *H pylori* respectively.

DISCUSSION

The presence of *Helicobacter* species DNA in the bile samples of patients with different hepato-biliary diseases is interesting since some reports in the past have suggested a positive association of *Helicobacter* and the evolution of liver diseases[9, 15, 18, 19]. Recent studies on *Helicobacter spp* in different diseases of liver and bile ducts have shown that *Helicobacter* can be detected not only in the extremely hostile milieu of the stomach but also in human bile[20, 19]. Although none of the previous studies including the present study have not been able to isolate *H pylori in vitro,* it has been proven that some of *Helicobacter* species live in the gall bladder. In a recent study[15], by PCR and subsequent sequencing of the 16S rDNA and amplification of *cag*A gene, *Helicobacter spp* was detected in 17 of 20 patients operated for hepatocellular carcinoma (HCC). The same study reported the presence of a 290 bp product of 128 KDa CagA protein specific only for type I *H pylori*. Further, it has been shown that several *Helicobacter spp*. secrete a liver specific toxin that causes hepatocyte necrosis in cell culture and might also be involved in damaging liver parenchyma *in vivo*[15]. In contrast, other authors did not detect any *Helicobacter* or *H pylori* DNA in the patients with similar diseases[21, 28]. These observations impelled us to explore a possible association of *Helicobacter* and hepato-biliary disease among Indian patients.

In the present study, which comprised of two groups (I & II), of the 30 subjects from group I with various hepato-biliary ailments, we could detect *Helicobacter* genus specific 16S rRNA sequence in 29 bile samples by nested PCR and only 1 sample did not give any amplification with the specific primers used. By contrast, in Group II subjects, i.e. those with no significant hepato-biliary disease but with various gastric disorders (Control subjects) only 2 subjects gave positive amplification with the *Helicobacter* genus specific primer used yielding the desired fragment. We carried out 16S rRNA amplification specific to *H pylori* on 29 subjects positive from group I and 2 from group II for *Helicobacter* genus, followed by subsequent sequencing of the amplified products to confirm the presence of *H pylori* DNA in the bile samples. We found that 33.3% samples from group I and 3.33% from group II were amplified giving a product of 534 bp (Figure 1C). Further, we also investigated the presence of *ure*A and *cag*A gene in all the bile specimens followed by sequencing of the 16S rRNA and *cag*A amplified products of 4 bile samples (3 from group I and 1 from group II). Sequence comparison of the sequenced samples confirmed the presence of *H pylori* DNA sequence in the bile samples.

The usage of less invasive ERCP procedure to obtain bile is an adequate method for this purpose compared with other invasive approaches currently in practice. This procedure also avoids contamination with *H pylori* colonizing the stomach, as the sampling devices are inserted inside the endoscope and hence never traverse the stomach[28].

This is the first Indian study to simultaneously investigate the presence of *Helicobacter* DNA in bile specimens and gastric tissues and underscore the association of *Helicobacter* in bile obtained from patients with various hepato-biliary disorders. We detected *Helicobacter* DNA by nested PCR using two sets of primer. Further, our study also successfully demonstrated the presence of *ure*A and virulence genes such as *cag*A specific to *H pylori* in the DNA isolated from bile samples. As evident from the results, 33.3% carried *ure*A gene whereas 30% were amplified with the primers used for *cag*A detection (Table 3). Of the 9 positive for *H pylori cag*A

gene, 5 belonged to cholangio-carcinoma, 2 belonged to common bile duct stones and the remaining subjects had pancreatico-biliary malignancies (Data not shown). In addition, we also found that among 10 subjects positive for *H pylori* in group I, *ure*A and *cag*A were simultaneously detected in 9 subjects, 1 subject gave amplification only for *ure*A gene and the only sample which was amplified with the 16S rRNA specific primer of *H pylori* from group II was found to possess both genes respectively (data not shown). The only subject whose bile sample gave positive results with 16S rRNA, *ure*A and *cag*A primers in group II was found to suffer from antral gastritis endoscopically and was co-incidentally positive for *H pylori* by culture and PCR of both the biopsy and culture DNA (data not shown). Every possible precautionary measure was taken to assure that laboratory contamination did not account for the positive amplification results such as diluting the bile with sterile distilled water, centrifuging the samples at 15 000 × *g* for 20 min, and the supernatant being discarded, thus by concentrating the bacterial cells in the pellet, enabling removal of some of the inhibitors predominantly present in the bile. Collection of bile in glycerol and immediate plating nevertheless did not prove to be successful for *in vitro* isolation of *Helicobacters* from any of the bile samples as we could not get any growth even after extended incubations for up to 15 d.

The present study also investigated the gastric *H pylori* status of the patients enrolled in both the sub-groups to see if at all the gastric *H pylori* status had any impact on the etiology of the hepato-biliary diseases. Unfortunately from the results we could neither associate the severity of the hepato-biliary disease with that of the gastric diseases nor could we link the gastric *H pylori* status and the detection of *H pylori* DNA in bile of the hepato-biliary diseases. Even though 29 subjects from group I showed the presence of *Helicobacter* species DNA, only 10 showed the presence of *H pylori* DNA in the bile thus signifying the possibility of the presence of the other bile-resistant *Helicobacters* that normally reside in the liver and biliary tract. Besides the above results obtained in this study, we noticed that patients with various hepato-biliary disorders had much greater probability of positive *Helicobacter* species DNA compared to those with no pathologically proven liver and biliary diseases. Why these intestinal *Helicobacters* have been identified in Chilean patients[26] and *H pylori* has been identified in patients in other geographical regions, as we observed in this study warrant further investigations. In fact, the typical finding of the present study, correlates well with those of Kuroki *et al*[22], who recently demonstrated that the level of epithelium proliferation was higher in *Helicobacter*-positive biliary epithelium than in bacterium-negative epithelium.

The results of our study also suggest that besides *Helicobacter spp* sequences, even sequences pertaining to the virulence genes of *H pylori* are consistently found at a high frequency in bile samples and that they may be a significant cause of biliary diseases. Several hypotheses have been proposed[23-25], by which these *Helicobacters* find their way into the liver and bile duct. But these hypotheses entail strong evidences to underline the precise mechanism by which the *Helicobacter* species anchor the liver and aggravate the clinical outcome.

The findings of this study are in concert to those obtained by Fox *et al*[26] and Linn *et al*[18] who reported *Helicobacter spp* in gall bladder tissue from Chileans with chronic cholecystitis but different from those of Fallone *et al*[28] and Mendez-Sanchez *et al*[21] who were not able to detect *Helicobacter* sequences in the bile samples of North Americans and Mexicans respectively. The raison d'être for these discordant results could be the regional variations in the distribution of bile-resistant *Helicobacter* species[20]. The other alternative reason for the inconsistent results in their studies could be the methodology used, the selection of primers used, as both the studies had used a single primer set for the amplification of the conserved 16S rRNA gene. In contrast, our study used nested PCR for 16S rRNA amplification of *Helicobacter* genus, which according to Stark *et al*[27] is 10^4 times more sensitive than a 1-step PCR. Though we used only one set of oligonucleotide primers each for amplifying *ure*A and *cag*A, the specificity and sensitivity of the selected primers were previously determined during our routine screening. The primers were found to possess the sensitivity and specificity of 90% and 95% for *ure*A and 89% and 85% for *cag*A, particularly in this geographical area.

In conclusion, this study demonstrated that *Helicobacter spp* DNA can be detected in bile by PCR and that gastric presence of *H pylori* in patients with proven hepato-biliary disease had no clinical correlation with the hepatic and biliary disease. However, like other previous studies, we were unable to isolate the bacterium in culture. There are different reasons to justify this finding. Firstly, this could be due to the bacterial conversion from viable helicals to non-viable coccoids in an adverse bile rich environment. It is also possible that the number of bacterium is very few and that they may have been partially inhibited by unfavorable environment that exists in the biliary milieu. In addition, our study also confirmed by DNA sequencing that sequences specific to *H pylori* (16S rRNA, *cag*A) can be found at a high frequency in the bile samples, thus instilling strong evidence that presence of *Helicobacter spp* may in someway aggravate the etio-pathogenesis of hepato-biliary diseases. However, mere detection of *Helicobacter* DNA from patients with different hepatic and biliary disease does not confirm the precise role played by these organisms. Further, future studies unraveling the molecular mechanisms by which these *Helicobacter* members contribute to the clinical outcome of hepato-biliary disorders would be helpful to assess the true impact of enterohepatic *Helicobacters* and its metabolites in the genesis of biliary diseases.

REFERENCES

1 Unidentified curved bacilli on gastric epithelium in active chronic gastritis. *Lancet* 1983; **1:** 1273-1275
2 **Buckley MJM,** O'Morain CA. *Helicobacter* biology- discovery. *Br Med Bull* 1998; **54:** 7-16
3 **Parsonnet J,** Friedman GD, Vandersteen DP, Chang Y, Vogelman JH, Orentreich N, Sibley RK. *Helicobacter pylori* infection and the risk of gastric carcinoma. *N Engl J Med* 1991; **325:** 1127-1131
4 **Wotherspoon AC**, Ortiz-Hidalgo C, Falzon MR, Isaacson PG. Helicobacter pylori-associated gastritis and primary B-cell

gastric lymphoma. *Lancet* 1991; **338:** 1175-1176
5 **Melito PL**, Munro C, Chipman PR, Woodward DL, Booth TF, Rodgers FG. Helicobacter winghamensis sp. nov., a novel Helicobacter sp. isolated from patients with gastroenteritis. *J Clin Microbiol* 2001; **39:** 2412-2417
6 **Tiwari SK**, Khan AA, Ahmed KS, Ali SM, Ahmed I, Habeeb A, Kauser F, Hussain MA, Ahmed N, Habibullah CM. Polymerase chain reaction based analysis of the cytotoxin associated gene pathogenicity island of Helicobacter pylori from saliva: an approach for rapid molecular genotyping in relation to disease status. *J Gastroenterol Hepatol* 2005; **20:** 1560-1568
7 **Tiwari SK,** Khan AA, Ahmed KS, Ahmed I, Kauser F, Hussain MA, Ali SM, Alvi A, Habeeb A, Abid Z, Ahmed N, Habibullah CM. Rapid diagnosis of *Helicobacter pylori* infection in dyspeptic patients using salivary secretion: A non-invasive approach. *Singapore Med J* 2005; **46**: 224-228
8 **Fox JG,** Drolet R, Higgins R, Messier S, Yan L, Coleman BE, Paster BJ, Dewhirst FE. *Helicobacter canis* isolated from a dog liver with multifocal necrotizing hepatitis. *J Clin Microbiol* 1996; **34:** 2479-2482
9 **Fox JG**, Dewhirst FE, Tully JG, Paster BJ, Yan L, Taylor NS, Collins MJ Jr, Gorelick PL, Ward JM. Helicobacter hepaticus sp. nov., a microaerophilic bacterium isolated from livers and intestinal mucosal scrapings from mice. *J Clin Microbiol* 1994; **32:** 1238-1245
10 **Fox JG**, Li X, Yan L, Cahill RJ, Hurley R, Lewis R, Murphy JC. Chronic proliferative hepatitis in A/JCr mice associated with persistent Helicobacter hepaticus infection: a model of helicobacter-induced carcinogenesis. *Infect Immun* 1996; **64:** 1548-1558
11 **Fox JG**, Yan LL, Dewhirst FE, Paster BJ, Shames B, Murphy JC, Hayward A, Belcher JC, Mendes EN. Helicobacter bilis sp. nov., a novel Helicobacter species isolated from bile, livers, and intestines of aged, inbred mice. *J Clin Microbiol* 1995; **33:** 445-454
12 **Avenaud P**, Marais A, Monteiro L, Le Bail B, Bioulac Sage P, Balabaud C, Megraud F. Detection of Helicobacter species in the liver of patients with and without primary liver carcinoma. *Cancer* 2000; **89:** 1431-1439
13 **Nilsson H,** Tanneera J, Castedal M, Glats E, Olssen R, Wadstrom T. Identification of *Helicobacter pylori* and *Helicobacter* species by PCR, hybridization and partial DNA sequencing in human liver samples from patients with primary sclerosing cholangitis or primary biliary cholangitis. *J Clin Microbiol* 2000; **38:** 1072-1076
14 **Ponzetto A**, Pellicano R, Leone N, Cutufia MA, Turrini F, Grigioni WF, D'Errico A, Mortimer P, Rizzetto M, Silengo L. Helicobacter infection and cirrhosis in hepatitis C virus carriage: is it an innocent bystander or a troublemaker? *Med Hypotheses* 2000; **54:** 275-277
15 **Pellicano R,** Mazzaferro V, Grigioni WF, Cutufia MA, Fagoonee S, Silengo L, Rizzetto M, Ponzetto A. *Helicobacter* species sequences in liver samples from patients with and without hepatocellular carcinoma. *World J Gastroenterol* 2004; **10:** 598-601
16 **Clayton CL,** Mobley HLT. Methods in molecular medicine, *Helicobacter pylori* protocols, (3rd eds.) *Humana Press Inc, Totowa*, 2002; 33
17 **Wilson IG**. Inhibition and facilitation of nucleic acid amplification. *Appl Environ Microbiol* 1997; **63:** 3741-3751
18 **Lin TT**, Yeh CT, Wu CS, Liaw YF. Detection and partial sequence analysis of Helicobacter pylori DNA in the bile samples. *Dig Dis Sci* 1995; **40:** 2214-2219
19 **Leong RW**, Sung JJ. Review article: Helicobacter species and hepatobiliary diseases. *Aliment Pharmacol Ther* 2002; **16:** 1037–1045
20 **Bulajic M**, Maisonneuve P, Schneider-Brachert W, Muller P, Reischl U, Stimec B, Lehn N, Lowenfels AB, Lohr M. Helicobacter pylori and the risk of benign and malignant biliary tract disease. *Cancer* 2002; **95:** 1946-1953
21 **Mendez-Sanchez N**, Pichardo R, Gonzalez J, Sanchez H, Moreno M, Barquera F, Estevez HO, Uribe M. Lack of association between Helicobacter sp colonization and gallstone disease. *J Clin Gastroenterol* 2001; **32:** 138-141
22 **Kuroki T,** Fukuda K, Yamanouchi K, Kitajima T, Matsuzaki S, Tajima Y, Furui J, Kanematsu T. *Helicobacter pylori* accelerates the biliary epithelial cell proliferation activity in hepatolithiasis. *Hepato-Gastroenterol* 2002; **49:** 648-651
23 **Cassell GH**. Infectious causes of chronic inflammatory diseases and cancer. *Emerg Infect Dis* 1998; **4:** 475-487
24 **Crabtree J**. Cytokine responses to *Helicobacter pylori*-induced infection. In: Riecken EO, Zeitz M, Stallmach A, Heise W editors. Malignancy and chronic inflammation in the gastrointestinal tract: new concepts. *Kluwer Academic publishers, Lancaster,* 2002; 25-36
25 **Hornick RB**. Enteric fever. In Blaser MJ, Smith PD, Ravdin JI, Greenberg HB and Guerrant RL (eds), Infections of the gastrointestinal tract. *New York, Raven Press, Ltd,* 1997; 325-332
26 **Fox JG,** Yan L, Dewhirst FE, Shen Z, Feng Y, Taylor NS, Paster BJ, Ericson RL, Lau CN, Correa P, Araya J, Roa I. Hepatic *Helicobacter* species identified in bile and gall bladder tissue from Chileans with chronic cholelithiasis. *Gastroenterology* 1998; **114:** 755-763
27 **Stark KD**, Nicolet J, Frey J. Detection of Mycoplasma hyopneumoniae by air sampling with a nested PCR assay. *Appl Environ Microbiol* 1998; **64:** 543- 548
28 **Fallone CA**, Tran S, Semret M, Discepola F, Behr M, Barkun AN. Helicobacter DNA in bile: correlation with hepato-biliary diseases. *Aliment Pharmacol Ther* 2003; **17:** 453-458

S- Editor Guo SY **L- Editor** Zhu LH **E- Editor** Bai SH

PO Box 2345, Beijing 100023, China
www.wjgnet.com
wjg@wjgnet.com

World J Gastroenterol 2006 April 14; 12(14): 2187-2194
World Journal of Gastroenterology ISSN 1007-9327

BASIC RESEARCH

Liver fibrosis and tissue architectural change measurement using fractal-rectified metrics and Hurst's exponent

Nicola Dioguardi, Fabio Grizzi, Barbara Franceschini, Paola Bossi, Carlo Russo

Nicola Dioguardi, Fabio Grizzi, Barbara Franceschini, Carlo Russo, Laboratori di Medicina Quantitativa, Istituto Clinico Humanitas IRCCS, Rozzano, Milan, and "Michele Rodriguez" Foundation, Institute for Quantitative Methods in Medicine, Milan, Italy
Paola Bossi, Department of Pathology, Istituto Clinico Humanitas IRCCS, Rozzano, Milan, Italy
Supported by the "Michele Rodriguez" Foundation, Institute for Quantitative Measures in Medicine, Milan, Italy
Correspondence to: Nicola Dioguardi, MD, Laboratori di Medicina Quantitativa, Istituto Clinico Humanitas IRCCS, Via Manzoni 56, 20089 Rozzano MI, Italy. nicola.dioguardi@humanitas.it
Telephone: +39-2-82244501 Fax: +39-2-82244590
Received: 2005-05-04 Accepted: 2005-08-26

Abstract

AIM: To provide the accurate alternative metrical means of monitoring the effects of new antiviral drugs on the reversal of newly formed collagen.

METHODS: Digitized histological biopsy sections taken from 209 patients with chronic C virus hepatitis with different grade of fibrosis or cirrhosis, were measured by means of a new, rapid, user-friendly, fully computer-aided method based on the international system meter rectified using fractal principles.

RESULTS: The following were described: geometric perimeter, area and wrinkledness of fibrosis; the collation of the Knodell, Sheuer, Ishak and METAVIR scores with fractal-rectified metric measurements; the meaning of the physical composition of fibrosis in relation to the magnitude of collagen islets; the intra- and inter-biopsy sample variability of these parameters; the "staging" of biopsy sections indicating the pathway covered by fibrosis formation towards its maximum known value; the quantitative liver tissue architectural changes with the Hurst exponent.

CONCLUSION: Our model provides the first metrical evaluations of the geometric properties of fibrosis and the quantitative architectural changes of the liver tissue. The representativeness of histological sections of the whole liver is also discussed in the light of the results obtained with the Hurst coefficient.

Key words: Liver; Fibrosis; Cirrhosis; Staging; Image analysis; Fractals

Dioguardi N, Grizzi F, Franceschini B, Bossi P, Russo C. Liver fibrosis and tissue architectural change measurement using fractal-rectified metrics and Hurst's exponent. *World J Gastroenterol* 2006; 12(14): 2187-2194

http://www.wjgnet.com/1007-9327/12/2187.asp

INTRODUCTION

Background

Experimental medical research based on reductionism retains in principle that the causes governing the processes and controls of the formation, growth and behavioral dynamics of living beings at macro-scalar levels can be derived from the processes and controls that take place at micro-scalar level.

This conception has led the hepatological disciplines to seek exact quantitative descriptions of the contents of liver fibrosis on the basis of the blood molecules related to the presence of the newly formed structure[1-5]. The basic idea is that the laws governing the set of processes and controls acting at the scale of the formation of septal and anular collagen structures can be translated into the set of laws that regulate the dynamics of these molecules at micro-scalar level when they enter the blood stream.

Sophisticated mathematical, physical and environmental studies suggest that these phenomena are governed by different multiple processes and controls (causality) at every larger or smaller scale rather than that of observation. The set of these multiple processes and controls is known as multiple scale causality (MSC)[6]. The macro-scalar growth of liver collagen fibres evolving into the septa and annuli of fibrosis is regulated by the physical events of diffusion, percolation, stratification and contraction of the extra-cellular matrix (ECM), and by the processes of neo-vascularisation. These physical processes are not involved in generation of microfibrils and fibrils, which is limited on ECM deposition. This phenomenon depends on the relationships between the processes of collagen synthesis and lyses, which are different from the biochemical processes that at a lower scale, regulate the quantitative and qualitative behaviors of the molecules formed during fibrogenesis and found in circulating blood. In other words, this means "what happens in the test tubes may be the same, the opposite, or bear no relationship at

all to what happens in the living cells, still less the living organisms".

In brief, the MSC-based conception rejects the idea that the laws regulating phenomena at one scale can in principle be derived from those regulating phenomena at a lower scale. In other words, every scale is characterized by different degrees of entropy[6].

As the characteristics of MSC are not universal, it is almost always impossible to establish a strict connection between the phases leading an observed object from micro- to macro-scalar positions and *vice versa*. Consequently, it is very difficult to identify a one-to-one relationship between the macro- and micro-scalar processes and controls of liver fibrosis production.

These considerations have convinced us to improve a direct, rapid and friendly method of measuring fibrosis using a meter that is suitable for its naturally irregular shape, provided that the biopsy procedures are performed by experts[7-12].

Liver biopsy is the only direct means of discovering the changes in liver tissue induced by chronic B or C virus-dependent inflammation and the fibrosis it causes[12-17]. Although it is the canonical point of reference for establishing the progression of the process, fibrosis has so far only been estimated on the basis of semi-quantitative evaluations[18-21] or morphometric methods[22-26] that must be considered approximate because of their use of the international system (IS) meter, which is unsuitable for measuring irregular shapes[7-11].

Like all natural objects, the collagen islets making up the fibrosis appear to be difficult to measure at all degrees of magnification because of their highly irregular shapes[7-11]. Furthermore, they do not have a single measurement because, at each enlargement (scale), their shape changes as a result of the addition of new details which are imperceptible at smaller scales. Mandelbrot have termed these irregular bodies fractal objects[27].

The studies of Perrin[28] in 1906, Hausdorff[29] in 1919, Richardson[30] in the 1950s, and Mandelbrot *et al*[26] in the 1970s and 1980s suggested a new geometry that has made it possible to measure such objects using a method that can be made simple with aid of computer technology.

The aim of this paper was to present the first results of the quantitative analysis of histological liver bioptical sections made using new metrics suggested by the concepts of fractal theory.

Our contribution to the quantitative evaluation of fibrosis in liver biopsies concerns: (1) the closest to real metric estimate of the surfaces covered by fibrosis and the quantitative classification of collagen islets; (2) the collation of metric and traditional semi-quantitative evaluations of collagen area; (3) considerations concerning the relationships depending on specific estimates defined by real numbers as a means of identifying the stadium of fibrosis; (4) the interior-to-edge metric relationship of the collagen islets used as an index of wrinkledness; (5) the definition of the harmonic state of the architectural structure of liver tissue, and the recognition and classification of its disharmonic states or architectural disorder using Hurst's exponent; (6) the intra-sample variability of fibrosis (area, wrinkledness and Hurst's exponent); and (7) the variability of the latter parameters in eight samples taken from the explanted liver of a transplant patient.

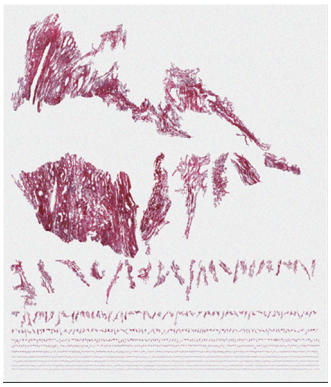

Figure 1 Prototypical catalogues of the Sirius-red stained collagen islets forming liver fibrosis, which consists of a set of irregularly shaped (wrinkled) objects.

Theory and objects

Characteristics of collagen islets The spaces occupied by the collagen islets making up fibrosis (Figure 1), and those occupied by the surviving fragments of parenchymal tissue, are both characterized by irregular shapes that exclude them from the application of Euclidean geometry[7-11]. However, their configurations make them members of the family of asymptotic statistical fractals (also called truncated fractals as they cannot be endlessly fracted)[31].

Dimension The dimension of an object indicates the Euclidean space it occupies. The fractionable "smooth" objects of classic geometry (a point, straight line, plane, and solid figure) occupy spaces whose dimensions are expressed by the whole numbers zo, 1, 2 and 3, whereas the irregular objects that are frangible into irregular pieces (sets of points, broken lines, undulating planes and irregular solids) occupy the intermediate spaces, and therefore have dimensions that cannot be expressed by whole numbers. In 1977, Mandelbrot[27] defined the objects whose dimensions are denoted by non-whole numbers as "fractals". The fractal dimension is indicated by D, and the Euclidean (or topological) dimension by Dγ.

Harmonic state of liver tissue The use of an analytical method based on a new geometry requires a brief formal description of the natural history of chronic virus-related hepatitis starting from the axiom that is defined by the persistence of a discreet necro-inflammatory process maintaining the activity of the ECM→collagen→fibrosis production system. The growth of fibrosis interrupts the continuity of the parenchyma, dissects it into irregular pieces, and compresses and atrophies the pieces enclosed in the fibrotic mass. This has two consequences: 1) it disrupts the natural harmonic state of the metric spaces covered by both natural fibrosis and the parenchyma, and 2) it alters the typical lobular architecture of hepatic tissue.

Using these axioms, the process can be represented by the first-order general equation:

$$z = f(x, y) \qquad 1)$$

in which z denotes the harmony of the natural architecture of liver tissue, x the metric space covered by fibrosis, and y the metric space covered by the parenchyma. The relationship of z to x and y can be indicated by the

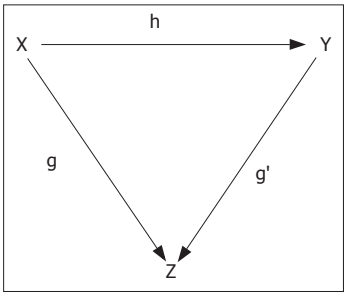

Figure 2 Categorial model of the harmonic state of liver tissue, in which z denotes the harmony of the natural architecture of liver tissue, x the metric space covered by fibrosis, and y the metric space covered by the parenchyma.

categorial representation (Figure 2), which shows the dependence of the state of z on the extension over z of the relationships between the "objects over" indicated by *x* and *y* in $f(x \rightarrow y)$.

As the variations in *x* and *y* are interconnected by the equality $(z\text{-}x)+(z\text{-}y)=1$, we can consider *x* and *y* as complementary spaces, and so the expression $z = f(x \rightarrow y)$ can be simplified to the form $z = f(x)$. The harmony of natural architecture of liver tissue is characterized by 3% fibrosis and 97% lobular parenchyma[32].

The evaluation of the metric space covered by the fibrosis induced by pathogenic agents is therefore sufficient by itself to describe the variations in the harmonic state of liver tissue architecture.

An alteration in the natural quantitative relationship between fibrosis and the parenchyma leads to the loss of the natural lobular architecture of hepatic tissue in a continuous but irregular progression that fractal geometry calls a random walk, or Brownian process[33,34].

MATERIALS AND METHODS

Patients

Two hundred and seven consecutive needle biopsy specimens (≥10 mm long) were taken from 74 female and 135 male patients (mean age: 52 ± 13 years) with chronic C virus-related liver disease. To evaluate the inter-sample variability of geometric characteristics of fibrosis, a total of six biopsy specimens were sampled from a liver explanted from a patient with clinically and histologically proved cirrhosis undergoing orthotopic liver transplantation. Each biopsy specimen was taken from a single segment of the liver.

Histological procedure

The study was performed in accordance with the guidelines of the Ethics Committee of the Istituto Clinico Humanitas, Rozzano and Ospedale Maggiore, Milan, Italy. All the patients were informed of the possible discomforts and risks of bioptic sampling. The liver specimens were fixed in 10% formalin and embedded in paraffin, and 2 μm thick sections were cut and stained with a freshly made 0.1% Sirius red staining solution[35].

Semi-quantitative evaluations

At least three expert pathologists independently staged the biopsies using Knodell's histology activity index (HAI), and the Sheuher, Ishak and METAVIR scoring systems. The number of available portal tracts in the liver fragment was assured on the basis of the indications established for the individual methods[18-21].

Quantitative image analysis

Our specially developed computer program could ensure: computer-driven microscopy focusing, digitation of the whole histological section and its fractal dimension and Hurst's exponent, less-biased measurements of each collagen islet and fibrosis mass raster perimeter length and area magnitude corrected by the fractal dimension, and wrinkledness of the fibrosis[7-11]. The time required for the whole analytical operation using this software was 30 s/mm^2, as determined on a standard reference needle specimen section, and was carried out at a microscopic magnification of ×200 (the measurements were valid only for that scale). The observed objects were measured using the IS meter rectified by their fractal dimension. When present, Glisson's capsule was included in the physiological amount of ECM, which was estimated as being 3% of the true area of the section[32].

Fractal dimension estimates

The fractal dimensions were automatically estimated using the box-counting method and the formula:

$$D_B = \lim_{\varepsilon \to 0} \frac{\mathrm{Log}N(\varepsilon)}{\mathrm{Log}(1/\varepsilon)} \qquad 2)$$

in which, D_B is the box-counting fractal dimension of the object, ε the side length of the box, and $N(\varepsilon)$ the smallest number of boxes of side ε required to cover the surface or the outline of the object completely[7-11,33,34]. As the zero limit could not be applied to biological objects, the dimensions were calculated as D = d, where d is the slope of the graph of log [N(ε)] against log 1/ε. The log-log graphs were plotted, and the linear segments were identified using least squares regression. Their gradients were calculated using an iterative resistant line method.

Computation of Hurst's exponent

Hurst's exponent, which gives a measure of the heterogeneous distribution of a set of irregularly-shaped objects[36-38], was obtained using the general relationship:

$$H = E + 1 - D \qquad 3)$$

where E indicates the Euclidean topological dimension, and D the fractal dimension of the surface covered by the extensions of all the collagen islets making-up the fibrosis. This exponent is capable of evaluating the loss of natural order that occurs in the histological picture as a result of the disruption of the natural quantitative relationship between the metric spaces covered by fibrosis and the parenchyma[11]. This could give the alterations the significance of a physical variable, make Hurst's exponent the descriptor of the configurational disorder of the hepatic tissue, and leave the fractal dimensions of the collagen islets and fibrosis the significance of an evaluation of how "densely" they occupy the metric space in which they lie and their spatial position.

In brief, Hurst's exponent values near to 1 quantitatively indicate a large loss of architectural harmony in the system (*i.e.* disordered states), whereas values near to zero indicate its preservation (*i.e.* states of structural order).

The reduction in Hurst's exponent could also be

interpreted as an index of the limited stability of a fractal object progressing towards more advanced states of stability.

Unit of measure

The construction of a meter with the most favorable spatial dimension for measuring the perimeter and area of the collagen islets was based on the assumptions that broken or mixed (in any case irregular) lines could be described as a "dilatative" (expanded) state of a straight line, and that their irregularity could be measured using the fractal dimension with similar criteria to those with which the coefficient of dilatation (λ) could be used to describe the length of a linear object before (s) and after (S) its exposure to the effect of heat expressed in the following formula:

$$S = s\,(1+\lambda t) \qquad 4)$$

where t is the duration of heat exposure[10].

According to this principle (which has been discussed elsewhere), the meter suitable for measuring a fractal object (m_F) could be obtained using the formula:

$$m_F = m\,[1 + \beta\,(D_P - D\gamma)] \qquad 5)$$

in which, m_F indicates the rectified meter, m the IS meter, β the dilatation constant of the unit of measure, D_P the fractal dimension of the perimeter, and $D\gamma$ the topological or Euclidean dimension[10]. The metric perimeter and area measurements were detected using the true liver biopsy area (indicated by the symbol A_B), by which we meant the surface area excluding any vascular, bile channel, sinusoidal or other empty spaces created by tissue loss during specimen manipulations.

Statistical analysis

All the data were expressed as mean±SD. The linear regression analysis was made using Spearman's correlation and Student's t test with Statistica software (StatSoft Inc., Tulsa, OK, USA). $P<0.05$ was considered statistically significant. The degree of intra- and inter-sample variability was quantitatively evaluated using the coefficient of variation (CV) given by the formula CV = SD/mean. Quantitative measures of fibrosis surfaces were compared (collated) with those of the score categories of the four currently used semi-quantitative methods.

RESULTS

Measurement of fractal dimension

By evaluating this parameter in our case-list of patients with chronic C virus-related hepatitis, we obtained dimensional values (D) ranging from 1.22 to 1.79. The value of this parameter increased depending on the extension of the fibrosis, with a regression curve ratio of $r=0.81$.

Perimeter measurements

The fibrosis perimeter (P_C) defined the sum of the perimeters all of the Sirius Red-stained areas of collagen in each biopsy section measured using the IS meter. The fractal fibrosis perimeter (P_{CF}) defined the same sum of perimeters measured using the fractal-rectified meter. The mean P_C was 860.64±588 μm, and the mean P_{CF} was 2966.1±2304.4 μm ($P<0.0005$). The marked difference

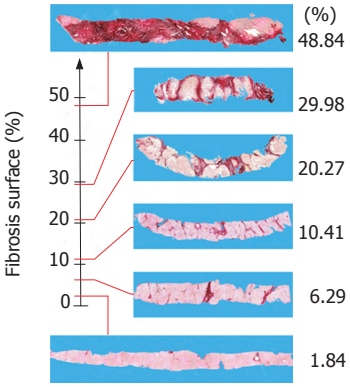

Figure 3 Trajectory of the dynamics of the fibrotic process considered as a continuous straight line going from *0%* to *48.84%* (the highest empirically observed percentage), without any jumps or abrupt swervings. The interaction of every experimental scalar expressing the state of the propositus fibrosis and the points of the geometric model gives the staging of fibrogenesis.

Δ was 225.21±38.69% due to the rectification, which included most of the fine, irregular particulars escaping the IS meter, thus making the result very close to reality. In this study, we only used the measurements corrected using the fractal dimension. The scalars indicating the length of the perimeters of fibrosis in each of the sections of the 209 bioptic samples fell within a range that was only closed at the zero point because the maximum value was not defined and could theoretically be greater.

Area measurements

The area of fibrosis (A_C) defined the sum of the areas of the Sirius Red-stained collagen islets measured using the IS meter. The fractal area of fibrosis (A_{CF}) was the sum of the areas of Sirius Red-stained collagen islets measured using the fractal-rectified meter. Both were expressed as a percentage of the total true area. The minimum and maximum values of A_C were 1.01% and 48.47% of the specimen area, the corresponding A_{CF} values were 1.34% and 48.84%. In this case, although statistically significant ($P<0.005$), the Δ(6.61%±4.79%) was small because histological sections were planar and the fractal measure of area depended only on its irregular contour. The scalars indicating the extent of the area of fibrosis in each of the sections of the 209 bioptic samples also fell within a range that was only closed at the zero point because the maximum value was not yet defined and could theoretically be greater.

Fibrosis staging of histological section

We constructed a geometrical model of the set of all states of ECM deposition on the line of real numbers as their state space using the scalars obtained from the fibrosis measured in our biopsies. The α (start) of the fibrotic process was fixed at 0% and the ω (end) at 48.84% of the area of the section (Figure 3). This model could represent a conventional interpretation of the ideal path that could be covered by potential fibrosis deposition in liver tissue. The staging observed in the histological section under examination was given by the relationship between the scalar expressing the actual fibrotic state of the section and the point indicated by this geometric model.

Classification of collagen islets

During the course of chronic hepatitis, fibrosis appeared under the control of stellate cells in the form of thin

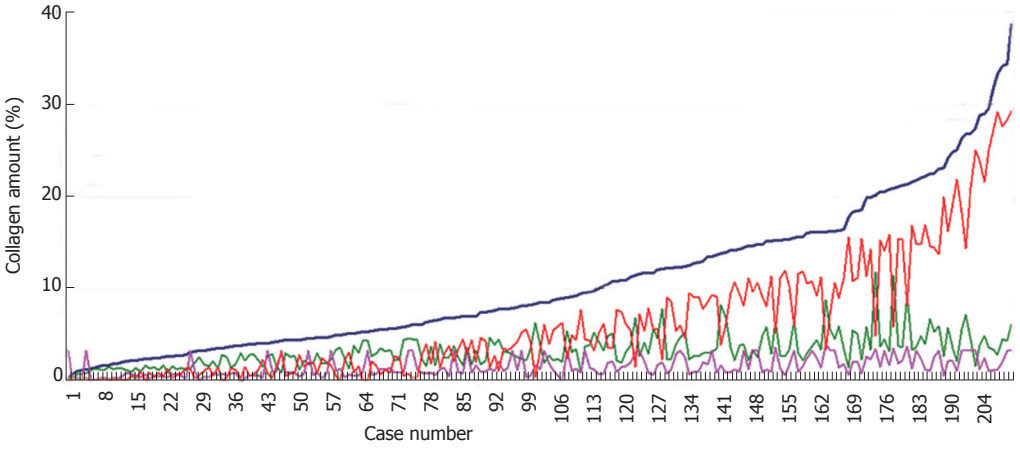

Figure 4 Comparative analysis of Markovian sequence of the amount of fibrosis, and the three sequences expressing the classes of magnitude of the collagen islets identified in 209 needle biopsy specimens. (1). Markovian sequence of the total amount of fibrosis in a histological biopsy section (blue line); (2). Percentage of collagen islets with a magnitude of 10^4-10^6 μm^2 (red line); (3). Percentage of collagen islets with a magnitude of 10^3-10^4 μm^2 (fuchsia line); (4). Percentage of collagen islets with a magnitude of 10^1-10^3 μm^2 (green line).

fibers that tended to grow in width and length within the portal space, around these structures and the central veins, and along the capillarised sinusoidal network. The three-dimensional interconnections of these collagen structures led to the formation of a fibrous network in which irregular meshes appeared as a set of collagen islets on different magnitudes on planar histological sections.

The logarithmic distribution of this set of 2.8 million collagen islets from 209 cases showed that it could be divided into three classes of elements of different magnitude: the collagen islets of 10-10^3 μm^2, those of between 10^3 and 10^4 μm^2, and those between 10^4 and 10^6 μm^2. All the histological sections contained islets with these classes of metrical values. In order to clarify the meaning of their presence, we first ordered the results of the fibrosis surface areas and constructed them in function of their magnitude as a Markovian curve (Figure 4).

The values of the islets belonging to the three subclasses in each bioptic section were plotted on the basis of the order of a Markovian curve, which generated the three irregular curves formed by the sets of islets belonging to each subclass. The fractal dimension of these curves showed that the Markovian reference curve had a fractal dimension of 1.1, whereas the curves of the three subclasses of the largest, medium-sized and smallest islets were respectively 1.9, 1.99 and 1.95. Fractal geometry suggested that the high fractal dimensions of the collagen islet subclasses could describe the instability of the collagen structure as it passed towards more stable fibrotic states[33].

Collagen area metric and semi-quantitative evaluations

The relationships between our measurements of fibrosis, the semi-quantitative Knodell histology activity index, and Sheuer, Ishak and METAVIR scores were investigated by comparing the portraits of each category of elements obtained by labeling the different semi-quantitative values on a geometric model using the line of real numbers as state space (Figure 5). The overlapping metric measures showed that samples with very similar metric surface areas fell into different categories while specimens with different metric surface areas fell into similar categories. Incidentally, our results reinforced the criticism by Rousselet *et al*[39] who have recently criticized the METAVIR system for evaluating fibrosis.

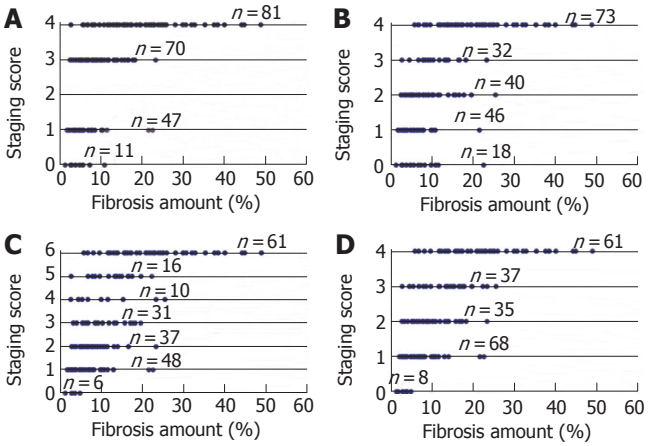

Figure 5 Comparison of the phase portraits obtained using the scalar values of the rectified areas of fibrosis projected onto the state spaces of each Knodell HAI (**A**), Sheuer (**B**), Ishak (**C**), and METAVIR category (**D**). All the graphs highlight the considerable overlapping of the data referring to different categories.

Wrinkledness

Wrinkledness (W), a typical characteristic of all natural fractal objects[11], could be obtained using the formula:

$$W = \frac{P_{CF} - R}{2\sqrt{\pi A_{CF}}} \qquad 6)$$

where R is the roundness coefficient of each islet.

The mean W value obtained by measuring the 209 biopsy sections was 731.3±298.72. As expected, this variable did not depend on the area of collagen (r=0.14), but was highly dependent on the length of its perimeter (r=0.80). Preliminary data showed that W was independent of the degree of necro-inflammatory activity (data not shown).

Measurement of Hurst's index

The same 209 patients provided us with H values ranging from 0.21 and 0.71. As said in the premises, we considered this index a quantitative variable of the alteration in hepatic tissue architecture. The ratio between H and the extension of the area of fibrosis indicated that the increased fibrotic area could lead to an extended loss of the natural harmony of this architecture (r=-0.81).

Table 1 Intra-sample variability in the area and wrinkledness of fibrosis

Patient number	*n*	A_{CF}(%)	CV	W	CV	H	CV
1	30	5.97±4.95	0.83	788.63±590.48	0.75	0.51±0.14	0.27
2	30	9.77±2.64	0.27	830.52±124.93	0.15	0.475±0.04	0.08
3	30	20.15±5.51	0.27	69±140.88	0.18	0.38±0.03	0.09

Note: Patient No.1 = Without pathology; Patient No.2 = Chronic hepatitis with intial fibrosis; Patient No.3 = Cirrhosis; *n* = number of sequential sections; A_{CF} = Fractal fibrosis area; CV = Coefficient of variability (standard deviation/mean); H = Hurst' exponent.

Intra-sample variability in area, wrinkledness and Hurst's exponent of fibrosis

In order to define the usefulness of generating numbers (or other kinds of invariants) to label the investigated structures in such a way that those with the same label could be considered alike and those with different labels could be considered different, the irregular tectonics of fibrosis was investigated in 30 sections taken at equal intervals from two patients with different degrees of disease severity and one was considered normal. The data (Table 1) showed the highly multifarious areas and wrinkledness of the collagen islets in the different sections. However, the Hurst's exponent was found less variable.

Inter-sample variability in area and wrinkledness of fibrosis

There was a high degree of inter-sample variability in the area (CV = 41%), outline perimeter (CV = 61%), and wrinkledness of fibrosis (CV = 38%). The inter-sample variability in Hurst's exponent was less (CV = 13%).

DISCUSSION

We have described a purely quantitative method of assessing liver fibrosis based on the theory of measure, which is the point of departure of all our concrete knowledge of the physical world, and the main reference for the construction of predictive and monitoring models[40].

During this study, our first difficulty was to measure the collagen islets making up liver fibrosis using standard metrics, because their irregularity excluded them from Euclidean geometry, which was created to describe smooth objects. Collagen islets can therefore only be measured using the principles of fractal mathematics and geometry[7-11].

Unlike the regular objects of Euclidean geometry, fractal objects do not have a single measure because it changes at every scale of observation as the result of the appearance of details that are imperceptible at lower magnifications, thus measurements have to be made at a well-defined scale[41].

The second difficulty was to identify the epistemological difference between the meanings of quantitative metric measures and the definition of a diagnosis of fibrosis in chronic inflammation or its progression to cirrhosis, which could be considered a radically different clinical condition. After making numerous experiments with our computer program, to analyze entire Sirius red-stained biopsy sections we established that the most favorable magnification was 200×, thus this magnification was used to digitize the microscope images.

After this methodological study, which considered the process of fibrogenesis as nothing rather than a physical phenomenon, we asked ourselves three basic questions, namely what have we learned about the meaning of liver tissue fibrosis? what new knowledge have we acquired after having measured the new canons of liver tissue architecture and classified their changes with scalars? and how much can these new notions be used in clinical practice to discriminate the progression or regression of fibrosis?

The first new notion was to extend the concept of the fractal dimension to metric measurements that might closely approximate the real magnitude of the irregular objects under observation.

Sensu stricto, the results of the intra-sample behavior and inter-sample variability study showed the non-representativeness of the perimeter and areas of fibrosis: the former due to its dependence on the extension of the bioptic specimen, and the latter for the high variability of the distribution of the inflammation process in the organ.

We added the staging of the evolution of ECM deposition towards stages of non-tolerability using the scalars obtained from the two-dimensional measurements of the area of the fibrotic mass. Although hardly representative and no more than a resonance of the mesomorphic process taking place in the environment, this information has some clinical interest if only as a very generic quantitative portrait of the general condition of the liver.

The quantitative relationships between the edge-interior of the fibrosis mass generated the new concept of its wrinkledness.

The collagen islets were categorized into three classes on the basis of the magnitude of their areas, which provided clues to their state of instability that indicated the activity of the fibrogenetic process. High presence of islets belonging to these subclasses according to the fractal geometry, is a signal of collagen structure instability in transition towards more stable states.

The distribution of the quantitative values of the areas covered by fibrosis in each category of the four semi-quantitative methods of evaluation clearly and simply confirmed the unreliability of the semi-quantitative systems themselves. This inadequacy could also be seen even when the histological preparations were analyzed by expert hepato-pathologists whose experience encompasses a large number of observed cases.

Interest in the collagen/parenchyma ratio led us to recognize the canons (mathematical laws) governing the natural "harmonic state of liver tissue", by which the order that characterizes its organized fibrous and parenchymal components (considered prime bodies) in such a way can provide a definition of the natural histological architecture of liver tissue. This can be defined in two dimensions on the basis of the extension of the metric spaces covered by fibrous tissue (no more than 3%) and the parenchyma (97%). It can be intuitively understood

that altered proportions between these spaces disrupt the natural harmonic state by creating disorder in the natural lobular structure of the liver tissue. In this sense, the words "measure" and "architectural alteration" in Ishak' s classical semi-quantitative definition (1995) …"[Staging] … is a measure of fibrosis, and architectural alteration, i.e. structural progression of the disease…" really indicate a rigorous metric value, and the term architectural alteration of this definition acquires the consistency of a measurable, scientific variable of state.

In order to quantify the architectural alteration, we used Hurst's exponent, and analysis of its variability gave the following promising results: the least variability in thirty sequential sections (intra-sample variability), the greatest representativeness in six samples of hepatic tissue obtained from different parts of the liver (it was not possible to speak of lobes because of the advanced structural alterations induced by cirrhosis). This last result is currently further investigated in our laboratories.

In conclusion, although a number of serum fibrosis markers have been discordantly proposed[1-5,42-46], the results of this study strongly underline the primary role of liver biopsy in the qualitative diagnosis of chronic liver disease and its usefulness in evaluating fibrosis in a metrically rigorous manner. The use of quantitative descriptors of irregularly-shaped fibrosis should shed new insights into the dynamics of viral and non-viral liver diseases. We are concentrating on the clinical use of Hurst's exponent after antiviral drug treatment as it can quantitatively demonstrate a drug's effect on fibrosis with a very low error.

REFERENCES

1 **Poynard T**, Imbert-Bismut F, Munteanu M, Messous D, Myers RP, Thabut D, Ratziu V, Mercadier A, Benhamou Y, Hainque B. Overview of the diagnostic value of biochemical markers of liver fibrosis (FibroTest, HCV FibroSure) and necrosis (ActiTest) in patients with chronic hepatitis C. *Comp Hepatol* 2004; **3**: 8

2 **Rosenberg WM**, Voelker M, Thiel R, Becka M, Burt A, Schuppan D, Hubscher S, Roskams T, Pinzani M, Arthur MJ. Serum markers detect the presence of liver fibrosis: a cohort study. *Gastroenterology* 2004; **127**: 1704-1713

3 **Patel K,** Gordon SC, Jacobson I, Hezode C, Oh E, Smith KM, Pawlotsky JM, McHutchison JG. Evaluation of a panel of non-invasive serum markers to differentiate mild from moderate-to-advanced liver fibrosis in chronic hepatitis C patients. *J Hepatol* 2004; **41**: 935-942

4 **Imbert-Bismut F,** Ratziu V, Pieroni L, Charlotte F, Benhamou Y, Poynard T. Biochemical markers of liver fibrosis in patients with hepatitis C virus infection: a prospective study. *Lancet* 2001; **357**: 1069-1075

5 **Lu LG**, Zeng MD, Wan MB, Li CZ, Mao YM, Li JQ, Qiu DK, Cao AP, Ye J, Cai X, Chen CW, Wang JY, Wu SM, Zhu JS, Zhou XQ. Grading and staging of hepatic fibrosis, and its relationship with noninvasive diagnostic parameters. *World J Gastroenterol* 2003; **9**: 2574-2578

6 **Rose S.** What is wrong with reductionist explanations of behaviour? *Novartis Found Symp* 1998; **213:** 176-186; discussion 186-192, 218-221

7 **Dioguardi N**, Grizzi F, Bossi P, Roncalli M. Fractal and spectral dimension analysis of liver fibrosis in needle biopsy specimens. *Anal Quant Cytol Histol* 1999; **21**: 262-266

8 **Grizzi F**, Dioguardi N. A fractal scoring system for quantifying active collagen synthesis during chronic liver disease. *Int J Chaos Theo Appl* 1999; **2-3**: 39-44, 1999

9 **Dioguardi N**, Grizzi F. Fractal dimension exponent for quantitative evaluation of liver collagen in bioptic specimens. In "Mathematics and Biosciences in interaction" ,Basel, Boston, Berlin: Birkhauser Press, 2001: 113-120

10 **Dioguardi N**, Franceschini B, Aletti G, Russo C, Grizzi F. Fractal dimension rectified meter for quantification of liver fibrosis and other irregular microscopic objects. *Anal Quant Cytol Histol* 2003; **25**: 312-320

11 **Dioguardi N**, Franceschini B, Russo C, Grizzi F. Computer-aided morphometry of liver inflammation in needle biopsies. *World J Gastroenterol* 2005; 11: 6995-7000

12 **Kleiner DE**. The liver biopsy in chronic hepatitis C: a view from the other side of the microscope. *Semin Liver Dis* 2005; **25**: 52-64

13 **Desmet VJ**. Liver tissue examination. *J Hepatol* 2003; **39 Suppl 1**: S43-S49

14 **Bravo AA**, Sheth SG, Chopra S. Liver biopsy. *N Engl J Med* 2001; **344**: 495-500

15 **Brunt EM**. Liver biopsy interpretation for the gastroenterologist. *Curr Gastroenterol Rep* 2000; **2**: 27-32

16 **Brunt EM**. Grading and staging the histopathological lesions of chronic hepatitis: the Knodell histology activity index and beyond. *Hepatology* 2000; **31**: 241-246

17 **Desmet V**, Fevery J. Liver biopsy. *Baillieres Clin Gastroenterol* 1995; **9**: 811-828

18 **Knodell RG**, Ishak KG, Black WC, Chen TS, Craig R, Kaplowitz N, Kiernan TW, Wollman J. Formulation and application of a numerical scoring system for assessing histological activity in asymptomatic chronic active hepatitis. *Hepatology* 1981; **1**: 431-435

19 **Scheuer PJ**. Classification of chronic viral hepatitis: a need for reassessment. *J Hepatol* 1991; **13**: 372-374

20 **Ishak K**, Baptista A, Bianchi L, Callea F, De Groote J, Gudat F, Denk H, Desmet V, Korb G, MacSween RN. Histological grading and staging of chronic hepatitis. *J Hepatol* 1995; **22**: 696-699

21 **Bedossa P**, Poynard T. An algorithm for the grading of activity in chronic hepatitis C. The METAVIR Cooperative Study Group. *Hepatology* 1996; **24**: 289-293

22 **Kage M**, Shimamatu K, Nakashima E, Kojiro M, Inoue O, Yano M. Long-term evolution of fibrosis from chronic hepatitis to cirrhosis in patients with hepatitis C: morphometric analysis of repeated biopsies. *Hepatology* 1997; **25**: 1028-1031

23 **Masseroli M**, Caballero T, O'Valle F, Del Moral RM, Perez-Milena A, Del Moral RG. Automatic quantification of liver fibrosis: design and validation of a new image analysis method: comparison with semi-quantitative indexes of fibrosis. *J Hepatol* 2000; **32**: 453-464

24 **Pilette C**, Rousselet MC, Bedossa P, Chappard D, Oberti F, Rifflet H, Maiga MY, Gallois Y, Cales P. Histopathological evaluation of liver fibrosis: quantitative image analysis vs semi-quantitative scores. Comparison with serum markers. *J Hepatol* 1998; **28**: 439-446

25 **Wright M**, Thursz M, Pullen R, Thomas H, Goldin R. Quantitative versus morphological assessment of liver fibrosis: semi-quantitative scores are more robust than digital image fibrosis area estimation. *Liver Int* 2003; **23**: 28-34

26 **O'Brien MJ**, Keating NM, Elderiny S, Cerda S, Keaveny AP, Afdhal NH, Nunes DP. An assessment of digital image analysis to measure fibrosis in liver biopsy specimens of patients with chronic hepatitis C. Am J Clin Pathol 2000; **114**: 712-718

27 **Mandelbrot BB** The fractal geometry of the nature: S. Francisco: Freeman, 1982

28 **Perrin J**. La discontinuité de la matière. *Revue du Mois* 1906; **1**: 323-344

29 **Hausdorff F**. Dimension and ausseres. *Mathematishe Annalen* 1919; **LXXIX**; 157-179

30 **Richardson L**. The problem of contiguity: an appendix of statistics of deadly quarrels *General Systems Yearbook* 1961; **6**: 139-187

31 **Rigaut JP**, Schoevaert-Brossault D, Downs AM, Landini G. Asymptotic fractals in the context of grey-scale images. *J Microsc* 1998; **189 (Pt 1):** 57-63

32 **Ruebner BH**. Collagen formation and cirrhosis. *Semin Liver Dis* 1986; **6**: 212-220

33 **Bassingthwaighte JB**, Liebovitch LS, West BJ: Fractal physiology. New York: Oxford University Press, 1994
34 **Hastings HM**, Sugihara G. Fractals. A User's Guide for the Natural Sciences. Oxford: Oxford Science Publications, 1993
35 **Junqueira LC**, Bignolas G, Brentani RR. Picrosirius staining plus polarization microscopy, a specific method for collagen detection in tissue sections. *Histochem J* 1979; 11: 447-455
36 **Hurst HE**. Long-term storage capacity of reservoirs. *Trans Amer Soc Civ Eng* 1951 ; **116**: 770-808
37 **Hurst HE**, Black RP, Simaiki YM. Long-term storage: an experimental study. London: Constable, 1965
38 **Bassingthwaighte JB**, Raymond GM. Evaluation of the dispersional analysis method for fractal time series. *Ann Biomed Eng* 1995; **23**: 491-505
39 **Rousselet MC**, Michalak S, Dupre F, Croue A, Bedossa P, Saint-Andre JP, Cales P. Sources of variability in histological scoring of chronic viral hepatitis. *Hepatology* 2005; **41**: 257-264
40 **Rosen R**. Fundamentals of measurements and representation of natural systems. Amsterdam: North-Holland, 1978
41 **Nonnenmacher TF**, Baumann G, Barth A, Losa GA. Digital image analysis of self-similar cell profiles. *Int J Biomed Comput* 1994; **37**: 131-138
42 **Lu LG**, Zeng MD, Mao YM, Li JQ, Qiu DK, Fang JY, Cao AP, Wan MB, Li CZ, Ye J, Cai X, Chen CW, Wang JY, Wu SM, Zhu JS, Zhou XQ. Relationship between clinical and pathologic findings in patients with chronic liver diseases. *World J Gastroenterol* 2003; **9**: 2796-2800
43 **Tao J**, Peng HQ, Cai WM, Dong FQ, Weng HL, Liu RH. Influence factors of serum fibrosis markers in liver fibrosis. *World J Gastroenterol* 2003; **9**: 2497-2500
44 **Zheng M**, Cai WM, Weng HL, Liu RH. ROC curves in evaluation of serum fibrosis indices for hepatic fibrosis. *World J Gastroenterol* 2002; **8**: 1073-1076
45 **Rosenthal-Allieri MA**, Peritore ML, Tran A, Halfon P, Benzaken S, Bernard A. Analytical variability of the Fibrotest proteins. *Clin Biochem* 2005; **38**: 473-478
46 **Rossi E**, Adams L, Prins A, Bulsara M, de Boer B, Garas G, MacQuillan G, Speers D, Jeffrey G. Validation of the FibroTest biochemical markers score in assessing liver fibrosis in hepatitis C patients. *Clin Chem* 2003; **49**: 450-454

S- Editor Wang J **L- Editor** Wang XL **E- Editor** Bi L

PO Box 2345, Beijing 100023, China
www.wjgnet.com
wjg@wjgnet.com

World J Gastroenterol 2006 April 14; 12(14):2195-2200
World Journal of Gastroenterology ISSN 1007-9327

BASIC RESEARCH

Comparison of protocatechuic aldehyde in *Radix Salvia miltiorrhiza* and corresponding pharmacological sera from normal and fibrotic rats by high performance liquid chromatography

Tao Lv, Xi-Xian Yao

Tao Lv, Xi-Xian Yao, Hebei Institute of Gastroenterology, Department of Gastroenterology, The Second Hospital of Hebei Medical University, Shijiazhuang 050000, Hebei Province, China
Correspondence to: Tao Lv, Hebei Institute of Gastroenterology, Department of Digestive Disease, The Second Affiliated Hospital of Hebei Medical University, No.215, Hepingxi Road, Shijiazhuang 050000, Hebei Province, China. taolv22@yahoo.com.cn
Telephone: +86-311-87222831 Fax: +86-311-87061012
Received: 2005-10-21 Accepted: 2005-12-23

Abstract

AIM: To observe the effect of protocatechuic aldehyde on the proliferation of hepatic stellate cells (HSCs).

METHODS: Liver fibrosis was induced in rats by carbon tetrachloride (CCl_4). Then normal and fibrotic drug sera were extracted from rats. The effects of protocatechuic aldehyde, raw *Radix Salvia miltiorrhiza* and drug sera of *Salvia miltiorrhiza* on HSC growth were determined by CCK-8. The protocatechuic aldehyde was separated by high performance liquid chromatography (HPLC) in a Alltima C18 column (250 mm × 4.6 mm, 5 μm) with a mobile phase of acetonitrile-4% glacial acetic acid solution (gradient elution) at the wavelength of 281 nm.

RESULTS: Protocatechuic aldehyde, raw *Radix Salvia miltiorrhiza* and drug sera of *Salvia miltiorrhiza* were found to have inhibitory effects on proliferation of rat HSCs. Raw Radix Salvia miltiorrhiza had a stronger inhibitory effect than the drug sera. The fibrotic drug sera showed a higher suppressive effect than the normal drug sera ($P < 0.05$). Protocatechuic aldehyde was found in crude materials of both *Radix Salvia miltiorrhiza* and its corresponding drug sera. The average recovery ($n = 6$) was 110.5% for raw *Salvia miltiorrhiza Bge,* 102% for normal drug sera and 105.2% for fibrotic drug sera. The relative standard deviation (RSD) was 0.37%, 1.96% and 1.51%, respectively ($n = 6$). The contents of protocatechuic aldehyde were 0.22%, 0.15% and 0.19%, respectively ($n = 6$) ($P < 0.05$). The RSD was 0.33%, 0.75% and 1.24% ($n = 6$) for raw material of *Radix Salvia miltiorrhiza,* normal drug sera and fibrotic drug sera, respectively. The samples were stable for 6 d.

CONCLUSION: Protocatechuic aldehyde can inhibit the growth of HSCs. HPLC is suitable for the determination of virtual bioactive components of Chinese herbal medicines *in vitro.*

Key words: *Radix Salvia miltiorrhiza;* Protocatechuic aldchyde; Seropharmacological method; High performance liquid chromatography

Lv T, Yao XX. Comparison of protocatechuic aldchyde in *Radix Salvia miltiorrhiza* and corresponding pharmacological sera from normal and fibrotic rats by high performance liquid chromatography. *World J Gastroenterol* 2006; 12(14): 2195-2200

http://www.wjgnet.com/1007-9327/12/2195.asp

INTRODUCTION

Radix Salvia miltiorrhiza is an important traditional Chinese medicine (TCM) for activating blood and eliminating stasis[1]. Its effects on chronic hepatic diseases, such as liver fibrosis and cirrhosis, have been proved in experiments *in vitro* (cell culture) and *in vivo* (animal experiment)[2-4]. Liver fibrosis is a necessary stage during the development of liver cirrhosis. The activation and proliferation of hepatic stellate cells (HSCs) are the critical steps in hepatic fibrogenesis[5,6]. *Radix Salvia miltiorrhiza* could markedly inhibit the activation and proliferation of HSCs. Protocatechuic aldchyde is one of the bioactive components of *Radix Salvia miltiorrhiza*, which could inhibit the proliferation of HSCs and might be one of the efficient components of *Radix Salvia miltiorrhiza* acting on HSCs.

"Traditional seropharmacological method" usually utilizes healthy animals (such as rats) as medicine takers. The effect *in vitro* can be studied by isolating the drug sera (normal drug sera) from healthy animals to clarify the functions of the components in drug sera [7]. But different functional status of liver, which is the biggest organ for biological metabolism, could lead to some differences in the conversion of the same drug. Therefore, we used rats with liver fibrosis as the drug receivers and drug serum resources in our study. The corresponding

drug sera (pathological drug sera) were drawn after oral administration of the herbs. We termed it "modified seropharmacological method".

We compared the contents of protocatechuic aldchyde in raw *Radix Salvia miltiorrhiza* in normal and fibrosis rats before and after administration. Whether this method could predict the curative effects of *Radix Salvia Miltiorrhiza* was evaluated.

MATERIALS AND METHODS

Materials

Twenty male Sprague-Dawley (SD) rats weighing 200-250 g were provided by the Laboratory Animal Center of Hebei Medical University. All rats were randomized into group A (normal rats) and group B (liver fibrotic rats), 10 in each group. The rats in group A were treated with saline, while the rats in group B were treated with 40% carbon tetrachloride (CCl_4). Hepatic fibrosis was induced in rats of group B by 40% CCl_4 4 mL/kg body weight for the first injection, then 2 mL/kg body weight, twice a week, for 9 wk.

HSC cell line was presented by Professor Greenwell, Marion Bessin Liver Research Center, Albert Einstein College of Medicine. The phenotype of *CFSC* was obtained from CCl4-cirrhotic liver of rats after spontaneous immortalization in culture.

RPMI-1640 was from GIBICO. CCl_4 was of analytical grade. *Radix Salvia miltiorrhiza* was provided by Hebei Lerentang Chinese Medicine DrugStore Co. Drug sera were drawn from rats.

Methods

Preparation of samples for HSC cultivation

Radix Salvia miltiorrhiza was ground into powder and filtered with a sieve plate. The powder was dissolved into pure RPMI-1640 media to make the concentration 15 times that of the decoction for adults (within the range of safe concentration for HSCs). Then the dissolution was filtered to remove the bacteria for HSC cultivation.

SD rats weighing 200-250 g were randomized into group A and group B, 10 in each group. Liver fibrosis was induced in rats of group B by 40% CCl_4, 4 mL/kg body weight first, then by 2 mL/kg body weight, twice a week, for 9 wk. The rats in group A were treated with saline. The decoction of *Radix Salvia miltiorrhiza* was administrated to all rats for 5 d. The quantity of raw *Radix Salvia miltiorrhiza* in solution was 1.33 g/mL. Blood was drawn from inferior vena cava 2 h after the drugs were given on the fifth day. Then drug sera were obtained by centrifugation at 3000 r/min for 20 min at 4 ℃. The sera were deactivated at 56 ℃ for 30 min. Then the drug sera were dissolved in RPMI-1640 to obtain 10% drug sera-1640 medium for analysis.

Detection of inhibitory rate of protocatechuic aldchyde, raw Radix Salvia miltiorrhiza and drug sera of Salvia miltiorrhiza on HSC growth by CCK-8

Cell suspension (100 μl) was incubated on a 96-well plate. When HSCs grew to 90% confluence they were incubated in pure RPMI-1640 overnight to synchronize HSCs into the G_0 period. The solutions of protocatechuic aldchyde, raw *Radix Salvia miltiorrhiza* and the corresponding 10% normal and fibrotic drug sera-1640 media in the wells were changed. The results were obtained. A group of controls was set at the same time. One hundred microliters of CCK-8 solution were added to each well of the plate after the drug sera were allowed to work for 24 h. Then the plate was incubated for 4 h. The absorbance (A) at 450 nm was measured with a microplate reader. The inhibitory rates (IR) of all solutions on the growth of HSCs were calculated (IR = experiment group-control group /control group×100%).

Systems for HPLC

Waters 810 controller, Waters 486 tunable absorbance detector, Waters 510 HPLC pump, Millipore Waters U6K, Waters system interface module, Waters baseline 810 chromatography workstation (America) were used for HPLC. Sep-Park C18 purification column, ultrafree-MC filters (10000 NMWL filter unit) and Autoscience ultrasonic producer were all from Millipore Corporation, America. Standard of protocatechuic aldchyde (NO. 110810-200205), glacial acetic acid and methanol were all special for HPLC. All reagents used in HPLC were filtered and deprived of vapor by ultrasound.

Preparation of samples for HPLC

Radix Salvia miltiorrhiza (100 g) was ground into powder and filtered with a sieve plate. The powder of *Radix Salvia miltiorrhiza* was put into a volumetric flask containing methanol. Then ultrasound was used to facilitate the dissolution of the powder for 5 min and methanol was added to obtain 100 mL solution. This solution was then filtered through filters with 0.45 μm Millipore, purified by Sep-Park C18 column, and repeatedly filtered through Ultrafree-MC filters. Finally, the filtered solution was used as samples of raw *Radix Salvia miltiorrhiza* and kept in darkness at 4 ℃.

Samples of Radix Salvia miltirrhiza drug sera (normal and fibrotic drug sera)

The preparation of drug sera was the same as that of the sera for HSC cultivation. After the drug sera were obtained by centrifugation at 3000 r/min for 20 min at 4 ℃, acetonitrile was mixed with the sera to get rid of protein by centrifugation. Then the supernatant was filtered through filters with 0.45 μm Millipore, purified by Sep-Park C18 column, and filtered through filters. Finally, the filtered solutions were kept in darkness at 4 ℃.

Parameters of HPLC

The parameters for HPLC included: HPLC column: Alltima C18 column (250 mm × 4.6 mm, 5 μm); velocity of flow: 0.5 mL/min; detection wavelength: 281 nm; temperature for HPLC column: 30 ℃; mobile phase: A: acetonitrile; B: 4% glacial acetic acid; gradient elution: A-B (2:98): 0-10min; A-B (10:90): 10-26 min.

Linear relation

Protocatechuic aldchyde (4.125 mg) was added into a volumetric flask. Then methanol was used to dissolve the powder to a final volume of 100mL (final concentration was

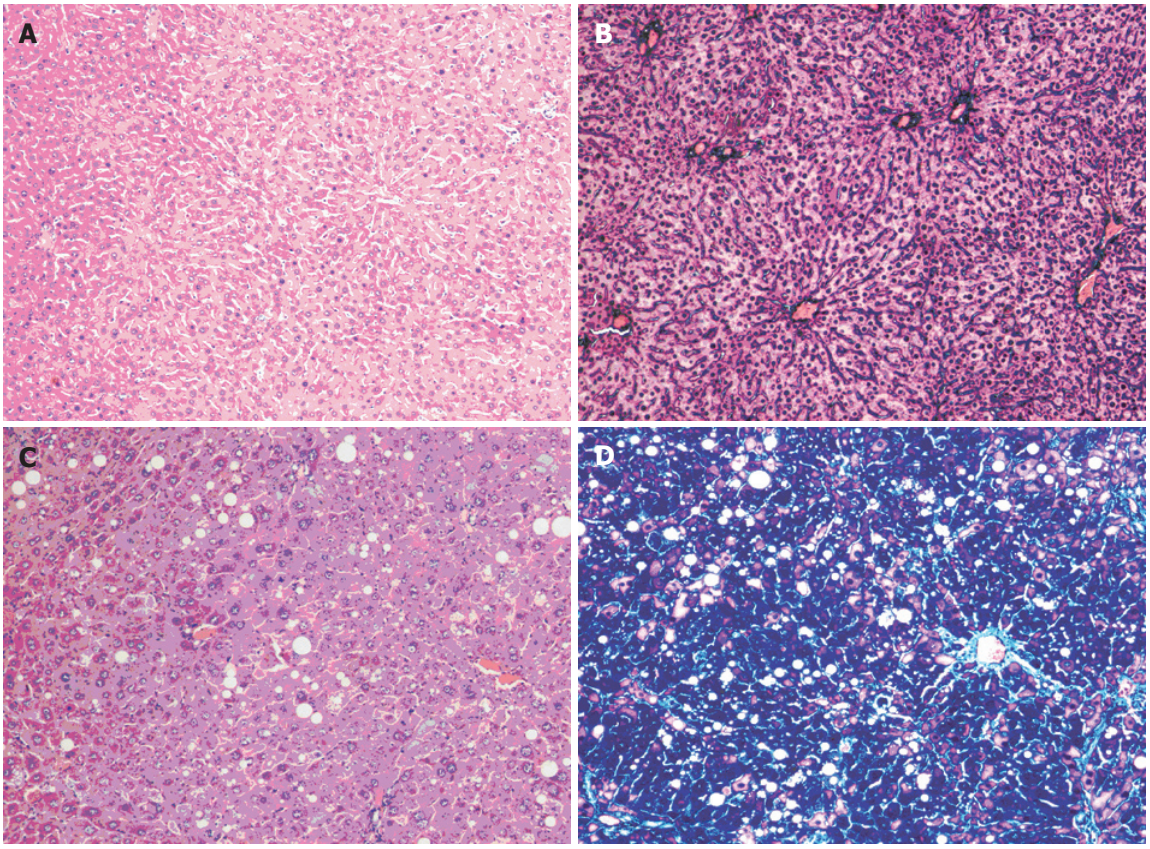

Figure 1 Healthy liver tissue of rats of group A (**A**, **B**) and fibrotic liver tissue of rats of group B (**C**, **D**). **A** and **C** (HE, 100×); **B** and **D** (Masson, 100×).

0.04125 mg/mL). Afterwards, 2, 5, 8, 10, 12, 15, 18 and 20 μL of protocatechuic aldchyde standard solution were injected into U6K for detection. Each volume was detected 3 times by HPLC under the conditions as described above. The standard curve was plotted with X axis (μg) to Y axis (mv.min).

Experiment of exactitude and evaluation of stability of samples

For the experiment of exactitude, 10 μL of protocatechuic aldchyde standard solution (41.25 μg/ml) was injected into U6K for detection. The detection was repeated 6 times, 10 μL for each time. Then the relative standard deviation (RSD) of the peak areas was calculated to evaluate the exactitude of the experiment.

For the experiment of stability, the same volume of standard solution was injected into U6K for detection, 6 times each day for 9 d. The RSD of the peak areas each day was calculated to evaluate the stability of the samples during the 9 d.

Experiment of recovery rate

In brief, 0.05 mg of protocatechuic aldchyde was put into 25 mg powder of raw *Salvia miltiorrhiza*. Then the samples for research were injected into U6K for detection. The average recovery rate ($n = 6$) was calculated.

Six samples of drug sera (400 μL for each sample) were taken out and 10 μL of protocatechuic aldchyde standard solution (0.04125 mg/mL) was dispensed into each sample of drug sera. Then the products were detected by HPLC ($n = 6$) to calculate the average recovery.

Experiment of repeatability

Radix Salvia miltiorrhiza (100 mg) was disposed as in preparation of samples of raw *Radix Salvia miltiorrhiza*. Then the samples were detected by HPLC for the content of protocatechuic aldchyde ($n = 6$). The detection was repeated 6 times independently. RSD of the peak areas was calculated to evaluate the repeatability of the experiment.

Four hundred μL of a certain drug serum was disposed as in preparation of samples of drug sera. The samples were detected for the content of protocatechuic aldchyde by HPLC ($n = 6$). RSD of the peak areas was calculated to evaluate the repeatability of the experiment.

The content of protocatechuic aldchyde in samples was detected by HPLC.

Statistical analysis

SPSS 10.0 was used to perform χ^2 test and $P < 0.05$ was considered statistically significant.

RESULTS

Obvious proliferation of fibers appeared in the livers when the rats in group B (Figures 1C and 1D) were treated with 40% CCl_4 for 9 wk. There were obvious signs of vacuole degeneration, lobular inflammation and necrosis in the tissues of fibrotic liver. No evident changes appeared in the rat liver of group A (Figures 1A and 1B).

It showed that protocatechuic aldchyde, raw *Radix Salvia miltiorrhiza*, the corresponding normal and fibrotic drug sera could all inhibit the proliferation of HSCs compared with blank control group ($P < 0.05$). The raw *Radix Salvia*

Table 1 Inhibitory rates of protocatechuic aldchyde, raw Radix Salvia miltiorrhiza and corresponding normal and fibrotic drug sera on proliferation of HSCs

Group	IR (%)	A
A (Protocatechuic aldchyde)	24.36	1.565±0.08[a]
B (raw Radix Salvia miltiorrhiza)	36.10	1.322±0.10[a]
C (Normal drug sera of Salvia miltiorrhiza)	16.14	1.735±0.12[ab]
D (Fibrotic drug sera of Salvia miltiorrhiza)	21.41	1.626±0.53[ab]
E (Control)	–	2.069±0.37

[a]$P < 0.05$ *vs* group E; [b]$P < 0.05$ *vs* group D

IR = (experiment group–control group) ÷ control group × 100%.

miltiorrhiza had a stronger inhibitory effect than the corresponding drug sera. The fibrotic drug sera of *Salvia miltiorrhiza* from fibrotic rats showed a higher suppressive effect on HSC growth than the normal drug sera from healthy rats ($P < 0.05$) (Table 1). The contents of protocatechuic aldchyde showed a nice linearity within the range of 0.1-0.8 μg ($Y=2.14\times10^4X+2.77$, $r=0.9999$).

Protocatechuic aldchyde standard solution was detected 6 times. The RSD was 0.33% for the peak areas of protocatechuic aldchyde. Within the 9 d of observation, the peak areas of protocatechuic aldchyde in standard solutions did not change significantly in the first 6 d. The RSD was 0.45% ($n=6$) for the peak areas of protocatechuic aldchyde in the first 6 d. It indicated that the solutions of standards could be kept in darkness at 4 ℃ for 6 d.

The average recovery of raw *Radix Salvia miltiorrhiza* was 110.5%. RSD was 0.37% ($n=6$). The average recovery of drug sera of *Salvia miltiorrhiza* was 102%, and the RSD was 1.96% ($n=6$). The average recovery of fibrotic drug sera was 105.2%, and the RSD was 1.51% ($n=6$).

Protocatechuic aldchyde in raw *Radix Salvia miltiorrhiza* was 0.22%, and the RSD was 0.33% ($n=6$). The ratio of protocatechuic aldchyde in normal drug sera was 0.15%, and the RSD was 0.75% ($n=6$). The ratio of protocatechuic aldchyde in fibrotic drug sera was 0.19% and the RSD was 1.24% (Table 2, Figures 2A-2C).

Table 2 Results of sample determination (mean±SD, %)

Group	Content of protocatechuic aldehyde
Salvia miltiorrhiza Bge	0.22±0.07
Normal drug sera of Salvia miltiorrhiza Bge	0.15±0.01[a]
Fibrotic drug sera of Salvia miltiorrhiza Bge	0.19±0.01[a c]

[a]$P < 0.05$ *vs* Salvia miltiorrhiza Bge; [c]$P < 0.05$ *vs* Normal drug sera of Salia miltiorrhiza Bge.

DISCUSSION

Radix Salvia miltiorrhiza is the dried root of labiate-*Salvia miltiorrhiza Bge,* an important drug in traditional Chinese medicine for activating blood flow and eliminating stasis. *Radix Salvia miltiorrhiza* has certain curative effect on coronary heart diseases and chronic liver diseases with few adverse effects. No ideal anti-fibrosis drugs in Western medicine have been developed so far. A series of blood-activating and stasis-eliminating Chinese medicines such as *Radix Salvia miltiorrhiza*, have a positive effect on prevention and reversion of fibrogenesis. However, it is difficult to clarify the working mechanism and real active components of Chinese anti-fibrosis herbs. *Radix Salvia miltiorrhiza* can improve liver function and ameliorate hepatic pathological changes in rats and humans. In our study, when the aqueous extract of *Radix Salvia miltiorrhiza* was given to rats before the injection of CCl_4, liver fibrosis was produced. On the other hand, in cell culture *in vitro*, *Radix Salvia miltiorrhiza* showed its inhibitory effect on lipid peroxidation and some key signal transduction circuits in HSCs, delaying the activation and proliferation of HSCs. A kind of extract from *Radix Salvia miltiorrhiza*-monomer IH764-3 could activate caspase-3 and induce apoptosis of HSCs.

Many bioactive components in *Radix Salvia miltiorrhiza*, including soluble and insoluble parts have various pharmacological effects such as blood-activating and stasis-eliminating and facilitate the circulation of blood and oxygen. The insoluble components mainly include compounds of phenanthrenequinone (PAQ), such as tanshinones I and II cryptotanshinone and isotanshinone. The soluble components are mainly composed of phenolic acids. Salvianolic acid B[8] is one of the bioactive parts of *Radix Salvia miltiorrhiza* to inhibit the activation and proliferation of HSCs by blocking the intracellular signal transduction of transforming growth factor-β1 (TGF-β1).

Protocatechuic aldchyde is one of the water-soluble components of *Radix Salvia miltiorrhiza* and can be used to treat dysmenorrhea in gynaecology. Protocatechuic aldchyde can inhibit the proliferation of HSCs (CCK-8) *in vitro* and might be used to treat liver fibrosis. In this study, the peak areas maintained stable for 6 d. Since the stability of protocatechuic aldchyde is much better than other components (such as salvianolic acid B) in *Radix Salvia miltiorrhiza*, protocatechuic aldchyde performs the pharmacological effects for a longer time *in vivo* and *in vivo*. The content of protocatechuic aldchyde in raw *Radix Salvia miltiorrhiza* is higher than that in the corresponding drug sera, which could explain the phenomenon that the inhibitory effect of raw *Radix Salvia miltiorrhiza* was stronger than that of drug sera. It indicates that only part of metabolites of protocatechuic aldchyde in raw *Radix Salvia miltiorrhiza* could enter blood to exert pharmacological effects after metabolism *in vivo*. If crude medicines are used to work on HSCs directly *in vitro*, the pharmacological effect of the medicine would be exaggerated. On the other hand, some other herbs could perform their pharmacological effect only after decocted *in vitro* and metabolized *in vivo*, because the process of decoction and metabolism would promote the activation of the bioactive components in this kind of crude medicines. Under this condition, the herbs seem useless if they are directly used on cells *in vitro*, suggesting that the effect of raw *Radix Salvia miltiorrhiza* is not equal to

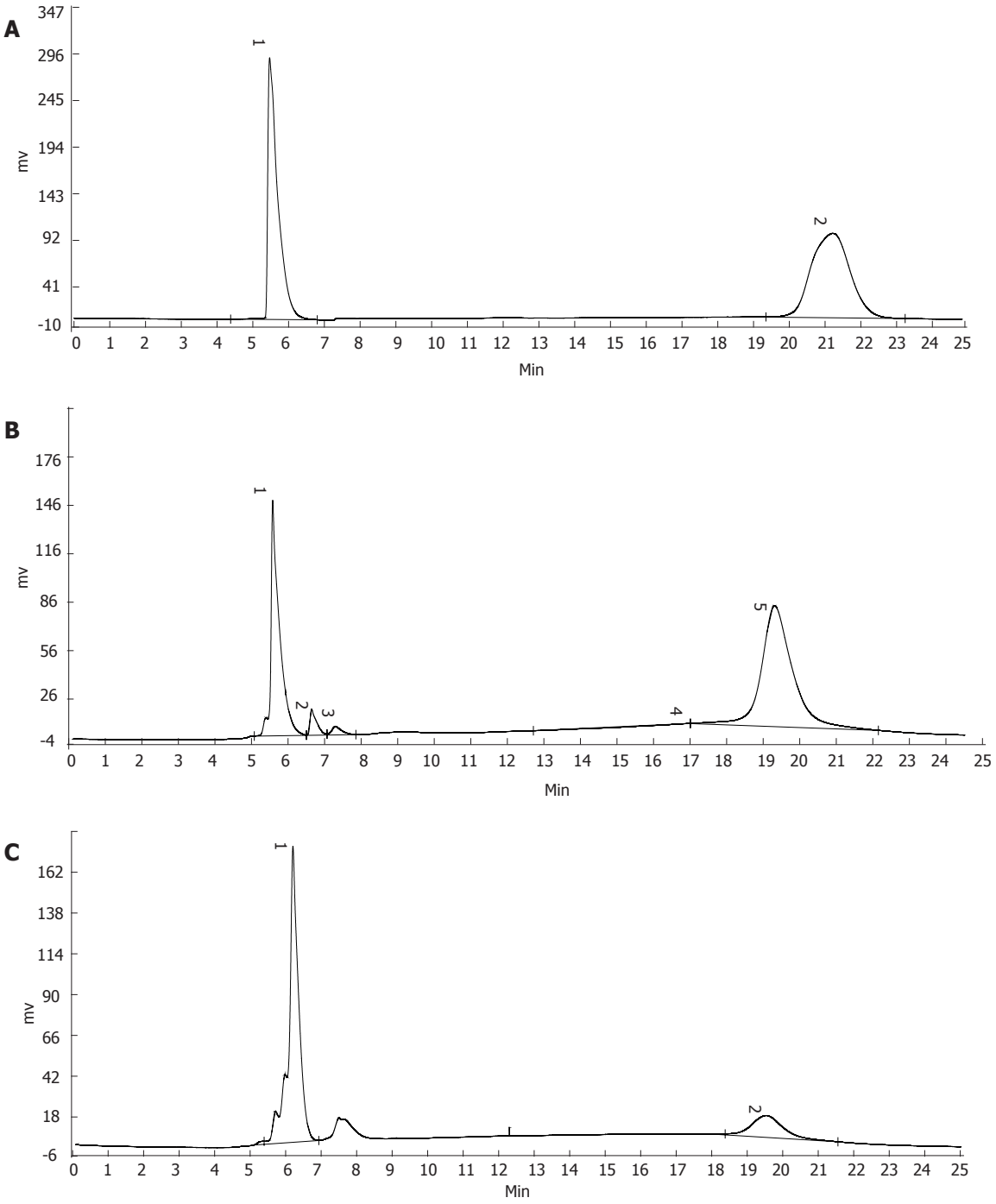

Figure 2 Chromatography of raw *salvia miltiorrhiza Bge* (**A**), pathological drug sera of *Salvia miltiorrhiza Bge* (**B**) and normal drug sera of *Salvia miltiorrhiza Bge* (**C**).

the effect of *Salvia miltiorrhiza in vivo*. The differences are related to the characteristics of herbs. Active constituents of TCM are influenced by soils, climates, growth stages, and factors *in vitro* and *in vivo*. So the "Pharmacological method" is more suitable for researching herbs.

Protocatechuic aldchyde in pathological drug sera is more than that in normal drug sera, which is in accordance with the different effects of normal and fibrotic drug sera [3]. Because of this difference between the two kinds of drug sera and the phenomenon that most of the medicine takers are patients with hepatic diseases, it is better to use "modified seropharmacological method" and " pathological drug sera" to carry out research on herbs *in vitro* (*vs* " traditional seropharmacological method" and "normal drug sera"). In this way, the impact of different liver functional status on herbs' metabolic process could be included as a parameter in experiment. The phenomenon that the content of protocatechuic aldchyde is higher in fibrotic drug sera than in normal sera, coincides with the working characteristics of herbs, which might be caused by different "first pass effect" of the liver under different liver conditions and metabolism of drugs. From the traditional Chinese medicinal theory of "diagnosis and treatment on the basis of an overall analysis of the illness and the patient's different symptoms and pathogenesis" and "bidirectional regulation", TCM works best only when

the symptoms and etiology are just their corresponding indications. *Radix Salvia miltiorrhiza* is one of the blood-activating and stasis-eliminating drugs. Liver fibrosis is considered as "blood obstruction"[9] in traditional Chinese medicine. Undoubtedly it is the indication for *Radix Salvia miltiorrhiza*. So the blood-activating and stasis-eliminating herbs such as *Radix Salvia miltiorrhiza* have better pharmacological effects on fibrotic rats. The active components in *Radix Salvia miltiorrhiza* might be activated and released more efficiently to perform stronger pharmacological effects. The ability of fibrotic liver to transform and inactivate drugs might decrease because the metabolic functions of fibrotic liver decrease, thus making the concentration of the effective components higher, prolonging the effective working period.

The value of this research lies in that we could get the real active components of *Radix Salvia miltiorrhiza* by "modified seropharmacological method" after they are metabolized *in vivo*. HPLC is a quick and sensitive method the determination of effective components in drugs *in vitro* and *in vivo*.

REFERENCES

1 **Sun J,** Huang SH, Tan BK, Whiteman M, Zhu YC, Wu YJ, Ng Y, Duan W, Zhu YZ. Effects of purified herbal extract of Salvia miltiorrhiza on ischemic rat myocardium after acute myocardial infarction. *Life Sci* 2005; **76:** 2849-2860

2 **Nan JX**, Park EJ, Kang HC, Park PH, Kim JY, Sohn DH. Anti-fibrotic effects of a hot-water extract from Salvia miltiorrhiza roots on liver fibrosis induced by biliary obstruction in rats. *J Pharm Pharmacol* 2001; **53:** 197-204

3 **Yao XX**, Lv T. Effects of pharmacological serum from normal and liver fibrotic rats on HSCs. *World J Gastroenterol* 2005; **11**: 2444-2449

4 **She SF**, Huang XZ, Tong GD. Clinical study on treatment of liver fibrosis by different dosages of Salvia injection. *Zhongguo Zhong Xi Yi Jie He Za Zhi* 2004; **24**: 17-20

5 **Vincent KJ**, Jones E, Arthur MJ, Smart DE, Trim J, Wright MC, Mann DA. Regulation of E-box DNA binding during in vivo and in vitro activation of rat and human hepatic stellate cells. *Gut* 2001; **49:** 713-719

6 **Siegmund SV**, Uchinami H, Osawa Y, Brenner DA, Schwabe RF. Anandamide induces necrosis in primary hepatic stellate cells. *Hepatology* 2005; **41**: 1085-1095

7 **Zhang QH,** Zhong B, Chen KJ. Effect of concentrated xuefu zhuyu pill on proliferation of vascular smooth muscle cells in experimental atheriosclerosis rabbits observed by serologic pharmacological test. *Zhongguo Zhong Xi Yi Jie He Za Zhi* 1996; **16:** 156-159

8 **Liu C,** Liu P, Hu Y, Zhu D. Effects of salvianolic acid-B on TGF-beta 1 stimulated hepatic stellate cell activation and its intracellular signaling. *Zhonghua Yi Xue Za Zhi* 2002; **82:** 1267-1272

9 **Yao XiX**, Xu KC. Liver fibrosis–basis and clinic. Shanghai; Shanghai Scientific and Technological Education Publishing House, 2003; 75-84

S- Editor Pan BR **L- Editor** Wang XL **E- Editor** Cao L

PO Box 2345, Beijing 100023, China
www.wjgnet.com
wjg@wjgnet.com

World J Gastroenterol 2006 April 14; 12(14): 2201-2204
World Journal of Gastroenterology ISSN 1007-9327

CLINICAL RESEARCH

Treatment of active steroid-refractory inflammatory bowel diseases with granulocytapheresis: Our experience with a prospective study

Bresci Giampaolo, Parisi Giuseppe, Bertoni Michele, Mazzoni Alessandro, Scatena Fabrizio, Capria Alfonso

Bresci Giampaolo, Parisi Giuseppe, Bertoni Michele, Mazzoni Alessandro, Scatena Fabrizio, Capria Alfonso, U.O. di Gastroenterologia, U.O. di Immunoematologia Azienda Ospedaliera-Universitaria Pisana, Pisa, Italy
Correspondence to: Giampaolo Bresci, Via A. Della Spina, 11 56125 Pisa, Italy. gbresci @ libcro. it
Telephone: +39-50-45227 Fax: +39-50-45227
Received: 2005-09-12 Accepted: 2005-10-26

Giampaolo B, Giuseppe P, Michele B, Alessandro M, Fabrizio S, Alfonso C. Treatment of active steroid-refractory inflammatory bowel diseases with granulocytapheresis: Our experience with a prospective study. *World J Gastroenterol* 2006; 12(14): 2201-2204

http://www.wjgnet.com/1007-9327/12/2201.asp

Abstract

AIM: To report our experience with the use of granulocytapheresis (GCAP) in 14 patients with active steroid-refractory inflammatory bowel disease (IBD) in order to evaluate its efficacy in achieving remission and maintaining a long lasting symptom-free period.

METHODS: The activity of the disease was evaluated by clinical activity index (CAI) and endoscopic index (EI) in ulcerative colitis (UC), while by Crohn's disease activity index (CDAI) in Crohn's disease (CD). The patients were treated using the Adacolumn™ system, an adsorption column which selectively binds to granulocytes and monocytes. One session/week of GCAP was performed for 5 wk. Steroids were stopped during apheresis.

RESULTS: All the patients completed the five-week course showing no complications. At the end of the last session, 93% of patients showed a clinical remission of the disease that persisted for 6 mo. Nine months after the end of the treatment, 60% of the cases maintained remission, while 23% of the patients were still in clinical remission after 12 mo.

CONCLUSION: Even if the number of our patients with steroid-refractory IBDs was not big, we can assert that GCAP is well tolerated and effective, especially in the first six months after the treatment, in a significant percentage of cases. The rate of sustained response drops slightly after 6 mo and significantly after 12 mo, however the absence of severe side effects can be a stimulus for further evaluating new schedules of treatment.

Key words: Granulocytapheresis; Ulcerative colitis; Crohn's disease; Steroid-refractory

INTRODUCTION

The term "inflammatory bowel disease (IBD)" usually means two similar but distinct chronic diseases of the gut: ulcerative colitis (UC) and Crohn's disease (CD) characterised by episodes of remission and exacerbation with systemic complications[1-4].

During the last 20 years the treatment of IBD has been greatly improved although it is still empirical due to its unknown aetiology[5-8]. It seems that both ulcerative colitis and Crohn's disease are multifactorial in origin. However, regardless of the cause, the final pathway of tissue damage in IBD is mediated by the cellular immune response through white blood cells in the intestinal mucosa. Corticosteroids are a mainstay of acute therapy for moderate to severe ulcerative colitis or Crohn's disease. However, up to 40% of patients do not respond to the high-dose steroid therapy. So, new therapeutic approaches are needed to improve the clinical outcome of active steroid-refractory IBD.

Classic immunosuppressant drugs like azathioprine or mercaptopurine need some weeks to exert their full activity, so they are useless during the acute phases of the disease. Moreover, newer immunosuppressants like cyclosporine A have shown only a temporary benefit and often serious side effects.

In recent years some trials have suggested that leukocytapheresis can be a useful and safe way to induce clinical remission in patients with IBD[9-11, 15]. Subsequent trials have proved that granulocytapheresis (GCAP), a technique that sequestrates much selectively granulocyte and monocyte subpopulations, is equally effective in patients with active IBD[16, 17].

Even if with a limited casuistry, we aimed at bulking the published data by referring our experience with GCAP. We analyzed the clinical, endoscopic and laboratory parameters of patients with active, steroid-refractory IBDs,

Table 1 Baseline characteristics of UC patients ($n = 8$) (mean ± SD)

Female/Male	3/5
Age (yr)	35.2±7.4
Colonic involvement	All PanUC
Disease duration (yr)	7.8±3.0
Basal CAI	10.0±3.4
Basal EI	10.5±2.5

CAI:clinical activing index;
EI: endoscopic index.

Table 2 Baseline characteristics of CD patients ($n = 6$) (mean ± SD)

Female/Male	3/3
Age (yr)	37.8±2.5
Disease location	All ileal CD
Disease duration (yr)	7.1±3.2
Basal CDAI	213.3±32.0

before and after the completion of GCAP during a follow-up period of 12 mo. This work was to get more information about the real effectiveness of GCAP in achieving remission and possibly in maintaining it.

MATERIALS AND METHODS

All the patients with UC or CD treated with GCAP in our department because of steroid-resistant IBD were followed up by monitoring clinical, laboratory and endoscopic parameters for UC.

Before admitted for GCAP, all patients signed an informed consent and underwent routine laboratory tests and basal ECG. Moreover, they were visited by a cardiologist in order to exclude serious cardiovascular diseases.

All patients received a 5-session (1 session/wk) treatment with GCAP. This was an extracorporeal procedure in which 1.8 L of blood was filtered through an Adacolumn™ (JIMRO, Takasaki, Japan). Adacolumn™ is a 335 mL capacity column filled with 35 000 cellulose diacetate beads (2 mm in diameter) that bind to granulocytes and monocytes via the CR3 receptors present on these cells. Each apheresis procedure required the addition of 1500 UI of sodium heparin as an anticoagulant. Blood was obtained by antecubital vein puncture. Methylprednisolone daily dose was progressively reduced until discontinuation in a 6-wk period (one week after the last apheresis procedure). Concomitant treatment with aminosalicylates was maintained during the treatment and follow-up at the same dosage.

In ulcerative colitis patients, the activity of the disease was evaluated by clinical activity index (CAI): Clinical remission was defined if less than 6 and endoscopic index (EI): endoscopic remission was defined if less than 4. In the subjects with Crohn's disease, the activity was measured by Crohn's disease activity index (CDAI): clinical remission was defined if less than 150.

After the end of the five-week course of granulocytapheresis and every 3 mo, each patient was visited for a clinical and endoscopic assessment, paying particular attention to the activity indices. The subjects who achieved clinical remission were followed up for 12 mo by the last session of GCAP.

Relapse was defined as an increase of clinical and endoscopic scores (CAI, EI, CDAI) more than 6, 4 or 150 respectively. Patients who were on 5-aminosalicylic acid continued this medication but no additional treatment.

Hemograms, biochemistry and coagulation were recorded during the apheresis treatment.

Statistical analysis

Data were expressed as mean ± SD if required. Student's t test for paired variables was performed. Statisticcal analyses were analysed with SPSS 11.5 (®SPSS inc. 2002).

RESULTS

We treated and followed up 14 patients (8 with ulcerative colitis and 6 with ileal Crohn's disease).

Baseline characteristics

Baseline characteristics of the 8 UC patients were mean age: 35.2±7.4 years; female/male ratio: 3:5; mean time of disease history: 7.8±3 years. All patients had an active pancolitis with a mean CAI of 10.0±3.4 at baseline and a mean endoscopic index (EI) score of 10.5±2.5 (Table 1). All the patients showed an active disease and were treated with 0.8-1 mg/kg pre d of i.v. or i.m. methylprednisolone and 2.4 g/d of oral mesalazine during the 8 wk period prior to GCAP initiation, without achieving response. None of the patients was under inmuno-supressor therapy at baseline but all of them were on mesalazine at 2.4 g/d.

Baseline characteristics of the 6 CD patients were mean age: 37.8±2.5 years; female/male ratio: 3:3; mean time of disease history: 7.1±3.2 years. All patients had an active ileal CD with a mean basal CDAI of 213.3±32.0 (Table 2).

Induction of remission in UC patients

One week after GCAP treatment, all UC patients achieved remission (Figures 1A and 1B) and stopped methylprednisolone treatment. The mean CAI decreased from 10.0 ± 3.4 to 3.5 ± 1.2 ($P < 0.001$). Also EI decreased from 10.5±2.2 to 2.6 ± 0.5 ($P < 0.001$). The mean values of CRP and ESR decreased from 32.5 ± 11.2 to 4.5 ± 4.7 mg/L ($P < 0.001$) and 48.5 ± 8.6 to 15.0 ± 2.3 mm/h respectively ($P < 0.001$) (Figures 3A and 2B).

Induction of remission in CD patients

One week after GCAP treatment, 5 out of 6 patients achieved remission (Figure 3A) and stopped methylprednisolone treatment. The mean CDAI decreased from 213.3 ± 32.0 to 135 ± 50 ($P < 0.015$). The mean CRP values decreased from 39.0 ± 12.6 to 9.5 ± 9.1 mg/L ($P < 0.01$) and ESR values from 52.3 ± 9.8 to 21.7 ± 18.0 mm/h ($P < 0.05$) (Figures 3B and 3C).

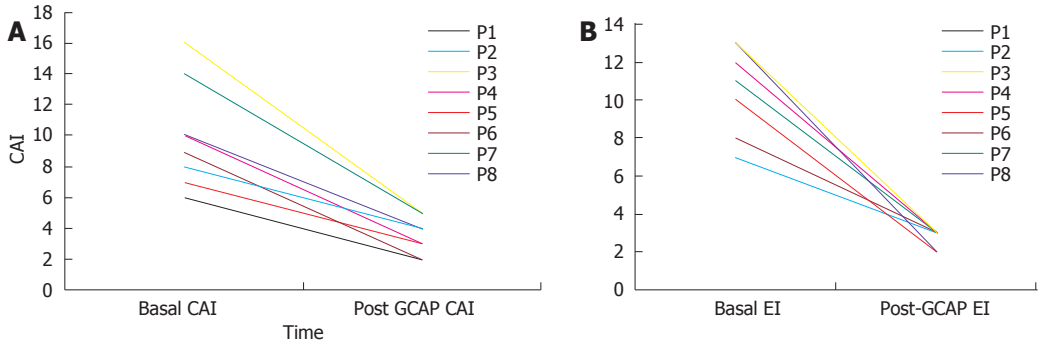

Figure 1 Evolution of CAI (**A**) and EI (**B**) in UC patients.

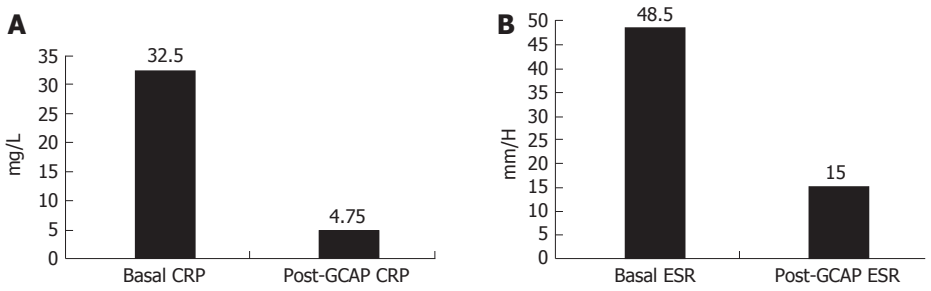

Figure 2 Mean evolution of CRP (**A**) and ESR (**B**) in UC patients.

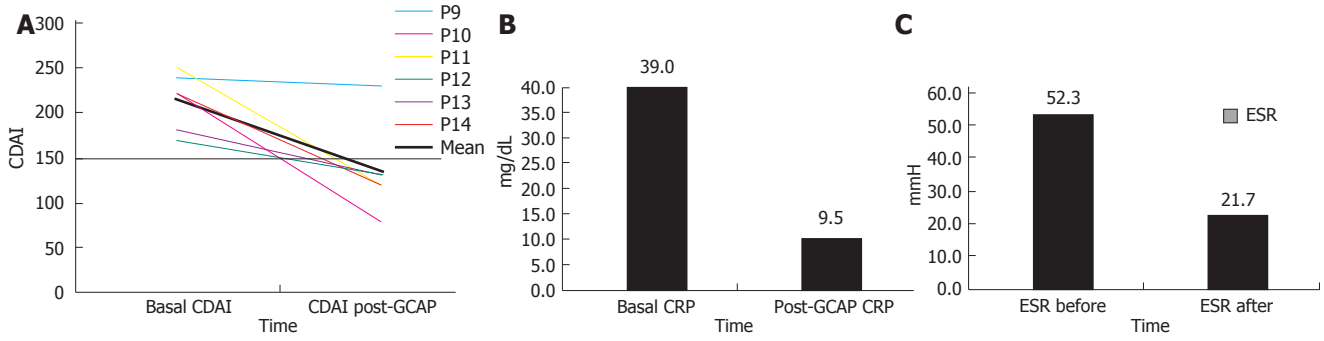

Figure 3 Mean evolution of CDAI (**A**), CRP (**B**) and ESR (**C**) in CD patients.

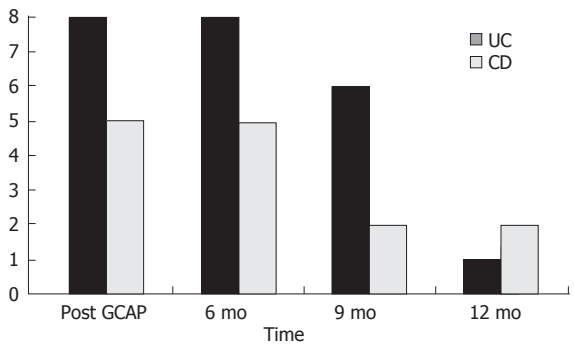

Figure 4 Remission during follow-up.

Adverse events

All the patients completed GCAP without severe side effects. Only a transient mild headache was recorded in two patients during the procedure.

Follow-up

All the patients were followed up for 12 mo after GCAP treatment and no additional treatment was added. Clinical remission persisted for 6 mo in all the patients and was achieved early after apheresis (93%). At the 9th mo of follow-up, 6 of 8 UC patients and 2 of 5 CD patients were still in clinical remission. At the 12th mo of follow-up, only 1 of 8 UC patients and 2 of 5 CD patients were in remission (Figure 4).

DISCUSSION

Currently, the use of steroid drugs is a common strategy for the treatment of acute inflammatory bowel disease. However, large doses of steroids are often necessary to control active diseases and some patients do not respond to this conventional treatment. Colectomy rate varies from 10% to 40% in these patients[12]. The treatment with cyclosporin in these patients can avoid acute colectomy in 57% of cases, but after a 6-mo follow-up period 73% of patients undergo surgery[13]. Azathioprine or 6-mercaptopurine has been reported to be beneficial for steroid resistant cases, but their use requires several weeks to get full effects[14].

Recent data from literature have pointed out that

granulocytapheresis, which acts on specific subpopulations of leukocytes involved in the inflammatory process, can represent a useful and probably much safe treatment for patients with ulcerative colitis or Crohn's disease[16, 17].

In fact it is well known that inflammatory bowel disease is associated with elevated circulating and tissue levels of leukocytes. Granulocytes are the first cells mobilizing to inflammation sites and interact with lymphocytes to orchestrate the inflammatory response. For these reasons the removal of granulocytes may be a logical therapeutic manoeuvre. Moreover, the good results obtained so far by granulocytapheresis have been attributed not only to the removal of granulocytes and monocytes, but also to its immunomodulatory effect[10, 11, 15, 16].

The goal of this study was to assess the safety and efficacy of GCAP in patients with active inflammatory bowel disease that was refractory to conventional drug therapy. In our small casuistry, the procedure was well tolerated and 93% of cases showed remission at the end of a five-week course of GCAP. No serious side effects were recorded and clinical/endoscopic remission lasted for six months in all the patients, achieved at the end of the therapeutic course ("responders"). Nine months after GCAP treatment, about 60% of responders were still in remission, without any significant difference between UC and CD patients. The remission rate dropped dramatically at the 12th mo, with slightly better outcome in CD patients.

In conclusion, this new approach to active steroid-refractory IBD seems an important innovation and a useful therapy after the failure of conventional treatments. GCAP is able to achieve clinical remission in a large proportion of "difficult" IBD patients. This new technique is virtually free of severe side effects and could be repeated more times if necessary.

We hope that our data could represent a stimulus for further trials aimed to evaluate the real usefulness of apheresis in IBD, to clarify the optimal length of treatment and to know which patients could get most benefit from it.

REFERENCES

1 **Sloan WP Jr,** Bargen JA, Gage RP. Life histories of patients with chronic ulcerative colitis: a review of 2,000 cases. *Gastroenterology* 1950; **16**: 25-38

2 **Mekhjian HS,** Switz DM, Melnyk CS, Rankin GB, Brooks RK. Clinical features and natural history of Crohn's disease. *Gastroenterology* 1979; **77**: 898-906

3 **Farmer RG**, Whelan G, Fazio VW. Long-term follow-up of patients with Crohn's disease. Relationship between the clinical pattern and prognosis. *Gastroenterology* 1985; **88**: 1818-1825

4 **Bresci G,** Parisi G, Gambardella L, Banti S, Bertoni M, Rindi G, Capria A. Evaluation of clinical patterns in ulcerative colitis: a long-term follow-up. *Int J Clin Pharmacol Res* 1997; **17**: 17-22

5 **Bresci G**, Parisi G, Bertoni M, Capria A. Long-term maintenance treatment in ulcerative colitis: a 10-year follow-up. *Dig Liver Dis* 2002; **34**: 419-423

6 **Summers RW,** Switz DM, Sessions JT Jr, Becktel JM, Best WR, Kern F Jr, Singleton JW. National Cooperative Crohn's Disease Study: results of drug treatment. *Gastroenterology* 1979; **77**: 847-869

7 **Riis P,** Anthonisen P, Wulff HR, Folkenborg O, Bonnevie O, Binder V. The prophylactic effect of salazosulphapyridine in ulcerative colitis during long-term treatment. A double-blind trial on patients asymptomatic for one year. *Scand J Gastroenterol* 1973; **8**: 71-74

8 **Ardizzone S**, Petrillo M, Imbesi V, Cerutti R, Bollani S, Bianchi Porro G. Is maintenance therapy always necessary for patients with ulcerative colitis in remission? *Aliment Pharmacol Ther* 1999; **13**: 373-379

9 **Yamaji K**, Fukunaga K, Yamane S, Sueoka A, Nose Y. Current therapeutic apheresis technologies for inflammatory bowel disease. *Ther Apher* 1998; **2**: 105-108

10 **Kawamura A**, Saitoh M, Yonekawa M, Horie T, Ohizumi H, Tamaki T, Kukita K, Meguro J. New technique of leukocytapheresis by the use of nonwoven polyester fiber filter for inflammatory bowel disease. *Ther Apher* 1999; **3**: 334-337

11 **Kohgo Y,** Ashida T, Maemoto A, Ayabe T. Leukocytapheresis for treatment of IBD. *J Gastroenterol* 2003; **38 Suppl 15**: 51-54

12 **Kjeldsen J.** Treatment of ulcerative colitis with high doses of oral prednisolone. The rate of remission, the need for surgery, and the effect of prolonging the treatment. *Scand J Gastroenterol* 1993; **28**: 821-826

13 **Kozarek R,** Bedard C, Patterson D, Justus P, Sandford R, Greene M, Gelfand M, Bredfeldt J, Brentnall T, Putnam W. Cyclosporin use in the precolectomy chronic ulcerative colitis patient: a community experience and its relationship to prospective and controlled clinical trials.Pacific Northwest Gastroenterology Society. *Am J Gastroenterol* 1995; **90**: 2093-2096

14 **Su C,** Lichtenstein GR. Treatment of inflammatory bowel disease with azathioprine and 6-mercaptopurine. *Gastroenterol Clin North Am* 2004; **33**: 209-234, viii

15 **Sawada K**, Muto T, Shimoyama T, Satomi M, Sawada T, Nagawa H, Hiwatashi N, Asakura H, Hibi T. Multicenter randomized controlled trial for the treatment of ulcerative colitis with a leukocytapheresis column. *Curr Pharm Des* 2003; **9**: 307-321

16 **Saniabadi AR**, Hanai H, Takeuchi K, Umemura K, Nakashima M, Adachi T, Shima C, Bjarnason I, Lofberg R. Adacolumn, an adsorptive carrier based granulocyte and monocyte apheresis device for the treatment of inflammatory and refractory diseases associated with leukocytes. *Ther Apher Dial* 2003; **7**: 48-59

17 **Suzuki Y**, Yoshimura N, Saniabadi AR, Saito Y. Selective granulocyte and monocyte adsorptive apheresis as a first-line treatment for steroid naive patients with active ulcerative colitis: a prospective uncontrolled study. *Dig Dis Sci* 2004; **49**: 565-571

S- Editor Wang J **L- Editor** Wang XL **E- Editor** Liu WF

PO Box 2345, Beijing 100023, China
www.wjgnet.com
wjg@wjgnet.com

World J Gastroenterol 2006 April 14; 12(14): 2205-2208
World Journal of Gastroenterology ISSN 1007-9327

CLINICAL RESEARCH

Echo-enhanced ultrasound with pulse inversion imaging: A new imaging modality for the differentiation of cystic pancreatic tumours

Steffen Rickes, Klaus Mönkemüller, Peter Malfertheiner

Steffen Rickes, Klaus Mönkemüller, Peter Malfertheiner, Department of Gastroenterology, Hepatology and Infectious Diseases, Otto-von-Guericke-University, Magdeburg, Germany
Correspondence to: Steffen Rickes, PD Dr, Otto-von-Guericke-University Magdeburg, Department of Gastroenterology, Hepatology and Infectious Diseases, Leipziger Str. 44, 39120 Magdeburg, Germany. steffen. rickes@medizin.uni-magdeburg.de
Telephone: +49-39-16713100 Fax: +49-39-16713105
Received: 2005-06-21 Accepted: 2005-08-26

Abstract

AIM: To describe and discuss echo-enhanced sonography in the differential diagnosis of cystic pancreatic lesions.

METHODS: The pulse inversion technique (with intravenous injection of 2.4 mL SonoVue®) or the power-Doppler mode under the conditions of the 2nd harmonic imaging (with intravenous injection of 4 g Levovist®) was used for echo-enhanced sonography.

RESULTS: Cystadenomas frequently showed many vessels along fibrotic strands. On the other hand, cystadenocarcinomas were poorly and chaotically vascularized. "Young pseudocysts" were frequently found to have a highly vascularised wall. However, the wall of the "old pseudocysts" was poorly vascularized. Data from prospective studies demonstrated that based on these imaging criteria the sensitivities and specificities of echo-enhanced sonography in the differentiation of cystic pancreatic masses were > 90%.

CONCLUSION: Cystic pancreatic masses have a different vascularization pattern at echo-enhanced sonography. These characteristics are useful for their differential diagnosis, but histology is still the gold standard.

Key words: Cystic pancreatic lesions; Differential diagnosis; Echo-enhanced sonography

Rickes S, Mönkemüller K, Malfertheiner P. Echo-enhanced ultrasound with pulse inversion imaging: A new imaging modality for the differentiation of cystic pancreatic tumours. *World J Gastroenterol* 2006; 12(14): 2205-2208

http://www.wjgnet.com/1007-9327/12/2205.asp

INTRODUCTION

Cystic tumours of the pancreas are rare, accounting for about 1% of all pancreatic neoplasms[1]. Cystadenomas and cystadenocarcinomas are the most frequently encountered cystic lesions[1-3]. There are problems in the differentiation of cystic pancreatic masses. It is obvious that the discrimination between these lesions is critical for prognosis and therapy[4].

Conventional transabdominal ultrasound displays no characteristic signs for the differentiation of cystic pancreatic tumours and the diagnostic accuracy is low[5-7]. The vascularization pattern is helpful for the tumour differentiation and can be investigated by fundamental power and colour Doppler sonography. However, there is a low sensitivity of these procedures for detecting low blood flow velocity or small vessels. The sensitivity can be increased by echo-enhancers, such as SonoVue®. Therefore, echo-enhanced sonography is an increasingly used procedure for the differentiation of pancreatic tumours[8, 9].

In this review, echo-enhanced sonography in the differential diagnosis of cystic pancreatic tumours is depicted and discussed.

MATERIALS AND METHODS

All patients were investigated first by conventional sonography using a dynamic sector scanner. A special preparation of the patients was not necessary. The pulse inversion technique or the power-Doppler mode under the conditions of the 2nd harmonic imaging was used for echo-enhanced sonography. The pulse inversion mode was used more frequently than the 2nd harmonic imaging.

For echo-enhanced sonography, the pulse inversion 2.4 mL SonoVue® (sulfur hexafluoride gas-based contrast agent, Bracco International B.V., Amsterdam, Netherlands) was injected intravenously, and the mechanical index varied between 0.1 and 0.2 (low MI procedure). The investigation could be done in real time, and lasted for approximately 2 min.

Echo-enhanced power Doppler sonography was started immediately after intravenous injection of 4 g

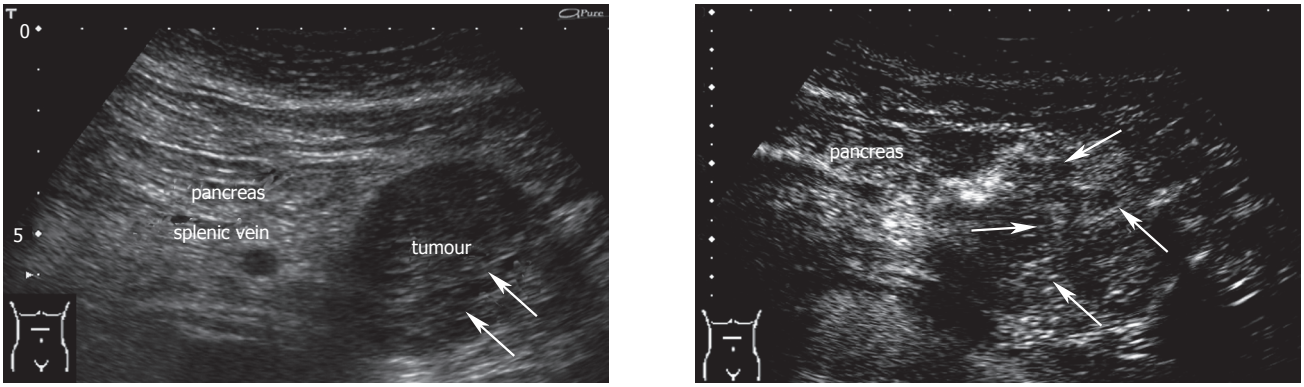

Figure 1 Cystadenoma at conventional and echo-enhanced ultrasound. **A**: A tumour at the pancreatic tail (5 cm in diameter) with small cystic areas (small arrows) and thin fibrotic strands; B: Highly vascularized tumour arteries (large arrows) along the fibrotic strands (maximum of contrastation 15 s after injection of the echo-enhancer).

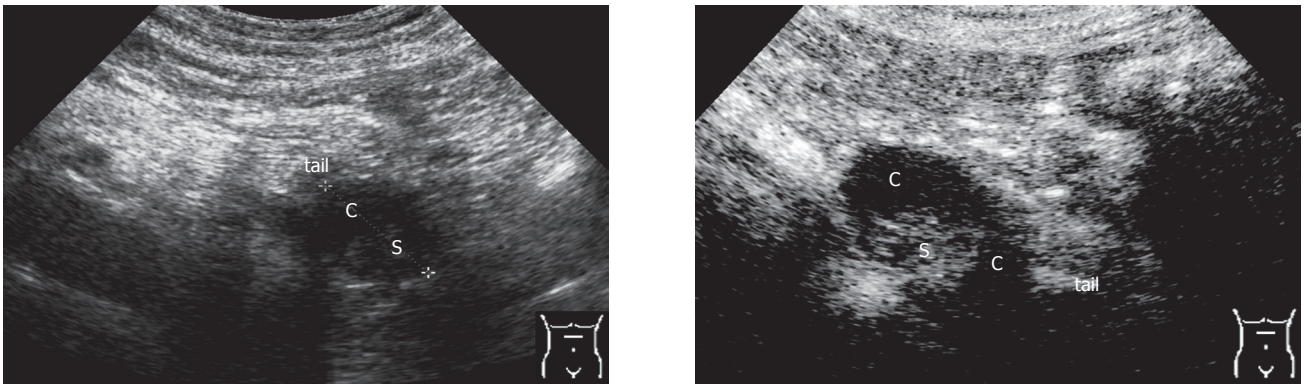

Figure 2 Cystadenoma at conventional and echo-enhanced ultrasound A: A tumour (7 cm in diameter) at the pancreatic tail with large cystic (c) and solid areas (s); **B**: A poorly vascularized solid (s) tumour (maximum of contrastation 15 s after injection of the echo-enhancer).

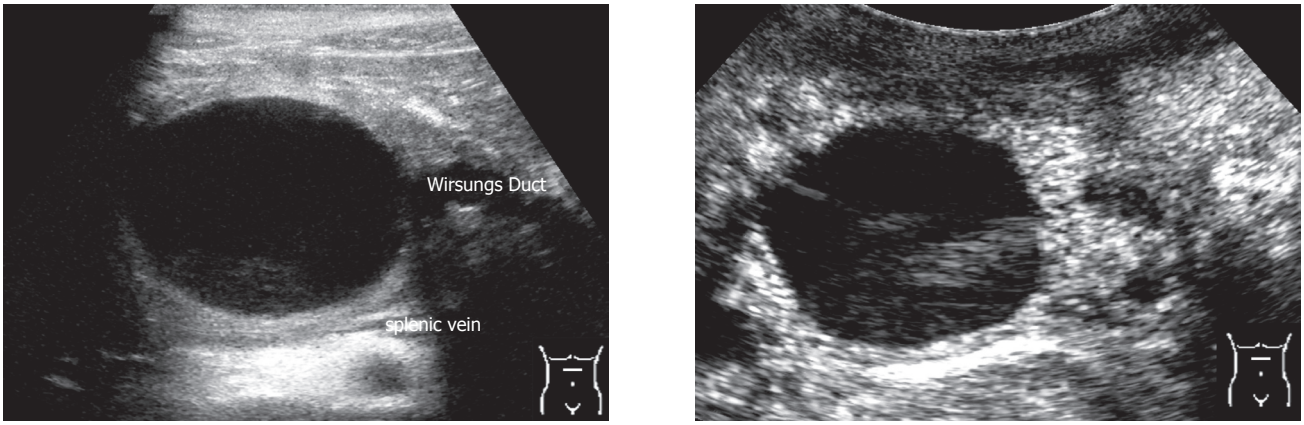

Figure 3 Pseudocust at conventional and echo-enhanced ultrasound A: A lesion with an echo-free pattern and a sharply delineated wall. The Wirsungs Duct is dilated; **B**: A highly vascularized wall (maximum of contrastation 20 s after injection of the echo-enhancer).

Levovist® (galactose-based contrast agent, concentration 300 mg/mL, Schering AG, Berlin, Germany). Intermittent sweeps were done, and the investigation lasted for approximately 2 min. One focus zone with depth adapted to the area of interest and a mechanical index of 0.8-1.3 (high MI procedure) should be used.

RESULTS

Criteria for the differentiation of pancreatic masses by conventional and echo-enhanced sonography[10, 11] are shown in Table 1. Cystadenomas consisting of small cystic areas (< 3 cm) and thin fibrotic strands are shown in Figure 1A. At echo-enhanced sonography highly vascularized solid tumour parts and arteries along the fibrotic strands are shown in Figure 1B. On the other hand, cystadenocarcinomas were found to have large cystic areas (about 5 cm) and solid tumour parts in the conventional ultrasound examination (Figure 2A). After injection of an echo-enhancer, poorly vascularized solid

Table 1 Criteria for differentiation of cystic pancreatic tumours with conventional ultrasound, fundamental power Doppler sonography, and echo-enhanced ultrasound[10, 11]

	Conventional ultrasound	Fundamental power Doppler sonography	Echo-enhanced sonography
Cystadenoma	• small cystic areas (often < 3 cm) • spoke-like pattern of fibrotic strands with small calcifications • no dilated Wirsung's duct	• no tumour vessels detectable	• highly vascularised tumour arteries along the fibrotic strands
Cystadeno-carcinoma	• large cystic areas (often > 5 cm) • solid areas • no dilated Wirsung's duct	• rarely tumour vessels with chaotic pattern detectable	• poorly and chaotic vascularised solid areas
Pseudocyst	• often echo-free pattern • sharply delineated wall • features of acute and/or chronic pancreatitis • signs of bleeding and/or calcifications • bowel infiltration is possible	• rarely tumour vessels detectable in "young cysts"	• "young cysts" (a few weeks of age) show often a highly vascular-ised wall • "old cysts" (a few months of age) show often a poorly vascularised wall

areas could be detectable (Figure 2B). Pseudocysts were found to be characterised by an echo-free pattern and a sharply delineated wall (Figure 3A). In the remaining pancreatic parenchyma features of chronic inflammation such as calcifications and a dilated Wirsung's duct could also be found. After injection of an echo-enhancer the wall of the pseudocysts was highly ("young cyst", Figure 3B) or poorly vascularized ("old cysts").

A recently published study with 31 patients showed that echo-enhanced sonography could differentiate cystic neoplasms from pseudocysts[12]. The sensitivity of echo-enhanced sonography with respect to diagnosing cyst adenomas was 95% and its specificity was 92%. The corresponding values for pseudocysts were both 100%. However, one cystadenoma was misdiagnosed as a cystadenocarcinoma, and vice-versa. The morphological variability of these cystic lesions at conventional ultrasound and the difficulties in the evaluation of the vascularization of cystic masses might be responsible for the false results. On the other hand, only 27% of cystadenomas and 67% of pseudocysts could be correctly classified by conventional ultrasound[12].

DISCUSSION

So far not a single ideal diagnostic procedure is available for the differentiation of cystic pancreatic tumours. Histology is the gold standard but nevertheless can produce false negative results. The correct differential diagnosis of cystic neoplasms of the pancreas has proven to be difficult and imaging techniques have low correct diagnosis percentages[5, 13-15], which can be attributed to the particular anatomicropathological features of these tumors and the difficulty to discriminate them from pseudocysts.

Conventional ultrasound cannot provide the reliable characteristics of different cystic pancreatic lesions. Thus, it is difficult to distinguish these tumours. Cystadenomas often consist of small cystic areas and a spoke-like pattern of fibrotic strands. In contrast, cystadenocarcinomas often show large cysts (frequently larger than 5 cm in size). Pseudocysts are frequently echo-free and have a sharply delineated wall.

The angiographic vascularization pattern contributes to the differentiation of pancreatic tumours[16-18]. Since cyst-adenomas are characterised by their hypervascularization, they are often found to be hypovascularized with a chaotic pattern. However, the diagnostic accuracy of angiography is low because it is not possible to investigate the macroscopic tumour features[17].

The vascularization of tumours may also be studied by fundamental power and colour Doppler sonography. However, the sensitivity of these procedures is low in detecting low blood flow velocity or small vessels. This sensitivity can be improved by echo-enhancers, such as SonoVue® and Levovist®. Levovist® consists of air-filled microbubbles which enhance the Doppler signal at 20-30 dB[19-21]. However, the signal intensity of echo-enhanced sonography from flowing blood is lower than that of tissue movements. To overcome these difficulties the technique of the 2nd harmonic imaging has been developed based on the property of microbubbles to resonate and emit harmonic waves in an ultrasound field with a frequency of 1-5 MHz. If the harmonic frequency is to be detected at twice the transmitted frequency, the procedure is called the 2nd harmonic imaging. Since tissue particles have fewer of the 2nd harmonic waves than microbubbles, the signals of echo-enhancers are better distinguishable[19].

The new contrast agent Sonovue® is used more frequently for echo-enhanced sonography. Furthermore, the 2nd harmonic imaging can be replaced partially by the pulse inversion imaging technique. There are observations that with this new procedure more favourable results can be achieved than with the 2nd harmonic imaging. The 2nd harmonic imaging cannot separate the transmitted and

received harmonic signals completely because of limited bandwidth. However, pulse inversion imaging avoids these bandwidth limitations using characteristics specific to microbubble vibrations to subtract rather than filter out the fundamental signals. Because this imaging technique transmits two reciprocal pulses, leading to a subtraction of the two fundamental signals, it allows the use of broader bandwidths for the transmission and reception yielding an improved resolution and can provide an increased sensitivity to contrast[22]. However, comparative results of large prospective studies are missing.

We want to point out that according to our experience, conventional ultrasound, power and colour Doppler sonography, and echo-enhanced sonography should not be used as single imaging techniques, exclusively. Conventional ultrasound is the basic sonographic method, and tumour differentiation is hardly possible based on an echo-enhanced sonographic examination alone. Echo-enhanced sonography offers more diagnostic criteria than conventional ultrasound alone, but similar to the angiography it is impossible to investigate macroscopic tumour features with this procedure alone. Therefore, all sonographic procedures should be performed in combination.

The characteristic signs of pancreatic tumours at echo-enhanced sonography have been published [10, 11]. Solid areas of cystadenocarcinomas and the wall of the " old pseudocysts" are found to be hypovascularized. In contrast, solid parts of cystadenomas and the wall of the "young pseudocysts" are mostly hypervascularized. A recently published study showed that echo-enhanced sonography can differentiate cystic neoplasms better than conventional ultrasound alone[12].

The successful treatment of cystic pancreatic tumours requires a highly sensitive and specific diagnostic procedure. Echo-enhanced sonography can fulfil this requirement. However, histology is still the gold standard for the differentiation of cystic pancreatic lesions.

REFERENCES

1 **Rall CJ**, Rivera JA, Centeno BA, Fernandez-del Castillo C, Rattner DW, Warshaw AL, Rustgi AK. Peritoneal exfoliative cytology and Ki-ras mutational analysis in patients with pancreatic adenocarcinoma. *Cancer Lett* 1995; **97:** 203-211

2 **Compagno J**, Oertel JE. Microcystic adenomas of the pancreas (glycogen-rich cystadenomas): a clinicopathologic study of 34 cases. *Am J Clin Pathol* 1978; **69:** 289-298

3 **Compagno J,** Oertel JE. Mucinous cystic neoplasms of the pancreas with overt and latent malignancy (cystadenocarcinoma and cystadenoma). A clinicopathologic study of 41 cases. *Am J Clin Pathol* 1978; **69:** 573-580

4 **Warshaw AL**, Compton CC, Lewandrowski K, Cardenosa G, Mueller PR. Cystic tumors of the pancreas. New clinical, radiologic, and pathologic observations in 67 patients. *Ann Surg* 1990; **212:** 432-443; discussion 444-445

5 **Torresan F**, Casadei R, Solmi L, Marrano D, Gandolfi L. The role of ultrasound in the differential diagnosis of serous and mucinous cystic tumours of the pancreas. *Eur J Gastroenterol Hepatol* 1997; **9:** 169-172

6 **Yang EY**, Joehl RJ, Talamonti MS. Cystic neoplasms of the pancreas. *J Am Coll Surg* 1994; **179:** 747-757

7 **de Calan L**, Levard H, Hennet H, Fingerhut A. Pancreatic cystadenoma and cystadenocarcinoma: diagnostic value of preoperative morphological investigations. *Eur J Surg* 1995; **161:** 35-40

8 **Rickes S,** Unkrodt K, Neye H, Ocran KW, Wermke W. Differentiation of pancreatic tumours by conventional ultrasound, unenhanced and echo-enhanced power Doppler sonography. *Scand J Gastroenterol* 2002; **37:** 1313-1320

9 **Rickes S,** Unkrodt K, Ocran K, Neye H, Wermke W. Differentiation of neuroendocrine tumors from other pancreatic lesions by echo-enhanced power Doppler sonography and somatostatin receptor scintigraphy. *Pancreas* 2003; **26:** 76-81

10 **Rickes S,** Unkrodt K, Ocran K, Neye H, Lochs H, Wermke W. Evaluation of doppler ultrasonography criteria for the differential diagnosis of pancreatic tumors. *Ultraschall Med* 2000; **21:** 253-258

11 **Rickes S**, Flath B, Unkrodt K, Ocran K, Neye H, Lochs H, Wermke W. Pancreatic metastases of renal cell carcinomas-evaluation of the contrast behavior at echo-enhanced power-Doppler sonography in comparison to primary pancreatic tumors. *Z Gastroenterol* 2001; **39:** 571-578

12 **Rickes S,** Wermke W. Differentiation of cystic pancreatic neoplasms and pseudocysts by conventional and echo-enhanced ultrasound. *J Gastroenterol Hepatol* 2004; **19:** 761-766

13 **Bunk A,** Herzog KH, Kunze P, Braun S. Ultrasound differential diagnostic aspects in cystadenoma of the pancreas. *Ultraschall Med* 1995; **16:** 210-217

14 **Le Borgne J,** de Calan L, Partensky C. Cystadenomas and cystadenocarcinomas of the pancreas: a multiinstitutional retrospective study of 398 cases. French Surgical Association. *Ann Surg* 1999; **230:** 152-161

15 **Fugazzola C**, Procacci C, Bergamo Andreis IA, Iacono C, Portuese A, Dompieri P, Laveneziana S, Zampieri PG, Jannucci A, Serio G. Cystic tumors of the pancreas: evaluation by ultrasonography and computed tomography. *Gastrointest Radiol* 1991; **16:** 53-61

16 **Goldstein HM,** Neiman HL, Bookstein JJ. Angiographic evaluation of pancreatic disease. A further appraisal. *Radiology* 1974; **112:** 275-282

17 **Reuter SR**, Redman HC, Bookstein JJ. Differential problems in the angiographic diagnosis of carcinoma of the pancreas. *Radiology* 1970; **96:** 93-99

18 **Appleton GV,** Bathurst NC, Virjee J, Cooper MJ, Williamson RC. The value of angiography in the surgical management of pancreatic disease. *Ann R Coll Surg Engl* 1989; **71:** 92-96

19 **Wermke W**, Gaßmann B. Tumour diagnostics of the liver with echo enhancers. Springer Verlag, Berlin, Heidelberg, New York 1998

20 **Calliada F**, Campani R, Bottinelli O, Bozzini A, Sommaruga MG. Ultrasound contrast agents: basic principles. *Eur J Radiol* 1998; **27** Suppl 2: S157-S160

21 **Correas JM,** Helenon O, Pourcelot L, Moreau JF. Ultrasound contrast agents. Examples of blood pool agents. *Acta Radiol Suppl* 1997; **412:** 101-112

22 **Kim AY,** Choi BI, Kim TK, Kim KW, Lee JY, Han JK. Comparison of contrast-enhanced fundamental imaging, second-harmonic imaging, and pulse-inversion harmonic imaging. *Invest Radiol* 2001; **36:** 582-588

S- Editor Wang J **L- Editor** Wang XL **E- Editor** Cao L

PO Box 2345, Beijing 100023, China
www.wjgnet.com
wjg@wjgnet.com

World J Gastroenterol 2006 April 14; 12(14): 2209-2216
World Journal of Gastroenterology ISSN 1007-9327

CLINICAL RESEARCH

Surgical anatomy of the innervation of pylorus in human and *Suncus murinus*, in relation to surgical technique for pylorus-preserving pancreaticoduodenectomy

Shuang-Qin Yi, Fei Ru, Tetsuo Ohta, Hayato Terayama, Munekazu Naito, Shogo Hayashi, Sichen Buhe, Nozomi Yi, Takayoshi Miyaki, Shigenori Tanaka, Masahiro Itoh

Shuang-Qin Yi, Hayato Terayama, Munekazu Naito, Shogo Hayashi, Sichen Buhe, Nozomi Yi, Takayoshi Miyaki, Masahiro Itoh, Department of Anatomy, Tokyo Medical University, 6-1-1 Shinjuku, Shinjuku-ku, Tokyo 160-8402, Japan
Fei Ru, Department of Medicine, Johns Hopkins Medical Institutions, 600 North Wolfe Street, Baltimore, Maryland 21287, United States
Tetsuo Ohta, Department of Gastroenterologic Surgery, Kanazawa University, 13-1 Takara-Machi, Kanazawa 920-8420, Japan
Shigenori Tanaka, Department of Anatomy and Neuroembryology, Kanazawa University, 13-1 Takara-Machi, Kanazawa 920-8420, Japan
Supported by Ministry of Education, Culture, Sports, Science and Technology of Japan Grant, No. 14570008
Correspondence to: Dr Shuang-Qin Yi, Department of Anatomy, Tokyo Medical University, 6-1-1, Shinjuku, Shinjuku-ku, Tokyo 160-8402, Japan. yixim@tokyo-med.ac.jp
Telephone: +81-3-33516141 Fax: +81-3-33411137
Received: 2005-09-23 Accepted: 2005-11-18

Abstract

AIM: To clarify the innervation of the antro-pyloric region in humans from a clinico-anatomical perspective.

METHODS: The stomach, duodenum and surrounding structures were dissected in 10 cadavers, and immersed in a 10mg/L solution of alizarin red S in ethanol to stain the peripheral nerves. The distribution details were studied to confirm innervations in the above areas using a binocular microscope. Similarly, innervations in 10 Suncus murinus were examined using the method of whole-mount immunohistochemistry.

RESULTS: The innervation of the pyloric region in humans involved three routes: One arose from the anterior hepatic plexus via the route of the suprapyloric/supraduodenal branch of the right gastric artery; the second arose from the anterior and posterior gastric divisions, and the third originated from the posterior-lower region of the pyloric region, which passed via the infrapyloric artery or retroduodenal branches and was related to the gastroduodenal artery and right gastroepiploic artery. For Suncus murinus, results similar to those in humans were observed.

CONCLUSION: There are three routes of innervation of the pyloric region in humans, wherein the route of the right gastric artery is most important for preserving pyloric region innervation. Function will be preserved by more than 80% by preserving the artery in pylorus-preserving pancreaticoduodenectomy (PPPD). However, the route of the infrapyloric artery should not be disregarded. This route is related to several arteries (the right gastroepiploic and gastroduodenal arteries), and the preserving of these arteries is advantageous for preserving pyloric innervation in PPPD. Concurrently, the nerves of Latarjat also play an important role in maintaining innervation of the antro-pyloric region in PPPD. This is why pyloric function is not damaged in some patients when the right gastric artery is dissected or damaged in PPPD.

Key words: Innervation; Quality of life; Pylorus-preserving pancreaticoduodenectomy; *Suncus murinus*; Whole mount immunohistochemistry

Yi SQ, Ru F, Ohta T, Terayama H, Naito M, Hayashi S, Buhe S, Yi N, Miyaki T, Tanaka S, Itoh M. Surgical anatomy of the innervation of pylorus in human and *Suncus murinus*, in relation to surgical technique for pylorus-preserving pancreaticoduodenectomy. *World J Gastroenterol* 2006; 12(14): 2209-2216

http://www.wjgnet.com/1007-9327/12/2209.asp

INTRODUCTION

With the concept of less invasive surgery, pylorus-preserving pancreaticoduodenectomy (PPPD) has taken the place of conventional Whipple pancreaticoduodenectomy as a standard operative procedure for the treatment of various benign and malignant diseases in the periampullary region, even pancreatic head carcinoma, since 1978[1-5]. Early delayed gastric emptying has been described as a common and frustrating complication after this procedure, which occurs in 20% to 46% of patients[6-16]. Although delayed gastric emptying is self-limiting, not life-threatening, and can be treated conservatively[7,9,17], it results in discomfort and a significant prolonging of

the hospital stay, and so contributes to increased hospital costs[7,8,18,19]. However, the pathogenesis of delayed gastric emptying after PPPD remains controversial.

The procedure may impair gastric peristalsis. The duodenal pacemaker, which is located 0.5 to 1 cm distally from the pylorus, should therefore be preserved to avoid disturbances in normal gastric peristalsis[20]. Gastric arrhythmias may be another cause of delayed gastric emptying in the early postoperative period, probably exacerbated by intra-abdominal complications[21]. Problems caused by the surgical procedure itself include injury to the nerves of Latarjat or the placement of suture material through the pyloric muscle. In addition, ischemia of the duodenal stump and antropyloric muscle mechanisms could influence gastric emptying, although mucosal edema at the site of anastomosis and peri-anastomotic fluid collection seem to be more common problems[22]. In regard to maintaining the pylorus as a functional unit, it is of paramount importance to maintain normal innervation of the antro-pylorus, an adequate blood supply and a pyloric muscle unimpeded by sutures[1,23].

Moreover, there has been no detailed description concerning clinico-anatomical and morphologic studies of the innervation of the antro-pyloric region in other literature, although there are some records of human pyloric innervation in literatures[24-27]. Therefore, we attempted to clarify the innervation of the antro-pyloric region in humans from a clinico-anatomical point of view, and to evaluate the innervation-preserving procedure of PPPD and its modified procedures, by using the peculiar method of labeling and dissecting the autonomic nerves of the viscera, not the current dissection of gross anatomy as in our previous studies[28-30]. Furthermore, the experimental animal, *Suncus murinus*, has been used for a comparative study to demonstrate general morphologic characteristics more similar to humans than other current laboratory animals, e.g., mouse, rat and rabbit[28-31].

MATERIALS AND METHODS

Cadavers

The study was performed on 10 cadavers (5 men and 5 women) with a mean age of 79.8 (range, 50 to 94) years. All cadavers were selected from bodies used for research and practice of anatomy at Kanazawa University School of Medicine during the years 1999-2000, and were free from diseases of the liver, stomach, duodenum, pancreas, and their surrounding areas (Table 1).

Animals and tissue preparation

Adult laboratory house musk shrews, *S. murinus*, were obtained and maintained from a closed breeding colony bred in our laboratories in the Department of Anatomy and Neuroembryology, Kanazawa University, Japan. The animals were housed and handled in accordance with the Guide for the Care and Use of Laboratory Animals and the Guide for the Care and Use of Experimental Animals of the Canadian Council on Animal Care. Briefly, all shrews were kept individually after weaning (20 d after birth) in plastic cages equipped with a wooden nestbox containing paper strips, and were kept in a conventionally conditioned animal room: 23 ℃ to 27 ℃, no humidity control, and 14 L: 10 D. Commercial trout pellets containing 45.0% protein, 3.5% fat, 3.0% fiber, 13.0% ash and 26.2% complex carbohydrate (Nippon Haigou Shiryou, Tokyo, Japan) and water were supplied *ad libitum*. The mother colony, JIc: CR, is maintained in the Central Institute for Experimental Animals, Kawasaki, Japan[28]. Adult animals (6 females and 4 males, weighing 45-80 g) were first anesthetized with ether and received an intraperitoneal injection of a solution of urethrane (sodium ethyl carbamate, 900 mg/kg). After each *S. murinus* was completely narcotized, the abdominal cavity was opened, and a catheter was inserted retrogradely into the abdominal aorta at the level immediately above the bifurcation of this artery into the common iliac arteries. Perfusion was commenced with normal saline containing heparin (10 KU/L), and thereafter with phosphate-buffered saline (PBS) containing 40 g/L paraformaldehyde. After perfusion, the animals were injected with neoprene latex to label the blood vessels in the pylorus region. Thereafter, the abdominal organs including the stomach, duodenum, common bile duct, and pancreas were extracted en bloc with the related nerves and vessels, postfixed with 40 g/L paraformaldehyde in PBS (pH 7.4) at 4 ℃ overnight to prepare for whole mount immunostaining.

Anatomical procedures of under-stereoscopic microscopy

The anatomical procedures of the cadavers were performed, according to our previous description[29,30], as follows. From the adult autopsy, the viscera of the upper abdomen (including the liver, pancreas, lower esophagus, stomach, and duodenum) were resected en masse with the abdominal aorta (region including the celiac artery and superior mesenteric artery), portal system, and nerves (including the vagus nerve, celiac ganglion, and plexus). The resected specimens were immersed in a 10 mg/L solution of alizarin red S (Wako, Osaka, Japan) in ethanol to melt the fat tissue and stain the peripheral nerves. The solution was changed 3 times every 2 to 3 d, in principle, but this process may be prolonged if necessary depending on the degree of progression of elimination of fat and staining. The area of each sample surrounded by the horizontal plane that passed through the portal region and the lower margin of the horizontal part of the duodenum and the sagittal plane that passed through the descending part of the duodenum and hilum of the spleen was dissected to the depth of the celiac plexus with the aid of a stereoscopic microscope (magnification, ×40), keeping the sample immersed completely in 100% ethanol. In dissection, the lymphatic vessels and lymph nodes were removed, and particular attention was paid to preserve not only the nerves but also the arteries and veins around the stomach including the hepatogastro mesenteriolum, hepatoduodenal ligament and lower esophagus. Figures 1 and 2 show two such dissections.

Whole mount immunohistochemistry

The whole mount immunostaining procedures for the *S. murinus* were performed as previously described[28,30]. Briefly, after rinsing in PBS, the fixed specimens were treated with 10 g/L periodic acid for 20 min to prevent

Table 1 Cadavers used in this study and pyloric innervation in the superior part

Case	Sex	Age	Death	Number[1]	Route I	Route II	Route III
A	F	94	Pneumonia	1	O		O
B	F	81	Cerebral hemorrhage	2	O	O	O
C	F	83	Myocardial infarction	1	O		O
D	M	87	Myocardial infarction	4	O	O	O
E	M	86	Pneumonia	4	O		O
F	M	73	Cerebral hemorrhage	3	O	O	O
G	M	87	Cerebral hemorrhage	4	O		O
H	M	75	Myocardial infarction	4	O		O
I	F	82	Subarachnoid hemorrhage	5	O	O	O
J	F	50	Pneumonia	3	O	O	O

[1]The number of hepatic divisions, a total of 46 hepatic divisions (average of 4.6). Route I, from the anterior hepatic plexus via the right gastric artery to the pyloric region; Route II, descending division from the hepatic division to the right gastric artery directly; Route III, from the nerves of Latarjat.

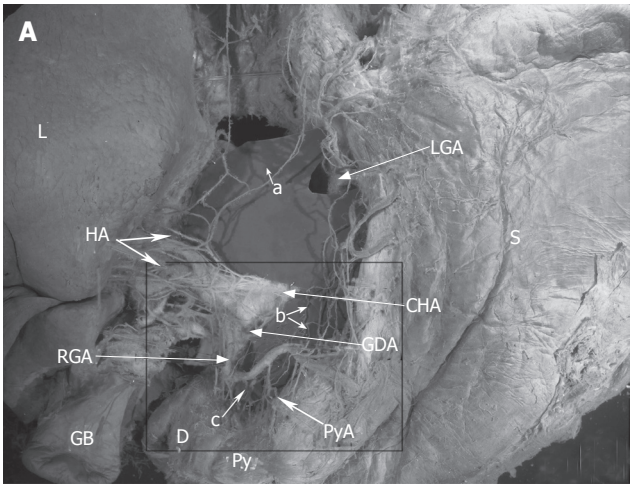

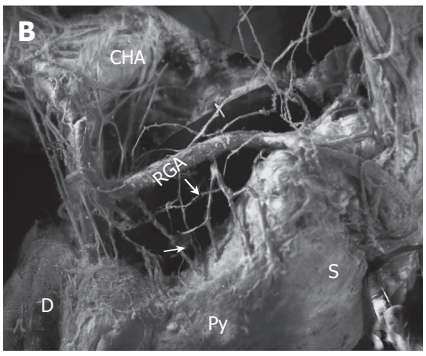

Figure 1 The innervation of the pyloric region from the view of the superior part of the pylorus, its schematic shows in Figure 3A. Hepatic divisions (a) join in the anterior hepatic plexus in the proper hepatic artery or the left/right hepatic artery (HA). The nerves ran along the right gastric artery (RGA) and its branches (PyA), and reached the pyloric region (Py) (c). The nerves (b) of Latarjet ran along the lesser curvature or the branches of the left gastric artery (LGA), intended for the antro-pyloric region. **B** is an enlargement of the box in **A**., the arrows show the nerves innervating the pyloric region from the right gastric artery. CHA, common hepatic artery; D, duodenum; E, esophagus; GB, gallbladder; GDA, gastroduodenal artery; L, liver; S, stomach.

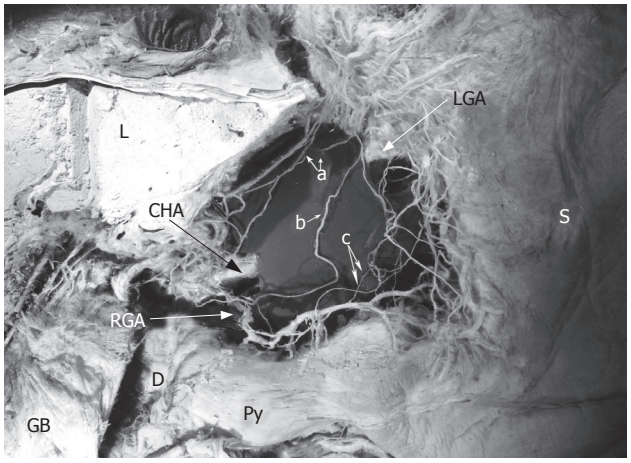

Figure 2 Another specimen, its schematic shows in Figure 3B, showing a descending branch (b) originating from the hepatic division of the anterior vagal trunk passing through the hepatogastric ligament, obliquely downward, reaching the right gastric artery (RGA), innervating the pyloric region (Py). a is similar to a in Figure 1A, indicating the hepatic divisions. c, indicating the branches for the pyloric region from the nerves of Latarjet. CHA, common hepatic artery; D, duodenum; GB, gallbladder; L, liver; LGA, left gastric artery; S, stomach.

any intrinsic peroxidase reaction. They were then incubated in freshly prepared 5 g/L papain (Sigma) in 0.025 mol/L Tris-HCl buffer (pH7.6) for 1 h and 25 g/L, 50 g/L, and 100 g/L sucrose in PBS for 30 min, respectively, followed by freezing and thawing thrice. The specimens were incubated with primary antibody (NFP-Ab) in PBS containing 2 g/L bovine serum albumin (BSA), 3 g/L Triton X-100, and 1 g/L sodium azide for 3 d at 4 ℃. After a thorough wash in PBS, the specimens were then incubated with secondary antibody labeled with peroxidase-conjugated affinity-purified sheep anti-mouse IgG (HRP) in PBS containing 2 g/L BSA and 3 g/L Triton X-100 for 3 d at 4 ℃. After a thorough wash in PBS, coloration was performed in 0.05 mol/L Tris-HCl buffer containing 20 mg/L 3,3'-diaminobenzidine (DAB) and 0.1 ml/L H_2O_2 for 1 to 3 d at 4 ℃. The stained preparations were then stored in glycerin to obtain transparency. The primary antibody was anti-neurofilament protein (NFP) antibody, a monoclonal mouse anti-all neurofilament consisting of three subunit proteins: NF-H (200 ku), NF-M (160 ku), and NF-L (70 ku) (M0762, lot 089, clone: 2F11, Dako).

RESULTS

In human

The innervation of the pyloric region in human involved three routes: via the right gastric artery, the nerves of Latarjet, and the infrapyloric artery.

Via the suprapyloric/supraduodenal branch of the right gastric artery

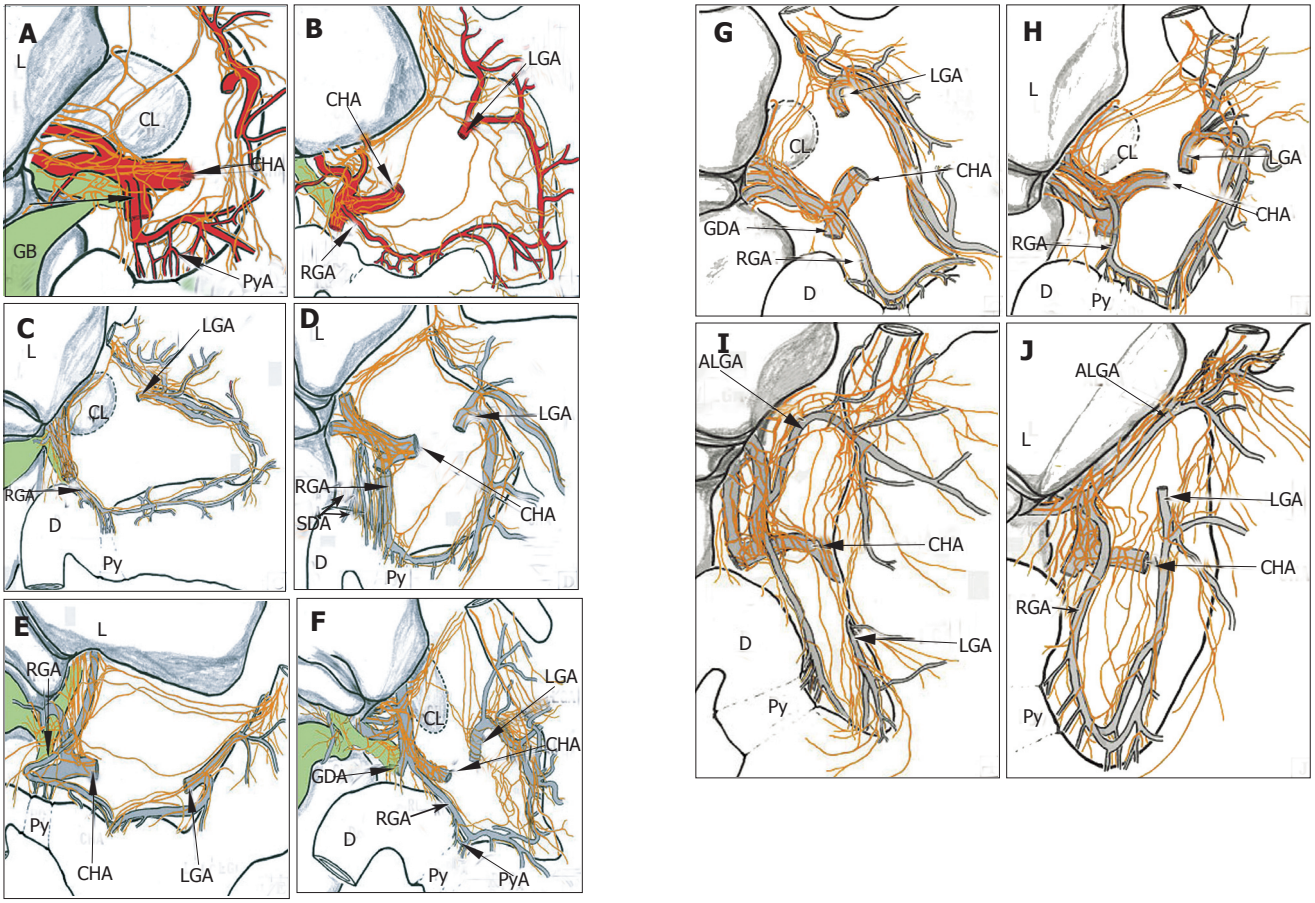

Figure 3 Diagram indicating the distribution in and around the cardia, the lesser curvature, the porta hepatica and the antro-pyloric region in 10 cadavers. Among them, **A** and **B** are diagrams of Figures 1A and 2, respectively. Five specimens, **B, D, F, I** and **J**, showed hepatic divisions joining directly to the right gastric artery, while, for the other specimens, after joining to the proper hepatic or hepatic artery, the nerves sent off some offshoots to the right gastric artery, and innervated the pyloric region. ALGA, accessory left gastric artery; CHA, common hepatic artery; CL, caudal liver; GB, gallbladder; L, liver; LGA, left gastric artery; Py, pylorus; PyA, pyloric artery; RGA, right gastric artery; SDA, supra-duodenal artery.

The hepatic division of the vagus, arising from the anterior vagal trunk, ran through the hepatogastric ligament near the edge of the liver (caudal liver), and joined the anterior hepatic plexus in the hepatoduodenal ligament. The plexus, containing the parasympathetic and sympathetic fibers (the latter originate from the celiac plexus), wound around the proper hepatic artery, then the suprapyloric or supraduodenal branch which comes from the right gastric artery, sent some branches to the pyloric region in the superior part of the pyloric regions (Figures 1, 2). This route was displayed in all ten specimens.

There was variation in the number of hepatic divisions. The total number of hepatic divisions was 46 (average, 4.6) in the 10 specimens in this study. The position where the hepatic division joined the anterior hepatic plexus occurred at different levels between the hepatic hilum and the root of the right gastric artery(Table 1, Figure 3). There were 2 cases of accessory left gastric artery in the 10 specimens. The hepatic division ran along the arteries to the hepatic hilum in these 2 cases(Figures 3I and 3J).

The branches, arising from the origin of the hepatic division, sent single or double descending branches of the hepatic division, ran in the lesser omentum, did not reach the proper hepatic artery or join the anterior hepatic plexus, joined directly to the right gastric artery, and then entered the pyloric region. Five cases of this route were observed in the 10 cadavers (Table 1, Figures 3B, 3D, 3F, 3I, and 3J).

Via the anterior and posterior gastric divisions

The anterior and posterior gastric divisions, namely the nerves of Latarjet, extended to and ran along the gastric lesser, while giving off some offshoots to the lesser curvature, sending some peripheral nerve fibers to the antro-pyloric region. The nerves of Latarjet passed through the lesser omentum, which lies 0.5 to 1.0 cm from the lesser curvature, or extended and anastomosed with the offshoots along the right gastric artery, or lay beneath the serosa of the gastric wall, entered the antro-pyloric region. The route was observed in all cases (Table 1, Figures 1, 2, and 3).

Via the infrapyloric artery or retroduodenal branches

There is always one or several infrapyloric arteries or/and retroduodenal branches, intended for the posterior-lower region of the pylorus. All of these arteries arise either from the gastroduodenal artery, or from one or the other of these two terminal branches, the right gastroepiploic

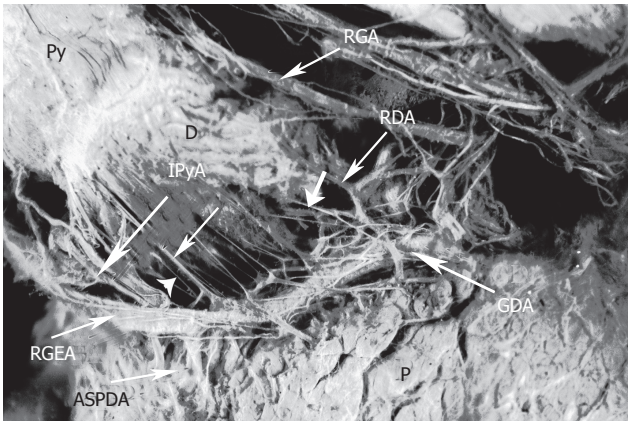

Figure 4 An example of innervation in the posterior part of the pylorus. The stomach was raised. The nerves originating from the right gastroepiploic artery (RGEA) or the gastroduodenal artery (GDA) running along the retroduodenal artery (RDA) (white arrow) or the infrapyloric artery (IPyA) (white arrowhead) reached the first duodenum posterior part and the pylorus of the posterior part.

artery, or the cranial and ventral pancreaticoduodenal artery.

This route with the arteries supplying the posterior-lower region of the pylorus, passed the nerve branches to the pyloric region. The nerve branches, arising from the anterior hepatic plexus, ran along the gastroduodenal artery, or the right gastroepiploic artery, to the infrapyloric artery or/and retroduodenal branches, reached the posterior-lower region of the pylorus. The route was observed in all cases (Figure 4).

In suncus murinus

Firstly, it is necessary to describe the morphological characters of the pyloric region in *S. murinus*. The pylorus closed the duodenal papilla, supplied by the branches of the gastroduodenal artery. The latter sent the branches to the duodenal papilla and the pyloric region. The arterial branch that supplied the pyloric region corresponded to the right gastric artery in humans. However, there existed no ramus anastomoticus between this artery and the left gastric arteries in *S. murinus* (Figure 5). There was the lesser omentum in this animal, and the right gastric artery sent anterior and posterior branches to the anterior and posterior of the pyloric region. Furthermore, there was no infrapyloric artery arising from the gastroduodenal artery in contrast to humans. Even though there are these differences, the innervation of the pyloric region in *S. murinus* was very similar to that in humans.

Via the branches of the right gastric artery

In *S murinus*, the nerves originating from hepatic plexus, ran along the gastroduodenal artery, the right gastric artery, and reached the pyloric region. This route was simple, and did not form the ramus anastomoticus with the anterior or posterior gastric branches, which originate from the vagal trunk or the left gastric artery. The innervation was observed in all cases (Figure 5).

Via the lesser omentum

In *S murinus*, the anterior and posterior gastric branches, corresponding to the Latarjet nerves in humans, while giving off some divisions to the lesser curvature and the gastric wall, sent some branches to the pyloric regions in all cases (Figure 5). The posterior-lower region of the pylorus in *S murinus* was innervated by nerve branches originating from the right gastric artery, in constrast to humans. The anterior and posterior gastric branches ran along the lesser omentum and close to the lesser curvature, or lay beneath the serosa of the gastric wall. Similarly, the route passing through the lesser omentum was also observed in some specimens, and these nerves originated from the anterior or posterior vagal trunk directly. The innervation was observed in all cases (Figure 5).

DISCUSSION

The present paper is concerned with a detailed observation of the innervation of the antro-pyloric region, with the objective of providing an anatomical basis for surgical operations in this region, especially concerning 'organ and function-preserving surgical procedures' like PPPD.

There are three routes of pyloric innervation in humans. One is the superior region of the pylorus, which is related to the hepatoduodenal ligament, whereby the nerve branches arose from the anterior hepatic plexus containing the branches coming from the hepatic division of vagus. The nerves ran along the right gastric artery, via the suprapyloric or supraduodenal branch, intended for the antro-pyloric region. The second route is the posterior-lower region of the pylorus, which is related to the gastro-pancreatic ligament. The nerves ran along the gastroduodenal or right gastroepiploic artery, to the infrapyloric artery, and reached the antro-pyloric region. The third route is the lower antrum region, which is related to the left gastric artery and the nerves of Latarjet. This route involves the branches of Latarjet nerves passing through the lesser curvature, and entering the antro-pyloric region. The animal model, *S murinus,* used in this study, allowed the complete anatomic observation of cadavers, exhibited the important arterial supply routes of the pylorus and anterior and posterior gastric divisions for the innervation of the pylorus.

The route of the superior region is the most important for pyloric innervation, in which the right gastric artery shows a core mission (main rule). The nerves of this route contain both sympathetic and parasympathetic fibers, originating from either the anterior hepatic plexus which arise from the celiac plexus, or the hepatic division of the anterior vagal trunk which joins the proper hepatic artery to the right gastric artery. The route was observed in all 10 cadavers. There were 4 cases of hepatic division distal to the hepatic edge, the division passing through the hepatogastric ligament, terminating in the right gastric artery in 10 cadavers. But only one case showed the pattern illustrated by McCrea[24], whereby a single descending branch of the hepatic division directly reached the pylorus. We agree with Skandalakis *et al*[27] that this pattern is typical but not universal. Namely, pyloric branches of the hepatic division do not, usually, directly reach the pyloric region, but pass via the arterial supply of the region, as the right hepatic artery and its branches.

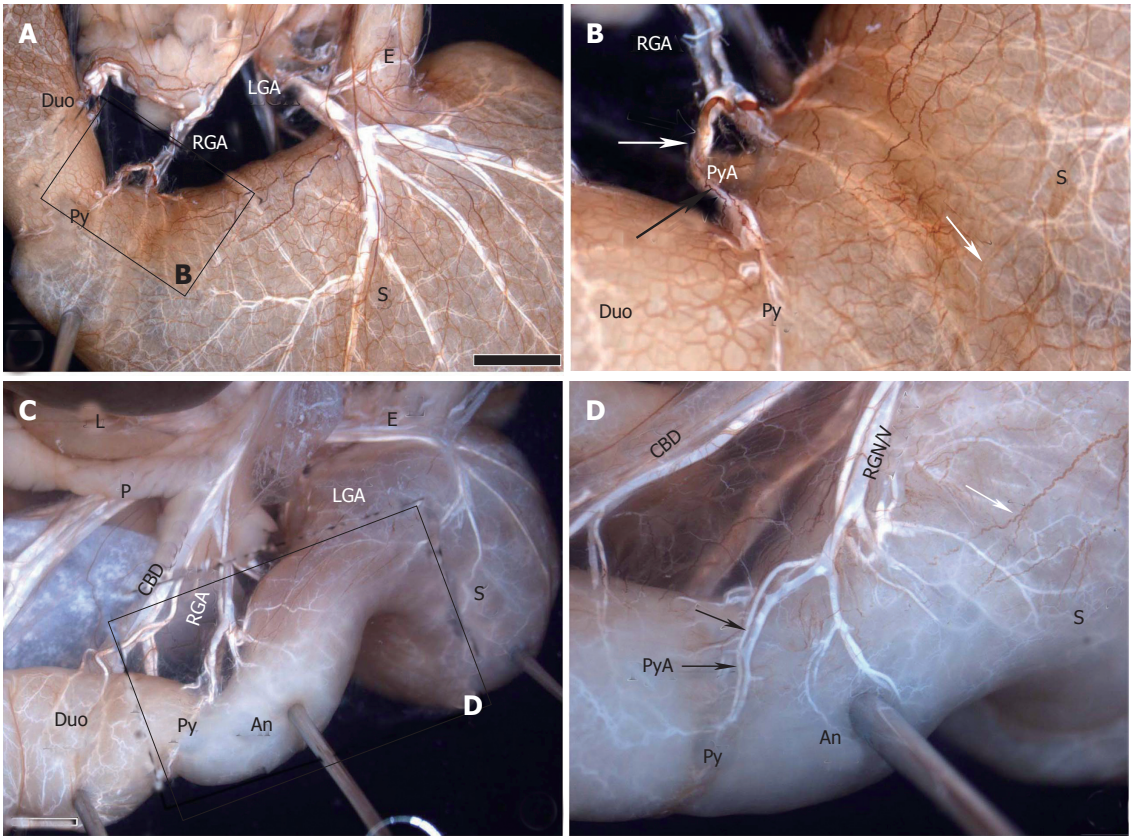

Figure 5 Two cases showing innervation of the pyloric region (Py) in *Suncus murinus* by whole-mount immunostaining. High magnifications of the boxed areas in **A** and **C** are shown in **B** and **D.** White arrows show the nerves of Latarjet intended for the antro-pyloric region. Black arrows indicate the nerves arising from the right gastric artery (RGA), running along the pyloric artery (PyA), and reaching the pyloric region. An, pyloric antrum; CBD, common bile duct; Duo, duodenum; E, esophagus; L, liver; LGA, left gastric artery; P, pancreas; RGA/V, right gastric artery/vein; S, stomach. Scale bar = 2 mm in A and B.

The right gastric artery arises from the hepatic artery and proceeds to the first portion of the duodenum (the supraduodenal artery), the pylorus and the antrum (the suprapyloric branch) along the lesser curvature. These routes via these arteries are important for pyloric innervation via the superior region of the pylorus. The preservation of the right gastric artery and its branches is potentially of great importance in providing earlier gastric emptying after operation. The drawback of pyloric preservation is a prolonged period of gastric suction. This time can be shortened by attention to the preservation of the supraduodenal artery and vagal innervation of the antrum, which is essential for gastric emptying[7]. In any event, as there was a reliable route of the right gastric artery, it is not necessary to preserve the hepatogastric ligament in order to preserve the route in clinic practice. In principle, it is only important to preserve the right gastric artery in order to preserve the innervation and function of the pylorus in PPPD.

For the route of the nerves of Latarjet, innervation originating from the anterior and posterior gastric branches of the nerves of Latarjet passed through the lesser omentum close to the lesser curvature, or extended to and anastomosed with the offshoots along the right gastric artery, or lay beneath the serosa of the gastric wall, and entered the antro-pyloric region. Skandalakis *et al* [26] reported that the nerves of Latarjet could be traced distally to about the level of the incisura in most specimens, but in many cases it reached the pylorus, and in six cases it was visible as far as the first part of the duodenum. It is possible that the nerves of Latarjet innervate the antro-pyloric region according to our observations in humans and *S. murinus*. Great care must be taken to preserve the blood supply from the left gastric artery to the lesser curvature of the stomach and pylorus in PPPD.

For the innervation of the posterior-lower region of the pylorus, it was disregard ordinarily. The route is via the arterial supply of the posterior-lower region of the pylorus. The branches are sent off by the gastroduodenal or the right gastroepiploic artery, termed by the infrapylorus branch or artery, or the retroduodenal branches. These branches come from the gastroduodenal artery in 30% of cases, from the right gastroepiploic artery in 44% of cases or from the ventral pancreaticoduodenal arch in 20% of cases[32]. The gastroduodenal artery should probably be severed distally to its first branch and should be preserved in cases of chronic pancreatitis where dissection could proceed by taking the pancreaticoduodenal artery at its origin from the gastroduodenal artery. Equal attention must also be given during the procedure to preserving innervations to the antrum and pylorus[9]. The gastroepiploic artery, with its large ascending pyloric branch, should probably be taken close to its origin from the gastroduodenal artery[9]. The origin of the innervation in

this route is similar to that of the superior region, coming from the anterior hepatic plexus. Hence, the innervation also contained both the sympathetic and parasympathetic fibers. If the right gastric artery is damaged, the route is able to compensate by its function in innervation. Grace *et al*[33] emphasized that an intact neurovascular supply to the pylorus and the first part of the duodenum is essential for the success of the pylorus preserving operation. By not ligating the gastroduodenal artery and right gastric artery at their origins and not freeing the tissues along the lesser curvature of the antrum and the gastrohepatic ligament-all these tissues remaining intact-the surgeon cannot rotate the proximal duodenum and antrum anteriorly and to the patient's left in PPPD. Thereby, it is advantageous to preserve all blood supply and innervation to antrum, pylorus, and proximal duodenum[16]. In fact, innervation of the antro-pyloric region takes several routes. When dissecting the lymph nodes in the hepatoduodenal ligament, the nerve branches originating from the anterior hepatic plexus to the right gastric artery could be damaged, however, as there are other routes of the posterior-lower region of the pylorus and the nerves of Latarjet, their influence on pyloric function may often be unclear.

In conclusion, we demonstrated the detailed description of the innervation of the antro-pyloric region from clinico-anatomical and morphologic perspectives in this study. The useful methods of whole mount immunostaining with a peripheral neuron marker for *S murinus*, and the alizarin red S staining technique for humans are effective for peripheral nerve labeling, as shown in our studies. There are three routes of pyloric innervation in humans, wherein the route of the right gastric artery is the most important for preserving pyloric region innervation. The function is preserved by more than 80% by preserving the artery in PPPD. However, the route of the infrapyloric artery should not be disregarded. This route is related to several arteries (the right gastroepiploic and gastroduodenal arteries), and the preservation of these arteries is advantageous for preserving pyloric innervation in PPPD. Concurrently, the nerves of Latarjet also perform an important role in maintaining innervation of the antro-pyloric region in PPPD. This is why the pyloric function is not damaged in some patients if the right gastric artery is dissected or damaged in PPPD.

ACKNOWLEDGMENTS

We thank Mr. Nakamura, Mr. Shiraishi and Mrs. Koizumi (Department of Anatomy and Neuroembryology, Kanazawa University) for their technical assistance, and Mrs Ogawa (Department of Anatomy, Tokyo Medical University) for her secretarial assistance during this study.

REFERENCES

1 **Traverso LW,** Longmire WP Jr. Preservation of the pylorus in pancreaticoduodenectomy. *Surg Gynecol Obstet* 1978; **146:** 959-962
2 **Ueno T,** Tanaka A, Hamanaka Y, Tsurumi M, Suzuki T. A proposal mechanism of early delayed gastric emptying after pylorus preserving pancreatoduodenectomy. *Hepatogastroenterology* 1995; **42:** 269-274
3 **Nagai H,** Ohki J, Kondo Y, Yasuda T, Kasahara K, Kanazawa K. Pancreatoduodenectomy with preservation of the pylorus and gastroduodenal artery. *Ann Surg* 1996; **223:** 194-198
4 **Yamaguchi K,** Kishinaka M, Nagai E, Nakano K, Ohtsuka T, Chijiwa K, Tanaka M. Pancreatoduodenectomy for pancreatic head carcinoma with or without pylorus preservation. *Hepatogastroenterology* 2001; **48:** 1479-1485
5 **Sugiyama M,** Abe N, Ueki H, Masaki T, Mori T, Atomi Y. A new reconstruction method for preventing delayed gastric emptying after pylorus-preserving pancreatoduodenectomy. *Am J Surg* 2004; **187:** 743-746
6 **Braasch JW,** Gongliang J, Rossi RL. Pancreatoduodenectomy with preservation of the pylorus. *World J Surg* 1984; **8:** 900-905
7 **Braasch JW,** Deziel DJ, Rossi RL, Watkins E Jr, Winter PF. Pyloric and gastric preserving pancreatic resection. Experience with 87 patients. *Ann Surg* 1986; **204:** 411-418
8 **Warshaw AL,** Torchiana DL. Delayed gastric emptying after pylorus-preserving pancreaticoduodenectomy. *Surg Gynecol Obstet* 1985; **160:** 1-4
9 **Itani KM,** Coleman RE, Meyers WC, Akwari OE. Pylorus-preserving pancreatoduodenectomy. A clinical and physiologic appraisal. *Ann Surg* 1986; **204:** 655-664
10 **Aonuma K.** Experimental studies on the gastroduodenojejunal motility and gastric emptying after duodenectomy with preservation of the total stomach and pylorus. *J Smooth Muscle Res* 1994; **30:** 147-164
11 **Yeo CJ**, Cameron JL, Sohn TA, Lillemoe KD, Pitt HA, Talamini MA, Hruban RH, Ord SE, Sauter PK, Coleman J, Zahurak ML, Grochow LB, Abrams RA. Six hundred fifty consecutive pancr eaticoduodenectomies in the 1990s: pathology, complications, and outcomes. *Ann Surg* 1997; **226:** 248-257; discussion 257-260
12 **Muller MW,** Friess H, Beger HG, Kleeff J, Lauterburg B, Glasbrenner B, Riepl RL, Buchler MW. Gastric emptying following pylorus-preserving Whipple and duodenum-preserving pancreatic head resection in patients with chronic pancreatitis. *Am J Surg* 1997; **173:** 257-263
13 **Yamaguchi K**, Tanaka M, Chijiiwa K, Nagakawa T, Imamura M, Takada T. Early and late complications of pylorus-preserving pancreatoduodenectomy in Japan 1998. *J Hepatobiliary Pancreat Surg* 1999; **6:** 303-311
14 **Murakami H,** Yasue M. A vertical stomach reconstruction after pylorus-preserving pancreaticoduodenectomy. *Am J Surg* 2001; **181:** 149-152
15 **Murakami H,** Suzuki H, Nakamura T. Pancreatic fibrosis correlates with delayed gastric emptying after pylorus-preserving pancreaticoduodenectomy with pancrea-ticogastrostomy. *Ann Surg* 2002; **235:** 240-245
16 **Gauvin JM**, Sarmiento JM, Sarr MG. Pylorus-preserving pancreaticoduodenectomy with complete preservation of the pyloroduodenal blood supply and innervation. *Arch Surg* 2003; **138:**1261-1263
17 **Patel AG,** Toyama MT, Kusske AM, Alexander P, Ashley SW, Reber HA. Pylorus-preserving Whipple resection for pancreatic cancer. Is it any better? *Arch Surg* 1995; **130:** 838-842; discussion 842-843
18 **Yeo CJ**, Barry MK, Sauter PK, Sostre S, Lillemoe KD, Pitt HA, Cameron JL. Erythromycin accelerates gastric emptying after pancreaticoduodenectomy. A prospective, randomized, placebo-controlled trial. *Ann Surg* 1993; **218:** 229-237; discussion 237-238
19 **Cameron JL**, Pitt HA, Yeo CJ, Lillemoe KD, Kaufman HS, Coleman J. One hundred and forty-five consecutive pancrea ticoduodenectomies without mortality. *Ann Surg* 1993; **217:** 430-435; discussion 435-438
20 **Tanaka M,** Sarr MG. Total duodenectomy: effect on canine gastrointestinal motility. *J Surg Res* 1987; **42:** 483-493
21 **Hocking MP,** Harrison WD, Sninsky CA. Gastric dysrhythmias following pylorus-preserving pancreaticoduodenectomy. Possible mechanism for early delayed gastric emptying. *Dig Dis Sci* 1990; **35:** 1226-1230
22 **Liberski SM,** Koch KL, Atnip RG, Stern RM. Ischemic gastroparesis: resolution after revascularization. *Gastroenterology* 1990; **99:** 252-257

23 **Traverso LW,** Longmire WP Jr. Preservation of the pylorus in pancreaticoduodenectomy a follow-up evaluation. *Ann Surg* 1980; **192:** 306-310
24 **McCrea ED.** The abdominal distribution of the vagus. *J Anat* 1924; **59:** 18
25 **Mitchell GA.** A macroscopic study of the nerve supply of the stomach. *J Anat* 1940; **75:** 50-63
26 **Skandalakis JE,** Gray SW, Soria RE, Sorg JL, Rowe JS Jr. Distribution of the vagus nerve to the stomach. *Am Surg* 1980; **46:** 130-139
27 **Skandalakis LJ**, Gray SW, Skandalakis JE. The history and surgical anatomy of the vagus nerve. *Surg Gynecol Obstet* 1986; **162:** 75-85
28 **Yi SQ**, Shimokawa T, Akita K, Ohta T, Kayahara M, Miwa K, Tanaka S. Anatomical study of the pancreas in the house musk shrew (Suncus murinus), with special reference to the blood supply and innervation. *Anat Rec A Discov Mol Cell Evol Biol* 2003; **273:** 630-635
29 **Yi SQ,** Miwa K, Ohta T, Kayahara M, Kitagawa H, Tanaka A, Shimokawa T, Akita K, Tanaka S. Innervation of the pancreas from the perspective of perineural invasion of pancreatic cancer. *Pancreas* 2003; **27:** 225-229
30 **Yi SQ,** Ohta T, Miwa K, Shimokawa T, Akita K, Itoh M, Miyamoto K, Tanaka S. Surgical anatomy of the innervation of the major duodenal papilla in human and *Suncus murinus*, from the perspective of preserving innervation in organ-saving procedures. *Pancreas* 2005; **30:** 211-217
31 **Yi SQ**, Akita K, Ohta T, Shimokawa T, Tanaka A, Ru F, Nakatani T, Isomura G, Tanaka S. Cellular localization of endocrine cells in the adult pancreas of the house musk shrew, Suncus murinus: a comparative immunocytochemical study. *Gen Comp Endocrinol* 2004; **136:** 162-170
32 **Wind P,** Chevallier JM, Sarcy JJ, Delmas V, Cugnenc PH. The infrapyloric artery and cephalic pancreatoduodenectomy with pylorus preservation: preliminary study. *Surg Radiol Anat* 1994; **16:** 165-172
33 **Grace PA,** Pitt HA, Longmire WP. Pylorus preserving pancreatoduodenectomy: an overview. *Br J Surg* 1990; **77:** 968-974

S- Editor Pan BR **L- Editor** Zhang JZ **E- Editor** Cao L

PO Box 2345, Beijing 100023, China
www.wjgnet.com
wjg@wjgnet.com

World J Gastroenterol 2006 April 14; 12(14): 2217-2222
World Journal of Gastroenterology ISSN 1007-9327

CLINICAL RESEARCH

Estimating liver weight of adults by body weight and gender

See Ching Chan, Chi Leung Liu, Chung Mau Lo, Banny K Lam, Evelyn W Lee, Yik Wong, Sheung Tat Fan

See Ching Chan, Chi Leung Liu, Chung Mau Lo, Banny K Lam, Evelyn W Lee, Sheung Tat Fan, Centre for the Study of Liver Disease, Department of Surgery, The University of Hong Kong, Pokfulam, Hong Kong, China
Yik Wong, Centre for the Study of Liver Disease, Department of Radiology, The University of Hong Kong, Pokfulam, Hong Kong, China
Supported by Sun C.Y. Research Foundation for Hepatobiliary and Pancreatic Surgery of the University of Hong Kong
Correspondence to: Professor Sheung Tat Fan, Department of Surgery, The University of Hong Kong, Queen Mary Hospital, 102 Pokfulam Road, Hong Kong, China. hrmsfst@hkucc.hku.hk
Telephone: +852-28554703 Fax: +852-28184407
Received: 2005-05-18 Accepted: 2005-08-22

Abstract

AIM: To estimate the standard liver weight for assessing adequacies of graft size in live donor liver transplantation and remnant liver in major hepatectomy for cancer.

METHODS: In this study, anthropometric data of body weight and body height were tested for a correlation with liver weight in 159 live liver donors who underwent donor right hepatectomy including the middle hepatic vein. Liver weights were calculated from the right lobe graft weight obtained at the back table, divided by the proportion of the right lobe on the computed tomography.

RESULTS: The subjects, all Chinese, had a mean age of 35.8 ± 10.5 years, and a female to male ratio of 118:41. The mean volume of the right lobe was 710.14 ± 131.46 mL and occupied 64.55% ± 4.47% of the whole liver on computed tomography. Right lobe weighed 598.90 ± 117.39 g and the estimated liver weight was 927.54 ± 168.78 g. When body weight and body height were subjected to multiple stepwise linear regression analysis, body height was found to be insignificant. Females of the same body weight had a slightly lower liver weight. A formula based on body weight and gender was derived: Estimated standard liver weight (g) = 218 + BW (kg) x 12.3 + gender x 51 (R^2 = 0.48) (female = 0, male = 1). Based on the anthropometric data of these 159 subjects, liver weights were calculated using previously published formulae derived from studies on Caucasian, Japanese, Korean, and Chinese. All formulae overestimated liver weights compared to this formula. The Japanese formula overestimated the estimated standard liver weight (ESLW) for adults less than 60 kg.

CONCLUSION: A formula applicable to Chinese males and females is available. A formula for individual races appears necessary.

Key words: Estimated standard liver weight; Liver tranplantation

Chan SC, Liu CL, Lo CM, Lam BK, Lee EW, Wong Y, Fan ST. Estimating liver weight of adults by body weight and gender. *World J Gastroenterol* 2006; 12(14): 2217-2222

http://www.wjgnet.com/1007-9327/12/2217.asp

INTRODUCTION

Small-for-size graft is a common problem in live donor liver transplantation[1]. In major hepatectomy, a small remnant liver is a key factor attributing to hospital mortality[2], even in the non-cirrhotic liver[3]. Size of the partial liver graft or the remnant liver is often expressed as a percentage of the estimated standard liver weight (ESLW) of the patient. Very often, the native liver of a transplant recipient is small and cirrhotic, and that of a patient undergoing major hepatectomy houses a large tumor. The size of the patient's liver, therefore, has little bearing on the preoperative assessment. Under both circumstances, reference to ESLW has a clinical relevance. The Shinshu group of Japan deduced a formula by drawing a relationship between the estimated standard liver volume (ESLV) and body surface area (BSA) from 96 patients who underwent abdominal computed tomography (CT), yet without liver diseases: ESLV (mL) = 706.2 × BSA (m^2) + 2.4[4]. BSA was derived from the clinical parameters of body weight (BW) and body height (BH) as described by DuBois and DuBois[5]. In view of the low mean age (11.1 years) of the patients in the study, the Shinshu group subsequently validated the formula by the same methodology in an independent sample of 96 adult live liver donors[6]. Nonetheless, this formula when applied to Caucasians underestimates the liver volume from studies based on autopsy data[7] and CT of patients without liver diseases[8].

Underestimation of liver volume was even found in another group of Asian population, the Koreans. In this Korean group the increase in liver volume in relation to BSA showed a nonlinear relationship. A piecewise linear model and a nonlinear model have thus been developed

in Korea[9]. In another study, a sample of 33 Chinese in-patients admitted for abdominal ailments apart from liver diseases were evaluated by CT. The main purpose of the study was to use them as control in comparison with cirrhotic livers and not intended for a broader application of liver size estimation[10]. As early as the sixties, it was pointed out that females of the same body size as males have a smaller liver[11]. A study of a wider scale recently has affirmed this concept[12]. Our study was to clarify the above issues by analyzing the right lobe graft weight which was measured directly on the back-table during donor right hepatectomy in healthy live liver donors. The weight of the whole liver was calculated by the measurements of the liver volumes from CT.

MATERIALS AND METHODS

Study design

From May 10, 1996 to October 25, 2004, 182 consecutive right lobe live donor liver transplants were performed at the University of Hong Kong, Queen Mary Hospital. These 182 live liver donors being evaluated and operated were healthy with normal liver biochemistry. None of them was hepatitis B or C carriers, or had the habit of alcohol consumption. Donor anthropometric data including age, gender, BW (measured to the nearest 0.5 kg), and BH (measured to the nearest 1 cm) were recorded prospectively and entered into a liver transplantation database by 2 designated liver transplant research assistants. BSA was calculated by the formula by DuBois and DuBois: BSA (m^2) = BW (kg)$^{0.425}$ × BH (cm)$^{0.725}$ × 0.007184[5]. Body mass index = BW/BH × BH. CT of the donors was performed before the donor operation. Estimation of the liver volumes on CT was done by 3 dedicated radiologists using the Heymsfield method[13]. They had no information of the body size of the live liver donors or the liver transplant recipients. All subjects underwent single slice spiral CT (HiSpeed Advantage System; General Electric Health Care, Milwaukee, WI) and multi-slice CT study (LightSpeed QX/i 4-MDCT or LightSpeed 16-MDCT, General Electric Health Care, Milwaukee, WI) from 2000. Cuts were made at 5 to 7.5 mm intervals and continuously. Demarcation of the right and left portions of the liver was made by tracing along the middle hepatic vein, corresponding to the Cantlie's line. Volumes of the right lobe plus right caudate lobe (segment 1r) and the left lobe plus left caudate lobe (segment 1l)[14,15], were measured independently. All but 1 donor underwent donor right hepatectomy including the middle hepatic vein. This donor's right lobe graft did not include the middle hepatic vein for anatomical reason (case no. 85). The donor was a non-Chinese, and was therefore excluded. Details of the donor right hepatectomy have been described elsewhere[16]. In short, the transection line was determined by temporary inflow control. Transection by Cavitron ultrasonic surgical aspirator (CUSA; Valleylab, Boulder, CO), was just onto the left of the middle hepatic vein, including the latter into the right lobe liver graft. The right lobe liver grafts were perfused with University of Wisconsin Solution (NPBI, Emmer-Compascuum, the Netherlands), and from case no. 110 of the series, with histidine-tryptophan-ketoglutarate solution (Dr. Franz Köhler, Chemie GmbH, Alsbach-Hähnlein, Germany). The gallbladder was removed in the early phase of the hepatectomy during hilar dissection. No parts of the inferior vena cava, triangular ligament, or coronary ligament were included. The right lobe liver grafts were then weighed at the back-table. The weight of the whole donor liver was calculated by the right lobe graft weight (GW) divided by the volume fraction of the right lobe in relation to the entire liver as measured on the CT.

Exclusion criteria

We excluded 23 donors over this entire period of 8 years from this study. These included fatty change of the liver over 10% as documented by biopsy of the liver graft intraoperatively (n = 9). Non-Chinese donors (n = 6) were also excluded. The above 2 conditions occurred in 1 of the donors (n = 1). Donors with missing data of height were also excluded (n = 4). Donors with BW (n = 2) or BH (n = 1) lying beyond 97.5% were excluded. The number of subjects for analysis thus became 159.

Statistical analysis

Following testing for normal distribution (Kurtosis and Skewness tests), data were expressed as mean ± SD. Simple linear regression analysis by the least-squares fit method was used to plot the relation between calculated liver weight against BSA. This was then done with BW, and also BH as independent variables. Male and female subjects were analyzed separately. By stepwise multiple linear regression analysis, the correlation between calculated liver weight as a dependent variable and with BW and BH as independent variables, and gender as a binary factor, was tested. Goodness of fit of the formula was tested by analysis of residuals. Formulae deduced from other studies and this study were used to calculate the ESLW using BW, BH, BSA, and gender of these 159 subjects as appropriate[4,7-9,11,12,17,18]. ESLV derived from the respective formulae[4,7-10,18] was converted to ESLW by a factor of 1.19 mL/g as derived from analysis of data from this study. This was obtained by plotting liver volume on CT against calculated liver weight of these 159 subjects. The ESLW so derived was compared with the calculated liver weight of this series by 2-sided paired-samples t test. $P < 0.05$ was considered statistically significant. Regression lines of representative series were drawn and compared with the regression line of this study[4,8,9,12]. All statistical analyses were performed by SPSS Version11.0 program (SPSS, Chicago, IL).

RESULTS

Baseline characteristics

Characteristics of the 159 subjects and their livers are listed in Table 1. They were young. Females outnumbered males by 2 fold. Such a female preponderance was attributed to a higher proportion of male recipients (n=118), and their wives volunteered as the donor (n=58). Donors who were healthy had normal built as reflected from the BMI.

Liver weights and volumes

From the measurements made on the preoperative CT,

Table 1 Characteristics of subjects (mean ± SD, *n* = 159)

Age (yr)	**35.8 ± 10.5 (18-57)**
Gender (M : F)	53 : 106
Body weight (kg)	56.3 ± 8.4 (41.0-78.5)
Body height (cm)	161.7 ± 7.5 (144.5-181.3)
Body mass index (kg/m^2)	21.5 ± 2.6 (16.5-29.1)
Body surface area (m^2)	1.59 ± 0.14 (1.30-2.13)
Computed tomography liver volume (mL)	1,099.10 ± 181.51
Right lobe graft volume on CT (mL)	710.14 ± 131.46
Right lobe to total liver volume on CT (%)	64.55 ± 4.47 %
Right lobe graft weight (g)	598.90 ± 117.39
Estimated whole liver weight (g)	927.54 ± 168.78

CT: computed tomography.

the mean volume of the right lobe was 710.14 ± 131.46 mL and the whole liver was 1099.10 ± 181.51 mL. On the back-table, the right lobe grafts after being perfused with preservation solution, weighed 598.90 ± 117.39 g. The right lobe accounted for an average of 64.55% ± 4.47% of the entire liver on the CT. The total liver weight calculated was 927.54 ± 168.78 g.

Regression models

When the calculated liver weight was plotted against BSA for males ($R^2 = 0.37$) and females ($R^2 = 0.26$), the linear relationships were distinctly different (Figure 1A). Those females with the same BSA as males had a lower calculated liver weight. When BW was used instead of BSA, a similar pattern occurred for males ($R^2 = 0.38$) and females ($R^2 = 0.34$) (Figure 1B). The correlation of calculated liver weight with BH was much weaker for males ($R^2 = 0.13$) and in particular for females ($R^2 = 0.02$) (Figure 1C).

By stepwise multiple linear regression analysis, the relation of calculated liver weight with BW, BH, and gender (male = 1, female = 0) was tested. BH was excluded by the collinearity statistics of tolerance from the following formula so derived:

ESLW (g) = 218.32 + BW (kg) × 12.29 + gender × 50.74 (R^2 = 0.48)

or more conveniently:

ESLW (g) = 218 + BW (kg) × 12.3 + gender × 51

The ESLW is predictably correlated with ESLV. Based on linear regression analysis, the relation between ESLW and ESLV is as follows: ESLV (mL) = 302.34 + ESLW (g) × 0.859 (R^2 = 0.64), ESLW (g) = 111.25 + ESLV (mL) × 0.743 ($R^2 = 0.64$). For simplicity, the conversion factor is 1.19 mL/g (Figure 1D).

Comparison of different formulae to estimated liver size

Using the formulae for ESLV and ESLW from other studies[4,7-9,11,12,17,18], and the anthropometric data of the 159 subjects of this study, the ESLV and ESLW were calculated. The ESLW was converted from ESLV by factor of 1.19 mL/g. The ESLWs calculated from each formula were compared with the calculated liver weight of these 159 subjects by two-sided paired-samples *t* test. All except that calculated from the Urata formula ($P = 0.098$) were found to deduce a higher ESLW, with statistically significant differences ($P < 0.000$, Table 2). Amongst these, 4 regression models were selected for comparison using the regression line of best-fit method. In one German study using autopsy data, the ESLW was markedly higher[12], whereas the other series had fairly close ESLWs[4,8,9]. The regression line of the model from Urata correlated nicely in subjects of the middle range of body weights. Nonetheless, divergence was seen in subjects with body weight less than 60 kg, resulting in a higher ESLW.

DISCUSSION

The results of this study demonstrate that in healthy Chinese adults, ESLW was positively related to BW, and such correlation was also gender-dependent. The liver of the male was slightly heavier than that of the female of the same body weight. Furthermore, BH was found to be not required in the estimation of the standard liver weight. Statistically, by the test of collinearity for tolerance, BH was eliminated as an independent factor. Though many studies have used BSA as the independent factor for liver size estimation, in which BH is a key component in calculating BSA, our findings here corroborate with those studies which evaluated BW, BH , and BSA independently[8,12]. This is also in concordance with the use of only body weight as reference in determining the adequacy of the size of the liver graft from studies of North America[19] and Europe[20]. In such convention, the graft weight to recipient body weight ratio is expressed as graft recipient weight ratio (GRWR). However, the intercept of the regression line in this study did not meet at zero, using body weight as denominator as in GRWR, accuracy may be compromised in subjects who deviate much from the mean body weight of the population.

The DuBois formula for calculating BSA[5] has been used for estimating liver size in 4 formulae[4,7,11,18]. The deficiency of the BSA formula is that it is published in 1916 and deduced from planometric measurements of the body castings made on 9 subjects spanning a wide age range[5]. Larger series of BSA estimation by geometric methods revealed that the DuBois equation can predict lower BSA values[21]. The Mosteller equation which illustrates that BSA (m^2) = square root BH (cm) × BW (kg) /3600[22] has been used in 2 series for the sake of easier calculation[8,17]. On the whole, convenience of using BSA is in using the simple formula from linear regression. The easy access to personal computer nowadays may make this point relatively invalid. Using BW and BH from which BSA is derived also evades all possibilities of using data not applicable to the local population from which BSA formulae are deduced. One study showed that liver volume had a curvilinear relation with BSA[9]. The formula for calculating BSA itself has a curvilinear nature with BW and BH. Thus, a pure relation with BW and BH should rather be addressed.

The gender factor in relation to liver weight is alluded to as early as in the sixties[11]. This has been recently validated by another study which included gender in the formula deduced in estimating the ESLW[12]. Such phenomenon of gender difference can be anticipated as the female has a smaller fat-free mass given the same BW and BH[23-25]. A slightly small liver is therefore required to

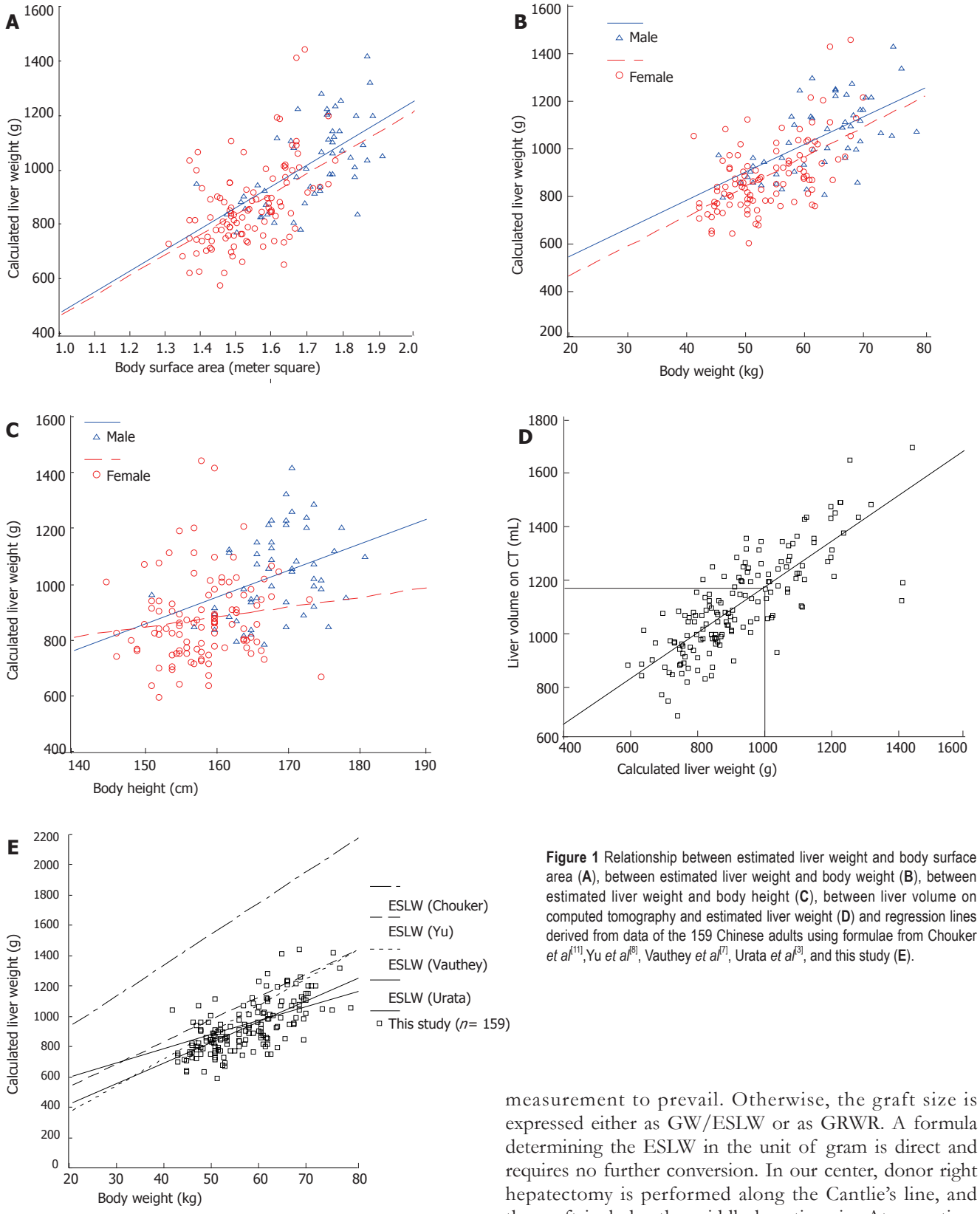

Figure 1 Relationship between estimated liver weight and body surface area (**A**), between estimated liver weight and body weight (**B**), between estimated liver weight and body height (**C**), between liver volume on computed tomography and estimated liver weight (**D**) and regression lines derived from data of the 159 Chinese adults using formulae from Chouker *et al*[11],Yu *et al*[8], Vauthey *et al*[7], Urata *et al*[3], and this study (**E**).

meet her metabolic need. The gender factor is also age-dependent, and becomes less important as the subjects become older[12]. This helps to explain why the gender factor was significant in our series in which the mean age of the subjects was 35.8 years.

Weight in gram is the common unit used in liver transplantation for quantifying the size of the liver graft. Handiness at the back-table enables this unit of measurement to prevail. Otherwise, the graft size is expressed either as GW/ESLW or as GRWR. A formula determining the ESLW in the unit of gram is direct and requires no further conversion. In our center, donor right hepatectomy is performed along the Cantlie's line, and the graft includes the middle hepatic vein. At operation, the line of demarcation between the right and left lobes is determined by temporary inflow control and marked by diathermy. It is our experience that the middle hepatic vein is predictably encountered during the course of liver transection employing the CUSA from the demarcation line to the mid portion of the inferior vena cava. Intraoperative ultrasonography certainly helps to define this plane and navigates the liver transection[26]. Weighing of the right lobe graft obviates the reliance on volume

Table 2 Comparison of regression models

Study	Formula	Mean ESLW (ESLV)	Difference in ESLW	*P*
Deland and North[11]	ESLW = 1020 × BSA^1 – 220	1400.41 g	- 472.86 g	0.000[a]
Heinemann[7]	ESLV = 1072.8 × BSA^1 - 345.7	1141.67 g (1358.59 mL)	- 214.12 g	0.000[a]
Yoshizumi[17]	ESLW = 772 × BSA^2	1225.50 g	- 297.95 g	0.000[a]
Yu[9]	ESLV = 21.585× $BW(kg)^{0.732}$ × $BH(cm)^{0.225}$	1087.32 g (1293.91 mL)	- 159.77 g	0.000[a]
Choukér[12]	ESLW = 452 + 16.434 × BW(kg) + 11.85 × age – 166 × gender (F=1, M=0)	1690.90 g	- 763.35 g	0.000[a]
Urata[4]	ESLV = 706.2 × BSA^1 + 2.4	944.79 g (1124.30 mL)	- 17.24 g	0.098
Vauthey[8]	ESLV = 1267.28 × BSA^2 -794.41	1022.95 g (1217.30 mL)	- 95.40 g	0.000[a]
Lee[18]	ESLV = 691 × BSA^1 + 95	1002.31 g (1192.75 mL)	- 74.76 g	0.000[a]
Lin[10]	ESLV = BH × 13 + BW × 12 - 1530	1048.85 g (1248.13 mL)	- 121.30 g	0.000[a]
This study	ESLW = 218.32 + BW × 12.29 + gender × 50.74 (M=1, F=0)	927.47 g	7.60E-2	0.994
Calculated liver weight		927.54 g		
Conversion factor 1.19 mL/g			paired samples *t* test	[a]$P < 0.05$

ESLV: estimated standard liver volume; ESLW: estimated standard liver weight; BSA: body surface area; BW: body weight; BH: body height; F, female; M, male.
[1]DuBois and DuBois[5]
[2]Mosteller[22]

determination of the liver by CT. Instead, it is the volume ratio of the right versus the left lobe that calculates the weight of the entire liver.

There is no perfect way of measuring the liver volume as this cannot be done with the organ *in-situ* in a healthy human subject. Many attempts have been made to get closest to the actual liver volume. ESLV can be obtained from measurement of the cadaveric internal organs. By definition, these measurements are acquired from non-healthy subjects with age bias, and influenced by sequelae of either the major illness leading to the demise, or the treatments like fluid resuscitation. Autopsy data excluding those with severe postmortem changes, extensive burns, blood transfusion, fluid infusion, and injury and pathological changes of the organ can minimize such errors[27]. By the principle of Archimedes, the liver volume is measured. An average tissue density of 1.04 kg/L[9] to 1.08 kg/L[7] is derived from correlation with the liver weight. Heinemann *et al*[7] have not pointed out the findings of the increase in liver volume in those with longer periods of survival before death. Furthermore, a gradual increase in liver volume has also been observed during the time interval between death and postmortem[7]. Deceased donor livers might be weighed with deduction of 2.3% for the weight of the gallbladder. The time from brain death to organ harvesting is usually short. Nonetheless, changes of volume status as a result of diabetes insipidus and fluid resuscitation, which are common in donors with intracerebral pathologies and perfusion with preservation solution, can still affect the liver size.

The accuracy of CT in assessing the liver volume has been evaluated. Inflow and outflow vessels of the liver from cadavers can be retrieved and dissected free of fascia and fat. They are weighed and underwent CT scan *ex-vivo*. A high correlation between the actual liver volume and the volume assessed by CT has been identified by Heymsfield *et al*[13]. Urata *et al*[4], reported that 19 children with end-stage liver disease undergoing liver transplantation also have their liver volume assessed preoperatively by CT. The liver volume obtained from CT is accurate. Another study reported the livers of fresh sheep can be scanned *in-vitro* and the volume can be measured by water displacement method[28]. All these 3 studies showed that the error of the CT is less than 5%. Nevertheless, it is worth noting that these are measurements of organs excised from deceased or diseased subjects. Misregistration errors made in tracing the peripheries of the liver on CT occur particularly in the thin portions such as the left lateral segment. Partial volume effect and respiratory movements are also possible sources of error. Overestimation for small livers and underestimation for large livers have also been observed[28]. Spiral CT which requires a shorter breath-holding period theoretically should minimize artifacts from breathing movements. This has, however, shown to be of no significance[29].

A potential major source of error in this study might come from the measurement of BW and BH in the ward. As donors were weighed wearing clothes, BW could be expected to have a systematic error of overestimation due to the weight of the clothes. As the BW and BH were measured in different wards over a long period, potential systematic errors from the equipments could be expected to be random instead of systematic. With continuous data collection, accuracy of the formula could be improved by more meticulous recording of BW and BH.

In comparison with ESLW/ESLV derived from other formulae, except that from Urata, the ESLW of the subjects in the current study was significantly smaller. Though statistically not significant, the Urata formula did overestimate liver weight in our adults less than 60 kg. The discrepancy between our formula and the others might be attributed to the fact that our liver grafts were weighed blood-free on the back-table. The liver already flushed with perfusion solution and devoid of back-perfusion via hepatic vein as *in-situ* is smaller and lighter. This nonetheless is the state at which the liver graft harvested is weighed. The conversion factor of 1.19 mL/g could be used for converstion of weight to volume. It is also possible that a smaller liver may be required to meet the metabolic need of the adult Chinese. The racial difference in the amount of visceral adipose tissue has been demonstrated by whole-body magnetic resonance imaging.

Asian Americans have a higher amount of visceral adipose tissue, thus less lean mass for the same body size[30]. A word of caution ought to be made in the application of data obtained from healthy and relatively young subjects to patients with various morbidities like wasting, edema, ascites, and perhaps to those of an older age.

In conclusion, these data demonstrate that ESLW can be derived from simple clinical parameters of weight and gender. The formulae for Caucasians may not be applicable to Chinese adults. Additional studies of more age- and weight-diverse subjects can provide additional information to this subject of interest.

REFERENCES

1 **Sugawara Y**, Makuuchi M. Small-for-size graft problems in adult-to-adult living-donor liver transplantation. *Transplantation* 2003; **75:** S20-S22
2 **Shirabe K**, Shimada M, Gion T, Hasegawa H, Takenaka K, Utsunomiya T, Sugimachi K. Postoperative liver failure after major hepatic resection for hepatocellular carcinoma in the modern era with special reference to remnant liver volume. *J Am Coll Surg* 1999; **188:** 304-309
3 **Shoup M**, Gonen M, D'Angelica M, Jarnagin WR, DeMatteo RP, Schwartz LH, Tuorto S, Blumgart LH, Fong Y. Volumetric analysis predicts hepatic dysfunction in patients undergoing major liver resection. *J Gastrointest Surg* 2003; **7:** 325-330
4 **Urata K**, Kawasaki S, Matsunami H, Hashikura Y, Ikegami T, Ishizone S, Momose Y, Komiyama A, Makuuchi M. Calculation of child and adult standard liver volume for liver transplantation. *Hepatology* 1995; **21:** 1317-1321
5 **Du Bois D**, DuBois EF. A formula to estimate the approximate surface area if height and weight be known.1916. *Nutrition* ;5:303-11; discussion 312-3
6 **Urata K**, Hashikura Y, Ikegami T, Terada M, Kawasaki S. Standard liver volume in adults. *Transplant Proc* 2000; **32:** 2093-2094
7 **Heinemann A**, Wischhusen F, Puschel K, Rogiers X. Standard liver volume in the Caucasian population. *Liver Transpl Surg* 1999; **5:** 366-368
8 **Vauthey JN**, Abdalla EK, Doherty DA, Gertsch P, Fenstermacher MJ, Loyer EM, Lerut J, Materne R, Wang X, Encarnacion A, Herron D, Mathey C, Ferrari G, Charnsangavej C, Do KA, Denys A. Body surface area and body weight predict total liver volume in Western adults. *Liver Transpl* 2002; **8:** 233-240
9 **Yu HC**, You H, Lee H, Jin ZW, Moon JI, Cho BH. Estimation of standard liver volume for liver transplantation in the Korean population. *Liver Transpl* 2004; **10:** 779-783
10 **Lin XZ**, Sun YN, Liu YH, Sheu BS, Cheng BN, Chen CY, Tsai HM, Shen CL. Liver volume in patients with or without chronic liver diseases. *Hepatogastroenterology* 1998; **45:** 1069-1074
11 **DeLand FH,** North WA. Relationship between liver size and body size. *Radiology* 1968; **91:** 1195-1198
12 **Chouker A**, Martignoni A, Dugas M, Eisenmenger W, Schauer R, Kaufmann I, Schelling G, Lohe F, Jauch KW, Peter K, Thiel M. Estimation of liver size for liver transplantation: the impact of age and gender. *Liver Transpl* 2004; **10:** 678-685
13 **Heymsfield SB**, Fulenwider T, Nordlinger B, Barlow R, Sones P, Kutner M. Accurate measurement of liver, kidney, and spleen volume and mass by computerized axial tomography. *Ann Intern Med* 1979; **90:** 185-187
14 **Kogure K**, Kuwano H, Fujimaki N, Makuuchi M. Relation among portal segmentation, proper hepatic vein, and external notch of the caudate lobe in the human liver. *Ann Surg* 2000; 231: 223-228
15 **Abdalla EK**, Vauthey JN, Couinaud C. The caudate lobe of the liver: implications of embryology and anatomy for surgery. *Surg Oncol Clin N Am* 2002; **11:** 835-848
16 **Fan ST**, Lo CM, Liu CL, Wang WX, Wong J. Safety and necessity of including the middle hepatic vein in the right lobe graft in adult-to-adult live donor liver transplantation. *Ann Surg* 2003; **238:** 137-148
17 **Yoshizumi T**, Gondolesi GE, Bodian CA, Jeon H, Schwartz ME, Fishbein TM, Miller CM, Emre S. A simple new formula to assess liver weight. *Transplant Proc* 2003; **35:** 1415-1420
18 **Lee SG**, Park KM, Hwang S, Lee YJ, Kim KH, Ahn CS, Choi DL, Joo SH, Jeon JY, Chu CW, Moon DB, Min PC, Koh KS, Han SH, Park SH, Choi GT, Hwang KS, Lee EJ, Chung YH, Lee YS, Lee HJ, Kim MH, Lee SK, Suh DJ, Kim JJ, Sung KB. Adult-to-adult living donor liver transplantation at the Asan Medical Center, Korea. *Asian J Surg* 2002; **25:** 277-284
19 **Ben-Haim M**, Emre S, Fishbein TM, Sheiner PA, Bodian CA, Kim-Schluger L, Schwartz ME, Miller CM. Critical graft size in adult-to-adult living donor liver transplantation: impact of the recipient's disease. *Liver Transpl* 2001; **7:** 948-953
20 **Troisi R**, de Hemptinne B. Clinical relevance of adapting portal vein flow in living donor liver transplantation in adult patients. *Liver Transpl* 2003; **9:** S36-S41
21 **Gehan EA**, George SL. Estimation of human body surface area from height and weight. *Cancer Chemother Rep* 1970; **54:** 225-235
22 **Mosteller RD**. Simplified calculation of body-surface area. *N Engl J Med* 1987; **317:** 1098
23 **Kotler DP**, Burastero S, Wang J, Pierson RN Jr. Prediction of body cell mass, fat-free mass, and total body water with bioelectrical impedance analysis: effects of race, sex, and disease. *Am J Clin Nutr* 1996; **64:** 489S-497S
24 **Kyle UG**, Pichard C, Rochat T, Slosman DO, Fitting JW, Thiebaud D. New bioelectrical impedance formula for patients with respiratory insufficiency: comparison to dual-energy X-ray absorptiometry. *Eur Respir J* 1998; **12:** 960-966
25 **Janssen I**, Heymsfield SB, Wang ZM, Ross R. Skeletal muscle mass and distribution in 468 men and women aged 18-88 yr. *J Appl Physiol* 2000; **89:** 81-88
26 **Fan ST**, Lo CM, Liu CL. Technical refinement in adult-to-adult living donor liver transplantation using right lobe graft. *Ann Surg* 2000; **231:** 126-131
27 **Ogiu N**, Nakamura Y, Ijiri I, Hiraiwa K, Ogiu T. A statistical analysis of the internal organ weights of normal Japanese people. *Health Phys* 1997; **72:** 368-383
28 **Kayaalp C**, Arda K, Oto A, Oran M. Liver volume measurement by spiral CT: an in vitro study. *Clin Imaging* 2002; **26:** 122-124
29 **Stapakis J**, Stamm E, Townsend R, Thickman D. Liver volume assessment by conventional vs. helical CT. *Abdom Imaging* 1995; **20:** 209-210
30 **Park YW**, Allison DB, Heymsfield SB, Gallagher D. Larger amounts of visceral adipose tissue in Asian Americans. *Obes Res* 2001; **9:** 381-387

S- Editor Guo SY **L- Editor** Wang XL **E- Editor** Cao L

PO Box 2345, Beijing 100023, China
www.wjgnet.com
wjg@wjgnet.com

World J Gastroenterol 2006 April 14; 12(14): 2223-2228
World Journal of Gastroenterology ISSN 1007-9327

CLINICAL RESEARCH

Gastrointestinal stromal tumors in a cohort of Chinese patients in Hong Kong

Kam Hoi Chan, Chun Wing Chan, Wai Hung Chow, Wai Keung Kwan, Chi Kwan Kong, Ka Fung Mak, Miu Yi Leung, Lin Kiu Lau

Kam Hoi Chan, Chun Wing Chan, Wai Hung Chow, Wai Keung Kwan, Department of Medicine, Yan Chai Hospital, Tsuen Wan, Hong Kong SAR, China
Chi Kwan Kong, Department of Surgery, Yan Chai Hospital, Tsuen Wan, Hong Kong SAR, China
Ka Fung Mak, Miu Yi Leung, Department of Radiology, Yan Chai Hospital, Tsuen Wan, Hong Kong SAR, China
Lin Kiu Lau, Department of Pathology, Yan Chai Hospital, Tsuen Wan, Hong Kong SAR, China
Co-first-author: Kam Hoi Chan and Chun Wing Chan
Correspondence to: Dr. Kam Hoi Chan, Department of Medicine, Yan Chai Hospital, Tsuen Wan, Hong Kong SAR, China. kamhoichan@gmail.com
Telephone: +852-94851466 Fax: +852-24116536
Received: 2005-08-17 Accepted: 2005-08-27

Abstract

AIM: To investigate the prevalence and clinical pattern of gastrointestinal stromal tumors (GISTs) in Hong Kong Chinese, and to assess the impact of introduction of CD117 on the disease incidence.

METHODS: From the database of the Department of Pathology of Yan Chai Hospital, 47 patients, with GISTs from September 1995 to December 2003 were included in this study. Ten GISTs were diagnosed before the introduction of CD117. The clinical features, tumor characteristics, and treatment were analyzed. Factors predicting tumor related death or recurrence were studied with Cox proportional hazard model.

RESULTS: The patients included 26 males and 21 females, with a mean age of 66.6 years (SD 13.1, range 29-87 years). The estimated prevalence of GISTs was 13.4-15.6 per 100 000 people, with an annual incidence of 1.68-1.96 per 100 000 people. The annual incidence of GISTs before and after the introduction of CD117 was 1.1 per 100 000 people and 2.1 per 100 000 people respectively. Stomach (34 patients, 72.3%) was the most common location for the tumor, followed by the small intestine (8 patients, 17.0%), esophagus (2 patients, 4.3%), omentum (2 patients, 4.3%) and colon (1 patient, 2.1%). Thirty-one patients (66%) had complete tumor resection. Eleven out of 16 deaths (23%) were tumor-related. The median survival time was 26 mo. Five-year survival rate was 61.3%. The significant factors associated with tumor-related death or recurrence were incomplete resection, tumor size 5 cm or above, invasion to the adjacent organ or presence of metastasis.

CONCLUSION: The incidence of GIST in Hong Kong is comparable to that in the United States but lower than that in Finland. The true incidence of GISTs could be underestimated before the introduction of CD117. Incomplete resection, tumor size 5 cm or above, invasion to the adjacent organ or presence of metastasis are factors predicting tumor-related death or recurrence.

Key words: Gastrointestinal tumor; GIST; Prognostic factors; Clinical features; Incidence

Chan KH, Chan CW, Chow WH, Kwan WK, Kong CK, Mak KF, Leung MY, Lau LK. Gastrointestinal stromal tumors in a cohort of Chinese patients in Hong Kong. *World J Gastroenterol* 2006; 12(14): 2223-2228

http://www.wjgnet.com/1007-9327/12/2223.asp

INTRODUCTION

Gastrointestinal stromal tumors (GISTs) are uncommon mesenchymal tumors that have been a controversial topic since their first description by Golden and Stoot in 1941[1]. In the past three decades, there has been considerable debate regarding its nomenclature, cellular origin, diagnosis, and prognosis[2]. Before the discovery of gain-of-function mutations in the *c-KIT* proto-oncogene in GISTs by Hirota and colleagues in 1998[3], most GISTs were thought to be smooth muscle neoplasm, and were classified as leiomyosarcoma due to their similar appearance by light microscopy. At present, GISTs are defined as spindle-cell, epithelioid, or occasionally pleiomorphic mesenchymal tumours of the gastrointestinal tract that express the *c-KIT* protein[4]. The precise cellular origin of GISTs recently has been proposed to be the interstitial cell of Cajal, an intestinal pacemaker cell[5]. The definition of *c-KIT*-negative GISTs remains a focus of research. In this study, we analyzed 47 Chinese patients with GISTs in Yan Chai Hospital to study their clinical, pathological characteristics, survival pattern and recurrence. The impact of introduction of CD117 on the incidence of this tumor was assessed, as well.

MATERIALS AND METHODS

Patient selection

From the database of the Department of Pathology of Yan Chai Hospital, we selected patients with the diagnoses of gastrointestinal stromal tumors (GISTs), leiomyoma, leiomyoblastoma and leiomyosarcoma from September 1995 to December 2003. Their histology slides were reviewed by a separate pathologist of the Department of Pathology. Patients with the diagnosis of GISTs were recruited to our study.

Clinical information including age, sex, comorbidity of the patients and presentation status of the tumor were recorded. The presentation status of the tumor reflected the extent of disease and the history of prior treatment when the patient was first seen in our hospital. The tumor was categorized as primary, metastatic or locally recurrent. Acute gastrointestinal haemorrhage was defined as significant blood loss requiring transfusion or haemodynamically significant blood loss. The criteria for chronic gastrointestinal haemorrhage were intermittent melena, guaiac-positive stool or iron deficiency anaemia. Ranges of diagnostic tests were used in these patients. They involved evaluating the gastrointestinal tract with contrast such as barium studies, endoscopies or ultrasound of abdomen. Computerized tomography scan and mesenteric angiography were used in some patients. Histology with or without adjacent organ involvement was also recorded. Histological subtype was determined by examination of light microscopy applying different staining methods. Immunohistochemistry stain included vimentin, alpha-smooth muscle actin, desmin, neuron-specific enolase (NSE), S100 protein and CD 34. CD117 was introduced to our Department of Pathology since October 1998. Electronic microscopy was also performed.

Tumor size was tabulated based on actual measurement of the gross surgical specimen or imaging when the tumor was inoperable. It was recorded as the largest diameter in any dimension of the primary tumor and was classified into < 5 cm, 5 to 10 cm, or >10 cm. Resection margins were checked closely for presence of microscopic disease. Tumors were also grouped according to their mitotic numbers as no mitosis (0/10 HPF), low mitotic index (1-4/10 HPF) and high mitotic index (≥5/10 HPF). Tumor cellularity, presence or absence of invasive growth, tumor necrosis and the presence or absence of haemorrhage were also examined.

Complete resection was defined as the excision of all gross disease regardless of microscopic margins. Resections were classified as incomplete when gross residual disease was present after resection. Inoperable was defined as when the tumor was unresectable at surgical exploration. Patients with incompletely resected tumor, metastatic or unresectable tumor were referred to oncology units for chemotherapy and radiation therapy as indicated. In total, 47 patients satisfied the diagnosis of GISTs.

Survival analysis

All times were calculated from the first presentation to the date of last follow-up or death. Time of last follow-up of dead patient was recorded as the time of certification of death. Others were censored at the time of last follow-up in specialist outpatient clinic or admission (clinical or emergency) whichever was later. Clinical variables, tumor characteristics, as well as modality of treatment were analyzed against tumor recurrence or death.

Statistic analysis

Statistical analyses were performed using SPSS 10.0(SPSS Inc., Chicago, USA). Influence of the factors in predicting tumor recurrence or death was assessed by univariate analyses. Multivariate analysis was performed with the Cox proportional hazards model to identify significant prognostic factors. $P<0.05$ was considered statistically significant.

RESULTS

Patient characteristics

Between September 1995 to December 2003, 47 patients (26 men and 21 women) were diagnosed with GIST. Mean follow up time in this cohort was 31 mo (range 0-99 mo). Mean age was 66.6 years (SD 13.1, range 29 to 87). Stomach (34 patients, 72.3%) was the most common site for the tumor, followed by the small intestine (8 patients, 17.0%), esophagus (2 patients, 4.3%), omentum (2 patients, 4.3%) and colon (1 patient, 2.1%). Gastrointestinal bleeding was the most common presenting symptom (28 patients, 60%), followed by epigastric pain (21 patients, 45%), and the presence of an abdominal mass (10 patients, 21%). Three patients (6%) with GIST were diagnosed incidentally. Endoscopically, the most common finding was a round tumor mass, either pedunculated or sessile, resembling a leiomyoma. Huge tumor usually presented as submucosal mass bulging into the lumen. Active bleeding ulcer or ulcer with stigmata of recent haemorrhage was present in 5 cases (71%) (Table 1). Radiological imaging including computerized tomography (CT) scan of the abdomen and barium studies were employed in most of our patients to identify the site and to assess the size of the lesions as well as the presence of any local invasion or distant metastases (Figure 1). Two patients had metastases delineated by CT scan, one in liver and one in omentum respectively, which precluded any curative surgical intervention.

Tumor characteristics

Tumor size ranged from 0.3 to 24 cm (median 4.5 cm, inter-quartile range 3-7.5 cm). Twenty-seven (57%) patients had tumor size less than or equal to 5 cm, 14 (30%) patients with tumor size between 5 cm to 10 cm, whereas 6 (13%) patients presented with tumor size greater than 10 cm. Seven (15%) patients had high mitotic index (≥ 5/10 HPF), 18 (38%) patients low (1-4/10 HPF) and 22 (47%) no mitotic index (0/10 HPF). Necrosis inside the tumor was found in 15 patients (32%) with GISTs. Seven out of 47 patients (15%) had presence of tumor metastases or invasion to adjacent organs. Immunohistochemical analyses were performed in all cases. Eleven (23%) GISTs had markers for neuronal and neuroendocrine tumors,

Table 1 Characteristics of patients with GISTs

Characteristics		*n* (%)
Number of patients		47
Male/Female (ratio)		26:21 (1.23:1)
Mean age at the time of diagnosis(SD)		66.60 (SD 19.1)
Median follow up time in months (IQR)		26.00 (10-43)
Presenting symptoms		
	GI bleeding	28 (60%)
	Epigastric pain	21 (45%)
	Abdominal mass	10 (21%)
	Incidental finding	3 (6.3%)
Locations		
	Stomach	34 (72.3%)
	Small bowel	8 (17.0%)
	Esophagus	2 (4.3%)
	Colon	1 (2.1%)
	Omentum	2 (4.3%)
Resection[1]		
	Complete	31 (66%)
	Incomplete	7 (14.9%)
	Inoperable	5 (10.6%)
Recurrence (after initial surgery)	Total	4 (8.5%)
	Local recurrence	1 (2.1%)
	Distal metastasis	3 (6.4%)
Death	Total	16 (34%)
	Tumor related	11 (23.4%)
	Tumor unrelated	5 (10.6%)

[1]Two patients refused resection of tumor. Two GISTs were discovered incidentally during autopsy. IQR: Inter-quartile range

Table 2 Tumor characteristics of 47 patients with GISTs

		n (%)
Number of patients		47
Median tumor size in cm (IRQ)		6.05 (3-7.5)
	≤5 cm	24 (51)
	>5-10 cm	13 (28)
	>10 cm	4 (9)
Mitotic index		
	High	7 (15)
	Low	18(38)
	No	22(47)
Presence of distal metastasis or local invasion		7 (15)

8(17%) demonstrated immunohistology markers for myoid series. Twenty-eight (60%) GISTs were undifferentiated tumors (Table 2).

Treatment

All patients were assessed for tumor resection either endoscopically or surgically. Thirty-one patients (66%) had complete resection of the tumor, and 7 patients (15%) underwent incomplete resection. In 5 patients (10%), resection of tumor was impossible because of extensive tumor metastases or poor general condition at the time of diagnosis. Endoscopic resection was possible only in 7 patients (15%) (5 gastric, 1 oesophageal and 1 colonic GISTs). All small bowel GISTs required surgical resection. Adjuvant chemotherapy by Imatinib (Glivec) was given in 2 patients post-operatively.

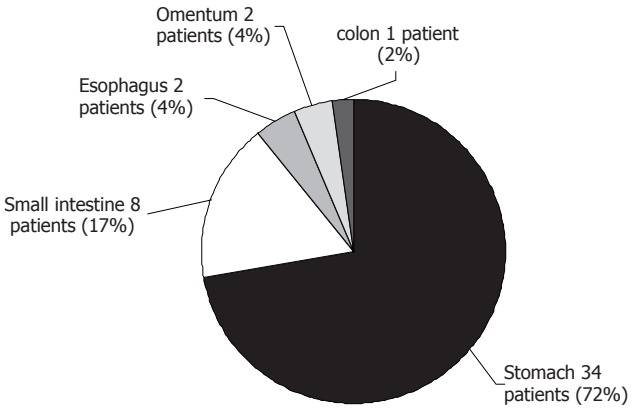

Figure 1 Tumor Locations of 47 GISTs

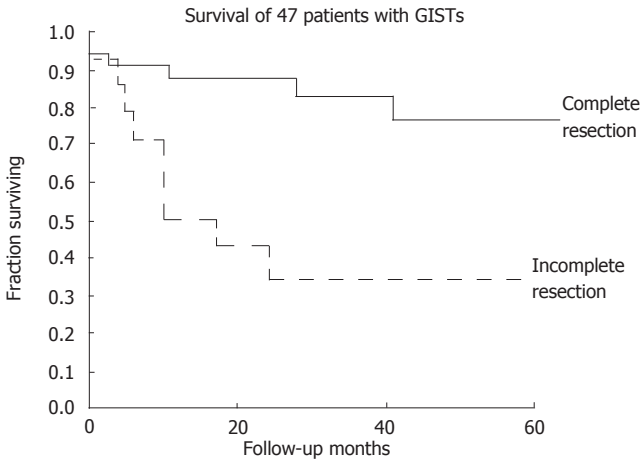

Figure 2 Kaplan-Meier survival curve of GIST patients with complete and incomplete tumor resection.

Survival

Totally 16 deaths were recorded in the study period, and 11 deaths were tumor related. The overall median survival was 26 mo. Five-year survival probability was 61.3% (SE 8.0%). The median survival time for completely resected GISTs was longer than that for incompletely resected or inoperable patients, 37 mo versus 10 mo respectively (log rank test, $P=0.0013$) (Figure 2). Two patients receiving imatinib were still alive at the end of the study, with liver metastatsis. Their survival time censored at the end of the study was 26 mo and 37 mo respectively.

Prognostic factors

By univariate analyses, the significant factors predicting tumor recurrence or tumor related death included tumor size 5 cm or above ($P=0.003$), presence of significant mitotic figures (1/10 HPF or above) ($P=0.021$), presence of necrosis ($P=0.005$), invasion to adjacent organ and/or presence of metastases at the time of diagnosis ($P<0.001$),

Table 3 Univariate analyses of factors predicting GISTs recurrence or tumor related death

Prognostic factors	Hazard ratios	*P* value
Tumor size 5 cm or above	20.5	0.003
Presence of significant mitotic figures (1/10 HPF or above)	3.8	0.021
Presence of necrosis	4.4	0.005
Invasion to adjacent organ and/or presence of metastases at the time of diagnosis	16.5	<0.001
Incomplete tumor resection	4.6	0.002

Table 4 Multivariate analyses of factors predicting GISTs recurrence or tumor-related death

Prognostic factors	Hazard ratios (CI)	*P* value
Tumor size 5 cm or above	9.6 (1.1-86.0)	0.042
Invasion to adjacent organ and/or presence of metastases at the time of diagnosis	14.0 (2.5-78.6)	0.003
Incomplete tumor resection	2.1 (1.1-86.0)	0.032

incomplete tumor resection ($P = 0.002$) (Table 3). By multivariate analyses, tumor size 5 cm or above (hazard ratio = 9.6, $P = 0.042$), invasion to adjacent organ and/or presence of metastases at the time of diagnosis (hazard ratio 14.0, $P = 0.003$), and incomplete tumor resection (hazard ratio = 2.1, $P = 0.032$) remained the significant factors predicting tumor recurrence or tumor related death (Table 4).

DISCUSSION

In this study, we summarized our 8 years' experience in the diagnosis and management of GISTs in a regional hospital in Hong Kong. Stromal tumors of the gastrointestinal tract are rare, accounting for less than 1% of all gastrointestinal tract malignancies. Their presumed origin from smooth muscle cells has led to the use of terms such as "leiomyoma", "leiomyoblastoma" and "epithelioid leiomyosarcoma". However, the exact origin of the tumor was difficult to determine in the early days until discovery of gain-of-function mutations in the *c-KIT* proto-oncogene in GISTs by Hirota and colleagues in 1998[3]. Therefore, the incidence of GISTs was rarely reported in the literature and was not reported in Chinese population.

Our hospital serves a local population of 300 000-350 000. The estimated prevalence of GISTs was 13.4-15.6 per 100 000 people, with an annual incidence of 1.68-1.96 per 100 000 people. This is comparable to that of the United States where the estimated annual incidence is 1-2 cases per 100 000 people, of which 20%-30% are malignant[4]. In contrast, Finland has higher annual incidence of malignant GISTs, 0.4 per 100 000 people[6], i.e. estimated 4 GISTs per 100 000 people.

The true incidence of GISTs could be underestimated before the introduction of CD117. In our hospital, all gastrointestinal tract tumors suspected to be GISTs were routinely tested for CD 117 marker since October 1998.

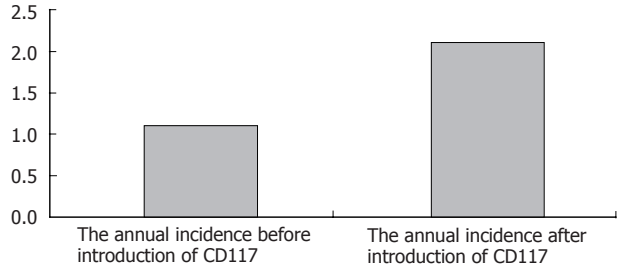

Figure 3 The annual incidence of GISTs before and after the introduction of CD117 was 1.1 per 100 000 people and 2.1 per 100 000 people respectively.

Interestingly, only 10 patients out of 47 (21%) were diagnosed as GISTs before the introduction of CD117. The annual incidence of GISTs after the introduction of CD117 increased from 1.1 per 100 000 people to 2.1 per 100 000 people (Figure 3). Similar trend was also noted in the United States. The estimated incidence of GISTs in the United States was around 0.6 per 100 000 people in the 1980s. The incidence increased to approximately 1-2 patients per 100 000 people after 2 000[4].

There existed some conflicting evidence on male predominance, however, most studies indicated no sex predilection[18, 21, 24, 31]. In our study, the occurrences of GISTs were similar in both sexes (1.2 male to 1 female). The age of presentation had a unimodal distribution, similar to the published data where the majority of patients presents in the fifth to seventh decade of life[4], the mean age of presentation of our patients was 66 years. GISTs are occasionally found in young adults, but they are very rare in children[7].

The vast majority of GISTs arise as a result of somatic mutation, but rare familial cases associated with mutated *c-KIT* have been identified[8, 10-12]. In our study, we could not identify any patient with familial relation. All the patients with GISTs were sporadic, and the predisposing factors were unknown.

Similar to other published data[7,13,14], the stomach was the most frequent site of involvement in our patients (72%), followed by small intestine (17%). The large bowel, esophagus and omentum were least likely involved. Symptomatic lesions have manifestations that depend on tumor size, location and growth pattern[7,13,14]. Ludwig and Traverso reported that GISTs with intraluminal nodule less than 2 cm was generally asymptomatic while tumors >4 cm were associated with symptoms[15]. In the literature approximately 50% of patients presented with acute or subacute gastrointestinal bleeding as the major symptom leading to diagnosis[25]. In our local patients, the most common presenting symptoms were gastrointestinal bleeding (60%), as results of overlying mucosal ulceration, followed by epigastric pain and abdominal mass. Other symptoms included fever, anorexia, dysphagia, obstruction and perforation of bowel were seldom seen in our series. Clinically palpable mass usually implies invasion to adjacent organs or distant metastasis, thus in turn predicts poor outcome of the patients. Surgical resection is the treatment of choice and should be performed with the intention to performing complete en bloc resection of the tumor, as it

is difficult or impossible to differentiate between benign or malignant lesions before or during operation[16]. Tumor size and frozen section during operation are not conclusive [17,18].

Prognostic factors

Gastrointestinal stromal tumors are unique in that their malignant potential is not always predictable. Most GISTs appear relatively low grade histologically, and it has been difficult to distinguish benign from malignant GISTs, especially at the low-grade end of the histological spectrum. Many previous studies suggest a single factor or even combinations of two factors are not sufficient to reliably predict the outcome of GISTs[19]. Currently no accepted staging system exists. Most pathologists use a multiparametric approach to predict the biological behavior of GISTs. The most reproducible predictor of malignancy has been mitotic rate >1-5 mitosis per 10 HPF[20-22]. Other poor prognostic factors include tumor size > 5 cm[23-27], mutation in the c-kit gene[28-30], necrosis[18, 20, 24, 31], infiltration and metastasis to other sites[13]. In our study, significant prognostic factors were tumor size 5 cm or above, invasion to adjacent organ and/or presence of metastases at the time of diagnosis as well as incomplete tumor resection. In contrast to previous studies[20-22], mitotic index did not appear as significant prognostic factor in our cohort. The different approaches to sample tissue from large tumors with considerable heterogeneity for microscopic assessment may explain such discrepancy between different studies. At present, the best method to adequately sample tumor tissue and report mitotic index is still controversial. In our hospital, our pathologists choose random sampling approach and report the highest mitotic index among different tissue samples. From the literatures, approximately 10% to 30% of all GISTs display malignant behavior[4, 14]. Our patients with GIST demonstrated similar ratio regarding malignant GISTs.

Survival

The overall survival appears to reflect the completeness of resection[7, 18, 32]. In Roswell Park Cancer Institute (RPCI), the United States, the median survival rate was significantly higher in those who underwent complete resection (33 mo) as compared to those who underwent palliative surgery (15 mo)[32]. Similarly in our center, the median survival time for completely resected GISTs was significantly longer than incompletely resected or inoperable patients, 37 mo versus 10 mo. The adjuvant therapy appeared to improve the survival and the quality of life in patients with incomplete tumor resections. Despite extensive metastasis, the 2 patients receiving imatinib were still alive at the end of the study. The survival times of 26 mo and 37 mo were much longer than the median 10 mo of other patients with incomplete tumor resection, although the number of patient in this group was too small for statistical analysis.

Recurrence is commonly local and peritoneal, often associated with liver metastasis. Peritoneal metastases are most probably a result of tumor cells seeding from the primary tumor directly into the peritoneal cavity. Liver metastases most probably result from haematogenous seeding into the portal vein[33]. Extra-abdominal disease in the absence of peritoneal involvement is rare[13]. There exist few reports in the literature describing a survival advantage after the resection of abdominal recurrence. In our hospital, local recurrence of GIST was not routinely operated again.

In conclusion, the incidence of GIST in Hong Kong is comparable to that of United States but lower than that in Finland. The true incidence of GISTs could be underestimated before the introduction of CD117. Incomplete resection, tumor size 5 cm or above, invasion to the adjacent organ or presence of metastasis are factors predicting tumor-related death or recurrence. The survival of the completely resected tumor is good. The introduction of medical adjuvant therapy appears to improve the survival and the quality of life in the unresectable and incompletely resected GISTs patients.

REFERENCES

1 **Golden T**, Stoot AP. Smooth Muscle tumors of the gastrointestinal tract and retroperitoneal tissue. *Surg Gynecol Obstet* 1941; **73:** 784-810
2 **Suster S**. Gastrointestinal stromal tumors. *Semin Diagn Pathol* 1996; **13:** 297-313
3 **Hirota S**, Isozaki K, Moriyama Y, Hashimoto K, Nishida T, Ishiguro S, Kawano K, Hanada M, Kurata A, Takeda M, Muhammad Tunio G, Matsuzawa Y, Kanakura Y, Shinomura Y, Kitamura Y. Gain-of-function mutations of c-kit in human gastrointestinal stromal tumors. *Science* 1998; **279:** 577-580
4 **Miettinen M**, Lasota J. Gastrointestinal stromal tumors--definition, clinical, histological, immunohistochemical, and molecular genetic features and differential diagnosis. *Virchows Arch* 2001; **438:** 1-12
5 **Kindblom LG**, Remotti HE, Aldenborg F, Meis-Kindblom JM. Gastrointestinal pacemaker cell tumor (GIPACT): gastrointestinal stromal tumors show phenotypic characteristics of the interstitial cells of Cajal. *Am J Pathol* 1998; **152:** 1259-1269
6 **Miettinen M**, Sarlomo-Rikala M, Lasota J. Gastrointestinal stromal tumours. *Ann Chir Gynaecol* 1998; **87:** 278-281
7 **DeMatteo RP**, Lewis JJ, Leung D, Mudan SS, Woodruff JM, Brennan MF. Two hundred gastrointestinal stromal tumors: recurrence patterns and prognostic factors for survival. *Ann Surg* 2000; **231:** 51-58
8 **Beghini A**, Tibiletti MG, Roversi G, Chiaravalli AM, Serio G, Capella C, Larizza L. Germline mutation in the juxtamembrane domain of the kit gene in a family with gastrointestinal stromal tumors and urticaria pigmentosa. *Cancer* 2001; **92:** 657-662
9 **Nishida T**, Hirota S, Taniguchi M, Hashimoto K, Isozaki K, Nakamura H, Kanakura Y, Tanaka T, Takabayashi A, Matsuda H, Kitamura Y. Familial gastrointestinal stromal tumours with germline mutation of the KIT gene. *Nat Genet* 1998; **19:** 323-324
10 **Maeyama H**, Hidaka E, Ota H, Minami S, Kajiyama M, Kuraishi A, Mori H, Matsuda Y, Wada S, Sodeyama H, Nakata S, Kawamura N, Hata S, Watanabe M, Iijima Y, Katsuyama T. Familial gastrointestinal stromal tumor with hyperpigmentation: association with a germline mutation of the c-kit gene. *Gastroenterology* 2001; **120:** 210-215
11 **Carney JA**. Gastric stromal sarcoma, pulmonary chondroma, and extra-adrenal paraganglioma (Carney Triad): natural history, adrenocortical component, and possible familial occurrence. *Mayo Clin Proc* 1999; **74:** 543-552
12 **Ishida T**, Wada I, Horiuchi H, Oka T, Machinami R. Multiple small intestinal stromal tumors with skeinoid fibers in association with neurofibromatosis 1 (von Recklinghausen's disease). *Pathol Int* 1996; **46:** 689-95
13 **Pidhorecky I**, Cheney RT, Kraybill WG, Gibbs JF. Gastrointestinal stromal tumors: current diagnosis, biologic behavior, and management. *Ann Surg Oncol* 2000; **7:** 705-712

14 **Miettinen M**, Sarlomo-Rikala M, Lasota J. Gastrointestinal stromal tumors: recent advances in understanding of their biology. *Hum Pathol* 1999; **30:** 1213-1220
15 **Ludwig DJ**, Traverso LW. Gut stromal tumors and their clinical behavior. *Am J Surg* 1997; **173:** 390-394
16 **Diamond T**, Danton MH, Parks TG. Smooth muscle tumours of the alimentary tract. *Ann R Coll Surg Engl* 1990; **72:** 316-320
17 **Langley JR**, Rosato FE, Vansant JH. Smooth muscle tumors of the stomach and small bowel. *Va Med* 1979; **106:** 272-275
18 **Shiu MH**, Farr GH, Papachristou DN, Hajdu SI. Myosarcomas of the stomach: natural history, prognostic factors and management. *Cancer* 1982; **49:** 177-187
19 **Bucher P**, Villiger P, Egger JF, Buhler LH, Morel P. Management of gastrointestinal stromal tumors: from diagnosis to treatment. *Swiss Med Wkly* 2004; **134:** 145-153
20 **Ballarini C**, Intra M, Ceretti AP, Prestipino F, Bianchi FM, Sparacio F, Berti E, Perrone S, Silva F. Gastrointestinal stromal tumors: a "benign" tumor with hepatic metastasis after 11 years. *Tumori* 1998; **84:** 78-81
21 **Evans HL**. Smooth muscle tumors of the gastrointestinal tract. A study of 56 cases followed for a minimum of 10 years. *Cancer* 1985; **56:** 2242-2250
22 **Yu CC**, Fletcher CD, Newman PL, Goodlad JR, Burton JC, Levison DA. A comparison of proliferating cell nuclear antigen (PCNA) immunostaining, nucleolar organizer region (AgNOR) staining, and histological grading in gastrointestinal stromal tumours. *J Pathol* 1992; **166:** 147-52
23 *Appelman HD*, Helwig EB. Sarcomas of the stomach. *Am J Clin Pathol* 1977; **67:** 2-10
24 **Chou FF**, Eng HL, Sheen-Chen SM. Smooth muscle tumors of the gastrointestinal tract: analysis of prognostic factors. *Surgery* 1996; **119:** 171-177
25 **Dougherty MJ**, Compton C, Talbert M, Wood WC. Sarcomas of the gastrointestinal tract. Separation into favorable and unfavorable prognostic groups by mitotic count. *Ann Surg* 1991; **214:** 569-574
26 **Emory TS**, Sobin LH, Lukes L, Lee DH, O'Leary TJ. Prognosis of gastrointestinal smooth-muscle (stromal) tumors: dependence on anatomic site. *Am J Surg Pathol* 1999; **23:** 82-87
27 **Franquemont DW**. Differentiation and risk assessment of gastrointestinal stromal tumors. *Am J Clin Pathol* 1995; **103:** 41-47
28 **Ernst SI**, Hubbs AE, Przygodzki RM, Emory TS, Sobin LH, O 'Leary TJ. KIT mutation portends poor prognosis in gastrointestinal stromal/smooth muscle tumors. *Lab Invest* 1998; **78:** 1633-1636
29 **Lasota J**, Jasinski M, Sarlomo-Rikala M, Miettinen M. Mutations in exon 11 of c-Kit occur preferentially in malignant versus benign gastrointestinal stromal tumors and do not occur in leiomyomas or leiomyosarcomas. *Am J Pathol* 1999; **154:** 53-60
30 **Taniguchi M**, Nishida T, Hirota S *et al*. Effect of c-kit mutation on prognosis of gastrointestinal stromal tumors. *Cancer Res* 1999; **59:** 4297-4300
31 **Ng EH**, Pollock RE, Munsell MF, Atkinson EN, Romsdahl MM. Prognostic factors influencing survival in gastrointestinal leiomyosarcomas. Implications for surgical management and staging. *Ann Surg* 1992; **215:** 68-77
32 **Carson W**, Karakousis C, Douglass H, Rao U, Palmer ML. Results of aggressive treatment of gastric sarcoma. *Ann Surg Oncol* 1994; 1: 244-251
33 **Joensuu H**, Fletcher C, Dimitrijevic S, Silberman S, Roberts P, Demetri G. Management of malignant gastrointestinal stromal tumours. *Lancet Oncol* 2002; **3:** 655-664

S- Editor Wang J **L- Editor** Zhu LH **E- Editor** Bai SH

PO Box 2345, Beijing 100023, China
www.wjgnet.com
wjg@wjgnet.com

World J Gastroenterol 2006 April 14; 12(14): 2229-2234
World Journal of Gastroenterology ISSN 1007-9327

CLINICAL RESEARCH

Establishment of risk model for pancreatic cancer in Chinese Han population

Xing-Hua Lu, Li Wang, Hui Li, Jia-Ming Qian, Rui-Xue Deng, Lu Zhou

Xing-Hua Lu, Jia-Ming Qian, Rui-Xue Deng, Lu Zhou. Department of Gastroenterology, Peking Union Hospital, Peking Union Medical College, Chinese Academy of Medical Sciences, Beijing, 100730, China
Li Wang, Hui Li. Department of Epidemiology, School of Basic Medical Sciences, Peking Union Medical College, Chinese Academy of Medical Sciences, Beijing, 100005, China
Supported by Clinical Subject Fund of the Ministry of Public Health of China, No. 20010102
Correspondence to: Xing-Hua Lu, Department of Gastroenterology, Peking Union Hospital, Peking Union Medical College, Chinese Academy of Medical Sciences, Beijing, 100730, China. lxhbj2000@yahoo.com.cn
Telephone: +86-10-65295016 Fax: +86-10-62622133
Received: 2005-07-07 Accepted: 2005-08-02

Abstract

AIM: To investigate risk factors for pancreatic cancer and establish a risk model for Han population.

METHODS: This population-based case-control study was carried out from January 2002 to April 2004. One hundred and nineteen pancreatic cancer patients and 238 healthy people completed the questionnaire which was used for risk factor analysis. Logistic regression analysis was used to calculate odds ratio (ORs), 95% confidence intervals (Cls) and β value, which were further used to establish the risk model.

RESULTS: According to the study, people who have smoked more than 17 pack-years had a higher risk to develop pancreatic cancer compared to non-smokers or light smokers (not more than 17 pack-years) (OR 1.98; 95% CI 1.11-3.49, $P=0.017$). More importantly, heavy smokers in men had increased risk for developing pancreatic cancer (OR 2.11; 95%CI 1.18-3.78, $P=0.012$) than women. Heavy alcohol drinkers (>20 cup-years) had increased risk for pancreatic cancer (OR 3.68; 95%CI 1.60-8.44). Daily diet with high meat intake was also linked to pancreatic cancer. Moreover, 18.5% of the pancreatic cancer patients had diabetes mellitus compared to the control group of 5.8% ($P=0.0003$). Typical symptoms of pancreatic cancer were anorexia, upper abdominal pain, bloating, jaundice and weight loss. Each risk factor was assigned a value to represent its importance associated with pancreatic cancer. Subsequently by adding all the points together, a risk scoring model was established with a value higher than 45 as being at risk to develop pancreatic cancer.

CONCLUSION: Smoking, drinking, high meat diet and diabetes are major risk factors for pancreatic cancer. A risk model for pancreatic cancer in Chinese Han population has been established with an 88.9% sensitivity and a 97.6% specificity.

Key words: Pancreatic cancer; Risk factor; High-risk model

Lu XH, Wang L, Li H, Qian JM, Deng RX, Zhou L. Establishment of risk model for pancreatic cancer in Chinese Han population. *World J Gastroenterol* 2006; 12(14): 2229-2234

http://www.wjgnet.com/1007-9327/12/2229.asp

INTRODUCTION

Pancreatic cancer is one of the most deadly cancers in the world. The mortality over morbidity ratio is 0.99:1. Only 10% patients have cancer cells confined in pancreas at the time of diagnosis, 40% have local invasion and 50% have distal metastasis. Although surgery, radiotherapy and chemotherapy have improved the life quality and survival rate in the cancer patients, only 10% patients show significant improvement. Most patients die from the cancer after 4 to 6 mo from diagnosis. Niederhuber *et al*[1] reported that one-year survival rate was less than 20%, decreasing to 7% for three-year and 3% for five-year. It is proposed that the best way to reduce the mortality is to improve early detection of this deadly cancer. In this paper we analyzed the possible risk factors and symptoms that correlated to pancreatic cancer based on a questionnaire survey among pancreatic patients and control subjects, and established a risk model for cancer estimation with weighted scores of risk factors and symptoms in an attempt to help early detection of pancreatic cancer in Chinese Han population.

MATERIALS AND METHODS

Subjects

A total of 119 cases of pancreatic cancer included in this study were diagnosed by Peking Union Medical College Hospital (PUMCH) between January 2002 and April

Table 1 Diagnostic standards for pancreatic cancer

A. Confirmed diagnosis by pathology
B. A valid confirmation requires at least 2 of the following listed items of imaging tests
(1) Ultrasound indicates there are low-density area in pancreas, as well as pancreatic duct dilation and common bile duct and gall bladder swelling
(2) CT indicates local enlargement and mass occupying lesion in pancreas
(3) ERCP indicates discontinuity of pancreatic duct, having mouse-tail ending, stiff and irregular duct wall, or any pull sign and double-duct sign
(4) MREP indicates there are stenosis and dilation in pancreatic duct and/or bile duct and space-occupying lesion in pancreas
(5) EUS indicates there is low-density, occupying lesion in pancreas
(6) IDUS
(7) Angiography
(8) PET
C. Palpable mass in surgery and at least an item of radiology evidence

ERCP: Endoscopic retrograde cholangiopancreatography
MREP: Magnetic resonance cholangiopancreatography
EUS: Endoscopic ultrasound sonography
IDUS: Intraductal ultrasound sonography
PET: Positron Emission Tomography

2004. The diagnosis was based on pathological, clinical and surgical evidence (Table 1). Among the 119 cases, 42 (35.3%) were confirmed by pathology; 17 (14.3%) by surgical findings; the rest (50.4%) by clinical findings. Those patients with a past history of chronic pancreatitis were diagnosed based on evidence of pancreatic calcification and pancreatic duct dilatation on imaging tests. All patients came from Beijing and its peripheral areas and were Han nationalities. The normal control group was randomly selected from normal general population in the same geographic area. The two groups were matched in gender and age and marriage status (Tables 2 and 3).

Methods

This is a case-controlled epidemiological study. We interviewed each subject in both groups based on a pre-determined questionnaire, which included questions about demographic data, smoking and drinking habits and family history of related diseases with pancreatic cancer. According to World Health Organization's definition of smoking, we defined the smokers as those who have smoked for 12 mo or more continuously or cumulatively in their lives. We measured the smoking history by the unit of pack-year which was defined as smoking of a package (20 pieces) of cigarette per day for one year. The number of pack-year = (the number of cigarette per day/20) × the number of years smoked. Because some persons used the pipe, we converted 50 g of pipe tobacco to 10 pieces of cigarettes. We defined the alcohol drinker as drinking at least twice a week and continuously for at least one year. Regarding the drinking volume, we adopted the unit of "drink", which was commonly used in North America. One drink contains 14 mL or 10.9 g of pure alcohol, which equals to 280 mL of beer (50 mL/L alcohol), 112 mL of wine (125 mL/L alcohol), 70 mL of rice wine (200 mL/L alcohol) or 35 mL of hard liquor (400 mL/L alcohol). In China, one bottle of beer is 640 mL, which is converted to 2.29 drinks. A glass of wine has 50 mL in volume, which is 0.45 drink unit. One cup of hard liquor is 55 mL, which equals to 1.57 drink units. One cup of rice wine having 50 mL in volume is converted to 0.71 drink unit. We assumed the subject drank the same amount of alcohol per day per year. The total drinking volume is calculated by the following formula: Total volume (drink-years) = (Numbers of bottle of beer × 2.29 + Numbers of glass of wine × 0.45 + Numbers of cup of hard liquor × 1.57 + Numbers of cup of rice wine × 0.71) × (Numbers of drinking years). Because a large number of subjects in this study did not drink or only drank once in several weeks or months, we did not adopt the calculating method of gr (alcohol)/per day, which is often used to define heavy drinking.

According to the relative amount of meat and vegetable intake during most time of one's life, diet habit was divided into high meat consumption, high vegetable consumption and equal meat and vegetable consumption.

The high-risk scoring model was established on the basis of multivariate logistic regression analysis. The variables included risk factors and symptoms of pancreatic cancer. Possible risk factors and symptoms described in the questionnaire were compared between two groups with the t test or χ^2 test. The OR value of each factor was also calculated and those with statistical significance were listed. Combined with our clinical findings, significant and borderline risk factors and symptoms were selected as variables. With multivariate logistic regression analysis, we obtained regression coefficient β of each independent variable. Selecting the minimal β value as radix, and through division of every β value by the radix, the weighted numerical scores of each variable were derived. We made small adjustments to some scores based on the suggestions of some experts of epidemiology and gastroenterology and established the risk scoring model. The risk score of each patient could be calculated through simple addition of weighted score of each variable. The risk scores were compared between two groups by the t test. Receiver operating characteristic (ROC) curve was used to set a cutoff value for high cancer risk.

RESULTS

Analysis of risk factors for pancreatic cancer

The body mass index of pancreatic cancer patient was distinctively higher than that of control group. After correction by age and gender, the average weight index of patient group was 24.89 (17.99-36.73), while that of control group was 23.99 (14.53-32.74), with significant difference ($P = 0.033$) between these two groups. A clinical manifestation of pancreatic cancer patient was weight loss in a short term. Among the 109 patients who had weight index, the average weight loss was 6.70 (-5-31) kg during the one-year period before diagnosis. However, among the 197 control subjects who had weight index, their body weight increased by an average of 0.33 (-10.5-5) kg during the same period. The weight changes between the two groups had significant difference ($P < 0.0001$). Therefore, we used the weight index of the subjects one year before they were recruited into the study group.

Heavy smoking was shown as a risk factor for pancreatic cancer. There was no significant difference

Table 2 Inclusion and exclusion criteria for patients and controls

	Inclusion criteria	Exclusion criteria
Patients	(1) The patient voluntarily took part in this research; agreed to take necessary clinical examinations and answer epidemiological questionnaire survey; and give consent to the publication of research data.	(1) The patient did not agree upon the conditions to participate in the study or the patient information was not available at the inclusion time.
	(2) Diagnosed by the pancreatic cancer team from PUMCH.	(2) Not diagnosed by the pancreatic cancer team from PUMCH.
	(3)Clinical examination and epidemiological investigation were acceptable for the patient's condition.	(3) The patient's condition did not allow the clinical examination and epidemiological investigation.
	(4) Patient was diagnosed for pancreatic cancer between 2002 and 2004.	(4) The patient was not diagnosed for pancreatic cancer for the first time between 2002 and 2004.
	(5) Patients did not undergo radiotherapy and anticancer therapy before surgery, and did not have other primary tumors.	(5) Patients whose pancreatic tumor was a metastatic carcinoma or who had other tumors.
	(6) Patients belonged to Han nationality.	(6) Patients were not from Han nationality.
Controls	(1) The person voluntarily took part in this research; agreeed to take necessary clinical examinations and answer epidemiological questionnaire survey; and give consent to the publication of research data.	(1) The person did not agree upon the conditions to participate in the study or the person's information was not available at the inclusion time.
	(2) The person did not have any kind of tumor.	(2) Person had any kind of malignant tumor.
	(3) The person matched with the patients for gender and age (±5 years).	(3) Person suffered from severe coronary heart disease or stroke.
	(4) Being the resident of Beijing or its peripheral area for at least 5 years.	(4) Person did not match with the patient group for gender and age (±5 years).
	(5) Han nationality.	(5) Not from Han nationality.

Table 3 Demographic characters of patients and controls

	Patients		Controls		χ^2	*P*
	n	(%)	*n*	(%)		
Age (yr)						
Male ≤50	16	(20.8)	36	(31.9)		
50-59	17	(22.1)	27	(23.9)	3.6583	0.1606
≥60	44	(57.1)	50	(44.3)		
Female ≤50	9	(21.4	28	(29.5)		
50-59	8	(19.1)	26	(27.4)	3.1297	0.2091
≥60	25	(59.5)	41	(43.2)		
Gender Male	77	(64.7)	113	(54.3)		
Female	42	(35.3)	95	(45.7)	3.3496	0.0672
Marriage status						
Married	115	(96.6)	183	(87.9)		
Divorced	0	(0)	7	(3.4)		
Widowed	4	(3.4)	16	(7.7)	8.093	0.082
Separated	0	(0)	1	(0.5)		
Spinsterhood	0	(0)	1	(0.5)		

between patient group (39.5%) and control group (35.92%) in terms of the percentage of smokers. After we divided each group into three subgroups (0, ≤17 package years and ≥17 package years) in terms of smoking history, we found significant differences between the patient group and control group. For those who smoked more than 17 package years (heavy smoker), the percentage of smokers accounted for 30.7% in patient group, which was 10% higher than that of control group. The risk of developing pancreatic cancer in the heavy smoker subgroup was 1.51 times that of the non-smokers (no statistic significance). When we combined the non-smoker and intermediate smoker subgroups (≤17 package years) together, it showed that the heavy smoker had increased risk of pancreatic cancer (OR, 1.98; 95% CI, 1.11-3.49; $P=0.017$). If divided by gender, there were more male heavy smokers in patient group (47.7%) than control group (30.3%). The risk of pancreatic cancer was increased for male heavy smokers (OR, 2.11; 95% CI, 1.18-3.87, $P=0.012$). However, no conclusion for females was made due to the low percentage of smokers within the patient group and control group.

Heavy drinking was shown as a risk factor for pancreatic cancer. According to the median total drinking volume of control group, we divided the drinkers into three subgroups: non-drinking, low-drinking (≤20 drink-years) and heavy-drinking (>20 drink-years). The result indicated that the distribution frequencies of three subgroups in patient group were 74.0% (88/109), 5.9% (7/109) and 20.2% (24/109) respectively, while in control group were 84.5% (175/207), 8.2% (17/207), 7.3% (15/207) respectively. The distribution in patient group had significant difference from control group. After correction of age, gender and smoking factors, the OR value of low-drinking compared to the non-drinking was 1.003, while for the heavy-drinking subgroup, it increased to 3.681. Therefore, heavy-drinking had higher risk to develop pancreatic cancer.

Diet with high meat consumption was shown as a high risk for pancreatic cancer. In this study, we only explored the relationship between dietary habit and pancreatic cancer. The results showed that those who claimed meat as their major daily diet accounted for 31.0% of patient group, while the number dropped significantly to 7.6% in control group. For those who claimed vegetable was their major daily diet accounted for 39.7% (46/116) in patient group and 28.9% (57/197) in control group. The diet containing half meat and half vegetable was reported by 25.9% (30/116) of patient group and 57.9% (114/197)

Table 4 Benign digestive diseases in patients and controls

Diseases	Patients				Controls				*P*
	n	Yes	No	Not stated	*n*	Yes	No	Not stated	
Chronic pancreatitis	119	2.5	95.0	2.5	205	0.5	99.5	0	0.012
Acute pancreatitis	119	0	98.3	1.7	205	0	100	0	0.06
Cholelithiasis	119	10.01	89.1	0.8	205	4.9	95.1	0	0.08
Cholecystitis	118	9.3	87.3	3.4	205	0.5	99.5	0	<0.0001
Cholecystectomy	119	3.4	95.8	0.8	205	2.9	97.1	0	0.41

Table 5 Clinical symptoms of patients and controls

Symptom	Symptom duration (mo)[a]	Patients				Controls				*P*
		n	Yes	No	Not stated	*n*	Yes	No	Not stated	
Anorexia	2	118	45.8	54.2	0	203	0.5	99.5	0	<0.0001
Epigastric pain	3	119	60.5	38.7	0.8	181	2.2	97.8	0	<0.0001
Backache	2	119	32.8	66.4	0.8	205	2.0	98.1	0	<0.0001
Hypogastralgia	3	119	16.0	82.4	1.7	205	3.4	96.6	0	<0.0001
Abdominal pain	2	119	38.7	61.3	0	205	4.9	95.1	0	<0.0001
Jaundice	1	119	42.0	58.0	0	205	0.5	99.5	0	<0.0001
Skin itch	1	119	13.5	86.6	0	205	8.7	91.3	0	0.0032
Weight loss	3	119	76.5	22.7	0.8	205	2.4	97.6	0	<0.0001

of control group. Therefore, people who had meat as their major diet faced higher risk of developing pancreatic cancer.

Also we found that 18.5% patients with pancreatic cancer had a history of diabetic mellitus; however this ratio dropped to 5.8% in the control group. There was significant difference between patient group and control group in having chronic pancreatitis, cholelithiasis and cholecystitis (Table 4). Moreover, we asked each subject for any cancer family history among the primary and secondary generation relatives, but no significant differences were found between the two groups. In patient group, those who had a family history of cancer accounted for 26.9%, while in the control group was 31.3% ($P=0.4064$). For those who lost weight in patient group, 48.9% patients lost weight within 3 mo, 33.3% in 4-6 mo, 16.7% in 7-12 mo, and 1.1% in more than 1 year. In addition, 45. 6% of patients had weight lost less than 5 kg, 30.0% between 6 to 10 kg, and 24.4% more than 10 kg (Table 5).

Although most factors had significant difference between two groups, their OR value did not show significance except for smoking and drinking due to relatively small sample of this study.

Establishment of the high-risk scoring model of pancreatic cancer

With multivariable logistic regression and some adjustments, we established the high-risk scoring model (as shown in Table 6).

The score of pancreatic cancer group was 80.6 ± 30.0 (95% CI 74.9-86.3), and the score of normal control group was 7.4 ± 11.9(95% CI 6.0-8.7), ($P<0.001$, Mann-Whitney test). According to the scores of pancreatic group and normal control group, we protracted ROC curve and the area below the curve was 0.981. When selecting $\geqslant 45$ as the differential cutoff between pancreatic cancer and normal control, the sensitivity and specificity of diagnosis were quite ideal, which were 88.9% and 97.6% respectively.

DISCUSSION

Because the two groups in our study were matched according to age and gender, there were no significant differences of the two factors. Based on previous studies on risk factors we included the two factors into high risk model. We have reported earlier that mortality of pancreatic cancer rises with age[2]. In a study involved 1619 cases of pancreatic cancer, 3.95% of the patients died before 40, but the mortality rate between 65 to 80 years was more than 5 times that of the average[2], which is consistent with other reports[3-6]. From 1991 to 2000, the epidemiological data of pancreatic cancer in China showed that the average male's mortality rate, revised mortality and standardized mortality grew 4.23%, 5.1% and 3.1% per year respectively, but the average growth rates for female were 7.7%, 8.6% and 6.74% respectively[2]. Although the gender disparity had been decreasing during this period, the increasing mortality rate in female has outpaced male. The age standardized mortality rate of male and female decreased from 1.97 in 1999 to 1.41 in 2000, which was consistent with report by Zheng *et al*[7].

Smoking is the only widely recognized risk factor for pancreatic cancer. Compared to non-smokers, the mortality rate of pancreatic cancer in smokers increased by 1.2-3.1 fold, and showed a dose-effect relationship. We found that the risk of pancreatic cancer occurrence increased in the heavy-smoking group (OR, 1.98; 95% CI, 1.11-3.49; $P=0.017$), which is consistent with previous literatures[4,8,9]. There was no consistent conclusion drawn for the risk of drinking associated with pancreatic cancer in literatures[4,10-12]. The OR value in the heavy-drinking

Table 6 Risk scoring model for pancreatic cancer

Risk factor	Criteria	Points
Gender	Male	2
Age (yr)	>60	7
Alcohol drinking	>20 drink-yr	4
Smoking	>17 pack-yr	5
Diabetic mellitus history		17
High meat consumption		7
Family history of pancreatic cancer		15
Chronic pancreatitis		12
Cholelithiasis history		8
Cholecystitis history		1
Anorexia		25
Epigastric pain		25
Weight loss		37
Jaundice		30

subgroup was 3.70 (95% CI, 1.604-8.443) compared to non-drinking subgroup. Therefore, we considered the risk of drinking associated with pancreatic cancer mainly existed in the heavy-drinking patients. Immigration epidemiological research showed that the mortality rate of pancreatic cancer among Asian and African populations in their homeland was low. However, for Asians and Africans who lived in western countries and adopted western diet habits, the risk of having pancreatic cancer was similar to or even higher than the Caucasians[13]. From our study, the percentage of people who had high meat consumption in their daily diet was much higher in the patient group than in control group ($P < 0.0001$). Currently, 35% of pancreatic cancers were attributed to the dietary factor. It was reported earlier that the vegetable abundant diet could prevent 33%-50% of pancreatic cancer cases[14].

Whether diabetes is the etiologic factor or the early manifestation of pancreatic cancer is still controversial. When probing into the relationship between them, we cannot draw a conclusion because it is impossible to carry out a randomized prospective research. At the same time, it is difficult to obtain evidence from animal experiments because of lacking credible animal model for type II diabetes. Currently, most investigations have used case-control study and prospective cohort study in general population. In our case-control study, 18.5% of pancreatic cancer patients had diabetes history, while only 5.8% of the control group did. This finding is in accordance with other researches[15-18].

The relationship between chronic pancreatitis and pancreatic cancer is still under debate. Our study showed that 22.5% of pancreatic cancer patients had chronic pancreatitis while only 0.49% of control group did. Karlsen reported that the risk of pancreatic cancer increased 13 times from a follow-up investigation of 715 chronic pancreatitis patients for an average of 10 years during 1971 to 1995[19]. At the same time, the author noticed that the incidence of pancreatic cancer was much higher than non-pancreatic tumors among those patients.

A population based case-control study showed that performing cholecystectomy a year before the diagnosis of pancreatic cancer was related to the occurrence of pancreatic cancer. However, the risk gradually decreased along with the delay of the surgery, but still positively related [11]. Because pancreas and bile duct tumors are difficult to distinguish, some researchers believed that patients with concealed pancreatic tumor were likely to have cholecystectomy performed because of presumed cholelithiasis. However, we did not discover any relation between pancreatic cancer and cholecystectomy in our study. Therefore, it still awaits further clarification.

We established the high-risk scoring model on the basis of the results of case-control study and clinical experience. The risk factors in the high-risk model including smoking, weight loss and diabetes are basically the same as that of overseas studies. For instance, in the cancer risk index established by Harvard University[20], the risk factors for pancreatic cancer are smoking (moderate to high dose), family history of pancreatic cancer, diabetes, chronic pancreatitis and carbohydrate ingestion. In that index, they mainly do allotment of fraction according to the OR value of each risk factor. However, our model is to confirm the fraction of each factor according to the result of logistic multivariate regression, and it reveals the relative contribution of each risk factor to pancreatic cancer. Our risk model is to help clinical diagnosis, which is different from the cancer risk index of Harvard University whose purpose is cancer prevention. So we added the associated symptoms of pancreatic cancer to the risk model. Although the main symptoms of pancreatic cancer such as abdominal pain and jaundice usually appear late when the tumor is already in advanced stage, there are some non-specific symptoms such as anorexia and weight loss which are very obscure and easy to be overlooked by patients and doctors or mistakenly diagnosed as other diseases and functional abnormity[21,22]. So tackling the symptom clues might be helpful for screening and early diagnosis of pancreatic cancer. Our research showed that weight loss, epigastric pain and diabetes all had significant differences in the two groups, but weight loss in mo offers the best indication for diagnosis, so its score is the highest.

In conclusion, we have established a risk factor model for early screening of pancreatic cancer in Chinese Han population through case-control study. In future, we will apply this model in areas that have high incidence of pancreatic cancer in Han population to further improve our model.

REFERENCES

1 **Niederhuber JE,** Brennan MF, Menck HR. The National Cancer Data Base report on pancreatic cancer. *Cancer* 1995; **76:** 1671-1677

2 **Wang L**, Yang GH, Lu XH, Huang ZJ, Li H. Pancreatic cancer mortality in China (1991-2000). *World J Gastroenterol* 2003; **9:** 1819-1823

3 **Devesa SS**, Blot WJ, Stone BJ, Miller BA, Tarone RE, Fraumeni JF Jr. Recent cancer trends in the United States. *J Natl Cancer Inst* 1995;**87**:175-182

4 **Nilsen TI,** Vatten LJ. A prospective study of lifestyle factors and the risk of pancreatic cancer in Nord-Trondelag, Norway. *Cancer Causes Control* 2000; **11**: 645-652

5 **Lillemoe KD.** Pancreatic disease in the elderly patient. *Surg Clin North Am* 1994; **74**: 317-344

6 **Hedberg M,** Anderson H, Borgstrom A, Janzon L, Larsson SA. Rising incidence of pancreatic carcinoma in middle-aged and older women-time trends 1961-90 in the city of Malmo,

Sweden. Br J Cancer 1996; **73**: 843-846
7 **Zheng T**, Holford TR, Ward BA, McKay L, Flannery J, Boyle P. Time trend in pancreatic cancer incidence in Connecticut, 1935-1990. *Int J Cancer* 1995; **61**: 622-627
8 **Coughlin SS**, Calle EE, Patel AV, Thun MJ. Predictors of pancreatic cancer mortality among a large cohort of United States adults. *Cancer Causes Control* 2000; **11**: 915-923
9 **Chiu BC**, Lynch CF, Cerhan JR, Cantor KP. Cigarette smoking and risk of bladder, pancreas, kidney and colorectal cancers in Iowa. *Ann Epidemiol* 2001;**11:** 28-37
10 **Lillemoe KD**, Yeo CJ, Cameron JL. Pancreatic cancer: state-of-the-art care. *CA Cancer J Clin* 2000; **50**: 241-268
11 **Silverman DT**. Risk factors for pancreatic cancer: a case-control study based on direct interviews. *Teratog Carcinog Mutagen* 2001; **21**: 7-25
12 **Zheng W,** McLaughlin JK, Gridley G, Bjelke E, Schuman LM, Silverman DT, Wacholder S, Co-Chien HT, Blot WJ, Fraumeni JF Jr. A cohort study of smoking, alcohol consumption, and dietary factors for pancreatic cancer (United States). *Cancer Causes Control* 1993; **4:** 477-482
13 **Stephens FO.** The increased incidence of cancer of the pancreas: is there a missing dietary factor? Can it be reversed?. *Aust N Z J Surg* 1999; **69**: 331-335
14 **Chen JS**, Wen ZM. Food, nutrition and cancer prevention. 1st ed. Shanghai: Shanghai Medical University Press, 1999:605
15 **Everhart J**, Wright D. Diabetes mellitus as a risk factor for pancreatic cancer: A meta-analysis. *JAMA* 1995; **273**: 1605-1609
16 **Fisher WE.** Diabetes: risk factor for the development of pancreatic cancer or manifestation of the disease? *World J Surg* 2001; **25**: 503-508
17 **Frye JN**, Inder WJ, Dobbs BR, Frizelle FA. Pancreatic cancer and diabetes: is there a relationship? A case-controlled study. *Aust N Z J Surg* 2000;**70**: 722-724
18 **Silverman DT,** Schiffman M, Everhart J, Goldstein A, Lillemoe KD, Swanson GM, Schwartz AG, Brown LM, Greenberg RS, Schoenberg JB, Pottern LM, Hoover RN, Fraumeni JF Jr. Diabetes mellitus, other medical conditions and familial history of cancer as risk factors for pancreatic cancer. *Br J Cancer* 1999; **80:** 1830-1837
19 **Karlson BM**, Ekbom A, Josefsson S, McLaughlin JK, Fraumeni JF Jr, Nyren O. The risk of pancreatic cancer following pancreatitis: an association due to confounding? *Gastroenterology* 1997; **113:** 587-592
20 **Colditz GA**, Atwood KA, Emmons K, Monson RR, Willett WC, Trichopoulos D, Hunter DJ. Harvard report on cancer prevention volume 4: Harvard Cancer Risk Index. Risk Index Working Group, Harvard Center for Cancer Prevention. *Cancer Causes Control* 2000; **11:** 477-488
21 **Gullo L**, Tomassetti P, Migliori M, Casadei R, Marrano D. Do early symptoms of pancreatic cancer exist that can allow an earlier diagnosis? *Pancreas* 2001; **22:** 210-213
22 Holly EA, Chaliha I, Bracci PM, Gautam M. Signs and symptoms of pancreatic cancer: a population-based case-control study in the San Francisco Bay area. *Clin Gastroenterol Hepatol* 2004; **2:** 510-517

S- Editor Pan BR **L- Editor** Zhu LH **E- Editor** Cao L

PO Box 2345, Beijing 100023, China
www.wjgnet.com
wjg@wjgnet.com

World J Gastroenterol 2006 April 14; 12(14): 2235-2238
World Journal of Gastroenterology ISSN 1007-9327

RAPID COMMUNICATION

Prevalence of hepatitis B virus precore stop codon mutations in chronically infected children

Philip Wintermeyer, Patrick Gerner, Stephan Gehring, Afshin Karimi, Stefan Wirth

Philip Wintermeyer, Patrick Gerner, Children's Hospital, Helios Klinikum Wuppertal, Witten-Herdecke University, Germany
Stephan Gehring, Children's Hospital, University of Mainz, Germany
Afshin Karimi, Stefan Wirth, Children's Hospital, Helios Klinikum Wuppertal, Witten-Herdecke University, Germany
Correspondence to: Professor Stefan Wirth, Children's Hospital, HELIOS Klinikum, Heusnerstr. 40, D-42283 Wuppertal, Germany. s-k-wirth@t-online.de
Telephone: +49-202-8963833 Fax: +49-202-8963834
Received: 2005-09-22 Accepted: 2005-11-18

Abstract

AIM: To find out whether there is a significant difference in the prevalence of the precore stop codon mutation between HBeAg positive and anti-HBe positive children.

METHODS: We investigated a large pediatric population of 155 European children (mean age 10.9 years) with chronic hepatitis B by PCR and direct sequencing. Ninety were HBeAg positive and 65 had seroconversion to anti-HBe. Additionally genotyping was performed.

RESULTS: Seventy-four (48%) of the sequenced HBV strains were attributed to genotype D and 81 (52%) to genotype A. In the group of 90 HBeAg positive patients, 2 (2.2%) 1896-G-to-A transitions leading to precore stop codon mutation were found, and in the group of 65 anti-HBe positive children, 5 (7.7%) were identified harbouring HBeAg-minus mutants. The difference was not statistically significant ($P = 0.13$).

CONCLUSIONS: HBeAg minus variants as predominant viral HB strains play a minor role in the course of chronic hepatitis B in European children.

Key words: Hepatitis B; Precore mutants; Children; HBeAg minus variants

Wintermeyer P, Gerner P, Gehring S, Karimi A, Wirth S. Prevalence of hepatitis B virus precore stop codon mutations in chronically infected children. *World J Gastroenterol* 2006; 12(14): 2235-2238

http://www.wjgnet.com/1007-9327/12/2235.asp

INTRODUCTION

Chronic hepatitis B (HB)-infection is a serious health problem worldwide and the leading cause of liver cirrhosis and hepatocellular carcinoma (HCC). In Germany 0.3%-0.5% of the population are HBsAg carriers and it is estimated that approximately 5% of them are children. Mutations preventing the expression of HBeAg, so-called precore stop codon mutations, have been reported to aggravate liver disease and to cause fulminant hepatitis in children as well as in adults[1-3]. Currently it is not yet clear whether these mutations influence the response to antiviral treatment. However, a recent study has shown a better outcome after interferon-alpha treatment for chronic hepatitis in individuals without precore mutant strains before treatment[4]. The most common stop-mutation is the G1896A-substitution in the precore region of HB-virus. A guanine (G) to adenine (A) mutation of the HBV precore gene at nucleotide 1896 (numbered from the EcoRI site) leads to a conversion of codon 28 from TGG (tryptophan) to TAG, which is a stop codon, thereby rendering HBV incapable of producing HBeAg[5]. In adults the prevalence of this mutation ranges between 20%-95%, whereas it is more common in HBeAg-negative than in HBeAg-positive patients[6]. Results of a cross-sectional multicenter study of adults with chronic HBV infection in the United States show an association of the presence of precore variants with higher serum HBV DNA levels in HBeAg-negative but not in HBeAg-positive patients[7]. The selection of precore variants is dependent on HBV genotype. It is most common in patients with genotype D and rare in patients with genotype A[8]. This phenomenon is related to base pairing in the stem-loop structure of the pregenome encapsidation sequence[9,10].

Fukuda *et al*[11] have postulated that hepatitis B virus exists mainly as a quasi species. On account of this, a correlation of nucleotide sequences with clinical and serological findings has to be made with caution. Available data about prevalence and significance of precore mutations in childhood are limited. A study of children with chronic HBV infection ($n = 60$) has shown the 1896-G-A-transition in 93% as mixed infection, with a similar prevalence of mixed viral populations in responders and non-responders to interferon treatment[12]. In the course of chronic HBV infection in children the frequency of precore mutant is increased after seroconversion from HBeAg to anti-HBe. It has been postulated that the higher

the aminotransferase levels are, the higher and the earlier the mutant emerges[13].

The aim of this study was to evaluate the prevalence of precore mutations in a large cohort of European children with chronic hepatitis B.

MATERIALS AND METHODS

Patients

A cross sectional testing of sera from 155 randomly assigned HBsAg positive chronic hepatitis B virus carriers was performed. The median age of the children at the time of blood sampling was 10.9 years. Ninety were HBeAg positive and 65 had seroconversion to anti-HBe 1 - 3 years before blood sampling. Fifty-four (35%) were female, 101 (65%) male; 108 (70%) of Caucasian, 42 (27%) of Mediterranean and 5 (3%) of Southeast Asian origin. ALT was elevated in 66 (73%) of HBeAg positive individuals (mean: 1100 nkat/L) and in 18 (28%) of anti-HBe positive individuals (mean: 367 nkat/L; normal <417 nkat/L).

HBV molecular analyses

DNA was extracted from sera with the QiaAmp blood kit (Qiagen, Chatsworth, CA, USA) and eluted with 50 μL distilled water according to the manufacturer's recommendations. The precore region of the HBV genome was amplified and re-amplified with a proof reading of expand-polymerase (Expand High Fidelity PCR System) by nested PCR. The following primers were used for amplification (nucleotide positions are according to the unique EcoRI site[14]: Sense P1: 5' -TGTCAACGACCGACCTTGAG-3' (nt 1683-1702), anti-sense P2: 5'-CAATGCTCAGGAGACTCTAAGGC-3' (nt 2045-2023); nested PCR: sense P3: 5'-GAGGAGT TGGGGTAGGACATT-3' (nt 1736-1756), anti-sense P4: 5'-TAGCTCCAAATTCTTTATA-3' (nt 1936-1918). PCR was performed in a 50-μL mixture with 20 pmol of each primer (Roth, Germany), 100 mmol/L of each dNTP, and 2.5 units of a Taq-Tgo polymerase mixture (Expand High Fidelity PCR System, Roche, Germany) diluted in 10 × expand polymerase buffer (Expand High Fidelity PCR System, Roche, Germany) in a DNA thermal cycler (Eppendorf Mastercycler personal). The amplified products were visualized by 20 g/L agarose electrophoresis and ethidium bromide staining.

Direct sequencing of PCR products

The amplified PCR products were purified by QIA Quick PCR-purification kit (Quiagen, Chatsworth, CA) according to the manufacturer's recommendations and precipitated with isopropanol to remove residual dNTPs and primers and re-suspended in a final volume of 10 μL distilled water. Nucleotide sequences of the PCR products were determined using a dye terminator cycle sequencing kit (big dye vs 3.1) in an automated sequencer (ABI PRISM, Foster City, CA, USA). The sequencing primers were the same as those used for DNA amplification.

Genotyping

The HBV-DNA sequences were assigned to the appropriate genotype based on the restriction fragment length polymorphism (RFLP) created by Ava2 and Dpn2 action on an amplified segment of the pres-S-region according to Lindh *et al*[15]. PCR of certain serum samples was performed under conditions as previously described with the following primers: Sense P1: 5'-CGA GGCAGGTCCCCTAGAAGAAGAA-3' (nt 2356-2380), anti-sense P2: 5'-GTCCTAGGAATCCTGAA-3' (nt 187-171); nested PCR: sense P3: 5'-TCACCATATTCT TGGGAACAAGA-3' (nt 2819-2841), anti-sense P4: 5' -TTCCTGAACTGGAGCCACCA-3' (nt 82-63). The PCR products were incubated with restriction enzymes Ava II and Dpn II (New England Biolabs, Inc., USA) for 3 h at 37 °C in a 15 μL reaction sample according to the manufacturer's recommendations. The products were visualized by 2 g/L agarose electrophoresis and ethidium bromide staining.

Statistical analysis

Fisher's exact test was used for statistical analysis $P < 0.005$ was taken as significant.

RESULTS

A total of 155 patients were enrolled. Seventy-four (48%) of the sequenced HBV strains were attributed to genotype D and 81 (52%) to genotype A. In the group of 90 HBeAg positive patients, 2 (2.2%) 1896-G-to-A transitions leading to precore stop codon were found, and in the group of 65 anti-HBe positive children, 5 (7.7%) were identified harbouring HBeAg-minus mutants. The difference was not statistically significant ($P = 0.13$).

First, all sera were randomly selected for analysis without association with patients' identities. We were then able to additionally investigate four HBeAg positive sera of the five patients who showed precore-mutations in anti-HBe positive status of the disease in order to find out if mutations already emerged in the HBeAg positive status. One of them was also positive for the G1896A-substitution in the HBeAg positive phase. All mutations identified were found in HBV DNA sequences of genotype D (Figures 1, 2).

The ALT levels in the two HBeAg positive sera with precore-mutation were 883 and 2983 nkat/L, reflecting a considerable elevation in one patient compared to the wild type sera of HBeAg positive status (mean: 1100 nkat/L). In the five anti-HBe positive individuals with the G1896A-substitution, the ALT levels were mildly elevated (mean: 467 nkat/L) compared to the group of 60 patients with wild type virus infection (mean: 367 nkat/L).

DISCUSSION

In contrast to previous studies with adults in particular, which reported HBeAg stop codon mutants in 20-95% of investigated patients (6, 16), we found a very low prevalence in children, both in the HBeAg (2.2%) and anti-HBe positive (8%) phase of the disease. However, our results demonstrated consistently that precore variants were more common in anti-HBe positive children, but the difference did not reach statistical significance. We were

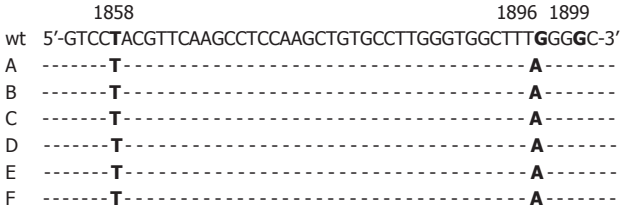

Figure 1 Precore region of HB virus with G1896A-substitution in 6 patients compared to the wild type-sequence (wt). Samples A and B were HBeAg positive. Samples while C-F were anti-HBe positive. All patients belonged to genotype D showing T at nucleotide position 1858.

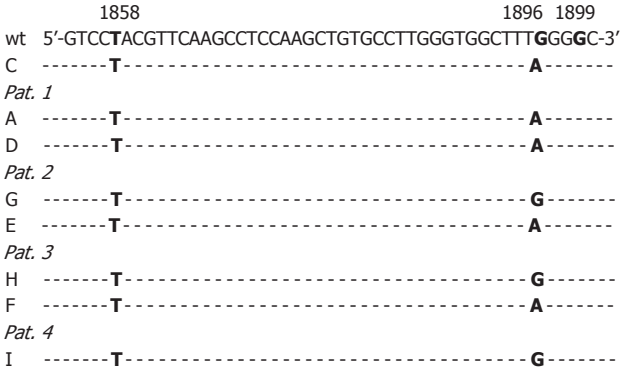

Figure 2 Precore region of HB virus in anti-HBe and HBeAg positive sera of 4 patients compared to the wildtype-sequence (wt). Samples A and C, G and D, H and E, I and F each belonged to one patient respectively. Samples C-F were anti-HBe positive, showing the G1896A-substitution. Samples A, G, H and I were HBeAg positive. All but sample A were negative for the mutant virus strain. Only one patient (No. 1) showed the G1896A-substitution both in anti-HBe and HBeAg positive serum (samples A and C). All patients belonged to genotype D showing T at nucleotide position 1858.

not able to show that mutations in anti-HBe positive sera have necessarily emerged already in the HBeAg positive phase of the disease. Thus, our data suggest that there is at least no strong evidence for the hypothesis that the mutant is selected by host immune pressure[13].

Due to the fact that the occurrence of the G1896A mutation is restricted to HBV genotypes with T at nucleotide position 1858 (genotype D)[17], it was not surprising that no mutations were identified in the group of genotype A virus strains. It has to be conceded that the existence of viral quasi-species including small amounts of precore stop mutations could not be excluded in our survey due to the method of direct sequencing. However, considering the high proportion of genotype D in our survey (48%), the postulation of a high prevalence of the G1896A precore mutation in these HBV strains[16] was not confirmed in chronically infected children.

It was reported that the precore mutation is common in Mediterranean and Asian populations, and two studies have shown a high prevalence of 16%-40% of the HBeAg minus variants in German adult populations as well[18,19]. It seems obvious that the age of the patients is more important than their ethnic origin.

Due to the elevated levels of transaminases in HBeAg positive sera, precore mutations may influence the inflammatory activity of the disease. But indeed, evidence is limited due to the small number of patients. In contrast to former studies, wherein a difference in clinical courses between genotypes B and C was described[20], this seems to be different for the most prevalent genotypes A and D in Europe, because they were equally distributed in our patients.

In summary, HBeAg minus variants as predominant viral HB strains play a minor role in the course of chronic disease in European children. Our results confirm the recent study of Söderström and colleagues who postulated that the most influential factors of HB-infection in childhood are epidemiologic parameters and the route of transmission[21].

REFERENCES

1 **Papatheodoridis GV**, Hadziyannis SJ. Diagnosis and management of pre-core mutant chronic hepatitis B. *J Viral Hepat* 2001; **8**: 311-321

2 **Omata M**, Ehata T, Yokosuka O, Hosoda K, Ohto M. Mutations in the precore region of hepatitis B virus DNA in patients with fulminant and severe hepatitis. *N Engl J Med* 1991; **324**: 1699-1704

3 **Friedt M**, Gerner P, Lausch E, Trubel H, Zabel B, Wirth S. Mutations in the basic core promotor and the precore region of hepatitis B virus and their selection in children with fulminant and chronic hepatitis B. Hepatology 1999; **29**: 1252-1258

4 **Seo Y**, Yoon S, Hamano K, Nakaji M, Yano Y, Katayama M, Ninomiya T, Hayashi Y, Kasuga M. Response to interferon-alpha in chronic hepatitis B with and without precore mutant strain detected by mutation site-specific assay. *J Clin Gastroenterol* 2004; **38**: 460-464

5 **Carman WF**, Jacyna MR, Hadziyannis S, Karayiannis P, McGarvey MJ, Makris A, Thomas HC. Mutation preventing formation of hepatitis B e antigen in patients with chronic hepatitis B infection. *Lancet* 1989; **2**: 588-591

6 **Gunther S**, Fischer L, Pult I, Sterneck M, Will H. Naturally occurring variants of hepatitis B virus. *Adv Virus Res* 1999; **52**: 25-137

7 **Chu CJ**, Keeffe EB, Han SH, Perrillo RP, Min AD, Soldevila-Pico C, Carey W, Brown RS Jr, Luketic VA, Terrault N, Lok AS. Prevalence of HBV precore/core promoter variants in the United States. *Hepatology* 2003; **38**: 619-628

8 **Rodriguez-Frias F**, Buti M, Jardi R, Cotrina M, Viladomiu L, Esteban R, Guardia J. Hepatitis B virus infection: precore mutants and its relation to viral genotypes and core mutations. *Hepatology* 1995; **22**: 1641-1647

9 **Junker-Niepmann M**, Bartenschlager R, Schaller H. A short cis-acting sequence is required for hepatitis B virus pregenome encapsidation and sufficient for packaging of foreign RNA. *EMBO J* 1990; **9**: 3389-3396

10 **Lok AS**, Akarca U, Greene S. Mutations in the pre-core region of hepatitis B virus serve to enhance the stability of the secondary structure of the pre-genome encapsidation signal. *Proc Natl Acad Sci USA* 1994; **91**: 4077-4081

11 **Fukuda R**, Mohammad R, Hamamoto S, Ishimura N, Ishihara S, Akagi S, Watanabe M, Kinoshita Y. Clinical relevance of precore and basal core promoter variants of hepatitis B virus during natural hepatitis B e antigen seroconversion may be overstated. *J Pediatr Gastroenterol Nutr* 2001; **32**: 301-306

12 **Cabrerizo M**, Bartolome J, Ruiz-Moreno M, Otero M, Lopez-Alcorocho JM, Carreno V. Distribution of the predominant hepatitis B virus precore variants in hepatitis B e antigen-positive children and their effect on treatment response. *Pediatr Res* 1996; **39**: 980-984

13 **Chang MH**, Hsu HY, Ni YH, Tsai KS, Lee PI, Chen PJ, Hsu YL, Chen DS. Precore stop codon mutant in chronic hepatitis B virus infection in children: its relation to hepatitis B e seroconversion and maternal hepatitis B surface antigen. *J Hepatol* 1998; **28**: 915-922

14 **Galibert F**, Mandart E, Fitoussi F, Tiollais P, Charnay P. Nucleotide sequence of the hepatitis B virus genome (subtype ayw) cloned in E. coli. *Nature* 1979; **281**: 646-650
15 **Lindh M**, Gonzalez JE, Norkrans G, Horal P. Genotyping of hepatitis B virus by restriction pattern analysis of a pre-S amplicon. *J Virol Methods* 1998; **72**: 163-174
16 **Funk ML**, Rosenberg DM, Lok AS. World-wide epidemiology of HBeAg-negative chronic hepatitis B and associated precore and core promoter variants. *J Viral Hep* 2002; **9**: 52-61
17 **Li JS**, Tong SP, Wen YM, Vitvitski L, Zhang Q, Trepo C. Hepatitis B virus genotype A rarely circulates as an HBe-minus mutant: possible contribution of a single nucleotide in the precore region. *J Virol* 1993; **67**: 5402-5410
18 **Knoll A**, Rohrhofer A, Kochanowski B, Wurm EM, Jilg W. Prevalence of precore mutants in anti-HBe-positive hepatitis B virus carriers in Germany. *J Med Virol* 1999; **59**: 14-18
19 **Tillmann H**, Trautwein C, Walker D, Michitaka K, Kubicka S, Boker K, Manns M. Clinical relevance of mutations in the precore genome of the hepatitis B virus. *Gut* 1995; **37**: 568-573
20 **Orito E**, Mizokami M, Sakugawa H, Michitaka K, Ishikawa K, Ichida T, Okanoue T, Yotsuyanagi H, Iino S. A case-control study for clinical and molecular biological differences between hepatitis B viruses of genotypes B and C. Japan HBV Genotype Research Group. *Hepatology* 2001; **33**: 218-223
21 **Söderström A**, Norkrans G, Conradi N, Krantz M, Horal P, Lindh M. Histologic activity of childhood chronic hepatitis B related to viremia levels, genotypes, mutations, and epidemiologic factors. *J Pediatr Gastroenterol Nutr* 2002; **35**: 487-494

S- Editor Pan BR **L- Editor** Wang XL **E- Editor** Bi L

PO Box 2345, Beijing 100023, China
www.wjgnet.com
wjg@wjgnet.com

World J Gastroenterol 2006 April 14; 12(14): 2239-2242
World Journal of Gastroenterology ISSN 1007-9327

RAPID COMMUNICATION

Copper toxicosis gene *MURR1* is not changed in Wilson disease patients with normal blood ceruloplasmin levels

Karl Heinz Weiss, Uta Merle, Mark Schaefer, Peter Ferenci, Joachim Fullekrug, Wolfgang Stremmel

Karl Heinz Weiss, Uta Merle, Mark Schaefer, Joachim Fullekrug, Wolfgang Stremmel, Department of Gastroenterology, University of Heidelberg, Germany
Peter Ferenci, Department of Gastroenterology and Hepatology, Medical University of Vienna, Austria
Correspondence to: Professor Wolfgang Stremmel, Medizinische Universitätsklinik Heidelberg, Abteilung Innere Medizin IV, Im Neuenheimer Feld 410, 69120 Heidelberg, Germany. wolfgang_stremmel@med.uni-heidelberg.de
Telephone: +49-6221-568705 Fax: +49-6221-564116
Received: 2005-10-21 Accepted: 2005-11-10

Abstract

AIM: To analyze our Wilson disease patient cohort ($n = 106$) for alterations in the gene coding for *MURR1*.

METHODS: Patients with an established diagnosis of Wilson disease but normal ceruloplasmin blood levels were chosen for our study ($n = 14$). Patients with two known disease-causing mutations in the *ATP7B* gene were not included. The three exons of the human *MURR1* gene were sequenced after amplification of the genomic DNA by polymerase chain reaction.

RESULTS: Our study did not reveal any mutations leading to an amino acid change in the *MURR1* sequence of Wilson disease patients. A polymorphism at 472 bp of the coding sequence could be confirmed.

CONCLUSION: The *MURR1* gene plays no role in the pathogenesis of Wilson disease patients with normal serum ceruloplasmin levels.

Key words: Wilson Disease; ATP7B; MURR1; COMMD1

Weiss KH, Merle U, Schaefer M, Ferenci P, Fullekrug J, Stremmel W. Copper toxicosis gene *MURR1* is not changed in Wilson disease patients with normal blood ceruloplasmin levels. *World J Gastroenterol* 2006; 12(14): 2239-2242

http://www.wjgnet.com/1007-9327/12/2239.asp

INTRODUCTION

In humans, Wilson disease (WD) is an autosomal recessively inherited disorder of copper metabolism[1, 2] characterized by the impaired biliary excretion of copper. Wilson disease leads to toxic copper accumulation predominantly in the liver and brain, causing liver cirrhosis and severe neurological defects. Common clinical findings in WD are low serum ceruloplasmin (CP) levels, elevated hepatic copper contents, elevated urine 24-h copper excretion and Kayser-Fleischer rings[3]. Homozygous or compound heterozygous mutations in the copper-transporting P-type ATPase ATP7B lead to Wilson disease[4, 5].

The genetic background is highly variable, with more than 300 mutations reported so far[6]. But not all cases are unambiguous because no mutations in the *ATP7B* gene have been found in some WD patients. It is unclear why no *ATP7B* mutations are detectable in a subgroup of patients presenting with typical features of Wilson disease. It might be due to an incomplete analysis of the *ATP7B* gene or due to other yet unidentified defects of genes involved in copper metabolism.

The clinical presentation is highly variable even among patients with the same mutation. In Wilson disease a low serum ceruloplasmin level is a typical finding and can be observed in 80%-90% of the patients. Ceruloplasmin is a copper binding ferroxidase in blood[1]. Today's understanding of the underlying molecular mechanisms[7] is that ATP7B is predominantly localized to the trans Golgi network and transports copper across the membrane to the lumen of the Golgi apparatus where apoceruloplasmin is loaded with copper. In case of a malfunction of ATP7B, apoceruloplasmin can not be loaded with copper and is degraded more rapidly, resulting in reduced blood levels of ceruloplasmin. Under elevated copper conditions, ATP7B translocates from the trans Golgi network to a vesicular compartment where it may facilitate biliary copper excretion[8, 9].

Recently, the autosomal recessively inherited canine copper toxicosis has been described in Bedlington terriers. Like in Wilson disease these dogs develop copper accumulation in the liver due to impaired biliary copper excretion leading to chronic hepatitis and cirrhosis. Neurological abnormalities have not been reported. The genetic basis of this defect is a deletion of the exon2 of the *Murr1* gene[10-12] mapped to 10q26 in Bedlington terriers. The human orthologous gene has been identified on chromosome 2p13-16 and is distinct from the *ATP7B* gene locus[11]. Furthermore, affected dogs present with normal ceruloplasmin serum levels, suggesting that the defect is beyond the trans-Golgi network. A direct interaction be-

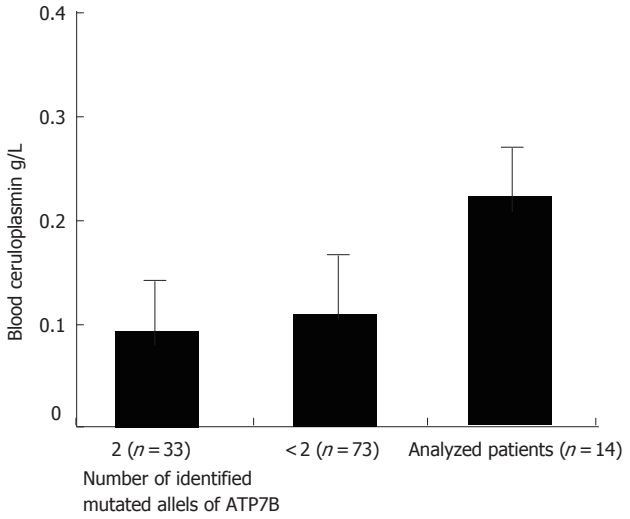

Figure 1 Mean ceruloplasmin blood levels in patients with two or less identified mutated alleles of ATP7B.

tween MURR1 and ATP7B has been reported[13]. There is biochemical evidence that decreased MURR1 levels lead to intracellular copper accumulation[14]. Based on these observations a role of MURR1 in the biliary copper excretion downstream of ATP7B has been suggested[15].

It would be interesting to identify a human disorder caused by defects in the human *MURR1* gene. Recently, a novel protein family (COMMD proteins) of structural and functional homologues of MURR1 (COMMD1) has been identified[16]. Recently, we reported an association between an *MURR1* polymorphism and onset of neurological and hepatic symptoms in WD patients homozygous for the most common *ATP7B* mutation H1069Q. Onset of disease was significantly earlier in patients with a heterozygous state at codon Asn 164 (GAT/GAC) than in patients with wild type (GAT/GAT)[17]. In the former study patients with low ceruloplasmin serum levels were included.

To identify possible disease related mutations in the *MURR1* gene in the current study we focused on patients with Wilson Disease but normal ceruloplasmin serum levels and at least one unknown mutation of *ATP7B*.

MATERIALS AND METHODS

Patients

Data of patients with an established diagnosis of Wilson disease were collected ($n = 106$). The diagnosis of Wilson disease was based on the criteria of the 8th International Conference on Wilson Disease and Menkes disease[19] (Leipzig, Germany April 16-18, 2001). For this study only patients with at least one undetermined mutation of the *ATP7B* gene were selected ($n = 73$), patients with two known disease defining mutations were excluded ($n = 33$). The *ATP7B* gene was sequenced in most patients in cooperation with Professor Ferenci, Department of Gastroenterology and Hepatology, Vienna, including the H1069Q mutation state in all patients. For our investigation out of the subset of WD patients without or with only one disease defining mutation, patients with normal or only slightly reduced ceruloplasmin levels were selected ($n = 14$) at the beginning of the study.

Ceruloplasmin cutoff was defined at a CP level of 0.15 g/L (normal in healthy persons: 0.2-0.6 g/L). Patients were excluded if the finding of a CP level above 0.15 g/L could be explained otherwise (e.g. contraceptive medication, pregnancy, acute phase reaction). A total of 14 patients with a CP level > 0.15 g/L and without any or with only one *ATP7B* mutation could be identified (Figure 1).

Mutation analysis of MURR1

Mutation analysis of *MURR1* was performed as described in detail previously[17]. In short, total DNA from the 14 selected patients was isolated and the three exons of the *MURR1* gene were amplified by polymerase chain reaction. The used primer combinations (exon 1 sense primer 5‘-GGT GGT TTT GCA CAG GCT ATT TAG-3‘, exon 1 anti-sense primer 5‘-GGC TTG TGA GGA CAG GGG AAG G-3‘; exon 2 sense primer 5‘-CAG TGA TTT AAG AGT CAC TC-3‘, exon 2 anti-sense primer 5‘-GCT GAA TAG ACA AGC TAA CAT GTA-3‘; exon 3 sense primer 5‘-GGG TAT TTT GAG TTT GGT CAT GC-3‘, exon 3 anti-sense primer 5’-TGA GAA CCT CTG CAC TGG AAC-3‘) resulted in PCR products covering the exons and parts of the 3` untranslated region and parts of the 5` region upstream of the start codon[17]. Additional putative exons or putative regulatory regions of the *MURR1* gene were not analyzed.

PCR products were purified as described previously[17]. Sequencing reactions were carried out by SEQLAB (Sequence Laboratories, Goettingen, Germany) or by MPI sequencing (Max Planck Institute, Dresden, Germany). For later analysis NM-152516 and AB17881 (NCBI sequence Viewer, http://www.ncbi.nlm.nih.gov/) were used as reference sequence. Nucleotide changes were numbered corresponding to their position in the *MURR1* mRNA beginning with the adenine of the ATG start codon.

RESULTS

The human orthologue of the *Murr1* gene encoded a protein of 190 amino acids. The gene spanned nearly 235 kb. Both introns were about 100 kb each in size (Figure 2). Therefore only the three exonic sequences were analyzed. In this study no mutations changing the amino acid sequence were found in the analyzed patients. A polymorphism at 472 bp of the coding sequence was detected (Table 1). Ten Patients (71%) were homozygous for wild-type GAT, 3 patients (21%) were heterozygous GAT/GAC and 1 patient was homozygous for GAC. The frequency of these variations was in line with previous reports[17]. We already reported a putative association between the GAT/GAC heterozygous state at codon Asn-164 with an earlier onset of disease in H1096Q *ATP7B* homozygous patients [17]. However, in the present study no significant genotype/phenotype correlation could be found, which might be due to the small number of patients.

DISCUSSION

Some patients with Wilson disease show no disease causing mutation in the *ATP7B* gene. Therefore other patho-

Table 1 MURR1 gene analysis in WD patients and associated CP blood values listed by WD gene mutation

Mutation in the *ATP7B* gene	*n*	*MURR1* gene base changes			CP level
		GAT/GAT	GAT/GAC	GAC/GAC	
2299InsC/ m n d.	1	1	-	-	0.15
3400DelC/ m n d.	1	1	-	-	0.18
G1030C/ m n d.	1	1	-	-	0.28
H1069Q/ m n d.	1	-	-	1	0.31
m.n.d./ m n d.	7	7	-	-	0.23 (± 0.09)
m.n.d./ m n d.	3	-	3	-	0.26 (± 0.08)

m n d: mutation not detected.

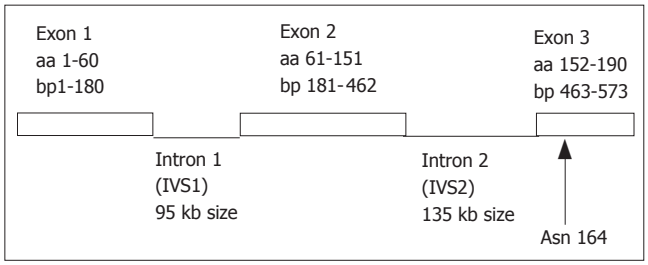

Figure 2 Map of the human *MURR1* gene. Localization of the reported polymorphism (492 T > C) in exon 3 is marked.

genetic factors might be involved. Due to the in part comparable phenotype of canine copper toxicosis and the reported interaction with *ATP7B*, the *MURR1* protein is an interesting candidate.

In this study we focused on Wilson disease patients showing a comparable phenotype to the copper toxicosis in dogs in regard to the normal ceruloplasmin serum level. However, in our group of patients with non-homozygous *ATP7B* mutation, no mutation in the coding sequence of the *MURR1* gene was found. Mutations in other parts of the Murr1 gene were not analyzed but could affect the gene expression and thus affect the phenotype. The finding that copper toxicosis gene *MURR1* is not changed in Wilson disease patients with normal blood ceruloplasmin levels needs to be evaluated in a larger clinical study.

Although our data do not necessarily rule out the possibility that MURR1 is involved in biliary copper excretion under physiological conditions, there is no direct evidence that it is indeed a disease-causing factor in human Wilson disease. This is in agreement with the findings of other investigators[17, 18]. In fact, a homozygous mutation of *ATP7B* resulting in the absence of this protein in the trans-Golgi network may be the only cause of Wilson disease. In our study population with detectable heterozygous or absent mutations of *ATP7B*, the other mutations may have not been identified yet. A low normal ceruloplasmin concentration was also observed in patients with homozygous mutations, suggesting that it may represent an undefined compensatory process by which apoceruloplasmin is loaded with copper by an *ATP7B* independent route, even outside the trans-Golgi network. This route seems to be less efficient but could result in low normal serum coeruloplasmin levels.

Although the possibility that *MURR1* is involved in biliary copper excretion in humans has not been ruled out, *MURR1* does not seem to play a role in the pathogenesis of Wilson disease.

ACKNOWLEDGMENTS

The authors thank the patients for their help and willingness to participate in this study and Dr. Bettina Stuehler for her advice and help with the sequencing reactions.

REFERENCES

1 **Harris ED**. Cellular copper transport and metabolism. *Annu Rev Nutr* 2000; **20**: 291-310
2 **Gitlin JD**. Wilson disease. *Gastroenterology* 2003; **125**: 1868-1877
3 **Riordan SM**, Williams R. The Wilson's disease gene and phenotypic diversity. *J Hepatol* 2001; **34**: 165-171
4 **Bull PC**, Thomas GR, Rommens JM, Forbes JR, Cox DW. The Wilson disease gene is a putative copper transporting P-type ATPase similar to the Menkes gene. *Nat Genet* 1993; **5**: 327-337
5 **Tanzi RE**, Petrukhin K, Chernov I, Pellequer JL, Wasco W, Ross B, Romano DM, Parano E, Pavone L, Brzustowicz LM. The Wilson disease gene is a copper transporting ATPase with homology to the Menkes disease gene. *Nat Genet* 1993; **5**: 344-350
6 URL: http://www.medgen.med.ualberta.ca/database.html
7 **Lutsenko S**, Petris MJ. Function and regulation of the mammalian copper-transporting ATPases: insights from biochemical and cell biological approaches. *J Membr Biol* 2003; **191**: 1-12
8 **Schaefer M**, Roelofsen H, Wolters H, Hofmann WJ, Muller M, Kuipers F, Stremmel W, Vonk RJ. Localization of the Wilson' s disease protein in human liver. *Gastroenterology* 1999; **117**: 1380-1385
9 **Roelofsen H**, Wolters H, Van Luyn MJ, Miura N, Kuipers F, Vonk RJ. Copper-induced apical trafficking of ATP7B in polarized hepatoma cells provides a mechanism for biliary copper excretion. *Gastroenterology* 2000; **119**: 782-793
10 **van De Sluis B**, Rothuizen J, Pearson PL, van Oost BA, Wijmenga C. Identification of a new copper metabolism gene by positional cloning in a purebred dog population. *Hum Mol Genet* 2002; **11**: 165-173
11 **van de Sluis BJ**, Breen M, Nanji M, van Wolferen M, de Jong P, Binns MM, Pearson PL, Kuipers J, Rothuizen J, Cox DW, Wijmenga C, van Oost BA. Genetic mapping of the copper toxicosis locus in Bedlington terriers to dog chromosome 10, in a region syntenic to human chromosome region 2p13-p16. *Hum Mol Genet* 1999; **8**: 501-507
12 **Klomp AE**, van de Sluis B, Klomp LW, Wijmenga C. The ubiquitously expressed MURR1 protein is absent in canine copper toxicosis. *J Hepatol* 2003; **39**: 703-709
13 **Tao TY**, Liu F, Klomp L, Wijmenga C, Gitlin JD. The copper toxicosis gene product Murr1 directly interacts with the Wilson disease protein. *J Biol Chem* 2003; **278**: 41593-41596
14 **Burstein E**, Ganesh L, Dick RD, van De Sluis B, Wilkinson JC, Klomp LW, Wijmenga C, Brewer GJ, Nabel GJ, Duckett CS. A novel role for XIAP in copper homeostasis through regulation of MURR1. *EMBO J* 2004; **23**: 244-254
15 **Wijmenga C**, Klomp LW. Molecular regulation of copper excretion in the liver. *Proc Nutr Soc* 2004; **63**: 31-39
16 **Burstein E**, Hoberg JE, Wilkinson AS, Rumble JM, Csomos RA, Komarck CM, Maine GN, Wilkinson JC, Mayo MW, Duckett CS. COMMD proteins, a novel family of structural and functional homologs of MURR1. *J Biol Chem* 2005; **280**: 22222-22232
17 **Stuehler B**, Reichert J, Stremmel W, Schaefer M. Analysis of the human homologue of the canine copper toxicosis gene MURR1 in Wilson disease patients. *J Mol Med* 2004; **82**: 629-634
18 **Muller T**, van de Sluis B, Zhernakova A, van Binsbergen E, Janecke AR, Bavdekar A, Pandit A, Weirich-Schwaiger H, Witt H, Ellemunter H, Deutsch J, Denk H, Muller W, Sternlieb

I, Tanner MS, Wijmenga C. The canine copper toxicosis gene MURR1 does not cause non-Wilsonian hepatic copper toxicosis. *J Hepatol* 2003; **38:** 164-168

19 **Ferenci P**, Caca K, Loudianos G, Mieli-Vergani G, Tanner S, Sternlieb I, Schilsky M, Cox D, Berr F. Diagnosis and phenotypic classification of Wilson disease. *Liver Int* 2003; **23:** 139-142

S- Editor Pan BR **L- Editor** Wang XL **E- Editor** Cao L

PO Box 2345, Beijing 100023, China
www.wjgnet.com
wjg@wjgnet.com

World J Gastroenterol 2006 April 14; 12(14): 2243-2244
World Journal of Gastroenterology ISSN 1007-9327

RAPID COMMUNICATION

Actigraphy: A new diagnostic tool for hepatic encephalopathy

Isabelle Hourmand-Ollivier, Marie-Astrid Piquet, Jean Pierre Toudic, Pierre Denise, Thông Dao

Isabelle Hourmand-Ollivier, Marie-Astrid Piquet, Jean Pierre Toudic, Thông Dao, Department of Nutrition and Hepatogastroenterology, CHU Côte de Nacre - 14033 cedex Caen, France
Pierre Denise, Physiology Laboratory, CHU Côte de Nacre - 14033 cedex Caen, France
Correspondence to: Dr. Isabelle Hourmand-Ollivier, Department of Nutrition and Hepatogastroenterology, CHU Côte de Nacre, 14033 Caen cedex, France. ollivierhourmand-i@chu-caen.fr
Telephone: +33-2-31064544 Fax: +33-2-31064545
Received: 2005-07-22 Accepted: 2005-12-22

Abstract

AIM: To assess the actigraphy, an ambulatory and continuous monitoring of wrist motor activity fitted to study sleep/wake patterns in hepatic encephalopathy (HE).

METHODS: Twenty-five cirrhotic patients (17 M, 8 F, mean age 56 ± 11 years, 24/25 alcoholic, Child-Pugh A , B, C: 2, 6, 17) were included. The patients were classified into 3 groups: stage 0 group ($n = 12$), stage 1-2 group ($n = 6$), and stage 3-4 group ($n = 7$) of encephalopathy. Over three consecutive days, patients had clinical evaluation 3 times a day with psychometric test, venous ammoniemia, flash visually evoked potentials (VEP), electroencephalogram and continuous actigraphic monitoring for 3 d, providing 5 parameters: mesor, amplitude, acrophase, mean duration of activity (MDAI) and inactivity (MDII) intervals.

RESULTS: Serum ammonia and VEP did not differ among the 3 groups. Electroencephalography mean dominant frequency (MDF) correlated significantly with clinical stages of HE ($r = 0.65$, $P = 0.003$). The best correlation with HE stage was provided by actigraphy especially with MDAI ($r = 0.7$, $P < 10^{-4}$) and mesor ($r = 0.65$, $P < 10^{-4}$). MDAI correlated significantly with MDF ($r = 0.62$, 0.004) and was significantly shorter in case of HE compared to patients without HE (stage 0: 5.33 ± 1.6 min; stage 1-2: 3.28 ± 1.4 min; stage 3-4: 2.52 ± 1.1 min; $P < 0.05$). Using a threshold of MDAI of less than 4.9 min, sensitivity, specificity, positive predictive value, negative predictive value for HE diagnosis were 85%, 67%, 73% and 80%, respectively.

CONCLUSION: Actigraphy may be an objective method to identify HE, especially for early HE detection. Motor activity at the wrist correlates well with clinical stages of HE. MDAI and mesor are the most relevant parameters.

Key words: Hepatic encephalopathy; Cirrhosis; Actigraphy

Hourmand-Ollivier I, Piquet MA, Toudic JP, Denise P, Dao T. Actigraphy: A new diagnostic tool for hepatic encephalopathy. *World J Gastroenterol* 2006; 12(14): 2243-2244

http://www.wjgnet.com/1007-9327/12/2243.asp

INTRODUCTION

Hepatic encephalopathy (HE) diagnosis is based on clinical criteria. Serum ammonia, evoked potentials and electroencephalogram (EEG) have low sensitivity[1-3]. Actigraphy allows ambulatory and continuous monitoring of motor activity and is fitted to study sleep/wake patterns. The actigraph worn on the non dominant wrist is based on a miniaturized acceleration sensor that translates physical motion to a numeric representation. It has already been successfully used in insomnia and extra pyramidal syndrome[4,5]. We assessed the actigraphy in HE.

MATERIALS AND METHODS

Twenty-five cirrhotic patients (17 M, 8 F, mean age 56 ± 11 years, 24/25 alcoholic, Child-Pugh A ,B, C: 2, 6, 17) were consecutively included. Patients with serum sedative or alcohol detection were excluded. Patients were classified into 3 groups: stage 0 group ($n = 12$), stage 1-2 group ($n = 6$), and stage 3-4 group ($n = 7$) of acute encephalopathy. HE causes were alcoholic hepatitis ($n = 5$), severe liver insufficiency ($n = 3$), digestive bleeding ($n = 1$), bacterial infection ($n = 1$), or undetermined ($n = 3$). Over three consecutive days, patients had clinical evaluation 3 times a day with the psychometric test Trail making test A when permitted by consciousness, venous ammoniemia using da Fonseca-Wollheim method, flash visual evoked potentials (VEP) with measurement of latencies of wavex N2, P2, N3, EEG and continuous actigraphic monitoring for 3 d using a small non dominant wrist-worn piezoelectric accelerometer (Gaehwiler electronic actimeter, CH 8634 Hombrechtiken, Switzerland) with a 0.1 G lower limit of sensitivity. Activity (wrist movements) measured at one-min intervals over a period of 24 h, was stored into the actigraph memory. Data downloaded to a compatible computer, were analysed by MONITOR software. The cosinor method or entire data linear adjustment by least-square method, provided 3 parameters: mesor (rhythm-adjusted mean), amplitude (half the variability between peaks to troughs), acrophase (peak time). Mean duration

of activity (MDAI) and inactivity (MDII) intervals independent of recording time, were measured. An activity interval was defined as a period during which the patient had more than 2 movements per minute, and an inactivity interval as a period during which the patient had less than 2 movements per minute. After 3 d, means of pooled data were calculated. Recording was made in hospitalized patients, so that physical activity was standardized.

Statistical analysis

Quantitative data were compared by ANOVA. Correlations were performed by Pearson test ($P<0.05$).

RESULTS

There was no difference between the 3 groups according to venous ammonia (41 ± 17 *vs* 46 ± 33 *vs* 65 ± 50 μmol/L respectively) or VEP (N3 = 201 ± 31 *vs* 205 ± 38 *vs* 227 ± 70 milliseconds). Electroencephalography mean dominant frequency (MDF) correlated significantly with clinical stages of HE ($r=0.65$, $P=0.003$). The best correlation with HE stage was provided by actigraphy especially with MDAI ($r=0.7$, $P<10^{-4}$) (Figure 1) and mesor ($r=0.65$, $P<10^{-4}$). Moreover MDAI correlated significantly with MDF ($r=0.62$, 0.004) and was significantly shorter in case of HE compared to patients without HE (stage 0: 5.33 ± 1.6 min versus stage 1-2: 3.28 ± 1.4 versus stage 3-4: 2.52 ± 1.1; $P<0.05$). In stages 0 and 1-2 of HE, MDAI correlated significantly with Trail making test A ($r=-0.61$; $P<0.05$). Using a threshold of MDAI of less than 4.9 min, sensitivity, specificity, positive predictive value, negative predictive value for HE diagnosis were 85%, 67%, 73% and 80%, respectively.

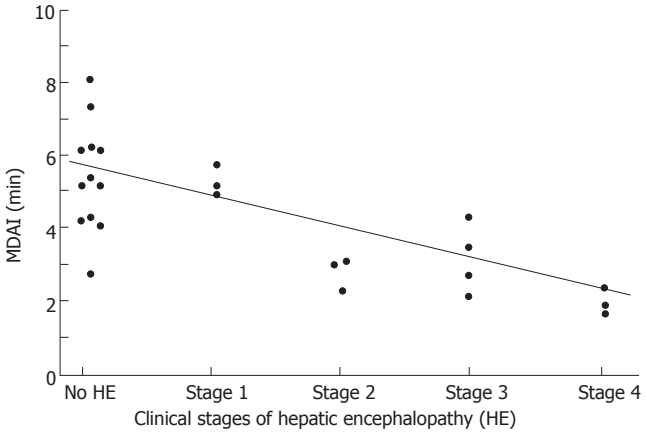

Figure 1 Correlation between clinical stages of hepatic encephalopathy and mean duration of activity intervals (MDAI), $r=0.7$, $P<0.0001$.

DISCUSSION

We suggest for the first time that actigraphy may be an objective method to identify HE. In our study, motor activity at the wrist recorded over three days, correlated well with clinical stages of HE. MDAI and mesor were the most relevant parameters. According to other works, neither serum ammonia[1] nor VEP[2] correlates with HE, contrary to EEG. However, EEG is a hospital procedure which has low specificity[3]. Using actigraphy, Cordoba *et al*[6] have previously shown a decrease of motor activity in cirrhotic patients without clinical evidence of HE. Seven out of 20 cirrhotic patients complained of unsatisfactory sleep, but they did not perform psychometric tests to screen subclinical encephalopathy. Actigraphy[4,5] is non invasive and simple to use. It can provide data under natural conditions over several days, which allows to take into account the oscillations in HE. One limit in our study is the decrease of motor activity due to bed-rest. However, we showed a significant relationship between actigraphy and encephalopathy. Actigraphy exhibits non specific changes in motor activity, but since we standardized physical activity, the observed changes might be due to HE. Our results suggest that actigraphy is especially fitted for early HE detection, since MDAI is significantly shorter in HE stage 1-2 patients compared to HE stage 0 patients. Moreover in cases of HE stages 0 and 1-2, MDAI, mesor, and acrophase correlate significantly with Trail making test A, a psychometric test routinely used to detect sub clinical encephalopathy. Further studies are needed to confirm actigraphy interest in sub clinical encephalopathy, a predictive factor of HE which is reversible by lactulose.

REFERENCES

1 **Basile AS**, Jones EA. Ammonia and GABA-ergic neurotransmission: interrelated factors in the pathogenesis of hepatic encephalopathy. *Hepatology* 1997; **25**: 1303-1305
2 **Sandford NL**, Saul RE. Assessment of hepatic encephalopathy with visual evoked potentials compared with conventional methods. *Hepatology* 1988; **8**: 1094-1098
3 **van der Rijt CC**, Schalm SW. Quantitative EEG analysis and evoked potentials to measure (latent) hepatic encephalopathy. *J Hepatol* 1992; **14:** 141-142
4 **Hauri PJ**, Wisbey J. Wrist actigraphy in insomnia. *Sleep* 1992; **15**: 293-301
5 **Van Hilten JJ**, Hoogland G, van der Velde EA, van Dijk JG, Kerkhof GA, Roos RA. Quantitative assessment of parkinsonian patients by continuous wrist activity monitoring. *Clin Neuropharmacol* 1993; **16**: 36-45
6 **Cordoba J**, Cabrera J, Lataif L, Penev P, Zee P, Blei AT. High prevalence of sleep disturbance in cirrhosis. *Hepatology* 1998; **27**: 339-345

S- Editor Wang J **L- Editor** Wang XL **E- Editor** Bi L

PO Box 2345, Beijing 100023, China
www.wjgnet.com
wjg@wjgnet.com

World J Gastroenterol 2006 April 14; 12(14): 2245-2249
World Journal of Gastroenterology ISSN 1007-9327

RAPID COMMUNICATION

Hepatoprotective effect of manual acupuncture at acupoint GB34 against CCl_4-induced chronic liver damage in rats

Yun-Kyoung Yim, Hyun Lee, Kwon-Eui Hong, Young-Il Kim, Byung-Ryul Lee, Tae-Han Kim, Ji-Young Yi

Yun-Kyoung Yim, Tae-Han Kim, Ji-Young Yi, Department of Meridian & Acupoint, College of Oriental Medicine, Daejeon University, #12407, 96-3, Yongun-dong, Dong-gu, Daejeon 300-716, South Korea
Hyun Lee, Kwon-Eui Hong, Young-Il Kim, Byung-Ryul Lee, Department of Acupuncture & Moxibustion, Dunsan Oriental Hospital of Daejeon University, 1136 Dunsan-dong, Seo-gu, Daejeon 302-122, South Korea
Correspondence to: Professor. Yun-Kyoung Yim, OMD, PhD, Department of Meridian abd Acupoint, College of Oriental Medicine, Daejeon University, #12407, 96-3, Yongun-dong, Dong-gu, Daejeon 300-716, South Korea. docwindy@dju.ac.kr
Telephone: +82-42-2802610 Fax: +82-42-2802610
Received: 2005-10-02 Accepted: 2005-12-22

Abstract

AIM: To investigate the hepatoprotective effect of manual acupuncture at Yanglingquan (GB34) on CCl_4-induced chronic liver damage in rats.

METHODS: Rats were injected intraperitoneally with CCl_4 (1 mL/kg) and treated with manual acupuncture using reinforcing manipulation techniques at left GB34 (Yanglingquan) 3 times a week for 10 wk. A non-acupoint in left gluteal area was selected as a sham point. To estimate the hepatoprotective effect of manual acupuncture at GB34, measurement of liver index, biochemical assays including serum ALT, AST, ALP and total cholesterol, histological analysis and blood cell counts were conducted.

RESULTS: Manual acupuncture at GB34 reduced the liver index, serum ALT, AST, ALP and total cholesterol levels as compared with the control group and the sham acupuncture group. It also increased and normalized the populations of WBC and lymphocytes.

CONCLUSION: Manual acupuncture with reinforcing manipulation techniques at left GB34 reduces liver toxicity, protects liver function and liver tissue, and normalizes immune activity in CCl_4-intoxicated rats.

Key words: Manual acupuncture; Yanglingquan (GB34); CCl_4-induced liver damage; Hepatoprotective effect

Yim YK, Lee H, Hong KE, Kim YI, Lee BR, Kim TH, Yi JY. Hepatoprotective effect of manual acupuncture at acupoint GB34 against CCl_4-induced chronic liver damage in rats. *World J Gastroenterol* 2006; 12(14): 2245-2249

http://www.wjgnet.com/1007-9327/12/2245.asp

INTRODUCTION

Herbal medicine and acupuncture are the two main methods to treat disease in oriental medicine. Because of chemical residue contamination, there is recent gaining suspicion that herbs may be harmful to the liver. Accordingly, acupuncture is getting more interest these days for the treatment of liver diseases in oriental medical clinics. In the present study, we tried to investigate the effects of manual acupuncture on long-term liver damage. To investigate the effects of manual acupuncture at GB34 on liver damage, we used CCl_4-intoxicated rat model and chose GB34 as an acupoint to protect liver and treat liver damage induced by CCl_4 administration.

GB34 is an acupoint located on the gall bladder meridian. In oriental medical theory, the liver and gall bladder corresponds to each other and their meridians are also closely related with each other in the 'interior-exterior relationship'[1,2]. Gall bladder meridian pertains to the gall bladder organ and connects with the liver organ. The liver meridian pertains to the liver organ and connects with the gall bladder organ. Therefore, the acupoints on the liver meridian are used to treat gall bladder organ diseases as well as liver organ diseases. Consequently, the acupoints on the gall bladder meridian are used to treat liver organ diseases as well as gall bladder organ diseases. Hence, GB34 is closely related with the liver as well as the gall bladder. It explains why GB34 is used to treat liver disease so often. Moreover, GB34 is the *He* (meaning "sea") point of gall bladder. In oriental medical theory, a "sea *He*" point is considered to be the entrance of the meridian energy to the corresponding organ[3]. Therefore, GB34 influences the liver and gall bladder more strongly than other acupoints. The functions of this point are regulating and tonifying the liver, regulating the gallbladder, spreading liver *Qi* (oriental medical term for "vital energy"), subduing liver *Yang*, draining liver pathogens, *etc*. GB34 has been clinically used for hypochondriac pain, jaundice, hepatitis, acute biliary tract diseases, cirrhosis of the liver and hypertension due to liver *Yang* excess, *etc*[1,4].

We presume that neuronal activity is involved in the transmission of acupuncture stimulation, so the animals were not anesthetized during the acupuncture administra-

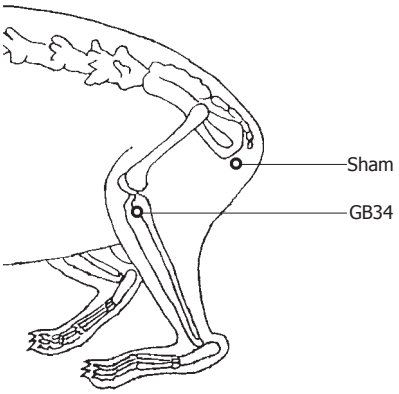

Figure 1 GB34 and sham point for acupuncture.

tion. To keep the animals from moving during the acupuncture administration, they were put in cages with five holes for tail and four limbs. To estimate and exclude the effect of stress from restriction within the cage, the rats in the control group were also kept in the cages in the same manner as the acupuncture group.

The action of acupuncture could be influenced by acupuncture techniques as well as point selection. There are two main categories of acupuncture techniques: reinforcing technique and reducing technique. Clockwise needle rotation, scraping downward of needles, and odd number of manipulating operations are considered as reinforcing techniques. On the other hand, counterclockwise needle rotation, scraping upward of needles, and even number of manipulating operations are considered as reducing techniques. Reinforcing acupuncture manipulation techniques are used for chronic and deficient syndrome, while reducing techniques are used for acute and excess syndrome [1]. Since the animals in the present study were injected with CCl_4 for a long period, we considered it as a chronic and deficient condition, and therefore, we administered acupuncture with reinforcing manipulation techniques.

MATERIALS AND METHODS

Animals

Sprague-Dawley male rats (200-250 g) were purchased from Deahan Biorink Co. The animals were adapted to the environment of 22±2℃ room temperature, 12-h light/dark cycle for 2 wk and had free access to water and food. Our animal experiment has been conducted in accordance with the Use of Laboratory Animals as adopted and promulgated by the U.S. National Institutes of Health.

Experimental design

Experimental animals were randomly divided into four groups: normal; control (CCl_4); Sham (CCl_4 + manual acupuncture at sham point); and GB34 (CCl_4 + manual acupuncture at left GB34). Each group consisted of 7 rats. Liver injury was induced by intraperitoneal injections with 500 mL/L CCl_4 (Sigma, USA) solution in olive oil (1 mL/kg), twice a week for 10 wk. Manual acupuncture was administered 3 times a week during the same period[5].

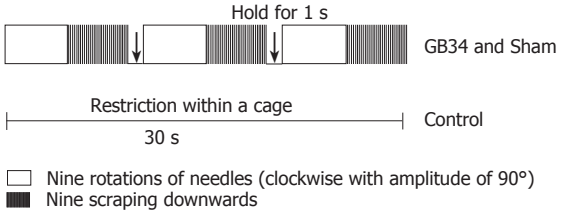

Figure 2 Acupuncture scheme.

Acupuncture

Cages with five holes for the tail and four limbs were manufactured for this study. During acupuncture administration, the animals were kept in the cage with left hind limb fastened to the wall of the cage with tape. Sterilized disposable stainless steel needles (0.25 mm × 30 mm, Dongbang Acupuncture Inc., Korea) were inserted perpendicularly as deep as 2-3 mm at left GB34 or sham point. Rat GB34 was determined according to human GB34 which locates on gall bladder meridian, in the depression anterior and inferior to the head of the fibula[1]. A non-acupoint in the gluteal region was selected as a sham point (Figure 1). After the needles were inserted, they were rotated clockwise with amplitude of 90° nine times, and scraped downward nine times. Nine rotations and nine scrapes constituted one manipulation unit, and three manipulation units constituted one treatment session. After each manipulation unit, there was a hold for about 1 s. The full manipulation took about 30 s. The rats in the control group were kept in a cage for 30 s with the left hind limb tied without acupuncture treatment (Figure 2). All acupuncture was administered by a trained and experienced oriental medical doctor who was unknown about the research protocol except the needle manipulating methods.

Liver index measurement

Rat's body weight was measured before the animals were sacrificed. Rat liver was removed and weighed right after the animal was sacrificed and the liver index (% of liver weight/body weight)[6,7] was estimated.

Biochemical analysis and blood counts

Forty-eight hours after the last administration with CCl_4, the rats were anesthetized with ethyl ether and blood samples were taken from the heart. Blood was centrifuged at 3000 r/min for 15 min and serum was taken. Alanine aminotransferase (ALT), aspartate aminotransferase (AST), alkaline phosphotase (ALP), total cholesterol in serum and the populations of RBC, WBC, lymphocytes in plasma were detected.

Histological analysis

The rats were sacrificed and the liver tissues were obtained individually from each group and fixed in 40 g/L formaldehyde. After decalcification in 50 mL/L formic acid, the specimens were processed for paraffin embedding. Tissue sections were obtained and stained with hematoxylin and eosin (HE) or masson's trichrome (MT). Tissue destruction and fatty changes of liver were observed at 400× magnification.

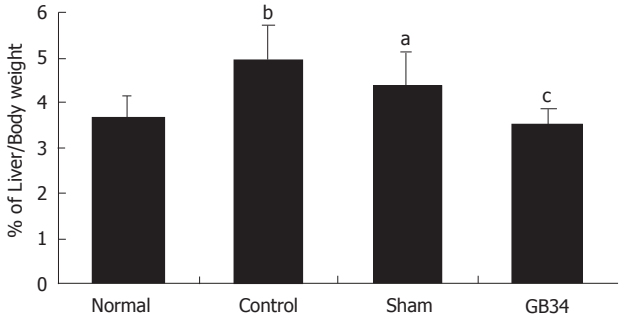

Figure 3 Effect of manual acupuncture at BG34 on liver index of CCl_4-intoxicated rats. [a]$P < 0.05$, [b]$P < 0.01$ *vs* normal group; [c]$P < 0.05$ *vs* control group.

Statistical analysis

Data were obtained from the rats which survived to the end of the experiment. All in normal group, 3 in control group, 3 in sham group and 5 in GB34 group survived to the end of the experiment. Data were expressed as mean ± SD. Statistical significance of difference between groups was determined using ANOVA, followed by *t*-test. $P < 0.05$ was considered statistically significant.

RESULTS

Liver index

CCl_4 injection induced a significant increase in liver index. On the other hand, manual acupuncture at GB34 lowered it similar to the normal value (Figure 3).

Serum ALT, AST, ALP and total cholesterol

ALT, AST, ALP and total cholesterol in serum were increased remarkably by long-term CCl_4 administration, indicating damage to the liver. Manual acupuncture at GB34 significantly reduced serum ALT, AST and total cholesterol in comparison with the control group. Serum ALP was also reduced by manual acupuncture at GB34 but no statistical significance was found (Figure 4).

Blood cell counts

The number of RBC was slightly reduced by CCl_4 intoxication and restored by manual acupuncture at GB34, though statistical significance was not observed. The number of WBC and the percentage of lymphocytes out of WBC was significantly reduced by CCl_4 intoxication and restored by manual acupuncture at GB34 close to the normal level (Figure 5).

Liver histology

Histological analysis using HE stain showed that necrosis of liver tissue and fatty changes were viciously induced by CCl_4 administration. The group treated with manual acupuncture at GB34 showed reduced feature of hepatocyte necrosis and fatty change compared to the control group and the sham group. In addition, MT staining showed lower accumulation of extracellular matrix in the GB34 group compared to the control group and sham group (Figure 6).

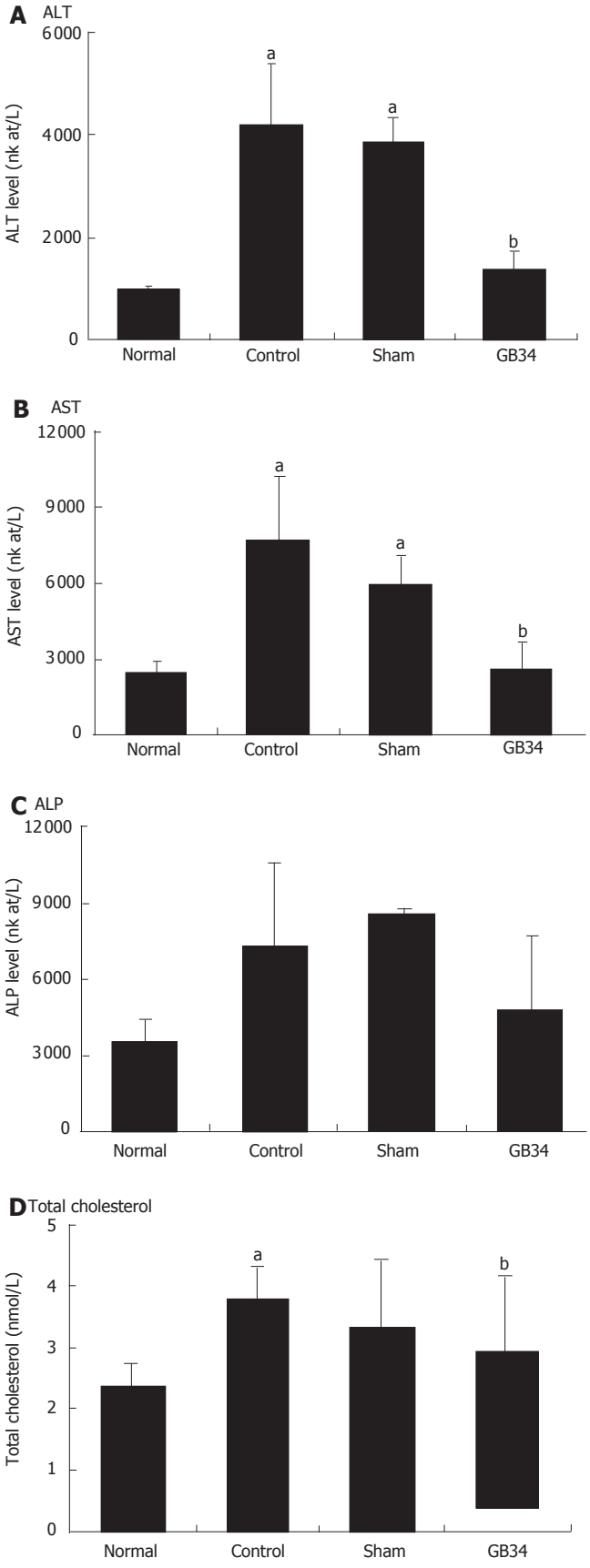

Figure 4 Effect of manual acupuncture at GB34 on serum ALT, AST, ALP and total cholesterol of CCl_4-intoxicated rats. [a]$P < 0.01$ *vs* normal group; [b]$P < 0.05$ *vs* control group

DISCUSSION

CCl_4 has been widely used to induce experimental hepatic

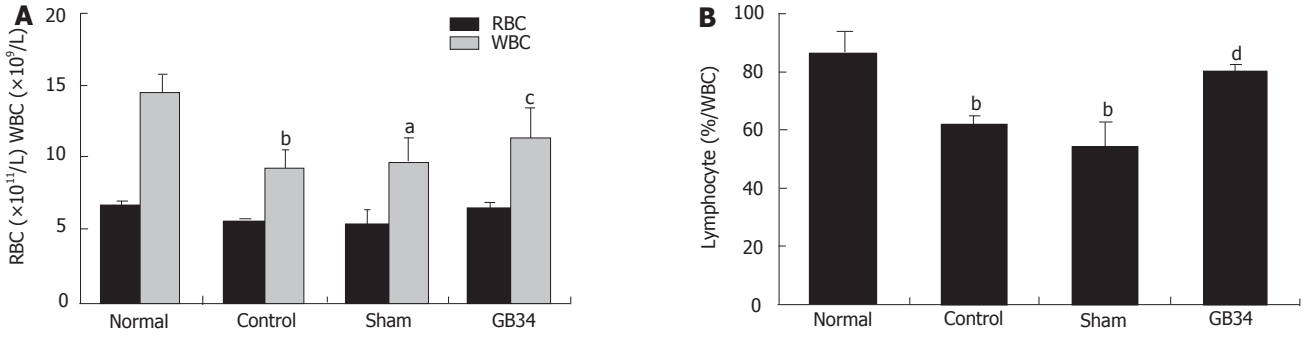

Figure 5 Effect of manual acupuncture at GB34 on RBC, WBC and lymphocytes in blood. $^{a}P<0.05$, $^{b}P<0.01$ *vs* normal group; $^{c}P<0.05$, $^{d}P<0.001$ *vs* control group.

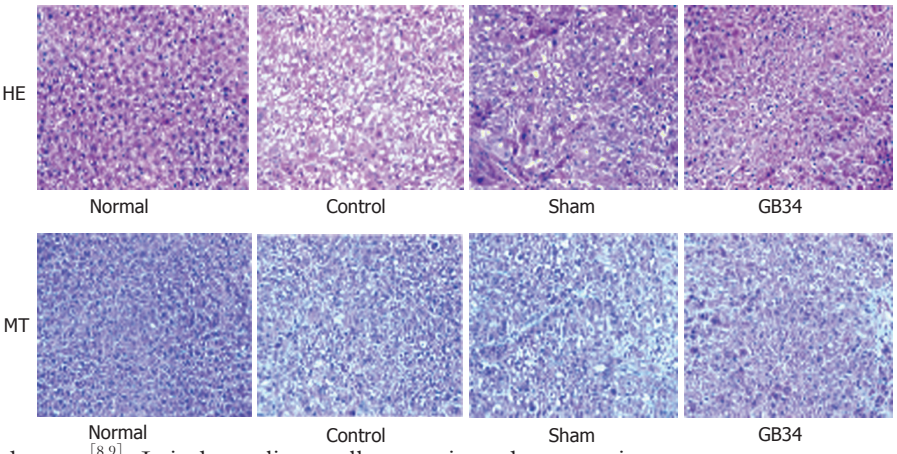

Figure 6 Histological results of liver tissue. Necrosis and fatty change could be found in the control group (top). GB34 group revealed lower accumulation of extracellular matrix compared to the control group and sham group (bottom) (× 400 magnification)

damage[8,9]. It induces liver cell necrosis and apoptosis, and can be used to induce hepatic fibrosis or cirrhosis by repetitive administration[10-12]. Liu *et al*[13] investigated the effect of manual acupuncture at ST36 and LR3 on CCl_4-induced acute liver damage. In the present study, we investigated the effect of manual acupuncture at GB34 on chronic liver damage induced by long-term CCl_4 administration.

ALT and AST are the specific markers to assess hepatocellular damage leading to liver cell necrosis[14]. Slight to moderate increases in ALP (1-2 times normal) occurred in liver disorders[15]. Serum cholesterol is one of the general indications of the synthetic and general metabolic capacity of the liver[16]. In the present study, CCl_4 injection significantly increased serum ALT, AST, ALP and cholesterol levels, indicating induction of hepatic damage. Manual acupuncture at GB34 inhibited the increases of these parameters, indicating that manual acupuncture at GB34 protected liver and reduced liver toxicity. Histological analysis also showed that the acupuncture at GB34 protected liver tissue against CCl_4-intoxication. Our histological analysis in this study was only qualitative. Quantitative assessment of anti-fibrotic effect of acupuncture, such as determination of hepatic hydroxyproline

content, would be meaningful in the next study.

In the present study, long-term CCl_4 administration reduced the population of leucocytes and lymphocytes in blood. We infer that this reduction was due to the decline of immune activity by long-term liver damage. Manual acupuncture at GB34 recovered the population of leucocytes and lymphocytes in blood. Therefore, we presume that manual acupuncture at GB34 restored the immune activity, which is also in agreement with Hau's report on the white cell increase by acupuncture[17]. However, the effect of acupuncture on inflammation in liver is not clear yet. It is known that inflammatory cells are infiltrated in CCl_4-intoxicated liver, and there exists an abnormality of cytokines in liver tissue. For instance, TNF-α and IL-10 are increased, and IL-2 and IFN-γ are reduced in CCl_4-intoxicated liver tissue[18,19]. More profound studies are required on how acupuncture influences the chronic inflammatory conditions of the liver.

Based on the results of the present study, we speculate that manual acupuncture at GB34 is beneficial to protect liver function and tissue, reduce hepatic toxicity and normalize immune activity against CCl_4-intoxication in rats. The hepatoprotective effect of manual acupuncture at GB34 in this study may be related to the immune reinforcing effect of acupuncture or neuro-immune interaction on the pathway of the transmission of acupuncture stimulation.

REFERENCES

1 **Deng L**, Gan Y, He S, Ji X, Li Y, Wang R, Wang W, Wang X, Xu H, Xue X, Yuan J. Chinese acupuncture and moxibustion. *Beijing: Foreign Languages Press,* 1997: 54, 71-74, 208, 325-327
2 **Captchuk TJ.** The web that has no weaver: understanding Chinese medicine. *NY: Contemporary books,* 2000: 8
3 **Choe YT**, Yu CH, Kim CH, Kim DH. Oriental medicine series. Vol 2; Acupuncture & moxibustion. *Seoul: Res Inst of Oriental Med Inc,* 1987: 160
4 **Lade A.** Acupuncture points images & functions. *Washington: Eastland Press*, 1998: 230
5 **Ulicna O,** Greksak M, Vancova O, Zlatos L, Galbavy S, Bozek P, Nakano M. Hepatoprotective effect of rooibos tea (Aspalathus linearis) on CCl4-induced liver damage in rats. *Physiol Res* 2003; **52**: 461-466
6 **Yang Q,** Xie RJ, Geng XX, Luo XH, Han B, Cheng ML. Effect of

Danshao Huaxian capsule on expression of matrix metalloproteinase-1 and tissue inhibitor of metalloproteinase-1 in fibrotic liver of rats. *World J Gastroenterol* 2005; **11**: 4953-4956
7 **Lin WC,** Lin WL. Ameliorative effect of *Ganoderma lucidum* on carbon tetrachloride-induced liver fibrosis in rats. *World J Gastroenterol* 2006; **12**: 265-270
8 **Tsukamoto H**, Matsuoka M, French SW. Experimental models of hepatic fibrosis: a review. *Semin Liver Dis* 1990; **10:** 56-65
9 **Yao XX**, Jiang SL, Tang YW, Yao DM, Yao X. Efficacy of Chinese medicine Yi-gan-kang granule in prophylaxis and treatment of liver fibrosis in rats. *World J Gastroenterol* 2005; **11**: 2583-2590
10 **Constandinou C**, Henderson N, Iredale JP. Modeling liver fibrosis in rodents. *Methods Mol Med* 2005; **117**: 237-250
11 **Chang ML**, Yeh CT, Chang PY, Chen JC. Comparison of murine cirrhosis models induced by hepatotoxin administration and common bile duct ligation. *World J Gastroenterol* 2005; **11**: 4167-4172
12 **Shi GF**, Li Q. Effects of oxymatrine on experimental hepatic fibrosis and its mechanism in vivo. *World J Gastroenterol* 2005; **11**: 268-271
13 **Liu HJ**, Hsu SF, Hsieh CC, Ho TY, Hsieh CL, Tsai CC, Lin JG. The effectiveness of Tsu-San-Li (St-36) and Tai-Chung (Li-3) acupoints for treatment of acute liver damage in rats. *Am J Chin Med* 2001; **29:** 221-226
14 **Amacher DE.** Serum transaminase elevations as indicators of hepatic injury following the administration of drugs. *Regul Toxicol Pharmacol* 1998; **27**: 119-130
15 **Isselbacher KJ**, Braunwald E, Wilson JD, Martin JB, Fauci AS, Kasper DL. Harrison's principles of internal medicine, 13th ed. *NY: McGraw-Hill*, 1994: 1444-1446
16 **Fregia A**, Jensen DM. Evaluation of abnormal liver tests. *Compr Ther* 1994; **20**: 50-54
17 **Hau DM**. Effects of electroacupuncture on leukocytes and plasma protein in the X-irradiated rats. *Am J Chin Med* 1984; **12**: 106-114
18 **Jeong DH**, Lee GP, Jeong WI, Do SH, Yang HJ, Yuan DW, Park HY, Kim KJ, Jeong KS. Alterations of mast cells and TGF-beta1 on the silymarin treatment for CCl(4)-induced hepatic fibrosis. *World J Gastroenterol* 2005; **11:** 1141-1148
19 **Yu XH**, Zhu JS, Yu HF, Zhu L. Immunomodulatory effect of oxymatrine on induced CCl4-hepatic fibrosis in rats. *Chin Med J (Engl) 2004*; **117**: 1856-1858

S- Editors Pan BR and Wang J **L- Editor** Kumar M **E- Editor** Bai SH

PO Box 2345, Beijing 100023, China
www.wjgnet.com
wjg@wjgnet.com

World J Gastroenterol 2006 April 14; 12(14): 2250-2253
World Journal of Gastroenterology ISSN 1007-9327

RAPID COMMUNICATION

Aberrant expression of krÜppel-like factor 6 protein in colorectal cancers

Yong-Gu Cho, Byung-Jun Choi, Jae-Whie Song, Su-Young Kim, Suk-Woo Nam, Sug-Hyung Lee, Nam-Jin Yoo, Jung-Young Lee, Won-Sang Park

Yong-Gu Cho, Byung-Jun Choi, Jae-Whie Song, Su-Young Kim, Suk-Woo Nam, Sug-Hyung Lee, Nam-Jin Yoo, Jung-Young Lee, Won-Sang Park, Department of Pathology, College of Medicine, The Catholic University of Korea, 505 Banpo-dong, Seocho-gu, Seoul 137-701, Korea
Byung-Jun Choi, Department of Pediatrics, College of Medicine, The Catholic University of Korea, 505 Banpo-dong, Seocho-gu, Seoul 137-701, Korea
Supported by the Korea Science and Engineering Foundation (KOSEF) through the Cell Death Disease Research Center at The Catholic University of Korea No. R13-2002-005-01004-0.
Co-first authors: Yong-Gu Cho and Byung-Jun Choi
Correspondence to: Dr. Won-Sang Park, Department of Pathology, College of Medicine, The Catholic University of Korea, 505 Banpo-dong, Seocho-gu, Seoul 137-701, Korea. wonsang@catholic.ac.kr
Telephone: +82-2-5901192 Fax: +82-2-5376586
Received: 2005-09-21 Accepted: 2005-11-18

Abstract

AIM: To investigate whether krÜppel-like factor 6 (KLF6) plays an important role in the development and/or progression of colorectal cancer.

METHODS: A total of 123 formalin-fixed and paraffin-embedded colorectal cancer specimens were analyzed by immunohistochemistry using tissue microarray for the expression of KLF6 protein. The specimens were collected over a 3-year period in the laboratories at our large teaching hospital in Seoul, Republic of Korea. The correlation of KLF6 expression with clinicopathologic parameters was analyzed by χ^2 test and Bartholomew test.

RESULTS: Normal colonic epithelium showed weak to moderate expression of KLF6, whereas reduced KLF 6 expression or loss of KLF6 expression was seen in 45 (36.6%) of the 123 colorectal carcinoma specimens. Interestingly, aberrant expression of KLF6 was detected in 25 (43.1%) of 58 cases with metastasis to regional lymph node and in 31 (47.0%) of 66 tumors more than 5 cm in size. Statistically, loss of KLF6 expression was significantly associated with tumor size ($P < 0.05$). However, there was no significant correlation between KLF6 expression and Dukes' stage (Bartholomew test, $P > 0.05$), tumor location and lymph node metastasis (χ^2 test, $P > 0.05$).

CONCLUSION: Loss of KLF6 expression may be a common and early event in colorectal carcinogenesis.

Key words: KLF6; Mutation; Immunohistochemistry; Aggressiveness; Tumor stage; Colorectal cancer

Cho YG, Choi BJ, Song JW, Kim SY, Nam SW, Lee SH, Yoo NJ, Lee JY, Park WS. Aberrant expression of krÜppel-like factor 6 protein in colorectal cancers. *World J Gastroenterol* 2006; 12(14): 2250-2253

http://www.wjgnet.com/1007-9327/12/2250.asp

INTRODUCTION

Colorectal cancer is the second leading cause of cancer-related death in the Western world[1]. In Korea, it accounts for an estimated 11.2% of all malignancies, with 11.6% in the male population and 10.7% in the female population[2]. Thus, colorectal cancer remains a significant contributor to the world's health burden. At a molecular level, great progress has been made in the last two decades in identification and characterization of the genetic changes involved in the malignant colorectal transformation process. Thus, the concept of multistage carcinogenesis is now widely accepted as a consequence of multiple genetic alterations accumulated in cancer cells [3]. However, the molecular mechanisms underlying dysregulated cell growth in colorectal cancer remain the subject of intensive investigation.

Krüppel-like factor 6 (KLF6) is a ubiquitously expressed zinc finger transcription factor that is part of a growing KLF family. The KLF family is broadly involved in growth-related signal transduction, cell proliferation, development and apoptosis, as well as angiogenesis[4, 5]. In functional analysis, wild-type KLF6 up-regulates the cell cycle inhibitor p21 in a TP53-independent manner and suppresses growth, whereas tumor-derived KLF6 mutants fail to upregulate p21 or suppress proliferation in prostatic and non-small cell lung cancer cells[6, 7]. In addition, introduction of KLF6 disrupts cyclin D1-dependent kinase 4 complexes and forces the redistribution of p21, which promotes G1 cell cycle arrest[8]. Furthermore, KLF6 plays

Table 1 Relationship between KLF6 expression and clinicopathologic parameters of colorectal carcinoma

Clinicopathologic parameters	KLF6 +	KLF6 -	Positive (%)	*P*
Stage				0.2969[1]
A	11	2	84.6	
B	29	18	61.7	
C	32	23	58.2	
D	6	2	75.0	
Lymph node metastasis				0.1754[2]
+	33	25	56.9	
-	45	20	69.2	
Site				0.0730[2]
Right	12	13	48.0	
Left	66	32	67.3	
Tumor size				0.0100[2]
> 5 cm	35	31	53.0	
≤ 5 cm	43	14	75.4	
Total	78	45	63.4	

[1]Bartholomew test; [2]χ^2 test.

a role as an inhibitor of cell proliferation by counteracting the function of the c-Jun protooncoprotein[9].

Recently, genetic alterations of *KLF6* gene have been identified in several human cancers, including colorectal cancer, hepatocellular carcinoma, prostate and gastric cancer[10-13]. Reduced expression of KLF6 protein has been found in non-small cell lung cancers and glioblastomas[7, 14]. Interestingly, the survey of gene expression in a panel of 60 NCI cancer cell lines showed that expression of KLF6 mRNA was reduced in colon cancer cell lines[15]. However, there is no report describing the expression pattern of KLF6 protein in colorectal cancers.

In the present study, to determine whether altered expression of the KLF6 protein is involved in colorectal cancer development, we analyzed the expression pattern of KLF6 on a series of 123 colorectal cancer specimens.

MATERIALS AND METHODS

Tissue samples

One hundred and twenty-three formalin-fixed and paraffin-embedded colorectal cancer specimens collected between 2002 and 2003 were enrolled in this study. No patient had a family history of colorectal cancer. Tumor stage was classified according to Dukes' criteria. Thirteen patients were classified as Dukes' A, 47 as Dukes' B, 55 as Dukes' C and 8 as Dukes' D[16]. Two pathologists screened histological sections and selected areas of the representative tumor cells. Three tissue cores (0.6 mm in diameter) were taken from each tumor sample and placed in a new recipient paraffin block using a commercially available microarray instrument (Beecher Instruments, Micro-Array Technologies, Silver Spring, MD) as previously described[17]. One cylinder of normal colonic mucosa adjacent to each tumor was also transferred to the recipient block.

Immunohistochemistry for KLF6

The primary polyclonal rabbit anti-KLF6 antibody (Santa Cruz Biotechnology, Santa Cruz, CA) was used. Immunostaining was performed on microarray tissue sections with a tyramide signal amplification kit (NEN Life Science, Boston, MA) for signal intensification. Antigen retrieval was performed by microwave heating in a citrate buffer (pH 6.0). Other procedures were performed as previously described[18]. Reaction products were developed with diaminobenzidine (Sigma, St Louis, MO) and counterstained with hematoxylin. Because all the corresponding normal colonic mucosae showed KLF6 expression, tumors were considered as negative when nuclear and cytoplasmic staining was seen in less than 20% of cancer cells. We calculated the KLF6 positive and negative cancer cells in three representative areas at X200 magnification. We only considered the percentage of stained nuclei in each tumor, independent of the intensity. Three pathologists independently reviewed the results and those cases with discrepant results were discussed until agreement was achieved. As a negative control, we used non-immune rabbit serum instead of the KLF6 antibody.

Statistical analysis

The correlation of KLF6 expression with clinicopathologic parameters, such as tumor site, size, lymph node metastasis and clinical stage, was analyzed by χ^2 test and Bartholomew test. $P < 0.05$ was considered statistically significant.

RESULTS

Expression of KLF6

We assessed the pattern of KLF6 protein expression in 123 colorectal carcinoma specimens by immunohistochemistry using tissue microarray. The KLF6 expression was positive in cytoplasm and nuclei of normal colonic mucosal epithelial cells, but weak to moderate in lymphocytes and fibroblasts. The expression of KLF6 in tumor cells was compared to the expression in their corresponding normal colonic mucosae. Interestingly, reduced KLF6 expression or loss of KLF6 expression was found in 45 (36.6%) of the 123 colorectal carcinoma specimens, in which immunostaining on cytoplasm and nuclei of tumor cells was predominantly (Figure 1). Unexpectedly, overexpression of the KLF6 in cancer was also found in 12 cases. Negative immunoreactivity was seen in 15.4% (2 of 13 cases) of stage A, 38.3% (18 of 47) of stage B, 41.1% (23 of 56) of stage C, and 25.0% (2 of 8) of stage D, respectively (Table 1). Loss of expression was found in 25 (43.1%) of 58 cases with metastasis to regional lymph nodes and 32 (32.7%) of 98 left-side colorectal cancers. In addition, immunostaining was negative in 31 (47.0%) of 66 cases with tumors >5 cm. Statistically, loss of KLF6 expression was closely associated with tumor size (χ^2 test, $P < 0.05$). However, there was no significant correlation between KLF6 expression and Dukes' stage (Bartholomew test, $P > 0.05$), tumor location and lymph node metastasis (χ^2 test, $P > 0.05$).

DISCUSSION

It has been reported that several KLFs play an essential role in maintaining the homeostasis of mammalian cells through the regulation of proliferation and

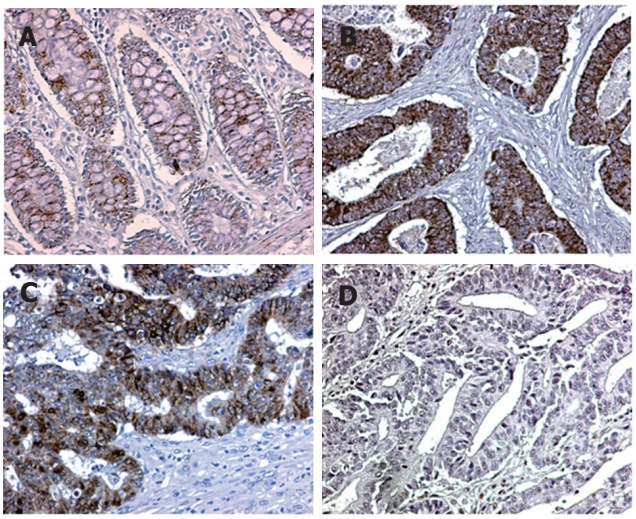

Figure 1 Expression of KLF6 protein in colonic mucosa and cancer. **A:** Positive reaction mainly in colonic glandular epithelial cells; **B:** Predominantly strong immunopositivity in cytoplasm of colon cancer cells; **C**: Predominantly strong immunopositivity in nuclei of colon cancer cells; **D**: Negative staining of KLF6 in cancer cells (original magnifications: X 200).

differentiation[4, 5]. The KLF6 is regulated during mammalian development and tissue regeneration, while its aberrant expression is associated with tumor formation. Recently, KLF6 has been identified as a tumor suppressor gene in several kinds of cancer because of reduced expression and its frequent genetic alterations, such as loss of heterozygosity and mutation, as well as functional suppression of cell proliferation. To further clarify the role of KLF6 in colorectal cancer, we examined loss of expression in 123 colorectal cancer samples.

In this study, reduced KLF6 expression or loss of KLF6 expression was found in 45 (36.6%) of the 123 colorectal adenocarcinoma specimens. Statistically, loss of KLF6 expression was closely associated with tumor size (χ^2 test, $P<0.05$). However, there was no significant correlation between reduced KLF6 expression and other clinicopathologic parameters, including Dukes' stage (Bartholomew test, $P>0.05$), tumor location and lymph node metastasis (χ^2 test, $P>0.05$). It has been reported that the expression of KLF6 protein is frequently down-regulated in non-small cell lung cancer and glioblastoma [7, 14]. Interestingly, down-regulation of KLF6 expression is not associated with the histology or surgical-pathological stages of lung tumors[7]. Taken together, these results further support that down-regulation of KLF6 may contribute to the development of human solid cancers and that inactivation of KLF6 may occur in the development of colorectal cancer as an early event.

Unexpectedly, upregulation of KLF6 was also seen in 14 colorectal cancer cases. Since KLF6 is broadly involved in growth-related signal transduction, cell proliferation, differentiation and apoptosis, upregulation of KLF6 might reflect compensatory mechanisms directed at reestablishing the equilibrium in proliferation, differentiation, and survival characteristics of colonic epithelial cells disrupted during carcinogenesis. Because mutation of the KLF6 is frequently found in colorectal cancer [13], over-expression of KLF6 might be caused by the genetic alteration of the *KLF6* gene. Further studies are necessary to investigate the precise molecular mechanisms underlying its over-expression.

Tissue microarray (TMA) consists of numerous tissues and tumor types. The use of TMA can stain a large number of cases at minimal cost and allow a rapid assessment of the staining profile. However, whether cores of tumor are representative of whole sections remains unclear. It was reported that immunostaining of one to four 0.6-mm cores is correlated with whole sections staining [19], suggesting that the use of small cores is equivalent to whole section immunohistochemistry. Another issue for consideration is that the scoring of TMA immunohistochemistry experiments remains subjective and not easily quantifiable. Significant efforts have been made to quantify protein expression levels on TMA sections [20], but most TMAs are subjectively scored by eyes. In this study, expression of KLF6 in three cores of tumor tissues was compared to their corresponding normal colonic mucosae by three pathologists. Although we did not perform immunohistochemistry on whole section, our results on TMA may be consistent with those of whole section immunohistochemistry.

Generally, the inactivation of a tumor suppressor associated with loss of expression results from genetic or epigenetic alterations, such as mutation, allelic loss or hypermethylation of the promoter region of the genes. Recently, genetic alterations of *KLF6* gene have been identified in several human cancers, including hepatocellular carcinoma, prostate, gastric and colon cancers[10-13]. However, no mutation of KLF6 has been found in human cancer[21-23]. Further studies on a large number of patients are necessary to find out the discrepancy in incidence of *KLF6* mutation. Interestingly, the *KLF6* mRNA is also frequently down-regulated in non-small cell lung cancer, glioblastoma, and colon cancer cell lines[7, 14, http://smd.stanford.edu/cgi-bin]. No mutation has been found in these cancer tissues and KLF6 is down-regulated in all samples with allelic loss[7]. Additionally, the *KLF6* is suggested to be a methylation-silenced gene in esophageal squamous cell carcinoma[24]. In the present study, we found that KLF6 expression was reduced or lost in 36.6% of colorectal cancers (Table 1). Although we did not perform the genetic or epigenetic analysis of the *KLF6* gene, our results suggest that reduced KLF6 expression or loss of KLF6 expression may be a common and early event in colorectal carcinogenesis.

REFERENCES

1 **Day DW**, Jass JR, Price AB, Shepherd NA, Sloan JM, Talbot IC, Warren BF, Williams GT. Epithelial tumors of the large intestinge. In Morson BC, Dawson IMP, and Day DW. Morson and Dawson's gastrointestinal pathology. 4th ed. *Oxford: Blackwell Pub* 2003: 551-609

2 **Shin HR**, Jung KW, Won YJ, Park JG, 2002 Annual report of the Korea central cancer registry: Based on registered data from 139 hospitals. *Cancer Research and Treatment* 2004; **36**: 103-114

3 **Fearon ER**, Vogelstein B. A genetic model for colorectal tumorigenesis. *Cell* 1990; **61**: 759-767

4 **Bieker JJ**. Kruppel-like factors: three fingers in many pies. *J Biol Chem* 2001; **276**: 34355-34358

5 **Black AR**, Black JD, Azizkhan-Clifford J. Sp1 and kruppel-like factor family of transcription factors in cell growth regulation and cancer. *J Cell Physiol* 2001; **188**: 143-160

6 **Narla G**, Heath KE, Reeves HL, Li D, Giono LE, Kimmelman AC, Glucksman MJ, Narla J, Eng FJ, Chan AM, Ferrari AC, Martignetti JA, Friedman SL. KLF6, a candidate tumor suppressor gene mutated in prostate cancer. *Science* 2001; **294:** 2563-2566

7 **Ito G**, Uchiyama M, Kondo M, Mori S, Usami N, Maeda O, Kawabe T, Hasegawa Y, Shimokata K, Sekido Y. Kruppel-like factor 6 is frequently down-regulated and induces apoptosis in non-small cell lung cancer cells. *Cancer Res* 2004; **64:** 3838-3843

8 **Benzeno S**, Narla G, Allina J, Cheng GZ, Reeves HL, Banck MS, Odin JA, Diehl JA, Germain D, Friedman SL. Cyclin-dependent kinase inhibition by the KLF6 tumor suppressor protein through interaction with cyclin D1. *Cancer Res* 2004; **64**: 3885-3891

9 **Slavin DA**, Koritschoner NP, Prieto CC, Lopez-Diaz FJ, Chatton B, Bocco JL. A new role for the Kruppel-like transcription factor KLF6 as an inhibitor of c-Jun proto-oncoprotein function. *Oncogene* 2004; **23:** 8196-8205

10 **Chen C**, Hyytinen ER, Sun X, Helin HJ, Koivisto PA, Frierson HF Jr, Vessella RL, Dong JT. Deletion, mutation, and loss of expression of KLF6 in human prostate cancer. *Am J Pathol* 2003; **162**: 1349-1354

11 **Kremer-Tal S**, Reeves HL, Narla G, Thung SN, Schwartz M, Difeo A, Katz A, Bruix J, Bioulac-Sage P, Martignetti JA, Friedman SL. Frequent inactivation of the tumor suppressor Kruppel-like factor 6 (KLF6) in hepatocellular carcinoma. *Hepatology* 2004; **40:** 1047-1052

12 **Cho YG**, Kim CJ, Park CH, Yang YM, Kim SY, Nam SW, Lee SH, Yoo NJ, Lee JY, Park WS. Genetic alterations of the *KLF6* gene in gastric cancer. *Oncogene* 2005; **24**: 4588-4590

13 **Reeves HL**, Narla G, Ogunbiyi O, Haq AI, Katz A, Benzeno S, Hod E, Harpaz N, Goldberg S, Tal-Kremer S, Eng FJ, Arthur MJ, Martignetti JA, Friedman SL. Kruppel-like factor 6 (KLF6) is a tumor-suppressor gene frequently inactivated in colorectal cancer. *Gastroenterology* 2004; **126:** 1090-1103

14 **Kimmelman AC**, Qiao RF, Narla G, Banno A, Lau N, Bos PD, Nunez Rodriguez N, Liang BC, Guha A, Martignetti JA, Friedman SL, Chan AM. Suppression of glioblastoma tumorigenicity by the Kruppel-like transcription factor KLF6. *Oncogene* 2004; **23:** 5077-5083

15 **Ross DT**, Scherf U, Eisen MB, Perou CM, Rees C, Spellman P, Iyer V, Jeffrey SS, Van de Rijn M, Waltham M, Pergamenschikov A, Lee JC, Lashkari D, Shalon D, Myers TG, Weinstein JN, Botstein D, Brown PO. Systematic variation in gene expression patterns in human cancer cell lines. *Nat Genet* 2000; **24:** 227-235

16 **Astler VB**, Coller FA. The prognostic significance of direct extension of carcinoma of the colon and rectum. *Ann Surg* 1954; **139**: 846-852

17 **Kononen J**, Bubendorf L, Kallioniemi A, Barlund M, Schraml P, Leighton S, Torhorst J, Mihatsch MJ, Sauter G, Kallioniemi OP. Tissue microarrays for high-throughput molecular profiling of tumor specimens. *Nat Med* 1998; **4**: 844-847

18 **Park WS**, Oh RR, Kim YS, Park JY, Shin MS, Lee HK, Lee SH, Yoo NJ, Lee JY. Absence of mutations in the kinase domain of the Met gene and frequent expression of Met and HGF/SF protein in primary gastric carcinomas. *APMIS* 2000; **108**: 195-200

19 **Simon R**, Mirlacher M, Sauter G. Tissue microarrays in cancer diagnosis. *Expert Rev Mol Diagn* 2003; **3**: 421-430

20 **Camp RL**, Chung GG, Rimm DL. Automated subcellular localization and quantification of protein expression in tissue microarrays. *Nat Med* 2002; **8**: 1323-1327

21 **Lievre A**, Landi B, Cote JF, Veyrie N, Zucman-Rossi J, Berger A, Laurent-Puig P. Absence of mutation in the putative tumor-suppressor gene KLF6 in colorectal cancers. *Oncogene* 2005; **24:** 7253-7256

22 **Koivisto PA**, Hyytinen ER, Matikainen M, Tammela TL, Ikonen T, Schleutker J. Kruppel-like factor 6 germ-line mutations are infrequent in Finnish hereditary prostate cancer. *J Urol* 2004; **172:** 506-507

23 **Boyault S**, Herault A, Balabaud C, Zucman-Rossi J. Absence of KLF6 gene mutation in 71 hepatocellular carcinomas. *Hepatology* 2005; **41:** 681-682; author reply 682-683

24 **Yamashita K**, Upadhyay S, Osada M, Hoque MO, Xiao Y, Mori M, Sato F, Meltzer SJ, Sidransky D. Pharmacologic unmasking of epigenetically silenced tumor suppressor genes in esophageal squamous cell carcinoma. *Cancer Cell* 2002; **2**: 485-495

S- Editor Wang J **L- Editor** Wang XL **E- Editor** Cao L

PO Box 2345, Beijing 100023, China
www.wjgnet.com
wjg@wjgnet.com

World J Gastroenterol 2006 April 14; 12(14): 2254-2258
World Journal of Gastroenterology ISSN 1007-9327

RAPID COMMUNICATION

Acute myopathy associated with liver cirrhosis

Ok-Jae Lee, Jee-Hyang Yoon, Eun-Jeong Lee, Hyun-Jin Kim, Tae-Hyo Kim

Ok-Jae Lee, Jee-Hyang Yoon, Eun-Jeong Lee, Hyun-Jin Kim, Tae-Hyo Kim, Department of Internal Medicine and Gyeongsang Institute of Health Science, Gyeongsang National University College of Medicine, Jinju, Republic of Korea
Correspondence to: Ok-Jae Lee, MD, Department of Internal Medicine, Gyeongsang National University College of Medicine, 90 Chilam-domg, Jinju, Gyongnam, 660-702, South Korea. ojlee@nongae.gsnu.ac.kr
Telephone: +82-55-7508056 Fax: +82-55-7508056
Received: 2005-05-14 Accepted: 2005-10-10

Abstract

AIM: Many cirrhotic patients have muscular symptoms and rhabdomyolysis. However, myopathy associated with liver cirrhosis has not been established as a disease entity. We evaluated the clinical significance of acute myopathy associated with liver cirrhosis.

METHODS: We retrospectively reviewed the medical records of 5440 cirrhotic patients who had been admitted to Gyeongsang National University Hospital from August 1997 to January 2003. Among these, 99 developed acute myopathies, and they were analyzed with respect to clinical and laboratory parameters, and outcomes.

RESULTS: The Child-Pugh classification at the time of myopathy onset was A in 3(3.1%) cases, B in 33(33.3%), and C in 63 (63.6%). Infection was identified as the most predisposing factor to myopathy. Fifty percent of 18 idiopathic cases who were tested for influenza antibody were positive. Forty-two of the 99 cases were complicated by acute renal failure, and 25 (59.5%) of these expired. Apart from 6 cases lost to follow-up, 64 of 93 recovered, giving a mortality rate of 31.2%. Mortality was higher in Child-Pugh class C than in B or A.

CONCLUSION: Acute myopathy can develop as a serious complication in liver cirrhosis. Its frequency, severity and mortality depend on underlying liver function, and are higher in decompensated liver cirrhosis. Influenza should be considered as an etiologic factor in idiopathic cases. It is proposed that acute myopathy associated with liver cirrhosis be called 'hepatic myopathy', and that careful monitoring for hepatic myopathy is necessary in the patients with advanced liver cirrhosis.

Key words: Myopathy; Rhabdomyolysis; Liver cirrhosis

Lee OJ, Yoon JH, Lee EJ, Kim HJ, Kim TH. Acute myopathy associated with liver cirrhosis. *World J Gastroenterol* 2006; 12(14): 2254-2258

http://www.wjgnet.com/1007-9327/12/2254.asp

INTRODUCTION

Since many investigators[1-3] had been interested in a causal relationship between alcohol ingestion and acute myonecrosis, Martin *et al*[4] systematically described the clinicopathological features of acute and chronic myopathy associated with alcoholism, and defined this as alcoholic myopathy. Now, it is well known that alcoholism and alcoholic liver diseases can be accompanied by alcoholic skeletal myopathy[5,6]. Moreover, a higher prevalence of muscle cramps was reported in patients with liver cirrhosis than in a matched population without cirrhosis, and it was suggested that muscle cramps be included as a recognized symptom of cirrhosis[7]. Muscular symptoms such as muscle cramps, weakness, aching and tenderness are also common in patients with liver cirrhosis, and even rhabdomyolysis can occur[8-10]. However, myopathy associated with liver cirrhosis has not been established as a disease entity. Here, we investigated the clinical characteristics of acute myopathy, which developed in patients with liver cirrhosis, and evaluated its clinical significance.

MATERIALS AND METHODS

Inclusion criteria

Of the 5440 patients with liver cirrhosis who had been admitted because of various problems related to cirrhosis to Gyeongsang National University Hospital from August 1997 to January 2003, 99 patients who developed acute myopathy were included. We reviewed and analyzed their medical records retrospectively so to find out predisposing or etiologic factors, and possible factors influencing the frequency, severity, and prognosis of acute myopathy associated with liver cirrhosis.

A diagnosis of liver cirrhosis was made based on liver biopsy, or clinical, laboratory and radiological evidence of chronic hepatocellular dysfunction and portal hypertension. Underlying liver function was assessed by Child-Pugh's classification based on laboratory data and physical signs at the time of most recent visit.

Acute myopathy was defined as an elevated serum muscle enzymes, i.e., creatine kinase (CK, 45-390 IU/L), lactate dehydrogenase (LDH, 30-170 IU/L), and aspartate

Table 1 Clinical characteristics of patients with liver cirrhosis who developed acute myopathy

Clinical parameters	Number of cases ($n=99$)
Sex (M:F)	74:25 (2.96:1)
Age (yr) range	27 - 76
mean	51 ± 10
Etiology of LC	
Alcohol	47
CVH (B)	41
CVH (C)	5
Wilson's disease	1
Idiopathic	5
Child-Pugh Class	
A:B:C	3:33:63

LC, Liver cirrhosis; CVH, Chronic viral hepatitis.

Table 2 Predisposing factors of acute myopathy in patients with liver cirrhosis ($n=99$)

Predisposing factors	Number of cases (%)
Infection	46 (46.5)
Respiratory infection	17
Gastrointestinal infection	12
Genitourinary infection	8
Septic shock	5
Alcohol	8 (8.1)
Exercise or trauma	8 (8.1)
Transarterial embolization	4 (4.0)
Herb medicine	3 (3.0)
Dehydration	2 (2.0)
Gastrointestinal bleeding	1 (1.0)
Idiopathic	27 (27.3)

transaminase (AST, 5-45 IU/L), and/or accompanied by acute muscular symptoms, such as muscle cramps, generalized or localized muscle weakness, muscle edema, muscle pain, or tenderness.

Possible predisposing factors were defined as the events occurring within one week prior to the onset time of myopathy.

Acute renal failure was diagnosed when the serum creatinine level increased by more than 50% of the baseline value, to above 1.5 mg/dL[11]. If there was no improvement in serum creatinine despite optimization of intravascular volume in azotemia, hepatorenal syndrome was diagnosed[12].

Exclusion criteria

Exclusion criteria were a history of myocardiac infarction, cardiomyopathy, cerebrovascular accident and other cardiovascular diseases, thyroid disease, peripheral neuropathy, phlebitis, primary muscle disease, heat stroke, and underlying kidney disease, and the ingestion of agents known as triggering agents of myopathy such as digitalis, cimetidine, clofibrate, lithium, opiate, nifedipine, beta 2-agonist, beta-blockers, penicillamine (except for Wilson's disease), cyclosporine, quinidine, antispastic drugs, verapamil, amphetamine, cocaine, vitamin E, or taurine[9,13].

RESULTS

General characterisitics

Ninety-nine (1.8%) of 5440 patients with liver cirrhosis developed acute myopathy. With exception of 4 patients who developed myopathy during hospitalization after transarterial embolization, 95 patients were admitted due to acute myopathy. Seventy-four patients were male, giving a male to female ratio of 2.96. Mean age of patients was 51 ± 10 years (range; 27-76 years), and most were in the 6th decade. The etiology of the liver cirrhosis was alcohol in 47, hepatitis B virus in 41, hepatitis C virus in 5, Wilson's disease in 1, and cryptogenic in 5 (Table 1).

Underlying liver function

Child-Pugh classification at the time of myopathy onset was A in 3 (3.0%), B in 33 (33.3%), and C in 63 patients (63.6%) (Table 1).

Etiologic factors

The most predisposing factor to myopathy was infection (46.5%); respiratory tract infections including common cold in 17, gastrointestinal infections in 12, urinary infection in 8, and septic shock in 5. Alcohol (8.1%), exercise or trauma (8.1%), transarterial embolization (4.0%), herb medicine (3.0%), dehydration (2.0%), and gastrointestinal bleeding (1.0%) were also possible predisposing factors of acute myopathy, and 27 cases (27.3%) were idiopathic (Table 2). In cases of transarterial embolization, acute myopathy developed after hepatic arterial embolization for primary liver cancer in two, and after splenic arterial embolization for splenomegaly with severe pancytopenia in two. Influenza antibody was checked in 18 of the 27 idiopathic cases and 9 (50%) had positive results.

Symptoms and signs

Patients presented with muscle pain (57.6%) and/or generalized muscle weakness (23.2%). However, in 19 patients (19.2%) muscular symptoms were masked with concomitant complications, namely, hepatic encephalopathy (15.2%) or spontaneous bacterial peritonitis (4%).

Muscle enzyme changes

Peak levels of AST, CK, and LDH in serum were 1264.8 IU/L, 20693.2 IU/L, and 1926.7 IU/L, respectively. The intervals from symptom onset to peak levels of these muscle enzymes were 5.1, 5.4, and 6.2 days. According to Child-Pugh class, AST, CK, LDH levels were 925, 6820.7, 1013 IU/L in A, 1359.8, 21083.3, 1991.7 IU/L in B, and 1231.2, 21147.9, 1936.1 IU/L in C, respectively. No statistically significant difference was found in muscle enzymes according to Child-Pugh class (Table 3).

Myoglobin

Sixty cases received a urine orthotolidine test for myoglobin; 38 (63.3%) were negative, and 22 (37.6%) positive. The incidence of myoglobinuria was not different significantly between patients with or without renal failure (41.2% *vs* 33.4%). Serum myoglobin concentrations were high in all patients, but did not differ in myoglobinuria-

Table 3 Muscle enzymes in patients with liver cirrhosis and acute myopathy

	AST (IU/L)	CPK (IU/L)	LDH (IU/L)
Class A	925	6820.7	1013
Class B	1359.8	21083.3	1991.7
Class C	1231.2	21147.9	1936.1
Total	1264.8	20693.2	1926.7
Peak day[a]	5.1	5.4	6.2

[a]The intervals from symptom onset to peak levels.

negative and -positive patients (565 ± 267 *vs* 575 ± 183 mg/dL, $P > 0.05$), or between patients with or without renal failure (616.3 ± 332.1 *vs* 629.9 ± 269.8 mg/dL, $P > 0.05$).

Radionuclide bone scan

A ^{99m}Tc-HDP (hydroxymethylene diphosphonate) radionuclide bone scan was performed in 28 patients, and radionuclide muscular uptake increased in 18 (64.3%) who received the test within a few days of onset. However, it should be noted that all 10 patients who did not show increased muscular uptake received the scan when they showed signs of symptomatic improvement rather immediately after onset.

Hospital course

Guidelines of discharge from hospital were the complete disappearance of muscular symptoms and a normalization or maintenance of muscle enzymes at < 1.5 times the normal value. Mean length of hospital stay was 20.8 ± 14.9 d, and this was longer for Child-Pugh B or C patients than for Child-Pugh A patients (21.6 ± 13.1 d, 20.4 ± 16 d *vs* 12.2 ± 3.1 d). Acute renal failure was a complication in 42 of the 99 (42.4%) acute myopathy patients.

Clinical outcomes

Of the 93 patients followed, i.e., except the 6 lost to follow-up, 64 (68.8%) recovered, and 29 (31.2%) expired. In-hospital mortality was higher in Child-Pugh class C (24/59, 40.7%) than in Child-Pugh class B (5/31, 16.1%) or A (0/3, 0%)(Table 4, Figure 1). Forty of the 93 cases (43.0%) were complicated by acute renal failure, and 25 (62.5%) of these expired. The incidences of renal failure were 0%, 30.3%, and 49.2% in Child-Pugh A, B, and C, respectively. The most common causes of death were hepatic failure (14, 48.3%), renal failure (6, 20.7%), septic shock (6, 20.7%), and upper gastrointestinal bleeding (3, 10.3%).

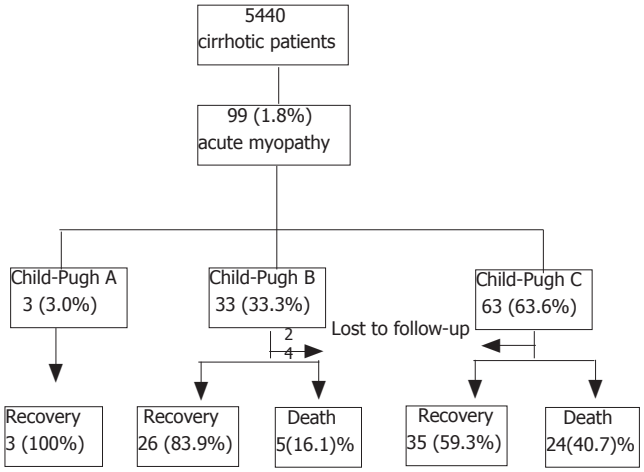

Figure 1 Clinical course of the patients with liver cirrhosis and acute myopathy.

DISCUSSION

Many investigators[7-9] have reported on the high prevalence of muscle cramps in patients with liver cirrhosis. Konikoff *et al*[7] found an 88% incidence of painful cramps in 33 cirrhosis patients, as compared to 21% in a matched population without liver disease. They concluded that the strikingly high incidence and uniformity of the phenomenon might justify the inclusion of painful muscle cramps among the recognized symptoms of cirrhosis. Abrams *et al*[8] suggested that cramps in cirrhotic patients are specifically related to the development of cirrhosis, and that a worsening liver function may be a risk factor for the development of cramps. Angeli *et al*[9] found that the prevalence of cramps was higher in cirrhotic patients than in controls, and that it was related to the duration of recognized cirrhosis and to the severity of liver function impairment. Moreover, they concluded that the pathophysiological link between cirrhosis and cramps may associate with a reduced effective circulating volume, and also indicated that weekly human albumin infusion may be an effective treatment for cramps in cirrhosis. However, these reports focused upon muscle cramps as a symptom observed in liver cirrhosis patients, and not on the clinical and laboratory findings associated with muscular symptoms. Moreover, in addition to muscular symptoms such as muscle cramps, weakness, aching and tenderness, rhabdomyolysis can also occur in liver cirrhosis patients[8-10]. However, no systematic investigation has been conducted on rhabdomyolysis development in cirrhotic patients.

Rhabdomyolysis may be defined as a clinical and laboratory syndrome resulting from skeletal muscle injury with the release of muscle cell contents into the plasma[14]. Increased concentrations of these released substances, such as CK, permit clinicians to diagnose this syndrome[14]. We found an incidence of acute myopathy of 1.8% among hospitalized liver cirrhosis patients. We investigated here cirrhotic patients with elevated muscle enzyme concentrations and/or muscular symptoms, i.e., rhabdomyolysis. And, we described this syndrome as acute myopathy rather than rhabdomyolysis, to better characterize the syndrome and to highlight its significance in liver cirrhosis patients, much like that of the myopathies of alcoholism and alcoholic liver diseases.

We observed that almost all cirrhotic patients who developed acute myopathy had a poor liver function, i.e., Child-Pugh B or C at the time of onset, with exception of 3 cases with Child-Pugh A. Therefore, patients with advanced liver cirrhosis and a poor liver function should be monitored carefully for acute myopathy, in addition to the better known complications of hepatic encephalopathy,

Table 4 Clinical outcome of patients with liver cirrhosis and acute myopathy by Child-Pugh's classification ($n=93$)

Outcome	Child-Pugh class (%)			
	A	B	C	Total
Recovery	3(100)	26(83.9)	35(59.3)	64(68.8)
Death	0(0)	5(16.1)	24(40.7)	29(31.2)
Total	3	31	59	93[a]

[a]Six patients (2 with Child-Pugh B and 4 with C) were lost to follow-up.

gastrointestinal bleeding, or hepatorenal syndrome.

Compared with rhabdomyolysis in the general population, in which drug overdose and septicemia are the most common etiologic factors[15], we found that the most predisposing factor to myopathy development in cirrhotic patients was infection (46.5%), including respiratory, spontaneous bacterial peritonitis (*E. coli*), urinary tract infection, and *Vibrio vulnificus* sepsis. Furthermore, 50% of idiopathic cases were positive for anti-influenza antibody, suggesting that an infectious etiology may account for over 50% of acute myopathy associated with liver cirrhosis, and that influenza should be considered an etiologic factor of acute myopathy developing in cirrhotic patients without a definite etiology. In addition to influenza, various viral and bacterial infections have been reported to be etiologic factors of rhabdomyolysis in the general population[16-20]. Although the precise pathophysiology underlying virus or bacteria-induced rhabdomyolysis is unknown, proposed pathophysiological mechanisms include direct viral or bacterial invasion of skeletal muscle and toxin generation[17]. Muscle biopsies performed on rhabdomyolysis patients found lymphocytic infiltrate or viral inclusions, which support the hypothesis of direct viral invasion[21-23]. Viral DNA PCR analysis of muscle specimens and the identification of viral particles and bacteria in the muscle biopsy specimens, and the isolation of virus by culture from muscle specimens provide more compelling evidence of direct viral or bacterial invasion[22-24].

As 19.2% of our subjects presented with symptoms of concurrent complications other than muscular symptoms, acute myopathy may be difficult to identify in some cirrhotic patients by symptoms alone, i.e., without testing muscle enzymes. Because cirrhotic patients can develop various complications, muscle enzymes investigations are recommended for the detection of acute myopathy. On this point, previous investigations[7-9] were limited because they evaluated only muscular symptoms.

Increased levels of muscle enzymes are the result of skeletal muscle injury and the consequent release of muscle cell contents into the plasma[14]. AST, CK, and LDH peaked 5-6 d after symptom onset, and symptom alleviation was followed by a reduction in muscle enzyme levels (data not shown). The patients with decompensated liver cirrhosis had higher plasma levels of muscle enzymes than cirrhotic patients with a well preserved liver function. These findings represent the natural course of acute myopathy development in cirrhotic patients.

Rhabdomyolysis may or may not result in myoglobinuria, depending on the amount of myoglobin released into plasma, the glomerular filtration rate, and the urine concentration[14]. In the present study, myoglobinuria was present in only 37.6% of subjects who took the urine orthotolidine test; however, serum myoglobin was elevated in all patients. Moreover, myoglobinuria and serum myoglobin levels were unrelated to each other or to the development of renal failure. Different urine sampling times may also have influenced the low incidence of myoglobinuria. Though myoglobinuria is an important clue for the diagnosis of rhabdomyolysis, it cannot be used alone to identify all myopathies. Increased levels of muscle enzymes and serum myoglobin are more sensitive for the diagnosis of rhabdomyolysis, and in particular, CK is a highly sensitive marker of muscle injury[25].

Many case reports have mentioned the usefulness of Tecnetium-99 m bone scintigraphy for the early diagnosis, and for determining the location and extent of the muscle damage in rhabdomyolysis[26-28]. In the present study, a ^{99m}Tc-HDP radionuclide bone scan was diagnostic in 64.3% of the patients evaluated. Patients evaluated within a few days after onset showed increased muscular uptake, but not all patients showing symptomatic improvement who received this test showed increased muscular uptake. Thus, ^{99m}Tc bone agent scintigraphy may be useful for the evaluation of the degree and extent of muscle injury, if it is timely performed.

The length of hospital stay was about 12 d in patients with Child-Pugh A and about 3 wk in the patients with Child-Pugh B or C. Over 40% of cirrhotic cases with acute myopathy were accompanied by acute renal failure. The incidence of renal failure depended on Child-Pugh class, and was highest in patients with Child-Pugh C. Although the pathophysiologic mechanisms of rhabdomyolysis-related acute renal failure are unknown, several mechanisms have been proposed, for example, tubular obstruction by myoglobin plugs and/or urate, renal vasoconstriction caused by the inhibitory effect of myoglobin on endothelial vasodilator production, and toxic free radical produced by ferrous compound, a metabolite of myoglobin[29, 30]. The frequency of acute renal failure in cases of rhabdomyolysis was reported to be 16%-33% in the general population[14,31], and 40.4% in acute myopathy associated with liver cirrhosis. In the present study, among rhabdomyolysis cases complicated by acute renal failure, 62.5% expired, and acute renal failure accounted for 20.7% of these mortalities. Thus, acute renal failure seems to have a prognostic role and its frequency was found to depend on Child-Pugh class. These findings suggest that the status of underlying liver function may be the most important prognostic factor in cases of acute myopathy associated with liver cirrhosis.

The mortality rate reported in the general population was 10%-12%[14, 15, 31], and the overall mortality rate in the present study was 31.2%, which is higher than those reported in cases of rhabdomyolysis in the general population. The mortality rate also depended on the status of underlying liver function. In particular, in-hospital mortality of Child-Pugh C patients was 40.7%. The most common cause of death in cirrhotic patients with acute myopathy was hepatic failure (48.3%).

There are some limitations in this study. First, since the present study was based on retrospective review of medi-

cal records of only symptomatic hospitalized patients, the incidence of acute myopathy was underestimated. In addition, all 5440 cirrhotic patients were hospitalized because of various problems related to cirrhosis so that a majority of them had advanced diseases and the patients with well compensated diseases were not included. Therefore, for all that an analysis of all cirrhotic patients including those without any complication is necessary for defining the predisposing factors for acute myopathy, we could not compare underlying disease function between the patients with myopathy and those without. Thirdly, the diagnosis of myopathy was based on the laboratory and clinical findings, not electromyography or muscle biopsy. However, the decompensated cirrhotic patients can hardly receive electromyography or especially muscle biopsy. Furthermore, the term 'myopathy' was used as rhabdomyolysis in this study.

We found that acute myopathy development is a serious complication in liver cirrhosis patients and that this has several predisposing factors. Moreover, its frequency, morbidity, and mortality were found to depend on underlying liver function and to be higher in decompensated liver cirrhosis. The authors propose that acute myopathy associated with liver cirrhosis be called 'hepatic myopathy' and that careful monitoring is required for its early recognition in the advanced liver cirrhosis patients. The avoidance of predisposing factors by identifying disease mechanisms is certain to reduce the occurrence and mortality of hepatic myopathy. Further studies on the pathophysiologic mechanism and treatment of hepatic myopathy are warranted.

Footnote: Abstract of this paper was presented at Digestive Disease Week 2004, New Orleans, USA

REFERENCES

1 **Hed R**, Larsson H, Wahlgren F. Acute myoglobinuria; report of a case with fatal outcome. *Acta Med Scand* 1955; **152**: 459-463
2 **Fahlgren H**, Hed R, Lundmark C. Myonecrosis and myoglobinuria in alcohol and barbiturate intoxication. *Acta Med Scand* 1957; **158**: 405-412
3 **Perkoff GT**, Hardy P, Velez-Garcia E. Reversible acute muscular syndrome in chronic alcoholism. *N Engl J Med* 1966; **274**: 1277-1285
4 **Martin FC**, Slavin G, Levi AJ. Alcoholic muscle disease. *Br Med Bull* 1982; 38: 53-56
5 **Martin F**, Ward K, Slavin G, Levi J, Peters TJ. Alcoholic skeletal myopathy, a clinical and pathological study. *Q J Med* 1985; **55**: 233-251
6 **Martin F**, Peters TJ. Alcoholic muscle disease. *Alcohol Alcohol* 1985; 20: 125-136
7 **Konikoff F**, Theodor E. Painful muscle cramps. A symptom of liver cirrhosis? *J Clin Gastroenterol* 1986; **8**: 669-672
8 **Abrams GA**, Concato J, Fallon MB. Muscle cramps in patients with cirrhosis. *Am J Gastroenterol* 1996; **91**: 1363-1366
9 **Angeli P**, Albino G, Carraro P, Dalla Pria M, Merkel C, Caregaro L, De Bei E, Bortoluzzi A, Plebani M, Gatta A. Cirrhosis and muscle cramps: evidence of a causal relationship. *Hepatology* 1996; **23**: 264-273
10 **Khokhar N**. Massive rhabdomyolysis in cirrhosis of liver. *J Pak Med Assoc* 2001; **51**: 331-332
11 **Sort P**, Navasa M, Arroyo V, Aldeguer X, Planas R, Ruiz-del-Arbol L, Castells L, Vargas V, Soriano G, Guevara M, Gines P, Rodes J. Effect of intravenous albumin on renal impairment and mortality in patients with cirrhosis and spontaneous bacterial peritonitis. *N Engl J Med* 1999; **341**: 403-409
12 **Arroyo V**, Gines P, Gerbes AL, Dudley FJ, Gentilini P, Laffi G, Reynolds TB, Ring-Larsen H, Scholmerich J. Definition and diagnostic criteria of refractory ascites and hepatorenal syndrome in cirrhosis. International Ascites Club. *Hepatology* 1996; **23:** 164-176
13 **Joekes AM**. Cramp: a review. *J R Soc Med* 1982; **75**: 546-549
14 **Gabow PA**, Kaehny WD, Kelleher SP. The spectrum of rhabdomyolysis. *Medicine* (Baltimore) 1982; **61:** 141-152
15 **Black C**, Jick H. Etiology and frequency of rhabdomyolysis. *Pharmacotherapy* 2002; **22**: 1524-1526
16 **Cunningham E**, Kohli R, Venuto RC. Influenza-associated myoglobinuric renal failure. *JAMA* 1979; **242**: 2428-2429
17 **Singh U**, Scheld WM. Infectious etiologies of rhabdomyolysis: three case reports and review. *Clin Infect Dis* 1996; **22**: 642-649
18 **Pesik NT**, Otten EJ. Severe rhabdomyolysis following a viral illness: a case report and review of the literature. *J Emerg Med* 1996; **14**: 425-428
19 **Morton SE**, Mathai M, Byrd RP Jr, Fields CL, Roy TM. Influenza A pneumonia with rhabdomyolysis. *South Med J* 2001; **94**: 67-69
20 **Fernandez A**, Justiniani FR. Massive rhabdomyolysis: a rare presentation of primary *Vibrio vulnificus* septicemia. *Am J Med* 1990; **89**: 535-536
21 **Foulkes W,** Rees J, Sewry C. Influenza A and rhabdomyolysis. *J Infect* 1990; **21:** 303-304
22 **Porter CB,** Hinthorn DR, Couchonnal G, Watanabe I, Caveny EA, Goldman B, Lash R, Holmes F, Liu C. Simultaneous Streptococcus and picornavirus infection. Muscle involvement in acute rhabdomyolysis. *JAMA* 1981; **245:** 1545-1547
23 **Pratt RD**, Bradley JS, Loubert C, LaRocco A Jr, McNeal RM, Newbury RO, Sawyer MH. Rhabdomyolysis associated with acute varicella infection. *Clin Infect Dis* 1995; **20**: 450-453
24 **Kessler HA**, Trenholme GM, Harris AA, Levin S. Acute myopathy associated with influenza A/Texas/1/77 infection. Isolation of virus from a muscle biopsy specimen. *JAMA* 1980; **243:** 461-462
25 **Hess JW**, MacDonald RP, Frederick RJ, Jones RN, Neely J, Gross D. Serum creatine phosphokinase (CPK) activity in disorders of heart and skeletal muscle. *Ann Inter Med* 1964; **61**: 1015-1028
26 **Delpassand ES**, Dhekne RD, Barron BJ, Moore WH. Evaluation of soft tissue injury by Tc-99m bone agent scintigraphy. *Clin Nucl Med* 1991; **16**: 309-314
27 **Yasuo M**, Yamamoto H. A case of rhabdomyolysis associated with influenza A viral infection given an useful early diagnosis by Tc-99m bone agent scintigraphy. *Kansenshogaku Zasshi* 2001; **75**: 568-572
28 **Bhargava P**, Bhutani C, Feng Q, Alavi A, Zhuang H. Varicella zoster infection associated rhabdomyolysis demonstrated by Tc-99m MDP imaging. *Clin Nucl Med* 2003; **28**: 594-595
29 **Abassi ZA**, Hoffman A, Better OS. Acute renal failure complicating muscle crush injury. *Semin Nephrol* 1998; **18**: 558-565
30 **Baliga R**, Ueda N, Walker PD, Shah SV. Oxidant mechanisms in toxic acute renal failure. *Drug Metab Rev* 1999; **31**: 971-997
31 **Kim HY**, Choi SO, Shin SJ, et al. Analysis of 250 cases of rhabdomyolysis. *Korean J Nephrology* 1994; **13**: 810-817

S- Editor Wang J **L- Editor** Zhu LH **E- Editor** Cao L

PO Box 2345, Beijing 100023, China
www.wjgnet.com
wjg@wjgnet.com

World J Gastroenterol 2006 April 14; 12(14): 2259-2263
World Journal of Gastroenterology ISSN 1007-9327

RAPID COMMUNICATION

Signal transduction of bombesin-induced circular smooth muscle cell contraction in cat esophagus

Sung-Uk Park, Chang-Yell Shin, Jung-Su Ryu, Hyen-O La, Sun-Young Park, Hyun-Ju Song, Young-Sil Min, Dong-Seok Kim, Uy-Dong Sohn

Sung-Uk Park, Chang-Yell Shin, Jung-Su Ryu, Sun-Young Park, Hyun-Ju Song, Young-Sil Min, Uy-Dong Sohn, Department of Pharmacology, College of Pharmacy, Chung Ang University, Seoul 156-756, Republic of Korea
Chang-Yell Shin, Research Laboratory, Dong-A Pharm. Co. Ltd, Yongin 449-905, Kyunggi-Do, Republic of Korea
Hyen-O La, Department of Pharmacology, College of Medicine, The Catholic University of Korea, Seoul 137-701, Republic of Korea
Dong-Seok Kim, Research Division for Human Life Sciences, Seoul National University, 28 Yongon-Dong, Chongno-Gu, Seoul 110-744, Republic of Korea
Correspondence to: Professor Uy Dong Sohn, Department of Pharmacology, College of Pharmacy, Chung Ang University, Seoul 156-756, Republic of Korea. udsohn@cau.ac.kr
Telephone: +82-2-8205614 Fax: +82-2-8268752
Received: 2005-05-13 Accepted: 2005-08-03

Abstract

AIM: To investigate the mechanism of bombesin-induced circular smooth muscle cell contraction in cat esophagus.

METHODS: Specific G protein or phospholipase C involved in cat esophagus contraction was identified, muscle cells were permeabilized with saponin. After permeabilization of muscle cells, the Gi3 antibody inhibited bombesin-induced smooth muscle cell contraction.

RESULTS: Incubation of permeabilized circular muscle cells with PLC-β3 antibody could inhibit bombesin-induced contraction. H-7, chelerythrine (PKC inhibitor) and genistein (protein tyrosine kinase inhibitor) inhibited bombesin-induced contraction, but DAG kinase inhibitor, R59949, could not inhibit it. To examine which mitogen-activated protein kinase (MAPK) was involved in bombesin-induced contraction, the specific MAPK inhibitors (MEK inhibitor, PD98059 and p38 MAPK inhibitor, SB202190) were used. Preincubation of PD98059 blocked the contraction induced by bombesin in a concentration-dependent manner. However, SB202190 had no effects on contraction.

CONCLUSION: Bombesin-induced circular muscle cell contraction in cat esophagus is madiated *via* a PKC or a PTK-dependent pathway or p44/p42 MAPK pathway.

Key words: Bombesin; G protein; Phospholipase C; Protein kinase C; Protein tyrosine kinase; MAP Kinase; Cell contraction

Park SU, Shin CY, Ryu JS, La HO, Park SY, Song HJ, Min YS, Kim DS, Sohn UD. Signal transduction of bombesin-induced circular smooth muscle cell contraction in cat esophagus. *World J Gastroenterol* 2006; 12(14): 2259-2263

http://www.wjgnet.com/1007-9327/12/2259.asp

INTRODUCTION

Bombesin is originally isolated from *Bombina bombina*, a European frog. Utilizing antibodies to amphibian bombesin, bombesin-like immunoreactivity has been identified in mammalian brain, lung, and gut[1]. Bombesin has a wide range of biological effects that include release of hormones, stimulation of pancreatic enzyme secretion, inhibition of gastric emptying, modulation of gastric acid secretion and contractions of various smooth muscle preparations from isolated gut[2]. Until now, four different subtypes of bombesin receptors have been discovered, which can lead to the activation of multiple cell signaling pathways[3]. The primary structures of all these receptor subtypes as deduced from corresponding cDNAs, display seven transmembrane domains coupled to signaling pathways via heterotrimeric G proteins[4-6].

Protein kinase C (PKC) is a family of homologous serine/threonine kinases and presents in cytoplasm. Upon agonist stimulation, it rapidly translocates to the particulate or membrane fraction[7,8]. PKC plays a role in the regulation of sustained agonist-induced contraction of various vascular smooth muscle preparations[9].

Increased protein tyrosine phosphorylation occurs rapidly (within seconds) in response to both polypeptide growth factors and vasoconstrictor hormones[10,11]. Furthermore, epidermal growth factor and platelet-derived growth factor increase vascular tone[12], and are blocked by genistein and typhostins, both of which are inhibitors of tyrosine kinases, indicating that tyrosine phosphorylation is involved in the contractile response[12].

The p44/42 MAP Kinase pathway consists of a protein kinase cascade linking growth and differentiation signals

with transcription in nuclei. Activated p44/p42 MAP kinase translocates to the nuclei and activates transcription by phosphorylation of transcription factors such as Elk-1 and Stat3. A selective and potent inhibitor of the p44/42 MAP kinase cascade, PD98059, has been identified[13]. This compound binds to inactive MEK and prevents phosphorylation and activation by Raf.

To test whether bombesin-induced contraction is mediated via a PKC- or PTK- or MAPK- dependent pathway and which G protein and phospholipase C isozyme is coupled to bombesin, we investigated the signals in mediating contraction induced by bombesin in cat esophageal circular muscle cells.

MATERIALS AND METHODS

Materials

R59949, PD98059 and SB202190 were purchased from Calbiochem (La jolla, CA). G protein antibodies (Gi1, Gi2, Gi3, Gq, and Go), and PLC isozyme antibodies (β1, β3, γ1) were purchased from Santa Cruz Biotechnology (Santa Cruz, CA). HEPES, collagenase type F, and other reagents were purchased from Sigma (St Louis, MO).

Preparation of dispersed muscle cells

Single muscle cells were isolated as previously described[14,15]. Muscle strip was incubated overnight in normal potassium HEPES buffer containing 1 g/L papain, 1 mmol/L DTT, 1 g/L bovine serum albumin (BSA) and 0.5 g/L collagenase (type F, Sigma) and equilibrated with 950 mL/L O2 and 5 mL/L CO_2 to maintain a pH of 7.0 at 31 ℃. The normal potassium-HEPES buffer contained 1 mmol/L CaCl2, 250 μmol/L EDTA, 10 mmol/L glucose, 10 mmol/L HEPES, 4 mmol/L KCl, 131 mmol/L NaCl, 1 mmol/L $MgCl_2$ and 10 mmol/L taurine. Next day we warmed up the tissue at room temperature for 30 min and incubated the tissue in water bath at 31 ℃ for 30 min. After incubation, the digested tissue was washed with 50 mL enzyme-free solution on 360 μm Nitex filter and reincubated in enzyme-free solution at 31 ℃ and gassed with 950 mL/L O_2 and 5 mL/L CO_2 and the cells were allowed to disperse spontaneously for 10-20 min. Suspensions of single muscle cells were harvested by filtration through 500 μm Nitex meshes. Before beginning the experiment, the cells were heated at 31 ℃ for at least 10 min to relax the cells. Throughout the entire procedure, care was taken not to agitate the fluid to avoid cell contraction in response to mechanical stress.

Preparation of permeabilized smooth muscle cells

Cells were permeabilized to diffuse the agents such as G protein antibodies or PLC isozyme antibodies. After completion of the enzymatic phase of the digestion process, the partly digested muscle tissue was washed with an enzyme-free cytosolic buffer containing 20 mmol/L NaCl, 100 mmol/L KCl, 5.0 mmol/L $MgSO_4$, 0.96 mmol/L NaH_2PO_4, 1.0 mmol/L EGTA, 0.48 mmol/L $CaCl_2$, and 2% bovine serum albumin. The cytosolic buffer was equilibrated with 950 mL/L O_2 and 5mL/L CO_2 to maintain a pH of 7.2 at 31 ℃. Muscle cells dispersed spontaneously in this medium. The cytosolic buffer contained 0.48 mmol/L $CaCl_2$ and 1 mmol/L EGTA, yielding 0.18 μmol/L free Ca^{2+} calculated as previously described[16]. After dispersion, the cells were permeabilized by incubation for 5 min in cytosolic buffer containing saponin (75 mg/L). After exposure to saponin, the cell suspension was centrifuged at 350 r/min and the resulting pellet was washed with saponin-free modified cytosolic buffer containing antimycin A (10 μmol/L), ATP (1.5 mmol/L) and an ATP-regenerating system consisting of creatine phosphate (5 mmol/L) and creatine phosphokinase (166.7μkat /L). After the cells were washed free of saponin, they were resuspended in modified cytosolic buffer.

Measurement of contraction by scanning micrometry

Contraction of isolated muscle cells was measured by scanning micrometry[17]. An aliquot of cell suspension containing 10^7 muscle cells/L was added to HEPES medium containing the test agents. The reaction was terminated by addition of formalin (10% final concentration). The length of 40-50 muscle cells treated with a contractile agent was measured at random by scanning micrometry, phase contrast microscope (model ULWCD 0.30 Olympus, Japan) and digital closed-circuit video camera (CCD color camera, Toshiba, Japan) connected to a Macintosh computer (Apple, Cupertino, CA) with a software program, NIH Image 1.57 (National Institutes of Health, Bethesda, MD) and compared with the length of untreated cells. Contraction was expressed as the percentage decrease in mean cell length from control.

Statistical analysis

Data were expressed as mean±SE. Data differences between means were determined by Student's *t* test.

RESULTS

Characterization of G protein subtype-coupled receptor of bombesin

Freshly isolated smooth muscle cells were stimulated for 30 s with bombesin (10^{-6}mol/L) and bombesin induced the contraction of smooth muscle cell (24.3%±2.2% decrease in cell length from control). G proteins, Gi1, Gi2, Gi3, G (40 ku), Gq (42 ku), Gs (46 ku) in cat esophagus cells were established as previously described[17,18]. To identify the specific G protein involved in cat esophagus contraction, muscle cells were permeabilized with saponin preincubated in cytosolic medium containing G protein antibody to allow the antibodies to diffuse into the cytosolic region of the cell membrane. These antibodies could block receptor-induced activation of G protein by binding to the terminal peptide region of G protein that could interact with the receptor. After permeabilization, the Gi3 inhibited contraction, but Gi1, Gi2, Go, Gq did not (Figure 1).

PLC-β3 mediated bombesin-induced contraction

We have previously shown that PC-PLC inhibitor D609 could block the bombesin-induced contraction[17]

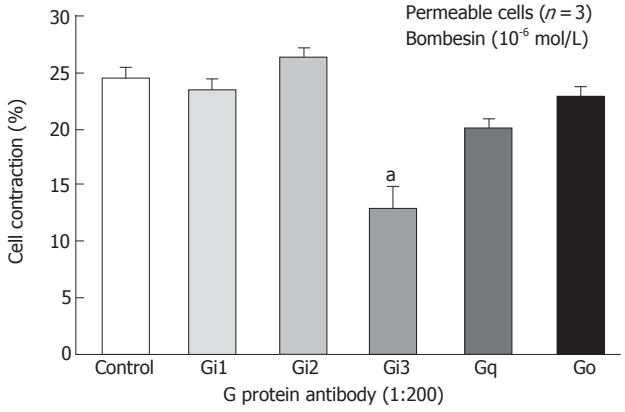

Figure 1 Inhibition of bombesin induced-contraction in permeabilized esophageal circular muscle cells by antibodies to G protein isoforms (Mean ± SE, Student's *t test*, $^aP < 0.05$ *vs* Control).

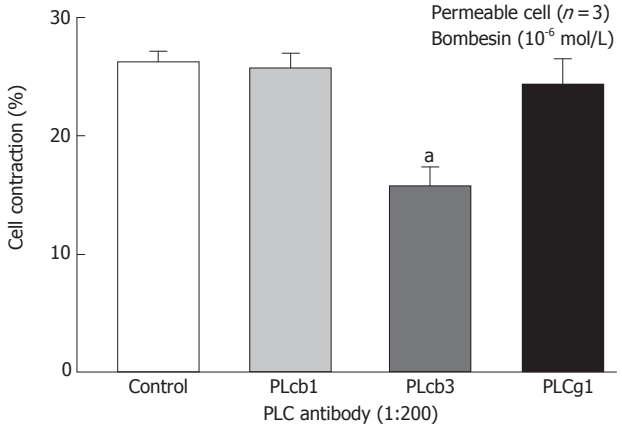

Figure 2 Inhibition of bombesin-induced contraction in permeabilized esophageal circular muscle cells by antibodies to PLC isoforms (Mean ± SE, Student's *t test*, $^aP < 0.05$ *vs* Control).

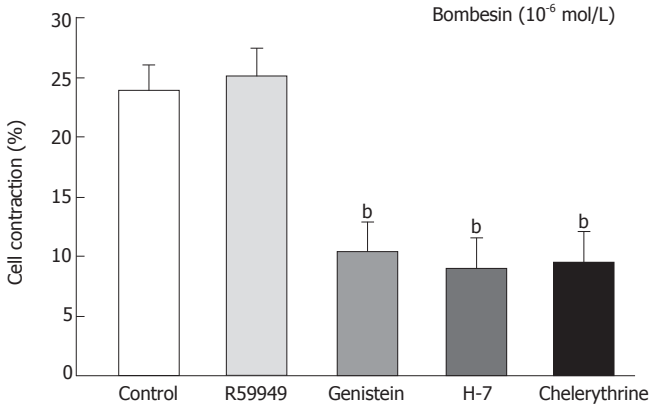

Figure 3 Contractile response of smooth muscle cells from cat esophagus to bombesin in presence of protein kinase C inhibitors (mean ± SE, $n = 4$, Student's *t test*, $^bP < 0.01$ *vs* Control).

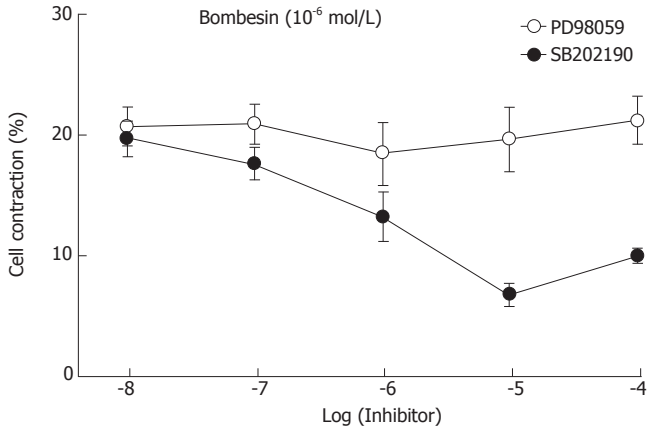

Figure 4 Effect of MEK inhibitor, PD98059 and p38 MAP kinase inhibitor, SB202190 on the bombesin-induced cat esophageal smooth muscle cell contraction (mean ± SE, $n = 4$).

and Western blot analysis of homogenates obtained from dispersed smooth muscle cells using monoclonal antibodies to PLC isozymes could demonstrate the presence of immunoreactive protein bands corresponding to 150 Ku PLC-β1, and PLC-β3 antibody, and 145 Ku PLC-β1 antibody[18]. Incubation of permeabilized circular muscle cells for 1 h with PLC- 3-specific antibody inhibited bombesin- (10^{-6} mol/L) induced contraction ($P < 0.05$). No other PLC-β3-specific antibodies had any significant effect on the contraction (Figure 2).

Role of protein kinase C and tyrosine kinase in bombesin-induced contraction

Cells were preincubated with either the tyrosine kinase inhibitor genistein (10^{-5} mol/L) for 20 min or with the protein kinase C inhibitor H-7 for 15 min (10^{-5} mol/L) or chelerythrine (10^{-5} mol/L) and diacylglycerol (DAG) kinase inhibitor R59949 (10^{-5} mol/L) for 1 min respectively, before the addition of bombesin (10^{-6}mol/L). Bombesin-induced contraction was inhibited by preincubation with genistein as follows: percent age decrease in cell length was 24.3% ± 2.2% *vs* 10.4% ± 2.5% and 9.1% ± 2.5% *vs* 9.5% ± 2.5% in the cells preincubated with H-7 and chelerythrine, respectively (Figure 3).

Role of MAPK in bombesin-induced smooth muscle cells contraction

To examine which MAPK was involved in bombesin-induced contraction, specific MAPK inhibitors were used. Preincubation of PD98059 (the MEK inhibitor) blocked the contraction induced by bombesin in a concentration-dependent manner. The maximal inhibition was observed in 10^{-5}mol/L (Figure 4). However, preincubation of SB202190 (the p38MAPK inhibitor) did not inhibit bombesin-induced concentration, suggesting that bombesin-induced concentration might be mediated via the p44/p42 MAPK pathway.

DISCUSSION

Bombesin is an amidated tetradecapeptide originally purified from the skin of the European frog *Bombina bombina*[1]. Exogenous introduction of this peptide into various organ systems elicits a wide range of responses including secretion of gastrointestinal, adrenal and

pituitary hormones and gastric acid, pancreatic enzyme and mucous, as well as regulation of smooth muscle contraction and modulation of neuronal firing rate[19]. Bombesin receptor is a member of the rhodopsin family of receptors containing seven transmembrane domains coupled to a G protein[20]. Molecular cloning studies have revealed the identity of three mammalian bombesin receptors: gastrin-releasing peptide (GRP receptor)[6], neuromedin B (NMB receptor)[21] and bombesin receptor subtype 3 (BRS-3)[4]. These three receptors share about 50% amino acid sequence identity. In adult animals, GRP-R and NMB-R are widely expressed in the central nervous system[21] and gastrointestinal tract[22,23], whereas BRS-3 shows limited expression in the hypothalamus but is expressed in secondary spermatocytes[4]. Peripheral administration of bombesin produces a variety of effects directly or indirectly linked to the activation of receptors for bombesin-like peptides in the gastrointestinal tract, including exocrine pancreatic secretion, gastrointestinal peptide hormone release, smooth muscle contraction and reduction of food intake. Bombesin receptor is activated after ligand binding and then catalyzes the exchange of GDP bound to the Gα subunit for GTP. After dissociation from Gβγ subunits, functional GTP binds to Gα subunit and activates β isoform of phospholipase C that catalyzes the hydrolysis of phosphatidyl inositol 4,5-bisphosphate (PIP2) in the cell membrane[24]. Gq (42 Ku), Gi1 (40 Ku), Gi2 (40 Ku), Gi3 (40 Ku), Go (40 Ku), Gs (46 Ku) in esophageal circular muscle have been detected by western blot[17]. In addition, when the same G protein antibodies are used to examine which G protein could mediate the contractile response of esophageal muscle, bombesin-induced contraction of esophageal muscles is inhibited by antibodies against the *alpha* subunits of Gi3[17].

We have previously shown that the response of esophageal cells to bombesin is blocked by the inhibitor of specific phosphatidylcholine-phospholipase C (PLC), D609[17] and Western blot analysis can demonstrate the presence of immunoreactive protein bands corresponding to 150 Ku PLC-β1, PLC-β3 antibody, and 145 Ku PLC-γ1 antibody[18]. Permeabilization was used to examine the participation of PLC isozymes in bombesin-induced muscle contraction in this study. Antibodies to PLC-β3, similarly to rabbit intestine[25], could inhibit bombesin-induced contraction. PLC-β1 and PLC-γ1 antibodies had no effect by themselves. The result suggests that PLC-β3 plays a role in mediating esophageal muscle contraction.

Many vasoconstrictor agonists increase protein tyrosine phosphorylation and ERK activity in smooth muscle preparations[26,27]. Furthermore, tyrosine kinase inhibitors block agonist-induced contraction[26,28,29], suggesting that this pathway is important for smooth muscle contraction. In this study, we investigated the regulation of tyrosine phosphorylation following bombesin stimulation and the role of this pathway in the contractile response. Genistein, a tyrosine kinase inhibitor, reduced contraction in response to bombesin in cat esophagus cells, suggesting that tyrosine kinases are involved in bombesin-induced contraction pathway.

Protein kinase C (PKC) is an enzyme activated by DAG, a second messenger produced by the PLC-catalyzed hydrolysis of PIP2. PIP2 hydrolysis produces two signaling molecules, DAG and IP3. DAG is the physiological activator of the classical and novel isoforms of PKC[30], whereas IP3 regulates intracellular Ca^{2+} movements[31]. DAG kinase plays an essential role in attenuation of DAG signals in agonist-stimulated cells. DAG kinase, which phosphorylates DAG to phosphatidic acid, is divided into a membrane bound and a soluble form. DAG kinase inhibitor increases PKC activity by blocking the phosphorylation of DAG to phosphatidic acid[32]. In this study, we showed that R59949 (the DAG kinase inhibitor) did not increase the bombesin-induced contraction. We found that PKC inhibitor, H-7 and chelerythrine, blocked the contraction induced by bombesin. This result is similar to those of Bitar *et al*[33].

MAP kinase is a serine/threonine-specific protein kinase, activation and phosphorylation of which are induced by a variety of extracellular factors such as mitogenic growth factors and neuropeptides[34,35]. In colonic smooth muscle cells[36,37], agonist-induced contraction involves a kinase cascade initiated by PKC and activation and redistribution of MAP kinase. The activation of MAP kinase by bombesin is rapid (within 15 s), reaching a maximum within 30 s, followed by a decline[37]. We found that p44/p42 MAP Kinase was involved in the bombesin-induced contraction in cat esophagus, indicating that the bombesin-induced signaling pathway progresses to p44/p42 MAP kinase to induce contraction.

In conclusion, bombesin induces circular muscle cell contraction in cat esophagus, which is mediated by protein kinase C and tyrosine kinase pathway. Bombesin induces contraction via Gi3 and PLC-β3. The contraction is mediated via p44/p42 MAP kinase pathway. Our findings provide the basic and clinical experimental data on bombesin-induced contraction and its signal transduction in esophagus.

REFERENCES

1 **Anastasi A**, Erspamer V, Bucci M. Isolation and structure of bombesin and alytesin, 2 analogous active peptides from the skin of the European amphibians Bombina and Alytes. *Experientia* 1971; **27**: 166-167

2 **Hampton LL**, Ladenheim EE, Akeson M, Way JM, Weber HC, Sutliff VE, Jensen RT, Wine LJ, Arnheiter H, Battey JF. Loss of bombesin-induced feeding suppression in gastrin-releasing peptide receptor-deficient mice. *Proc Natl Acad Sci USA* 1998; **95**: 3188-3192

3 **Ganter MT,** Pittet JF. Bombesin-like peptides: modulators of inflammation in acute lung injury? *Am J Respir Crit Care Med* 2006; **173**: 1-2

4 **Fathi Z**, Corjay MH, Shapira H, Wada E, Benya R, Jensen R, Viallet J, Sausville EA, Battey JF. BRS-3: a novel bombesin receptor subtype selectively expressed in testis and lung carcinoma cells. *J Biol Chem* 1993; **268**: 5979-5984

5 **Nagalla SR**, Barry BJ, Creswick KC, Eden P, Taylor JT, Spindel ER. Cloning of a receptor for amphibian[Phe13]bombesin distinct from the receptor for gastrin-releasing peptide: identification of a fourth bombesin receptor subtype (BB4). *Proc Natl Acad Sci USA* 1995; **92**: 6205-6209

6 **Spindel ER**, Giladi E, Brehm P, Goodman RH, Segerson TP. Cloning and functional characterization of a complementary DNA encoding the murine fibroblast bombesin/gastrin-releasing peptide receptor. *Mol Endocrinol* 1990; **4**: 1956-1963

7 **Sohn UD**, Zoukhri D, Dartt D, Sergheraert C, Harnett KM,

Behar J, Biancani P. Different protein kinase C isozymes mediate lower esophageal sphincter tone and phasic contraction of esophageal circular smooth muscle. *Mol Pharmacol* 1997; **51**: 462-470

8 **Crabos M**, Fabbro D, Stabel S, Erne P. Effect of tumour-promoting phorbol ester, thrombin and vasopressin on translocation of three distinct protein kinase C isoforms in human platelets and regulation by calcium. *Biochem J* 1992; **288 (Pt 3):** 891-896

9 **Khalil RA,** Morgan KG. Phenylephrine-induced translocation of protein kinase C and shortening of two types of vascular cells of the ferret. *J Physiol* 1992; **455**: 585-599

10 **Abedi H**, Dawes KE, Zachary I. Differential effects of platelet-derived growth factor BB on p125 focal adhesion kinase and paxillin tyrosine phosphorylation and on cell migration in rabbit aortic vascular smooth muscle cells and Swiss 3T3 fibroblasts. *J Biol Chem* 1995; **270**: 11367-11376

11 **Tsuda T**, Kawahara Y, Shii K, Koide M, Ishida Y, Yokoyama M. Vasoconstrictor-induced protein-tyrosine phosphorylation in cultured vascular smooth muscle cells. *FEBS Lett* 1991; **285**: 44-48

12 **Hollenberg MD.** Tyrosine kinase pathways and the regulation of smooth muscle contractility. *Trends Pharmacol Sci* 1994; **15**: 108-114

13 **Payne DM**, Rossomando AJ, Martino P, Erickson AK, Her JH, Shabanowitz J, Hunt DF, Weber MJ, Sturgill TW. Identification of the regulatory phosphorylation sites in pp42/mitogen-activated protein kinase (MAP kinase). *Embo J* 1991; **10**: 885-892

14 **Bitar KN**, Makhlouf GM**.** Receptors on smooth muscle cells: characterization by contraction and specific antagonists. *Am J Physiol* 1982; **242**: G400-407

15 **Biancani P**, Hillemeier C, Bitar KN, Makhlouf GM**.** Contraction mediated by Ca^{2+} influx in esophageal muscle and by Ca^{2+} release in the LES. *Am J Physiol* 1987; **253**: G760-766

16 **Fabiato A**, Fabiato F**.** Calculator programs for computing the composition of the solutions containing multiple metals and ligands used for experiments in skinned muscle cells. *J Physiol (Paris)* 1979; **75**: 463-505

17 **Sohn UD**, Han B, Tashjian AH Jr, Behar J, Biancani P. Agonist-independent, muscle-type-specific signal transduction pathways in cat esophageal and lower esophageal sphincter circular smooth muscle. *J Pharmacol Exp Ther* 1995; **273**: 482491

18 **Yang SJ**, An JY, Shim JO, Park CH, Huh IH, Sohn UD**.** The mechanism of contraction by 2-chloroadenosine in cat detrusor muscle cells. *J Urol* 2000; **163**: 652-658

19 **Milusheva EA**, Kortezova NI, Mizhorkova ZN, Papasova M, Coy DH, Balint A, Vizi ES, Varga G**.** Role of different bombesin receptor subtypes mediating contractile activity in cat upper gastrointestinal tract. *Peptides* 1998; **19**: 549-556

20 **Battey JF**, Way JM, Corjay MH, Shapira H, Kusano K, Harkins R, Wu JM, Slattery T, Mann E, and Feldman RI**.** Molecular cloning of the bombesin/gastrin-releasing peptide receptor from Swiss 3T3 cells. *Proc Natl Acad Sci USA* 1991; **88**: 395-399

21 **Wada E**, Way J, Shapira H, Kusano K, Lebacq-Verheyden AM, Coy D, Jensen R, Battery J**.** cDNA cloning, characterization, and brain region-specific expression of a neuromedin-B-preferring bombesin receptor. *Neuron* 1991; **6**: 421-430

22 **Moran TH**, Moody TW, Hostetler AM, Robinson PH, Goldrich M, McHugh PR**.** Distribution of bombesin binding sites in the rat gastrointestinal tract. *Peptides* 1988; **9**: 643-649

23 **Von Schrenck T**, Heinz-Erian P, Moran T, Mantey SA, Gardner JD, Jensen RT**.** Neuromedin B receptor in esophagus: evidence for subtypes of bombesin receptors. *Am J Physiol* 1989; **256**: G747-758

24 **Ohki-Hamazaki H.** Neuromedin B. *Prog Neurobiol* 2000; **62**: 297-312

25 **Murthy KS**, Makhlouf GM**.** Phosphoinositide metabolism in intestinal smooth muscle: preferential production of Ins(1,4,5)P3 in circular muscle cells. *Am J Physiol* 1991; **261**: G945-951

26 **Ohanian J**, Ohanian V, Shaw L, Bruce C, Heagerty AM**.** Involvement of tyrosine phosphorylation in endothelin-1-induced calcium-sensitization in rat small mesenteric arteries. *Br J Pharmacol* 1997; **120**: 653-661

27 **Khalil RA**, Menice CB, Wang CL, Morgan KG**.** Phosphotyrosine-dependent targeting of mitogen-activated protein kinase in differentiated contractile vascular cells. *Circ Res* 1995; **76**: 1101-1108

28 **Horowitz A**, Menice CB, Laporte R, Morgan KG**.** Mechanisms of smooth muscle contraction. *Physiol Rev* 1996; **76**: 967-1003

29 **Watts SW**, Yeum CH, Campbell G, Webb RC**.** Serotonin stimulates protein tyrosyl phosphorylation and vascular contraction via tyrosine kinase. *J Vasc Res* 1996; **33**: 288-298

30 **Nishizuka Y.** Protein kinase C and lipid signaling for sustained cellular responses. *FASEB J* 1995; **9**: 484-496

31 **Berridge MJ.** Inositol trisphosphate and calcium signalling. *Nature* 1993; **361**: 315-325

32 **Sohn UD**, Hong YW, Choi HC, Ha JH, Lee KY, Kim WJ, Biancani P, Jeong JH, Huh IH**.** Increase of[Ca(2+)]i and release of arachidonic acid via activation of M2 receptor coupled to Gi and rho proteins in oesophageal muscle. *Cell Signal* 2000; **12**: 215-222

33 **Bitar KN**, Kaminski MS, Hailat N, Cease KB, Strahler JR**.** Hsp27 is a mediator of sustained smooth muscle contraction in response to bombesin. *Biochem Biophys Res Commun* 1991; **181**: 1192-1200

34 **Pelech SL**, Sanghera JS**.** Mitogen-activated protein kinases: versatile transducers for cell signaling. *Trends Biochem Sci* 1992; **17**: 233-238

35 **Granot Y**, Erikson E, Fridman H, Van Putten V, Williams B, Schrier RW, Maller JL**.** Direct evidence for tyrosine and threonine phosphorylation and activation of mitogen-activated protein kinase by vasopressin in cultured rat vascular smooth muscle cells. *J Biol Chem* 1993; **268**: 9564-9569

36 **Bitar KN**, Yamada H**.** Modulation of smooth muscle contraction by sphingosylphosphorylcholine. *Am J Physiol* 1995; **269**: G370-377

37 **Yamada H**, Strahler J, Welsh MJ, Bitar KN**.** Activation of MAP kinase and translocation with HSP27 in bombesin-induced contraction of rectosigmoid smooth muscle. *Am J Physiol* 1995; **269**: G683-G691

S- Editors Wang J and Pan BR **L- Editor** Wang XL **E- Editor** Bi L

PO Box 2345, Beijing 100023, China
www.wjgnet.com
wjg@wjgnet.com

World J Gastroenterol 2006 April 14; 12(14): 2264-2268
World Journal of Gastroenterology ISSN 1007-9327

RAPID COMMUNICATION

Molecularly defined adult-type hypolactasia in school-aged children with a previous history of cow's milk allergy

Heli Rasinperä, Kristiina Saarinen, Anna Pelkonen, Irma Järvelä, Erkki Savilahti, Kaija-Leena Kolho

Heli Rasinperä, Irma Järvelä, Department of Medical Genetics, University of Helsinki, Finland
Kristiina Saarinen, Erkki Savilahti, Kaija-Leena Kolho, Hospital for Children and Adolescents, University of Helsinki, Finland
Anna Pelkonen, Department of Allergology, Skin and Allergy Hospital, Helsinki University Central Hospital, Helsinki, Finland
Irma Järvelä, Laboratory of Molecular Genetics, Helsinki University Hospital, Helsinki, Finland
Supported by The Sigrid Jusélius Foundation, Helsinki, Finland; The Helsinki University Hospital Research Funding, Helsinki, Finland; The Helsinki University Science Foundation, Helsinki, Finland and The Foundation of Nutrition Research, Helsinki, Finland
Correspondence to: Dr. Kaija-Leena Kolho, Hospital for Children and Adolescents, Box 281, 00290 Helsinki, Finland. kaija-leena.kolho@helsinki.fi
Telephone: +358-9-47174787 Fax: +358-9-47175299
Received: 2005-09-15 Accepted: 2005-10-26

Abstract

AIM: To assess the role of lactase non-persistence/persistence in school-aged children and their milk-related symptoms.

METHODS: The genotypes for the C/T$_{-13910}$ variant associated with lactase non-persistence/ persistence were determined using PCR-minisequencing in a group of 172 children with a mean age of 8.6 years (SE = 0.02, 93 boys) participating in a follow-up study for cow's milk allergy. The parents were asked to assess their children's milk consumption and abdominal symptoms.

RESULTS: The presence of allergy to cow's milk was not associated with the C/C$_{-13910}$ genotype related with a decline of lactase enzyme activity during childhood (lactase non-persistence). The frequency of the C/C$_{-13910}$ genotype (16%) was similar to published figures for the prevalence of adult-type hypolactasia in Finland. The majority of the children (90%) in this series consumed milk but 26% of their families suspected that their children had milk-related symptoms. Forty-eight percent of the children with the C/C$_{-13910}$ genotype did not drink milk at all or consumed a low lactose containing diet prior to the genotyping ($P < 0.004$ when compared to the other genotypes).

CONCLUSION: Analysis of the C/T$_{-13910}$ polymorphism is an easy and reliable method for excluding adult-type hypolactasia in children with milk-related symptoms. Genotyping for this variant can be used to advise diets for children with a previous history of cow's milk allergy.

Key words: Adult-type hypolactasia; Primary lactose malabsorption; Genetic testing; Cow's milk allergy

Rasinperä H, Saarinen K, Pelkonen A, Järvelä I, Savilahti E, Kolho KL. Molecularly defined adult-type hypolactasia in school-aged children with a previous history of cow's milk allergy. *World J Gastroenterol* 2006; 12(14): 2264-2268

http://www.wjgnet.com/1007-9327/12/2264.asp

INTRODUCTION

Lactase deficiency (LD, lactase non-persistence) is the most common cause of milk intolerance in children and adolescents world-wide[1]. It plays a significant role in recurrent abdominal pain in populations with common consumption dairy products[2]. Immunologically mediated adverse reaction to ingested proteins of cow's milk is referred to as cow's milk allergy (CMA), the symptoms of which usually appear under one year of age[3]. CMA affects 1.9%-3.2% of infants[4] though recent studies suggest that allergy to cow's milk protein may have an impact on abdominal symptoms at schoolage also[5]. CMA is easily differentiated from LD if it manifests at an early age with skin and/or respiratory symptoms[6]. In cases of CMA that present with gastrointestinal symptoms, the clinical picture may overlap with symptoms caused by low lactase activity especially at schoolage, when the downregulation of lactase enzyme activity occurs[7].

The differential diagnosis of milk-related symptoms in children is difficult to establish because of the variability of clinical symptoms and inaccurate diagnostic laboratory tests[8]. The diagnosis of lactose malabsorption is based on the measurement of disaccharidase activities in intestinal biopsy specimens, a method which is not suitable for every day clinical practice. The indirect commonly used lactose-tolerance test (LTT) is not reliable in children and results in up to 30% of false positive results, thus reducing its value in clinical use[9]. In addition, children with normal lactose digestion complain of symptoms during LTT[10].

Recently, a C to T single nucleotide polymorphism residing 13 910 base pairs upstream of the lactase-phlorizin

hydrolase (LCT) gene has been shown to associate with lactase persistence/non-persistence, the C/C-13910 genotype defining lactase non-persistence as well as C/T-13910 and T/T-13910 genotype lactase persistence[11]. The association of the C/T-13910 variant with disaccharidase activities and lactase/sucrase ratio (L/S) has been verified in a total of >600 intestinal biopsy specimens[7, 11, 12]. In Finnish children (8-20 years of age) the mean level of lactase activity among subjects with the C/C-13910 genotype is 6.5 U/g protein. The C/T-13910 genotype is 29.9 U/g protein and 50.0 U/g protein respectively, showing a trimodal distribution of the lactase activity[7]. Functional evidence for the C/T-13910 variant in regulation of lactase activity has been obtained in several studies[12-15] and a greater increase in LCT promoter activity was reported for the T-13910 variant[13, 14]. The down-regulation of intestinal lactase varies according to ethnicity but the differences at the timing of down-regulation are not marked and most commonly start to appear around 5-6 years of age[7]. At the age of 12 years, all children with the C/C-13910 genotype have low lactase activity in their intestines[7].

The aim of the present study was to evaluate the role of lactase non-persistence in milk consumption and milk-related clinical symptoms by analysing the C/T-13910 genotypes of lactase persistence/non-persistence in a group of 172 school-aged children from eight to nine years of age with or without a previous history of CMA.

MATERIALS AND METHODS

Subjects

This study was part of a prospective follow-up study of children with a history of CMA diagnosed at a mean age of seven months [16]. The present study group comprised 172 school-aged children (mean age 8.6 years; SE = 0.02, 93 boys, 79 girls) who were clinically examined during August 2003-March 2004 at the Helsinki University Central Hospital, Helsinki, Finland. Ninety-three children (54%) had a previous diagnosis of CMA and 79 children comprised the control group. All these children were subjects in the study by Saarinen and collaborators[17], in which 6209 unselected infants born between August 1994 and November 1995 in the Helsinki region were followed up from birth for the development of CMA. The presence of CMA was confirmed by a challenge test[17]. At the time of the present visit, the families were asked about the children's milk consumption and possible milk-related symptoms and those agreeing to participate in genetic testing of adult-type hypolactasia were included in the study. IgE-mediated hypersensitivity to cow's milk was measured by skin prick test. A diameter >3 mm exceeding the negative control was considered as a positive response[18]. Those children who were still avoiding milk due to previous CMA were re-challenged by cow's milk[16]. A supplementary questionnaire on the amount of milk consumed and possible abdominal symptoms during the preceding week was mailed later. Celiac disease was screened as previously described[19].

Ethics

The study was approved by the Ethical Committee of the Hospital for Children and Adolescents, University of Helsinki. The families/children gave their informed consent.

Genotyping

DNA was isolated from blood by phenol-chloroform extraction as previously described[20] and DNA fragments spanning the C/T-13910 variant were amplified using one biotinylated primer and one unbiotinylated primer (primer sequences available on request). Briefly, PCR amplifications were carried out in a 50-μL volume with genomic DNA (100 ng), primers (20 ng), dNTPs (200 μmol/L), and 0.5 U of Taq polymerase in a standard buffer (Dynazyme, Finnzymes, Espoo, Finland). The PCR cycle conditions were as follows: an initial round of denaturation at 94 ℃, then 35 cycles at 94 ℃ for 30 s, at 53 ℃ for 30 s, at 72 ℃ for 1.25 min and a final extension at 72 ℃ for 10 min. Ten μl of the PCR product was captured in a streptavidin-coated microtiter well (Thermo Electron, Vantaa, Finland) and two parallel minisequencing reactions were carried out for each PCR-product. The minisequencing reaction contained 10 pmoles of the minisequencing primer (primer sequence available on request), 0.1 μL of tritium-labelled dNTP (Amersham Biosciences, Little Chalfont, Buckinghamshire, UK), and 0.05 U of DNA polymerase (Dynazyme, Finnzymes, Espoo, Finland). The microtiter wells were incubated for 15 min at 56 ℃ and finally the wells were washed. The detection primer was eluted and the eluted radioactivity was measured in a liquid scintillation counter (Rackbeta 1209, Wallac, Finland) as previously described [21].

Statistical analysis

The Mann-Whitney *U* test and Spearman's rank correlation test were used for nonparametric comparisons. Fisher's exact 2-sided test was also used.

RESULTS

Twenty-six percent of the families (45/172) suspected that their children had milk-related symptoms at 8-9 years of age at the time of this study. A significantly greater proportion of these came from those diagnosed to have CMA (76%, 34/45) at a mean age of seven months[17] than those serving as controls ($P < 0.003$).

Skin-prick test with cow's milk was positive (> 3 mm) in 12% of the children undergoing these tests (20/168) and all these children had a previous history of CMA (Table 1). At the time of this study, the challenge test with cow's milk was positive in 11 of the 16-challenged children[16].

The frequency of C/C-13910 genotype defining adult-type hypolactasia was 16% in the total study group of 172 children. There was no correlation with the genotype and positive reaction in the skin prick test or food challenge. Of the 27 children with the C/C-13910 genotype, two were challenged with cow's milk at the time of this study and one of them had a positive challenge for cow's milk. The milk consumption of different genotypes is presented in Table 2. Screening for celiac disease was negative in 170/172 of the children. The two children with a positive screening test consumed milk and reported no abdominal symptoms. The genotypes in these two children were C/

Table 1 Milk consumption and abdominal symptoms in school-aged children with a history of cow's milk allergy[1] and their controls

	Previous allergy[1]	Controls
Questionnaire completed	92% (n=86)	97% (n=77)
Milk product consumption	80% (n=69)	100%[a] (n=77)
Milk consumption < 1 dL/d	36% (23/69)	16%[b] (12/77)
Low lactose content in diet	14% (10/69)	8% (6/77)
Abdominal symptoms: Flatulence	13% (11/86)	8% (6/77)
Loose stools	5% (4/86)	4% (3/77)
Skin prick test >3 mm to cow's milk	22%[2] (20/91)	0 (0/77)

[1]milk challenge positive at a mean age of 7 mo; [a]P < 0.0001 *vs* milk consumption; [b]P < 0.02 *vs* milk product consumption.

Table 2 Milk consumption and abdominal symptoms in school-aged children genotyped for adult-type hypolactasia

	T/T1-13910	C/T[1]-13910	C/C[2]-13910
Total number of children			
n=172	n=68	n=77	n=27
Milk products consumed	95%	95%	93%
(n=163)	(54/62)	(67/74)	(25/27)
Drinks milk < 1 dL/day	22%	18%	44%[a]
(n=146)	(12/54)	(12/67)	(11/25)
Low lactose content in the diet	7%	4%	36%[b]
(n=146)	(4/54)	(3/67)	(9/25)
Skin prick test >3 mm to cow's milk	13%[5]	11%[5]	12%[3]
(n=168)	(9/67)	(8/75)	(3/26)

[1]lactase persistence; [2]defines adult-type hypolactasia; [a]P < 0.02 *vs* genotypes associated with lactase persistence (T/T-13910 plus C/T-13910); [b]P < 0.002 *vs* T/T-13910 genotype or C/T-13910 genotype; [3]each of these prick positive children had a diagnosis of cow's milk allergy at a mean age of seven mo[17].

Table 3 Abdominal symptoms during a one-week period in school-aged children genotyped for adult-type hypolactasia

	Total	T/T[1]-13910	C/T[1]-13910	C/C[2]-13910
Questionnaire completed	n=163	n=62	n=74	n=27
Abdominal symptoms	(n=38)	15% (n=9)	27% (n=20)	33%[a] (n=9)
Flatulence	(n=17)	5% (n=3)	12% (n=9)	19%[b] (n=5)
Periumbilical pain	(n=10)	6.5% (n=4)	5.4% (n=4)	7.4% (n=2)
Loose stools	(n=7)	3.2% (n=2)	5.4% (n=4)	3.7% (n=1)
Upper epigastric pain	(n=7)	5% (n=3)	4.0% (n=3)	3.7% (n=1)
Constipation	(n=5)	0	5.4% (n=4)	3.7% (n=1)
Dyspepsia	(n=1)	0	1.4% (n=1)	0

[1]lactase persistence; [2] defines adult-type hypolactasia; [a]P=0.05, [b]P<0.04 *vs* T/T-13910 genotype.

Table 4 Probable changes in milk consumption of families after receiving the results of genetic testing for adult-type hypolactasia in school-aged children

	T/T[1]-13910	C/T[1]-13910	C/C[2]-13910
Questionnaire completed	94% (62/68)	97% (74/77)	100% (27)
No change in milk consumption	89% (n=54)	81% (n=61)	59%[3] (n=16)
Less lactose containing milk	0	0	33% (n=9)
More lactose containing milk	8% (n=5)	11% (n=8)	0
Not decided	5% (n=3)	7% (n=5)	7% (n=2)

[1]lactase persistence; [2]defines adult-type hypolactasia; [3]33% of the families consumed low lactose containing diet prior to genetic testing.

T-13910 and T/T-13910 (data not shown).

Fifty-two children out of the total study group of 172 children drank less than one dL of milk per day or did not consume milk products. The C/C-13910 genotype defining adult-type hypolactasia was present in 25% (13/52) and CMA in 21% (11/52, confirmed in a challenge test) of these children. Each child with CMA had a previous diagnosis of CMA. Milk consumption did not have any significant effect on body mass index (BMI, kg/m^2) and BMI was similar in children with different genotypes for adult-type hypolactasia (data not shown).

The questionnaire on daily milk consumption and abdominal symptoms was filled in by 95% (163/172) of the families (Table 3). Adult-type hypolactasia was suspected in 9% (15/163) of the children by their parents but was confirmed by genotyping in not more than 20% of these children (3/15 with the C/C-13910 genotype). One of these three children with the C/C-13910 genotype had a diagnosis of lactose malabsorption based on intestinal biopsy at the age of 7 years and the other two were noticed to have lactose-related symptoms at the age of 1.5 and 7 years. Two of the 27 children with the C/C-13910 genotype did not consume milk because of CMA. Eighty percent of the children (20/25) with the C/C-13910 genotype who had no CMA at this age had a low lactose containing diet at home or drank quantities of milk less than one dL/day already prior to the genetic testing (Table 2). A similar diet with milk restriction was practiced more rarely among children with genotypes associated with lactase persistence (31/119 of the children with C/T-13910 or T/T-13910 genotypes who answered the question and did not have allergy to milk, P< 0.004). Children with the C/C-13910 genotype did not report significantly more abdominal pains than children with the C/T-13910 or T/T-13910 genotypes but there was a difference in the presence of flatulence (P< 0.04, Table 3). Among the children with the C/C-13910 genotype, 4/15 children had milk restriction beyond two years of age because of milk allergy. Two of these four children experienced lactose-related symptoms.

The acceptance of genetic testing was good, as only two families did not participate in the study. Based on the interviews of the families among the children with the C/C-13910 genotype, 30% of the families reported to have another family member with symptoms of adult-type hypolactasia. Thirteen percent of the families of the total series and one third of the children with the C/C-13910 genotype reported that the result of the genetic test for adult-type hypolactasia had a probable effect on their milk consumption (Table 4). Of the families with genotypes associating with lactase persistence (C/T-13910 or the T/T-13910 genotype), 10% reported that the result of the genetic test was helpful in avoiding unnecessary restrictions on milk consumption.

DISCUSSION

Our results show that the overlap of IgE-mediated cow's milk allergy, CMA, and lactase non-persistence is unlikely

to occur at schoolage. The prevalence of adult-type hypolactasia in our study was 16% corresponding to the reported frequency in our population[7,11,22,23] and was not associated with CMA but correlated with the consumption of low lactose containing diets and the presence of flatulence. All children with a positive skin prick test for cow's milk at this age (12%) had a previous diagnosis of CMA, settled at a mean age of seven months as previously reported in detail[16]. It is noteworthy that not a single child in the non-CMA group turned IgE-positive for milk at schoolage, further confirming that IgE-mediated reactions with cow's milk develops at an early age. Tolerance to cow's milk develops in the majority of children with CMA (70%) by the age of three and eight to nine years. At the time of the present study, 85% of the children recovered from CMA[16].

It was reported that one third of the Finnish children at the age of eight years with the genotype C/C$_{-13910}$ have a high intestinal lactase activity[7] and are unlikely to develop symptoms caused by adult-type hypolactasia. It should however be borne in mind that in children the decline of intestinal lactase occurs slowly and depends on ethnicity [7]. Based on our previous study about the timing of down-regulation of lactase activity[7], we can estimate that about 10% (0.63 × 16%) of the children being studied have a reduced lactase activity (<10 U/g/protein) and all the others have a high lactase activity (>10 U/g/protein). In the present study, 60% of the children with the C/C$_{-13910}$ genotype consumed a low lactose containing diet or had milk-related symptoms at this age and 40% of those with the C/C$_{-13910}$ genotype were considered milk-tolerant. The avoidance of milk and consumption of low lactose containing diet was much more common among children with the C/C$_{-13910}$ genotype than among those with the genotypes associated with lactase persistence. This confirms our preliminary finding[7] and suggests that the children have experienced milk-related symptoms triggering a reduced lactose intake.

It is common, however, that children with abdominal dysfunction after consuming milk are unaware of its cause[24, 25]. This was also obvious in our series as the suspicion of milk-related symptoms was not increased in the families of the children with the C/C$_{-13910}$ genotype defining adult-type hypolactasia. However, restricted lactose intake was more common in these families. Although this dietary modification, the children with the C/C$_{-13910}$ genotype reported more flatulence when compared to those with the genotype T/T$_{13910}$ associated with lactase persistence ($P < 0.04$). There was no difference in the frequency of abdominal pain between the children with either CMA or lactose malabsorption and the control children.

It is common that only some individuals who self-report them as lactose intolerants are in fact lactose maldigesters when tested objectively[26-30]. The data on children, however, are limited. In our series, every fifth child suspected not to tolerate lactose was confirmed to have the predisposing genotype for adult-type hypolactasia. The lack of awareness of lactose maldigestion may increase abdominal symptoms in children as reported by Webster *et al*[31] who noticed that after a proper diagnosis of lactose malabsorption, the avoidance of milk products is more rigorous and results in a decrease in complaints. It is unclear whether individuals with adult-type hypolactasia and lactose maldigestion but without obvious symptoms of lactose intolerance should avoid milk or not. A recent double-blind study suggested that lactose maldigesters might benefit from lactose avoidance even though the diagnostic criteria for lactose intolerance are not fulfilled[32]. On the other hand, studies in adults reported that as many as 32% of lactose mal-absorbers experience no symptoms from lactose containing milk products[26], but at present there are no means to predict this at an individual level.

In the present study, 10% of the children with the C/T$_{-13910}$ genotype reported symptoms such as flatulence and loose stools suggestive of milk intolerance. One of these children had CMA (milk challenge positive) but in the other cases the causes for these symptoms were unknown. It is possible that some of these children are carriers of a mutation of congenital lactase deficiency (CLD), a rare congenital disorder which may result in low lactase activity but no disease manifestations in heterozygotes[33, 34]. Celiac disease may cause secondary hypolactasia but screening tests for the disease are negative in these children.

Parents easily suspect milk as a causative agent for abdominal symptoms in countries where dairy products are widely used. In the present study, 26% of the families reported a suspicion of milk-related symptoms in their school-aged children. The majority of these children did not drink milk nor had low lactose containing diets. When milk-related symptoms were suspected, the parents recognized CMA easily due to the previous history of CMA but their suspicion of adult-type hypolactasia was seldom confirmed. Accurate diagnosis of possible milk-related symptoms poses a challenge for clinicians as the elimination of milk and a proper challenge test for milk proteins or tolerance test for lactose are both time-consuming and may give unsatisfactory results[8]. The genetic testing of adult-type hypolactasia performed from a drop of blood was accepted well by the families as 99% of the families agreed to test their children. About 10% of the families reported that a negative result for adult-type hypolactasia was helpful as they may now avoid unnecessary restrictions on milk consumption.

In conclusion, a suspicion of milk-related symptoms is common in everyday clinical practice. The genetic test of C/T$_{-13910}$ polymorphism is reliable in excluding adult-type hypolactasia in children with milk-related symptoms. Genotyping for this variant may help in planning the diet for children with a suspicion of milk-related symptoms.

ACKNOWLEDGMENTS

The authors are grateful to the children and their families for their participation in this study. The authors thank Eija Hämäläinen, Hanna Komu and Sirkku Kristiansen for excellent help in performing the laboratory work.

REFERENCES

1 **Semenza G**, Auricchio S, Mantei N. Small-intestinal disaccharidases. In: Scriver CR, Beaudet AL, Sly D, Valle D, eds. The metabolic and molecular basis of inherited disease, New York: McGraw-Hill, 2001; 1623-1650

2 **Gudmand-Hoyer E.** The clinical significance of disaccharide maldigestion. *Am J Clin Nutr* 1994; **59:** 735S-741S
3 **Sampson HA**. Food allergy. *JAMA* 1997; **278**: 1888-1894
4 **Sicherer SH**. Food allergy. *Lancet* 2002; **360**: 701-710
5 **Kokkonen J**, Haapalahti M, Laurila K, Karttunen TJ, Maki M. Cow's milk protein-sensitive enteropathy at school age. *J Pediatr* 2001; **139**: 797-803
6 **Bahna SL.** Cow's milk allergy versus cow milk intolerance. *Ann Allergy Asthma Immunol* 2002; **89:** 56-60
7 **Rasinpera H**, Savilahti E, Enattah NS, Kuokkanen M, Totterman N, Lindahl H, Jarvela I, Kolho KL. A genetic test which can be used to diagnose adult-type hypolactasia in children. *Gut* 2004; **53:** 1571-1576
8 **Arola H**. Diagnosis of hypolactasia and lactose malabsorption. *Scand J Gastroenterol Suppl*. 1994; **202**: 26-35
9 **Krasilnikoff PA,** Gudman-Hoyer E, Moltke HH. Diagnostic value of disaccharide tolerance tests in children. *Acta Paediatr Scand* 1975; **64:** 693-698
10 **Lebenthal E**, Rossi TM, Nord KS, Branski D. Recurrent abdominal pain and lactose absorption in children. *Pediatrics* 1981; **67**: 828-832
11 **Enattah NS,** Sahi T, Savilahti E, Terwilliger JD, Peltonen L, Jarvela I. Identification of a variant associated with adult-type hypolactasia. *Nat Genet* 2002; **30:** 233-237
12 **Kuokkanen M,** Enattah NS, Oksanen A, Savilahti E, Orpana A, Jarvela I. Transcriptional regulation of the lactase-phlorizin hydrolase gene by polymorphisms associated with adult-type hypolactasia. *Gut* 2003; **52:** 647-652
13 **Olds LC**, Sibley E: Lactase persistence DNA variant enhances lactase promoter activity in vitro: functional role as a *cis* regulatory element. *Hum Mol Genet* 2003; **12**: 2333-2340
14 **Troelsen JT,** Olsen J, Moller J, Sjostrom H. An upstream polymorphism associated with lactase persistence has increased enhancer activity. *Gastroenterology* 2003; **125**: 1686-1694
15 **Arika T**, Amemiya K, Nomoto K. Combination therapy of radiation and Sizofiran (SPG) on the tumor growth and metastasis on squamous-cell carcinoma NR-S1 in syngeneic C3H/He mice. *Biotherapy* 1992; **4:** 165-170
16 **Saarinen KM,** Pelkonen AS, Makela MJ, Savilahti E. Clinical course and prognosis of cow's milk allergy are dependent on milk-specific IgE status. *J Allergy Clin Immunol* 2005; **116:** 869-875
17 **Saarinen KM**, Juntunen-Backman K, Jarvenpaa AL, Kuitunen P, Lope L, Renlund M, Siivola M, Savilahti E. Supplementary feeding in maternity hospitals and the risk of cow's milk allergy: A prospective study of 6209 infants. *J Allergy Clin Immunol* 1999; **104:** 457-461
18 **Saarinen KM**, Savilahti E. Infant feeding patterns affect the subsequent immunological features in cow's milk allergy. *Clin Exp Allergy* 2000; **30**: 400-406
19 **Sulkanen S,** Halttunen T, Laurila K, Kolho KL, Korponay-Szabo IR, Sarnesto A, Savilahti E, Collin P, Maki M. Tissue transglutaminase autoantibody enzyme-linked immunosorbent assay in detecting celiac disease. *Gastroenterology* 1998; **115:** 1322-1328
20 **Sambrook J**, Fritch EF, Maniatis T. Molecular cloning: A laboratory manual. 2nd ed. Cold Spring Harbor Laboratory Press, Cold Spring Harbor, NY, 1989.
21 **Syvanen AC**, Landegren U. Detection of point mutations by solid-phase methods. *Hum Mutat* 1994; **3:** 172-179
22 **Enattah NS**, Forsblom C, Rasinpera H, Tuomi T, Groop PH, Jarvela I. The genetic variant of lactase persistence C (-13910) T as a risk factor for type I and II diabetes in the Finnish population. *Eur J Clin Nutr* 2004; **58:** 1319-1322
23 **Rasinpera H,** Forsblom C, Enattah NS, Halonen P, Salo K, Victorzon M, Mecklin JP, Jarvinen H, Enholm S, Sellick G, Alazzouzi H, Houlston R, Robinson J, Groop PH, Tomlinson I, Schwartz S Jr, Aaltonen LA, Jarvela I. The C/C-13910 genotype of adult-type hypolactasia is associated with an increased risk of colorectal cancer in the Finnish population. *Gut* 2005; **54:** 643-647
24 **Barr RG**, Levine MD, Watkins JB. Recurrent abdominal pain of childhood due to lactose intolerance. *N Engl J Med* 1979; **300:** 1449-1452
25 **Scrimshaw NS**, Murray EB. The acceptability of milk and milk products in populations with a high prevalence of lactose intolerance. *Am J Clin Nutr* 1988; **48**: 1079-1159
26 **Carroccio A,** Montalto G, Cavera G, Notarbatolo A. Lactose intolerance and self-reported milk intolerance: relationship with lactose maldigestion and nutrient intake. Lactase Deficiency Study Group. *J Am Coll Nutr* 1998; **17:** 631-636
27 **de Vrese M**, Stegelmann A, Richter B, Fenselau S, Laue C, Schrezenmeir J. Probiotics--compensation for lactase insufficiency. *Am J Clin Nutr* 2001; **73:** 421S-429S
28 **Suarez FL**, Savaiano DA, Levitt MD. A comparison of symptoms after the consumption of milk or lactose-hydrolyzed milk by people with self-reported severe lactose intolerance. *N Engl J Med* 1995; **333**: 1-4
29 **Saltzman JR**, Russell RM, Golner B, Barakat S, Dallal GE, Goldin BR. A randomized trial of Lactobacillus acidophilus BG2FO4 to treat lactose intolerance. *Am J Clin Nutr* 1999; **69**: 140-146
30 **Vesa TH**, Seppo LM, Marteau PR, Sahi T, Korpela R: Role of irritable bowel syndrome in subjective lactose intolerance. *Am J Clin Nutr* 1998; **67**: 710-715
31 **Webster RB**, DiPalma JA, Gremse DA. Lactose maldigestion and recurrent abdominal pain in children. *Dig Dis Sci* 1995;**40**: 1506-1510
32 **Gremse DA**, Greer AS, Vacik J, DiPalma JA. Abdominal pain associated with lactose ingestion in children with lactose intolerance. *Clin Pediatr (Phila)* 2003; **42:** 341-345
33 **Savilahti E,** Launiala K, Kuitunen P. Congenital lactase deficiency. A clinical study on 16 patients. *Arch Dis Child* 1983; **58:** 246-252
34 **Jarvela I,** Enattah NS, Kokkonen J, Varilo T, Savilahti E, Peltonen L. Assignment of the locus for congenital lactase deficiency to 2q21, in the vicinity of but separate from the lactase-phlorizin hydrolase gene. *Am J Hum Genet* 1998; **63:** 1078-1085

S- Editor Wang J **L- Editor** Wang XL **E- Editor** Cao L

PO Box 2345, Beijing 100023, China
www.wjgnet.com
wjg@wjgnet.com

World J Gastroenterol 2006 April 14; 12(14): 2269-2275
World Journal of Gastroenterology ISSN 1007-9327

RAPID COMMUNICATION

Gilbert's syndrome: High frequency of the $(TA)_7$ TAA allele in India and its interaction with a novel CAT insertion in promoter of the gene for bilirubin UDP-glucuronosyltransferase 1 gene

Shabana Farheen, Sanghamitra Sengupta, Amal Santra, Suparna Pal, Gopal Krishna Dhali, Meenakshi Chakravorty, Partha P Majumder, Abhijit Chowdhury

Shabana Farheen, Sanghamitra Sengupta, Partha P Majumder, Human Genetics Unit, Indian Statistical Institute, Kolkata, India
Amal Santra, Suparna Pal, Gopal Krishna Dhali, Abhijit Chowdhury, Department of Gastroenterology, Institute of Postgraduate Medical Education & Research, Kolkata, India
Meenakshi Chakravorty, Human Genetics & Genomics Division, Indian Institute of Chemical Biology, Kolkata, India
Supported by grants from the Department of Biotechnology, Government of India (to PPM) and the Department of Science & Technology, Government of West Bengal (to AC)
Co-correspondents: Partha P Majumder
Correspondence to: Abhijit Chowdhury, MD, Department of Gastroenterology, Institute of Postgraduate Medical Education and Research, Kolkata 700020, India. achowdhury@apexmail.com
Telephone: +91-332553209
Received: 2005-06-04 Accepted: 2005-10-10

Abstract

AIM: To identify the variants in UDP-glucuronosyltransferase 1 (UGT1A1) gene in Gilbert's syndrome (GS) and to estimate the association between homozygosity for TA insertion and GS in India, as well as the frequency of TA insertion and its impact among normal controls in India.

METHODS: Ninety-five GS cases and 95 normal controls were selected. Liver function and other tests were done. The promoter and all 5 exons of UGT1A1 gene were resequenced. Functional assessment of a novel trinucleotide insertion was done by *in silico* analysis and by estimating UGT1A1 promoter activity carried out by luciferase reporter assay of appropriate constructs in Hep G2 cell line.

RESULTS: Among the GS patients, 80% were homozygous for the TA insertion, which was several-fold higher than reports from other ethnic groups. The mean UCB level was elevated among individuals with only one copy of this insertion, which was not significantly different from those with two copies. Many new DNA variants in UGT1A1 gene were discovered, including a trinucleotide (CAT) insertion in the promoter found in a subset (10%) of GS patients, but not among normal controls. *In-silico* analysis showed marked changes in the DNA-folding of the promoter and functional analysis showed a 20-fold reduction in transcription efficiency of UGT1A1 gene resulting from this insertion, thereby significantly elevating the UCB level.

CONCLUSION: The genetic epidemiology of GS is variable across ethnic groups and the epistatic interactions among UGT1A1 promoter variants modulate bilirubin glucuronidation.

Key words: Unconjugated hyperbilirubinemia; UGT1A1 gene; DNA resequencing; Luciferase reporter assay

Farheen S, Sengupta S, Santra A, Pal S, Dhali GK, Chakravorty M, Majumder PP, Chowdhury A. Gilbert's syndrome: High frequency of the $(TA)_7$TAA allele in India and its interaction with a novel CAT insertion in promoter of the gene for bilirubin UDP-glucuronosyltransferase 1 gene. *World J Gastroenterol* 2006; 12(14): 2269-2275

http://www.wjgnet.com/1007-9327/12/2269.asp

INTRODUCTION

Gilbert's syndrome (GS) is generally considered to be an autosomal recessive disorder (OMIM #143500) characterized by mild, chronic, non-hemolytic unconjugated hyperbilirubinemia in the absence of liver disease. Although it has long been perceived to be an innocuous clinical entity with a benign course, recent data suggest that affected individuals may be predisposed to development of liver injury following treatment with various drugs and xenobiotics and that the genetic defect in GS may influence the outcome of liver transplantation and other clinical conditions. The disorder due to a deficiency in bilirubin glucuronidation, is commonly caused by dinucleotide (TA) insertions and [TA $(TA)_7$TAA] alleles in the promoter region of the bilirubin UDP-glucuronosyltransferase 1 (UGT1A1) gene. This dinucleotide insertion reduces the efficiency of transcription of the gene and decreases hepatic UDP-glucuronosyltransferase activity to about 30% of normal levels in homozygous subjects[6-9]. The prevalence of GS, the frequency of the $(TA)_7$TAA allele in the UGT1A1 promoter and the proportion of GS patients who are homozygous for the $(TA)_7$TAA allele vary widely

across populations[10-19]. Recent data have also shown that variants in UGT1A1 gene other than the classical dinucleotide insertion in its promoter, can contribute to hyperbilirubinemia, including the milder form as in GS, although their effects appear to be variable across populations[5,20-24]. Thus, as recently emphasized[20], detailed investigations into genetic polymorphisms of UGT1A1 gene in Asian populations may provide a better understanding of unconjugated hyperbilirubinemia.

The objectives of our case-control study were to estimate the association between homozygosity for the $(TA)_7TAA$ allele and GS in India, to identify and study the impact of this and other polymorphisms in the promoter and exons of the UGT1A1 gene on serum bilirubin levels, and to estimate the frequency of the $(TA)_7TAA$ homozygous genotype in the general population in India.

MATERIALS AND METHODS

Participant recruitment and clinical biochemistry analysis

This study was conducted in 95 consecutive patients presenting to the Liver Clinic at the Department of Gastroenterology of the Institute of Postgraduate Medical Education & Research, Kolkata, India, for evaluation of persistent unconjugated hyperbilirubinemia (serum bilirubin greater than 1.2 mg/dL) documented at least twice over a period of one month. Serum total bilirubin and its unconjugated fraction were estimated in fasting condition. Each of these individuals had a normal finding on physical examination, normal hepatobiliary ultrasound, normal liver function test excluding hyperbilirubinemia and a normal reticulocyte count. A total of 95 adult healthy volunteers from the same ethnic population as the GS patients were included as controls. Each control also underwent the same set of investigations as the patients. Their fasting serum bilirubin level estimated twice at intervals of fifteen days was consistently less than 1.0 mg/dL. Patients were excluded if they were under any medication during the past one month or consumed alcohol regularly or had present or past history of hepatic/hematological disease. Additionally, quantitative estimation of hemoglobin fractions (A_0, A_2 and F) was carried out on each patient and control by cation-exchange HPLC using the Variant™ Hemoglobin Testing System Beta Thalassemia Short Program (Bio-Rad Diagnostics, Hercules, USA). A 5 mL blood sample was collected from each patient by venipuncture and DNA was isolated using a standard protocol[25]. Data and samples were collected with written informed consent of the patients and controls, after the approval was obtained from the Human Research Ethics Committee of the Institute of Postgraduate Medical Education & Research, Kolkata.

DNA re-sequencing and identification of variant alleles

DNA re-sequencing of the promoter and exon 1*1 encoding the substrate-specific region of bilirubin-UGT1 gene as well as the 4 common exons (exons 2-5) was carried out using an automated DNA sequencer (ABI-3100; Applied Bio-systems, Foster City, USA.). DNA samples were first amplified by the polymerase chain reaction technique using an ABI-9700 thermal cycler. PCR products were then cleaned using exonuclease-I (USB. Corporation, Cleveland, USA) and shrimp alkaline phosphatase (Amersham, Freiburg, Germany), and sequencing reactions were carried out. DNA resequencing was carried out in both forward and reverse directions. Raw DNA sequences were analyzed as previously described[26], and variant genotypes were identified.

Functional analysis of a novel trinucleotide insertion by luciferase reporter assay

UGT1A1 promoter fragments, 331-336 bp in length depending on the number of TA repeats and CAT insertion, were amplified using primers (F: 5'-tgtagatcttcct ctctggtaacact-3') and (R: 5'-atgaagctttgctcctgccagaggttc-3') from genomic DNA of individuals homozygous for six and seven TA repeats, and CAT insertion on $(TA)_7TAA$ background. DNA amplification was carried out with polymerase chain reaction (PCR) using FastStart Taq DNA polymerase (Roche, Mannheim, Germany) with an initial denaturation at 95℃ for 10 min, followed by 35 cycles at 94℃ for 1 min, at 56℃ for 45 s and at 72℃ for 30 s on an ABI-9700 (Applied Bio-systems, Foster City, USA.) thermal cycler. To facilitate subcloning of the PCR products in the reporter gene construct, oligonucleotides F and R were designed with a *Bgl* II and a *Hind* III restriction enzyme site at the 5' end, respectively. PCR products were doubly digested with *Bgl* II and *Hind* III, purified by Qiagen gel purification kit (Qiagen, Hilden, Germany) and subcloned into pGL3-basic vector (Promega, Madison, USA). The integrity of the resulting plasmids was confirmed by restriction mapping and sequencing analyses. Promoter activity of each construct was measured in HepG2 cell line. Cells were grown in MEM medium supplemented with 2 mmol/L L-glutamine, 0.1 mmol/L non-essential amino acids, 1 mmol/L sodium pyruvate and 10% fetal calf serum (GIBCO -BRL, Grand Island, USA) at 37℃ with 50 mL/L CO_2. Exponentially growing cells were trypsinized, seeded at 2.5×10^5 cells, and incubated overnight prior to transfection. Transfection was carried out by lipofectamin (Invitrogen, Carlsbad, USA) using 2 μg of each of the constructs (namely $(TA)_6$ TAA, $(TA)_7$ TAA and CAT insertion on $(TA)_7$ TAA background), as well as the pGL3-basic and pGL3-control as positive controls $(TA)_7TAA$, the luciferase gene was under the control of SV40 promoter and enhancer. After 48 h of transfection, the cells were lysed and centrifuged in cell culture lysis buffer (Promega, Madison, USA). Luciferase activity was assayed in the cell lysate by measuring the photoluminescence in a Monolight 2010 single channel luminometer and the total cellular protein content was measured by the standard Bradford's method. Luciferase activity was normalized to total cell protein concentration. Normalized luciferase activity of each construct was expressed as a ratio to that of the pGL3-basic vector. Three independent experiments were performed for each construct and all measurements were determined in duplicate.

Statistical analysis

Equality of proportions was statistically tested by the standard normal test procedure[27]. Equalities of mean

values of various hematological parameters for individuals belonging to different genotypes at various polymorphic loci were statistically tested using the Student *t*-test or the analysis of variance (ANOVA) procedure, as appropriate. Regression analysis was performed to test the significance of dependence of un-conjugated serum bilirubin level on some relevant variables. Allele frequencies were estimated using the gene-counting method.

RESULTS

Characteristics of patients and controls

No statistically significant ($P > 0.05$) differences in the proportions of males and females were observed between the patients (87 males, 8 females) and controls (77 males, 18 females). The mean ages of male and female patients (30.1 ± 1.1 years of males, 26.8 ± 5.1 years of females) and controls (30.2 ± 1.1 years of males, 31.1 ± 2.9 years of females) were not significantly different ($P > 0.05$). Since elevated HbA_2 levels could potentially increase the unconjugated bilirubin level, we tested the significance of the regression coefficient of HbA_2 level on unconjugated bilirubin, separately for patients and controls. In both sets, there was no statistically significant impact of HbA_2 (*P*-values for patients and controls were 0.638 and 0.106, respectively). The difference in the mean values of HbA_2 between patients and controls was not significantly different ($t = 1.76$, d.f. $= 128$, $P > 0.05$). The 8 GS patients, but none of the normal controls, who were habitual smokers were asked to refrain from smoking for 24 h prior to blood collection. We tested whether the inclusion of these 8 GS patients had a significant impact on our findings. We therefore, examined whether the mean value of un-conjugated bilirubin among patients who were smokers ($n = 8$) was significantly higher than that among patients who were not smokers ($n = 87$). No significant difference was found (mean for smoker patients $= 2.67 \pm 0.33$, mean for non-smoker patients $= 3.38 \pm 0.30$, $t = 0.696$, d.f. $= 93$, $P = 0.488$). We have performed all analyses that were reported below with and without the inclusion of the 8 GS patients who were habitual smokers. No differences in inferences were found (results not shown). Therefore, we presented all results including these 8 GS subjects.

UGT1A1 sequence variants and their relation with bilirubin level

Eleven sequence variants in UGT1A1 gene was observed, of which 3 each were in the promoter, 3 in exon 1, 2 in exon 2, 1 in exon 3 and 2 in exon 4. No variant was found in exon 5. The genotype and variant allele frequencies at these positions in patients and controls are given in Table 1. Of these 11 variant sites, 2 were non-polymorphic (frequency of the rarer allele $< 1\%$), while the remaining 9 sites were polymorphic either among patients or among controls or in both. One of the polymorphic sites was the TA insertion [$(TA)_7TAA$ allele] in the TATA box of the UGT1A1 promoter[2,3]. The frequencies of the $(TA)_7TAA$ allele (0.879) and the 7/7 genotype (80%) among the patients were significantly higher ($P < 0.005$) than those among the controls (0.384 and 10%, respectively). The un-conjugated serum bilirubin values for GS patients belonging to the 6/6, 7/6 and 7/7 genotypes are presented in Figure 1. The mean values of un-conjugated bilirubin for GS patients and normal controls were 2.5 ± 0.25 mg/dL and 0.61 ± 0.09 mg/dL respectively. The mean±SE value of un-conjugated bilirubin among patients with the 7/6 genotype was 3.46 ± 0.54 mg/dL, which was not significantly different ($P = 0.05$) from patients with the 7/7 genotype (3.31 ± 0.33 mg/dL). The mean un-conjugated serum bilirubin values for these genotypes among controls were only 0.59 ± 0.10 mg/dL and 0.64 ± 0.15 mg/dL, respectively.

No significant differences ($P = 0.05$) were found in the mean bilirubin levels among individuals belonging to the various genotypes at the remaining single nucleotide polymorphic loci. With respect to the C6844G polymorphism resulting in a non-synonymous amino acid change (A321G), all patients were CC homozygotes, while about 30% of the controls were CG heterozygotes (Table 1). We did not find any significant effect of the G71R polymorphism on un-conjugated bilirubin level. This polymorphism also showed no significant interaction with the TATA box insertion polymorphism (results not shown). These findings are discordant with those reported among the Japanese[19].

A novel human-specific trinucleotide insertion in Gilbert's syndrome patients and its impact on bilirubin level

Among the polymorphic variants described in Table 1, aside from the familiar TA insertion, the most striking was the CAT insertion (nucleotide positions -85 to -83) in the CAAT box of UGT1*1 promoter. Normally, there is one copy of the CAT trinucleotide present in human Genbank (http://www.ncbi.nlm.nih.gov/Genbank/). We found two copies of this trinucleotide in some GS patients. To confirm that this was an insertion we searched the chimpanzee (gi|6456543|gb|AF135463.1|AF135463) and gorilla (gi|6456545|gb|AF135464.1|AF135464) databases. In both species there is only copy, confirming that the single copy is the ancestral state. This CAT insertion was found only among nine (10%) GS patients, who were all homozygous for the TA insertion. We found that GS patients with the CAT-insertion had a significantly ($P < 0.001$) elevated mean level (6.13 ± 1.61 mg/dL) compared to those without the insertion (2.93 ± 0.28 mg/dL). Individuals who possessed the CAT insertion did not consistently possess a variant allele at any of the other sites. One individual who was heterozygous for the CAT insertion was also heterozygous for the I322V variant, and other three CAT-insertion heterozygotes were also heterozygotes for the H376R variant.

Functional analysis of CAT insertion

Since about 10% of the $(TA)_7TAA$ homozygotes carried the CAT insertion and the insertion significantly elevated the bilirubin level, we postulated that the insertion had a functional impact. To examine this, we studied the change in DNA-folding of the promoter region caused by this insertion. The most stable structures, namely those with lowest free energy (dG) values, are given in Figure 2 for the UGT1A1 promoter region without (dG = -14.4) and

Table 1 DNA sequence variations observed among Gilbert's syndrome patients and normal controls

Location of variant and nucleotide position (np)	Description of variant[1]	Genotype/Allele frequency (p)	Patients (%)	Control (%)
UGT1*1 promoter	CAT insertion	Insertion/Insertion	3	0
nps -85 to -83		Insertion/non-insertion	6	0
		Non-insertion/non-insertion	86	95
		p(Insertion)	0.063	0.000
UGT1*1 promoter	G→C	GG	93	95
np -63		GC	2	0
		p(C)	0.011	0.000
UGT1*1 promoter	$(TA)_6$ TAA→	$(TA)_6$ TAA /$(TA)_6$ TAA	4	32
nps -53 to -38	$(TA)_7$ TAA	$(TA)_7$ TAA /$(TA)_6$ TAA	15	53
		$(TA)_7$ TAA/$(TA)_7$ TAA	76	10
		p[$(TA)_7$ TAA]	0.879	0.384
Exon 1	G→A	GG	85	90
np +211	(G71R)	GA	9	5
		AA	1	0
		p(A)	0.058	0.026
Exon 1	T→C	TT	93	94
np +476	(I159T)	TC	2	1
		p(C)	0.011	0.005
Exon 1	T→C	TT	94	95
np +625	(*R209W*)	TC	1	0
		p(C)	0.005	0.000
Exon 2	C→G	CC	95	66
np +6844	(*A321G*)	CG	0	29
		p(G)	0.000	0.152
Exon 2	A→G	AA	87	89
np +6846	(*I322V*)	AG	7	6
		GG	1	0
		p(G)	0.042	0.032
Exon 3	G→A	GG	94	95
np +7640	(*D359N*)	GA	1	0
		p(A)	0.005	0.000
Exon 4	C→T	CC	93	95
np +7939	(*P364L*)	CT	2	0
		p(T)	0.011	0.000
Exon 4	A→G	AA	92	95
np +7975	(H376R)	AG	3	0
		p(G)	0.016	0.000

[1]Amino acid changes resulting from nucleotide changes in the exons are indicated in parentheses.

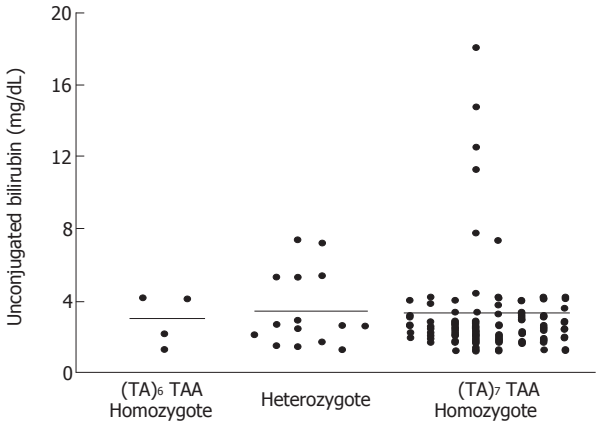

Figure 1 Distributions of un-conjugated serum bilirubin values among Gilbert's syndrome patients classified by the genotype of the common TA insertion in the TATA box of the UGT1A1 promoter.

with (dG = -14.8) the additional CAT insertion. A striking structural change was found around the region of the insertion, the loops were converted to stems. It is well known that formation of stems in the promoter could reduce transcription of the gene. A detailed functional analysis of the UGT1A1 promoter by luciferase reporter assay confirmed that there was a two-fold decrease in transcription efficiency for the variant $(TA)_7$TAA promoter allele, and a 20-fold decrease when there was a CAT insertion in the promoter on the background of the $(TA)_7$TAA allele compared to the normal $(TA)_6$TAA promoter allele (Figure 3).

DISCUSSION

Genetically determined un-conjugated hyperbilirubinemia constitutes a spectrum of clinical entities characterized by incremental serum bilirubin values related to graded reduction of UGT1A1 enzyme activity. The most novel finding of our study is that a trinucleotide (CAT) insertion in the nucleotide positions -85 to -83 of the UGT1A1 promoter was present in GS patients who were homozygous for the causal TA insertion, but not in other GS patients or in controls. This insertion significantly ($P < 0.001$) elevated the un-conjugated bilirubin level (mean = 6.13 mg/dL) in the patients to the range usually seen in Crigler-Najjar (CN) II syndrome. We have

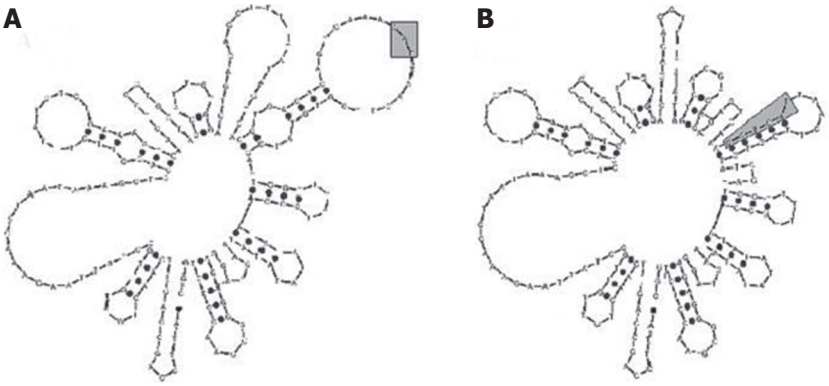

Figure 2 Folded DNA structures of the UGT1A1 promoter region with one copy of the CAT trinucleotide (shaded region) (**A**) and two copies of the CAT trinucleotide (CAT insertion allele, shaded region) (**B**).

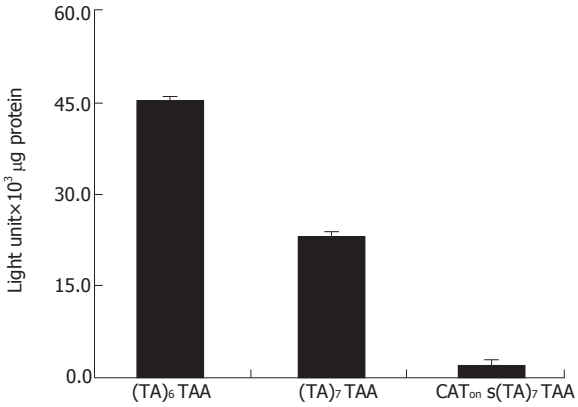

Figure 3 Transcriptional activities of the (TA)$_6$TAA, (TA)$_7$ TAA and CAT alleles as assessed by a luciferase reporter assay.

demonstrated that this insertion in the background of the (TA)$_7$ allele classically described in GS, diminishes UGT1A1 transcriptional activity to about 5% (2.4 light units/10^3 μg protein) of the normal (44.9 light units/10^3 μg protein), much lower than the 50% reduction (22.9 light units/10^3 μg protein) observed for (TA)$_7$ alone. Thus the combined biological effect of the CAT and TA insertions is a further elevation in the un-conjugated bilirubin level compared to that of the TA insertion alone, which is exactly what we have observed in the GS patients carrying the CAT insertion. This initial description of the interactive influence of a novel trinucleotide insertion and the GS-type abnormality in the promoter region alone, in the absence of a consistent exonic mutation, to quantitatively elevate un-conjugated bilirubin to levels observed in Crigler-Najjar II (CN II) provides further evidence of genetic heterogeneity and overlap of the clinical syndromes of un-conjugated hyperbilirubinemia. Thus, Gilbert's, Crigler-Najjar I (CN I) and CN II syndromes may not be mutually exclusive clinical-genetic entitities but are different windows of the quantititative spectrum of elevated serum unconjugated bilirubin levels.

The association (80%) between homozygosity for the (TA)$_7$TAA allele and GS is much stronger in India than reported earlier from most other ethnic groups[14,15,16,20]. Graded reduction of UGT1 activity has been demonstrated with increasing length of the TA repeats in a recent study[28]. It was demonstrated that 7/7 homozygotes and 7/6 heterozygotes have, respectively, a 52% and a 37% reduction of UDP glucuronyl transferase activity in liver tissue homogenates. In our study, serum un-conjugated bilirubin values among 7/6 heterozygote GS patients were high but not significantly different from the 7/7 homozygotes. The finding of increased serum bilirubin values among the 7/6 heterozygote GS patients to the same extent as those homozygous for the classically described 7/7 genotype, even in the absence of any other consistent change in the UGT1A1 gene, is intriguing. We could not explain this finding, but speculate the role of other interacting non-UGT1A1 genetic variants.

Although the insertion of additional TA repeats in the (TA)$_6$ TAA promoter, sequence of the UGT1A1 gene is the most common variation associated with Gilbert's syndrome, (TA)$_5$ and (TA)$_8$ sequences in the TATAA box have also been found[4,14]. We did not find (TA)$_5$ and (TA)$_8$ alleles in our study participants. Moreover, several mutations in the exons have been found in other populations, particularly from Asia, in association with GS and hyperbilirubinemia, either as the only abnormality or in addition to the more common promoter defect[20-22,29-31]. We have identified several promoter and coding region (all non-synonymous) variants of the gene (Table 1). The G71R variant has been reported earlier[19, 22-24], and the P364L variant has recently been reported in one Japanese GS patient[19]. Contrary to the finding among the Japanese[32], the G71R change had no impact on un-conjugated bilirubin level in our samples, nor did it interact with the dinucleotide (TA) insertion in the TATA box of the UGT1A1 gene. Many variants discovered in this study have not been reported earlier and many variants reported earlier were not found in the present sample. Although all the observed variations in exons could result in amino acid substitutions, none of these significantly altered the mean bilirubin level. Thus, the UGT1A1 gene appears to tolerate a large number of mutations without any significant deleterious effect. None of these was strongly associated with the (TA)$_7$TAA allele in our study. However, the amino acid change from isoleucine to valine at the amino acid position 322 was only found among the controls and not among the GS patients. Further studies are necessary to test whether this change helps bilirubin glucuronidation by the UGT1A1 gene.

The UGT1A1 polymorphisms have recently acquired significance because they predispose individuals to altered metabolism and enhanced toxicity of several drugs like paracetamol, propofol, irinotecan, indinavir, *etc*, which are

substrates for glucoronidation by UGT1A1[33-36]. Exons 2-5 are shared by other UGT1A transcripts and isozymes that mediate metabolism of xenobiotics apart from A1 involved in bilirubin glucuronidation[37]. The new variants in these exons may be relevant to drug metabolism, but we have not tested this. Our findings reveal that it is crucial to carry out detailed surveys on genetic variations in and around the UGT1A1 gene and functional studies on these variants for a deeper understanding of quantitative anomalies of bilirubin.

ACKNOWLEDGMENTS

The authors thank Dr. S. Roy Choudhury for permitting us to carry out the cell-biology work in his laboratory at the Indian Institute of Chemical Biology, Kolkata.

REFERENCES

1 **Powell LW**, Hemingway E, Billing BH, Sherlock S. Idiopathic unconjugated hyperbilirubinemia (Gilbert's syndrome). A study of 42 families. *N Engl J Med* 1967; **277**: 1108-1112
2 **Bosma PJ**. Inherited disorders of bilirubin metabolism. *J Hepatol* 2003; **38**: 107-117
3 **Sampietro M**, Lupica L, Perrero L, Comino A, Martinez di Montemuros F, Cappellini MD, Fiorelli G. The expression of uridine diphosphate glucuronosyltransferase gene is a major determinant of bilirubin level in heterozygous beta-thalassaemia and in glucose-6-phosphate dehydrogenase deficiency. *Br J Haematol* 1997; **99**: 437-439
4 **Doyama H**, Okada T, Kobayashi T, Suzuki A, Takeda Y, Mabuchi H. Effect of bilirubin UDP glucuronosyltransferase 1 gene TATA box genotypes on serum bilirubin concentrations in chronic liver injuries. *Hepatology* 2000; **32**: 563-568
5 **Jansen PL**, Bosma PJ, Bakker C, Lems SP, Slooff MJ, Haagsma EB. Persistent unconjugated hyperbilirubinemia after liver transplantation due to an abnormal bilirubin UDP-glucuronosyltransferase gene promoter sequence in the donor. *J Hepatol* 1997; **27**: 1-5
6 **Bosma PJ**, Chowdhury JR, Bakker C, Gantla S, de Boer A, Oostra BA, Lindhout D, Tytgat GN, Jansen PL, Oude Elferink RP. The genetic basis of the reduced expression of bilirubin UDP-glucuronosyltransferase 1 in Gilbert's syndrome. *N Engl J Med* 1995; **333**: 1171-1175
7 **Koiwai O**, Nishizawa M, Hasada K, Aono S, Adachi Y, Mamiya N, Sato H. Gilbert's syndrome is caused by a heterozygous missense mutation in the gene for bilirubin UDP-glucuronosyltransferase. *Hum Mol Genet* 1995; **4**: 1183-1186
8 **Burchell B**, Hume R. Molecular genetic basis of Gilbert's syndrome. *J Gastroenterol Hepatol* 1999; **14**: 960-966
9 **Clarke DJ**, Moghrabi N, Monaghan G, Cassidy A, Boxer M, Hume R, Burchell B . Genetic defects of the UDP-glucuronosyltransferase-1 (UGT1) gene that cause familial non-haemolytic unconjugated hyperbilirubinaemias. *Clin Chim Acta* 1997; **266**: 63-74
10 **de Morais SM**, Uetrecht JP, Wells PG. Decreased glucuronidation and increased bioactivation of acetaminophen in Gilbert's syndrome. *Gastroenterology* 1992; **102**: 577-586
11 **McGurk KA**, Brierley CH, Burchell B. Drug glucuronidation by human renal UDP-glucuronosyltransferases. *Biochem Pharmacol* 1998; **55**: 1005-1012
12 **Owens D**, Evans J. Population studies on Gilbert's syndrome. *J Med Genet* 1975; **12**: 152-156
13 **Sieg A**, Arab L, Schlierf G, Stiehl A, Kommerell B. Prevalence of Gilbert's syndrome in Germany. *Dtsch Med Wochenschr* 1987; **112**: 1206-1208
14 **Beutler E**, Gelbart T, Demina A. Racial variability in the UDP-glucuronosyltransferase 1 (UGT1A1) promoter: a balanced polymorphism for regulation of bilirubin metabolism? *Proc Natl Acad Sci USA* 1998; **95**: 8170-8174
15 **Monaghan G**, Ryan M, Seddon R, Hume R, Burchell B. Genetic variation in bilirubin UPD-glucuronosyltransferase gene promoter and Gilbert's syndrome. *Lancet* 1996; **347**: 578-581
16 **Lampe JW**, Bigler J, Horner NK, Potter JD. UDP-glucuronosyltransferase (UGT1A1*28 and UGT1A6*2) polymorphisms in Caucasians and Asians: relationships to serum bilirubin concentrations. *Pharmacogenetics* 1999; **9**: 341-349
17 **Ando Y**, Chida M, Nakayama K, Saka H, Kamataki T. The UGT1A1*28 allele is relatively rare in a Japanese population. *Pharmacogenetics* 1998; **8**: 357-360
18 **Biondi ML**, Turri O, Dilillo D, Stival G, Guagnellini E. Contribution of the TATA-box genotype (Gilbert syndrome) to serum bilirubin concentrations in the Italian population. *Clin Chem* 1999; **45**: 897-898
19 **Takeuchi K**, Kobayashi Y, Tamaki S, Ishihara T, Maruo Y, Araki J, Mifuji R, Itani T, Kuroda M, Sato H, Kaito M, Adachi Y. Genetic polymorphisms of bilirubin uridine diphosphate-glucuronosyltransferase gene in Japanese patients with Crigler-Najjar syndrome or Gilbert's syndrome as well as in healthy Japanese subjects. *J Gastroenterol Hepatol* 2004; **19**: 1023-1028
20 **Kamisako T**. What is Gilbert's syndrome? Lesson from genetic polymorphisms of UGT1A1 in Gilbert's syndrome from Asia. *J Gastroenterol Hepatol* 2004; **19**: 955-957
21 **Kaplan M**, Hammerman C, Rubaltelli FF, Vilei MT, Levy-Lahad E, Renbaum P, Vreman HJ, Stevenson DK, Muraca M. Hemolysis and bilirubin conjugation in association with UDP-glucuronosyltransferase 1A1 promoter polymorphism. *Hepatology* 2002; **35**: 905-911
22 **Soeda Y,** Yamamoto K, Adachi Y, Hori T, Aono S, Koiwai O, Sato H. Predicted homozygous mis-sense mutation in Gilbert's syndrome. *Lancet* 1995; **346:** 1494
23 **Sato H**, Adachi Y, Koiwai O. The genetic basis of Gilbert's syndrome. *Lancet* 1996; **347**: 557-558
24 **Aono S**, Adachi Y, Uyama E, Yamada Y, Keino H, Nanno T, Koiwai O, Sato H. Analysis of genes for bilirubin UDP-glucuronosyltransferase in Gilbert's syndrome. *Lancet* 1995; **345**: 958-959
25 **Miller SA**, Dykes DD, Polesky HF. A simple salting out procedure for extracting DNA from human nucleated cells. *Nucleic Acids Res* 1988; **16**: 1215
26 **Gordon D**, Abajian C, Green P. Consed: a graphical tool for sequence finishing. *Genome Res* 1998; **8**: 195-202
27 **Snedecor GW**, Cochran WG. Statistical Methods. 8th Edition. Iowa State University Press, Ames, 1989
28 **Raijmakers MT,** Jansen PL, Steegers EA, Peters WH. Association of human liver bilirubin UDP-glucuronyltransferase activity with a polymorphism in the promoter region of the UGT1A1 gene. *J Hepatol* 2000; **33:** 348-351
29 **Kadakol A,** Sappal BS, Ghosh SS, Lowenheim M, Chowdhury A, Chowdhury S, Santra A, Arias IM, Chowdhury JR, Chowdhury NR. Interaction of coding region mutations and the Gilbert-type promoter abnormality of the UGT1A1 gene causes moderate degrees of unconjugated hyperbilirubinaemia and may lead to neonatal kernicterus. *J Med Genet* 2001; **38:** 244-249
30 **Parvez MK**, Goyal A, Kazim N, Hasnain SE, Sarin SK. TA insertion mutation in bilirubin UDP- glucoronyl transferase gene (UGT1A1) promoter in Indian patients with Gilbert's syndrome . *J Hepatol* 2002; **36(S1)**: 159-160
31 **Borlak J**, Thum T, Landt O, Erb K, Hermann R. Molecular diagnosis of a familial nonhemolytic hyperbilirubinemia (Gilbert's syndrome) in healthy subjects. *Hepatology* 2000; **32:** 792-725
32 **Sugatani J**, Yamakawa K, Yoshinari K, Machida T, Takagi H, Mori M, Kakizaki S, Sueyoshi T, Negishi M, Miwa M. Identification of a defect in the UGT1A1 gene promoter and its association with hyperbilirubinemia. *Biochem Biophys Res*

Commun 2002; **292**: 492-497
33 **Ostrow JD**, Tiribelli C. New concepts in bilirubin neurotoxicity and the need for studies at clinically relevant bilirubin concentrations. *J Hepatol* 2001; **34:** 467-470
34 **Esteban A**, Perez-Mateo M. Heterogeneity of paracetamol metabolism in Gilbert's syndrome. *Eur J Drug Metab Pharmacokinet* 1999; **24**: 9-13
35 **Le Guellec C**, Lacarelle B, Villard PH, Point H, Catalin J, Durand A. Glucuronidation of propofol in microsomal fractions from various tissues and species including humans: effect of different drugs. *Anesth Analg* 1995; **81**: 855-861
36 **Ando Y**, Saka H, Ando M, Sawa T, Muro K, Ueoka H, Yokoyama A, Saitoh S, Shimokata K, Hasegawa Y. Polymorphisms of UDP-glucuronosyltransferase gene and irinotecan toxicity: a pharmacogenetic analysis. *Cancer Res* 2000; **60**: 6921-6926
37 **Zucker SD**, Qin X, Rouster SD, Yu F, Green RM, Keshavan P, Feinberg J, Sherman KE. Mechanism of indinavir-induced hyperbilirubinemia. *Proc Natl Acad Sci USA* 2001; **98**: 12671-12676

S- Editor Wang J **L- Editor** Wang XL **E- Editor** Bi L

PO Box 2345, Beijing 100023, China
www.wjgnet.com
wjg@wjgnet.com

World J Gastroenterol 2006 April 14; 12(14): 2276-2279
World Journal of Gastroenterology ISSN 1007-9327

RAPID COMMUNICATION

Ultrasonic characterization of porcine liver tissue at frequency between 25 to 55 MHz

Xiao-Zhou Liu, Xiu-Fen Gong, Dong Zhang, Shi-Gong Ye, Bing Rui

Xiao-Zhou Liu, Xiu-Fen Gong, Dong Zhang, Shi-Gong Ye, State Key Laboratory of Modern Acoustics, Institute of Acoustics, Nanjing University, Nanjing 210093, Jiangsu Province, China
Bing Rui, Nanjing Meat Processing Plant, Nanjing 210015, Jiangsu Province, China
Supported by the National Natural Science Foundation of China, No. 10204014
Correspondence to: Associate Professor Xiao-Zhou Liu, State Key Laboratory of Modern Acoustics, Institute of Acoustics, Nanjing University, Nanjing 210093, Jiangsu Province, China. xzliu@nju.edu.cn
Telephone: +86-25-83594503 Fax: +86-25-83315557
Received: 2005-6-24 Accepted: 2005-08-02

Abstract

AIM: To study the relation between acoustic parameters and histological structure of biological tissue and to provide the basis for high-resolution image of biological tissues and quantitative ultrasonic diagnosis of liver disease.

METHODS: Ultrasonic imaging and tissue characterization of four normal porcine liver and five cirrhotic liver tissue samples were performed using a high frequency imaging system.

RESULTS: The acoustic parameters of cirrhotic liver tissue were larger than those of normal liver tissue. The sound velocity was 1577 m/s in normal liver tissue and 1631 m/s in cirrhotic liver tissue. At 35 MHz, the attenuation coefficient was 3.0 dB/mm in normal liver tissue and 4.1 dB/mm in cirrhotic liver tissue. The backscatter coefficient was 0.00431 dB/Srmm in cirrhotic liver tissue and 0.00303 dB/Srmm in normal liver tissue. The backscatter coefficient increased with the frequency. The high frequency images coincided with their histological features.

CONCLUSION: The acoustic parameters, especially the sound backscatter coefficient, are sensitive to the changes of liver tissues and can be used to differentiate between the normal and pathological liver tissues. High frequency image system is a useful device for high-resolution image and tissue characterization.

Key words: Porcine liver tissue; Hepatocirrhosis; High frequency imaging; Tissue characterization; Acoustic parameter

Liu XZ, Gong XF, Zhang D, Ye SG, Rui B. Ultrasonic characterization of porcine liver tissue at frequency between 25 to 55 MHz. *World J Gastroenterol* 2006; 12(14): 2276-2279

http://www.wjgnet.com/1007-9327/12/2276.asp

INTRODUCTION

Ultrasonic diagnosis has been widely used in the clinical medicine. However, contemporary ultrasonic diagnosis technique is limited to the qualitative description at frequency ranging between 0.5-10 MHz based on the gray scale presentation in ultrasonic image. Due to the longer wavelength at a low frequency, the image resolution is not very high. Besides, the physical quantity using the ultrasonic image is the amplitude of the echo while the spectrum of the echo is overlooked.

The research on the ultrasound scatter spectrum has begun since 1970s. Shung and Reid[1] conducted an experimental study of ultrasound backscatter in calf liver and muscle using the pulse insert-substitution method. The backscatter coefficients for calf heart, kidney, pancreas and spleen were studied by Ten and Shung[2] at frequency between 2-7 MHz using bandwidth pulse insert-substitution measurement system. The ultrasound backscatter in myocardial muscle of dog was studied by Donnell *et al*[3]. The anisotropy for ultrasound backscatter in myocardial muscle was reported by O'Mottley and Miller[4], which coincides with the theoretical prediction. The backscatter coefficient for human brain was studied at frequency between 0.5-1.5 MHz by Barger[5], who successfully differentiated the white from the gray matters in the brain. Nicholas[6] studied the backscatter coefficient of human tissues using spectrum technique. However, the frequency used in these researches is below 10 MHz. To increase the resolution of imaging, the frequency of ultrasound must be increased. D'Astous *et al*[7] and Foster *et al*[8] have achieved the high frequency imaging of breast. Turnbull[9-12] studied mouse embryos using ultrasound backscatter microscopy. Ye *et al*[13] and Pavlin *et al*[14,15] studied the ocular tissue using high frequency imaging. The ultrasonic properties of vascular tissues and blood were measued from 35 to 65 MHz by Lockwood *et al*[16] and Meyer *et al*[17]. Yano *et al*[18] and Liu *et al*[19] studied the high frequency imaging of skin and thyroid. Ultrasound backscatter microscopy images of the internal structure of living tumor spheroids have been

obtained[20,21].

Liver is the important organ for metabolism. Hepatic lobule is the basic element in liver, and is surrounded by connective tissue. Most blood capillaries pass through the boundary of its connective tissues. Hepatic tissue regeneration and connective tissue hyperplasia induce change of the normal structure of hepatic lobule. The liver becomes deformed and stiff, known as hepatocirrhosis. Common liver diseases can be diagnosed by B- ultrasound. However, it is difficult to diagnose diffuse diseases of liver.

The present study was to investigate the relation between acoustic parameters and histological structure of biological tissue and to provide the basis for high-resolution image of biological tissues and quantitative ultrasonic diagnosis of liver disease.

MATERIALS AND METHODS

Experimental system

High frequency imaging system was set up in our laboratory. The sample was fixed in the sample-holder between quartz and a thin plastic membrane and then mounted in water bath. The focused ultrasound transducer (center frequency 35 MHz, -3dB bandwidth from 25 MHz to 55 MHz, f-number 1.6, focus depth 1 mm, beam width 70 μm) was excited with a pulse (300 Vpp in amplitude, 15 ns in width). The ultrasonic pulse passing through the membrane, sample reflected from the quartz flat was received by the same transducer. The transducer and the step motor were carefully moved, the region of interest in the sample was located in the focus area and in the focal depth of the transducer. The scan parameters for raster motion were downloaded by MTM2500 pp (Newport Co, USA). The attenuation signal and backscatter signal were recorded by a 400 MHz digital scope (HP54502A, USA). The information about the C-scan imaging was acquired by sampling the backscatter signal after a specified delay corresponding to the focus and stored in a hard disk for software scan conversion after data collection was completed. An IEEE-488 bus transferred the digitized signals to the control computer for further processing

The transducer in a raster fashion over a 3 mm × 5 mm area was removed and a backscatter image of the sample was generated using C-scan mode. The region of homogenous tissue was selected for quantitative measurement. The incident direction of the sound beam was perpendicular to the surface of the sample during the measurement. The interest region containing 16 points in 4 by 4 grids was selected to measure the velocity of sound, 64 points in 8 by 8 grids were selected to measure the attenuation and backscatter coefficients of the sample and each grid was separated by 80 μm.

Sample preparation

Liver tissue samples were obtained from the Meat Processing Plant. In the experiment, the sample was clamped between plastic membrane and reflector quartz flat in a specially designed sample holder and both sides of the sample were cut at -10℃ using Cryostat 2700 (Frigocut, Reichert-june, Germany) to make the surface with a homogenous thickness between 0.5-1.5 mm. Then the sample was thawed in saline solution and sealed with a thin plastic membrane. In the study, four normal liver tissue samples and five cirrhotic liver tissue samples (hepatocirrhosis) were used. A slice from each sample was stained. The corresponding histological diagram and ultrasound image were obtained.

Table 1 Sound speed and attenuation and acoustic backscatter coefficient (mean ± SD)

		Normal liver	Cirrhotic liver
Sound speed (m/s)		1577 ± 7	1631 ± 5
Attenuation	α_1	0.121 ± 0.045	0.082 ± 0.023
(dB/mm)	α_{35}	3.0 ± 0.6	4.1 ± 0.8
	m	0.9	1.1
Backscatter coefficient	μ_1	$2.66 \times 10^{-6} \pm 1.43 \times 10^{-6}$	$4.85 \times 10^{-6} \pm 1.52 \times 10^{-6}$
(1/Srmm)	μ_{35}	0.00303 ± 0.00015	0.0043 ± 0.00025
	n	1.98	1.91

RESULTS

Images

The ultrasound imaging of normal and cirrhotic liver tissues and their corresponding pathological slices are shown in Figure 1A-1D. From the images, some microstructures of the tissue could be observed. However, the image of normal liver tissue (Figures 1A, 2B) was different from that of cirrhotic liver tissue (Figures 1C, 1D). The image of normal liver tissue was ultrasonically homogenous while the image of cirrhotic liver tissue was contrary to that of normal liver tissue. From the imaging, we could see the hyperecho of the cirrhotic liver. Some short and strong echoes caused by hyperplasia of connective tissue occurred.

Sound velocity, attenuation and backscatter coefficient

A summary of the acoustic parameters measured in the liver are listed in Table 1.The experimental results showed that the acoustic parameters from cirrhotic liver were larger than those from normal liver. The sound velocity in normal liver was 1 577 m/s and 1 631 m/s in cirrhotic liver, which coincides with the sound velocity (1 600 m/s) in bovine liver[22]. At 35 MHz, the attenuation coefficient was 3.0 dB/mm in normal liver and 4.1 dB/mm in cirrhotic liver. However, it has been reported to be 9.73 dB/mm at 70 MHz[22] and 0.89 dB/mm at 10.0 MHz respectively in liver[23]. The backscatter coefficient was 0.00431/Srmm at 35 MHz in cirrhotic liver and 0.00303/Srmm in normal liver. The power-law fits with the backscatter coefficient in normal liver as a function of frequency. However, it has been reported to be $(2.66\times10^{-6}\pm1.43\times10^{-6})^{f1.98}$/Srmm) and $(4.85\times10^{-6}\pm1.52\times10^{-6})^{f1.91}$/Srmm in cirrhotic liver[24]. The increase of backscatter coefficient is caused by hyperplasia of the connective tissue in cirrhotic liver (Figure 2). The backscatter occurs when the size of backscatter structure is similar to the wavelength of the sound beam, suggesting that the size of backscatters is within the wavelength of the ultrasound wave and the size of porcine liver lobules may be similar to it. The frequency-dependent decrease in cirrhotic liver reflects the increase of scattering elements

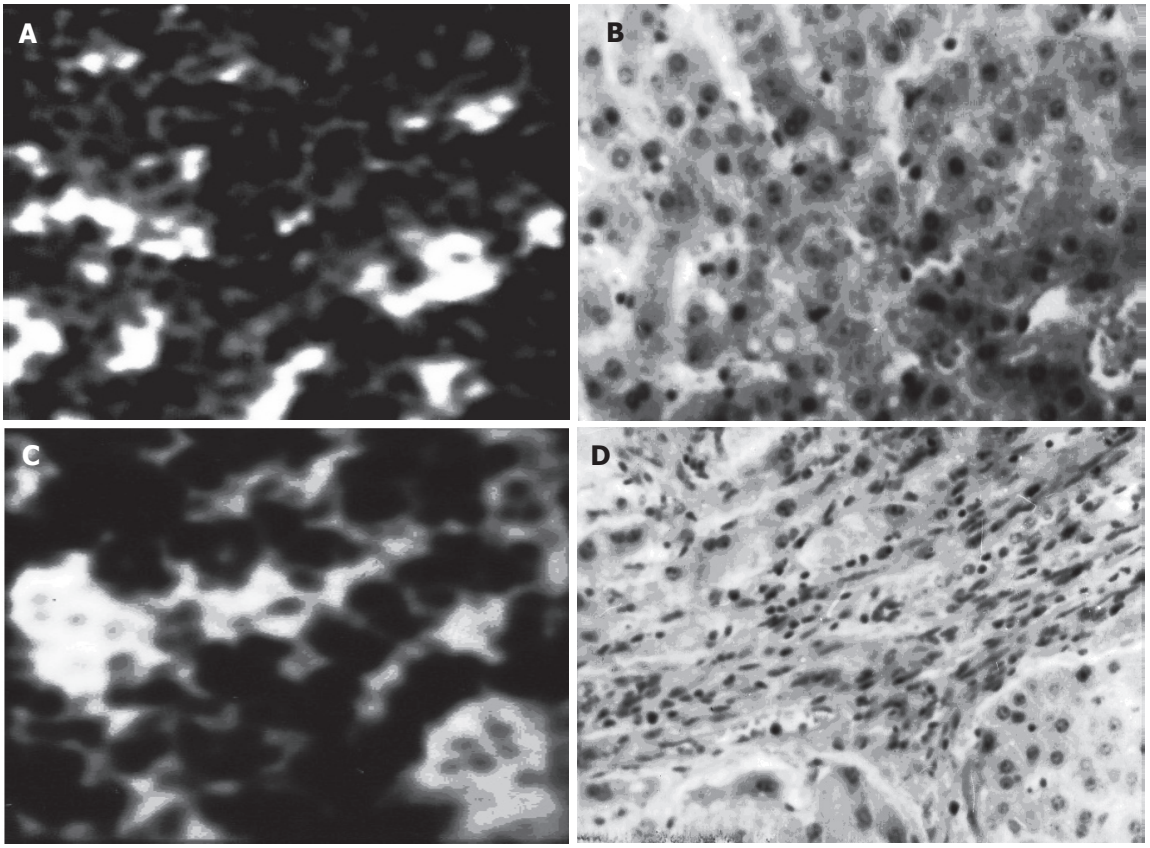

Figure 1 Ultrasound images of normal and cirrhotic liver and their corresponding pathological slices **A:** ultrasound imaging of normal liver; **B:** pathological slice of normal liver; **C:** ultrasound imaging of cirrhotic liver; **D:** pathological slice of cirrhotic liver.

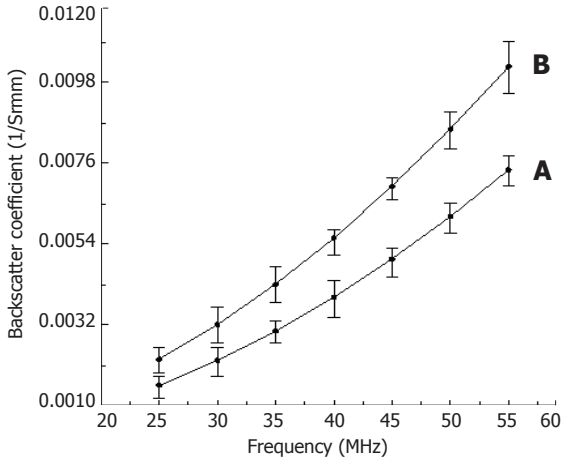

Figure 2 Backscatter coefficients changing with frequency in normal liver (**A**) and cirrhotic liver (**B**).

in the liver.

DISCUSSION

Ultrasonic tissue characterization based on spectrum analysis of backscattered radio frequency (RF) echo signals provides information regarding the acoustic properties of tissue, such as the size, concentration, and acoustic impedance of scatterers that are not available by conventional imaging methods[25,26]. The ultrasonic backscatter coefficient in human liver was measured in the range of 2.0-4.0 MHz[24]. The ultrasonic propagation properties at 100 MHz in excessively fatty rat liver were studied[27]. Strong correlation of ultrasonic speed with both water concentration and fat concentration in the liver was observed. The ultrasonic attenuation and velocity in rat liver as a function of fat concentration at 100 MHz were investigated[28] and the acoustic properties of freshly excised bovine liver were characterized at the frequency range between 20-200 MHz by the ultrasonic spectroscope system[22].

On the other hand, ultrasonic imaging systems in medicine depend fundamentally upon analysis of the ultrasonic scattering properties of the soft tissues investigated. However, the mechanism governing ultrasonic scattering within most soft tissues have not been delineated. In many cases the absolute magnitude of the scattering process has not been accurately quantified. The relationship between collagen and ultrasonic backscatter in myocardial tissue was evaluated[3]. The dependence of the ultrasonic scatter coefficient on collagen concentration in mammalian tissues was addressed[29]. And the mean-scatter spacing estimated with spectral correlation was used for tissue characterization[30]. However, there is little report on tissue characterization of hepatic tissues in the range between 25-55 MHz.

In this study, ultrasound images and sound parameters for hepatic tissues were studied by using C-scan ultrasound system at the frequency between 25-55 MHz. The above experimental results indicate that the resolution of high frequency image is much better than that obtained at low ultrasound frequency because some microstructure of the tissue can be seen. The information obtained from the ultrasound image is coincided with the histological feature of the sample. Furthermore, the samples need not to be stained. The acoustic parameters especially the sound backscatter coefficient are sensitive to the changes of the

tissues and can be used to differentiate between the normal and pathological tissues, the frequency dependence of backscatter coefficient could be reflected by the change of scattering elements and may be employed as a parameter for characterizing tissues and their physiological states. Therefore the high frequency image system is a useful device for high-resolution image and tissue characterization within the high frequency range.

REFERENCES

1 **Shung KK**, Reid JM. Ultrasound Scattering from tissues. *Ultrasonic Symposium proceedings (IEEE Cat. 77 CH1264-ISU)* 1977; 203

2 **Fei DY,** Shung KK. Ultrasonic backscatter from mammalian tissues. *J Acoust Soc Am* 1985; **78:** 871-876

3 **O'Donnell M,** Mimbs JW, Miller JG. The relationship between collagen and ultrasonic attenuation in myocardial tissue. *J Acoust Soc Am* 1979; **65:** 512-517

4 **Madaras EI,** Perez J, Sobel BE, Mottley JG, Miller JG. Anisotropy of the ultrasonic backscatter of myocardial tissue: II. Measurements in vivo. *J Acoust Soc Am* 1988; **83:** 762-769

5 **Barger JE.** Brain tissues classification by its ultrasonic backscatter. *IEEE Trans on sonics & ultrasonics* 1981; **28:** 311-315

6 **Nicholas D.** Evaluation of backscattering coefficient for excised human tissues: results interpretations and associated measurement. *Ultrasound in Med and Biol* 1982; **1:** 17-28

7 **D'Astous FT,** Foster FS. Frequency dependence of ultrasound attenuation and backscatter in breast tissue. *Ultrasound Med Biol* 1986; **12:** 795-808

8 **Foster FS**, Strban M, Austin G. The ultrasound macroscope: initial studies of breast tissue. *Ultrason Imaging* 1984; **6:** 243-261

9 **Turnbull DH.** Ultrasound backscatter microscopy of mouse embryos. *Methods Mol Biol* 2000; **135:** 235-243

10 **Turnbull DH,** Ramsay JA, Shivji GS, Bloomfield TS, From L, Sauder DN, Foster FS.Ultrasound backscatter microscope analysis of mouse melanoma progression. *Ultrasound Med Biol* 1996; **22:** 845-853

11 **Turnbull DH,** Bloomfield TS, Baldwin HS, Foster FS, Joyner AL. Ultrasound backscatter microscope analysis of early mouse embryonic brain development. *Proc Natl Acad Sci USA* 1995; **92:** 2239-2243

12 **Turnbull DH,** Starkoski BG, Harasiewicz KA, Semple JL, From L, Gupta AK, Sauder DN, Foster FS. A 40-100 MHz B-scan ultrasound backscatter microscope for skin imaging. *Ultrasound Med Bio*l 1995; **21:** 79-88

13 **Ye SG,** Harasiewicz KA, Pavlin CJ, Foster FS. Ultrasonic characterization of normal ocular tissue in the frequency range from 50MHz to 100MHz. *IEEE Transactions on ultrasonics, ferroelectrics and frequency control* 1995; **42:** 8-14

14 **Pavlin CJ,** Harasiewicz K, Sherar MD, Foster FS. Clinical use of ultrasound biomicroscopy. *Ophthalmology* 1991; **98:** 287-295

15 **Pavlin CJ,** Sherar MD, Foster FS. Subsurface ultrasound microscopic imaging of the intact eye. *Ophthalmology* 1990; **97:** 244-250

16 **Lockwood GR,** Ryan LK, Hunt JW, Foster FS. Measurement of the ultrasonic properties of vascular tissues and blood from 35-65 MHz. *Ultrasound Med Biol* 1991; **17:** 653-666

17 **Meyer CR**, Chiang EH, Fechner KP, Fitting DW, Williams DM, Buda AJ. Feasibility of high-resolution, intravascular ultrasonic imaging catheters. *Radiology* 1988; **168:** 113-116

18 **Yano T,** Fukukita H, Umeo S, Fukumoto A. 40MHz ultrasound diagnostic system for dermatology examination. *Proc IEEE Ultrason Symp* 1987; 875-878

19 **Liu XZ,** Ye SG, Gong XF, Zhang WY, Jia YQ. High frequency ultrasound image and tissue characterization for human thyroid. *Zhonghua Shenwu Yixue Gongcheng* 2001; **20:** 110-115

20 **Sherar MD,** Starkoski BG, Taylor WB, Foster FS. A 100 MHz B-scan ultrasound backscatter microscope. *Ultrason Imaging* 1989; **11:** 95-105

21 **Sherar MD,** Noss MB, Foster FS. Ultrasound backscatter microscopy images the internal structure of living tumour spheroids. *Nature* 1987; **330:** 493-495

22 **Akashi N,** Kushibiki J, Chubachi N, Dunn F. Acoustic properties of selected bovine tissues in the frequency range 20-200 MHz. *J Acoust Soc Am* 1995; **98:** 3035-3039

23 **Frizzell LA,** Carstensen EL, Davis JD. Ultrasonic absorption in liver tissue. *J Acoust Soc Am* 1979; **65:** 1309-1312

24 **Wear KA,** Garra BS, Hall TJ. Measurements of ultrasonic backscatter coefficients in human liver and kidney in vivo, *J Acoust Soc Am* 1995; **98:** 1852-1857

25 **Hosokawa T**, Sigel B, Machi J, Kitamura H, Kolecki RV, Justin JR, Feleppa EJ, Tuszynski G, Kakegawa T. Experimental assessment of spectrum analysis of ultrasonic echoes as a method for estimating scatterer properties. U*ltrasound Med Biol* 1994; **20:** 463-470

26 **Lizzi FL**, Greenebaum M, Feleppa EJ, Elbaum M, Coleman DJ. Theoretical framework for spectrum analysis in ultrasonic tissue characterization. *J Acoust Soc Am* 1983; **73:** 1366-1373

27 **O'Brien WD Jr**, Erdman JW Jr, Hebner TB. Ultrasonic propagation properties (@ 100 MHz) in excessively fatty rat liver. *J Acoust Soc Am* 1988; **83:** 1159-1166

28 **Tervola KM**, Gummer MA, Erdman JW Jr, O'Brien WD Jr. Ultrasonic attenuation and velocity properties in rat liver as a function of fat concentration: a study at 100 MHz using a scanning laser acoustic microscope, *J.Acoust.Soc.Am* 1985; **77:** 307-313

29 **Pohlhammer J,** O'Brien WD Jr. Dependence of the ultrasonic scatter coefficient on collagen concentration in mammalian tissues. *J Acoust Soc Am* 1981; **69:** 283-285

30 **Varghese T**, Donohue KD. Mean-scatterer spacing estimates with spectral correlation. *J Acoust Soc Am* 1994; **96:** 3504-3515

S- Editor Guo SY **L- Editor** Wang XL **E- Editor** Cao L

PO Box 2345, Beijing 100023, China
www.wjgnet.com
wjg@wjgnet.com

World J Gastroenterol 2006 April 14; 12(14): 2280-2283
World Journal of Gastroenterology ISSN 1007-9327

RAPID COMMUNICATION

Antiviral effect of Chinese medicine jiaweisinisan in hepatitis B virus transgenic mice

Xiao-Yin Chen, Guang-Dong Tong, Fang Xia

Xiao-Yin Chen, Fang Xia, Department of Traditional Chinese Medicine, Medical College, Jinan University, Guangzhou 510632, Guangdong Province, China
Guang-Dong Tong, Department of Gastroenterology, Shenzhen Traditional Chinese Medical Hospital, Shenzhen 518000, Guangdong Province, China
Supported by the National Natural Science Foundation of China, No. 30000217 and the Natural Science Foundation of Guangdong Province, No. 000359 and No. 2005B30101012
Correspondence to: Professor Xiao-Yin Chen, Department of Traditional Chinese Medicine, Medical College, Jinan University, 601 Huangpu Road, Guangzhou 510632, Guangdong Province, China. tchenxiaoyin@jnu.edu.cn
Telephone: +86-20-85226410
Received: 2005-09-23 Accepted: 2005-10-26

Abstract

AIM: To study the antiviral effect of Chinese medicine jiaweisinisan (JWSNS) on hepatitis B virus (HBV) infection in transgenic mice (TGM).

METHODS: Twenty two 6-8 wk old HBV TGM in the third generation were divided into TGM control group and TGM treated group randomly. The normal control group included ten normal BC 57L/6 mice at the same age. The mice in treated group were administrated with JWSNS at the concentration of 4 g/mL and the dosage of 50 g/kg per d for 30 d, while the mice in TGM control group and normal control group were administrated with normal saline at the same dosage and the same time. Polymerase chain reaction (PCR) was used to assess the contents of HBV DNA in serum of HBV TGM before and after treatments, whereas blot hybridization was utilized to measure the contents of HBV DNA in the liver of both HBV TGM and normal BC 57L/6 mice.

RESULTS: The levels of serum HBV DNA in TGM treated group were remarkably decreased after the treatment of JWSNS (7.662 ± 0.78 *vs* 5.22 ± 3.14, $P < 0.05$), while there was no obvious change after administration of normal saline in TGM control group (7.125 ± 4.26 *vs* 8.932 ± 5.12, $P > 0.05$). The OD values of HBV DNA in the livers of the mice in TGM treated group were significantly lower than those of TGM control group (0.274 ± 0.096 *vs* 0.432 ± 0.119, $P < 0.01$).

CONCLUSION: JWSNS exerts suppressive effects on HBV DNA in the serum and liver of TGM.

Key words: Traditional Chinese herbs; Hepatitis B virus; Transgenic mice; PCR; Blot hybridization; Chronic hepatitis B

Chen XY, Tong GD, Xia F. Antiviral effect of Chinese medicine jiaweisinisan in hepatitis B virus transgenic mice. *World J Gastroenterol* 2006; 12(14): 2280-2283

http://www.wjgnet.com/1007-9327/12/2280.asp

INTRODUCTION

In this *in vivo* study, HBV transgenic mice (HBV TGM) models were established to detect the antiviral effects of traditional Chinese medicine, jiaweisinisan (JWSNS) on HBV TGM, so to further confirm the inhibitory effects of this traditional Chinese herb on HBV infection.

MATERIALS AND METHODS

Experimental animals

Normal C57BL/6 mice and the HBV transgenic mice, living in the same cote, were provided by Department of Transgenic Engineering in Hepatopathy Research Center of Guangzhou Military Hospital. All the non-transgenic mice were under close surveillance to ensure the HBV DNA in serum and tissue to be negative.

Traditional Chinese herbs

JWSNS, including buplerum chinense DC, flea body, prunus persica (L.) batsch, of 10 grams each, and radix paeoniae alba, fructus aurantii immaturus, dipsacus asper wall, rhizoma dryopteris crassirhizomae, eupatorium adenophorum sprengel, of 12 grams each, as well as 5 grams of glycyrrhizaglabral, and 30 grams of loranthus parasiticus, was prepared according to the traditional procedures. Five compounds of drugs were mixed together, 141 grams per compound, and dissolved into the water to distil twice, yielding 1500 mL distillation solution, followed by inspissation of the distillation to 180 mL. The final concentration was 4 g/mL, stored in refrigerator for use.

PCR primer and reagent

PCR primers and relevant reagents were provided by

Shanghai Bioengineering Research Center of Chinese Academy of Sciences. The sequence of PCR primer one is 5'-TGGCACTAGTAAACTGAGCC-3' and that of PCR primer two is 5'-ACATCAGGATTCCTAGGACC-3'. Other reagents such as $MgCl_2$, dNTP, buffer, Tag enzyme, and paraffin oil were purchased from Promega Company (Madison, USA). Quantitative diagnostic kit (batch number 1000-902-1) for HBV DNA was provided by Biotromcs Technological Company (San Francisco, USA).

DNA extraction kit

DNA extraction kit was obtained from Maikang Biotechnological Company of Zhongshan Medical University.

Recombinant plasmid PBR322-2.0 HBV rapid extraction reagents

The reagents included host strain, antibiotics, peptone, yeast extract, gelose, buffer Ⅰ (50 mmol/L glucose, 25 mmol/L Tris HCl, 10 mmol/L EDTA), buffer Ⅱ (0.2 mol/L NaOH, 1% SDS), and buffer Ⅲ (5 mol/L potassium acetate 60 mL, iced acetic acid 11.5 mL, water 28.5 mL).

α-^{32}P-DNA probe labeled reagents

It included NEN kit (Promega Co., Madison, USA), Sephaclex G-50 columniation, purified recombinant plasmid PBR322-2.0 HBV (100 ng/μL), 0.5 mol/L EDTA.

Blot hybridization reagents

It included nitrate fibrous membrane (aperture 0.45 μm, Amersham Co., Buckinghamshire, UK), Formamide 20×SSC buffer, 37% formaldehyde, dyestuff (25% Bromophenolblue dissolved into Ficoll), TE buffer.

Apparatus

Gene amp PCR system (Techne, England), AG-9600 equipment for analytical fluorescence microscope (USA), low-temperature freeze centrifuge (Biofuge 22R, Germany), water bath, pH meter, magnetic shaker, vacuum pump, refrigerator, balance (China), constant temperature rocker, constant temperature incubator, superclean working table (China), ZXZ-4 gyral vacuum pump (Zhejiang Linhai Vacuum Apparatus Factory), 721 spectrophotometer (The Third Spectrophotometry Factory, Shanghai) were used.

Establishment of HBV TGM model

P2.0 HBV plasmid passed through a series of *Eco*RI/*Sal*I restriction enzyme digestion, and electrophoresis, followed by the collection of 7.0 kb DNA fraction, which contained two end-to-end 3.2 kb HBV entire genes, and 0.6 kb PBR322 DNA vector. After electrophoresis quantitative analysis, the collected DNA fractions were dissolved in TE buffer under bioclean condition to ensure the concentration to be 1 mg/L, then respectively packed and stored at -20 ℃ to wait for micro- injection. C57BL/6 mice injected entire genome plasmid which contained HBV were identified to be G0 generation. Positively integrating male mice of G0 generation were selected to hybridise with infraspecific normal female mice, producing G1 generation. In similar manner, positively integrating male mice of G1 generation were selected to copulate with infraspecific normal female mice, producing G2 generation. Mice of G3 generation were produced in the same way[1].

Selecting procedures of HBV TGM

A total of one hundred and fifteen 6-8 wk old mice of G3 generation, weighing 20 g, were provided by Department of Transgenic Engineering in Guangzhou Military Hospital. HBV DNA detection kit was purchased from Baosheng Bioengineering Company (Dalian). Tissues were firstly detected to select HBV DNA positive mice, followed by serum detections. Twenty-two serum HBV DNA positive mice were eventually selected from 115 mice of G3 generation to be labeled as HBV DNA transgenic mice.

Grouping

Twenty-two HBV TGM, whose serum HBV DNA was positive, and 10 normal C57BL/6 mice were grouped into TGM treated group, 12 TGM mice; TGM control group, 10 TGM mice; normal control group, 10 normal C57BL/6 mice; and then registered. Additional six 6–8 wk old C57BL/6 mice, weighing (20 ± 2) g, whatever male or female, were also prepared. All the mice were fed in Experimental Animal Center of Guangzhou Military Hospital. Auto-supply of water and standard food were offered as well as air condition to maintain the constant temperature during the whole experimental procedures.

Administration

Mice in TGM treated group were administrated with JWSNS at 50 g/kg per d, in 0.3-0.4 mL JWSNS solution (about 4 g/mL, ig) once a day for four weeks, while the mice in the other two control groups were administrated with the same dosage of normal saline at the same time.

Sample collection

Two hours after the last administration, eyeballs were extirpated to collect peripheral blood before the execution of the mice followed and sera were then separated for detection of HBV markers. Promptly, livers were removed and broken, frozen by liquid nitrogen and stored at -70 ℃ for detection.

Detection method

PCR quantitative analysis[2, 3] was used to detect the serum contents of HBV DNA of TGM at the moment when the total contents had reached up to 1.0×10^5 kb/mL, while blot hybridization[4, 5] was utilized to analyze the contents of HBV DNA in liver of mice. The extraction of DNA in liver tissue was processed according to the instruction provided by the manufacturer of the kit. The rapid extraction of recombinant plasmid PBR322-2.0 HBV was performed by alkali fission method[6]. α-^{32}P-DNA probe was labeled according to instructions of Promega Co. reagent kit. Blot hybridization was performed as follows: 40 μL α-^{32}P-DNA probe labeled solutions was used

Table 1 Changes of serum levels of HBV DNA in HBV TGM before and after treatment of JWSNS (mean±SD)

Group		*n*	Serum HBV DNA	
			Case transformed from DNA positive to negative	Content of HBV[1]
TGM controlled group	Prior to administration of normal saline	10	0	7.125±4.26
	After administration of normal saline	10	0	8.932±5.12
TGM treated group	Prior to JWSNS treatment	10	0	7.662±0.78
	After JWSNS treatment	10	3	5.122±3.14

[1]Analyzed by *t*-test. TGM treated group, [1]$P<0.05$ *vs* TGM controlled group, [1]$P>0.05$.

Table 2 Effect of JWSNS on levels of HBV DNA in the liver of HBVTGM (mean±SD)

Group	*n*	HBV DNA blot hybridization
Normal control group	9	0
TGM control group	9	0.432±0.119
TGM treated group	9	0.274±0.096[b]

[b]$P<0.01$ *vs* TGM control group.

to dot on the membrane, which was then dipped in the metamorphic solution, and baked in the oven at 80 ℃ for two hours. After pre-interaction, membrane washing, slice nipping, the positive degree was justified according to the OD value of each blot.

Statistical analysis

Statistical data was analyzed by SPSS software. The comparability prior to and after disposal of the same sample was verified by paired-samples *t*-test, whereas the difference of the mean value among various groups was analyzed by χ^2 test. *P* less than 0.05 was taken as significant.

RESULTS

Effects of JWSNS on serum contents of HBV DNA in HBVTGM

The levels of serum HBV DNA in TGM treated group displayed considerable distinction before and after treatment of JWSNS ($P<0.05$), compared with those in TGM controlled group in which no significant difference was shown before and after administration with normal saline ($P>0.05$) (Table 1).

Effect of JWSNS on levels of HBV DNA in the liver of HBV TGM

HBV DNA blot hybridization was positive in HBV TGM both before and after treatment. The OD value showed extremely significant difference between TGM controlled group and TGM treated group ($P<0.01$), whereas blot hybridization in normal control group appeared to be negative (Table 2).

DISCUSSION

Value of HBV TGM model in the study of inhibitory effect of the traditional Chinese medicine on HBV

The host infected by HBV showed violent phyletic and tissue specificity, resulting in the remarkable restriction in the establishment of the animal model infected by HBV and anti-HBV study. In the past, data related to anti-HBV entirely came from HBV-infected patients, orangutan or cell *in vitro*. In addition, significant distinction existed between experimental data of other hepatophilic DNA virus such as duck or groundhog HBV and those of human HBV[7,8].

In 1980, microinjection HBVTGM model was successfully established which obviously overcame the limitation described above. Chissari [9] established TGM model and claimed that HBV DNA and HBsAg granules were detected in TGM blood and congregated in a fraction of hepatocyte, inducing tumefaction and dysfunction of the endoplasm as well as the ground glass hepatocytes, besides enhancing the sensitivity of hepatocytes to the lipopolysaccharide and IFN-γ, resulting in the damnification, necrosis and regeneration of the hepatocyte, or even the occurrence of hepatocarcinoma. Thus, HBVTGM model was, to a great extent, similar to the immune interaction between virus and host during natural infection of HBV[10].

HBVTGM is viewed as an immune tolerance condition. Despite limited damnification of hepatocytes in some mice, inflammation was not obvious, which is consistent with the pathologic change in human beings infected with HBV. The objective of our study emphasized on suppressive effect of JWSNS on HBV including the change of HBV contents in blood and tissue rather than the inflammatory level in liver. Thus, it is appropriate that HBVTGM served as the anti-HBV model.

Anti-HBV effect of traditional Chinese medicine and significance of HBV DNA detection

The symptom in different stage of HBV persistent infection varies from chronic asymptomatic HBV carrier and chronic hepatitis to hepatocirrhosis and hepatocarcinoma[11,12]. According to modern medicine chronic asymptomatic HBV carrier is viewed as the earlier stage of chronic persistent infection of HBV, in which the immune system is inhibited, leading to the inefficacy of interferon and lamivudine, the traditional antivirus drugs. Thus it is a widespread viewpoint that there is no effective treatment for earlier stage of HBV infection. However, it does not mean that there is no need for treatment[13,14]. Of note, at this stage, viruses copy themselves constantly, accompanied with the obvious viraemia, and approximately

normal liver function. However, as the copying process continues, a series of immune reaction of the host would be triggered to damage the liver and other organs. This stage may be a chance for traditional Chinese medicine to act as antivirus agent[15]. Pioneering clinical experiences indicated that traditional Chinese medicine such as phyllanthus urinaria L., matrine could endow the host in immune tolerance condition advantage in antivirus effect and protective effect on liver, and the detection of HBV DNA contents could help evaluate the antivirus effect of traditional Chinese medicine.

Theoretic basis for treatment of HBV infection by JWSNS

The treatment regimen of chronic hepatitis B by JWSNS is rooted in pathologic hypothesis of traditional Chinese medicine proposed by Bao Yi Liu, a famous doctor in ancient China who stated that whenever the *nephric qi* is inadequate, the protective function of human body against disease would decline, whereas *sick qi* would take the chance to invade the human body, weakening the *hepatic qi*, inducing the damp and the heat, which then attack the spleen and stomach, leading to the disfunction of both liver and spleen. This main pathologic process persists during the whole course of disease. According to this pathologic hypothesis, nothing but nourishing *nephric qi* is the key step to cure chronic hepatitis B. JWSNS, a famous compound, is used to enrich *nephric qi,* thus to reinforce the protective effect of the human body, and to overcome the state of immune tolerance.

Inhibitory effect of JWSNS on HBV of HBVTGM

In this study, HBVTGM model was used to observe the change of HBV DNA content both in serum and in hepatic tissue before and after the JWSNS treatment. The contents of HBV DNA in liver reflect the contents of HBV in hepatocyte. HBV, a hepatophilic virus, invades into the hepatocyte, in which they copy themselves, and then migrate into the peripheral circulation, inducing the diffuse chronic infection of HBV. The contents of HBV DNA reflect the level of virus copy. In the study, hepatocellular DNAs were extracted, and with the probe of P^{32} labeled plasmid P2.0 HBV, blot hybridization proceeded in nitrate fibrous membrane. The results of blot hybridization showed that no blot could be seen in normal control group, in striking contrast with the obvious blot appearing in both TGM control group and TGM treated group. The measurement of OD value of the blot demonstrated that the contents of HBV DNA in hepatocyte dramatically decreased four weeks after JWSNS treatment, compared with HBVTGM control group ($P < 0.01$).

PCR, a comparatively sensitive method was utilized in detecting the change of serum HBV DNA before and after JWSNS treatment in treated group or before and after administration of normal saline in control group. Four weeks later, no significant change could be seen in TGM control group administrated with normal saline, whereas HBV DNA of three mice was converted from positive to negative after treatment with JWSNS, and the serum contents of HBV DNA showed significant decline before and after treatment ($P < 0.05$).

The detection of HBV DNA contents in both liver tissue and serum shows that JWSNS could, to certain extent, inhibit HBV DNA, which provides the experimental proof for treatment of chronic hepatitis B with JWSNS.

REFERENCES

1 **Cheng GX,** Cheng Y, Li DZ. Artificial hepatic virus entire genome transgenic mice. Nanjing Jiaoyu Daxue Xuebao (Ke xue bao) 1995; **18:** 129-135

2 **Pfaffl MW**, Gerstmayer B, Bosio A, Windisch W. Effect of zinc deficiency on the mRNA expression pattern in liver and jejunum of adult rats: monitoring gene expression using cDNA microarrays combined with real-time RT-PCR. *J Nutr Biochem.* 2003; **14:** 691-702

3 **Hata J**, Ikeda E, Uno H, Asano S. Expression of hepatocyte growth factor mRNA in rat liver cirrhosis induced by N-nitrosodimethylamine as evidenced by in situ RT-PCR. *J Histochem Cytochem* 2002; **50**: 1461-1468

4 **Fukushima A**, Okubo K, Sugino H, Hori N, Matoba R, Niiyama T, Murakawa K, Yoshii J, Yokoyama M, Matsubara K. Chromosomal assignment of HepG2 3'-directed partial cDNA sequences by Southern blot hybridization using monochromosomal hybrid cell panels. *Genomics* 1994; **22:** 127-136

5 **Phromjai J,** Boonsaeng V, Withyachumnarnkul B, Flegel TW. Detection of hepatopancreatic parvovirus in Thai shrimp Penaeus monodon by in situ hybridization, dot blot hybridization and PCR amplification. *Dis Aquat Organ*. 2002; **51:** 227-232

6 **Jin DY,** Li MF. Experimental instruction for molecular clone. Beijing: scientific publishing company, 1996; 19

7 **Julander JG**, Sidwell RW, Morrey JD. Characterizing antiviral activity of adefovir dipivoxil in transgenic mice expressing hepatitis B virus. *Antiviral Res* 2002; **55:** 27-40

8 **Kimura K**, Kakimi K, Wieland S, Guidotti LG, Chisari FV. Activated intrahepatic antigen-presenting cells inhibit hepatitis B virus replication in the liver of transgenic mice. *J Immunol* 2002; **169**: 5188-5195

9 **Chisari FV.** Analysis of hepadnavirus gene expression, biology, and pathogenesis in the transgenic mice. *Curr Top Microbiol Immunol* 1991; **168:** 85-101

10 **Chisari FV.** Hepatitis B virus transgenic mice: insights into the virus and the disease. *Hepatology* 1995; **22:** 1316-1325

11 **Nuez M,** Garcia-Samaniego J, Soriano V. Advances in the diagnosis and treatment of the infection by the hepatitis B virus. *Enferm Infecc Microbiol Clin*. 2004; **22:** 539-549

12 **Karayiannis P**. Current therapies for chronic hepatitis B virus infection. *Expert Rev Anti Infect Ther*. 2004; **2:** 745-760

13 **Akuta N,** Kumada H. Corticosteroid withdrawal therapy in patients with chronic hepatitis B virus infection. *Nippon Rinsho*. 2004; **62** Suppl 8: 345-348

14 **Fujisawa T**, Inui A, Sogo T, Komatsu H. Long-term history of chronic hepatitis B virus infection in children. *Nippon Rinsho*. 2004; **62** Suppl 8 : 303-308

15 **Yao JL**. Clinical treatise of infectious disease. Guangzhou: Guangdong superior pedagogic publishing company, 2000: 2

S- Editor Wang J **L- Editor** Zhu LH **E- Editor** Cao L

PO Box 2345, Beijing 100023, China
www.wjgnet.com
wjg@wjgnet.com

World J Gastroenterol 2006 April 14; 12(114): 2284-2287
World Journal of Gastroenterology ISSN 1007-9327

RAPID COMMUNICATION

Effect of explosive noise on gastrointestinal transit and plasma levels of polypeptide hormones

Zhen-Bin Mu, Yu-Xin Huang, Bao-Min Zhao, Zhen-Xiong Liu, Bing-Hua Zhang, Qing-Li Wang

Zhen-Bin Mu, Yu-Xin Huang, Bao-Min Zhao, Zhen-Xiong Liu, Bing-Hua Zhang, Qing-Li Wang, Department of Gastroenterology, Tang Du Hospital of the Fourth Military Medical University, Xi'an 710038, Shaanxi Province, China
Co-correspondence: Yu-Xin Huang
Correspondence to: Dr. Zhen-Bin Mu, Department of Gastroenterology, Tang Du Hospital of the Fourth Military Medical University, Xi'an 710038, Shaanxi Province, China. mzb-999@163.com
Telephone:+86-29-83377597
Received: 2005-09-21 Accepted: 2005-10-26

Abstract

AIM: To investigate the effect of firing noise on gastrointestinal transit and probe its mechanism by measuring the levels of plasma polypeptide hormones.

METHODS: A total of 64 SD rats were randomly divided into a control group and three stimulating groups. Firing noise of different intensity by sub-machine guns was used as inflicting factor. The effect of firing noise on liquid substance gastrointestinal transit and solid substance gastrointestinal transit was observed by measuring the ratio of carbon powder suspension transmitting and barium sticks transmitting respectively. Plasma levels of polypeptide hormones were measured by radio-immunoassay.

RESULTS: The noise accelerated gastrointestinal transit of solid food by more than 80 db;and accelerated gastrointestinal transit of liquid food significantly by more than 120 db. Meantime, plasma levels of plasma motilin (MTL)(157.47±16.08; 151.90±17.08), somatostatin (SS)(513.97±88.77; 458.25±104.30), substance P (SP)(115.52±20.70; 110.28±19.96) and vasoactive intestinal peptide (VIP) (214.21±63.17; 251.76±97.24) remarkably changed also.

CONCLUSION: Within a certain intensity range, the firing noise changes the levels of rat plasma gastrointestinal hormones, but the gastrointestinal transit is still normal. Beyond the range, the noise induces plasma hormone levels disturbance and gastrointestinal transit disorder.

Key words: Explosive noise; Gastrointestinal transit; Gastrointestinal hormone
Mu ZB, Huang YX, Zhao BM, Liu ZX, Zhang BH, Wang QL. Effect of explosive noise on gastrointestinal transit and plasma levels of polypeptide hormones. *World J Gastroenterol* 2006; 12(14): 2284-2287

http://www.wjgnet.com/1007-9327/12/2284.asp

INTRODUCTION

Explosive noise may produce an adverse effect on gastrointestinal tract, and there is higher incidence of digestive system disease in war time. Current studies mainly focus on morphological changes of gastrointestinal tract[1], and there is little information available in literature about the effect of firing noise on the gastrointestinal transit. The aim of this study was to show the effects of explosive noise on gastrointestinal transit, and probe its mechanism by measuring the levels of plasma polypeptide hormones.

MATERIALS AND METHODS

Materials

Healthy SD rats were purchased from Animal Center of the Fourth Military Medical University (FMMU). The ND2 volume level meter was provided by the School of Aerospace Medicine of FMMU. Radioimmunoassay kits were supplied by Naval Radioimmunoassay Technology Center. An FJ-2003/8PS radioimmunity counter and a high-speed and low-temperature centrifuge were used in this experiment.

Experimental procedures

After an adaptive phase of 7 d, 64 SD male rats were randomly divided into 4 groups: Group A, consisting of 16 rats, which were not stimulated; Group B, which were stimulated with 40 dB noise; Group C, which were stimulated with 80 dB noise; and Group D, which were stimulated with 120 dB noise. Different groups received different intensity noise stimulations respectively. Then 8 rats of each group (including Group A) were intragastricly administrated with carbon powder suspension[2,3], anesthetized 20 min later, and then decapitated. Blood was sampled and the ratio of carbon powder suspension transmitting measured. The other 8 rats were intragastricly administrated with barium small sticks[4], anesthetized 10 h later, and decapitated. Blood was sampled in the same way and the ratio of barium sticks transmitting observed under X-ray.

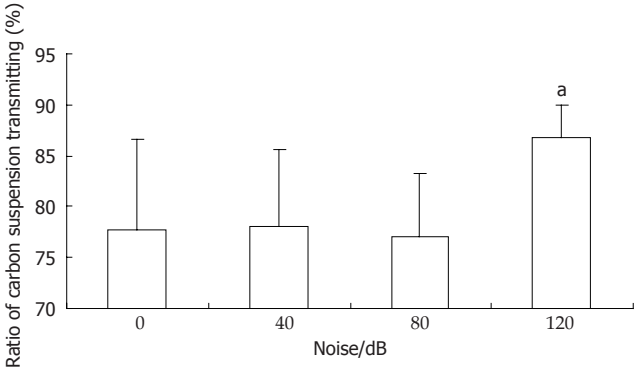

Figure 1 Effect of explosive noise on liquid substance gastrointestinal transit ($n=8$, *vs* 0 dB), $^aP<0.05$.

Noise stimulation

After 12-h abrosia, rats were put into sound-proof room. Firing noise of submachine guns acted as an inducing factor which had been recorded and was played to rats through a loudspeaker at a distance of 20-30 cm for 12 h. Examined with ND2 volume level meter and frequency spectrum analyzer, the intensity of the firing noise was measured as 0 dB (Group A), 40 dB (Group B), 80 dB(Group C) and 120 dB(Group D) respectively and their frequency as 0.25-4.00 kHz.

Liquid substance gastrointestinal transit

Rats were intragastricly administrated with 1 mL carbon powder suspension, consisting of carbon powder (50 g/L), gum arabic (100 g/L) and water(850 g/L), then anesthetized and dissected 20 min later. Small intestine was taken out of abdomen and tiled on the bench. The distance of carbon powder transmission from pyloric sphincter to the end of small intestine was measured, and the ratio of carbon powder suspension transmitting calculated [5,6] (distance of carbon powder transmission/ total length of small intestine ×100%).

Solid substance gastrointestinal transit

Rats were intragastricly administrated with 10 barium small sticks (length: 5 mm, diameter: 1 mm), then anesthetized and dissected 10 h later. The sticks were taken out of gastrointestinal tract. Barium small sticks which remained in each segment of the gastrointestinal tract were counted.

Measurement of plasma MTL, SS, VIP and SP

Rats were decapitated to sample the blood. Blood plasma was separated by centrifugation at 3500 r/min at 4 ℃, then concentrations of MTL, SS, SP and VIP were tested by radio-immunoassay[7], according to instruction of RIA kits strictly.

Statistical analysis

Analysis of variance was performed to investigate the effects of firing noise on gastrointestinal transit and plasma polypeptide hormone level in rats of four groups. All data were presented as mean ± SD. $P<0.05$ was taken as significant.

Table 1 Plasma polypeptide hormones after noise stimulation (mean ± SD, $n=8$, μg/L)

Noise/dB	MTL	SP	SS	VIP
0	128.0±5.1	52.5±20.1	184.6±49.6	254.3±129.1
40	130.6±15.6	74.4±17.4	382.8±79.1^b	471.1±145.4^a
80	133.2±30.5	86.6±15.2^b	386.6±59. 6^b	460.6±173.8^a
120	157.5±16.1^b	115.5±20.7^b	514.0±88.8^b	214.2±63.2

$^aP<0.05$. $^bP<0.01$ *vs* 0 dB(control).

RESULTS

Liquid substance gastrointestinal transit and plasma peptides levels

Ratios of carbon powder suspension transmitting in groups B and C were 78.1%±7.6% and 77.1%±6.1% respectively, and were not significantly different from that of group A (control group, 77.8%±8.8%). Ratio of carbon powder suspension transmitting in group D was 86.7%±3.3%, significantly higher than that of group A ($P<0.05$). The liquid substance gastrointestinal transit of group D (120 dB noise stimulated group) was accelerated significantly (Figure 1).

At the same time, all of the plasma MTL, SS, SP and VIP concentrations in groups B and C were increased compared with that of group A. In group D, plasma MTL, SS and SP concentrations were increased, but plasma VIP concentration decreased to some extent (Table 1). It could be seen that plasma peptides in groups B and C were increased gradually, but plasma peptides in group D were changed irregularly.

Solid substance gastrointestinal transit and plasma peptides levels

Percentage of barium sticks remained in the gastrointestinal tract in group A was 40.6%±25.4%, and that of group B was 36.9%±22.1%. There was no significant difference between groups A and B. Percentage of barium sticks remained in groups C and D was 16.2%±10.8% and 22.5%±16.1% respectively, significantly lower than that of group A(control group) ($P<0.05$) (Figure 2). There was smaller percentage of barium sticks remained in the gastrointestinal tract, indicating that barium sticks gastrointestinal transmit was faster. So the solid substance gastrointestinal transit of groups C and D (80,120 dB noise stimulated group) was accelerated.

All of the plasma peptide concentrations in group B was increased compared with that of group A. In groups C and D, plasma MTL, SS and SP concentrations were increased, but plasma VIP concentration decreased to some extent(Table 2). It could be seen that plasma peptides in group B were increased stepwise, but plasma peptides in groups C and D were irregularly disturbed.

DISCUSSION

There is a higher incidence of digestive system disease in war time than in peace time. Explosive noise is one of important factors that induce human body stress

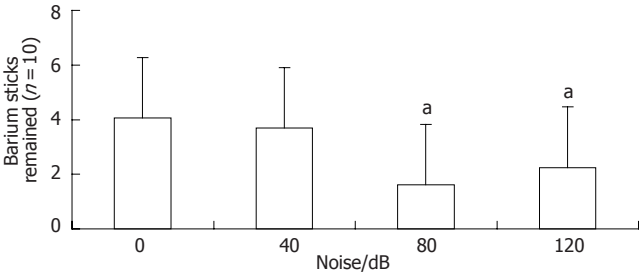

Figure 2 Effect of explosive noise on gastrointestinal transit $^{a}P<0.05$ *vs* 0 dB.

Table 2 Plasma polypeptide hormones after noise stimulation (mean ± SD, $n = 8$, μg/L)

Noise/dB	MTL	SP	SS	VIP
0	128.0±5.1	52.3±23.0	308.9±222.8	275.5±125.5
40	130.2±8.9[a]	82.6±15.7[b]	329.3±95.6	359.2±227.8
80	134.9±12.6[b]	110.3±20.0[b]	458.3±104.3[a]	251.8±97.2
120	151.9±17.1[b]	115.2±20.4[b]	503.7±65.3[b]	257.8±142.2

$^{a}P<0.05$. $^{b}P<0.01$ *vs* 0 dB (control).

in war time, and it may produce an adverse effect on gastrointestinal tract[8-10]. Liu found that explosive noise could injure gastric mucosa. Our results indicated that explosive noise could accelerate gastrointestinal transit, and that the effect was related to the intensity of the noise. There was no apparent change in gastrointestinal transit ($P>0.05$), after stimulated with lower intensity noise; however, not only solid substance but also liquid substance gastrointestinal transits were accelerated significantly ($P<0.05$), after stimulated with high level noise.

Gut hormone is a main factor in regulatory mechanism of gastrointestinal motility, and plays an important regulatory role in gastrointestinal function in stress state[11-13]. Gut hormone is generally divided into two categories, erethitic hormone and inhibitive hormone. They are contradictory regulating factors in the blood. When balance between them is lost, the disturbance of gastrointestinal motility occurs[14]. We observed plasma concentrations of two kinds of erethitic braingut peptides and two kinds of inhibitive braingut peptides, after stimulation of rats with different intensity noise, so as to probe the mechanism of explosive noise impacting gastrointestinal transit.

We found that concentrations of all four plasma peptides were increased, when rats were stimulated by low level noise, and the balance between stimulatory and inhibitory gut hormones was normal. When rats were stimulated with high level noise, three of peptides (including MTL, SS and SP) were increased in comparison with normal controls, but plasma VIP was decreased.

It is well known that MTL and SP are erethitic gut hormones. They could promote GI transit[15,16]. Our results showed that plasma MTL and SP concentration increased after stimulation with firing noise. After lower intensity sound stimulations, their plasma levels increased to some extent and after high intensity sound stimulations, their plasma levels increased obviously. In all, we found that plasma erethitic gut hormones concentration was increased and was positively correlated with intensity of noise.

SS exerts depressive effect on GI motility[17]. Previous findings showed that plasma SS level was higher in stress state[18,19]. Similarly, we found that plasma SS concentration increased along with the augmentation of the sound intensity. VIP is another kind of inhibitive gut hormone[20]. In our study, after lower intensity sound stimulation, plasma VIP concentration increased also; but it declined after stimulation by high intensity noise.

Rats, after stimulation by low intensity noise, could keep the GI transit normal, and the balance between the erethitic and inhibitive gut hormones was kept under moderate stress still, which helped to keep GI transmission function normal. At same time, we found that disturbance of GI transmission function occurred after stimulation with high intensity noise, and that the balance between the erethitic and inhibitive gut hormones was lost because of severe stress, which induced GI transmission function disorder. Therefore we presumed that changes of plasma gut hormone level were related to GI transmission function disorder induced by explosive noise and were one of the important underlying reasons.

In summary, our results indicate that explosive noise could induce stress in rats and exert some negative effect upon gastrointestinal transit. After explosive noise stimulation, secretion of many kinds of gut hormone is chaotic, which plays an important role in occurrence of gastrointestinal transmission disorder.

REFERENCES

1 **Liu GS**, Huang YX, Li SW, Pan BR, Wang X, Sun DY, Wang QL. Experimental study on mechanism and protection of stress ulcer produced by explosive noise. *World J Gastroenterol* 1998; **4:** 519-523
2 **Mittelstadt SW**, Hemenway CL, Spruell RD. Effects of fasting on evaluation of gastrointestinal transit with charcoal meal. *J Pharmacol Toxicol Methods* 2005; **52**: 154-158
3 **Lee HT**, Chung SJ, Shim CK. Small intestinal transit does not adequately represent postoperative paralytic ileus in rats. *Arch Pharm Res* 2002; **25**: 978-983
4 **Zhan SQ**, Luo JY, Gong J, Yang WD, Song CY, Wang SJ. The physiological and pathophysiological study of gastrointestinal transit time. *Xi'an Yike Daxue Xuebao* 1998; **19**: 590-592
5 **Appelbaum BD**, Holtzman SG. Restraint stress has no effect on morphine-induced inhibition of gastrointestinal transit in the rat. *Physiol Behav* 1985; **34**: 995-997
6 **Dong DL**, Wang QH, Chen W, Fan JJ, Mu JW, Ke J, Yang BF. Contrasting effects of tetraethylammonium and 4-aminopyridine on the gastrointestinal function of mice. *Eur J Pharmacol* 2005; **509**: 179-185
7 **Demling L**, Strunz U. Gastro-intestinal hormones. What remains? *Arq Gastroenterol* 1978; **15:** 130-135
8 **Al Moutaery AR**. Effect of centrophenoxine on water-immersion restraint stress- and chemically-induced gastric ulcers in rats. *Res Commun Mol Pathol Pharmacol* 2003; **113-114:** 39-56
9 **Yates DA**, Santos J, Soderholm JD, Perdue MH. Adaptation of stress-induced mucosal pathophysiology in rat colon involves opioid pathways. *Am J Physiol Gastrointest Liver Physiol* 2001; **281:** G124- G128
10 **Beglinger C**, Degen L. Role of thyrotrophin releasing hormone and corticotrophin releasing factor in stress related alterations of gastrointestinal motor function. *Gut* 2002; **51 Suppl 1:**

i45-i49
11 **Bunnett NW**. The stressed gut: contributions of intestinal stress peptides to inflammation and motility. *Proc Natl Acad Sci USA* 2005; **102**: 7409-7410
12 **Muelas MS**, Ramirez P, Parrilla P, Ruiz JM, Perez JM, Candel MF, Aguilar J, Carrasco L. Vagal system involvement in changes in small bowel motility during restraint stress: an experimental study in the dog. *Br J Surg* 1993; **80**: 479-483
13 **Fukudo S**, Suzuki J. Colonic motility, autonomic function, and gastrointestinal hormones under psychological stress on irritable bowel syndrome. *Tohoku J Exp Med* 1987; **151**: 373-385
14 **Plourde V.** Stress-induced changes in the gastrointestinal motor system. *Can J Gastroenterol* 1999; **13 Suppl A:** 26A-31A
15 **Depoortere I**, Van Assche G, Thijs T, Geboes K, Peeters TL. Differential changes in ACh-, motilin-, substance P-, and K(+)-induced contractility in rabbit colitis. *Am J Physiol* 1999; **277**: G61- G68
16 **Liu CQ**, Sun T, Li ZX, Liu ZF, Fu SF, Shen JL. Plasma polypeptide hormone levels in rats with gastric ulcer after exposure to intense noise *Zhonghua Lao Dong Wei Sheng Zhi Ye Bing Za Zhi* 2003; **21:** 48-50
17 **Eisenbraun J**, Ehrlein HJ. Effects of somatostatin on luminal transit and absorption of nutrients in the proximal gut of minipigs. *Dig Dis Sci* 1996; **41**: 894-901
18 **Gui X**, Pan G, Ke M. Potential role of gut peptides in stress-induced colonic motor disorder *Zhonghua Yi Xue Za Zhi* 1997; **77:** 31-34
19 **Wang JJ**, Huang YX, Guo QD, Qin M, Gao W, Wang QL. Protective and therapeutic effects of electroacupuncture on gastric motor disorders and acute gastric mucosal lesions under psychological stress in rats. *Disi Junyi Daxue Xuebao* 2001; **22**: 806-810
20 **Li LS**, Qu RY, Guo H, Wang W, Meng Y. Changes of SP and VIP in blood and ileum of cool stress rats. *Shoudu Yike Daxue Xuebao* 2002; **23**: 113-114

S- Editors Pan BR and Wang J **L- Editor** Zhu LH **E- Editor** Bai SH

PO Box 2345, Beijing 100023, China
www.wjgnet.com
wjg@wjgnet.com

World J Gastroenterol 2006 April 14; 12(14): 2288-2290
World Journal of Gastroenterology ISSN 1007-9327

RAPID COMMUNICATION

Assay of gastrin and somatostatin in gastric antrum tissues of children with chronic gastritis and duodenal ulcer

Xiao-Zhi Xie, Zhi-Guang Zhao, Dan-Si Qi, Zong-Min Wang

Xiao-Zhi Xie, Zhi-Guang Zhao, Dan-Si Qi, Zong-Min Wang, Department of Pathology, Children's Hospital of Wenzhou Medical College, Wenzhou 325027, Zhejiang Province, China
Correspondence to: Xiao-Zhi Xie, Pathological Department of Children's Hospital, Wenzhou Medical College, Wenzhou 325027, Zhejiang Province, China. xiaozhixie@126.com
Telephone: +86-577-88816335
Received: 2005-09-29 Accepted: 2005-11-18

Abstract

AIM: To study the expressions of gastrin (GAS) and somatostatin (SS) in gastric antrum tissues of children with chronic gastritis and duodenal ulcer and their role in pathogenic mechanism.

METHODS: Specimens of gastric antrum mucosa from 83 children were retrospectively analyzed. Expressions of GAS and SS in gastric antrum tissues were assayed by the immunohistochemical En Vision method.

RESULTS: The expressions of GAS in chronic gastritis Hp+ group (group A), chronic gastritis Hp- group (group B), the duodenal ulcer Hp+group (group C), duodenal ulcer Hp- group (group D), and normal control group (group E) were 28.50+4.55, 19.60+2.49, 22.69+2.71, 25.33+4.76, and 18.80+2.36, respectively. The value in groups A-D was higher than that in group E. The difference was not statistically significant. The expressions of SS in groups A-E were 15.47+1.44, 17.29+ 2.04, 15.30+1.38, 13.11+0.93 and 12.14+1.68, respectively. The value in groups A-D was higher than that in group E. The difference was also not statistically significant.

CONCLUSION: The expressions of GAS and SS are increased in children with chronic gastritis and duodenal ulcer.

Key words: Chronic gastritis; Duodenal ulcer; Gastrin; Somatostatin

Xie XZ, Zhao ZG, Qi DS, Wang ZM. Assay of gastrin and somatostatin in gastric antrum tissues of children with chronic gastritis and duodenal ulcer. *World J Gastroenterol* 2006; 12(14): 2288-2290

http://www.wjgnet.com/1007-9327/12/2288.asp

INTRODUCTION

Infantile chronic gastritis and peptic ulcer are frequently encountered in children. The gastroscopic diagnostic rate accounts for 85%-94.5% for chronic gastritis and 8%-22% of peptic ulcer. The causes of these diseases and pathogenic mechanisms are not completely clear. The digestive tract is the largest and most complicated secretory organ in human bodies. Gastrointestinal hormones not only play an important regulatory role in secretory and motor functions of the digestive tract, but also have an important effect on its growth, development and damage repair. It has been shown that abnormity of GAS and SS plays an important role in causing chronic gastritis and duodenal ulcer in children[1]. We examined the expression of GAS and SS in gastric antrum tissues from 83 children with chronic gastritis and duodenal ulcer using immunohistochemical method (Table 1). The changes in GAS and SS and Hp infection and their effect on chronic gastritis and duodenal ulcer in children were studied, in order to provide a theoretical basis for the gastrointestinal hormone drugs used in the treatment of chronic gastritis and duodenal ulcer in children.

MATERIALS AND METHODS

Materials

Paraffin specimens of gastric antrum mucosa were obtained from the children during the period of 2002-2003 in our hospital. All the subjects did not receive gastrointestinal kinetic drugs and H2 receptor agonists. The biopsy tissues were fixed in 10% neutral formalin, routinely dehydrolyzed, paraffin-embedded and cut into sections which were stained with HE. Hp infection was diagnosed by rapid urease test and microscopy. The cases were regarded as strongly positive when the test paper of urease test became cherry-red from yellow within 1 min, weakly positive when the test paper turned cherry-red and negative when the test paper did not change color. The weakly positive specimens were excluded from the study. Microscopy at 400 × magnification revealed positive rod-shaped bacteria in the gastric pit and body (Figure 1). A case was considered Hp+ when it was positive in the two methods and Hp- when it was negative in the two methods. The experimental samples were divided into group A: chronic superficial gastritis, Hp+; group B: chronic superficial gastritis, Hp-; group C: duodenal ulcer, Hp+; group D: duodenal ulcer, Hp-; and group E: normal gastric antrum tissues with no obvious pathologic

Table 1 Expression of GAS and SS in gastric antrum mucosa from children with chronic gastritis and duodenal ulcer (mean ± SD)

Groups	*n*	GAS	SS
Chronic gastritis Hp+ group	20	28.50±4.55	15.47±1.44
Chronic gastritis Hp- group	19	19.60±2.49	17.29±2.04
Duodenal ulcer Hp+ group	21	22.69±2.71	15.30±1.38
Duodenal ulcer Hp- group	12	25.33±4.76	13.11±0.93
Normal control group	11	18.80±2.36	12.14±1.68

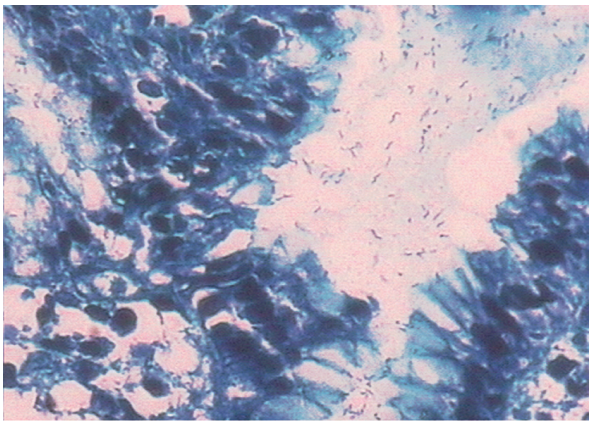

Figure 1 *Helicobacter pylori* in gastric pit (Giemasa ×400).

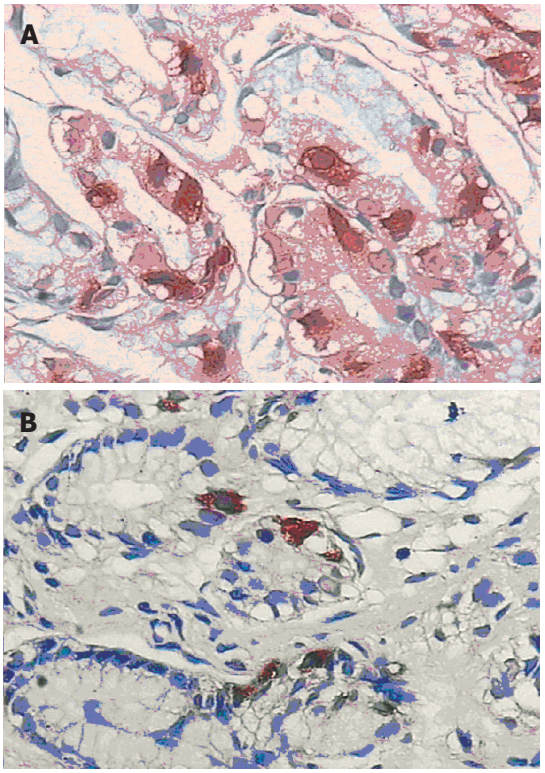

Figure 2 Expression of GAS (**A**) and SS (**B**) in glands. Brown particles were identified in cytoplasm (En Vision ×400).

changes, Hp-. Patients with other diagnoses such as chronic atrophic gastritis were excluded from the study. Thirty experimental samples were then randomly taken from each group. After specimens from patients with intestinal metaplasia or superficial specimens and very tiny specimens were excluded, the exact number of samples used in groups A-E was 20, 19, 21, 12 and 11, respectively.

Methods

Immunohistochemical method (En Vision method) was used and each paraffin sample was labeled with GAS and SS, respectively. When GAS and SS were located in cytoplasm, samples displaying brownish yellow particles or balls were regarded as positive. Positive cell bands of each sample were observed and lymph follicle areas were avoided. The number of positive cells within a sample was counted.

Statistical analysis

Statistical analysis was carried out with SPSS10.0 software package. The count of GAS and SS was in conformity with a normal distribution and expressed as mean ± SD. $P < 0.05$ was considered statistically significant.

RESULTS

GAS and SS expression was higher in groups A-D than in group E with no significant difference (Figures 2A, 2B).

DISCUSSION

GAS is a kind of peptides secreted by G cells located in the gastric antrum and duodenal mucosa, whose main function is to stimulate gastric acid secretion. It is of physiopathologic importance in occurrence of duodenal diseases. Since Levi *et al*[2] found that Hp could lead to increase in serum GAS of Hp-infected persons, a flood of studies have found that the level of serum GAS is higher in Hp positive children with chronic gastritis than in Hp negative children. After anti-Hp treatment, the level of GAS in children decreases[3]. It is held that Hp infection may lead to increase in GAS released by G cells, making damages to gastric and duodenal mucosa. Hp stimulates inflammatory cell factors such as IL-21, IL-28, TNF, IFN and G cells to release GAS[4]. SS secretion is reduced by the inhibition of D cell functions by Hp infection, which results in decrease in inhibition of G cells by SS[5]. The increased Hp level on surface of the gastric antrum by ammonia interferes with the normal feedback mechanism of inhibition of GAS secretion by acids in the stomach, which results in increase in GAS secretion. Hp or its products (ammonia or peptides) have direct effects on G cells[6]. The present study showed that the expression of GAS in chronic gastritis Hp+ group (group A) and chronic gastritis Hp- group (group B) was higher than that in the normal control group (group E) and the expression of GAS in chronic gastritis Hp+ group (group A) was higher than that in chronic gastritis Hp- group (group B), indicating that chronic inflammation, especially Hp infection, can result in increase in GAS, which may be one of the pathogenic mechanisms underlying chronic gastritis.

The causes of duodenal ulcer are associated with various factors. Digestion of local mucosal tissues by gastric acid and peptase is an important cause of ulcer occurrence. Therefore, ulcer is closely associated with

GAS. Smith *et al* [7] reported that the basal and postprandial concentrations of serum GAS are increased in adults with duodenal ulcer. Wu *et al* [8] reported that the level of serum GAS in children with duodenal ulcer was much higher than that in the control group. Increased GAS release, which results in increased secretion of gastric acid and occurrence of ulcer, is one of the mechanisms underlying duodenal ulcer in children.

SS widely exists in the gastrointestinal tract, with its highest concentration in the gastric pylorus area. D cells in the gastric pylorus secrete SS. SS has an inhibitory effect on secretion of gastrointestinal hormones such as GAS, motilin and gastric acid. Therefore, SS is regarded as a defensive factor for local mucosa.

Geller *et al*[9] showed the level of fasting serum SS was higher in DU patients than in normal persons, suggesting that the increased level of SS in DU patients is a compensatory mechanism caused by the feedback stimulation with high concentrations of acids. Lucey *et al* [10] showed hydrochloric acid can increase the level of SS in DU patients. Erton *et al*[11] found that high concentrations of acids could stimulate SS release. Mihaljevic *et al*[3] showed that the level of serum SS in Hp+ patients was lower than that in Hp- patients. Zavros *et al*[12] found that the content of SS in specimens of gastric mucosa from chronic gastritis Hp+ patients was 6 times lower than that in chronic gastritis Hp- patients. Chavialle *et al*[13] showed that the content of SS in gastric antrum mucosa of DU patients was lower than that in the control group. However, Jensen *et al* [14] reported that the content of SS in bulb mucosa of DU patients was higher than that in the control group. Therefore, the true meaning of changes in the content of SS in gastroduodenal mucosal tissues of DU patients and their role in the pathogenic mechanism of DU are unclear. The extent of various damages and regulating function may be different in human tissues during different phases. Our study showed that the number of SS positive cells in groups A-D was higher than that in group E, indicating that inflammation, especially Hp infection, can stimulate release of GAS and SS as well as secretion of gastric acid under high concentrations of acids. The reason why there was no significant difference may be the insufficient cases of experiment. Due to relatively small amount of biopsy tissues from superficial or relatively superficial mucosa and the abandoned sections whose immunohistochemical staining was not clear, the valid cases for the experiment were greatly reduced. Besides, because the size of biopsy tissues from children was smaller than that from adults, the observed number of cells was also smaller. Therefore, our studies necessitate further efforts to perfect them.

REFERENCES

1 **Haruma K**, Sumii K, Okamoto S, Yoshihara M, Sumii M, Kajiyama G, Wagner S. Helicobacter pylori infection is associated with low antral somatostatin content in young adults. Implications for the pathogenesis of hypergastrinemia. *Scand J Gastroenterol* 1995; **30:** 550-553

2 **Levi S,** Beardshall K, Haddad G, Playford R, Ghosh P, Calam J. Campylobacter pylori and duodenal ulcers: the gastrin link. *Lancet* 1989; **1:** 1167-1168

3 **Dawes C,** O'Connor AM, Aspen JM. The effect on human salivary flow rate of the temperature of a gustatory stimulus. *Arch Oral Biol* 2000; **45:** 957-961

4 **Calam J**. The somatostatin-gastrin link of Helicobacter pylori infection. *Ann Med* 1995; **27**: 569-573

5 **Sumii K,** Sumioka M, Yoshihara M, Tari A, Haruma K, Kajiyama G. Somatostatin in gastric juice in normal subjects and patients with duodenal ulcer. *Dig Dis Sci* 1992; **37**: 1020-1024

6 **DelValle J,** Yamada T. Amino acids and amines stimulate gastrin release from canine antral G-cells via different pathways. *J Clin Invest* 1990; **85:** 139-143

7 **Smith JT,** Pounder RE, Nwokolo CU, Lanzon-Miller S, Evans DG, Graham DY, Evans DJ Jr. Inappropriate hypergastrinaemia in asymptomatic healthy subjects infected with Helicobacter pylori. *Gut* 1990; **31:** 522-525

8 **Wu Xiuying**, Ou Biyou, Chen Xiaoxiao. Determination of the contents of gastrin, motilin and somatostatin in blood of DU children with chronic gastritis. *Zhonghua Erke Zazhi* 2000; **38**: 685-688

9 **Fujii M**, Shirasawa Y, Kondo S, Sawanobori K, Nakamura M. Cardiovascular effects of nipradilol, a beta-adrenoceptor blocker with vasodilating properties. *Jpn Heart J* 1986; **27:** 233-250

10 **Lucey MR**, Wass JA, Fairclough PD, O'Hare M, Kwasowski P, Penman E, Webb J, Rees LH. Does gastric acid release plasma somatostatin in man? *Gut* 1984; **25:** 1217-1220

11 **Ertan A,** Arimura A. Regulation of gastric somatostatin secretion. *Gastroenterology* 1988; **95:** 847-848

12 **Zavros Y,** Paterson A, Lambert J, Shulkes A. Expression of progastrin-derived peptides and somatostatin in fundus and antrum of nonulcer dyspepsia subjects with and without Helicobacter pylori infection. *Dig Dis Sci* 2000; **45**: 2058-2064

13 **Chayvialle JA,** Descos F, Bernard C, Martin A, Barbe C, Partensky C. Somatostatin in mucosa of stomach and duodenum in gastroduodenal disease. *Gastroenterology* 1978; **75:** 13-19

14 **Jensen SL**, Holst JJ, Christiansen LA, Shokouh-Amiri MH, Lorentsen M, Beck H, Jensen HE. Effect of intragastric pH on antral gastrin and somatostatin release in anaesthetised, atropinised duodenal ulcer patients and controls. *Gut* 1987; **28**: 206-209

S- Editor Wang J **L- Editor** Wang XL **E- Editor** Cao L

PO Box 2345, Beijing 100023, China
www.wjgnet.com
wjg@wjgnet.com

World J Gastroenterol 2006 April 14; 12(14): 2291-2292
World Journal of Gastroenterology ISSN 1007-9327

CASE REPORT

Cholelithiasis associated with haemolytic-uraemic syndrome

Deepak Kejariwal

Deepak Kejariwal, Norfolk and Norwich University Hospital, Norwich NR4 7UY, United Kingdom
Correspondence to: Dr. Deepak Kejariwal, Specialist Registrar, Gastroenterology, Norfolk and Norwich University Hospital, Norwich NR4 7UY, United Kingdom. dkejariwal@aol.com
Telephone: +44-7789774975
Received: 2005-10-16 Accepted: 2005-11-18

Abstract

Cholelithiasis occurs infrequently in the paediatric age group. Hereditary spherocytosis, sickle cell anaemia and thalassemia are the haemolytic disorders most commonly associated with development of gall stones in paediatric age group. The question is whether an isolated episode of haemolysis can cause gallstones.

Key words: Cholelithiasis; Haemolytic anaemia; Haemolytic uraemic syndrome

Kejariwal D. Cholelithiasis associated with haemolytic-uraemic syndrome. *World J Gastroenterol* 2006; 12(14): 2291-2292

http://www.wjgnet.com/1007-9327/12/2291.asp

INTRODUCTION

Haemolytic uraemic syndrome (HUS) is characterised by acute haemolytic anaemia, thrombocytopenia and acute oliguric renal failure. Often the patient has a prodrome of gastroenteritic bloody diarrhoea caused by *Escherichia coli* (*E. coli*). We report a patient who presented with biliary colic four months after recovery from HUS and her abdominal ultrasound revealed gallstones.

CASE REPORT

A 15-year-old girl presented with a 10-day history of watery diarrhoea, oliguria, haematuria and vomiting. A diagnosis of HUS was made based on renal failure, anaemia, thrombocytopenia and the presence of schistocytes on peripheral smear. Stool culture grew *E. coli* O157, phage type 21. She received packed cell transfusion, but did not need any dialysis. Following satisfactory clinical and biochemical improvement, she was discharged a week after admission. On follow-up, she was doing well.

Four months after admission, she presented with an episode of intermittent colicky right upper quadrant abdominal pain and nausea. Clinical and biochemical examination was normal. An ultrasound examination revealed marginally dilated common bile duct (diameter 9 mm) and common hepatic ducts. Gall bladder contained a small amount of sludge, but was otherwise normal. She was treated conservatively with analgesics and intravenous fluids and was doing well at discharge, a couple of days later.

She was readmitted 2 mo later for another episode of colicky right upper quadrant abdominal pain and nausea. A repeat abdominal ultrasound revealed multiple small gall bladder calculi. Rest of the ultrasound examination was normal. She had a magnetic resonance cholangiopancreatography (MRCP), which revealed a normal biliary duct and a common bile duct, besides gallstones. She had an elective laparoscopic cholecystectomy 6 wk later. Multiple pigment gallstones were found. On follow-up, she remained asymptomatic and was doing well.

DISCUSSION

Gallstones are classified into three types according to their chemical composition, namely cholesterol, pigment and mixed stones. Mixed and cholesterol gallstones usually contain more than 70% cholesterol monohydrate plus an admixture of calcium salts, bile acids and bile pigments, proteins, fatty acids and phospholipids. Pigment stones are composed primarily of calcium bilirubinate containing less than 10% cholesterol.

Although cholelithiasis occurs infrequently in the paediatric age group, its incidence has increased during the last few decades. The reason why gall stones are not considered as a possible cause of jaundice or right upper quadrant discomfort in the past is the emphasis placed on the belief that haemolytic disease is a necessary prerequisite for gall stone formation in children[1].

Currently only about 20% of cholelithiasis cases in children are attributed to haemolytic conditions. Hereditary spherocytosis, sickle cell anaemia and thalassemia are the haemolytic disorders most commonly associated with development of gall stones. The question is whether an isolated episode of haemolysis can cause gallstones. The answer is yes because there are many reports in the literature.[2, 3] while the answer is no because none of the textbooks mentions it as a cause of gallstones. Hence, there is relatively low awareness that self-limiting haemolytic episodes can predispose to gall stones.

There are a few case reports of gall stones associated with HUS[2, 3]. Brandt *et al*[4] reported a high incidence of

gastrointestinal sequelae following typical HUS. Cholelithiasis might be related to haemolysis during the acute phase of HUS leading to pigment gall stones or to the use of parenteral nutrition. Parenteral nutrition was not used in the case presented.

In conclusion, neither is cholelithiasis mentioned as a complication of the HUS, nor is an acute haemolytic process listed as aetiology of gallstones. But gallstones should be suspected in both settings. An abdominal ultrasound examination can easily and readily confirm the diagnosis.

REFERENCES

1 **Holcomb GW Jr**, Holcomb GW 3rd. Cholelithiasis in infants, children, and adolescents. *Pediatr Rev* 1990; **11**: 268-274
2 **Schweighofer S Jr**, Primack WA, Slovis TL, Fleischmann LE, Slovis TL, Hight DW. Cholelithiasis associated with the hemolytic-uremic syndrome. *Am J Dis Child* 1980; **134:** 622
3 **Parida SK**, Hollman AS, Beattie TJ. Cholelithiasis associated with hemolytic uremic syndrome. *Clin Nephrol* 1991; **35**: 86
4 **Brandt JR**, Joseph MW, Fouser LS, Tarr PI, Zelikovic I, McDonald RA, Avner ED, McAfee NG, Watkins SL. Cholelithiasis following Escherichia coli O157:H7-associated hemolytic uremic syndrome. *Pediatr Nephrol* 1998; **12**: 222-225

S- Editor Wang J **L- Editor** Wang XL **E- Editor** Cao L

PO Box 2345, Beijing 100023, China
www.wjgnet.com
wjg@wjgnet.com

World J Gastroenterol 2006 April 14; 12(14): 2293-2296
World Journal of Gastroenterology ISSN 1007-9327

CASE REPORT

Extended surgical resection for xanthogranulomatous cholecystitis mimicking advanced gallbladder carcinoma: A case report and review of literature

Antonino Spinelli, Guido Schumacher, Andreas Pascher, Enrique Lopez-Hanninen, Hussain Al-Abadi, Christoph Benckert, Igor M Sauer, Johann Pratschke, Ulf P Neumann, Sven Jonas, Jan M Langrehr, Peter Neuhaus

Antonino Spinelli, Guido Schumacher, Andreas Pascher, Hussain Al-Abadi, Christoph Benckert, Igor M Sauer, Johann Pratschke, Ulf P Neumann, Sven Jonas, Jan M Langrehr, Peter Neuhaus, Department of General, Visceral and Transplantation Surgery, Charitè-Universitatsmedizin Berlin, Campus Virchow Klinikum, Augustenburger Platz 1, 13353 Berlin, Germany
Enrique Lopez-Hanninen, Department of Radiology, Charitè-Universitatsmedizin Berlin, Campus Virchow Klinikum, Augustenburger Platz 1, 13353 Berlin, Germany
Correspondence to: Antonino Spinelli, MD, Department of General, Visceral and Transplantation Surgery, Charitè-Universitatsmedizin Berlin, Campus Virchow Klinikum, Augustenburger Platz 1, 13353 Berlin, Germany. antoninospinelli@email.it
Telephone: +49-30-450552001 Fax: +49-30-450552900
Received: 2005-09-02 Accepted: 2005-11-18

Abstract

Xanthogranulomatous cholecystitis (XGC) is a destructive inflammatory disease of the gallbladder, rarely involving adjacent organs and mimicking an advanced gallbladder carcinoma. The diagnosis is usually possible only after pathological examination. A 46 year-old woman was referred to our center for suspected gallbladder cancer involving the liver hilum, right liver lobe, right colonic flexure, and duodenum. Brushing cytology obtained by endoscopic retrograde cholangiography (ERC) showed high-grade dysplasia. The patient underwent an en-bloc resection of the mass, consisting of right lobectomy, right hemicolectomy, and a partial duodenal resection. Pathological examination unexpectedly revealed an XGC. Only six cases of extended surgical resections for XGC with direct involvement of adjacent organs have been reported so far. In these cases, given the possible coexistence of XGC with carcinoma, malignancy cannot be excluded, even after cytology and intraoperative frozen section investigation. In conclusion, due to the poor prognosis of gallbladder carcinoma on one side and possible complications deriving from highly aggressive inflammatory invasion of surrounding organs on the other side, it seems these cases should be treated as malignant tumors until proven otherwise. Clinicians should include XGC among the possible differential diagnoses of masses in liver hilum.

Key words: Xanthogranulomatous cholecystitis; Gallbladder cancer; Gallbladder carcinoma

Spinelli A, Schumacher G, Pascher A, Lopez-Hanninen E, Al-Abadi H, Benckert C, Sauer IM, Pratschke J, Neumann UP, Jonas S, Langrehr JM, Neuhaus P. Extended surgical resection for xanthogranulomatous cholecystitis mimicking advanced gallbladder carcinoma: A case report and review of literature. *World J Gastroenterol* 2006; 12(14): 2293-2296

http://www.wjgnet.com/1007-9327/12/2293.asp

INTRODUCTION

The term xanthogranulomatous cholecystitis (XGC) describes a rare inflammatory lesion of the gallbladder, characterized by marked proliferative fibrosis and infiltration of macrophages and foam cells involving the wall of the gallbladder[1]. Although a fair number of cases of this pathological condition have already been described, so far very few reports have described XGC with aggressive tumor-like inflammation pattern directly involving adjacent structures and organs[2-7].

We herein report a case of XGC presenting as advanced gallbladder carcinoma with involvement of liver, common bile duct, duodenum and transverse colon, review the characteristics of patients with XGC involving adjacent organs who underwent extended surgery, and discuss the different diagnostic and surgical options in cases of massive extra-gallbladder involvement.

CASE REPORT

A 46-year-old woman with no prior medical history was admitted to a local hospital due to progressively increasing upper abdominal discomfort for some weeks, lately associated with jaundice. No weight loss was reported. No mass was palpable at the physical examination. Ultrasound showed a gallbladder hydrops with gallstone in the infundibulum and bilateral dilation of intrahepatic bile ducts. An endoscopic retrograde cholangiography (ERC) demonstrated a filiform stenosis of the proximal common bile duct and the bifurcation with upstream intrahepatic bile duct dilation, and no visualisation of cystic duct and

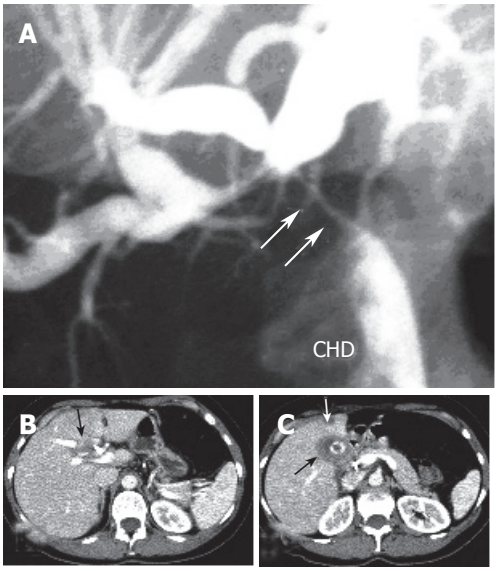

Figure 1 Proximal obstruction (arrows) of the common hepatic bile duct (CHD) with upstream dilatation of both left and right intrahepatic bile ducts (**A**), a soft tissue mass at the hepatic hilum (**B**), and thickened gallbladder wall (black arrow) with a concretion and hepatic lesion in liver segment 4 (**C**).

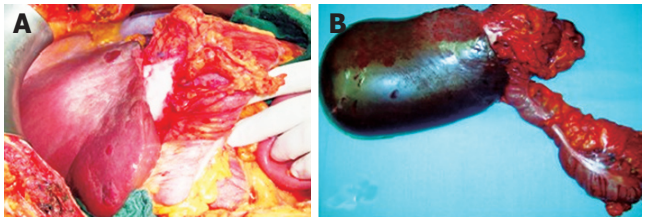

Figure 2 Intraoperative finding in situ (**A**) and surgical specimen ex situ (**B**).

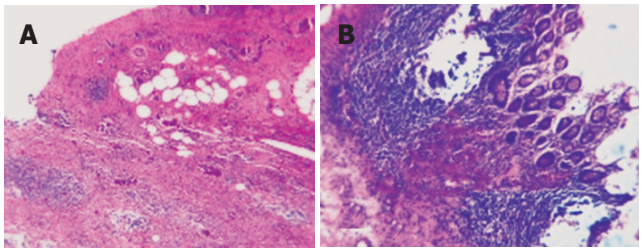

Figure 3 Xanthogranulomatous cholecystitis (**A**) and xanthogranulomatous cholecystitis involving the wall of the transverse colon (**B**). There is destruction of the submucosa and muscular coat of the transverse colon by extensive macrophage infiltrates, the mucosa is intact and exhibits no cellular atypia (HE, 200x).

gallbladder. A complete sphincterotomy was performed with insertion of an internal stent draining the left main bile duct. Magnetic resonance imaging (MRI) confirmed the presence of a hilar mass with two liver lesions in the right lobe of the liver, suspicious of metastases. MRI-vascular reconstruction excluded an infiltration of the portal vein and the hepatic artery. The patient was then transferred to our clinic with the diagnosis of advanced gallbladder cancer with differential diagnosis from Mirizzi's syndrome type I (i.e., secondary stenosis of the common hepatic duct caused by inflammatory fusion of gallbladder infundibulum and common bile duct due to gallstone impaction, without presence of a fistula). On admission to our centre, the patient was icteric after internal drainage of the left and common bile duct. Serum concentrations of total bilirubin (4.2 mg/dL, ref <1.1 mg/dL), alkaline phosphatase (325 U/L, ref <170 U/L), gamma glutamyl transpeptidase (55 U/L, ref <18 U/L), were all elevated. The tumor marker carbohydrate antigen 19-9 (CA19-9) was 42 U/mL (ref <33 U/mL) while carcinoembryonic antigen (CEA) was normal. We repeated ERC (Figure 1A) to attain cytological material and removed the internal stent. Brushing cytology revealed atypical epithelial cells with high-grade dysplasia. Computed tomography (CT-scan) with liver volumetry (Figures 1B, 1C) confirmed the presence of two hypodense lesions in the right liver lobe, suspicious of metastases, already detected by the MRI performed in the first hospital. Clinical, serological, cytological and imaging data were highly indicative of malignancy. Surgical exploration confirmed the diagnostic findings (Figure 2A): the mass completely involved the hepatic hilum, the transverse colon and the second duodenal portion, seeming to originate from the gallbladder bed, since the gallbladder itself was not distinguishable from the surrounding inflammatory tissue. The preoperatively suspected liver metastases were intraoperatively identified as hemangiomas. Assuming an advanced gallbladder carcinoma, we performed an anatomic right lobectomy en-bloc with gallbladder and extrahepatic bile duct resection, segmental duodenal resection, right hemicolectomy and partial omentectomy. Reconstruction was achieved by a hepaticojejunostomy protected by transhepatic drainage through the left biliary system, and an ileotransversostomy. Gross examination of the specimen (Figure 2B) demonstrated a bright white, hard mass, inseparable from the adjacent structures. A 2.5 cm × 3 cm × 2.5 cm biliary stone was packed in the infundibulum of the gallbladder. Histological examination unexpectedly revealed a xanthogranulomatous cholecystitis (Figure 3A), with tumor-like inflammatory tissue invading the liver as well as the proximal common bile duct, the right flexure of the colon (Figure 3B) and the second duodenal portion, with no evidence of malignancy.

The postoperative course was completely uneventful and the patient was discharged on the 15th postoperative day. One year after surgery, the patient was asymptomatic and in good health.

DISCUSSION

XGC is found after approximately 1.46% of cholecystectomies and affects men and women equally[8], almost always in presence of gallstones (91%-100%)[1]. Even if aetiology is unknown, some authors suggest that in the presence of gallstones, obstruction, and cholestasis, XGC results from the extravasation of bile into the gallbladder wall. With involvement of Rokitansky-Aschoff sinuses[8], the process is supposed to start as an initial inflammatory process, followed by a granulomatous reaction, similarly to the aetiopathogenesis of xanthogranulomatous pyelonephritis, in which chronic infection and calculi are common findings. Macroscopically, XGC is characterized by formation of multiple yellowish nodules within the gallbladder wall. Histologically, abundant so-called foam-cells (histiocytes)

Table 1 Characteristics of the patients with XGC who underwent extended surgical resections

Author Year	Age (Sex)	Symptoms	Tumor markers	Involvement of	Performed resection	Follow-up
Okamoto 1990	70 (F)	Fever, general malaise	CA19.9 ↑, CEA normal	Liver, bile duct, transverse colon	Cholecystectomy, local atypical liver resection, bile duct resection and transverse colectomy	Uncomplicated postoperative course, alive 6 mo after surgery
Maeda 1994	75 (F)	No complaints	CA19.9 ↑, CEA normal	Liver bed and transverse colon	Cholecystectomy with local atypical liver resection and transverse colectomy	Uncomplicated postoperative course, follow-up not reported
Furuta 1996	46 (M)	Epigastric pain	CA19.9 and CEA normal	Liver, bile duct, duodenum, right hepatic artery, right portal vein	Right hepatectomy and pancreatoduodenectomy	-
Natori 1997	55 (M)	No complaints	CA19.9 normal, CEA ↑	Liver (gallbladder bed) and bile duct	Cholecystectomy with local atypical liver resection and bile duct resection	-
Enomoto 2003	64 (M)	High fever, hypochondralgia	CA19.9 and CEA normal	Liver, bile duct, duodenum, transverse colon, right hepatic artery and right portal vein	Right hepatectomy, pancreatoduodenectomy and transverse colectomy	Uncomplicated postoperative course, alive 4 yr after surgery
Pinocy 2003	64 (M)	Hypochondralgia, fever	-	Right colonic flexure	Cholecystectomy and resection of the right colonic flexure	-
Present case 2005	46 (F)	Epigastric pain, sense of fullness, jaundice	CA19.9 ↑, CEA normal	Right liver, right colonic flexure, second duodenal portion	Right hepatectomy, partial duodenectomy and right hemicolectomy	Uncomplicated postoperative course, alive 1 yr after surgery

are mixed with chronic and acute inflammatory cells[9]. With regard to imaging of a liver hilar mass, ultrasound, CT, MRI and ERC can be considered. In the case of XGC, ultrasound can detect focal or diffuse thickening of the hyperechoic gallbladder wall[10] with the presence of characteristic intraluminal hypoechoic nodules in 35-73% of the cases[11]. Other commonly reported findings are cholecystitis-like fluid collections near the gallbladder and dilation of intra- and extra hepatic bile ducts in case of choledocolithiasis. Chun *et al*[12] analyzed CT-patterns of XGC in a series of patients, with emphasis on differential diagnosis of gallbladder carcinoma and stated that intramural hypodense nodules occur more often in XGC than in cancer patients. However, these characteristic findings are inconstant in patients with XGC, as highlighted by more recent studies[11, 13-14]. Visualisation of the biliary anatomy through direct (percutaneous or endoscopic) cholangiography or magnetic resonance cholangiopancreatography (MRCP) is particularly important if a direct involvement of the common bile duct is suspected. Furthermore, ERC allows brushing cytology. The potential role of positron emission tomography in the differential diagnosis of cholecystitis from gallbladder carcinoma is unclear, because only a few studies in small series are available up to now[15,16] with a patient with XGC being the only false positive case in one study[15].

Concerning tumor markers, our patient had only a slightly elevated (42 U/mL) serum level of CA 19.9 (reference = 33 U/mL), which persisted even after resolution of jaundice through placement of an endoscopic stent preoperatively. Adachi *et al*[17] argued that serum-CA 19.9 may be elevated even greatly in both carcinoma and XGC patients, thus being not helpful in the differential diagnosis between the two conditions. Even in cases of XGC with extended involvement of other organs[3,5] elevations of tumor markers concentrations (CA 19.9, CEA) are inconsistent.

Although XGC is not an exceptional finding, a direct involvement of extra-gallbladder organs and structures is very rare. To the best of our knowledge, only six cases of extended surgical resections for XGC have been reported so far. In these cases (Table 1), additional procedures such as bile duct resections, segmental resections of colon or duodenum, partial pancreatoduodenectomies have been performed. It can be discussed if such extended surgical procedures could be avoided in presence of a benign disease. Our patient exhibited severe, destructive, tumor-like xanthogranulomatous inflammation, with extensive invasion of adjacent organs (right lobe of the liver, extrahepatic bile ducts, colon and duodenum). The clinical and radiological findings were suggestive of a gallbladder carcinoma. ERC was indicative of hilar cholangiocarcinoma (Klatskin tumor). However, after confrontation with CT findings (gallbladder hydrops, gallbladder wall thickened over 1.8 cm, presence of suspect lesions in the right liver lobe, suspected infiltration of adjacent organs- all uncharacteristic findings in cases of Klatskin tumors), the most probable diagnosis was a locally advanced gallbladder cancer, with infiltration of the proximal common bile duct and the bile duct bifurcation. In addition, cytology obtained during ERC showed high-grade dysplasia and CA 19.9 was slightly but persistently elevated after stenting. Under these conditions, a radical resection of the mass was the only reasonable option. According to the published data on gallbladder cancer and hilar cholangiocarcinoma, radical surgery offers the only chance to achieve long-term survival[18-23]. The necessity of radical surgery in those cases of XGC with extensive extra-gallbladder involvement is not cleared. We agree with Houston *et al*[24] emphasizing the necessity of a complete resection of the involved structures in order to treat symptoms like jaundice and cholangitis and to prevent possible complications like bowel obstruction and perforation, potentially life threatening.

Intraoperative frozen section investigation or fine needle aspiration cytology has been suggested to confirm the

diagnosis. In cases with no invasion of adjacent organs these tools are indicated because they can change the surgical strategy (e.g, simple cholecystectomy versus associated liver resection). Nevertheless, in cases of extensive invasion of other organs, like in our patient, it can not alter our approach. Even in the case of a negative or inconclusive result, radical surgery can be performed since gallbladder carcinoma and XGC may coexist [24-26] and the patient had jaundice and cholangitis, which needed a treatment. Furthermore, even assuming an advanced gallbladder carcinoma, we believe it is essential to minimize the intraoperative tumor cell spread by avoiding any unneeded manipulation or dissection in the liver hilum.

Two different risks are linked to misjudgement of this pesudotumoral condition. On the one hand, excessive surgical resection is inevitably linked with a certain perioperative mortality and morbidity. On the other hand, this condition may be misinterpreted as not being radically operable. Especially in this latter case, before deciding for inoperability, it is essential to gain specimens for frozen section biopsy.

In conclusion, preoperative or intraoperative differential diagnosis of XGC from gallbladder carcinoma remains a challenge, especially in patients with extensive pseudotumoral involvement of surrounding structures and organs. From our point of view, radical resection is mandatory as long as malignancy can not be ruled out after a complete preoperative diagnostic examination. Preoperative fine needle aspiration biopsy and intraoperative frozen section are valuable tools for differential diagnosis when there is no invasion of adjacent organs, otherwise they would not influence the surgical strategy. The presence of symptoms such as jaundice and cholangitis, as well as the potential risk of life-threatening complications like bowel obstruction and subsequent perforation, supports a radical surgical approach.

REFERENCES

1 **Kwon AH**, Matsui Y, Uemura Y. Surgical procedures and histopathologic findings for patients with xanthogranulomatous cholecystitis. *J Am Coll Surg* 2004; **199**: 204-210
2 **Furuta A**, Ishibashi T, Takahashi S, Sakamoto K. MR imaging of xanthogranulomatous cholecystitis. *Radiat Med* 1996; **14**: 315-319
3 **Enomoto T**, Todoroki T, Koike N, Kawamoto T, Matsumoto H. Xanthogranulomatous cholecystitis mimicking stage IV gallbladder cancer. *Hepatogastroenterology* 2003; **50**: 1255-1258
4 **Pinocy J**, Lange A, Konig C, Kaiserling E, Becker HD, Krober SM. Xanthogranulomatous cholecystitis resembling carcinoma with extensive tumorous infiltration of the liver and colon. *Langenbecks Arch Surg* 2003; **388**: 48-51
5 **Maeda T**, Shimada M, Matsumata T, Adachi E, Taketomi A, Tashiro Y, Tsuneyoshi M, Sueishi K, Sugimachi K. Xanthogranulomatous cholecystitis masquerading as gallbladder carcinoma. *Am J Gastroenterol* 1994; **89**: 628-630
6 **Natori S,** Takimoto A, Endoh K, Ishikawa T, Yamaguchi S, Fjii Y, Takahashi T, Takeda K, Watarai S, Nakano A, Kitamura H, Shimada H. A case of xanthogranulomatous cholecystitis difficult to be differentiated from gallbladder cancer. *Tann to Sui* 1997; **18**: 593-596.
7 **Okamoto S,** Konan T, Yamaguchi K, Nakamura K, Maeda S, Kitamura K. Xanthogranulomatous cholecystitis masquerading as gallbladder carcinoma. *Tann to Sui* 1990; **11**: 1415-1419
8 **Guzman-Valdivia G**. Xanthogranulomatous cholecystitis: 15 years' experience. *World J Surg* 2004; **28**: 254-257
9 **Fligiel S**, Lewin KJ. Xanthogranulomatous cholecystitis: case report and review of the literature. *Arch Pathol Lab Med* 1982; **106**: 302-304
10 **Muguruma N**, Okamura S, Okahisa T, Shibata H, Ito S, Yagi K. Endoscopic sonography in the diagnosis of xanthogranulomatous cholecystitis. *J Clin Ultrasound* 1999; **27**: 347-350
11 **Parra JA**, Acinas O, Bueno J, Guezmes A, Fernandez MA, Farinas MC. Xanthogranulomatous cholecystitis: clinical, sonographic, and CT findings in 26 patients. *Am J Roentgenol* 2000; **174**: 979-983
12 **Chun KA**, Ha HK, Yu ES, Shinn KS, Kim KW, Lee DH, Kang SW, Auh YH. Xanthogranulomatous cholecystitis: CT features with emphasis on differentiation from gallbladder carcinoma. *Radiology* 1997; **203**: 93-97
13 **Vetto RM,** Burger DR, Nolte JE, Vandenbark AA, Baker HW. Transfer factor therapy in patients with cancer. *Cancer* 1976; **37:** 90-97
14 **Iannicelli E**, Rossi G, Almberger M, Salvi PF, David V. A case of xanthogranulomatous cholecystitis: integrated US-CT imaging. *Radiol Med* (Torino) 2002; **104:** 106-110
15 **Koh T**, Taniguchi H, Yamaguchi A, Kunishima S, Yamagishi H. Differential diagnosis of gallbladder cancer using positron emission tomography with fluorine-18-labeled fluorodeoxyglucose (FDG-PET). *J Surg Oncol* 2003; **84**: 74-81
16 **Holmberg L**, Ekbom A, Zack M. Do screening-detected invasive breast cancers have a natural history of their own? *Eur J Cancer* 1992; **28A**: 920-923
17 **Adachi Y**, Iso Y, Moriyama M, Kasai T, Hashimoto H. Increased serum CA19-9 in patients with xanthogranulomatous cholecystitis. *Hepatogastroenterology* 1998; **45**: 77-80
18 **Kokudo N,** Makuuchi M, Natori T, Sakamoto Y, Yamamoto J, Seki M, Noie T, Sugawara Y, Imamura H, Asahara S, Ikari T. Strategies for surgical treatment of gallbladder carcinoma based on information available before resection. *Arch Surg* 2003; **138:** 741-750; discussion 750
19 **Dixon E**, Vollmer CM Jr, Sahajpal A, Cattral M, Grant D, Doig C, Hemming A, Taylor B, Langer B, Greig P, Gallinger S. An aggressive surgical approach leads to improved survival in patients with gallbladder cancer: a 12-year study at a North American Center. *Ann Surg* 2005; **241**: 385-394
20 **Neuhaus P**, Jonas S, Settmacher U, Thelen A, Benckert C, Lopez-Hanninen E, Hintze RE. Surgical management of proximal bile duct cancer: extended right lobe resection increases resectability and radicality. *Langenbecks Arch Surg* 2003; **388**: 194-200
21 **Behari A**, Sikora SS, Wagholikar GD, Kumar A, Saxena R, Kapoor VK. Longterm survival after extended resections in patients with gallbladder cancer. *J Am Coll Surg* 2003; **196**: 82-88
22 **Capildeo R,** Court C, Rose FC. Social network diagram. *Br Med J* 1976; **1:** 143-144
23 **Kondo S**, Nimura Y, Kamiya J, Nagino M, Kanai M, Uesaka K, Hayakawa N. Mode of tumor spread and surgical strategy in gallbladder carcinoma. *Langenbecks Arch Surg* 2002; **387**: 222-228
24 **Houston JP**, Collins MC, Cameron I, Reed MW, Parsons MA, Roberts KM. Xanthogranulomatous cholecystitis. *Br J Surg* 1994; **81**: 1030-1032
25 **Goodman ZD**, Ishak KG. Xanthogranulomatous cholecystitis. *Am J Surg Pathol* 1981; **5**: 653-659
26 **Lopez JI**, Elizalde JM, Calvo MA. Xanthogranulomatous cholecystitis associated with gallbladder adenocarcinoma. A clinicopathological study of 5 cases. *Tumori* 1991; **77**: 358-360

S- Editor Guo SY **L- Editor** Wang XL **E- Editor** Cao L

PO Box 2345, Beijing 100023, China
www.wjgnet.com
wjg@wjgnet.com

World J Gastroenterol 2006 April 14; 12(14): 2297-2300
World Journal of Gastroenterology ISSN 1007-9327

CASE REPORT

Development of multiple myeloma in a patient with chronic hepatitis C: A case report and review of the literature

Peter Laszlo Lakatos, Sandor Fekete, Margit Horanyi, Simon Fischer, Margit E Abonyi

Peter Laszlo Lakatos, Simon Fischer, Margit E Abonyi, 1st Department of Medicine Semmelweis University, Budapest, Hungary
Sandor Fekete, Department of Hematology, Szent Laszlo Hospital, Budapest, Hungary
Margit Horanyi, Virus Laboratory,OGYK, Budapest, Hungary
Correspondence to: Peter Laszlo Lakatos, MD, PhD, 1st Department of Medicine, Semmelweis University, Koranyi str. 2/A, H-1083, Hungary. kislakpet@bel1.sote.hu
Telephone: +36-1-9117727 Fax: +36-1-3130250
Received: 2005-10-07 Accepted: 2005-11-10

Key words: HCV; Multiple myeloma; Non-Hodgkin Lymphoma; Extrahepatic manifestation

Lakatos PL, Fekete S, Horanyi M, Fischer S, Abonyi ME. Development of multiple myeloma in a patient with chronic hepatitis C: A case report and review of the literature. *World J Gastroenterol* 2006; 12(14): 2297-2300

http://www.wjgnet.com/1007-9327/12/2297.asp

Abstract

An association between chronic hepatitis C virus (HCV) infection and essential mixed cryoglobulinaemia and non-Hodgkin lymphoma (NHL) has been suggested. However, a causative role of HCV in these conditions has not been established. The authors report a case of a 50 year-old woman with chronic hepatitis C (CHC) who has been followed up since 1998 due to a high viral load, genotype 1b and moderately elevated liver function tests (LFTs). Laboratory data and liver biopsy revealed moderate activity (grade: 5/18, stage: 1/6). In April 1999, one-year interferon therapy was started. HCV-RNA became negative with normalization of LFTs. However, the patient relapsed during treatment. In September 2002, the patient was admitted for chronic back pain. A CT examination demonstrated degenerative changes. In March 2003, multiple myeloma was diagnosed (IgG-kappa, bone marrow biopsy: 50% plasma cell infiltration). MRI revealed a compression fracture of the 5th lumbar vertebral body and an abdominal mass in the right lower quadrant, infiltrating the canalis spinalis. Treatment with vincristine, adriamycin and dexamethasone (VAD) was started and bisphosphonate was administered regularly. In January 2004, after six cycles of VAD therapy, the multiple myeloma regressed. Thalidomide, as a second line treatment of refractory multiple myeloma (MM) was initiated, and followed by peginterferon-α2b and ribavirin against the HCV infection in June. In June 2005, LFTs returned to normal, while HCV-RNA was negative, demonstrating an end of treatment response. Although a pathogenic role of HCV infection in malignant lymphoproliferative disorders has not been established, NHL and possibly MM may develop in CHC patients, supporting a role of a complex follow-up in these patients.

INTRODUCTION

Numerous clinical syndromes have been reported in association with hepatitis C virus (HCV) infection. Some are well established while others remain a speculation (Table 1)[1], Fourteen to seventy percent of patients with HCV have detectable cryoglobulins in their serum even in the absence of rash, weakness or arthralgias[1], whereas 50-90% of patients with mixed cryoglobulinaemia are reported to have HCV infection[2]. It is suggested that approximately 10% of type II mixed cryoglobulinaemiae can evolve into malignant lymphoma several years after diagnosis.

Epidemiological studies from Europe, Japan and North America also implicate that HCV plays a role in the pathogenesis of non-Hodgkin lymphomas (NHL)[3-7]. HCV infection is detectable in a significant proportion of NHL (14%-52%), nonetheless, it has not been confirmed[8]. A 50-fold elevation in the risk for NHL of the liver or salivary glands has been reported in an Italian case-control study, which is greater than the relative risk of hepatocellular carcinoma. The relative risk for NHL of other sites is increased about 4-fold[9]. An association between multiple myeloma (MM) and chronic HCV infection has been suggested by some epidemiological studies[2,9].

CASE REPORT

The authors report a case of a 50 year-old woman with chronic HCV infection who has been followed up since 1998 due to high viral load (13.47 MEq/mL), genotype 1b and moderately elevated liver function tests (LFTs). The patient received treatment of chronic backache and tonsillectomy prior to admission to our hospital. Laboratory data and liver biopsy revealed moderate activity (grade 5/18, stage I). In April 1999, one-year interferon therapy (3x3ME/wk) was initiated. HCV-RNA became negative with normalization of the LFTs. However, the

Table 1 Extrahepatic diseases associated with hepatitis C virus infection

Association: strong	Intermediate	Weak
-Cryoglobulinemic syndrome (Cutaneous leukocytoclastic vasculitis, arthritis, weakness) -Renal disease (membranoproliferative glomerulo- nephritis) -Peripheral neuropathy -Non-Hodgkin lymphoma -Sjörgen's syndrome	-Porphyria cutanea tarda -Diabetes	-Thyroid disease -Corneal ulcers -Lichen planus -Pulmonary fibrosis

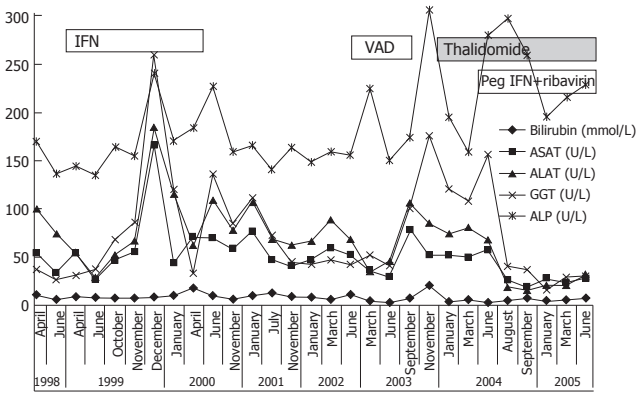

Figure 1 Liver function tests from April 1998 to July 2005.

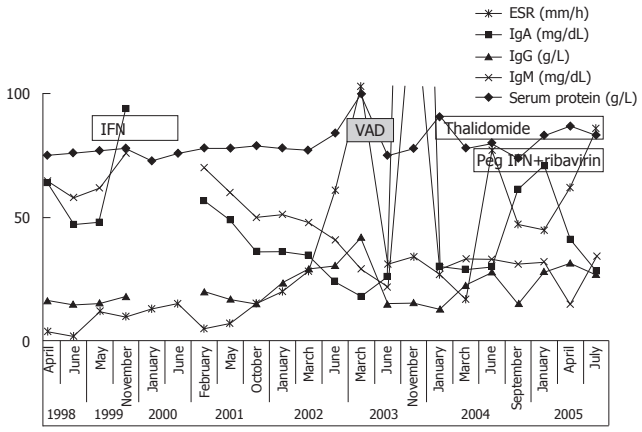

Figure 2 ESR and serum immunoglobulin levels from April 1998 to July 2005.

patient relapsed in the 7th mo of treatment (HCV-RNA became positive, LFTs increased). The liver function tests are summarized in Figure 1. In February 2000, hypothyroidism was diagnosed, substitution was initiated and follow-up was scheduled.

In September 2002, the patient was admitted for chronic backpain. CT examination revealed degenerative changes of the 5th lumbar vertebral body. Subsequently, the patient was not monitored until March 2003, when she was again hospitalized due to chronic backache and weakness of the right lower limb. Based on laboratory results, IgG-κ multiple myeloma was diagnosed (erythrocyte sedimentation rate; ESR): 104 mm/h, IgA: 0.18 g/L, IgG: 41.86 g/L, IgM: 0.29 g/L and 12.8% M-component on serum immunoelectrophoresis; bone marrow biopsy: 50% plasma cell infil). Mixed cryoglobulins were detected in the serum. Anemia, low platelet count or hypercalcaemia did not occur during follow-up. Serum IgG was elevated from 1998. However, monoclonality was not detected prior to March 2003. The serum immunoglobulin data and ESR are presented in Figure 2. MRI revealed a compression fracture of the 5th lumbar vertebral body and an abdominal mass in the right lower quadrant, infiltrating the canalis spinalis, ileum and sacroiliac joint (osteolytic lesions).

An aggressive treatment regimen was implemented with vincristine, adriamycin and dexamethasone (VAD). From April to October 2003, she received six cycles of VAD therapy followed by multiple myeloma's regression. The presence of compression fracture also prompted the regular adminis of bisphosphonate (Aredia). In January 2004, 22.2% M-components were detected by immunoelectrophoresis, yet the ESR was normal (17mm/h). Methyl prednisolone (100 mg b.i.d) and cytoxane (100 mg o.d.) p.o. therapy was started.

In April 2004, she was admitted to the Haematological Department for paraparesis. Laminectomy (Th VII-IX) with myelin decompression and tumor resection was performed. Therapy was amended with thalidomide (100mg o.d.) orally. In August, repeated CT scans demonstrated compression fractures at L5 and S2 accompanying narrowing of the spinal canal at L5. In September, due to worsening of the paraparesis, a second laminectomy was performed (L5-S1) followed by insertion of a stabilizing prosthesis (L4-S1).

In June 2004, weekly peginterferon-α2b (1.5 μg/kg) and 800 mg ribavirin (daily) were prescribed (HCV PCR 145000 IU/mL, Roche TaqMan). No further dose adjustment was necessary. The LFTs became normal and PCR returned negative after three months of therapy, indicating an early viral response (EVR). In June 2005, the LFTs were normal with a negative HCV-PCR, demonstrating an end of treatment response (ETR).

DISCUSSION

In recent years, major advances have been made in the treatment of HCV infection with the sustained response rate of 52%-63% achieved[11-13]. A major disadvantage in Hungary is that the hard-to-treat genotype 1 is almost universal (90%-95%) and occurs much more frequently compared to that in other European countries[13, 14].

Apart from hepatocellular carcinoma, HCV infection is also associated with various extrahepatic diseases, including mixed cryoglobulinaemia and NHL. Fourteen to seventy percent of patients with HCV have detectable cryoglobulins in their serum[1, 2], while 50%-90% of patients with mixed cryoglobulinaemia are reported to have HCV infection.

Epidemiological case-control studies from the 1990s suggest that chronic HCV infection is associated with the development of NHL. It was reported that 9% and 11.5% of NHL patients are HCV-antibody positive[15,16]. Germanidis *et al*[4] investigating 201 NHL patients found that the prevalence of HCV infection was 2-fold higher

than that in controls[4]. More recent studies have further confirmed this finding. A Japanese study showed that 17% of patients with B-cell NHL were HCV-antibody positive compared to 6.6% of controls[6]. Moreover, an East European study[7] reported that 6 out of 42 (24.3%) NHL patients were HCV-antibody positive. In contrast, Rabkin *et al*[8] investigated the stored sera of 57 NHL patients, 24 MM patients and fourteen Hodgkin's disease patients, and found that only four patients were HCV-antibody positive.

An association between chronic HCV infection and MM was also found in epidemiological studies. Gharagozloo *et al*[2] showed that HCV antigens were detectable in 11% of patients with MM, 69% of patients with essential mixed cryoglobulinaemia and 4.3% of patients with NHL, using recombinant immunoblot assay (RIBA) and enzyme-linked immunosorbent assay (ELISA). Another study revealed that HCV infection was found in 32% of MM patients[10]. The former was associated with 4.3-fold risk for MM.

The possible mechanism by which HCV infection leads to stimulation of B cells is starting to unravel. It is well documented that HCV infection, as observed in our case, usually precedes NHL by many years[9]. Hepatitis C is lymphotropic and may replicate in lymphocytes and hepatocytes[17]. The second portion of the HCV envelope (E2 protein) binds to CD81[18], suggesting that this phenomenon is associated with CD19 and CR2 as well as MHC class II molecules on lymphocytes. The binding of CD81 to B cells can activate this complex, which lowers the antigen threshold necessary for antibody stimulation, thus rendering the B cell hyper-responsive. Sequencing of the antigen-binding region of immunoglobulin produced by malignant lymphocytes demonstrates that it has a high degree of homology to both antibodies specific for E2, as well as the antibodies produced by B cells that secrete RF. Furthermore, 88% of patients with HCV infection and cryoglobulinaemia demonstrate over-expression [t(14,18)translocation] of the anti-apoptotic *bcl-2* gene, compared with 8% of patients with HCV infection, 2% of patients with other liver diseases, and 3% of individuals with other rheumatoid disorders, which cause enhanced B cell survival[19]. In addition, over-expression of NF-kB has been reported in lymphocytes and liver samples of patients with chronic HCV infection and those with NHL[20, 21]. This is an important finding, as NF-kB plays a key role in virus-induced lymphomagenesis. Mutations of the NF-kB gene are common in lymphoid malignancies[22] and alterations of NF-kB could initiate changes in downstream regulatory pathways. A second mutation (e.g. myc, NF-kB) could possibly initiate the progression to lymphoma[23].

In conclusion, although a pathogenic role of HCV infection in malignant lymphoproliferative disorders has not been established, NHL and possibly MM may develop in cases of CHC, supporting the need for a complex follow-up in these patients.

REFERENCES

1 **Agnello V,** De Rosa FG. Extrahepatic disease manifestations of HCV infection: some current issues. *J Hepatol* 2004; **40**: 341-352

2 **Gharagozloo S,** Khoshnoodi J, Shokri F. Hepatitis C virus infection in patients with essential mixed cryoglobulinemia, multiple myeloma and chronic lymphocytic leukemia. *Pathol Oncol Res* 2001; **7**: 135-139

3 **Agnello V,** Chung RT, Kaplan LM. A role for hepatitis C virus infection in type II cryoglobulinemia. *N Engl J Med* 1992; **327**: 1490-1495

4 **Germanidis G,** haioun C, Dhumeaux D, Reyes F, Pawlotsky JM. Hepatitis C virus infection, mixed cryoglobulinemia, and B-cell non-Hodgkin's lymphoma. *Hepatology* 1999; **30**: 822-823

5 **Trejo O,** Ramos-Casals M, Lopez-Guillermo A, Garcia-Carrasco M, Yague J, Cervera R, Font J, Ingelmo M. Hematologic malignancies in patients with cryoglobulinemia: association with autoimmune and chronic viral diseases. *Semin Arthritis Rheum* 2003; **33**: 19-28

6 **Mizorogi F,** Hiramoto J, Nozato A, Takekuma Y, Nagayama K, Tanaka T, Takagi K. Hepatitis C virus infection in patients with B-cell non-Hodgkin's lymphoma. *Intern Med* 2000; **39**: 112-117

7 **Gasztonyi B,** Par A, Szomor A, Nagy A, Kereskai L, Losonczy H, Pajor L, Horanyi M, Mozsik G. Hepatitis C virus infection and B-cell non-Hodgkin's lymphoma. *Orv Hetil* 2000; **141**: 2649-2651

8 **Rabkin CS,** Tess BH, Christianson RE, Wright WE, Waters DJ, Alter HJ, Van Den Berg BJ. Prospective study of hepatitis C viral infection as a risk factor for subsequent B-cell neoplasia. *Blood* 2002; **99**: 4240-4242

9 **De Vita S,** Zagonel V, Russo A, Rupolo M, Cannizzaro R, Chiara G, Boiocchi M, Carbone A, Franceschi S. Hepatitis C virus, non-Hodgkin's lymphomas and hepatocellular carcinoma. *Br J Cancer* 1998; **77**: 2032-2035

10 **Montella M,** Crispo A, Russo F, Ronga D, Tridente V, Tamburini M. Hepatitis C virus infection and new association with extrahepatic disease: multiple myeloma. *Haematologica* 2000; **85**: 883-884

11 **Manns MP,** McHutchison JG, Gordon SC, Rustgi VK, Shiffman M, Reindollar R, Goodman ZD, Koury K, Ling M, Albrecht JK. Peginterferon alfa-2b plus ribavirin compared with interferon alfa-2b plus ribavirin for initial treatment of chronic hepatitis C: a randomised trial. *Lancet* 2001; **358**: 958-965

12 **McHutchison JG,** Manns M, Patel K, Poynard T, Lindsay KL, Trepo C, Dienstag J, Lee WM, Mak C, Garaud JJ, Albrecht JK. Adherence to combination therapy enhances sustained response in genotype-1-infected patients with chronic hepatitis C. *Gastroenterology* 2002; **123**: 1061-1069

13 **Abonyi ME,** Lakatos PL. Ribavirin in the treatment of hepatitis C. *Anticancer Res* 2005; **25**: 1315-1320

14 **Cenci M,** De Soccio G, Recchia O. Prevalence of hepatitis C virus (HCV) genotypes in central Italy. *Anticancer Res* 2003; **23**: 5129-5132

15 **Silvestri F,** Pipan C, Barillari G, Zaja F, Fanin R, Infanti L, Russo D, Falasca E, Botta GA, Baccarani M. Prevalence of hepatitis C virus infection in patients with lymphoproliferative disorders. *Blood* 1996; **87**: 4296-4301

16 **Kashyap A,** Nademanee A, Molina A. Hepatitis C and B-cell lymphoma. *Ann Intern Med* 1998; **128**: 695

17 **Ferri C,** Monti M, La Civita L, Longombardo G, Greco F, Pasero G, Gentilini P, Bombardieri S, Zignego AL. Infection of peripheral blood mononuclear cells by hepatitis C virus in mixed cryoglobulinemia. *Blood* 1993; **82**: 3701-3704

18 **Pileri P,** Uematsu Y, Campagnoli S, Galli G, Falugi F, Petracca R, Weiner AJ, Houghton M, Rosa D, Grandi G, Abrignani S. Binding of hepatitis C virus to CD81. *Science* 1998; **282**: 938-941

19 **Zignego AL,** Giannelli F, Marrocchi ME, Mazzocca A, Ferri C, Giannini C, Monti M, Caini P, Villa GL, Laffi G, Gentilini P. T(14;18) translocation in chronic hepatitis C virus infection. *Hepatology* 2000; **31**: 474-479

20 **Tai DI,** Tsai SL, Chen YM, Chuang YL, Peng CY, Sheen IS, Yeh CT, Chang KS, Huang SN, Kuo GC, Liaw YF. Activation of nuclear factor kappaB in hepatitis C virus infection: implications for pathogenesis and hepatocarcinogenesis. *Hepatology* 2000; **31**: 656-664

21 **Gasztonyi B,** Par A, Kiss K, Kereskai L, Szomor A, Szeberenyi J, Pajor L, Mozsik G. Activation of the nuclear factor kappa B--

key role in oncogenesis? Chronic hepatitis C virus infection and lymphomagenesis. *Orv Hetil* 2003; **144**: 863-868

22 **Neri A,** Fracchiolla NS, Migliazza A, Trecca D, Lombardi L. The involvement of the candidate proto-oncogene NFKB2/ lyt-10 in lymphoid malignancies. *Leuk Lymphoma* 1996; **23**: 43-48

23 **Ellis M,** Rathaus M, Amiel A, Manor Y, Klein A, Lishner M. Monoclonal lymphocyte proliferation and bcl-2 rearrangement in essential mixed cryoglobulinaemia. *Eur J Clin Invest* 1995; **25**: 833-837

S- Editor Guo SY **L- Editor** Wang XL **E- Editor** Liu WF

PO Box 2345, Beijing 100023, China
www.wjgnet.com
wjg@wjgnet.com

World J Gastroenterol 2006 April 14; 12(14): 2301-2304
World Journal of Gastroenterology ISSN 1007-9327

CASE REPORT

A rare case of enteropathy-associated T-cell lymphoma presenting as acute renal failure

Milena Bakrac, Branka Bonaci, Miodrag Krstic, Sanja Simic, Milica Colovic

Milena Bakrac, Milica Colovic, Institute of Hematology, Clinical Center of Serbia, Serbia
Branka Bonaci, Institute of Allergology and Immunology, Clinical Center of Serbia, Serbia
Miodrag Krstic, Institute of Gastroenterology, Clinical Center of Serbia, Serbia
Sanja Simic, Institute of Nephrology, Clinical Center of Serbia, Serbia
Correspondence to: Milena Bakrac, MD, PhD, Institute of Hematology, Clinical Center of Serbia, Koste Todorovica 2, 11000 Belgrade, Serbia donmil@eunet.yu
Telephone: +381-11-3065112 Fax: +381-11-3065112
Received: 2005-08-05 Accepted: 2005-10-26

Abstract

Enteropathy-associated T-cell lymphoma (EATCL) is a high grade, pleomorphic peripheral T-cell lymphoma usually with cytotoxic phenotypes. We describe a first case of patient with EATCL that is remarkable for its fulminant course and invasion of both kidneys manifested as acute renal failure. The patient was a 23 year old woman with a long history of celiac disease. She was presented with acute renal failure and enlarged mononuclear infiltrated kidneys. Diagnosis of tubuloi-nterstitial nephritis and polyserositis was confirmed with consecutive pulse doses of steroid therapy. After reco-very, she had disseminated disease two months later. Magnetic resonance imaging showed thickened intestine wall, extremely augmented kidneys, enlarged intra-abdominal lymph nodes with extra-luminal compression of common bile duct. Laparotomy with mesenterial adipous tissue and lymph glands biopsy was done. Consecutive pathophysiological and immunohistochemical analyses confirmed the diagnosis of EATCL: CD45RO+, CD43+, CD3+. The revision of renal pathophysiology sub-stantiated the diagnosis. The patient received chemotherapy, but unfortunately she died manifesting signs of pulmonary embolism caused by tumor cells.

Key words: EATCL; Acute renal failure; Celiac disease; Anti-endomisial antibodies

Bakrac M, Bonaci B, Krstic M, Simic S, Colovic M. A rare case of enteropathy-associated T-cell lymphoma presenting as acute renal failure. *World J Gastroenterol* 2006; 12(14): 2301-2304

http://www.wjgnet.com/1007-9327/12/2301.asp

INTRODUCTION

Intestinal enteropathy associated T-cell lymphoma (EATCL) is highly aggressive, pleomorphic peripheral T-cell lymphoma (PTL), usually with cytotoxic immunological phenotypes (TdT-, CD3+, CD5-, CD7+, CD4-, CD8±, CD45RO+, CD103+, HLA-DR-)[1-3]. This type of PTL originates from intraepithelial T-lymphocytes of small intestine mucosa and is associated with celiac disease (CD) in about 50% of the time[4,5]. Intestinal lymphoma develops in 7%-12% of CD cases[6]. It may even occur without any previous CD[6]. Infiltration of the kidneys is commonly found in disseminated lymphoma but rarely in primary renal lymphoma[7]. Acute renal failure (ARF) arising from bilateral renal infiltration is also uncommon[8,9]. Primary renal failure may occur and is usually of B-cell lineage[7]. It is rare for patients with lymphoma to develop ARF as their initial clinical presentation. The first report in which the phenotype of non-Hodgkin's lymphoma was established using renal biopsy was published by Miyake *et al*[10]. Renal lymphoma is commonly secondary due to lymphomatous infiltration of the kidneys in disseminated lymphoma and advanced stage IV of the disease. Different pathophysiological aggressive types of B-cell lymphoma such as Burkitt[11], precursor B-lymphoblastic lymphoma/leukemia[12], mantle cell lymphoma, diffuse large B-cell lymphoma[13] as well as PTL[14,15], T-cell rich B-cell lymphoma[8], make parenchymal neoplastic invasion of the kidneys. We present, as far as we know for the first time, ARF as the initial manifestation of EATCL.

Nevertheless, the intestinal lymphomas account for 20%-35% of non-Hodgkin's lymphomas (NHL) of the gastrointestinal tract (GIT) and serological screening for CD is not recommended generally in people with lymphoma[16]. In patients with primary small intestinal disease, 9% are found to have small intestinal lymphoma[17]. Lymphomas involving the small intestine represent a heterogenous group with diverse pathogenic mechanisms[18] and high-risk MALT lymphoma is most frequently considered for differential diagnosis. EATCL, a type of PTL is most commonly localized in jejunum (70% of cases) but rarely in the colon and stomach. Gross examination can reveal multiple ulcers of jejunal

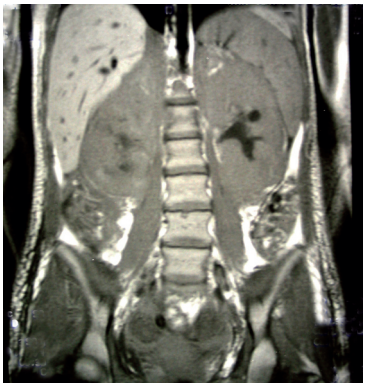

Figure 1 Magnetic resonance imaging shows extremely augmented kidneys.

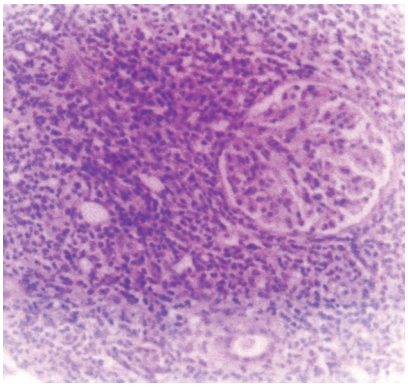

Figure 3 Renal infiltration with monomorphous lymphoid infiltration (H&E, x 40).

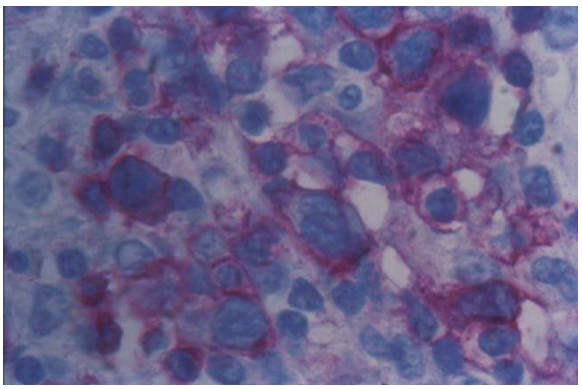

Figure 2 Neoplastic mesenterial lymph node infiltration with staining of lymphoma cells (APAAP with anti-CD3 Ab x 400).

mucosa frequently associated with perforation of intestinal wall or solitary lymph nodes[19]. Microscopy can show solitary epithelial lesions in the form of microabscess or lymphoepithelial lesions. In the adjacent mucosa, alterations are seen in CD such as crypt elongation, flattened mucosa and villi which are shortened, blunted or missing[2]. Tumor cells of the respective immunological phenotype have genetic characteristics as clonally rearranged TCR β and γ[5,6] can be arrested in varying stages of activation[1].

CASE REPORT

We report a case of female patient who was 23 years old with CD diagnosed at her age of 3 and had regular gluten-free diet regime. In March 1999, she was admitted to the Institute of Nephrology due to anemia and ARF. Clinical examination revealed excessive pallor of the skin and apparent mucous membranes with fever, splenomegaly +1 cm and ascites. A history was negative for exposure to nephrotoxins and hereditary renal diseases. Laboratory tests showed Hb = 65 g/L (120-170), WBC = 5.3×10^9/L (4-10), Platelet = 401×10^9/L (150-450), MCV = 90 fl (80-100), Hct = 0.34 (0.36-0.42), and normal differential count. In biohumoral status, the following pathological values were found: ESR = 90 mm/h, urea = 17.9 mmol/L (2.5-7.5), Cr = 476 μmol/L (53-106), ClCr = 13.3mL/min, tubular proteinuria=0.82 g/24h without erythrocyturia, total protein = 60 g/L (62-81), albumin = 6 g/L (40-55), Fe = 4.6 μmol/L (7-26), TIBC = 36.3 μmol/L (44.8-75.1), LDH = 590 IU/L(160-320). Immunological analyses showed CRP 28.9 mg/L (<9), ANA negativity, RF 37.3 IU/mL (<25) WR 1:40+. Virusological and bacteriological analyses were normal. Hemostasis screening did not display any detectable abnormalities. X-ray of the lungs and heart was normal, too. Abdominal echosonography showed craniocaudal splenomegaly of 14 cm, ascites and enlarged kidneys, the right of 14.5 cm and the left of 13.7 cm, without corticomedullary border. Echosonography of the heart showed pericardial effusion. Thereupon, ultrasound-guided biopsy of kidneys was performed and pH finding indicated tubulointerstitial nephritis (TIN). There were no criteria for connective tissue disease, drug-or infection-induced acute TIN**.** The diagnosis of idiopathic acute TIN with polyserositis was made and urbason at pulse doses of 3×1 g/d was administered, followed by prednisolone 45 mg/d for another month. After a short recovery, in May 1999, the patient was rehospitalized for jaundice, pains under the right costal arch, nausea and vomiting. Endoscopic retrograde cholangiopancreatography showed extra-luminal compression of ductus pancreaticus and ductus hepaticus which was moved to the right, while choledochus was filamentary narrowed distally from the site of compression. Proximal of stricture was a huge biliary duct dilatation with changes of intrahepatical biliary ducts [as in cholangitis]. Magnetic resonance imaging of the abdomen and small pelvis revealed the enlarged retroperitoneal and mesenterial lymph glands, thickened small intestine wall, extremely augmented kidneys with destroyed corticomedullary structure, as well as infiltration of the right sacral bone (Figure 1). Choledochotomy and cholecystectomy with choledochojejunostomy and biopsy of mesenterial lymph glands and adipous tissue were performed. Pathohistological (PH) and immunohistochemical (IHC) analyses of mesenterial lymph nodes and adipous tissue from transfersal mesocolon showed the PTL infiltration (anti-CD45RO+, anti-CD43+, CD3+ as well as anti-EMA- /epithelial membrane antigen/, anti-vimentin-) (Figure 2). The revision of renal PH findings substantiated the diagnosis (Figure 3). Neoplastic lymphoid cells were also found in the ascites (Figure 4). Antiendomysial serum IgA antibodies (EmA) in high titer +++ were (Figure 5) detected by indirect immunofluorescence on monkey oesophagus. Anti-nuclear, anti-microsomal, anti- tireoglobulin antibodies were negative and serum levels of IgM, IgG and IgA were normal. Upon complete staging of the disease, it was

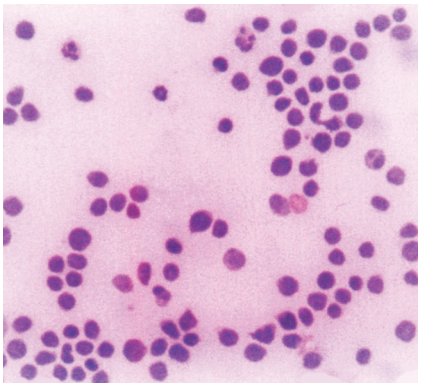

Figure 4 Neoplastic lymphoid cells in ascites (MGG, x100).

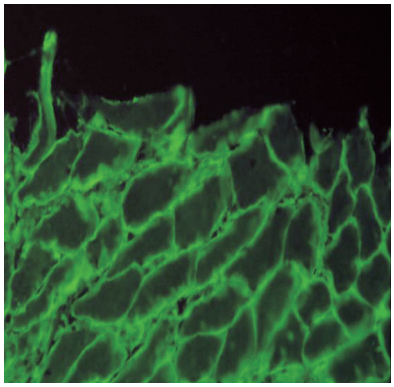

Figure 5 IgA antiendomysial antibodies surrounding sarcolemma of smoth muscle fibers in lamina muscularis mucosae of monkey esophagus (IIF, x 400).

verified that it was EATCL with infiltration of intestines, intraabdominal lymph glands, kidneys and sacral bone (CS IVB). The patient was transferred to the Institute of Hematology, where she received chemotherapy with cyclophosphamide (1200 mg, D1), doxorubicin (90 mg, D1), vincristine (2 mg, D1), prednisolone (100 mg, D1-5. On the second day of therapy, the patient died manifesting the signs of cardiorespiratory insufficiency and picture of pulmonary embolism, most probably caused by tumor cells.

DISCUSSION

EATCL is a relatively rare disease with the incidence rate less than 1% of all NHL[20]. By nature, it is aggressive whether it occurs as de novo disease or results from long-term untreated or refractory CD. Usually, the jejunum is involved with presence of multiple circumferential ulcerations but without formation of homogenous tumor mass. In addition, the involvement of mesenterial lymph glands is frequently seen. In fact, refractory CD is considered as lymphoma of low grade malignancy resulting from clonal expansion of intraepithelial lymphocytes and represents an intermediate stage between CD and EATCL[21,22].

The moment when CD converts to intestinal lymphoma is sometimes difficult to recognize. Diffuse bilateral infiltration of the kidneys by lymphoma cells is a rare but well documented cause of ARF[23]. The diagnosis should be suspected in a patient with ARF, bilateral enlargement of the kidneys, minimal proteinuria, non-specific findings on urine analysis, and absence of other features (fever, skin rush, eosinophilia) typical of drug-induced TIN. Renal imaging techniques may suggest the possibility of lymphomatous infiltration, but only renal biopsy or autopsy can provide a definitive diagnosis[24]. Diffuse bilateral renal cell lymphoma sometimes presents as ARF of unknown cause. Signs of extrarenal lymphomatous involvement were detected in 44% patients at the time of kidney biopsy or shortly thereafter[25] and often clinically mimic primary renal disease or systemic connective disease.

In our patient who was diagnosed with CD 20 years prior to the development of lymphoma, CD was in subclinical form for years. This is a key point for misdiagnosis of TIN instead of lymphoma renal infiltration. At the time of aggravation of general condition, renal failure with signs of TIN and polyserositis predominated in the clinical picture of disease. Short-term improvement after the corticosteroid treatment was followed by stasis icterus but without any symptoms typical of intestinal lymphoma. Diagnostic dilemma was resolved by complete PH and IHC examinations of bioptic specimens of mesenterial lymph glands and mesocolic adipous tissue tumor. Time loss due to unrecognized intestinal lymphoma, and dissemination into abdominal organs and small pelvis, brought about the extreme progression of the disease. Because of huge tumor mass, it led to lethal outcome with pulmonary embolism by tumor cells after the chemotherapy. Actually, this was a long-term CD, which like the premalignant condition gave rise to highly aggressive T-cell lymphoma with striking propagation and short survival median.

Our case demonstrated that in this point of view, serological follow-up was very useful and could reduce the time of possible subclinical or refractory CD. It is necessary to determine serum IgA EmA not only to monitor the activity but also to predict the gluten-free diet compliance. IgA EmA should disappear after a gluten free diet is started and about 90% of patients who have characteristic findings of CD respond to complete dietary gluten restriction[26]. In the early stages of EATCL, serological, immunohistochemical and molecular biological analyses may lead to the correct diagnosis and better prognosis[27].

The target cells in EATCL as a member of uniform subclass T-cytotoxic lymphocytes are also target cells in the intestinal lesion in CD patients, indicating that the evolution of genetically controlled autoimmune disease as pre-malignant condition to highly risk and aggressive lymphoma of small intestine is the evidence confirming that autoimmunity is a risk factor for malignancy.

Our case revealed very aggressive atypical clinical onset of EATCL patient, which was presented as ARF without intestinal symptoms at presentation. This is a first case in published literature, which describes ARF as an initial manifestation of EATCL. Although it was a case of misdiagnosis of idiopathic TIN with polyserositis instead of lymphoma, our study has confirmed that subjects with persistent high IgA EmA should be regularly re-examined concerning possible evolution of CD towards EATCL. Although good serological predictors are not yet available, IgA EmA assessment may help to detect individuals at higher risk to develop EATCL.

REFERENCES

1 **de-Bruin PC**, Conolly CE, Qudejans JJ, Kummer JA, Jansen W, McCarthy CF, Meijer CJ. Enteropathy-associated T-cell lymphomas have a cytotoxic T- cell phenotype. *Histopathology* 1997; **31**: 313-317

2 **Murray A**, Cuevas EC, Jones DB, Wright DH. Study of the immunohistochemistry and T cell clonality of enteropathy-associated T cell lymphoma. *Am J Pathol* 1995; **146**: 509-519

3 **Sutcliffe SB**, Gospodarowicz. Primary Extranodal lymphomas. In: The Lymphomas. Canellos GP, Lister TA, Sklar JL. W.B. Philadelphia: Saunders Company, 1998: 449-479

4 **Harris NL**, Jaffe ES, Diebold J, Flandrin G, Muller-Hermelink HK, Vardiman J. Lymphoma classification--from controversy to consensus: the R.E.A.L. and WHO Classification of lymphoid neoplasms. *Ann Oncol* 2000; **11 Suppl 1:** 3-10

5 **Harris NL**, Jaffe ES, Diebold J, Flandrin G, Muller-Hermelink HK, Vardiman J, Lister TA, Bloomfield CD. World Health Organization classification of neoplastic diseases of the hematopoietic and lymphoid tissues: report of the Clinical Advisory Committee meeting-Airlie House, Virginia, November 1997. *J Clin Oncol* 1999; **17**: 3835-3849

6 **Jones D**, Levin B, Salem P. Primary small intestinal lymphomas. In: Almy T. Gastrointestinal Disease. W. B. Philadelphia: Saunders Company, 1997: 1378-1392

7 **Brouland JP**, Meeus F, Rossart J, Hernigon A, Gentric C, Jacquot C, Diebold J, Nochy D. Primary bilateral B-cell lymphoma: a case report and review of the literature. *Am J Kidney Dis* 1994; **24**: 586-589

8 **Chin KC**, Perry GJ, Dowling JP, Thomson NM. Primary T-cell-rich B-cell lymphoma in the kidney presenting with acute renal failure and a second malignancy. *Pathology* 1999; **31**: 325-327

9 **Ozaltin F**, Yalcin B, Orhan D, Sari N, Caglar M, Besbas N, Bakkaloglu A. An unusual cause of acute renal failure: renal lymphoma. *Pediatr Nephrol* 2004; **19**: 912-914

10 **Miyake JS**, Fitterer S, Houghton DC. Diagnosis and characterization of non-Hodgkin's lymphoma in a patient with acute renal failure. *Am J Kidney Dis* 1990; **16**: 262-263

11 **Gianviti A**, Boldrini R, Bosman C, Rizzoni G. Chronic renal failure due to kidney infiltration by Burkitt type lymphoma. *Pediatr Nephrol* 1989; **3**: 448-450

12 **Boueva A**, Bouvier R. Precursor B-cell lymphoblastic leukemia as a cause of a bilateral nephromegaly. *Pediatr Nephrol* 2005; **20**: 679-682

13 **Porcaro AB**, D'Amico A, Novella G, Curti P, Ficarra V, Antoniolli SZ, Martignoni G, Matteo B, Malossini G. Primary lymphoma of the kidney. Report of a case and update of the literature. *Arch Ital Urol Androl* 2002; **74**: 44-47

14 **Neuhauser TS**, Lancaster K, Haws R, Drehner D, Gulley ML, Lichy JH, Taubenberger JK. Rapidly progressive T cell lymphoma presenting as acute renal failure: case report and review of the literature. *Pediatr Pathol Lab Med* 1997; **17**: 449-460

15 **Srinivasa NS**, McGovern CH, Solez K, Poppema S, Halloran PF. Progressive renal failure due to renal invasion and parenchymal destruction by adult T-cell lymphoma. *Am J Kidney Dis* 1990; **16**: 70-72

16 **Farre C**, Domingo-Domenech E, Font R, Marques T, Fernandez de Sevilla A, Alvaro T, Villanueva MG, Romagosa V, de Sanjose S. Celiac disease and lymphoma risk: a multicentric case--control study in Spain. *Dig Dis Sci* 2004; **49**: 408-412

17 **Zhan J**, Xia ZS, Zhong YQ, Zhang SN, Wang LY, Shu H, Zhu ZH. Clinical analysis of primary small intestinal disease: A report of 309 cases. *World J Gastroenterol* 2004; **10**: 2585-2587

18 **Yuan CM**, Stein S, Glick JH, Wasik MA. Natural killer-like T-cell lymphoma of the small intestine with a distinct immunophenotype and lack of association with gluten-sensitive enteropathy. *Arch Pathol Lab Med* 2003;**127**: e142-e146

19 **Jones D**, Levin B, Salem P. Primary small intestinal lymphomas. In: Almy T. Gastrointestinal Disease. W. B. Philadelphia: Saunders Company, 1997: 1378-1392

20 **Hoffmann M**, Vogelsang H, Kletter K, Zettinig G, Chott A, Raderer M. 18F-fluoro-deoxy-glucose positron emission tomography (18F-FDG-PET) for assessment of enteropathy-type T cell lymphoma. *Gut* 2003; **52**: 347-351

21 **Culliford AN**, Green PH. Refractory sprue. *Curr Gastroenterol Rep* 2003; **5**: 373-378

22 **Verkarre V**, Asnafi V, Lecomte T, Patey Mariaud-de Serre N, Leborgne M, Grosdidier E, Le Bihan C, Macintyre E, Cellier C, Cerf-Bensussan N, Brousse N. Refractory coeliac sprue is a diffuse gastrointestinal disease. *Gut* 2003; **52**: 205-211

23 **Kanfer A**, Vandewalle A, Morel-Maroger L, Feintuch MJ, Sraer JD, Roland J. Acute renal insufficiency due to lymphomatous infiltration of the kidneys: report of six cases. *Cancer* 1976; **38**: 2588-2592

24 **Truong LD**, Soroka S, Sheth AV, Kessler M, Mattioli C, Suki W. Primary renal lymphoma presenting as acute renal failure. *Am J Kidney Dis* 1987; **9**: 502-506

25 **Tornroth T**, Heiro M, Marcussen N, Franssila K. Lymphomas diagnosed by percutaneous kidney biopsy. *Am J Kidney Dis* 2003; **42**: 960-971

26 **Bider HJ**. Disorders of absorption. In: Kasper DL, Braunwald E, Fauci AS et al (Eds) Harrison's Priciples of Internal Medicine (16th Edition). Mc Graw Hill New York. 2005: 1763-1776

27 **Bachle T**, Ruhl U, Ott G, Walker S. Enteropathy-associated T-cell lymphoma. Manifestation as diet-refractory coeliac disease and ulcerating jejunitis. *Dtsch Med Wochenschr* 2001; **126**: 1460-1463

S- Editor Wang J **L- Editor** Wang XL **E- Editor** Bi L

PO Box 2345, Beijing 100023, China
www.wjgnet.com
wjg@wjgnet.com

World J Gastroenterol 2006 April 14; 12(14): 2305-2307
World Journal of Gastroenterology ISSN 1007-9327

CASE REPORT

An interesting cause of esophageal ulcer etiology: Multiple myeloma of IgG kappa subtype

Yavuz Pehlivan, Alper Sevinc, Ibrahim Sari, Murat T Gulsen, Mehmet Buyukberber, Mehmet E Kalender, Celalettin Camci

Yavuz Pehlivan, Alper Sevinc, Ibrahim Sari, Murat T Gulsen, Mehmet Buyukberber, Mehmet E Kalender, Celalettin Camci, Gaziantep University, School of Medicine, Departments of Internal Medicine, Medical Oncology, Pathology, and Gastroenterology, Sahinbey Medical Center, Gaziantep, TR-27310, Turkey
Correspondence to: Dr. Alper Sevinc, Gaziantep University, School of Medicine, Department of Medical Oncology, Sahinbey Medical Center, Gaziantep, TR-27310, Turkey. sevinc@gantep.edu.tr
Telephone: +90-342-3601314 Fax: +90-342-3601617
Received: 2005-09-22 Accepted: 2005-11-18

Abstract

Multiple myeloma is a neoplasm of mature and immature plasma cells. A 50-year-old woman with lumbago, dysphagia, and left arm pain was presented. Upper endoscopical examination was performed. There was an exudate-covered ulcer in the distal esophagus, located at 30-32 cm from the incisors, covering the whole mucosa. Histopathological examination of the specimens obtained from the lesion showed the involvement of plasma cells consistent with multiple myeloma of IgG kappa subtype. Esophageal involvement of multiple myeloma should be kept in mind in patients presenting with dysphagia.

Key words: Multiple myeloma; Esophageal ulcer; Dysphagia; Endoscopy

Pehlivan Y, Sevinc A, Sari I, Gulsen MT, Buyukberber M, Kalender ME, Camci C. An interesting cause of esophageal ulcer etiology: Multiple myeloma of IgG kappa subtype. *World J Gastroenterol* 2006; 12(14): 2305-2307

http://www.wjgnet.com/1007-9327/12/2305.asp

INTRODUCTION

Multiple myeloma (MM) is a plasma-cell neoplasm characterized by skeletal destruction, renal failure, anemia and hypercalcemia. The most common symptoms at presentation are fatigue, bone pain and recurrent infections. New diagnostic criteria require the presence of at least 10% plasma cells on examination of the bone marrow (or biopsy of tissue with monoclonal plasma cells), monoclonal protein in the serum or urine, and evidence of end-organ damage[1].

Apart from the bone marrow, MM may involve any part of the body including spleen, liver, lymph nodes, thyroid, adrenal glands, ovary, testis, lung, pleura, pericardium, skin, pancreas and intestinal tract. Esophageal involvement by multiple myelomas is uncommon in the English literature. Here we report an extremely rare involvement in MM.

CASE REPORT

A 50-year-old woman was admitted to Gaziantep University Hospital with lumbago, dysphagia and left arm pain. She complained of lumbago in the last 3 mo, which deteriorated but was relieved by non-steroid anti-inflammatory drugs (NSAIDs). Dysphagia was particularly associated with solid foods over a period of month. Her severe arm pain began after lifting a heavy weight. She also complained of fatigue.

Her medical history revealed a 10-year history of hypertension and one year of type 2 diabetes mellitus. No abnormal signs were detected apart from the pale conjunctivas and the left arm pain during physical examination. She was taking gliclazide 3 mg/d and amlodipine 10 mg/d.

Biochemical examination and complete blood count showed (normal reference ranges are given in parenthesis) hemoglobin:102 g/L (110-180 g/L); hematocrit: 0.32 (0.35-0.60); ESR: 110 mm/h (1-18 mm/h); glucose: 160 mg/dL (70-110 mg/dL); total serum protein: 144 g/L (64-82 g/L); albumin: 22 g/L (34-50 g/L); globulin: 122 g/L (14-30 g/L); calcium: 12.6 mg/dL (8.5-10.1); (BUN, Cr, Na, Cl, and P were in the normal limits). IgG: 46.7 g/L (7-16); IgA:0.29 g/L (0.7-4); IgM:0.171 IU/mL (0.4-2.3); and IgE:184 g/L (0-100). Bone marrow aspiration and biopsy confirmed multiple myeloma (30% plasma cells) besides hyperglobulinemia, hypercalcemia, anaemia, elevated ESR, and bone pain. Multiple lytic lesions were encountered on radiographic examination of the arms, the vertebras, and the cranium. Endoscopic examination showed exudate-covered ulcer in the distal esophagus located at 30-32 cm from the incisors, covering the whole mucosa (Figure 1) and no pathological finding in the stomach. Histopathologic examination of the specimens obtained from the lesion showed the involvement of plasma cells in the ulcerated esophageal mucosa (Figure 2). Immunohistochemically, plasma cells revealed positive reaction with CD38, CD56, and kappa light chain and (Figure 3)

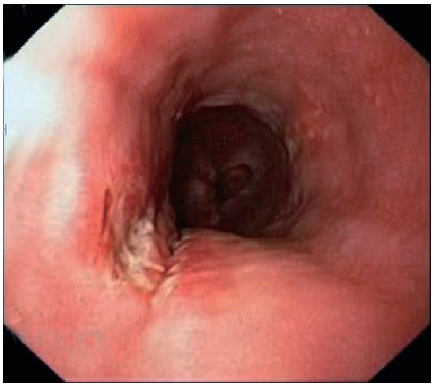

Figure 1 Exudate-covered ulcer in distal esophagus.

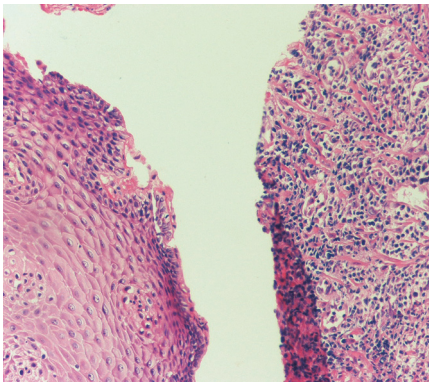

Figure 2 Plasma cells infiltrating esophageal mucosa (hematoxylin & eosin staining, x 200).

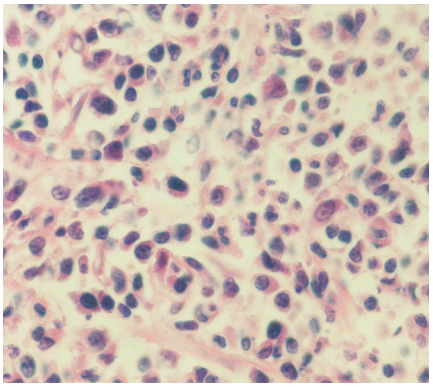

Figure 3 Myeloma cells in lamina propria of esophagus (hematoxylin & eosin staining, x 400).

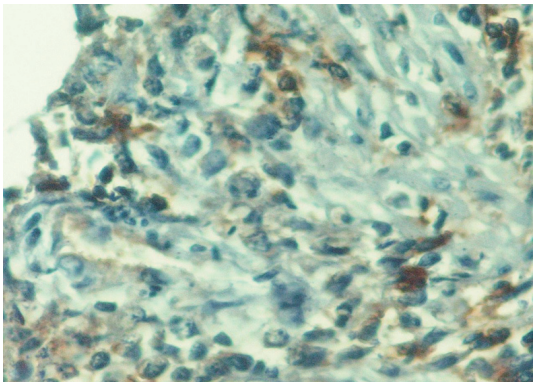

Figure 4 Immunohistochemically stained kappa light-chain showing monoclonality of plasma cells (x400).

negative reaction with CD20 and lambda light chain both in the bone marrow and in the esophagus (Figure 4). It was consistent with MM of IgG kappa subtype. Left upper extremity MRI revealed an irregularly shaped 5 cm × 4 cm × 6 cm mass on the humeral head. Total excision of the mass in the left arm was performed. It was also consistent with MM.

The patient was diagnosed with MM of IgG kappa subtype, and chemotherapy regimen of VAD was applied (vincristine 0.4 mg for 24 h infusion on days 1-4, adriablastina 9 mg/m^2 for 24 h infusion on days 1-4, dexamethasone 40 mg po on days 1-4, 9-12, 17-20). Dysphagia was relieved after administration of the chemotherapy regimen. Control endoscopical examination revealed that the formerly detected ulcers on admission were improved.

DISCUSSION

Multiple myeloma is a neoplastic proliferation of monoclonal plasma cells that can result in osteolytic bone lesions, hypercalcemia, renal impairment, bone marrow failure, and the production of monoclonal gammopathy. Although it is usually restricted to the bone marrow, extramedullary involvement can occur in the form of plasmacytomas in up to 20% of cases. The most common site of extramedullary involvement is the upper respiratory tract, including the oropharynx, nasopharynx, nasal cavity, paranasal sinuses, and larynx[1,2]. Gastrointestinal involvement by plasma cells is rare, representing less than 5% of all extramedullary plasmacytomas. Presentation may be either primary or secondary. Before a diagnosis of multiple myeloma is made it is mandatory to exclude primary extramedullary plasmacytoma (PEMP) by performing the necessary investigations. The differential diagnosis of PEMP from multiple myeloma is important because these two entities are thought to be biologically different and their prognoses are not the same.

Most of the reported cases represent involvement of the gastrointestinal tract by solitary plasmacytomas. All segments of the gastrointestinal tract may be involved by plasma cell infiltration. Small bowel is the most common site of involvement, followed by stomach, large bowel and esophagus[2-5]. Esophageal involvement by multiple myeloma is uncommon (Figure 3). A search of the English literature for plasmacytoma of the esophagus has revealed only four previous reports. The case reported by Morris and Pead[6] occurred in a 59-year old woman who presented with weight loss and intermittent dysphagia that progressively worsened over a 4- 5-mo period. Plasmacytoma is a protuberant mass occurring in the lower esophagus and involving the full thickness of the wall. Ahmed *et al*[7] encountered an esophageal PEMP in a 67-year-old man who, in addition to dysphagia, had weakness and weight loss. The lower third of the esophagus was invaded by an 8 cm tumour that extended to the gastric cardia and penetrated the entire thickness of the esophageal wall. Davis and Boxer[8] described a PEMP of esophagus in a 69-year-old man who only had a two-week history of dysphagia. Furthermore, this patient did not have weight loss, malaise or constitutional symptoms. The tumour was polypoid,

measured 4 cm in diameter, and involved the distal third of the esophagus. Recently, Chetty *et al*[9] described a PEMP of esophagus in a 58-year-old man. Dysphagia occurs particularly with consumption of solid foods over a period of 2 mo. Gross examination of esophagus can reveal large polypoid tumour. In the present case, however, dysphagia was particularly with solid foods over a period of one month. The lesion was in the form of ulcer and was probably induced by impairment of the esophageal mucosa due to replacement of the stromal tissue by the plasma cells (Figure 4).

The presenting features of esophageal plasmacytoma are similar to esophageal carcinoma, i.e., progressive dysphagia, profound weight loss, signs of malnutrition, and anemia. Diagnosis on clinical grounds alone is impossible and the radiologic appearance does not seem distinctive. Endoscopic biopsy is the earliest opportunity for diagnosis.

Diffuse plasma cell infiltration may also be seen in Barrett's esophagus that should be ruled out in the differential diagnosis. Plasma cells are positive for monoclonal light chain in MM as in the present case, but they are polyclonal in Barrett's esophagus. Additionally, there was no intestinal glandular metaplasia in the present case.

In conclusion, multiple myeloma is a systemic disease which may be rarely presented with esophageal involvement. It should be kept in mind that esophageal ulcers in patients diagnosed with MM may be related to the myeloma involvement and these patients should be examined further.

REFERENCES

1 **Kyle RA**, Rajkumar SV. Multiple myeloma. *N Engl J Med* 2004; **351**: 1860-1873

2 **Dolin S**, Dewer JP. Extramedullary plasmacytoma. *Am J Pathol* 1956; **32**: 83-103

3 **Sloyer A**, Katz S, Javors FA, Kahn E. Gastric involvement with excavated plasmacytoma: case report and review of endoscopic criteria. *Endoscopy* 1988; **20**: 267-269

4 **Pimentel RR**, van Stolk R. Gastric plasmacytoma: a rare cause of massive gastrointestinal bleeding. *Am J Gastroenterol* 1993; **88**: 1963-1964

5 **Goeggel-Lamping C**, Kahn SB. Gastrointestinal polyposis in multiple myeloma. *JAMA* 1978; **239**: 1786-1787

6 **Morris WT**, Pead JL. Myeloma of the oesophagus. *J Clin Pathol* 1972; **25:** 537-538

7 **Ahmed N**, Ramos S, Sika J, LeVeen HH, Piccone VA. Primary extramedullary esophageal plasmacytoma: First case report. *Cancer* 1976; **38:** 943-947

8 **Davies RA**, Boxer DI. Primary plasmacytoma of the oesophagus. *Br J Radiol* 1988; **61**: 1180-1181

9 **Chetty R**, Bramdev A, Reddy AD. Primary extramedullary plasmacytoma of the esophagus. *Ann Diagn Pathol* 2003; 7: 174-179

S- Editor Wang J **L- Editor** Wang XL **E- Editor** Bi L

PO Box 2345, Beijing 100023, China
www.wjgnet.com
wjg@wjgnet.com

World J Gastroenterol 2006 April 14; 12(14): 2308
World Journal of Gastroenterology ISSN 1007-9327

ACKNOWLEDGMENTS

Acknowledgments to Reviewers of *World Journal of Gastroenterology*

Many reviewers have contributed their expertise and time to the peer review, a critical process to ensure the quality of *World Journal of Gastroenterology*. The editors and authors of the articles submitted to the journal are grateful to the following reviewers for evaluating the articles (including those were published and those were rejected in this issue) during the last editing period of time.

Seyed Alireza Taghavi, Associate Professor
Department of Internal Medicine, Nemazee Hospital, No.23, 59th Alley, Ghasrodasht St., Shiraz 71838-95453

Masahiro Arai, MD, PhD
Department of Gastroenterology, Toshiba General Hospital, 6-3-22 Higashi-ooi, Shinagawa-ku,Tokyo 140-8522, Japan

SØren MØller, Chief Physician
Department of Clinical Physiology 239, Hvidovre Hospital, Kettegaard alle 30, DK-2650 Hvidovre, Denmark

Yuan Yuan, Professor
Cancer Institute of China Medical University, 155 North Nanjing Street, Heping District, Shenyang 110001, Liaoning Province, China

Tomohiko Shimatani, Assistant Professor
Department of General Medicine, Hiroshima University Hospital, 1-2-3 Kasumi, Minami-ku, Hiroshima 7348551, Japan

Manuel Romero-Gómez, MD
Professor, Hepatology Unit, Hospital Universitario de Valme, Ctra de Cádiz s/n, Sevilla 41014, Spain

Mark S Pearce, Dr
Sir James Spence Institute, University of Newcastle Upon Tyne, Royal Victoria Infirmary, Newcastle Upon Tyne, NE1 4LP, United Kingdom

Rainer Haas, PhD
Max von Pettenkofer Institut, Pettenkoferstrasse 9a, D-80336 Munich, Germany

Xian-Ming Chen, MD
Center for Basic Research in Digestive Diseases, Division of Gastroenterology and Hepatology, Mayo Clinic College of Medicine, 200 First Street, SW, Rochester, MN 55905, United States

Yutaka Inagaki, Dr
Department of Community Health, Yokai University School of Medicine, Bohseidai, Isehara 259-1193, Japan.

Giovanni Monteleone, MD
Professor, Dipartimento di Medicina Interna, Università Tor Vergata, Via Montpellier, 1, 00133 Rome, Italy

Yoshio Shirai, Associate Professor
Division of Digestive and General Surgery, Niigata University Graduate School of Medical and Dental Sciences, 1-757 Asahimachi-dori, Niigata City 951-8510, Japan

Alan W Hemming MD
MSc, FRCSC, FACS, Professor of Surgery, Director of Hepatobiliary Surgery, Department of Surgery, Division of Transplantation, PO Box 100286, University of Florida,Gainesville, FL, 32610, United States

Lee Bouwman, Dr
Leiden University Medical Centre, department of surgery, Albinusdreef 2 PO Box 9600, 230 RC Leiden, The Netherlands

Hans Scherubl, Professor
Charité, Universitatsmedizin Berlin, Campus Benjamin Franklin, Medical Clinic, Mindenburgdamm 30, 122000 Berlin, Germany

Josep M Bordas, MD
Department of Gastroenterology IMD, Hospital Clinic", Llusanes 11-13 at, Barcelona 08022, Spain

Ian C Roberts-Thomson, Professor
Department of Gastroenterology and Hepatology, The Queen Elizabeth Hospital, 28 Woodville Road, Woodville South 5011, Australia

Fritz von Weizsacker, Professor
Department of Medicine Schlosspark-Klinik, Humboldt University, Heubnerweg 2, Berlin D-14059, Germany

Figen Gurakan, Professor
Department of Pediatric Gastroenterology, Hacettepe University Medical Faculty, Ankara 06100, Turkey

Peter Laszlo Lakatos, MD, PhD, Assistant Professor
1st Department of Medicine, Semmelweis University, Koranyi S 2A, Budapest H1083, Hungary

Shiu-Ming Kuo, MD
University at Buffalo, 15 Farber Hall, 3435 Main Street, Buffalo 14214, United States

Dariusz Marek Lebensztejn, Associate Professor
IIIrd Department of Pediatrics, Medical University of Bialystok, 17 Waszyngtona Str, Bialystok 15-274, Poland

Mauro Bernardi, Professor
Internal Medicine,Cardioangiology,Hepatology, University of Bologna, Semeiotica Medica - Policlinico S. Orsola-Malpighi - Via Massarenti, 9, Bologna 40138, Italy

Markus W Büchler, MD
Department of General Surgery, University of Heidelberg, Im Neuenheimer Feld 110, Heidelberg D-69120, Germany

Eric M Yoshida, MD
Department of Medicine, University of British Columbia, 100-2647 Willow Street, Vancouver V5Z 3P1, Canada

Luigi Bonavina, Professor
Department of Surgery, Policlinico San Donato, University of Milano, via Morandi 30, Milano 20097, Italy

María Isabel Torres López, Professor
Experimental Biology, University of Jaen, araje de las Lagunillas s/n, Jaén 23071, Spain

Bo-Rong Pan, Professor
Departmant of Oncology, Xijing Hospital, Fourth Military Medical University, No.1, F. 8, Bldg 10, 97 Changying East Road, Xi'an 710032, Shaanxi Province,China

Inge Irma Depoortere, PhD
Centre for Gastroenterological Research, Gasthuisberg OandN, bus 701, Leuven 3000, Belgium

Leonard R Johnson, Professor
Department of Physiology, University Tennessee College of Medicine, 894 Union Ave, Memphis, TN 38163, United States

Satoshi Kondo, Professor and Chairman
Department of Surgical Oncology, Hokkaido University Graduate School of Medicine, N15 W7, Kita-ku, Sapporo 060-8638, Japan

Tetsuo Ohta, MD
Department of Gastroenterologic Surgery, Kanazawa University Hospital, Takara-machi 13-1, Kanazawa 920-0934, Japan

Gustav Paumgartner, Professor
University of Munich, Klinikum Grosshadern, Marchioninistr. 15, Munich, D-81377, Germany

Dong-Wan Seo, Professor
Department of Internal Medicine, Division of Gastroenterology, Asan Medical Center, Univeristy of Ulsan College of Medicine, 388-1 Pungnapdong, Songpagu, Seoul 138-736, South Korea

Bernardino Rampone, Dr
Department of General Surgery and Surgical Oncology, University of Siena, viale Bracci, Siena 53100, Italy

Giovanni Maconi, MD
Department of Gastroenterlogy, 'L.Sacco' University Hospital, Via G.B. Grassi, 74, Milan 20157, Italy

PO Box 2345, Beijing 100023, China
www.wjgnet.com
wjg@wjgnet.com

World J Gastroenterol 2006 April 14; 12(14):2309
World Journal of Gastroenterology ISSN 1007-9327

Meetings

MAJOR MEETINGS COMING UP

Digestive Disease Week
107th Annual of AGA, The American Gastroenterology Association
20–25 May 2006
Loas Angeles Converntion Center, California

American College of Gastroenterology
Annual Scientific
20-25 October 2006
Las Vegas, NV

14th United European Gastroenterology Week, UEGW
21-25 October 2006
Berlin, Germany

APDW 2006: Asian Pacific Digestive Week 2006
26-29 November 2006
Lahug Cebu City, Philippines

EVENTS AND MEETINGS IN THE UPCOMING 6 MONTHS

Falk Symposium 151: Emerging Issues in Inflammatory Bowel Diseases
24–25 March 2006
Sydney - NSW
Falk Foundation e.V.
symposia@falkfoundation.de

10th International Congress of Obesity
3–8 September 2006
Sydney
Event Planners Australia
enquiries@ico2006.com
www.ico2006.com

Easl 2006 - the 41st annual
26–30 April 2006
Vienna, Austria
Kenes International

Prague hepatology 2006
14–16 September 2006
Prague
Foundation of the Czech Society of Hepatology
veronika.revicka@congressprague.cz
www.czech-hepatology.cz/phm2006

12th International Symposium on Viral Hepatitis and Liver Disease
1–5 July 2006
Paris
MCI France
isvhld2006@mci-group.com
www.isvhld2006.com

Falk Symposium 152: Intestinal Disease Part I, Endoscopy 2006 - Update and Live Demonstration
4–5 May 2006
Berlin
Falk Foundation e.V.
symposia@falkfoundation.de

Falk Symposium 153: Intestinal Disease Part II, Immunoregulation in Inflammatory Bowel Disease - Current Understanding and Innovation
6–7 May 2006
Berlin
Falk Foundation e.V.
symposia@falkfoundation.de

ILTS 12th Annual International Congress
3–6 May 2006
Milan
ILTS
www.ilts.org

Internal Medicine: Gastroenterology
22 July 2006–1 August 2006
Amsterdam
Continuing Education Inc
jbarnhart@continuingeducation.net

6th Annual Gastroenterology And Hepatology
15–18 March 2006
Rio Grande
Office of Continuing Medical Education
cmenet@jhmi.edu
www.hopkinscme.net

World Congress on Gastrointestinal Cancer
28 June 2006–1 July 2006
Barcelona, Spain
c.chase@imedex.com

International Conference on Surgical Infections, ICSI2006
6–8 September 2006
Stockholm
European Society of Clinical Microbiology and Infectious Diseases
icsi2006@stocon.se
www.icsi2006.se/9/23312.asp

7th World Congress of the International Hepato-Pancreato-Biliary Association
3–7 September 2006
Edinburgh
Edinburgh Convention Bureau
convention@edinburgh.org
www.edinburgh.org/conference

Society of American Gastrointestinal Endoscopic Surgeons
26–29 April 2006
Dallas – TX
www.sages.org

Digestive Disease Week 2006
20–25 May 2006
Los Angeles
www.ddw.org

Annual Postgraduate Course
25–26 May 2006
Los Angeles, CA
American Society of Gastrointestinal Endoscopy
www.asge.org/education

American Society of Colon and Rectal Surgeons
3–7 June 2006
Seatlle - Washington
www.fascrs.org

EVENTS AND MEETINGS IN 2006

10th World Congress of the International Society for Diseases of the Esophagus
22–25 February 2006
Adelaide
isde@sapmea.asn.au
www.isde.net

Falk Symposium 151: Emerging Issues in Inflammatory Bowel Diseases
24–25 March 2006
Sydney - NSW
Falk Foundation e.V.
symposia@falkfoundation.de

10th International Congress of Obesity
3–8 September 2006
Sydney
Event Planners Australia
enquiries@ico2006.com
www.ico2006.com

Easl 2006 - the 41st annual
26–30 April 2006
Vienna, Austria
Kenes International

VII Brazilian Digestive Disease Week
19–23 November 2006
www.gastro2006.com.br

International Gastrointestinal Fellows Initiative
22–24 February 2006
Banff, Alberta
Canadian Association of Gastroenterology
cagoffice@cag-acg.org
www.cag-acg.org

Canadian Digestive Disease Week
24–27 February 2006
Banff, Alberta
Digestive Disease Week Administration
cagoffice@cag-acg.org
www.cag-acg.org

Prague Hepatology 2006
14–16 September 2006
Prague
Foundation of the Czech Society of Hepatology
veronika.revicka@congressprague.cz
www.czech-hepatology.cz/phm2006

12th International Symposium on Viral Hepatitis and Liver Disease
1–5 July 2006
Paris
MCI France
isvhld2006@mci-group.com
www.isvhld2006.com/

Falk Seminar: XI Gastroenterology Seminar Week
4–8 February 2006
Titisee
Falk Foundation e.V.
symposia@falkfoundation.de

European Multidisciplinary Colorectal Cancer Congress 2006
12–14 February 2006
Berlin
Congresscare
info@congresscare.com
www.colorectal2006.org

Falk Symposium 152: Intestinal Disease Part I, Endoscopy 2006 - Update and Live Demonstration
4–5 May 2006
Berlin
Falk Foundation e.V.
symposia@falkfoundation.de

Falk Symposium 153: Intestinal Disease Part II, Immunoregulation in Inflammatory Bowel Disease - Current Understanding and Innovation
6–7 May 2006
Berlin
Falk Foundation e.V.
symposia@falkfoundation.de

14th United European Gastroenterology Week
21–25 October 2006
Berlin
United European Gastroenterology Federation
www.uegw2006.de

World Congress on Controversies in Obesity, Diabetes and Hypertension
25–28 October 2006
Berlin
comtec international
codhy@codhy.com
www.codhy.com

Asia Pacific Obesity Conclave
1–5 March 2006
New Delhi
info@apoc06.com
www.apoc06.com/

ILTS 12th Annual International Congress
3–6 May 2006
Milan
ILTS
www.ilts.org

XXX Panamerican Congress of Gastroenterology
11–16 November 2006
Cancun
www.panamericano2006.org.mx

Internal Medicine: Gastroenterology
22 July 2006–1 August 2006
Amsterdam
Continuing Education Inc
jbarnhart@continuingeducation.net

6th Annual Gastroenterology And Hepatology
15–18 March 2006
Rio Grande
Office of Continuing Medical Education
cmenet@jhmi.edu
www.hopkinscme.net

Hepatitis 2006
25 February 2006–5 March 2006
Dakar
hepatitis2006@mangosee.com
mangosee.com/mangosteen/hepatitis2006/hepatitis2006.htm

World Congress on Gastrointestinal Cancer
28 June 2006–1 July 2006
Barcelona, Spain
c.chase@imedex.com

International Conference on Surgical Infections, ICSI2006
6–8 September 2006
Stockholm
European Society of Clinical Microbiology and Infectious Diseases
icsi2006@stocon.se
www.icsi2006.se/9/23312.asp

5th International Congress of The African Middle East Association of Gastroenterology
24–26 February 2006
Sharjah
InfoMed Events
infoevent@infomedweb.com
www.infomedweb.com

7th World Congress of the International Hepato-Pancreato-Biliary Association
3–7 September 2006
Edinburgh
Edinburgh Convention Bureau
convention@edinburgh.org
www.edinburgh.org/conference

13th International Symposium on Pancreatic & Biliary Endoscopy
20–23 January 2006
Los Angeles - CA
laner@cshs.org

2006 Gastrointestinal Cancers Symposium
26–28 January 2006
San Francisco - CA
Gastrointestinal Cancers Symposium Registration Center
giregistration@jspargo.com

Society of American Gastrointestinal Endoscopic Surgeons
26–29 April 2006
Dallas – TX
www.sages.org

Digestive Disease Week 2006
20–25 May 2006
Los Angeles
www.ddw.org

Annual Postgraduate Course
25–26 May 2006
Los Angeles, CA
American Society of Gastrointestinal Endoscopy
www.asge.org/education

American Society of Colon and Rectal Surgeons
3–7 June 2006
Seatlle - Washington
www.fascrs.org

71st ACG Annual Scientific and Postgraduate Course
20–25 October 2006
Venetian Hotel, Las Vegas, Neveda
The American College of Gastroenterology

AASLD 57th Annual – The Liver Meeting™
27–31 October 2006
Boston, MA
AASLD

New York Society for Gastrointestinal Endoscopy
13–16 December 2006
New York
www.nysge.org

EVENTS AND MEETINGS IN 2007

9th World Congress on Gastrointestinal Cancer
20–23 June 2007
Barcelona
Imedex
meetings@imedex.com

Gastro 2009, World Congress of Gastroenterology and Endoscopy London, United Kingdom 2009

PO Box 2345, Beijing 100023, China
www.wjgnet.com
wjg@wjgnet.com

World J Gastroenterol 2006 April 14; 12(14):2310-2311
World Journal of Gastroenterology ISSN 1007-9327

Instructions to authors

GENERAL INFORMATION

World Journal of Gastroenterology (*WJG, World J Gastroenterol* ISSN 1007-9327 CN 14-1219/R) is a weekly journal of more than 48 000 circulation, published on the 7th, 14th, 21st and 28th of every month.

Original Research, Clinical Trials, Reviews, Comments, and Case Reports in esophageal cancer, gastric cancer, colon cancer, liver cancer, viral liver diseases, *etc.*, from all over the world are welcome on the condition that they have not been published previously and have not been submitted simultaneously elsewhere.

Published by
The WJG Press

SUBMISSION OF MANUSCRIPTS

Manuscripts should be typed double-spaced on A4 (297 mm×210 mm) white paper with outer margins of 2.5 cm. Number all pages consecutively, and start each of the following sections on a new page: Title Page , Abstract, Introduction, Materials and Methods, Results, Discussion, acknowledgements, References, Tables, Figures and Figure Legends. Neither the editors nor the Publisher is responsible for the opinions expressed by contributors. Manuscripts formally accepted for publication become the permanent property of The WJG Press, and may not be reproduced by any means, in whole or in part without the written permission of both the authors and the Publisher. We reserve the right to put onto our website and copy-edit accepted manuscripts. Authors should also follow the guidelines for the care and use of laboratory animals of their institution or national animal welfare committee.

Authors should retain one copy of the text, tables, photographs and illustrations, as rejected manuscripts will not be returned to the author(s) and the editors will not be responsible for the loss or damage to photographs and illustrations in mailing process.

Online submission
Online submission is strongly advised. Manuscripts should be submitted through the Online Submission System at: http://www.wjgnet.com/index.jsp. Authors are highly recommended to consult the ONLINE INSTRUCTIONS TO AUTHORS (http://www.wjgnet.com/wjg/help/instructions.jsp) before attempting to submit online. Authors encountering problems with the Online Submission System may send an email you describing the problem to wjg@wjgnet.com for assistance. If you submit your manuscript online, do not make a postal contribution. A repeated online submission for the same manuscript is strictly prohibited.

Postal submission
Send 3 duplicate hard copies of the full-text manuscript typed double-spaced on A4 (297 mm×210 mm) white paper together with any original photographs or illustrations and a 3.5 inch computer diskette or CD-ROM containing an electronic copy of the manuscript including all the figures, graphs and tables in native Microsoft Word format or *.rtf format to:

Editorial Office
World Journal of Gastroenterology
Editorial Department: Apartment 1066, Yishou Garden,
58 North Langxinzhuang Road,
PO Box 2345, Beijing 100023, China
E-mail: wjg@wjgnet.com
http: //www.wjgnet.com

MANUSCRIPT PREPARATION

All contributions should be written in English. All articles must be submitted using a word-processing software. All submissions must be typed in 1.5 line spacing and in word size 12 with ample margins. The letter font is Tahoma. For authors from China, one copy of the Chinese translation of the manuscript is also required (excluding references). Style should conform to our house format. Required information for each of the manuscript sections is as follows:

Title page
Full manuscript title, running title, all author(s) name(s), affiliations, institution(s) and/or department(s) where the work was accomplished, disclosure of any financial support for the research, and the name, full address, telephone and fax numbers and email address of the corresponding author should be included. Titles should be concise and informative (removing all unnecessary words), emphasize what is new, and avoid abbreviations. A short running title of less than 40 letters should be provided. List the author(s)' name(s) as follows: initial and/or first name, middle name or initial(s) and full family name.

Abstract
An informative, structured abstract of no more than 250 words should accompany each manuscript. Abstracts for original contributions should be structured into the following sections: AIM: Only the purpose should be included. METHODS: The materials, techniques, instruments and equipments, and the experimental procedures should be included. RESULTS: The observatory and experimental results, including data, effects, outcome, *etc.* should be included. Authors should present *P* value where necessary, and the significant data should accompany. CONCLUSION: Accurate view and the value of the results should be included.

The format of structured abstracts is at: http://www.wjgnet.com/wjg/help/11.doc

Key words
Please list 3-10 key words that could reflect content of the study mainly from *Index Medicus*.

Text
For most article types, the main text should be structured into the following sections: INTRODUCTION, MATERIALS AND METHODS, RESULTS and DISCUSSION, and should include in appropriate Figures and Tables. Data should be presented in the body text or in Figures and Tables, but not in both.

Illustrations
Figures should be numbered as 1, 2, 3 and so on, and mentioned clearly in the main text. Provide a brief title for each figure on a separate page. No detailed legend should be involved under the figures. This part should be added into the text where the figures are applicable. Digital images: black and white photographs should be scanned and saved in TIFF format at a resolution of 300 dpi; color images should be saved as CMYK (print files) but not as RGB (screen-viewing files). Place each photograph in a separate file. Print images: supply images of size no smaller than 126 mm×76 mm printed on smooth surface paper; label the image by writing the Figure number and orientation using an arrow. Photomicrographs: indicate the original magnification and stain in the legend. Digital Drawings: supply files in EPS if created by freehand and illustrator, or TIFF from photoshops. EPS files must be accompanied by a version in native file format for editing purposes. Existing line drawings should be scanned at a resolution of 1200 dpi and as close as possible to the size where they will appear when printed. Please use uniform legends for the same subjects. For example: Figure 1 Pathological changes of atrophic gastritis after treatment. A: ...; B: ...; C: ...; D: ...; E: ...; F: ...; G: ...

Tables
Three-line tables should be numbered as 1, 2, 3 and so on, and mentioned clearly in the main text. Provide a brief title for each table. No detailed legend should be included under the tables. This part should be added into the text where the tables are applicable. The information should complement but not duplicate that contained in the text. Use one horizontal line under the title, a second under the column heads, and a third below the Table, above any footnotes. Vertical and italic lines should be omitted.

Notes in tables and illustrations
Data that are not statistically significant should not be noted. $^{a}P<0.05$, $^{b}P<0.01$ should be noted ($P>0.05$ should not be noted). If there are other series of *P* values, $^{c}P<0.05$ and $^{d}P<0.01$ are used. Third series of *P* values can be expressed as $^{e}P<0.05$ and $^{f}P<0.01$. Other notes in tables or under illustrations should be expressed as ^{1}F, ^{2}F, ^{3}F; or some other symbols with a superscript (Arabic numerals) in the upper left corner. In a multi-curve illustration, each curve should be labeled with ●, ○, ■, □, ▲, △, *etc.* in a certain sequence.

Acknowledgments
Brief acknowledgments of persons who have made genuine contributions to the manuscripts and who endorse the data and conclusions are included. Authors are responsible for obtaining written permission to use any copyrighted text and/or illustrations.

REFERENCES

Coding system

The author should code the references according the citation order in text in Arabic numerals, put references codes in square brackets, superscript it at the end of citation content or the author name of the citation. For those citation content as the narrate part, the coding number and square brackets should be typeset normally. For example, Crohn's disease (CD) is associated with increased intestinal permeability[1,2]. If references are directly cited in the text, they would be put together with the text, for example, from references [19,22-24], we know that...

When the authors code the references, please ensure that the order in text is the same as in reference part and also insure the spelling accuracy of the first author's name. Do not code the same citation twice.

PMID requirement

PMID roots in the abstract serial number indexed by PubMed (http://www.ncbi.nlm.nih.gov/entrez/query.fcgi?db=PubMed). The author should supply the PMID for journal citation. For those references that have not been indexed by PubMed, a printed copy of the first page of the full reference should be submitted.

The accuracy of the information of the journal citations is very important. Through reference testing system (http://www.aushome.cn/cgi-bin/index.pl), the authors and editor could check the authors name, title, journal title, publication date, volume number, start page, and end page. We will interlink all references with PubMed in ASP file so that the readers can read the abstract of the citations online immediately.

Style for journal references

Authors: the first author should be typed in bold-faced letter. The surname of all authors should be typed with the initial letter capitalized and followed by their name in abbreviation (For example, Lian-Sheng Ma is abbreviated as Ma LS, Bo-Rong Pan as Pan BR). Title of the cited article and italicized journal title (Journal title should be in its abbreviation form as shown in PubMed), publication date, volume number (in black), start page, and end page [PMID: 11819634]

Note: The author should test the references through reference testing system (http://www.aushome.cn/cgi-bin/index.pl)

Style for book references

Authors: the first author should be typed in bold-faced letter. The surname of all authors should be typed with the initial letter capitalized and followed by their name in abbreviation (For example, Lian-Sheng Ma is abbreviated as Ma LS, Bo-Rong Pan as Pan BR) Book title. Publication number. Publication place: Publication press, Year: start page and end page.

Format

Standard journal article (list all authors and include the PubMed ID [PMID] where applicable)

1 **Das KM,** Farag SA. Current medical therapy of inflammatory bowel disease. *World J Gastroenterol* 2000; 6: 483-489 [PMID: 11819634]

2 **Pan BR**, Hodgson HJF, Kalsi J. Hyperglobulinemia in chronic liver disease: Relationships between *in vitro* immunoglobulin synthesis, short lived suppressor cell activity and serum immunoglobulin levels. *Clin Exp Immunol* 1984; 55: 546-551 [PMID: 6231144]

3 **Lin GZ,** Wang XZ, Wang P, Lin J, Yang FD. Immunologic effect of Jianpi Yishen decoction in treatment of Pixu-diarrhoea. *Shijie Huaren Xiaohua Zazhi* 1999; 7: 285-287

Books and other monographs (list all authors)

4 **Sherlock S,** Dooley J. Diseases of the liver and billiary system. 9th ed. Oxford: Blackwell Sci Pub, 1993: 258-296

Chapter in a book (list all authors)

5 **Lam SK.** Academic investigator's perspectives of medical treatment for peptic ulcer. In: Swabb EA, Azabo S. Ulcer disease: investigation and basis for therapy. New York: Marcel Dekker, 1991: 431-450

Electronic journal (list all authors)

6 **Morse SS.** Factors in the emergence of infectious diseases. Emerg Infect Dis serial online, 1995-01-03, cited 1996-06-05; 1(1):24 screens. Available from: URL: http//www.cdc.gov/ncidod/EID/eid.htm

Inappropriate references

Authors should always cite references that are relevant to their article, and avoid any inappropriate references. Inappropriate references include those that are linked with a hyphen and the difference between the two numbers at two sides of the hyphen is more than 5. For example, [1-6], [2-14] and [1, 3, 4-10, 22] are all considered as inappropriate references. Authors should not cite their own unrelated published articles.

Statistical data

Present as mean ± SD or mean ± SE.

Statistical expression

Express *t* test as *t* (in italics), *F* test as *F* (in italics), chi square test as χ^2 (in Greek), related coefficient as *r* (in italics), degree of freedom as γ (in Greek), sample number as *n* (in italics), and probability as *P* (in italics).

Units

Use SI units. For example: body mass, m (B) = 78 kg; blood pressure, *p*(B)= 16.2/12.3 kPa; incubation time, t (incubation) = 96 h, blood glucose concentration, c (glucose) 6.4 ± 2.1 mmol/L; blood CEA mass concentration, p (CEA) = 8.6 24.5 μg/L; CO_2 volume fraction, 50 mL/L CO_2 not 5% CO_2; likewise for 40 g/L formaldehyde, not 10% formalin; and mass fraction, 8 ng/g, *etc.* Arabic numerals such as 23, 243, 641 should be read 23 243 641.

The format about how to accurately write common units and quantum is at: http://www.wjgnet.com/wjg/help/15.doc

Abbreviations

Standard abbreviations should be defined in the abstract and on first mention in the text. In general, terms should not be abbreviated unless they are used repeatedly and the abbreviation is helpful to the reader. Permissible abbreviations are listed in Units, Symbols and Abbreviations: A Guide for Biological and Medical Editors and Authors (Ed. Baron DN, 1988) published by The Royal Society of Medicine, London. Certain commonly used abbreviations, such as DNA, RNA, HIV, LD50, PCR, HBV, ECG, WBC, RBC, CT, ESR, CSF, IgG, ELISA, PBS, ATP, EDTA, mAb, can be used directly without further mention.

Italics

Quantities: *t* time or temperature, *c* concentration, *A* area, *l* length, *m* mass, *V* volume.

Genotypes: *gyr*A, *arg* 1, *c myc*, *c fos*, *etc.*

Restriction enzymes: *Eco*RI, *Hin*dI, *Bam*HI, *Kbo* I, *Kpn* I, *etc.*

Biology: *Helicobacter pylori, H pylori, E coli, etc.*

SUBMISSION OF THE REVISED MANUSCRIPTS AFTER ACCEPTED

Please revise your article according to the revision policies of *WJG*. The revised version including manuscript and high-resolution image figures (if any) should be copied on a floppy or compact disk. Author should send the revised manuscript, along with printed high-resolution color or black and white photos, copyright transfer letter, the final check list for authors, and responses to reviewers by a courier (such as EMS) (submission of revised manuscript by e-mail or on the *WJG* Editorial Office Online System is NOT available at present).

Language evaluation

The language of a manuscript will be graded before sending for revision. (1) Grade A: priority publishing; (2) Grade B: minor language polishing; (3) Grade C: a great deal of language polishing; (4) Grade D: rejected. The revised articles should be in grade B or grade A.

Copyright assignment form

It is the policy of *WJG* to acquire copyright in all contributions. Papers accepted for publication become the copyright of *WJG* and authors will be asked to sign a transfer of copyright form. All authors must read and agree to the conditions outlined in the Copyright Assignment Form (which can be downloaded from http://www.wjgnet.com/wjg/help/9.doc).

Final check list for authors

The format is at: http://www.wjgnet.com/wjg/help/13.doc

Responses to reviewers

Please revise your article according to the comments/suggestions of reviewers. The format for responses to the reviewers' comments is at: http://www.wjgnet.com/wjg/help/10.doc

Proof of financial support

For paper supported by a foundation, authors should provide a copy of the document and serial number of the foundation.

Publication fee

Authors of accepted articles must pay publication fee.

EDITORIAL and LETTERS TO THE EDITOR are free of change.

PO Box 2345, Beijing 100023, China
www.wjgnet.com
wjg@wjgnet.com

World J Gastroenterol 2006 April 14; 12(14):2312
World Journal of Gastroenterology ISSN 1007-9327

World Journal of Gastroenterology standard of quantities and units

Number	Nonstandard	Standard	Notice
1	4 days	4 d	In figures, tables and numerical narration
2	4 days	four days	In text narration
3	day	d	After Arabic numerals
4	Four d	Four days	At the beginning of a sentence
5	2 hours	2 h	After Arabic numerals
6	2 hs	2 h	After Arabic numerals
7	hr, hrs,	h	After Arabic numerals
8	10 seconds	10 s	After Arabic numerals
9	10 year	10 years	In text narration
10	Ten yr	Ten years	At the beginning of a sentence
11	0,1,2 years	0,1,2 yr	In figures and tables
12	0,1,2 year	0,1,2 yr	In figures and tables
13	4 weeks	4 wk	
14	Four wk	Four weeks	At the beginning of a sentence
15	2 months	2 mo	In figures and tables
16	Two mo	Two months	At the beginning of a sentence
17	10 minutes	10 min	
18	Ten min	Ten minutes	At the beginning of a sentence
19	50% (*V/V*)	500 mL/L	
20	50% (m/*V*)	500 g/L	
21	1 M	1 mol/L	
22	10 μM	10 μmol/L	
23	1N HCl	1 mol/L HCl	
24	1N H_2SO_4	0.5 mol/L H_2SO_4	
25	4rd edition	4^{th} edition	
26	15 year experience	15- year experience	
27	18.5 kDa	18.5 ku,18 500u or M_r18 500	
28	25 $g.kg^{-1}/d^{-1}$	25 g/(kg·d) or 25 g/kg per day	
29	6900	6 900	
30	1000 rpm	1 000 r/min	
31	sec	s	After Arabic numerals
32	1 pg $\cdot L^{-1}$	1 pg/L	
33	10 kilograms	10 kg	
34	13 000 rpm	13 000 *g*	High speed; *g* should be in italic and suitable conversion.
35	1000 *g*	1 000 r/min	Low speed. *g* cannot be used.
36	Gene bank	GenBank	International classified genetic materials collection bank
37	Ten L	Ten liters	At the beginning of a sentence
38	Ten mL	Ten milliliters	At the beginning of a sentence
39	umol	μmol	
40	30 sec	30 s	
41	1 g/dl	10 g/L	10-fold conversion
42	OD_{260}	A_{260}	"OD" has been abandoned.
43	One g/L	One microgram per liter	At the beginning of a sentence
44	*A*260 nm	A_{260} nm	*A* should be in italic.
	^bP<0.05	^aP<0.05	In Table, no note is needed if there is no significance instatistics: ^aP<0.05, ^bP<0.01 (no note if *P*>0.05). If there is a second set of *P* value in the same table, ^cP<0.05 and ^dP<0.01 are used for a third set: ^eP<0.05, ^fP<0.01.
45	**F*=9.87, $^§F$=25.9, $^\#F$=67.4	^1F=9.87,^2F=25.9, ^3F=67.4	Notices in or under a table
46	KM	km	kilometer
47	CM	cm	centimeter
48	MM	mm	millimeter
49	Kg, KG	kg	kilogram
50	Gm, gr	g	gram
51	nt	N	newton
52	l	L	liter
53	db	dB	decibel
54	rpm	r/min	rotation per minute
55	bq	Bq	becquerel, a unit symbol
56	amp	A	ampere
57	coul	C	coulomb
58	HZ	Hz	
59	w	W	watt
60	KPa	kPa	kilo-pascal
61	p	Pa	pascal
62	ev	EV	volt (electronic unit)
63	Jonle	J	joule
64	J/mmol	kJ/mol	kilojoule per mole
65	$10\times10\times10cm^3$	10 cm×10 cm×10 cm	
66	N·km	KN·m	moment
67	$x\pm s$	mean±SD	In figures, tables or text narration
68	Mean±SEM	mean±SE	In figures, tables or text narration
69	*im*	im	intramuscular injection
70	*iv*	iv	intravenous injection
71	Wang et al	Wang *et al.*	
72	EcoRI	*Eco*RI	*Eco* in italic and RI in positive. Restriction endonuclease has its prescript form of writing.
73	Ecoli	*E.coli*	Bacteria and other biologic terms have their specific expression.
74	Hp	*H pylori*	
75	Iga	*Iga*	writing form of genes
76	*igA*	IgA	writing form of proteins
77	-70 kDa	~70 ku	